

Excellentia ante omnia

ABSTRACT BOOK

Twenty-Sixth Annual Meeting

Omni Shoreham Hotel, Washington, DC 20008

June 20 – 24, 2004

1978-2004

26 Years of Excellence

FOREWORD

The following abstracts were reviewed by the Technical Program Committee and approved for presentation at the Twenty-Sixth Annual Meeting. While the Technical Program Committee reviewed the content of these abstracts, they may not present completed work nor were they formally peer-reviewed for technical content.

Individuals wishing to reference or quote from these abstracts in whole or part should obtain permission from the author(s).

Some abstracts were optically scanned for this compilation. This process is not perfect and errors may have been introduced, for which we apologize.

*The BEMS copyright on the following abstracts does not extend
To any government work that is in the public domain.*

ABSTRACTS

PLENARY SESSION I:
NIH FUNDING UPDATE
PULSED HV FIELDS
Chair: Bruce McLeod

NIBIB/NIH EXTRAMURAL RESEARCH PROGRAMS UPDATE. W.J. Heetderks. NIBIB, NIH, Bethesda, MD 20892, USA.

The National Institute of Biomedical Imaging and Bioengineering (NIBIB) is the newest institute at the NIH having been formed just over 3 years ago. Our mission is to improve public health through the discovery of new devices and application of technologies to biomedical research and clinical applications. The bulk of our funds provide grants to researchers at universities and research centers for support of research and technology development. In this presentation, I will highlight some of our ongoing projects in the area of sensing and imaging that depend on the interaction of the biological tissue with electromagnetic energy. I will also outline the support mechanisms we have available to support research and training. Emphasis will be on the unique aspects of the NIBIB.

ULTRASHORT ELECTRICAL PULSES OPEN A NEW GATEWAY INTO CELLS. K.H. Schoenbach. Center for Bioelectrics, Old Dominion University and Eastern Virginia Medical School, Norfolk, VA 23510 USA.

Results of simple electrical models of biological cell indicate that ultrashort pulses, with pulse durations of less than the charging time constant of the plasma membrane, affect intracellular structures. The primary targets of such pulses are the membranes of organelles. Charging these membranes allows us to induce and control intracellular membrane processes, such as intracellular electroporation. Experimental studies in which human cells were exposed to pulsed electric fields of up to 30 MV/m amplitude with durations as short as 10 ns, have confirmed this hypothesis. The observed effects include the breaching of intracellular granule membranes without permanent damage to the cell membrane, abrupt rises in intracellular free calcium levels, and enhanced expression of genes. At increased electric fields, the application of submicrosecond pulses induces apoptosis in biological cells.

Modeling of the ultrashort pulse effects has so far focused on microdosimetry; the modeling of the electric field and energy distribution in cells when exposed to ultrashort pulses. The calculations utilize measured electrical parameters of cells such as the complex permittivity of membranes and cytoplasm or nucleoplasm, and assumptions on critical voltages, for which the resistivity of the membranes changes. First attempts to address field-induced changes on the molecular level are underway. Such modeling studies coupled with experimental studies on the pairing of primary effects (charging of subcellular membranes) with secondary effects, such as apoptosis, are the topic of a Multidisciplinary University Research Initiative (MURI) project.

In spite of our still limited understanding of electric field interactions with subcellular structures, applications for the observed effects are already being considered. Apoptosis induction by means of ultrashort pulses has already been tested as a way to reduce or inhibit the growth of tumors. Calcium release has been shown to cause temporary immobilization of cells; an effect that we feel is the cause for the observed immobilization of certain aquatic species. Another possible application of intracellular electroeffects is gene therapy. Initial studies that used electroporation to open the outer plasma membrane, followed by ultrashort pulses, resulted in increased expression of a reporter gene. In addition to

environmental and medical applications, intracellular electroporation opens a new field of research of electrical effects on the subcellular level. By utilizing electrical pulses, which generate electric fields on the same order and higher than the inherent electric fields in membranes, and using pulses with durations long enough to charge membranes of subcellular structures, but short enough to avoid thermal effects, the ultrashort pulses serve as electrical probes, allowing us to expand our knowledge about the electrical parameters of cells.

Research on this topic has been supported by an AFOSR/DOD MURI grant on subcellular responses to narrowband and wideband radiofrequency radiation, administered through Old Dominion University.

The initial focus for the day will be funding and the exciting new research area of ultrashort electrical pulses. We will continue with the results of major studies focusing on the assessment of the biological effects of electromagnetic field exposure from the animal level to humans.

SESSION 1: PULSED HV RESEARCH and APPLICATION

Chairs: Joe Roti Roti and Marty Meltz

1-1

INTRACELLULAR EFFECTS DUE TO EXTREMELY LARGE, SUBMICROSECOND ELECTRIC FIELD PULSES: THEORY AND MODELING. J.C. Weaver, D.A. Stewart,* Z. Vasilkoski* and T.R. Gowrishankar*. Harvard-MIT Division of Health Sciences and Technology, Massachusetts Institute of Technology, Cambridge, MA 02139, USA

INTRODUCTION: Several groups have described experiments in which nonthermal electric field pulses with durations of 10 to 300 ns and magnitudes of 1 to 150 kV/cm cause effects associated with subcellular structures. Field-induced apoptosis is the most striking effect.

OBJECTIVES: We are creating progressively more realistic models of cells, such that models contain not only the outer plasma membrane (PM), but also models for subcellular structures such as the nucleus, endoplasmic reticulum and several mitochondria. This provides microdosimetry at the cellular and subcellular level. With suitable biophysical coupling models this also provides estimates of chemical change by predicting molecular and ionic transport within a cell model.

METHODS: We use a transport lattice approach (Gowrishankar and Weaver, PNAS, 2003) to create two dimensional (2D) mammalian cell models that include subcellular structures. These models include local models for conductive and dielectric properties of membranes and of the extra- and intracellular electrolytes, with the dielectric properties of electrolytes important for short pulses with high frequency components. The membrane also contains local models for the resting potential and a local nonlinear, hysteretic model for lipid membrane electroporation, which involves solving an ordinary differential equation at ~600 local sites within the cell model (Stewart et al, submitted). We also use a 3 μm X 3 μm membrane planar patch model with a Smoluchowski equation-based model to investigate local electroporation behavior due to pulses of a wide range of durations and amplitudes.

RESULTS: The planar patch model shows that supra-electroporation (two to three orders of magnitude more pores per area than conventional electroporation) is expected for the very large, submicrosecond pulses (Vailkoski et al., in preparation), and that only minimum size pores ($r \sim 1$ nm) are involved in preventing the transmembrane voltage from exceeding ~ 1.5 V. The 2D cell models show that the PM is supra-electroporated. Both displacement and conductive currents create sufficiently large intracellular fields that the mitochondrial inner membrane is electroporated, with the postpulse, slowly decaying pore population sufficient to create a quasi-voltage clamp of ~ 0 V (transmembrane voltage). This should open the mitochondrial permeability transition pore (MPTP), one proposed mechanism for initiating apoptosis by a permeability transition (Halestrap et al. Biochimie, 2002; Zamzami and Kroemer, Curr. Biol. 2003). A general feature of our models is that supra-electroporation occurs extensively in the PM and less but significant electroporation occurs in membranes of the nucleus, endoplasmic reticulum and both the inner and outer mitochondrial membranes. The small, residual pores have lifetimes of order seconds, which is a mechanism for translating submicrosecond interactions to the physiological time scale of 0.1 ms to seconds. Translocation of membrane components is expected for both conventional (pulses with > 100 microsecond durations and ~ 1 kV/cm magnitudes) and supra-electroporation, and the persistence of translocated phospholipids or proteins generates signals that can last for even longer times. Both molecular and ionic transport of residual pores and signaling by translocated membrane molecules may contribute to diverse and potentially specific intracellular effects that are caused by the exposure of cells and tissues to extremely large, submicrosecond pulses.

Support: AFOSR/DOD MURI grant on Subcellular Responses to Narrowband and Wideband Radio Frequency Radiation, administrated through Old Dominion University and NIH grant RO1-GM63857.

HUMAN GENE EXPRESSION IN RESPONSE TO NANOSECOND PULSED ELECTRIC FIELDS. C.C. Tseng*¹, Z-M. Wang*¹, D.S. Johnson*¹, S.J. Beebe*², and K.H. Schoenbach*³. ¹Purdue University Calumet, Hammond, Indiana 46323, USA; ²Eastern Virginia Medical School, Norfolk, Virginia 23510, USA; ³Old Dominion University, Norfolk, Virginia 23510, USA.

INTRODUCTION: The responses of human cells to nanosecond pulsed electric fields (nsPEF) depend on exposure conditions (field intensity, pulse duration, and pulse number), and the effects range from alterations of gene expression (without immediate apoptosis) to necrosis. The present work focuses on gene expression using exposure conditions below the thresholds that cause apoptosis and membrane electroporation.

OBJECTIVES: 1) To determine the 6 h response of 20,000 human genes from a cell line exposed to 3 consecutive 60 ns pulses at 15kV/cm. 2) To classify the up-regulated and down-regulated genes based on functions. 3) To use the current results as a basis for additional work, including the study of time-dependent expression of affected genes.

METHODS: Human HL-60 cells were grown in RPMI + 10% FBS, and 10×10^6 cells/ml were transferred to a cuvette (1 mm) for a total volume of 130 μ l RPMI medium with FBS. Cells were exposed to 3 consecutive 60 ns pulses at 15kV/cm. Exposed cells from 5 cuvettes were pooled (650 μ l), diluted 10-fold with RPMI + 10% FBS, and incubated for 6 hours in a T75 flask. Under this nsPEF condition, there was no membrane electroporation as determined by ethidium homodimer uptake, no immediate apoptosis as indicated by the lack of caspase activation and the absence of annexin-V-FITC binding, and no cell death (near 100% survival). After nsPEF exposure and incubation, RNA was extracted in a single-step phenol-chloroform process. Amersham's CodeLink Expression Bioarray System (Human 20K genes) was used to determine genome-wide gene expression. The procedure involved 1) the preparation of total RNA, 2) first strand cDNA synthesis, 3) 2nd strand cDNA synthesis, 4) cDNA purification, 5) *in vitro* transcription and biotin-labeling of cRNA, 6) cRNA purification, 7) fragmentation of cRNA, 8) hybridization of cRNA with probes on the microarray, 9) washing and staining with fluorophore, 10) scanning, and 11) data analysis.

RESULTS: From a total of 20489 genes analyzed, 603 genes are up- or down-regulated using the minimum value of a 2-fold difference. Of the affected genes, 1/3 is down-regulated and 2/3 are up-regulated. Many of the affected genes are involved in important biological activities such as signal transduction, cell adhesion, apoptosis, cell defense, immunity, inflammatory and stress response, transcriptional control, DNA binding, ion transport, protein folding, phosphorylation and modification, and cell death. These results clearly indicate that the nsPEF condition we applied can have significant impact on gene expression, although the immediate cellular and subcellular changes leading to apoptosis are not apparent. The data will be compared with the results from both longer and shorter periods of incubation (2h, 12h, and 24h) in order to follow the sequential changes of gene activity after nsPEF exposure.

CONCLUSIONS: 1) Genes are sensitive to environmental conditions (e.g., nsPEF) as shown by genome-wide expression analysis. 2) Current PEF conditions represent a minimum level that may alter gene expression in HL-60 cells. 3) Gene expression may occur at different time intervals, e.g., 2h, 6h, 12h, and 24h. 4) Current data will be compared with the affected genes expressed at different intervals.

This research is supported by two AFOSR DOD MURI grants.

DYNAMIC EFFECTS OF NANOSECOND PULSED ELECTRIC FIELDS ON HUMAN CELL SIGNAL TRANSDUCTION AND FUNCTION. S.J. Beebe*^{1,2,4}, C.C. Tseng³, P.F. Blackmore*², J. White*¹, E. Hall*¹, and K.H. Schoenbach*⁴ ¹Center for Pediatric Research, Eastern Virginia Medical School, Norfolk Virginia 23510 USA; ²Department of Physiological Sciences, Eastern Virginia Medical School, Norfolk Virginia, 23501 USA; ³Purdue University Calumet, Hammond Indiana 46323 USA; ⁴Center for Bioelectrics Old Dominion University and Eastern Virginia Medical School, Norfolk Virginia, 23510 USA

INTRODUCTION: Nanosecond, high intensity pulsed electric fields with rapid rise and fall times [nsPEF] that are below the plasma membrane [PM] charging time constant have decreasing effects on the PM and increasing effects on intracellular structures and functions as the pulse duration decreases [1, 2, 3].

OBJECTIVES: These studies were designed to investigate nsPEF-induced intracellular electro-effects [ICE²] that modulate intracellular signaling mechanisms and regulate cell function and fate in human cells.

METHODS: Human cells in suspension were exposed in cuvettes to nsPEF with durations between 10 and 300 nanoseconds and electric fields between 4-300 kV/cm. Cells were analyzed for apoptosis markers, intracellular calcium using fura-2 and fluorometry, green fluorescent protein [GFP] expression by flow cytometry, or gene expression by microarray analysis. B10.2 mouse fibrosarcoma tumors were exposed to nsPEF *in vivo* with needle electrodes and analyzed for apoptosis markers, size, and weight.

RESULTS: When electric fields were high enough, apoptosis signaling pathways were activated in several cell culture models as defined by phosphatidylserine externalization [PSE], caspase activation, DNA fragmentation, and cytochrome *c* release into the cytoplasm. B10.2 mouse fibrosarcoma tumors exposed *in vivo* to nsPEF exhibited DNA fragmentation and elevated caspase activity and were reduced in size and weight compared to contralateral sham-treated control tumors. However, in adherent HCT116 colon carcinoma cells, PSE and caspase activation were present but cells did not die, suggesting that these two markers serve non-apoptotic functions in these cells. When ICE² were below the thresholds for apoptosis and classical plasma membrane electroporation in HL-60 cells (60ns, 15kV/cm), signaling was initiated by mobilizing calcium from the endoplasmic reticulum and subsequently by capacitive calcium entry through store-operated channels in the PM. These responses mimicked calcium mobilization induced by purinergic agonists that bind to receptors in the PM. Under these same ICE² conditions, out of a total of 20,500 genes analyzed, the expression of 603 genes (~3%) was up regulated (~67%) or down-regulated (~33%) by ≥2-fold. The expression of ~60 genes were affected by ≥4-fold. The affected genes were involved in signal transduction, ion transport, DNA binding, and transcription control, among others. Finally, when ICE² conditions followed classical electroporation-mediated transfection of a green fluorescent protein [GFP] plasmid, the expression intensity and number of GFP-expressing cells were enhanced above electroporation conditions alone.

CONCLUSIONS: These studies demonstrate that nsPEF-induced ICE² can serve as basic science and/or as therapeutic tools that can profoundly modulate cell signaling mechanisms involving second messenger actions, ion transport, and transcription/translation that determine survival or death functions.

The Air force Office of Scientific Research and the American Cancer Society supported these studies.

[1] Schoenbach KH, Beebe SJ, and Buescher ES (2001) *Bioelectromagnetics* 22: 440-448.

[2] Beebe SJ, Fox PM, Rec LJ, Willis EI, and Schoenbach KH (2003) *FASEB J*.17: 1493-5.

[3] Beebe SJ, White J, Blackmore, PF, Deng Y, Somers, K, Schoenbach KH (2003) *DNA Cell Biol.* 22: 785-96.

THE RULES OF CELL SURVIVAL AFTER EXPOSURE TO HIGH-INTENSITY, ULTRASHORT ELECTRICAL PULSES. A. Pakhomov^{1,3}, K. Walker III¹, J. Kolb³, K.H. Schoenbach³, B. Stuck², and M. Murphy⁴. ¹McKesson BioServices Corporation, ^{1,2}US Army Medical Research Detachment, Brooks City-Base, San Antonio, TX, USA; ³Center for Bioelectrics, Old Dominion Univ., Norfolk, VA, USA; ⁴Directed Energy Bioeffects Division, Human Effectiveness Directorate, Air Force Research Laboratory, Brooks City-Base, San Antonio, TX, USA.

OBJECTIVES: The study was aimed to: (1) analyze the dependence of cytotoxic effect of 10-ns electrical pulses (EP) on their voltage, number, and repetition rate, (2) characterize the time dynamics and general mechanisms of cell death, and (3) develop quantitative criteria of sensitivity of different cell lines to 10-ns EP.

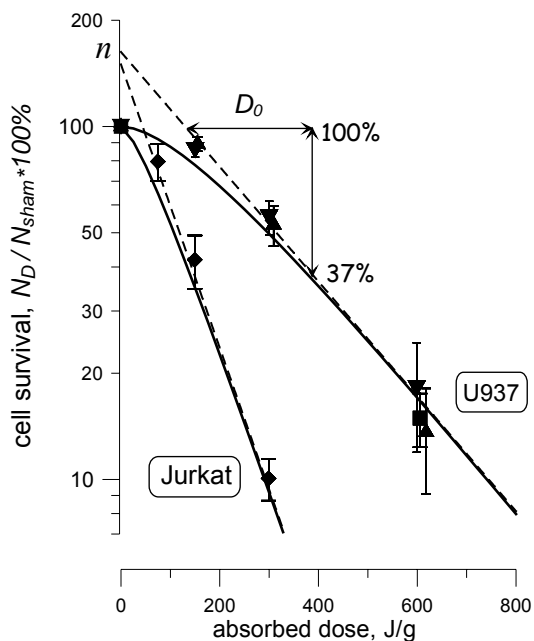


Figure 1. Survival of Jurkat (left) and U937 cells as a function of the absorbed dose. Different symbols for U937 cells correspond to mean survival values (\pm s.e.) for different pulse voltages (87, 125, and 174 kV/cm). Datapoints at doses producing average survival under 10% have not been included. Dashed and solid lines are the best fits approximations using equations (1) and (2), respectively (see text). Calculation of D_0 is illustrated for U937 cells only. See text for more detail.

METHODS: Experiments were performed in two cell lines, U937 (human histiocytic lymphoma) and Jurkat (human T-cell leukemia). Cells were grown at 37 °C with 5% CO₂ in air in ATCC-modified RPMI 1640 medium with 10% fetal bovine serum. Cells were exposed in the growth medium at 0.2×10^6 cells/ml in gene transfer cuvettes (BIORAD) with a 1- or 2-mm gap between the electrodes. High-intensity 10-ns EP were applied using a Blumlein line generator manufactured at the Old Dominion University. Pulse shape and amplitude were monitored with a 500-MHz TDS3052B Tektronix digital oscilloscope using a custom-made high-voltage probe. All exposures were performed at a room temperature of 24-25 °C, and even under the most intensive EP treatment the temperature of exposed samples did not exceed 37 °C. Live and dead cell densities were determined by hemocytometer cell counts after Trypan blue staining, at intervals from 0.5 to 72 hr post exposure. The induction of apoptosis by EP was evaluated by the specific cleavage of poly(ADP-ribose) polymerase (PARP) using Western blot, and by internucleosomal DNA

fragmentation using agarose gel electrophoresis.

RESULTS: In U937 cells, exposure to brief pulse trains (e.g., 100 pulses at 100 kV/cm, or 200 pulses at 75 kV/cm) killed only few cells, if any. Longer pulse trains and/or higher voltages caused both immediate (necrotic) and delayed (at least partially apoptotic) cell death. Live cell density reached its minimum at 8-16 hr after the exposure; afterwards, surviving cells proliferated at a regular pace. Jurkat cells showed the same immediate and delayed types of cell death, but were far more sensitive to the same EP treatment than U937. Jurkat survivors failed to restore normal proliferation rate within 72 hr of post-exposure observation. Analysis of the cytotoxic efficiency of varied EP treatments (different E-field values, numbers of pulses, and pulse repetition rates) established that, in most cases, same values of the absorbed dose (D , J/g) caused the same decrease in cell survival. For both tested cell lines, the survival decreased exponentially with increasing D , with an initial shoulder at lower doses (Fig.1). However, at survival rates under 10%, the mean survival values often were situated above the exponential fit line, either due to the presence of a resistant cell fraction in the population, or because of nonuniform exposure of samples. The survival curves such as shown in Fig. 1 closely resemble well-known types of dose response for bioeffects of ionizing radiation, and can be conveniently described in the same terms. Disregarding the initial shoulder, the surviving cell fraction $N_{(D)}/N_{(sham)}$ can be calculated as:

$$N_{(D)}/N_{(sham)} = e^{(-\frac{D}{D_0})} \quad (1),$$

where D_0 is the dose that decreases the survival to 37%. The initial shoulder can be taken into account using the function:

$$N_{(D)}/N_{(sham)} = 1 - (1 - e^{(-\frac{D}{D_0})})^n \quad (2),$$

where n is the extrapolated intercept of the exponential portion of the curve with the ordinate axis. (See Fig. 1 for illustration of procedures employed to calculate n and D_0 .)

SUMMARY: The indices D_0 and n can be used for quantitative comparison of EP sensitivity of different cell lines. Their respective values in our study were 108 J/g and 1.5 for Jurkat cells, and 266 J/g and 1.63 for U937. Cellular mechanisms responsible for so different sensitivity of these cell lines to EP have yet to be understood. It is important to note, however, that, even at the highest tested doses, heating of samples was not the cause of cell death. The similarity of the dose-response curves with those of the ionizing radiation effect may be pointing to common interaction principles and/or cell killing mechanisms. The possibility of selective killing of certain cell types with little impact on other cells may have potential applications in biotechnology and medicine.

The work was supported by the U.S. Army Medical Research and Materiel Command and the U.S. Air Force Research Laboratory under U.S. Army contract DAMD17-94-C-4069 awarded to McKesson BioServices Corporation, and by an AFOSR/DOD MURI grant on Subcellular Responses to Narrowband and Wideband Radiofrequency Radiation, administered through Old Dominion University.

1-5

ULTRAWIDEBAND ELECTROMAGNETIC RADIATION (UWB EMR) EXPOSURES AND ACTIVATION OF SIGNAL TRANSDUCTION PATHWAY. M. Natarajan¹, B.K. Nayak^{1*}, S.P. Mathur², C. Galindo^{1*}, M.L. Meltz¹. ¹Dept of Radiation Oncology, University of Texas Health Science Center at San Antonio, ²McKesson BioServices, US Army Med Res Detachment, Brooks City-Base, San Antonio, TX 78235 USA.

OBJECTIVE: The study of cell signaling mechanisms continues to move forward at a prodigious rate. Signal transduction is a fundamental process that cells and organisms use to respond to external stimuli, and thereby attempt to maintain normal function and homeostasis. Since a subtle change in the environment can initiate and transduce signals, it has immense value for (a) estimating an agent's biological

activity, (b) defining an agent's mode of action and (c) establishing an agent's antagonism or synergism with other agents. In an attempt to identify and understand the biological effects initiated by electromagnetic radiation exposure of mammalian cells, our focus is directed towards examining the activation of signaling mechanisms. In this presentation we will review the studies on signaling mechanisms induced/inhibited by ultrawide band exposures. Second, we will discuss the current studies undergoing in our laboratory on cell signaling upon UWB exposure of human Cells.

METHODS: For the current study, the following exposure parameters are used: human monocytes were exposed intermittently to UWB pulses for a total of 90 minutes (three recurring exposures of 30 minute on and 30 minute off). The pulse width was 0.8 ns pulse rise time was between 258 to 273 ps, pulse E-field was 100 kV/m, and the pulse repetition rate was 250pps. The temperature of the medium was maintained at 37°C in both sham and RFR-exposed flasks. Immediately after exposure the cells were transferred to 37°C Air/CO2 incubator and harvested after 10 min, 0.5 h, 4 h, 8 h, 24 h, and 48 h. Initiation of the NF-κB signaling pathway was analyzed by EMSA analysis. To examine the downstream effect of the NF-κB signaling pathway, cells transiently transfected either with NFκB-luciferase reporter vector or control vector were exposed as described above and harvested after 16 h. The whole cell extract was examined for NFκB-dependent transcriptional activation of downstream genes by luciferase reporter assay. The differential expression of NFκB dependent genes was screened at 8 and 24 h after UWB exposure by NFκB super array.

RESULTS: Cells exposed to UWB and incubated for 24 h post-irradiation showed a marked increase in the NFκB DNA-binding activity compared to mock-irradiated controls. The results provide evidence that UWB can initiate NFκB-dependent cell signaling pathway. The cell signaling response after UWB exposure appears to be a delayed effect, since, unlike UWB, Mono Mac cells exposed to 2.5 and 8.2 GHz microwave radiation, showed the activation of NFκB at much earlier time point (4 and 8 h). Cells transiently transfected with Mercury Pathway™ constructs containing 4X NFκB binding sites associated with luciferase reporter system did not induce NFκB driven luciferase activity indicating that the activation of NFκB after UWB exposure is functionally inactive. Similarly, the transcriptional regulation of κB-dependent target gene expression in response to UWB investigated by Human TranSignal™ NFκB target gene array revealed no difference in the gene expression profile, which further confirms that the UWB-induced NFκB is only a transient response with minimal or no downstream effect.

This work was supported by the AFOSR Grant No. F49620-01-1-0349

1-6

POTENTIAL EFFECTS OF SHORT {1-5 SECOND} THERMOEXPOSURES {+ 15°C} FROM 95 GHZ RADIATION ON DNA REPAIR. J.L. Roti Roti, J. Mueller*, M. Xu*, E. Moros. Radiation Oncology Dept, Washington Univ School of Medicine, St. Louis, Missouri 63108 USA.

The ability of cells to effectively repair DNA damage arising from environmental hazards such as ionizing radiation, ultraviolet radiation and other environmental genotoxic agents is thought to be critical for the maintenance of long term genomic stability. Loss of genomic stability is thought to be an early step in the development of cancer. Therefore, agents, which increase genomic instability, are potentially carcinogenic. Recent knowledge of the proteins involved in DNA repair has made new methods available to study the heat effects on the DNA repair processes, particularly those processes following exposure to ionizing radiation. These new approaches will be reviewed in this presentation. Traditional estimates of thermal hazards have relied on the concept of thermal dose which utilizes time-temperature conversions. However, it is possible that short (1 -5 sec) exposures to high temperature (+10 -15oC) may not follow the traditional time temperature conversions. This is an important fact to ascertain in the ongoing research. However, assuming for the sake of experimental design that such conversions are valid, we find that a +15oC exposure returning exponentially to ooC in 20 sec might result in a thermal dose that would be equivalent

to approximately 6 min at 43oC for cells that were adapted to growing at 37oC. This exposure has potential biological effects and it can be further converted into temperatures for which thermal effects on DNA repair systems have been studied in our laboratory, particularly 41oC. We find that at 41oC there are heat effects on both the DNA repair protein, MRE11 and the modified chromatin protein, yH2AX, which marks chromatin at the site of DNA damage. Aspects of the heat-induced effects of these changes correlate linearly with increases in radiosensitivity of the heated cells. Interestingly, these changes do not correlate with DNA damage or repair as measured by the comet assay. Future studies are designed to look at the potential interaction between UV and the thermal effects from 95 GHz because it is likely that exposed personnel will have simultaneous UV and thermal exposures. We have chosen a rat system and the current plan is to look at the induction and repair of DNA damage following UV exposure with and without exposure to 95 GHz. We expect that the results from this study will either identify a potential thermal hazard in terms of DNA repair or provide knowledge of a safety margin should the thermal dose be sufficiently low that no thermal effects on DNA repair are anticipated.

This study was supported by the Non-lethal Technology Innovation Center.

SESSION 2: EPIDEMIOLOGY
Chairs: Leeka Kheifets and C.K. Chou

2-1

COMPARATIVE ANALYSIS OF RF EXPOSURE FROM MOBILE PHONES IN DIFFERENT GEOGRAPHICAL LOCATIONS. J.J. Morrissey, M. Kanda. Motorola Florida Research Labs, 8000 West Sunrise Blvd., Ft. Lauderdale, Florida, USA 33322.

OBJECTIVE: Characterize and compare nominal RF exposure from mobile phone use in Motorola engineers residing in different geographical locations in the US, Europe, and Asia using modified dosimeter phones.

BACKGROUND: In assessing the potential adverse health risk of a physical or chemical agent, significant weight is generally placed on epidemiologic studies if they are available and have satisfactory study design. Existing epidemiologic studies that have analyzed mobile phone use and the incidence of various forms of cancer will undoubtedly play a role in upcoming risk assessment efforts, including that of the International Agency for Research on Cancer (IARC) in ~2005 to evaluate mobile phone use as a potential carcinogen. Dose assessment strategies in previous mobile phone epidemiologic studies have involved analysis of billing records or reconstruction of mobile phone use through questionnaire. Although such methods can provide some general information on the amount of time an individual may have used a mobile phone, the extent of recall accuracy and bias, and the contribution of many other variables that can influence the actual RF dose absorbed by a mobile phone user, are largely unknown. One of these variables, the influence of different geographical locations, may affect RF dose as a result of variations in the communication network, terrain, volume of communication traffic, average distance to work / time of travel, etc. In the following study, we have attempted to compare nominal RF exposure from the use of mobile phones in similar groups of Motorola engineers as a result of their location in different geographical areas.

METHODS & RESULTS: Software modified dosimeter phones were developed as described previously (BEMS 2001, 2002, 2003) and sent contacts at Motorola facilities in Ft. Lauderdale Florida, Arlington Heights Illinois, Libertyville Illinois, Phoenix Arizona, Austin Texas, Basingstoke UK, Taunusstein Germany, Paris France, and Penang Malaysia. Phones were then handed out to Motorola engineers that had pre-existing GSM network accounts. The volunteers were able to swap their existing GSM network SIM card into the modified dosimeter phone and use it for 2 weeks as their normal phone without changing their user information or calling habits. During the data collection period, a date and time stamp was assigned to each call and average transmit power levels ranging between a few up to 250 milliwatts were recorded every 2.5 seconds. At the end of the 2-week data collection period, information on number of calls and transmit power was downloaded and analyzed. The results demonstrate significant differences in average transmit power levels between locations, as well as due to other variables that correlated with responses on a questionnaire given immediately before each study. By inference, this would suggest potential variations of similar magnitude in SAR between otherwise similar groups of mobile phone users in epidemiologic studies.

DISCUSSION AND CONCLUSION: Based upon this data, dose assessment for mobile phone use might be strengthened in epidemiologic studies if additional information, such as the effect of different geographical locations, is characterized and incorporated. In addition age, time spent inside buildings vs. outdoors, time spent driving, RF signal type, metropolitan vs. rural residence and/or workplace, and other factors may also provide useful information that might strengthen dose assessment data.

This study supported by Motorola, Inc.

EFFECT OF GSM CELLULAR PHONES ON HUMAN HEARING: METHODOLOGICAL APPROACH AND PRELIMINARY RESULTS. S.L. Bell*¹, N. Thomas *¹, M. Parazzini*², G. Thuroczy³, M.E. Lutman*¹, P. Ravazzani².¹Inst of Sound and Vibration Res, Univ of Southampton, Hi SO17 1BJ, Southampton, UK; ²Inst di Ingegneria Biomedica CNR, 20133 Milano, Italy; ³Nat'l Res Inst for Radiobiology and Radiohygiene, Dept. of Non-Ionising Rad,122 Budapest, Anna u.5, Hungary.

INTRODUCTION: The purpose of this paper is to present the experimental protocol and the work in progress performed in the framework of the European project GUARD to assess potential changes of the hearing function of humans after exposure to low-intensity electromagnetic fields produced by GSM cellular phones. This study has entailed development of protocols to identify small changes in auditory function. That is why, in addition to conventional measures of hearing threshold level, which require a subjective response, the study focuses on two types of objective response: otoacoustic emissions and the auditory brainstem response. The study design, test protocols and preliminary analysis of data from the first recordings will be presented.

MATERIALS AND METHODS In this study two experimental paradigms are used: the within-subject paradigm and the between-subject paradigm. The first entails measurements immediately before and immediately after exposure to EMF via a commercial mobile phone. The procedure is conducted twice in a double-blind design: once with a genuine exposure and once with a sham exposure. The second utilises two groups: heavy users and light users of mobile telephones. The differences between groups are assessed to determine if there may be any chronic effects of mobile telephone use. Participants are healthy young adults (18-30 years old) without any evidence of hearing or ear disorder. Additionally, for the between-subject study, participants are screened either as high or as low users of mobile telephones, where high users are defined as typically speaking for at least 30 minutes per day using a mobile phone held to the ear and low users are defined as typically speaking for less than 5 minutes per day. The tests for assessment of auditory function are: transient otoacoustic emissions (TEOAE) using click stimuli, distortion product otoacoustic emissions (DPOAE) using DP-gram and I/O function, auditory brainstem response (ABR) using clicks at medium and high rates. For the within-subject study, they are performed immediately before and after exposure to EMF and only the exposed ear is tested. For the between-subject study, they are performed only once on both ears. For the within-subject study only, the exposure, double blind and counterbalanced in order, consists of speech at a typical conversational level delivered via an earphone to one ear, plus EMF exposure in either genuine (test) or sham (control) conditions to simulate the normal use of a phone. Genuine and sham exposures are on separate days (at least 24 hours apart) EMF exposure utilises the normal output of a consumer mobile phone (NOKIA 6310) at full power for 10 minutes. Half of the participants receive GSM exposure at 900 MHz (full power = 2W) and the other half receive GSM exposure at 1800 MHz (full power = 1W). The sham or genuine exposure is performed using a "load" or a "dummy load". A system of phone fixation with a possibility of freely moving of the subjects' head but without any replacement of the phone from the adjusted position was designed. During the exposure the phone is placed so that its longitudinal axis follows an imaginary line from the entrance to the ear canal to the corner of the mouth.

RESULTS: A pilot study has confirmed the practicality both of the study design and of the test protocols. No problems were found with performing the two recording and exposure sessions. The longest test session is around 2 hours. All mobile phones included in the project have passed validation tests before use. During the tests the power, the frequency and the spatial distribution of the radio frequency exposure was processed. The variation in results, i.e. before and after exposure or between the two groups of mobile phone user, appears small at this stage and individual variability is within the limits at which the effect should be notified to the ethics committee.

CONCLUSIONS: These preliminary findings show no significant effects of GSM electromagnetic fields on the hearing system of humans neither in the case of acute effect nor in the case of chronic effect. The experiments, results evaluation and statistical analysis are currently in progress.

This work was partially financed by the Project GUARD “Potential adverse effects of GSM cellular phones on hearing” (European Commission, 5th Framework Programme, QLK4-CT-2001-00150, 2002-2004).

2-3

METHODS FOR ASSESSING OCCUPATIONAL EXPOSURES TO ELECTRIC AND MAGNETIC FIELDS FOR THE INTERPHONE STUDY OF MOBILE PHONES AND CANCERS OF THE HEAD. J.D. Bowman¹, D.L. Conover¹, S. Mann^{2*}, D. McLean*, L. Nadon^{3*}, P. Vecchia^{4*}, I. Deltour*, E. Cardis*. Int’l Agency for Res on Cancer, 150 Cours Albert Thomas, 69008 Lyon, France. ¹Nat’l Inst for Occupational Safety and Hlth, Cincinnati, OH, USA. ²Nat’l Radiological Protection Board, Didcot, Oxon, OX11 0RQ, UK. ³INRS—Inst Armand Frappier, Laval de Rapides, Quebec, Canada. ⁴Nat’l Inst of Hlth, Rome, Italy.

BACKGROUND: The INTERPHONE study of mobile phones cancers of the head is a population-based case-control study which is being conducted in 13 countries. In addition to mobile phone radiation, the personal interviewers from the INTERPHONE study also ask subjects about their exposures to other known or possible risk factors for cancers of the head, including occupational sources of electric and magnetic fields (EMF) from 0 Hz through the microwave frequency range.

OBJECTIVE: This presentation summarizes methods developed by the INTERPHONE study to estimate the cumulative exposure and frequency range of workplace EMF exposures from the interview results.

METHODS: Cases in the INTERPHONE study are adults, age 30-59, who have verified cases of brain cancer, salivary gland tumors, or acoustic neurinomas. Controls are randomly drawn from the general population and matched to cases by age and gender. Study centers in Australia, Canada, Denmark, Finland, France, Germany, Israel, Italy, Japan, New Zealand, Norway, Sweden, and the United Kingdom have different methods for identifying cases and controls, but they all conform to a common protocol that ensures the subjects are drawn from the general population of a clearly defined region. Each subject who met the study criteria and gave their informed consent received a Computer-Assisted Personal Interview (CAPI). In addition to queries about demographics and mobile phone use, the CAPI questionnaire includes a structured interview on occupational EMF sources throughout the subject’s work history, including the type of source, product, work process, frequency of use, duration of employment, distance from the source, and whether the source involved an automated process. To evaluate exposures, the published exposure data on EMF magnitudes and frequencies measured at all sources reported during the interviews were reviewed. For sources where measurement data were not found, measurements or expert judgments on the frequency bands and magnitudes will be made. From these judgments and reviews, a database is being created with all sources in the CAPI linked to their mean EMF exposures and frequency range. For this exposure assessment, the EMF frequency spectrum is divided into six bands which probably have different biological coupling mechanisms: static (0 Hz) magnetic fields, ELF, VLF-LF, MF-HF<10MHz, HF>10MHz-VHF, and UHF-microwave ranges. By linking this occupational exposure measurement database with the replies to CAPI, a subject’s EMF exposure and frequency band can be estimated for most reported sources, and adjusted for the subject’s reported distance from the source and automation of the process. Using the frequency of use and duration of employment information from CAPI, a subject’s cumulative exposure will be calculated for each of the six frequency bands. These cumulative exposure estimates will be divided into tertiles so that prevalences and disease risks can be calculated for high, medium, and low EMF magnitudes.

RESULTS: The INTERPHONE study began identification and interviewing of subjects in 2000 and will finish interviews in early 2004. As of November 2003, 5767 cases and 2364 controls had been interviewed. By the 2004 Annual Meeting of the Bioelectromagnetics Society, occupational EMF exposures will be estimated for some of these subjects and summarized in our presentation.

DISCUSSION: With about 10,000 subjects expected to be interviewed, the INTERPHONE study is the largest case-control study ever conducted on cancer and EMF at or below the microwave frequencies, and

the largest epidemiologic study of any kind to interview all subjects about their workplace EMF exposures. As a population-based study, INTERPHONE is an unprecedented opportunity to estimate the prevalence of EMF exposures in the workforces of 13 industrialized countries, as well as looking for any brain cancer risks from these fields. These prevalence estimates will be semi-quantitative because of the difficulties in linking interview replies with published measurements taken in other places with a wide variety of methods. The outcome depends on the reliability of the subject's answers, which might be poor, and the quality of the measurements in the literature data, that might be low. In addition, some sources such as induction heaters have such a wide range of reported frequencies (0 Hz – 3.8 MHz) and magnitudes (E-field: 3-1580 V/m, H-field: 0.02-12,100 A/m) that any exposure estimate for this source cannot be accurate for all subjects. To take into account all kinds of inaccuracies in our exposure assessment process, the quality of the published papers and the other steps in the process are being systematically evaluated, and will be used to assign a quality rating (high, medium or low) to each exposure estimate.

This study was made possible by the contract QLK4-1999-01563 from the European Union and a contract from the International Union Against Cancer (UICC).

IMPROVING RADIOFREQUENCY EXPOSURE ASSESSMENT IN EPIDEMIOLOGIC STUDIES OF MOBILE PHONE USERS: AN OVERVIEW OF RESEARCH DESIGN AND PRELIMINARY DATA. M.A. Kelsh¹, A.R. Sheppard², N. Kuster³, M. Shum*¹, J. Fröhlich³, M. McNeeley*¹. ¹Exponent, Inc., Menlo Park, CA, USA; ²Asher Sheppard Consulting, Redlands, CA, USA; ³Information Tech in Society (IT²IS) Zurich, Switzerland.

OBJECTIVE: To identify aspects of cell phone systems and use that can yield practical and reliable proxy measures for radiofrequency (RF) exposure in epidemiologic studies.

BACKGROUND: Handset power control (PWC) can rapidly change power radiated from the handset over a range between maximum and levels reduced 100-fold or more. Although exposure is a function of duration and RF energy, most epidemiologic studies have concentrated on duration of use as the sole surrogate for RF exposure. Our study incorporates the RF energy component by recording PWC data from GSM-based software modified phones (SMPs). In addition, we will obtain SAR measurements using “mobile phantom heads” for a variety of field conditions and wireless technology factors (handset type, service provider). We have classified mobile phone user RF energy exposures into four broad dimensions: 1) characteristics of the user, 2) technical characteristics of the mobile phone (e.g. design, specific cellular technology and position of the phone relative to the head or other body region), 3) environmental factors (e.g. network, distance to base station, base station density, terrain), and 4) duration and frequency of use. Numerous factors may affect each of these dimensions (Table 1).

METHODS: Our study incorporates four major research elements: a questionnaire-based recall study, SMP-based survey of power control settings, a field study, and SAR modeling. We also organized an expert panel of epidemiologists, engineers, and RF dosimetry experts to review and provide input to our proposed study designs and protocols. Key aspects of the four substudies include:

Recall Study: We will determine the accuracy of recall of phone use from comparison of questionnaire data to billing record data in an occupational population. This recall study will help determine how accurately duration, frequency, and usage habits can be obtained from questionnaires over recent (1 week, 1 month) and more distant periods (1-5 years).

SMP Study: Data from SMPs used by individuals in an occupational population who are normally issued cell phones for work-related use, and activity logbooks will be evaluated to assess which factors affect PWC.

Field Study: SAR measurements in phantom heads fitted with phones and E-field probes will assess the influence of phones, network conditions, and being stationary or in motion. Parameters with the greatest influence on SAR may qualify as exposure predictors.

SAR Modeling Study: PWC and SAR will be evaluated through empirical measurements and modeling using phantoms for different types and models of phones, technologies, positions, and anatomies to determine their influences on RF exposure.

RESULTS: There are 215 employees for whom company billing records are available in a central database. Preliminary analysis of data for a one-year period of use indicated that the average number of calls made per day was approximately 5 and average minutes per day of usage was approximately 15.5 minutes. The results of a pilot field study that will be used to refine the design of the Field Study and SMP survey data are also presented.

DISCUSSION: This research focuses on RF exposure assessment issues only with the goal of providing guidelines for future epidemiologic research. Based on data developed from the four substudies, RF exposure parameters will be ranked by how much exposure variability is captured by that specific parameter. Such information will be valuable for future health risk assessments of the use of wireless technologies.

Technical Oversight: Radiation Biology Branch, Center for Devices and Radiological Health, U.S. Food & Drug Administration (FDA). **Research Funding:** Cellular Telephone and Internet Association (CTIA)

Table 1: Overview of Exposure Parameters Affecting SAR That Will be Assessed in the Questionnaire Recall/Billing Records Study, SMP Survey, Field Studies and SAR Modeling.

Factors	Exposure Parameter
1. Head/Body	Anatomy (height, weight, density) Metal-rim glasses and jewelry
2. Cell Phone	Technology (CDMA, GSM, etc.) Service provider Phone type (candy bar, flip phone) Model Frequency (900, 1800, 1900 MHz) Antenna up/down, antenna type Position of phone (i.e., cheek, tilt, hands-free)
3. Environment	Base station density Indoor/Outdoor Rural/Urban Upstairs/Downstairs Weather Building type Building construction material Cell traffic Duration of call Time of day
4. Personal Behavior	Duration as user Frequency of calls Circumstances of calls

2-5

FEASIBILITY OF FUTURE EPIDEMIOLOGICAL STUDIES ON POSSIBLE HEALTH EFFECTS OF MOBILE PHONE BASE STATIONS. G.G. Neubauer¹, M. Rössli², M. Feychting³, Y. Hamnerius⁴, L. Kheifets⁵, N. Kuster⁶, J. Schüz⁷, J. Wiart⁸. ¹Seibersdorf research, Austria, ²Univ Bern, Switzerland, ³Karolinska Institutet, Sweden, ⁴Chalmers Univ, Sweden, ⁵UCLA, USA, ⁶IT IS Switzerland, ⁷Univ of Mainz, Germany, ⁸France telecom research center, France.

BACKGROUND: The introduction of mobile phones using the digital GSM 900 / DCS 1800 systems in the 1990s led to a wide use of this technology and subsequently to an increase in the environmental exposures to RF fields. Latest developments in mobile communications, e.g. UMTS, will intensify this process. Today about 1 billion people are using mobile telephones world-wide, about 400 million people of them in Europe. The frequent use of mobile phones has necessitated an increased deployment of base stations. Such installations are often situated close to dwellings or houses and have become the focus of concerns of parts of the population in recent years. These concerns resulted in the demand for epidemiological studies on the potential health effects of the RF emissions of such base stations. However, several scientific problems, e.g. availability of reliable estimates of exposure have to be solved before feasibility of such studies can be determined. Within the scientific community the usefulness of

epidemiological studies to investigate health effects related to the RF fields from mobile base stations has been debated controversially. Up to now only a few cross sectional surveys on possible effects of base stations were performed. These surveys do not allow any conclusions and sound large scale studies are lacking. In addition, several cluster investigations and other studies that looked at the potential health effects of populations residing near TV and radio transmitters have to be considered. Several questions remain open, e.g. the adequate type of study design, the endpoints to be investigated, the adequate exposure metric and the methodology how to deal with the emissions from other RF sources.

OBJECTIVE: This research project brings together in a collaborative effort leading international scientists in RF-engineering/dosimetry and epidemiology to jointly assess the feasibility of epidemiological studies on health impacts of RF-exposure from mobile phone base stations.

METHODOLOGY: The project consists of three parts:

1) Analysis of existing study designs of epidemiological studies

Existing epidemiological studies on RF sources and health are analysed to describe existing study designs and to identify strengths and weaknesses. The current scientific evidence of a relationship between RF fields arising from base stations and health effects is investigated.

2) Comparison and analysis of dosimetric concepts

Existing exposure assessment methodologies are evaluated. More data on individual's exposure is urgently needed; little is known to what extent different exposure sources contribute to a subject's overall exposure. The suitability of existing concepts of dosimeters for epidemiological studies is examined. Present day exposure assessment techniques and existing data on exposure of the population are analysed. The contribution from other RF sources to the total exposure is taken into account.

3) Expert workshop

In the last step the developed specifications are evaluated by experts in different fields in the frame of a workshop. Specifications not suitable are identified, cost analysis are undertaken. Finally (a) reliable concept(s) should be available describing the methods and the equipment which have to be used to describe exposure from base stations in a way that is useful for epidemiological studies.

EXPECTED RESULTS: The purpose of this study is to investigate the feasibility of future epidemiological studies on health effects, or effects on well being, of mobile communication base stations by evaluating existing studies and dosimetric concepts, contributions from other RF sources have to be taken into account. If possible a list of recommendations and specifications for such studies will be developed and a cost analysis will be performed. A comprehensive rationale for the conclusion will be given in any case.

This project is sponsored by the Swiss Research Foundation on Mobile Communication, the Swiss Agency for the Environment, Forests and Landscape and the Swiss Federal Office of Public Health

2-6

NEW CONCEPT FOR RISK ASSESSMENT AND MANAGEMENT OF RADIO FREQUENCY ELECTROMAGNETIC FIELD EXPOSURE HEALTH EFFECTS ON THE BASIS OF NEURO-FUZZY NETWORKS. O.P. Molchanova. Dept of General Hygiene and Basics of Ecology, M.I. Pirogov Vinnytsya Nat'l Med Univ, Vinnytsya, 21018, Ukraine.

INTRODUCTION: Subcommittee 4 of the IEEE International Committee on Electromagnetic Safety is now reviewing the IEEE Standard for Safety Levels with Respect to Human Exposure to Radio Frequency (RF) Electromagnetic Fields C95.1-1991. It was stated among the criteria offered as the guiding principles of the revision that the maximum exposure limits should be based on established adverse effects after inclusion of the appropriate safety factors that should consider uncertainties in the biological database, e.g. environmental conditions, individual variability, exposure duration, and other factors.

OBJECTIVES: The objective of the study was to develop, substantiate scientifically, and propose the approach to risk assessment and risk management of RF fields' effects on various aspects of human health

by creation of an expert system based on a neuro-fuzzy network.

METHODS: The multifactor model is based on fuzzy sets theory proposed by L.Zadeh. Knowledge about relations between RF field exposure, exposure conditions and the established adverse effects can be obtained from expert opinions and from experimental data followed by the building of a cause-effect relations tree. Fuzzy knowledge has to be described as a hierarchic set of suggestions like IF/Input/ THEN/Output/, and formalized by the analytic-linguistic approximation to create a fuzzy model. The model created has to be fine-tuned by its tutoring on experimental data using a neural network.

RESULTS: Use of fuzzy sets theory allows the creation of a model of the process being investigated by formalization of knowledge of experts (highly qualified professionals who are familiar with risk assessment of RF field exposure) presented in terms of linguistic variables. The main requirements (rules) for RF field exposure health effects risk assessment can be developed based on maximum exposure limits for different frequencies that are already established. Influence of different safety factors can be evaluated based on reliable experimental data obtained from literature or experiments specially designed for this purpose. The cause-effect relations tree can be built in such a way that it will take into account both exposure limits and conditions. The multifactor fuzzy model of RF field exposure effects on human health can be created on the basis of this knowledge. Fuzzy sets created can be entered into the formula of risk. Fine-turning of the model by use of the neural network on experimental data will increase risk assessment model reliability, optimize work of the model, and will probably reveal new relations inside the system being modeled. Knowledge generated by the neural network can be extracted and used for better understanding of relations inside the system under investigation. An expert system for risk assessment of RF field exposure effects on human health can be created on the basis of the neuro-fuzzy network developed.

CONCLUSIONS: The use of neuro-fuzzy networks for risk assessment and risk management of RF fields health effects has the following advantages: a) it unites exposure limits for wide range of frequencies; b) it allows consideration of different safety factors; c) it formalizes the knowledge of experts about the established and possible adverse effects; d) it allows future improvement of the risk assessment by teaching the network on the basis of new data obtained; e) it allows the extraction of new knowledge about RF field health effects from relations revealed by neuro-fuzzy network.

We suggest that the expert system for RF fields exposure health effects risk assessment may be used for both the substantiation of maximum exposure limits for different environments and for advanced risk management.

SESSION 3: EMF THERAPIES
Chairs: Art Pilla and Gabi Nindl

3-1 STUDENT

LOW FIELD MAGNETIC STIMULATION: ANTI-DEPRESSANT EFFECTS WITH MRI STRENGTH FIELDS. M.L. Rohan*, W.A. Carlezon Jr.*, B.M. Cohen* , P.F. Renshaw*. Dept of Psychiatry, Harvard Medical School and Mclean Hospital. Belmont, Massachusetts 02478 USA.

OBJECTIVES:

1. Report on the observation of mood effects in depressed bipolar subjects during an Echo Planar Spectroscopic Imaging (EP-MRSI) experiment in a clinical MRI system.
2. Report on the subsequent observation of anti-depressant effects observed in rats in the Forced Swim Test (FST) using a table-top sized low field magnetic stimulation device that was designed to deliver the same induced electric fields as the EP-MRSI scan in the MRI system.

METHODS: – **EPMRSI** Fifty-four human subjects were examined for immediate mood change in the EP-MRSI study. 30 depressed bipolar subjects had EP-MRSI, 14 normal comparison subjects had EP-MRSI, and 10 depressed bipolar subjects had a sham EP-MRSI which consisted of standard anatomic MRI exam, in a single-blind experiment. Mood change was measured with the “Brief Affect Scale” (BAS), administered to all subjects immediately before and after the MR scanning session. The BAS measures change in immediate mood state on a 7-point scale. These numerically ranked responses were grouped into the ordinal categories for statistical treatment. Ordered logistic regression modeling methods were used to examine the differences in BAS scores among the study groups.

RESULTS: – **EPMRSI** Twenty-three of 30 bipolar subjects receiving EP-MRSI, three of 10 bipolar subjects receiving sham EP-MRSI, and four of 14 healthy comparison subjects receiving EP-MRSI reported improvement in mood after MR exams. Table 1 summarizes the BAS improvement scores.

Ordinal BAS ratings were compared for bipolar subjects receiving EP-MRSI scans vs. those receiving sham EP-MRSI (significant ($z=2.63$, $p=0.009$); between medication naïve bipolar EP-MRSI subjects scans vs medicated bipolar EP-MRSI subjects (significant $z=2.02$, $p=0.044$); between bipolar EP-MRSI subjects and healthy EP-MRSI subjects (significant $z=2.61$, $p=0.009$); and between bipolar sham EP-MRSI subjects and healthy EP-MRSI subjects (not significant $z=0.29$, $p=0.77$). A summary of these results is listed in Table 2.

METHODS: – **FST** A table-top sized LFMS device was constructed, based on a surplus MRI gradient head coil. The antidepressant effects of LFMS were also investigated using this device in a rodent model with the forced swim test (FST), an animal model often used in the study of depression. Standard antidepressant drugs (e.g., tricyclics, fluoxetine) modify forced swim behavior in this test, an effect that is correlated with the clinical efficacy of these agents (Porsolt et al 1977).

Male Sprague-Dawley rats (46 rats, 325-350 g) ($N = 7-10$ rats per group) were used in this experiment. Six 6 groups of rats were used to test LFMS or pharmacological conditions. Between the first and second exposure to forced swimming, rats received on each of 3 occasions 20 min of exposure to either (1) LFMS within the focal point of the field ($N=9$), (2) LFMS outside the focal point of the field ($N=6$), (3) sham 1: no fields ($N=9$), (4) sham 2: constant Y magnetic field gradient (1.5 G/cm) ($N=9$). These tests mimicked antidepressant administration regimens typically used with pharmacological treatments (Carlezon et al 2002). For comparison, the effects of (5) desipramine (DMI) ($N=6$) and (6) fluoxetine (FLX) ($N=7$) were examined in parallel, using all of the same conditions as were used for LFMS. Mean latency to immobility and mean number of samples for immobility, swimming and climbing behaviors were compared between all groups using ANOVA. Fisher’s post hoc tests were used to examine specific LFMS, DMI and FLX measures in comparison to the sham groups.

RESULTS: – FST LFMS dramatically reduced immobility, suggesting antidepressant-like effects. Immobility was affected in this test ($F(4,40)=5.0$, $p<0.01$) with LFMS ($p<0.01$) and DMI ($p<0.05$) treatments having reduced immobility. The effects of LFMS were qualitatively similar to, but larger than, those of FLX, the effects of which may have been reduced by the additional stress associated with repeatedly restraining the rats for the LFM. These are shown in Fig 1.

LFMS Fields – The changing magnetic fields of LFMS induce electric fields; waveforms for these fields are shown in Fig. 2. Electric fields are 0.25ms square pulses delivered with alternating polarity at 1 kHz. They are 0.7V/m – 1.0V/m, uniformly in the right-to-left orientation.

CONCLUSIONS: – This effect was unexpected, particularly at these low fields. However, it has been observed in two very different experiments. We suggest that the timing waveform of these fields has optimal parameters for interaction with some neural circuits, and are planning further studies of this surprising situation.

Table 1. Mood Improvement in Bipolar and Normal Subjects with EP-MRSI

	N	# improved	# worse	mean BAS
Bipolar, EP-MRSI	30	23	1	0.87±0.68
subgroup: medication naïve	11	11	0	1.18±0.41
subgroup: on medication	19	12	1	0.68±0.75
Bipolar, sham EP-MRSI	10	3	2	0.30±1.06
Comparison, EP-MRSI	14	4	0	0.29±0.47

Table 2. Significance of Mood Improvement with EP-MRSI

	Z	p
Bipolar, EP-MRSI vs. Bipolar, sham EP-MRSI	2.63	0.009
subgroups: Bipolar, EP-MRSI, medication naïve vs. Bipolar, EP-MRSI, on medication	2.02	0.044
Bipolar, EP-MRSI vs. Comparison, EP-MRSI	2.61	0.009
Comparison, EP-MRSI vs. Bipolar, sham EP-MRSI	0.29	0.77

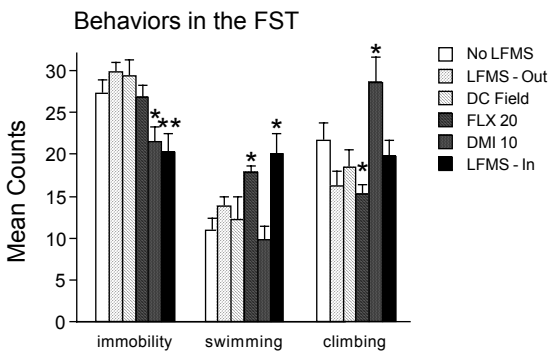


Figure 1. Results of behavior sampled every 5 seconds during the FST for 6 conditions

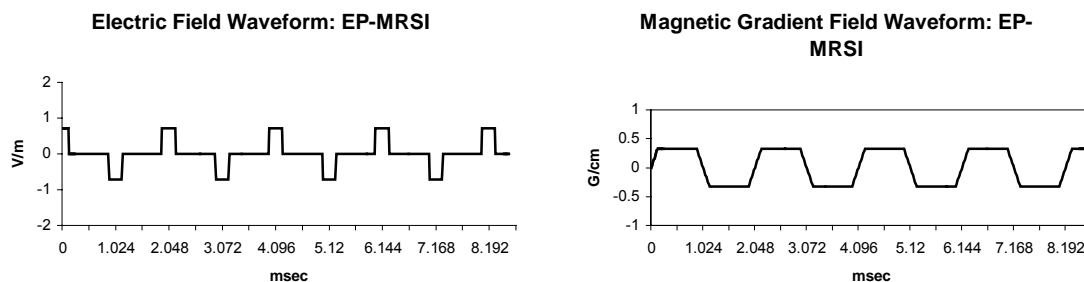


Figure 2. LFMS / EP-MRSI electric and magnetic field waveforms

3-2

STATIC MAGNETIC FIELDS MODULATE THE EFFECT OF CHEMOTHERAPY IN THE TREATMENT OF HUMAN MALIGNANCY. J.R. Salvatore, J. Harrington, T. Kummet. Division of Hematology/Oncology, Hayden VA Medical Center, Phoenix, AZ 85012 USA.

INTRODUCTION: Electromagnetic fields have wide application in clinical medicine and are used in the diagnosis and treatment of human disease. Laboratory studies in cell and animal systems using both static and time-varying magnetic fields have shown effects on tumor growth characteristics and on the efficacy of anti-neoplastic chemotherapy against malignant cells. However, there have been few studies on the application of static magnetic fields during the treatment of human cancer. We have been conducting a Phase I study of the combination of a static magnetic field and chemotherapy during the clinical therapy of human malignancy.

METHODS: Participants selected were starting a chemotherapy program for advanced cancer and signed informed consent. A static magnet was placed over the liver for 15 minutes before chemotherapy, for the duration of chemotherapy, and for 0 minutes(level 1), 15 minutes(level two), or 30 minutes(level three) after the completion of chemotherapy. There were 12 evaluable subjects in each level who were monitored by history, physical examination, and blood tests, and the data obtained from these evaluations was assessed using the National Cancer Institute’s Common Toxicity Criteria v.2.0.

RESULTS: No subject withdrew from the study because of discomfort or inconvenience from placement of the magnet. Each piece of data was a discrete event which could be assigned a severity number based on the toxicity criteria. We have been able to compare the results of subjects in all three levels of application and have found that the magnetic field applied for progressively longer time periods appears to protect the liver from the effects of chemotherapy and to reduce the severity of abnormalities of the complete blood count(CBC).

CONCLUSIONS: The purpose of a Phase I study is to establish the safety and toxicity profile of a new therapy. The data from this study suggest that application of a static magnetic field during the treatment of human malignancy with anti-neoplastic chemotherapy is safe and may in fact reduce the severity of some of the effects of chemotherapy on the liver and the CBC. Since the combination of a static magnetic field and anti-neoplastic chemotherapy appears safe, we can begin studies that look at the anti-tumor efficacy of this combination.

3-3 STUDENT

STATIC MAGNETS REDUCE MYOFASCIAL TRIGGER POINT PAIN. M. Brantley*, D. Cheben*, H. Gay*, L. Wright*, A. Thompson*, D. Lake*. Department of Physical Therapy, Armstrong Atlantic State University, Savannah, Georgia, USA 31415.

INTRODUCTION: A previous study (Valbona, et al., 1997, Arch Phys Rehabil, 78, 1200-1203) reported a decrease in myofascial trigger point (MTP) pain following a 45-minute exposure to a static magnet. That study involved a highly specialized population of post-polio patients.

OBJECTIVE: The objective of this study was to test the effects of therapeutic static magnets on MTP pain in a general myofascial pain population. The hypothesis was there would be a significant reduction in pain in the magnet group but no change in the sham control group

METHODOLOGY: This study was a randomized, double blind, clinical trial. Thirty subjects with MTPs were randomly assigned to active (14) or sham magnet control (16) groups. Both the experimenters and subjects were blinded to group assignment. A single identified MTP on each subject was tested with a pressure algometer, and the subjects were asked to indicate the maximum pressure that could be tolerated (pain tolerance). Algometer pressure readings were recorded. The subjects then filled out the McGill pain questionnaire (MPQ), the Present Pain Index (PPI) from the McGill pain questionnaire and a visual analog scale (VAS) indicating pre-treatment pain level. Subjects were then exposed to either an active or sham magnet (BIOflex Medical Magnetics, FL) for 45 minutes. Both active and sham magnets were 40 mm diameter circles, 3 mm thick and looked identical. The active magnet was a composite of bipolar and axially magnetized flexible ferrite. The average magnetic field at the surface of the magnet was 450 G. The magnetic field decayed (normal to the magnet surface) to an average of 45 G at 1 cm, 10 G at 3.5 cm and background at 9 cm. The magnetic field at the surface of the sham magnet was not significantly different from background. Identical pressure was then applied to the same MTP using the pressure algometer, and the subjects again filled out the MPQ, the PPI and the VAS. Pre-test/Post-test differences in pain levels for each measurement were compared using the one-tailed, paired t-tests for both control and magnet groups. Pre-test measures between the magnet and control groups were compared using two-tailed, unpaired t-test.

RESULTS: The results of the Kolmogorov-Smirnov normality test indicated that parametric analysis could be used for all 3 pain measures. There were no significant differences using the two-tailed, unpaired t-test in the pain level upon algometer pressure application between the pre-test measures for all measures between the active and control groups ($p = .111$, $p = .621$, $p = .202$ for the McGill, PPI and VAS respectively). There was a significant pre-post decline measured using the one-tailed, paired t-test in all 3 pain measures in the active group. The McGill pain score was reduced by 55% ($p=.011$), The PPI score was reduced by 39% ($p=.020$) and the VAS score was reduced by 23% ($p=.044$). A moderate effect size was seen in the McGill total score ($d=.69$), a large effect size was seen in the PPI ($d=.88$) and a moderate effect size was seen in the VAS (0.68). There were no significant changes in any pre-test to post-test measures in the subjects treated with the sham control magnets.

CONCLUSIONS: This study suggests that 500 gauss therapeutic static magnetic fields with the configuration utilized in this study can decrease the pain associated with pressure applied to myofascial trigger points after one 45 minute treatment. This confirms a previous study by Vallbona, et al. (1997) who reported a decrease in pain in myofascial trigger points in a post-polio population. This study expands upon those results to suggest that static therapeutic magnets may have a beneficial effect in reducing pain in a wider range of patients with myofascial trigger points.

3-4 **P-B-23 Moved to Session 3-4.**

EFFECTS OF PULSED ELECTROMAGNETIC FIELDS (PEMFs) ON EXPERIMENTAL DEGENERATIVE OSTEOARTHRISIS. S. Setti¹, M. Fini², F. Cavani³, R. Cadossi¹. ¹Laboratorio di Biofisica Clinica, IGEA, 41012 Carpi (Mo), Italy; ²Laboratorio di Chirurgia Sperimentale, Istituti Ortopedici Rizzoli, 40126 Bologna, Italy; ³Università degli Studi di Modena e Reggio Emilia, Dipartimento di Anatomia e Istologia, Policlinico di Modena, 41100 Modena, Italy.

INTRODUCTION. Pulsed electromagnetic fields (PEMFs) have been shown to increase chondrocyte proliferation (1) and to reduce proteoglycan degradation (2) suggesting a potential application as a treatment for osteoarthritis (3).

OBJECTIVE. The aim of this study was to evaluate the effects of pulsed electromagnetic fields on the degeneration of articular cartilage, typical of osteoarthritis, in Dunkin-Hartley guinea pigs that spontaneously develop osteoarthritis with age.

METHODS. Ten Dunkin-Hartley guinea pigs, aged 12 months, were included in the study. Each of them was placed in a cage with a coil underneath. Five animals were stimulated with PEMFs (75 Hz, 1.8mT) generated by a pulse generator (ONE, IGEA S.r.l., Carpi, Italy) and the other animals were sham treated. The animals were stimulated six hours/day for three months and then sacrificed. Knee joints were harvested, embedded in methylmethacrylate and were sectioned. For each animal eight sections were microradiographed and further cut for histological analysis. Toluidine blue-fast green staining was performed and a score was given taking into consideration articular cartilage structure and toluidine blue staining (marker of proteoglycan content). The possible total score ranged from 0 (normal cartilage) to 14 (severe structural damage and complete loss of toluidine blue staining). Moreover, the number of histological sections that showed signs of articular cartilage degeneration was calculated. The presence of superficial fibrillation on the cartilage of the medial tibial plateau was the parameter considered as sign of articular cartilage degeneration.

RESULTS. The histomorphometrical analysis showed in all animals signs of articular cartilage degeneration. While the average number of section showing signs of articular cartilage degeneration was 3.4 ± 1.14 in the stimulated group, it was 5.4 ± 1.01 in the control group ($p < 0.01$). Moreover a significant difference ($p < 0.05$) in articular cartilage score was observed between the treatment and control group.

DISCUSSION. The results showed that PEMFs exposure seems to reduce articular cartilage degeneration by decreasing the extension of the damage and the progression of the pathology. In fact in the treatment group the superficial fibrillation of the cartilage is limited and the proteoglycan content of the matrix is preserved with respect to the control group. PEMFs treatment seems to exert a beneficial effect on cartilage, thus confirming the potentiality of the stimulation as a treatment to reduce osteoarthritis progression.

References.

- 1) De Mattei M, et al., Connect Tissue Res. 2001; 42(4):269-79.
- 2) Liu H. et al., Biochim Biophys Acta 1997; 1336(2):303-14.
- 3) Trock, DH et al. J. Rheumatol. 1994, 21: 1903-11.

3-5

EXPOSURE TO A SPECIFIC PULSED EXTREMELY LOW FREQUENCY MAGNETIC FIELD: A HISTORY OF INDUCED ANALGESIA IN ANIMALS, AND A DOUBLE-BLIND PLACEBO CONTROLLED STUDY IN FIBROMYALGIA PATIENTS. A.W. Thomas, N.M. Shupak, F.S. Prato. Department of Medical Biophysics, University of Western Ontario; Lawson Health Research Institute and Department of Diagnostic Imaging, St. Joseph's Health Care (London), London, Ontario, Canada, N6A 4V2.

INTRODUCTION: One of the most reproducible effects of extremely low frequency (ELF) magnetic field (MF) exposure has been the effect on opioid-related behaviors. It has been shown that a specific

pulsed ELFMF induces analgesia in snails, rodents, and healthy human volunteers. In a double-blinded placebo-controlled study, we investigated the effects of 30-minute MF exposure ($\leq 400 \mu\text{T}$; $<1 \text{ kHz}$) on pain ratings in fibromyalgia patients attending an in-hospital resident pain treatment program.

OBJECTIVE: Determine the effects of exposure to a specific pulsed extremely low frequency magnetic field on pain ratings in fibromyalgia patients.

METHODOLOGY: Female Fibromyalgia patients attending a resident pain treatment program within a hospital out-patient service were given 30 min acute treatments. Patients completed the McGill Pain Questionnaire (MPQ) and pain and anxiety visual analog scales (VAS) before and after a 30-minute (MF or sham) exposure period. Muscle tension and heart rate were recorded throughout the experiment to assess possible physiological correlates of MF exposure.

RESULTS: A repeated measures analysis revealed a significant overall pre-post effect for the MPQ Pain Rating Index (Total), $F(1,15) = 16.16$, $p < 0.01$, $\eta^2 = 0.519$, $\text{power} = 0.963$. The MF group, $F(1,8) = 17.60$, $p < 0.01$, $\eta^2 = 0.688$, $\text{power} = 0.955$, but not the sham group, $F(1,7) = 3.98$, $p = 0.09$, $\eta^2 = 0.362$, $\text{power} = 0.406$ showed a decrease in the PRI. Similar findings were found for the sensory, affective, and emotional components of pain as measured by the MPQ; comparable findings existed for the VAS pain ratings. Patients in the MF group also had significantly reduced variability in heart rate post-exposure relative to patients in the sham group. A significant condition by time interaction existed for the minute immediately following the 30-minute exposure, $F(1,15) = 8.137$, $p < 0.05$, $\eta^2 = 0.352$, $\text{power} = 0.760$.

CONCLUSION: Results confirm past findings that exposure to a specific pulsed MF induces a significant degree of analgesia. The significantly lower pain ratings following MF, but not sham exposure, indicate the potential clinical use of MF exposure for reducing pain in patients with fibromyalgia.

This study was supported in part by the Canadian Institutes of Health Research, the Natural Science and Engineering Research Council, Lawson Health Research Institute, FrAlex Therapeutics Inc., the Ontario Research and Development Challenge Fund, the Canadian Foundation for Innovation, Ontario Innovation Trust, and St. Joseph's Health Care Foundation. Special thanks to Dr. Warren Nielson, Director, Rheumatology Day Program, St. Joseph's Care (London).

3-6 STUDENT

DEBRIDEMENT AND ANTIBACTERIAL EFFECTS OF 25 KHZ ULTRASOUND. L.C. Kloth*, C.H. Schulze*. Marquette Univ and Froedtert Memorial Lutheran Hospital, Milwaukee, Wisconsin, USA and Endotoxin Laboratory for Surgical Research, Christian-Albrechts-Universitat, Kiel, Germany.

INTRODUCTION: Chronic human wounds share common impediments to healing that include recurring amounts of necrotic tissue and levels of microorganisms that compete with healthy cells for oxygen and nutrients. It is established that debridement of necrotic tissue plays an essential role in the healing process by reducing the wound bio-burden which aids in preventing wound infection. Current methods of debridement include autolytic, enzymatic, mechanical and sharp surgical and non-surgical techniques. Each of these methods has disadvantages, for example the autolytic, enzymatic and mechanical methods remove dead tissue very slowly and/or incompletely. Sharp debridement is also unable to completely remove necrotic fibrin and overly aggressive excision of viable tissue can cause excessive bleeding and the need for anesthesia.

Recently, 25 kHz ultrasound (US) has emerged as a viable alternative for wound bed preparation and debridement. When US vibrations at 25 kHz are transmitted to wound tissues through a fluid coupling medium (e.g. 0.9% saline or tissue fluid), micro-size gas bubbles are created. During the debridement procedure thousands of gas bubbles implode and release energy as the US pressure wave impacts upon them. The energy from this microcavitation effect¹ enables 25 kHz US to rapidly solubilize necrotic fibrin² in vivo and destroy bacteria^{3,4} in vitro.

OBJECTIVES: Objectives are to describe the in vivo use of low frequency (25 kHz) ultrasound in debridement of necrotic tissue from chronic wounds and to present in vitro bactericidal effects of this

modality on several bacterial strains.

METHODS: The US device used for in vivo and in vitro procedures was the Sonoca Ultrasonic/Dissector® (Soring GMB – Germany). US was delivered to the wound via a Sonotrode® handpiece that contains lead zirconate titanate ceramic discs, which convert electrical input to mechanical 25 kHz US vibrations at the probe tip. To evaluate this modality for its debridement effect the probe tip which supplies the saline coupling medium, was moved slowly and continuously and either immersed in saline / wound fluid or in light direct contact with the necrotic fibrin for 1-3 minutes at 60% of maximum power. To evaluate its antibacterial effect 4 bacterial strains were cultured and treated at 5 US outputs (20, 40, 60, 80, 100%) and 6 exposure times (20, 40, 60, 80, 100, 120 sec).

RESULTS: 25 kHz US demonstrated its fibrinolytic effects by selectively destroying necrotic fibrin and slough within minutes without harming healthy cells and tissues. Several cases will be presented to illustrate debridement effects. Bactericidal effects were found to be dependent on US output level and exposure time with the greatest killing effect occurring at 100% US output for 120 seconds. However, 15 of 16 culture plates treated at 100% US output for 60 seconds were found to be sterile.

References.

Young, S. Ultrasound Therapy. In Kitchen, S (ed), Electrotherapy: Evidence-Based Practice, 11th edition. Churchill Livingstone, London, UK, p 214, 2002.

Suchkova V, Carstensen EL, Francis CW. Ultrasound enhancement of fibrinolysis at frequencies of 27 to 100 kHz. *Ultrasound in Med and Biol.* 2002; 28(3): 377-82.

Gostishchev VK, Oganessian SS, Tarverdian NA. Effect of low frequency ultrasound on non-clostridial anaerobic microflora. *Vestnik khirurgii imeni I. I. Grekova (Russian)* 1987; 138(4): 38-42.

Schulze CH. Endotoxin Laboratory for Surgical Research, Christian-Albrechts-Universitat, Kiel, Germany (unpublished data)

3-7

BASIC STUDY OF THE EFFECTS OF LOW INTENSITY PULSED ULTRASOUND FOR BONE FORMATION. T. Sorimachi¹, K. Yamamoto¹, T. Masaoka¹, N. Miyagawa¹, K. Morishita¹, D. Kimura¹, S. Asahi¹, E. Fukada². ¹Dept. of Orthop. Surg., Tokyo Medical Univ. 6-7-1 Nishi-Shinjyuku Shinjyukuku Tokyo Japan, 160-0023 ²Kobayashi Inst of Physical Research.

INTRODUCTION : Many previous studies have reported the effect of low intensity pulsed ultrasound (LIPUS) exposure for acceleration of the fracture repair. So far, We have investigated the effects of low intensity pulsed ultrasound (LIPUS) for differentiation and proliferation on mouse osteoblast-like cell line, MC3T3-E1.

OBJECTIVE : In this study, we examined the production of Interleukin-6 (IL-6) and Vascular Endothelial Growth Factor (VEGF) in bone metabolism by LIPUS exposure, in comparison with unexposed sample.

MATERIALS & METHODS : Cell culture. MC3T3-E1 cells, a mouse osteoblast-like cell line, were cultured in α -modified essential medium (α -MEM) containing 10% heat-inactivated fetal bovine serum (FBS), penicillin and streptomycin in a humidified atmosphere of 5% CO₂ at 37°C. Cells were plated in 6-well culture plates at a density of 1×10^5 cells/cm², and after incubation for 24 hrs, the medium was replaced with α -MEM, with 10% FBS. LIPUS input signal was a 200 microsecond burst sine wave of 1.5 MHz repeating at a frequency of 1.0 kHz, and intensity of 40mW/cm². Exposure times were 20 minutes in all cultures. All experiments were performed in a water tank at 37°C. At intervals of 30 min from 0 to 180 min, and intervals of 3 hrs from 3 to 48 hrs. After LIPUS exposure, cells and medium were separately collected for the following IL-6, VEGF ELISA assay and RT-PCR. Unexposed samples were also subjected to the same operations without LIPUS exposure in the same condition. Significance was tested using Student's T test with $p < 0.05$.

RESULTS : Results of ELISA assay, the up-regulation of IL-6 reached a peak at 60min., and subsided at

24hour by LIPUS exposure. In another, regulation of VEGF increased with times. Besides, RT-PCR analysis, the expression of IL-6 and VEGF m-RNAs increased by LIPUS exposure, in comparison with unexposed sample. This results suggest that not only bone resorption but also vascularity have been accelerated by LIPUS exposure.

CONCLUSIONS : LIPUS has stimulated the acceleration of bone formation, bone resorption and vascularity in early time. Then bone remodeling has revitalized, inducing all sorts of chemical mediator.

3-8

MECHANISM AND THERAPEUTIC POTENTIAL OF NON-IONIZING ELECTROMAGNETIC.

M.T. Johnson¹ and G. Nindl². Indiana Univ School of Med, ¹Dept of Microbiology and Immunology and ²Department of Cellular and Integrative Physiology Terre Haute, IN 47809.

Magnets, electric current and time varying magnetic fields have played a role in human medicine for a number of years. Modern clinical practice would be far less effective without devices like cardiac pacemakers and bone growth stimulators, nuclear magnetic resonance imaging and electrodiagnostic tools. This paper presents a summary of natural and artificial electromagnetic field (EMF) characteristics that are currently in use or under investigation for several therapeutic applications. This background provides a basis for discussion of emerging and novel EMF therapies. Although awareness of alternative and complementary medicine has existed for centuries in some cultures, such methods have become an area of heightened interest for western healthcare practitioners, partially because of a growing understanding of how EMFs interact with cellular systems. EMF therapies for the treatment of pain, cancer, epilepsy, and inflammatory diseases like psoriasis, tendinitis and rheumatoid arthritis are currently being explored. The long-term success of this new area of medicine is still unknown. However, EMF therapy optimized for individual applications through specific dosimetry analysis has the potential to revolutionize western medicine, which is currently dominated by pharmaceutical and surgical interventions. We have developed a working hypothesis that some EMF signals have clinically significant anti-inflammatory properties stemming from down-regulation of T lymphocytes that are activated through the T cell receptor during inflammation. Further exploration of this idea may provide a basis for the development of therapeutic tools for noninvasive treatment of inflammatory diseases.

SESSION 4: IN VIVO STUDIES
Chairs: Rene De Seze and Larry Anderson

4-1

THERMOPHYSIOLOGICAL RESPONSES OF SEATED HUMAN VOLUNTEERS TO WHOLE-BODY RADIO FREQUENCY (RF) EXPOSURE AT 220 MHZ. E.R. Adair¹, D.W. Blick², S.J. Allen³, K.S. Mylacraine³, J.M. Ziriaux⁴, D.M. Scholl⁵. ¹Air Force Senior Scientist Emeritus, Hamden, CT 06517; ²Independent Consultant, San Antonio, TX 78218; ³Advanced Eng Information Sys, a General Dynamics Co., Brooks City-Base, TX 78235; ⁴Naval Hlth Cntr Detachment, Brooks City-Base, TX 78235; ⁵AFRL/HEDR, Brooks City-Base, TX 78235 USA.

INTRODUCTION: The goal of much research on the interaction of RF energy with living systems ultimately concerns the effects of human exposure to such fields. Over the past 10 years, our research has characterized how thermophysiological responses are mobilized in human volunteers exposed to several radio frequencies, i.e., 100, 450, and 2450 MHz. A significant gap in the range of frequencies selected for study is now neatly filled by the present study conducted at 220 MHz, a frequency in the transition range from deep body heating (resonance) to more superficial energy deposition.

OBJECTIVE: Our objective was to quantify the basic thermophysiological responses of heat loss and heat production in human volunteers during periods of controlled RF exposure (220 MHz CW) in controlled thermal environments for comparison with published results at 100 and 450 MHz.

METHODS: Thermoregulatory responses were measured in 6 adult volunteers (5 males, 1 female, aged 24 - 63 years) during 45-min whole-body dorsal exposures to 220 MHz RF fields. Three power densities (PD = 9, 12, and 15 mW/cm²; whole-body average normalized specific absorption rate [SAR] = 0.044 [W/kg]/[mW/cm²]) were tested in each of 3 ambient temperatures (T_a = 24, 28, and 31 °C) plus T_a controls (no RF). Measured responses included esophageal (T_{esoph}) and 7 skin temperatures, metabolic rate (M), local sweat rate, and local skin blood flow. Derived measures included heart rate, respiration rate, and total evaporative water loss. FD-TD modeling of a seated 70 kg human exposed to 220 MHz compared predictions with physiological data.

RESULTS: No changes in M occurred under any test condition, confirming published results of studies at 100, 450, and 2450 MHz. During RF exposure at 220 MHz, T_{esoph} showed small changes (≤ 0.14 °C) and never exceeded 37.2 °C. As with similar exposures at 100 MHz, local skin temperatures changed little, except for the ankle temperature that rose in proportion to the PD. Modest increases in skin blood flow were often recorded, especially at the higher PD and in the warm T_a . At 220 MHz, vigorous sweating was mobilized rapidly at PD = 12 and 15 mW/cm² and to higher levels than observed for equivalent PD at 100 MHz. Based on FD-TD modeling of a 70 kg adult human, the local SAR in deep neural tissues that harbor temperature-sensitive neurons (e.g., medial preoptic hypothalamus, spinal cord) was greater at 220 than at 100 MHz. These new data strengthen the evidence that small temperature increases in the circulating cerebrospinal fluid trigger central thermosensitive cells to initiate heat loss responses.

CONCLUSIONS: Exposure of humans at 220 MHz, like exposure at 100 MHz, results in far less skin heating than occurs during exposure at a higher frequency (450 MHz). Nevertheless, the exposed subjects thermoregulate efficiently because of greatly increased sweating and modest increases in skin blood flow. It is now clear that these responses are controlled principally by neural signals from thermosensors deep in the body, rather than those in the skin.

Supported by USAF Research Laboratory.

LIFE-LONG EXPOSURE TO 50 HZ MAGNETIC FIELDS DOES NOT INCREASE THE RISK OF LYMPHOMA IN AKR/J MICE. A. Lerchl, A.M. Sommer*. School of Engineering and Science, International Univ Bremen, D-28759 Bremen, Germany.

BACKGROUND: Some epidemiological studies suggest that exposure to 50 or 60 Hz magnetic fields might increase the risk of leukemia, especially in children with a high residential exposure. To investigate this possibility experimentally, the influence of 50 Hz magnetic field exposure on lymphoma induction was determined in a mouse strain that is genetically predisposed to this disease. The AKR/J mouse genome carries the AK-virus, which leads within one year to spontaneous development of thymic lymphoblastic lymphoma in approximately 90% of all animals.

OBJECTIVE: To investigate experimentally whether 50 Hz magnetic field exposure influences lymphoma induction in a mouse strain that is genetically predisposed to this disease.

METHODOLOGY: Groups of 160 unrestrained female AKR/J mice were sham-exposed or exposed to sinusoidal 50 Hz magnetic fields at 1 or 100 μ T for 24 hours per day, 7 days per week. Animals were visually checked daily for signs of developing disease and were weighed and palpated weekly to detect swollen lymph nodes. Starting at the age of 6 months, blood samples were taken monthly from the tail to perform differential leucocyte counts. Animals with signs of disease or with an age of about 42 weeks were sacrificed and a gross necropsy was performed.

RESULTS: There was no effect from magnetic field exposure on body weight gain or survival rate, and lymphoma incidence did not differ between exposed and sham-exposed animals.

CONCLUSION: These data do not support the hypothesis that exposure to sinusoidal 50 Hz magnetic fields is a significant risk factor for developing leukemia.

This study was part of a project supported by the Bundesamt für Strahlenschutz, St. Sch 4323: "Beeinflussung der spontanen Leukämierate bei AKR-Mäusen durch niederfrequente Magnetfelder".

ANALYSIS OF LITERATURE (ABSTRACTS) ON BIOLOGICAL EFFECTS OF EMF IN THE FREQUENCY RANGE 2 – 3 GHZ. L. Haberland*¹, M. Simeonova*¹, W. Alsbach*², S. Brandt*³, W. Dubois*². ¹Inst of Cellular Bio and Biosystems Tech, Univ of Rostock, D-18057 Rostock, Germany, ²Forschungsgemeinschaft Funk e.V. (FGF), D-53111 Bonn, Germany, ³rubitec GmbH, D-44801 Bochum, Germany.

BACKGROUND: The frequency range 2 – 3 GHz is designated for new communication tools (e.g. UMTS, bluetooth), but is already widely used by devices, such as microwave ovens and diathermy units. Therefore, a lot of experimental research on biological effects and medical applications has already been carried out in this frequency range. The present data analysis has been undertaken to get an overview of this research, with a focus on biological effects.

METHODS: Abstracts were used to minimize effort and to complete this evaluation in a manageable timeframe. 3 databases were scanned: PubMed-Database: MEDLINE-Database of the "National Center for Biotechnology Information (NCBI)", EMF-Database of Information Ventures, USA, and WBLDB (Wissensbasierte Literaturdatenbank) of FEMU at RWTH Aachen, Germany. Found abstracts from 1975 through 2003 were processed in an Excel sheet. Each abstract was split into specific parts: bibliographic data, exposure and biological parameters, different classifications (*in vivo/in vitro*, biological endpoint, biological category), results, and main focus. Abstracts were classified according to their biological category (e.g. genetics, nervous system). To better illustrate similarities and differences in the data, abstracts were further divided into: "*in vivo / in vitro*", and "main focus". Comparison of abstracts with the same main focus concentrating on specific parameters, like biological object and exposure condition, gave

hints on research gaps in the particular category.

RESULTS: 809 abstracts met the conditions of experimental work in the defined frequency range. We found that research on microwave effects occurs in practically all biological systems without a clear concentration on a special issue or hypothesis. Published results are often controversial or have no replication. Thus, no category can be regarded as “fully investigated” with respect to the biological effects that may occur and their mechanisms, especially concerning exposure conditions near or below valid threshold values. Only the influence on spermatogenesis, the influence of acute exposure on permeability of the blood brain barrier, and the influence of continuous wave exposure on heartbeat seem to be satisfactorily investigated. In all three cases most likely, no effects occur below valid safety thresholds.

CONCLUSION: Our analysis of literature allows a detailed comparison of all publications from three databases in a special field of interest – based on their abstracts. In most biological categories different investigators have been reporting controversial results on possible microwave field effects in the frequency range of 2-3 GHz – sometimes even though they applied similar exposure conditions and biological parameters. This situation is calling for an analysis of the full publications and additional research at the same time. Other publications deal with special topics, their results are neither verified or disproved by other researchers. Therefore, our database can give hints for desirable future research projects. At the moment we are searching for a way to make the database publicly available.

This work has been supported by Forschungsgemeinschaft Funk e.V. (FGF) and by Bundesamt für Strahlenschutz (BfS), grant no. StSch 2002 0418A.

4-4

TRANSCRANIAL MAGNETIC STIMULATION SUPPRESS THERMAL BUT NOT MECHANICAL HYPERSENSITIVITY IN AN INFLAMMATORY PAIN RAT MODEL. H. Harada. Asahimachi 67, Dept of Anesthesiology, Kurume Univ School of Med, Kurume, Fukuoka, 8300011 Japan.

BACKGROUND: Pain refractory to conventional treatments is a big problem for patients and doctors. Interventions such as electroconvulsive therapy and deep brain stimulation have been clinically adopted to control such pain. However, those means are sometimes harmful and invasive with limited success. On the other hand, transcranial magnetic stimulation (TMS) has a capability to activate deep brain tissue without any pain or injury even under an wakeful state. TMS has been actually in clinical trial for Parkinson's disease. We have tested whether TMS could suppress hypersensitivity to thermal and mechanical stimuli in an inflammatory pain model.

MATERIAL AND METHODS: Experimental pain model was produced by injecting 150 μ g with complete Freund Adjuvant(FA) into the left hindpaw of 18 Wister rats. The same amount of serum was injected to the right hindpaw, which served as a control. At the 6th day after FA injection, changes in response for radiant heat and von Frey's hair stimuli were examined. TMS was applied for 30 min with a frequency of 0.1 Hz and a strength of 0.7 tesla. The responses were determined every 2 hours for the following 6 hours after TMS and then once a day for the subsequent 4 days.

RESULTS: The thermal response time after induction of the inflammatory pain was shorter on the FA-injected left hindpaw(7.2 \pm 0.8sec) than on the control right hindpaw (10.7 \pm 0.7sec). The shortened response time on the right side was restored for the following period; at 6 hrs (9.1 \pm 1.7sec) and at 2nd day (9.1 \pm 2.0sec) after TMS, though it returned to the pre-TMS level(8.3 \pm 1.4sec) at the 4th day after TMS. The mechanical response after induction of the inflammatory pain was also shortened on the FA- injected hindpaw(left vs right; 14.3 \pm 3.3g vs 25.1 \pm 2.7g). However, TMS did not affected on the mechanical hypersensitivity.

CONCLUSION: The present study has demonstrated in an inflammatory pain model that the hypersensitive state to heat was restored temporarily from 6 hrs through 2 days after TMS, while the hypersensitive state to touch was not affected. The results imply a possibility of TMS therapy for refractory

pain.

4-5

TWO GENERATION RF EXPERIMENT WITH NON-RESTRAINED RATS OF VARIOUS BODY MASS: DOSIMETRIC ANALYSIS USING HIGH RESOLUTION MODELS. T. Reinhardt*¹, A. Bitz*¹, J. Streckert*¹, V. Hansen¹, J. Buschmann*². ¹Chair of Electromagnetic Theory, Univ of Wuppertal, 42097 Wuppertal, Germany ²Fraunhofer Institute of Toxicology and Experimental Med, 30625 Hannover, Germany.

Ever since the decision was reached to launch the wideband UMTS in Europe connected with a substantial increase of the number of base station antennas, the public discussion about hypothetical health risks of weak electromagnetic fields has been reinforced.

As a contribution to the scientific work concerning this question, the Forschungsgemeinschaft Funk (FGF) has initiated the present project designed to investigate a number of endpoints during the development of Wistar rats which will be exposed for two generations to electromagnetic fields around 2 GHz modulated by a typical UMTS signal [1]. 20 hours/day exposure is applied during the complete period of the experiment of approx. 9 months including the exposure of rats during mating and pregnancy of the first generation, as well as lactation, weaning, maturation, mating and pregnancy of the second generation.

The biological design implies that during the study rats of different age and body mass are kept in the same cage and that up to 9 rats are able to move freely within one cage.

The exposure must be chosen in such a way that thermal effects are avoided in any stage of the experiment. The rat's body temperature as a function of power density was determined in a pilot study.

In order to evaluate the variation of the whole body SAR and the value and location of the maximum local SAR respectively, extensive numerical computations were performed under consideration of differently sized animals and for a wide range of their positions and postures within the cages. Detailed models with a resolution of 1mm³ for adult and young rats were used. The large number of computations enables a reasonable statistical examination.

Results of the dosimetry are shown for the animals located in an ideal homogeneous electromagnetic field and in the actual exposure field. The latter was generated by a new exposure set-up developed from a radial waveguide that excites an array of sector horns with high-impedance side walls which were inserted in order to yield propagation of TEM-waves. Each sector horn contains one cage, thus the fields of different cages are decoupled and the field variations due to the movement of the rats in one cage cannot influence the fields in adjacent cages. Each device contains 16 cages. In total 128 cages with up to 256 adult rats and up to 1000 pups are exposed during the experiment. The concept of the exposure setup was presented in [2, 3].

References.

[1] Ndoumbè Mbonjo Mbonjo, H., Streckert, J., Bitz, A., Hansen, V., Glasmachers, A., Gencol, S., Rozic, D.: A generic UMTS test signal for RF bio-electromagnetic studies. Accepted for publication in Bioelectromagnetics, December 2003.

[2] Bitz, A., Streckert, J., Reinhardt, T., Hansen, V., Buschmann, J.: „Exposure Setup for UMTS Two-Generation Study with up to Thousand Rats”, 25th BEMS Annual Meeting, Maui, Hawaii, USA, June 2003, 44.

[3] Reinhardt, T., Bitz, A., Streckert, J., Hansen, V., Buschmann J.: “Dosimetry for two generation experiment: RF exposure of up to nine non-restrained rats of various body mass kept in the same cage”, 6th International Congress of the European Bioelectromagnetics Association (EBEA), Budapest, Hungary, November 2003,74.

PROLIFERATION RATES IN MAMMARY GLAND TISSUE AND ADJACENT SKIN OF DIFFERENT RAT STRAINS AFTER 50 – HERTZ, 100 microT MAGNETIC FIELD EXPOSURE.

M. Fedrowitz* and W. Löscher. Dept of Pharmacology, Toxicology, and Pharmacy, School of Veterinary Med, Bünteweg 17, 30559 Hannover, Germany.

INTRODUCTION: In order to explain differing results of tumor-promoting magnetic field (MF) effects in the DMBA breast cancer model in female Sprague-Dawley rats (SD) from different countries (USA and Germany), the use of different substrains was considered to be the most important factor (Anderson et al., *Environ. Health Perspect.* 108, 797-802, 2000). In line with these considerations, we recently described differences in sensitivity of neoplastic response to DMBA between two different MF-exposed SD substrains from the same breeder (Fedrowitz et al., *Cancer Res.*, 2004, in press). The SD substrain (SD1) that we used in previous MF studies over many years showed robust and reproducible tumor-promoting MF effects in the DMBA model (Thun-Battersby et al., *Cancer Res.* 59, 3627-3633, 1999). We also found a cell-proliferation enhancing effect in the mammary gland tissue of this substrain after a MF exposure (100 μ T, 50-Hz) of two weeks which could explain the findings in the DMBA model (Fedrowitz et al., *Cancer Res.*, 62, 1356-1363, 2002). The other SD substrain (SD2) was never used by us for MF experiments before and could be considered MF-insensitive because these rats failed to show MF effects in the DMBA breast cancer model. Furthermore, this SD2 substrain had a higher sensitivity to DMBA and resembled the SD substrain used in the US studies.

OBJECTIVES: In the present study, we are searching for further MF-sensitive rat strains by determination of cell proliferation after MF exposure using the *in vivo* proliferation marker BrdU (bromodeoxyuridine) to get more information about rat strain differences in sensitivity to MF exposure.

METHODS: Female rats from two outbred (a “new“ SD substrain [SD3] and Wistar rats) and one inbred strain (Lewis) were examined up to now. All rats were obtained from Charles River, Sulzfeld, Germany. The rats were either exposed or sham-exposed to a 50-Hz, 100 μ T MF for 2 weeks. The thymidine analogue BrdU was administered i.v. at a dose of 50 mg/kg one h before killing the rats for marking cells in the S-phase of the cell cycle. BrdU positive cells in the cranial thoracic mammary glands, skin, and hair follicles were counted in a blind manner. The persons involved in the experiments were not aware whether rats were MF- or sham-exposed.

RESULTS: In contrast to SD1 rats MF exposure failed to produce a cell-proliferation enhancing effect in SD2, SD3, Wistar, and Lewis rat strains. There was a significantly decreased cell proliferation in the skin and hair follicles of female Wistar rats after MF exposure.

CONCLUSIONS: The data indicate that the MF-sensitive SD1 substrain we used over years seems to be a “fortunate“ exception for studies of tumor-promoting and cell-proliferation enhancing MF effects among several other strains and substrains of rats. However, we are determining cell proliferation in more rat strains at the moment, e.g. Fischer 344 and Copenhagen rats, to identify another strain, particularly an inbred one, that shows robust MF effects. Data for these two additional strains will be available at the BEMS meeting. Although MF-sensitive rat strains or substrains seem to be the minority, it might be very useful to find and examine these rats because knowledge about the role of the genetic background and the mechanisms of MF exposure could be helpful to explain strain differences in MF sensitivity and for the choice of rats for future experiments.

This work is funded by the Deutsche Forschungsgemeinschaft (Bonn, Germany).

THE EFFECTS OF RADIOFREQUENCY RADIATION ON BRAIN PHYSIOLOGY AND FUNCTION: A STUDY IN MICE. ¹J.E.H. Tattersall, ^{1*}A.J. Smith, ^{1*}P.K. Harrison, ^{1*}G. Underwood, ^{2*}J.B. Uney, ^{2*}R.J. Hobson, ^{3*}A.L. Bottomley, ^{3*}R. Bartram and ^{3*}Z.J. Sienkiewicz. ¹Biomedical Sci Dept, Dstl Porton Down, Salisbury, Wiltshire, SP4 0JQ, UK ²Henry Wellcome L.I.N.E, Dorothy Hodgkin Bldg, Whitson St, Bristol, BS1 3NY, UK; ³Nat'l Radiological Protection Board, Chilton, Didcot, Oxfordshire, OX110RQ, UK.

OBJECTIVE: This work tests the possibility that pulsed radiofrequency (RF) radiation associated with mobile telephones can induce changes in brain physiology and function. The specific objectives are to seek evidence of RF-induced changes in gene expression, electrophysiological responses and learned behaviour in mice. This abstract reports studies on acute exposures to 900MHz fields.

METHODS: Adult male C57BL mice were restrained in Perspex "rockets" (to which they had previously been habituated) and exposed to unmodulated 900MHz or 900MHz GSM fields (3.6, 18 and 36 W.kg⁻¹) for 1 hour using a head-only loop antenna system. The exposure system parameters were controlled by PC using customised software, which also recorded the history of each exposure to file. SAR values were determined using computer modelling (FDTD) and measurements on mouse cadavers with Luxtron thermometers. Sham-exposed and cage control groups were also used. For studies of gene expression, messenger RNA was extracted from the hippocampi of mice killed immediately after exposure to RF and changes in gene expression were analysed using the recently developed Affymetrix 430A mouse chip. For electrophysiological assessment, slices of hippocampus were prepared immediately after exposure of the animal to RF. Extracellular field potentials were recorded in CA1 stratum pyramidale using glass microelectrodes filled with 2M NaCl. Slices were characterised by determining stimulus-response relationships for the field potentials, the relationship between field excitatory postsynaptic potential (fEPSP) and population spike (PS), paired-pulse facilitation and inhibition, and the ability to express long term potentiation (LTP). For behavioural studies, following habituation to restraint, animals were trained over 4 days on the Morris water maze task. Performance was assessed using latency to escape as well as swim pattern and swimming speed. Immediately before the probe trial, animals were exposed for 60 minutes to the RF field.

RESULTS: A double blind study was carried out to investigate the effect of acute (restraint) stress and restraint habituation on gene expression in the mouse brain. Preliminary analysis suggested that following habituation (a 10-day repetition of the restraint) there were no significant stress mediated changes in gene expression in the hippocampus and therefore our ability to discern RF mediated changes in gene expression would not be compromised. Analysis of the effects of exposure to 900MHz fields on gene expression is still in progress. No significant changes were found in any of the electrophysiological parameters measured in hippocampal slices following exposure of mice to 900MHz unmodulated or GSM fields at 36 W.kg⁻¹. The results from the water maze indicated that there were no apparent field-dependent effects on the indices of performance examined during the probe trial. Animals from all treatments spent more time in the quadrant where the platform was located during acquisition, suggesting there were no impairments in spatial memory. The cage controls were slightly less active in the pool than the sham and RF exposed animals.

DISCUSSION: The results of this work will provide an integrated assessment of the effects of GSM fields on the brain at three levels: gene expression, neuronal physiology and behaviour. Future experiments will examine the effects of exposure to TETRA (400MHz) and UMTS (2200MHz) signals on these parameters, as well as the effects of repeated exposures.

The work was supported by the Mobile Telecommunications and Health Research Programme but the views expressed are those of the authors.

INVESTIGATION OF DOSE IN STUDIES OF PROTECTIVE EFFECTS OF ELF MAGNETIC FIELDS ON CHICK EMBRYOS EXPOSED TO UV-IRRADIATION. A.C. Mannerling*¹, K.H. Mild^{1,2}, M.O. Mattsson¹. Dept of Natural Sciences, Örebro Univ, SE-701 82 Örebro, Sweden. ²Nat'l Inst for Working Life, SE-907 13 Umeå, Sweden.

OBJECTIVE: The present study was undertaken to see if ELF magnetic fields (MF) at different frequencies, flux densities, and polarisations can confer protection against UV-exposure in chick embryos.

INTRODUCTION: We and others have previously demonstrated that ELF MF can protect against the lethal outcome of several stressors, including UV-irradiation in chick embryos. A possible mechanistic explanation in induction of the hsp70 gene. Here we report on experiments that are 1) investigating the replicability of our earlier studies 2) designed to investigate various flux densities in combination with different time frames for MF exposure.

METHODS: Fertilised hen eggs (White Leghorn) were incubated for 96 h (37.7°C). Subsequently, embryos were either exposed or sham-exposed to the chosen MF (50 Hz sinusoidal, vertical or horizontal polarisations, 50-200 μ T) for various times, followed by UV-irradiation for 75 min (0.4 μ W/cm² at 254 nm) after which vitality (as judged by beating heart) was checked every 30 min for 3 h. The possible induction of hsp70 was semiquantitatively investigated by immunoblotting. All experiments were performed in a blinded fashion, and in the presence of the local geomagnetic field.

SUMMARY AND CONCLUSION: Results in the present study confirm earlier observations in our laboratory. Thus, there is a significant protective effect against UV-induced death after MF exposure. The protective effect varies due to polarization, flux densities, and exposure times. In addition, there seems to be a threshold level at which the protection occurs. Work is in progress to more accurately determine what constitutes dose, and to establish when MF exposure is protective or not.

PLENARY SESSION II: Thz RESEARCH

Chair: Bruce McLeod

Thz RESEARCH: AN OVERVIEW. R. Osiander. JHU/APL, Johns Hopkins Road 2-255, Laurel, MD 20723, USA.

Electromagnetic waves in the frequency range between approximately 100 GHz and 10 THz, sometimes referred to as terahertz radiation or “T-rays”, are bridging the gap between the microwave and optical regimes. The increased attention to this technology within recent years is primarily due to the wider availability of sources and detectors for this frequency range. In parallel with the source and detector development a number of applications for THz technology have surfaced, many of them sparked by the need for new technologies in homeland security applications. Examples are the detection of explosives, biological and chemical agents, and buried mines. Many of these applications rely on the ability of THz technology to “see” through envelopes, cardboard or clothing. Another field for THz applications is the biomedical arena, where the non-ionizing nature of the THz radiation holds considerable potential for diagnosis of cancer cells or tooth decay.

The field of THz technology can be divided into a number of different disciplines depending on the source/detector technology and the application. Spectroscopy utilizing mm-wave technology is routinely applied to remote sensing of chemical processes in the upper atmosphere as well as identification of interstellar molecular species in “radio” astronomy. The expansion of the THz region into the far infrared, by electronic as well as optical means, offers new approaches to identify important chemical compounds such as explosives or proteins. Another important aspect of THz technology is the high imaging resolution capability when compared to microwave applications such as ground penetrating radar (GPR). This has been applied to ranging as well as to imaging of buried or hidden object such as mines in shallow ground or bio-agents in mailing envelopes. The latter image application utilizes the spectroscopic capability, which provides a contrast between different chemical compounds or bio-agents. Nondestructive evaluation (NDE) of dielectric materials such as thermally insulating foams for defects and interfaces, almost impossible for standard NDE methods such as ultrasound and thermal imaging, is another application where THz imaging promises a solution.

This presentation will review different source and detector technologies for THz radiation, discuss a number of examples for THz spectroscopy and imaging, and provide an introduction into the capabilities of T-rays for biomedical applications.

SESSION 5: THz APPLICATIONS IN BIOLOGY and MEDICINE

Chairs: Mays Swicord and Joe Spadaro

5-1 STUDENT

TERAHERTZ RADIATION SPECTROSCOPY ON MOLECULAR COMPLEXES, POLYPEPTIDES, AND PROTEINS.

A. Oka¹, K. Yamamoto¹, H. Kandori², and K. Tominaga¹
¹Molecular Photoscience Res Center, Kobe Univ, Nada, Kobe, 657-8501 Japan, Dept of Applied Chem, Nagoya Inst of Tech, Gokiso-cho, Showa-ku, Nagoya, 466-8555 Japan, ³CREST/JST Nada, Kobe, 657-8501 Japan. Res Cntr for Superconductor Photonics, Osaka Univ, 2-1 Yamadaoka, Suita, Osaka, 565-0871 Japan.

INTRODUCTION: There has been dramatic progress in generation and detection techniques of freely propagating terahertz (THz) radiation in these two decades (1 THz corresponds to 33.3 cm^{-1}). THz time-domain spectroscopy (TDS) is an attractive technique to study dynamics in sub-picoseconds and picoseconds time scales in condensed phases.

OBJECTIVES: In this report, THz radiation spectroscopy has been applied to measure far infrared (FIR) absorption spectra of molecular complexes in solution, polypeptides, and proteins such as cytochrome *c* and bacteriorhodopsin.

METHODS: The THz radiation was generated by surface photocurrent in a semiconductor placed in a magnetic field, and an electro-optic sampling method is utilized for detection.

RESULTS: In the region from 7 cm^{-1} to 55 cm^{-1} FIR absorption cross sections of polyglycine and poly-L-alanine in powder are greater than those of glycine and L-alanine in powder. On the other hand, FIR absorption spectra of cytochrome *c* in lyophilized powder show little dependence on protein structures. FIR spectral features of biopolymers in the THz frequency region are qualitatively discussed in terms of density of states and homogeneous/inhomogeneous broadening. We have measured the low-frequency spectra of electron donor-acceptor complexes consisting of hexamethylbenzene and tetracyanoethylene in carbontetrachloride by THz time-domain spectroscopy. The 1:1 and 2:1 complexes show quite different spectra of the extinction coefficient, reflecting different dynamics, fluctuations, and intermolecular interactions of these complexes. We have also performed THz spectral measurement on bacteriorhodopsin in a film.

5-2

THz-BRIDGE: A EUROPEAN PROJECT FOR THE STUDY OF THE INTERACTION OF TERAHERTZ RADIATION WITH BIOLOGICAL SYSTEMS.

G.P. Gallerano¹, E. Grosse², R. Korenstein³, M. Dressel⁴, W. Mäntele⁵, M.R. Scarfi⁶, A.C. Cefalas⁷, P. Taday⁸, R.H. Clothier⁹, P. Jepsen¹⁰.
¹ENEA-UTS TechFisiche Avanzate, 00044 Frascati-Italy on behalf of the THz-BRIDGE partners, ²Inst für Kern-und Hadronenphysik-Forschungszentrum Rossendorf, Germany, ³Dept of Phys. and Pharmacol Fac of Med, Tel-Aviv Univ, Israel, ⁴Physikalisches Inst Univ Stuttgart, Germany, ⁵Inst für Biophysik-J. W. Goethe-Univ Frankfurt am Main, Germany, ⁶CNR - IREA, Napoli, Italy, ⁷Nat'l Hellenic Res Found, Athens, Greece, ⁸Teraview Limited, Cambridge, UK, ⁹Sch of Biomedical Sci, Univ of Nottingham, UK, ¹⁰Albert-Ludwigs Univ Freiburg, Germany.

The recent technological break-through of electromagnetic radiation sources, components and devices in the Terahertz (THz) region has triggered a variety of applications in the field of material science, biology and biomedicine. Biological applications are based on the specific spectroscopic fingerprints of biological matter in this spectral region. However, very little is known of the effects of THz radiation in biological

systems and of potential damages that could be induced by the radiation. Despite the fact that there is not a wide public exposition to THz radiation with the present state of the technology, a timely assessment of potential hazards and health effects at specific occupational sites of research laboratories and industries is required.

A research project has been funded in the Quality of Life programme of the European Union to study the interaction of THz radiation with biological matter. The THz-BRIDGE project involves ten research groups of five European countries and takes advantage of the complementary expertise of its partners, from spectroscopy to optics and microwave engineering, from biophysics to biology and medicine, to analyse the physical mechanisms of interaction, to assess the risk of potential damage to biological activity, and to guide the development of microscopic biological imaging at THz frequencies.

As a part of the project activity, several spectroscopic techniques, from Fourier Transform to Time Domain Spectroscopy have been employed for the investigation of a variety of biological systems in the THz region. Spectroscopic measurements are crucial for a clear definition of the external parameters to be kept under control in irradiation studies.

Irradiation studies have been performed on whole blood in the frequency band from 110 to 140 GHz. Following irradiation, the Micronucleus assay was performed on human lymphocytes. Additional studies have included the Comet assay on human lymphocytes, in blood samples where the shielding effect of serum had been reduced, and the FISH assay on lymphocytes cultures.

A database on the irradiation of epithelial cell cultures has also been completed and a systematic investigation of the effects of 130 GHz exposure of liposomes at different modulation conditions has been carried out.

A summary of the project results will be presented together with some considerations on the safety issues raised by the use of THz radiation.

This work has been carried out with financial support from the Commission of the European Communities, specific RTD programme "Quality of Life and Management of Living Resources", QLK4-CT2000-00129 "Tera-Hertz Radiation In Biological Research, Investigation on Diagnostics and study on potential Genotoxic Effects".

5-3

DETERMINATION OF P53 PROTEIN STABILIZATION, LOSS OF MITOCHONDRIAL MEMBRANE POTENTIAL, AND THE RELEASE OF CYTOCHROME C INTO THE CYTOSOL IN RESPONSE TO UWB EMR EXPOSURE IN HUMAN LYMPHOBLASTOID CELLS. B.K. Nayak, C. Galindo*, M. Natarajan, S.P. Mathur¹*, M.L. Meltz. Dept of Radiation Oncology, Univ of Texas Health Sci Center at San Antonio, San Antonio, TX 78229, USA. ¹McKesson BioServices, USA Army Medical Res Detachment, Brooks Air Force Base, San Antonio, TX 78235, USA.

OBJECTIVE: The aim of the study was to determine the effect of ultrawideband electromagnetic radiation (UWB EMR) exposure on p53 protein stabilization, loss in mitochondrial membrane potential, and the release of cytochrome C into the cytoplasm, which are molecular alterations associated either with induction of apoptosis or inhibition of cell cycle progression when DNA is damaged.

METHODS: The studies were performed in 244B human lymphoblastoid cells. The cells were exposed to UWB EMR pulses intermittently for a total of 90 minutes (30 min on, 30 min off). The UWB EMR pulses had an average peak amplitude of 100 kV/m, an average pulse width of 0.80 ns, an average rise time of 200 ps, and a pulse repetition frequency of 250 pps. The frequencies ranged from D.C. to ~2 GHz. The stabilization of p53 protein was examined by western blot analysis. The transactivation of p53 target genes (p21, gadd45, Bax) was analyzed using the RNase protection assay. Further, evidence of the induction of apoptosis in response to UWB EMR exposure was determined by measuring a change in mitochondrial membrane potential using JC1 staining, and by detecting the release of cytochrome C into the cytoplasm (western blot analysis).

RESULTS: The p53 protein was not stabilized after the UWB EMR exposure of the 244B cells, i.e., there was no increase in the p53 protein level as compared to the sham and incubator control. There was no evidence of transcriptional induction of the p53 responsive genes p21, gadd45, and Bax after the UWB EMR exposure. In the positive control cells exposed to ionizing radiation, the p53 protein level was increased and there was an induction of the p53 target genes p21 and Bax. These are molecular responses associated with cell cycle arrest and apoptosis after this type of irradiation.

There was no loss of mitochondrial membrane potential and there was no release of cytochrome C into the cytoplasm in response to UWB EMR exposures (suggesting that apoptosis was not occurring), while in the positive control cells treated with staurosporine (1 μ g/ml), there was a loss of mitochondrial membrane potential accompanied with the release of cytochrome C into the cytosol, indicating the onset of apoptosis.

CONCLUSION: The analysis of several different molecular parameters, such as p53 protein stabilization, loss of mitochondrial membrane potential, and cytochrome C release into the cytosol, indicates that after this type of UWB EMR exposure, induction of apoptosis and effects on cell cycle progression in human lymphoblastoid cells do not occur. The evidence is not supportive of the hypothesis that this type of exposure induces DNA strand breaks.

This work was supported by AFOSR Grant No. F49620-01-1-0349.

5-4

NANOSECOND UWB EMF PULSES AFFECT CELL RECOVERY AND VIABILITY, AND RESULT IN THE INDUCTION OF C-FOS ONCOGENE EXPRESSION IN HUMAN LYMPHOBLASTOID CELLS. M.L. Meltz, B.K. Nayak, C. Galindo*, M. Natarajan. Dept of Radiation Oncology, Univ of Texas Health Sci Center at San Antonio, San Antonio, TX 78229, USA.

OBJECTIVE: The aim of this study was to examine the expression of p53 responsive genes in human lymphoblastoid cells after exposure to nanosecond pulses of UWB EM, under conditions where both cell recovery and viability are known to occur.

METHODS: The 244B human lymphoblastoid cells were exposed to a series of 10, 25, 50 or 100 pulses at an average peak field intensity of 200kV/cm using the 10 ns Pulse Device. The pulses had an average rise time of <2 ns, with a frequency range of D.C to >1 GHz. The cell viability was evaluated by the trypan blue dye exclusion method and microscope counting. The expression of the p53 target genes p21, gadd45, Bax, and the c-fos oncogene was analyzed using the RNase protection assay.

RESULTS: Both the recovery and viability of 244B cells increasingly decreased with increasing numbers of pulses (compared to sham exposed cells) within 30 minutes of 10 ns UWB EMF exposure. At 2 h post-exposure, the viability continued to decrease for all exposure conditions (numbers of pulses). However, at 24 hrs post-exposure, the viability of cells in all exposure conditions had increased. The induction of the p53 target genes p21, gadd45, and Bax was not observed to occur at 2 h and 4 h after 50 pulses of 10 ns pulse width. However, the induction of the c-fos oncogene was observed at 2 and 4 hour post-exposure (50 pulses).

CONCLUSION: The studies show that at conditions of nanosecond pulses where an effect on cell recovery and viability is observed, an induction of the c-fos oncogene occurs in 244B human lymphoblastoid cells. The nanosecond UWB EMF pulses might induce apoptosis via a c-fos-dependent pathway. This work was supported by AFOSR MURI Grant No. F49620-02-10320, by AFOSR Grant No. F49620-01-1-0349, and by the Department of Radiation Oncology (UTHSCSA).

NANOELECTROPULSE PERTURBATIONS OF CALCIUM AND PHOSPHOLIPID DISTRIBUTION IN HUMAN LYMPHOCYTES. P.T. Vernier^{*1,2}, Y. Sun^{*3}, L. Marcu^{*1,4,5}, C.M. Craft^{*6}, M.A. Gundersen^{*1}. ¹Dept of Electrical Engineering-Electrophysics, Univ of Southern CA, Los Angeles, CA, USA; ²MOSIS, Information Sci Inst, Univ of Southern CA, Los Angeles, CA, USA; ³Dept of Materials Sci, Univ of Southern CA, Los Angeles, CA, USA; ⁴Dept of Biomedical Engineering, Univ of Southern CA, Los Angeles, CA, USA; ⁵Biophotonics Res and Tech Development, Cedars-Sinai Medical Center, Los Angeles, CA, USA; ⁶Dept of Cell and Neurobiology, Keck School of Med, Univ of Southern CA, Los Angeles, CA, USA.

INTRODUCTION: Nanosecond, megavolt-per-meter pulsed electric fields cause intracellular calcium release and scramble the asymmetric arrangement of phospholipids in the external membranes of mammalian cells without the permeabilizing effects associated with longer, lower-field pulses. Real-time microscopic evidence associates these events directly and immediately with nanoelectropulse exposure. We establish a threshold amplitude for this pulsed electric field for Jurkat T lymphoblasts, below which calcium bursts and phosphatidylserine externalization do not occur, and we show that this threshold field strength corresponds closely to the induced transmembrane potential (≥ 0.5 V) that causes increased conductance when much longer (microsecond) pulses are applied (conventional electroporation). The ability to activate this signal remotely, with non-ionizing, non-thermal (high power, but low total energy), non-invasive electric pulses may be useful in both research and clinical settings.

OBJECTIVE: Characterize the immediate, electrophysical effects of nanosecond, megavolt-per-meter pulsed electric fields on the phospholipid bilayers of cell membranes and on the structures and regulatory mechanisms comprising intracellular calcium compartments in order to improve biophysical models and set boundaries on potential applications.

METHODS: Observations of live cells during pulse exposures were made with a Zeiss Axiovert 200 epifluorescence microscope. Images were captured and analyzed with a LaVision PicoStar HR12 camera and software (LaVision, Goettingen, Germany). Cells were placed in a rectangular channel 100 μm wide, 30 μm deep, and 12 mm long, with gold-plated electrode walls, microfabricated with photolithographic methods on a glass microscope slide. A fast MOSFET MicroPulser (Behrend *et al.*, 2003) was mounted on the microscope stage for delivery of pulses directly to the microchamber electrodes in ambient atmosphere at room temperature (Fig. 2).

RESULTS: Calcium bursts and PS externalization in Jurkat T cells appear within milliseconds of exposure to a single, 30 ns, 2.5 MV/m pulse. PS externalization, which occurs with or without calcium in the external medium is polarized along an axis of the cell aligned with the external field, indicating an immediate and direct interaction between the electric field and components of the membrane lipid bilayer. Propidium, sodium, calcium, and manganese ion influx under these conditions is below the level of detection with fluorescence microscopic methods, arguing against a significant role for facilitated phospholipid diffusion at transient, field-induced membrane nanopores. PS translocation occurs only at the anode pole of the cell, not at the cathode end, supporting the hypothesis that the energy for transporting PS across the lipid bilayer is provided by an electrostatic (dipole or electrophoretic) interaction between the pulsed field and the negatively charged head group of PS. Exploration of these possibilities promises to uncover not only basic cell biology and bioelectrics information but also pathways to practical applications. The ability to flip the membrane phospholipid switch with remotely delivered nanosecond electric pulses suggests the development of pulse exposure recipes (with pulse trains of varying amplitude, duration, and pattern) for selectively triggering responses in different cell types depending on their dielectric properties, leading to the elimination of undesirable cell populations by inducing them to advertise for phagocytic engulfment or to initiate directly their own apoptotic demise.

This work was made possible by support from the Air Force Office of Scientific Research and the Army Research Office.

THz HETERODYNE INSTRUMENT FOR BIOMEDICAL IMAGING APPLICATIONS. P.H. Siegel^{1,2} and R.J. Dengler², ¹California Institute of Technology, Division of Biology, Pasadena, CA 91125, ²Jet Propulsion Laboratory, Pasadena, CA 91109

INTRODUCTION: The submillimeter-wave frequency bands: 300-3000 GHz (wavelengths from 1mm to 100 microns), have long been the purview of far-IR spectroscopists. Thousands of important molecular line vibrational and rotational transitions have been calculated, measured and catalogued, with the goals of a basic understanding of quantum chemistry. Equally important applications for THz measurements have dominated Earth, planetary and space science [1]. Due largely to the recent availability of ultra-fast-pulsed time domain spectrometers (TDS), there has been a growing interest in this wavelength range for biological and biomedical work [2,3,4]. TDS systems yield wide spectral coverage but have limited frequency resolution and signal-to-noise ratio (limited penetration depth in “wet” tissue). As a contrast to TDS, CW heterodyne imaging is a more traditional technique that offers the potential for extremely large dynamic range and high signal-to-noise ratio while maintaining fast data acquisition, stable magnitude and phase measurements, reasonable frequency flexibility and millimeter scale penetration in wet tissues and other biomaterials.

The authors present a description and early measurement results from a unique CW terahertz heterodyne imaging system based around two custom fabricated 2.5 THz planar Schottky diode mixers [5] and two commercially available optically pumped far IR lasers [6]. One laser is used for the signal beam and supplies as much as 70mW at 2.5 THz. The other laser acts as a local oscillator (LO) source for the two mixers. Line pairs very close to each other (CH₃OH and CH₂F₂) are chosen to provide a workable intermediate frequency output (IF) of 24 GHz. A frequency stabilization scheme has been implemented to track and calibrate the laser power (magnitude and phase) over a sample run. The system uses the second THz mixer, a low frequency (GHz) reference oscillator and a lock-in amplifier to monitor and normalize the two lasers (LO and **signal**). Stability of ~0.05 dB and <5 degrees of phase have been achieved with a dynamic range (S/N) of **110 dB**. The system has been employed on both biological (mammalian and human) tissues as well as materials of interest to NASA space science applications. The instrumentation is briefly described and some representative images appear in this short abstract. A more complete description of the test system can be found in [7].

THz HETERODYNE IMAGER: The recent introduction of commercial CO₂ pumped far-IR lasers [6] and high sensitivity room temperature THz planar Schottky diode downconverters [5] makes a high dynamic range THz heterodyne imaging system realizable. In order to achieve an optimal signal-to-noise ratio (S/N), the pre-detection bandwidth must be made as narrow as possible. However, in order to obtain an image of reasonable resolution (many scanned pixels), it is desirable to use the largest possible pre-detection bandwidth (maximum signal strength). In addition to these conflicting requirements, there is the added complication of the stability of the THz sources (better than 1 part in 10⁹ is required, i.e. kHz). The minimum frequency drift of the commercial CO₂ pumped far IR lasers, over a 5 minute period, is about 150 kHz. Bearing these limitations in mind and taking advantage of space sensor technology that we have developed for several NASA missions, a system for imaging the transmission loss and phase of thin (< 10 mm thick) biosamples at 2.522 THz has been constructed and successfully tested in the laboratory. Dynamic range as great as **110 dB** has been measured to date with a 3 dB pixel size of <0.4 mm (this can be improved with different optics). The noise in the phase measurements is less than +/- 5 degrees. A block diagram of the imager appears in Fig. 1. The large dynamic range and amplitude stability have been obtained using a locking scheme patterned after Doane [8] wherein the two intermediate frequencies (reference and signal) are mixed with each other and filtered through a very narrow band phase-locked-loop tracking circuit. The transmission system relies on scanning the object through the fixed THz beam and building up an image pixel-by-pixel. Representative biological and materials images appear in Figure 2. The system is particularly sensitive to water absorption, both an advantage (for contrast) and a hindrance

Fig. 1. Amplitude stabilized heterodyne imager with 24 GHz IF (laser locking scheme not shown).

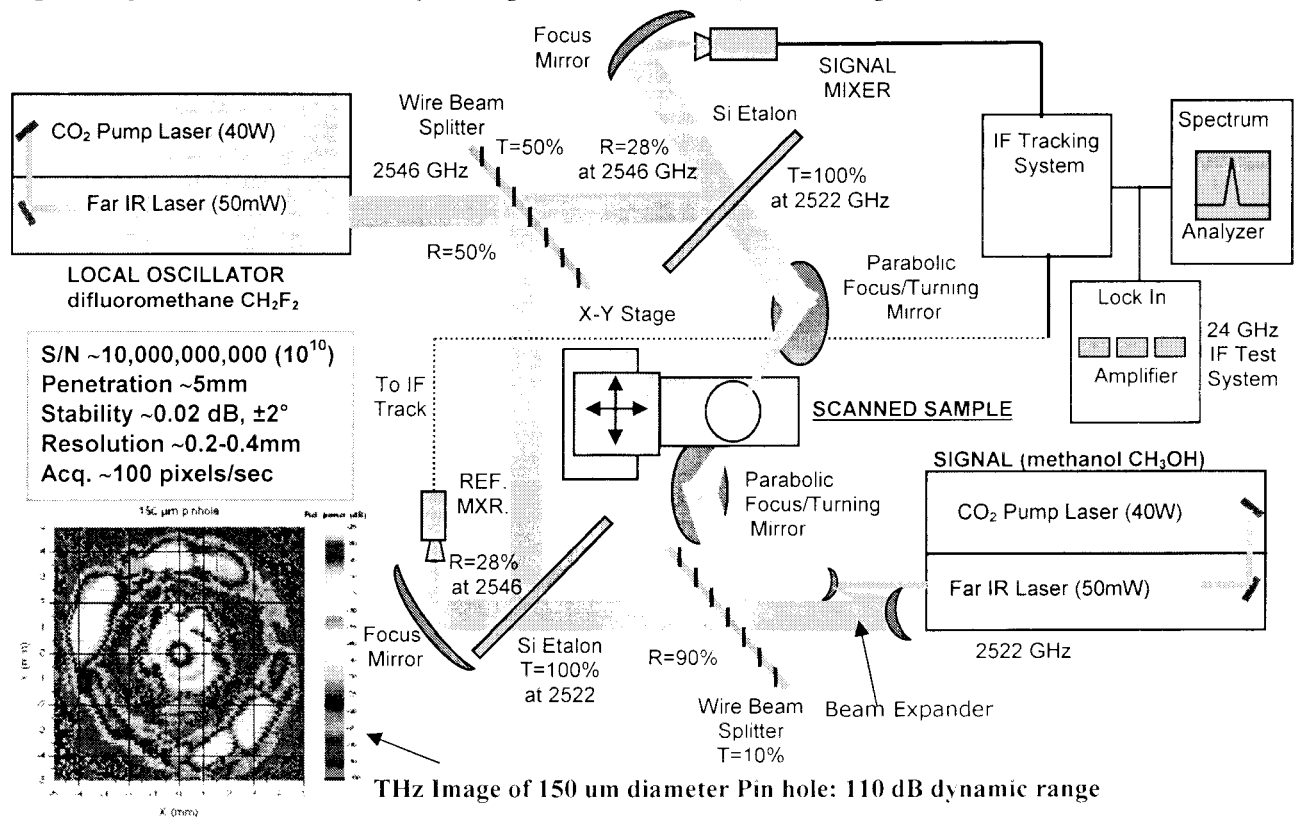
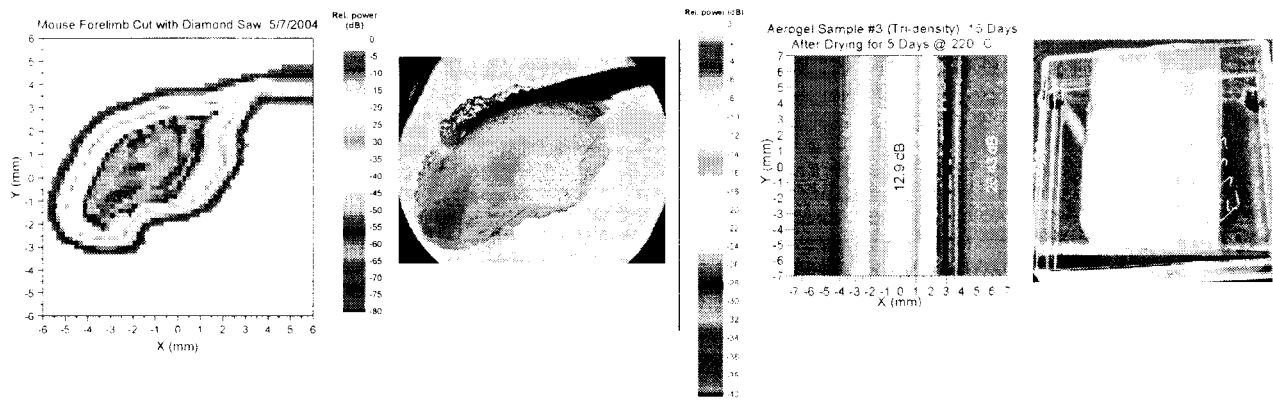


Fig 2. Representative biological and materials science images constructed at 2.5 THz by scanning samples through the fixed RF beam. *Left:* THz and Optical images of mouse forelimb section. *Right:* THz and optical images of tri-density aerogel sample after bake-out to remove trapped water.



(poor transmission throughput) and is therefore being used for a range of differing applications. This work was performed at the Jet Propulsion Laboratory under contract with the National Aeronautics and Space Administration and the California Institute of Technology. Funding was supplied jointly by NASA Code R and NIH through a K25 EB00109-02 grant.

References.

- [1]. P. H. Siegel, "Terahertz Technology," IEEE Trans. MTT, Special 50th Anniversary Issue, vol. MTT-50, no. 3, March 2002.
- [2]. Terahertz Sensing Technology, Volume 1, Editors: D.L. Woolard, et.al., World Scientific Publishing Co. Pte., Ltd., Singapore, 2003.
- [3]. Sensing with Terahertz Radiation, editor: D. Mittelman, Springer Series in Optical Sciences, Springer-

Verlag, Berlin, 2003.

[4]. P.H. Siegel, "THz Technology in Biology and Medicine," submitted to IEEE Trans. Microwave Theory and Techniques, Jan. 2004.

[5]. P.H. Siegel, R. Smith, S. Martin, M. Gaidis, "2.5 THz GaAs Monolithic Membrane-Diode Mixer", IEEE Trans. MTT, v.47, pp.596-604, May 1999.

[6]. E.R. Mueller et.al., "2.5 THz laser local oscillator for the EOS Chem I satellite," 9th. Int. Conf. Sp. THz Tech, p.563, Pasadena, CA, March 1998.

[7]. P.H. Siegel and R.J. Dengler, "Terahertz Heterodyne Imager for Biomedical Applications," SPIE , vol. 5354, San Jose, CA, Jan 25-26, 2004.

[8]. J. L. Doane, "Broadband superheterodyne tracking circuits for millimeter-wave measurements," Rev. Sci. Instr., vol. 51, pp. 317-20, March 1980.

5-7

THE USE OF TERAHERTZ RADIATION IN THE BIOLOGICAL AND MEDICAL SCIENCES.

D.A. Crawley, Y. Shen, P.C. Updaha and E.H. Linfield. University of Cambridge, Cavendish Laboratory, Madingley Road, Cambridge CB3 0HE, England.

The terahertz (10^{11} - 10^{13} Hz) region of the electromagnetic spectrum lies between the microwave and the infrared region. Imaging systems that exploit this region of the electromagnetic spectrum are extremely sensitive to water content and hydrogen-bonded materials in general, leading to one mode of contrast. Furthermore, unlike systems that operate in the mid-IR systems that operate in the Terahertz region are sensitive to intermolecular modes as well as intramolecular modes of large molecules.

Traditionally it has been difficult to build sources and detectors that operate in the terahertz region of the electromagnetic spectrum. However, the emergence of coherent detection as a technology for accessing the terahertz spectral range has lead to numerous proposals for the use of terahertz radiation in the biological and medical sciences. Demonstrated applications include caries detection in dentistry[1], [2] , cancer detection in dermatology[3] and "lab on a chip" DNA analysis[4]. These applications will be reviewed, including discussion of the first disease tissue detection using terahertz radiation, the first tomographic images of biological samples using terahertz and some of the earliest *in vivo* studies of human tissue. Recent results in bio-spectroscopy, of DNA and glucose using coherent detection techniques will also be presented.

There remain, however, considerable challenges in conducting systematic *in vivo* studies as compact, reliable and fast imaging systems are required. The current state of the art in coherent detection systems will be reviewed. A proposal for a novel, pseudo-holographic imaging technique will be discussed as well as the design of a compact probe head that will offer the possibility for *in vivo* studies using near field imaging in three dimensions.

References.

1. Crawley D, Longbottom C, Wallace VP, *et al.* Three-Dimensional Terahertz Pulse Imaging Of Dental Tissue J BIOMED OPT 8 (2): 303-307 APR 2003
2. Crawley D Longbottom C, Cole B, *et al.* Terahertz Pulse Imaging: A Pilot Study Of Potential Applications In Dentistry CARRIES RES 2003;37:352-359
3. Shankar S, Flanagan N, Pye R, *et al.* Terahertz Pulse Imaging For Basal Cell Carcinoma BRIT J DERMATOL 149: 108-108 Suppl. 64 JUL 2003
4. Nagel M, Bolivar PH, Brucherseifer M, *et al.* Integrated Planar Terahertz Resonators For Femtomolar Sensitivity Label-Free Detection Of DNA Hybridization APPL OPTICS 41 (10): 2074-2078 APR 1 2002

EFFECTS OF THz RADIATION ON CARBONIC ANHYDRASE LOADED LIPOSOMES. L. De Gregori¹, M. D'Arienzo², A. Doria², G.P. Gallerano², E. Giovenale², G. Messina², A. Ramundo-Orlando¹. ¹INEMM-CNR, Via Del Fosso del Cavaliere, 100, 00133 Roma, Italy, ²ENEA C.R. Frascati, Via Enrico Fermi 45, 00044 Frascati, Italy.

INTRODUCTION: Several in vitro studies indicate that millimeter waves radiation may alter structural and functional properties of the cell membrane [1]. Previous studies in our laboratory have indicated that cationic liposomes loaded with carbonic anhydrase offers a good system for evaluating permeability alteration of lipid membrane induced by EMFs both at high (2.45 GHz) and extremely low frequency (7-13 Hz) [2, 3]. Studies at higher frequencies are desirable both in the CW and pulsed regime. Here we report that THz radiation may induce alteration of liposome bilayer permeability.

OBJECTIVE: Evaluate the effect on liposome permeability induced by THz radiation at 130 GHz composed of 4 μ s pulses at different repetition rate between 1 to 10 Hz.

METHODOLOGY: Cationic liposomes consisting of dipalmitoylphosphatidyl choline, cholesterol and positive charged stearylamine (SA) at 5:3:2 molar ratio, entrapping Carbonic Anhydrase (CA) were used. The THz irradiation was generated by the Compact Free Electron Laser at ENEA-Frascati [4]. We used two different irradiation set up, referred to as A or B (Fig. 1). In both cases, the influx of the p-nitrophenyl acetate (p-PNA) across intact liposome bilayer was followed by means of spectrophotometric measurement of CA enzymatic activity. In the A apparatus, liposomes were irradiated for 60 minutes, and at the end of the irradiation time p-PNA was added and the CA activity rate was measured. In the B apparatus, real time kinetic measurements of CA activity were carried out during 2 minutes of the THz irradiation. In both cases, the hydrolysis rate of p-PNA ($\Delta A/\text{min}$), expressed as the absorbance change at 400 nm, was computed on the slope of the linear fitting of the recorded curve.

RESULTS: A significant increase of the p-NPA hydrolysis rate ($\Delta A/\text{min}$) from 0.0027 ± 0.0014 to 0.0058 ± 0.0014 ($p = 8.6E-10$ $df=47$) at 7 Hz resulted, while there was no significant increase at other frequencies of pulse repetition rate. The observed differences, reported as % of CA activity in Fig. 2, were significantly higher in setup B than in setup A, indicating that real time exposures might reveal possible reversible effects induced by the field. In spite of an intrinsic variability of the membrane system due to the use of several liposome preparations throughout all the experiments, the observed effects cannot be merely due to a difference of average power delivered to the system. No effect resulted for THz irradiation at 150 GHz without modulation.

CONCLUSION: Our results indicate that the membrane model used in these studies appears to be a sensitive system to THz exposures, especially regarding the frequencies of pulse repetition rate. Resonance effects on these cationic liposomes entrapping carbonic anhydrase have already been observed in the ELF (Extremely Low Frequencies) region at 7 Hz [5]. Future studies will provide further information about any possible correlation between resonance effects observed at a pulse repetition rate of 7 Hz and the previous effects observed in the ELF region.

References:

- [1] Pakhomov A. G., *et al (review) Bioelectromagnetics* 19: 393-413 (1998).
- [2] Ramundo-Orlando, A., Mossa, G., and d'Inzeo, G. *Bioelectromagnetics* 15: 303-313 (1994).
- [3] Ramundo-Orlando A., Morbiducci U., Mossa G., d'Inzeo, G. *Bioelectromagnetics* 21: 491-498 (2000).
- [4] Gallerano G.P., Doria A., Giovenale E., Renieri A. *Infrared Phys. and Tech.* 40, 161-174 (1999).
- [5] Ramundo-Orlando A., Mattia F., Palombo A., d'Inzeo G. *Bioelectromagnetics* 21:499-507 (2000).

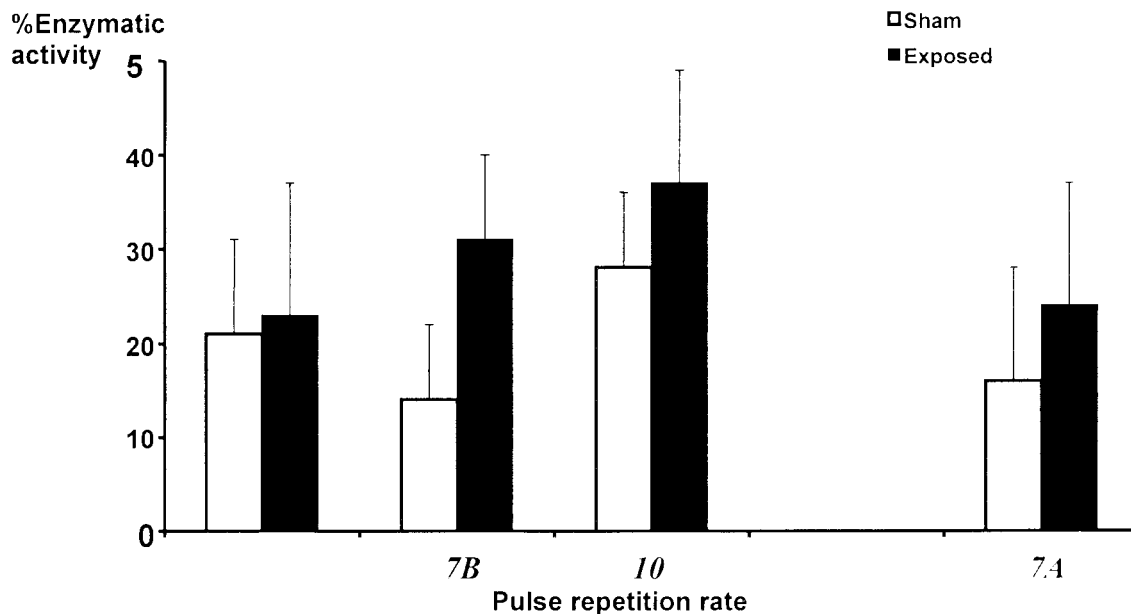


Fig.1 Irradiation set up A (left) showing one cuvette placed in. Set up B (right) for kinetic measurement in real time during THz irradiation

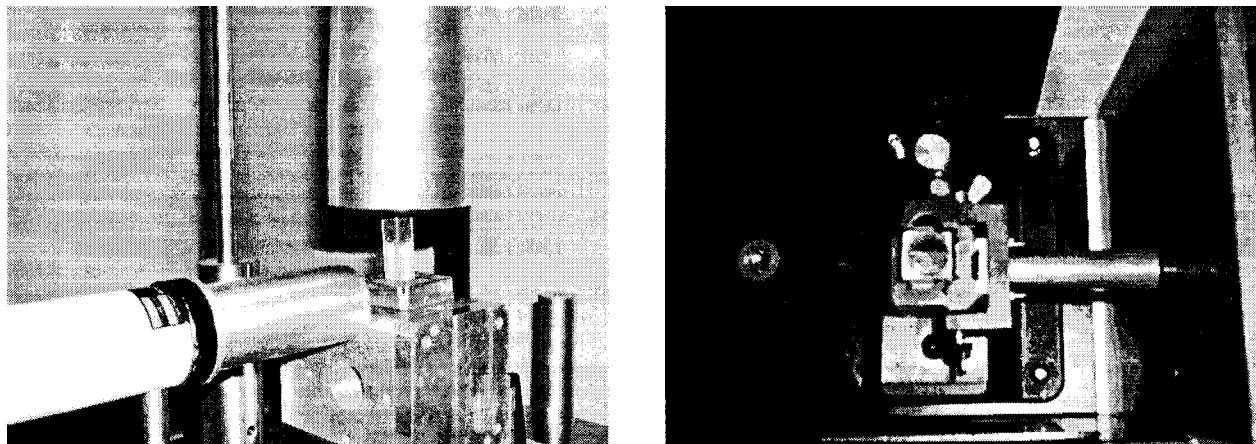


Fig. 2) THz-stimulated diffusion of *p*-NPA through CA-loaded liposomes at different pulse repetition rates (the suffix A or B refers to the exposure setup A and B, respectively). The total enzymatic activity of CA liposomes, after detergent rupture, was taken as 100%. CA activity at 7Hz pulse repetition rate sham 14 ± 8 , exposed 31 ± 9 ($p = 1,72E-09$).

This work has been carried out with financial support from the Commission of the European Communities, specific RTD programme "Quality of Life and Management of Living Resources", QLK4-CT2000-00129 "Tera-Hertz Radiation In Biological Research, Investigation on Diagnostics and study on potential Genotoxic Effects".

SESSION 6: MECHANISMS and MODELING
Chairs: Frank Barnes and Stefan Engström

6-1

A VOXEL-BASED WHOLE-BODY MODEL INCORPORATING ACTIVE THERMO-REGULATION FOR SIMULATING RF HEATING IN MAN. A.R. Curran^{*1}, E.A. Marttila^{*1}, D.A. Nelson², J.M. Ziriak³, P.A. Mason⁴, W.D. Hurt⁴. ¹ThermoAnalytics, Inc., Calumet, MI 49913, USA; ²Dept of Biomedical Engineering, Michigan Tech Univ, Houghton, MI 49931, USA; ³Naval Hlth Res Center Detachment, Brooks City Base, TX 78235, USA; ⁴Air Force Res Lab, Directed Energy Bioeffects Div, Brooks City Base, TX 78235, USA.

INTRODUCTION: Tissue heating is an established bioeffect of exposure to radio frequency (RF) fields of sufficient power density [1]. The ability to accurately predict the magnitude of tissue heating effects, has been limited by the lack of detailed models, with adequate spatial resolution, which incorporate known heat transfer and thermoregulatory mechanisms. Recent research by Curran, et al [2] the development of a three-dimensional voxel-based model [2], which has the spatial resolution and heat transfer mechanisms necessary to accurately predict tissue heating was developed. However, the model does not have an active thermoregulatory control system, which is needed to compute tissue heating in a living human.

OBJECTIVE: The objective of this work is to enhance a voxel-based code for simulation of RF heating of anatomically realistic models to include the effects of physiological heat sources and active thermoregulatory mechanisms and clothing.

METHODS: The thermal code solves a variation of Pennes' bio-heat equation [32] that includes the effects of local blood flow, metabolic heating, convective heat transfer, and the heating effects of EM irradiation:

$$k_t \nabla^2 T + \dot{m}_b c_b (T_b - T) + \dot{q}_m + \dot{q}_{conv} + \dot{q}_{sar} = \rho_t c_t \frac{\partial T}{\partial t}$$

The left-hand side terms of equation above represent, respectively, conduction through tissue with thermal conductivity k_t , heat advection associated with blood flow rate per unit tissue volume \dot{m}_b , metabolic heating, convective heat transfer (for voxels in contact with exterior air) and RF heating. The right-hand side term describes the rate of energy increase of the tissue volume. A multi-segmented human thermoregulatory model was developed by Fiala, et al [4], which includes the effects of peripheral vasomotion, shivering metabolism, working metabolism and sweating, [3]. This multi-segmented model was adapted for the voxel-based model to include the effects of peripheral vasomotion, shivering metabolism, working metabolism, and sweating. The effects of peripheral vasomotion are included by evaluating the blood flow rate for a tissue volume (\dot{m}_b) as a function of local skin temperature, mean skin temperature, and basal blood flow rate. The metabolic heat rate for non-muscle voxels is composed of a basal metabolic heat rate and a local change in basal metabolic rate given by according to the van't Hoff "Q10" effect. For muscle voxels, the metabolic heat rate also includes shivering and working metabolism. The shivering metabolic rate is computed using the mean skin temperature and the hypothalamus temperature, and the working metabolic rate is computed using the user-specified activity level of the subject. The temperature of the blood pool is calculated by applying an energy balance of the heat stored in the blood supply and with the advective heat exchange of the blood with each tissue volume. The effects of sweating are accounted for by applying mass and energy balances at the surface voxels. Clothing is modeled using localized insulation and evaporation coefficients to account for resistance to transfer of heat and moisture. The primary output from the program are three dimensional temperature files at specified

simulation times. Additional output includes temperature versus time for selected tissue volumes, average temperature for each tissue type, and whole-body average temperature.

RESULTS: The code development of the thermoregulation model is a work-in-progress. In its current state, the current version of the model accounts for active metabolic heating and mechanical thermogenesis (shivering (including shivering and working), as well as peripheral vasomotion effects. Preliminary results using the 5mm voxelized human model are promising in that reasonable metabolic rates are predicted, and the metabolic rates respond appropriately to influences of EM irradiation. More definitive results will be available once code development is complete.

DISCUSSION: The thermoregulation code will enable high-resolution determinations of thermal effects of exposure to EM fields for living humans. A tool that enables the accurate prediction of tissue temperatures will be useful for establishing safety standards and ensuring equipment compliance that relate to tissue heating.

References.

[1] CH Durney, H Massoudi, MF Iskander, Radiofrequency radiation dosimetry handbook, 4th ed. Brooks AFB, TX: USAF School of Aerospace Medicine, Aerospace Medical Division, 1986.

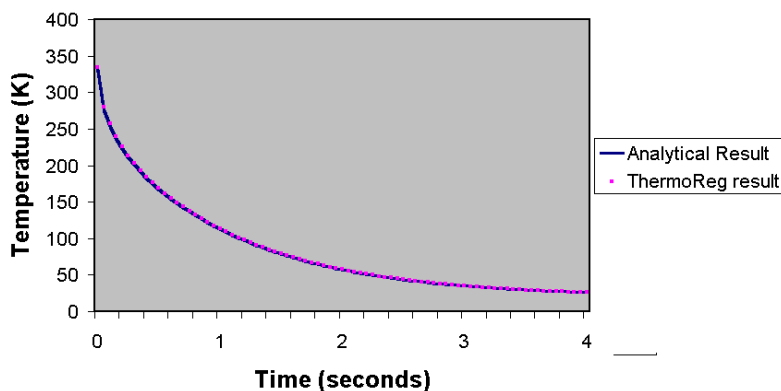
[2] A.R. Curran, E.A. Marttila, D.A. Nelson, J.M. Ziriak, P.A. Mason, W.D. Hurt, A three dimensional, voxel-based bio-heat transfer code for whole-body simulation of RF heating. 25th Annual Meeting of the Bioelectromagnetics Society, June 22-27, 2003.

[3] HH Pennes, Analysis of tissue and arterial blood temperatures in the resting human forearm. J Appl Physiol 1:93-122; 1948..

[43] D. Fiala, K.J. Lomas, M. Stohrer, Computer prediction of human thermoregulatory and temperature responses to a wide range of environmental conditions. *Int J Biometeorol* 45:143-159, 2001

This work was supported by the Small Business Innovation Research (SBIR) Program and administered through the Office of Naval Research (ONR). The Program Officer was CDR Stephen Ahlers of ONR and the Technical Monitor was Dr. John Ziriak of the Naval Health Research Center Detachment at Brooks Air Force Base.

Sphere Edge Temperature Comparison



6-2 STUDENT

DEVELOPMENT OF A FLAT PHANTOM SETUP FOR THE COMPLIANCE TESTING OF BODY-MOUNTED, WEARABLE AND PORTABLE TRANSMITTERS OPERATING IN THE FREQUENCY RANGE FROM 30MHz TO 5800MHz. M. Loeser.^{*1}, A. Christ^{*2}, A. Klingenböck^{*2}, N. Kuster², ¹Swiss Federal Inst of Tech (ETH), 8092 Zurich, Switzerland, ²Foundation for Res on Information Tech in Society, 8004 Zurich, Switzerland.

INTRODUCTION: Recent years have seen a steady growth in wireless devices operating in close proximity to the human body, such as WLAN transmitters in laptop computers or body-mounted health

support systems. In order to minimize the health risk due to the radiation to which the user is exposed, existing compliance testing standards need to be extended to cover a large variety of devices, frequencies and usage patterns. For this purpose, a novel phantom setup is being developed and characterized with respect to SAR assessment. This setup is to yield a conservative estimate of the local SAR caused by electromagnetic radiation operating at close distances from the human body (10mm to 200mm). The frequency range of interest spans from 30MHz up to 5800MHz.

OBJECTIVE: The goal of this study was to determine the characteristics of a generic human body phantom setup which yield a conservative estimate for the specific absorption rate (SAR) inside the human body when exposed to electromagnetic radiation. This includes:

- determine worst- case tissue compositions for body tissue covering the frequency range between 30MHz up to 5800MHz
- rigorously characterize the absorption mechanism in the phantom setup depending on antenna size and type
- propose a phantom setup which yields a conservative exposure estimate for the application range of interest
- benchmark the phantom setup using high resolution human models of different ages/sexes and different antenna positions (spine, kidney, leg, heart)

METHODS: For the human body the worst-case tissue composition (for incident plane waves) was derived by means of numerical optimization. Based on these data worst-case phantom setup liquids were computed and validated for different phantom designs, antennas (e.g., dipole, loop, PIFA), frequencies and distances. Specifically electrically small and large antennas were compared, as their SAR patterns show significant differences. Theoretical, numerical (FDTD platform SEMCAD) and experimental techniques (DASY4 near-field scanner) were applied for validation. For comparison with the energy absorption inside the human body, the same antennas were simulated operating in front of several high-resolution anatomical models.

RESULTS and DISCUSSION: It could be shown that the phantom shape only plays a minor role with respect to peak SAR. Accordingly, a flat phantom was chosen, because of its simple geometry. By optimizing its parameters, the tissue simulating liquid of the setup could be modified in such way that the flat phantom yields a conservative estimate for a range of distances covering the normal usage patterns of the devices of interest.

6-3

REAL-TIME MONITORING OF EFFECTS OF ELECTRIC FIELDS ON KINETICS OF MEMBRANE TRANSPORT IN SINGLE LIVING CELLS. X.N. Xu¹, Q. Wan¹, J. Kolb² and K.H. Schoenbach², ¹Department of Chemistry and Biochemistry; ²Department of Electrical and Computer Engineering; Old Dominion University, Norfolk, Virginia 23529, USA.

INTRODUCTION: Cellular and sub-cellular membrane transports play a key role in cellular and sub-cellular function and define the fate of living cells. It is well known that electric fields can be used to gate the cellular membrane transport. However, the detailed mechanism remains essentially unknown. Furthermore, it is still unclear whether electric fields can be used to tune the membrane transport of sub-cellular compartments without causing cell death. Moreover, it remains unknown whether one can selectively tune the specific transport pathway using desired electric fields. These are crucial questions to be addressed in order to achieve the possible application of electric fields for therapy and drug delivery.

OBJECTIVES: The goal of this study is to address some of these questions, such as, whether electric fields can be used to tune the membrane transport of sub-cellular compartments without leading to cell death, and whether one can selectively tune the specific transport pathway using desired electric fields. The outcome of this work will advance the understanding of the effects of electric fields on subcellular membrane transport. The possible applications include the selective eradication of specific cellular pathways and intelligent drug delivery.

METHODS: We have developed the microfabricated electrochemical cells and interfaced these electrochemical systems with our real-time single nanoparticle and single living cell imaging station, and a nanosecond pulser system. This unique unification allows the narrowband (nano-second) high electric fields at 100-1000 KV/cm to be applied in situ while real-time monitoring of the change of membrane transport kinetics at the cellular and subcellular level.

RESULTS: The results have demonstrated that the cellular and subcellular membrane transport kinetics are highly dependent upon the electric field strength, showing the promise of real-time tuning of cellular and subcellular membrane transport. In addition, it appears that the cellular membrane transport kinetics and subcellular transport kinetics can be selectively controlled by specific electric field strength because their responses to the electric field strengths are substantially different. This opens up the new opportunity to selectively control the subcellular membrane permeability. Furthermore, we find that we can increase the membrane transport kinetics while maintaining the viability of the cells, showing the possibility of using electric fields for tuning the cellular function and potential drug delivery. The experimental approach, updated research results and prospective applications will be discussed in detail.

This work is supported by an AFOSR/DOD MURI grant on Subcellular Responses to Narrowband and Wideband Radiofrequency Radiation, administered through Old Dominion University

6-4

FINITE-DIFFERENCE TIME-DOMAIN (FDTD) ANALYSIS AND DOSIMETRY OF A GIGAHERTZ TEM CELL. Z. Ji*, S.C. Hagness, J.H. Booske*, S. Mathur*,¹ and M. Meltz,² Dept of Electrical and Computer Engineering, Univ of Wisconsin-Madison, 1415 Engineering Drive, Madison, WI 53706, ¹McKesson BioServices, 8355 Hawks Road, Brooks City-Base, TX 78235, and ²Dept of Radiation Oncology, Univ of Texas Health Sci Center at San Antonio, San Antonio, TX 78229.

INTRODUCTION: A Gigahertz TEM (GTEM) cell has been designed and adopted for ultrawideband (UWB) baseband electromagnetic pulse (EMP) exposure studies of biological specimens [1]. The objective of the recent experiments are to examine cellular and molecular responses occurring after exposure of mammalian cells to biological cells high average peak power to ~ 1 ns, intense EMPs (~ 1 ns pulse width). In these experiments, the GTEM cell is by inserting loaded with T-25 flasks containing cells suspended in cell culture media inside the GTEM cell. Important information about the spatial uniformity and temporal transients of electromagnetic fields within the media in the flasks is very difficult to obtain experimentally. FDTD simulations are regarded as a practical means of acquiring the required dosimetry information. While FDTD models of a few unloaded GTEM cells have been previously reported [1,2], recent advances in computing power and FDTD algorithms [3] permit the modeling of UWB EMP propagation in GTEM cells with increased accuracy.

OBJECTIVE: The ultimate objective of this study is to obtain transient dosimetry information in a GTEM cell loaded with T-25 flasks containing cell culture media. The first phase objective of the first phase of this study is to develop a realistic three-dimensional (3D) simulation model of the unloaded GTEM cell and to validate the simulation results by comparison with experimental measurements of the electric field pulses at several points within the GTEM cell. Upon successful completion of the first phase, the computational model will be used to study field distributions in space and time within the specimen T-25 flasks.

METHOD: The FDTD method was used to simulate the GTEM cell. Several GTEM FDTD models were built and compared. The final FDTD simulation model was built by terminating the GTEM cell at the load end of the GTEM cell is terminated with Perfectly Matched Layer (PML) absorbing boundary conditions. The source end of the modeled GTEM cell was extended beyond the experimental source plane to form using a model an apex similar to that of Refs. [21, 32]. This choice permits accurate simulations excitations of UWB pulses excitation without having to model the complex feed structure of the actual experimental assembly [1]. The experimentally generated waveform is approximated using a

double exponential pulse with a width of Based on the pulsewidth of ~ 1 ns, excited between the septum and the outer ground plane of the GTEM cell. This source waveform is plotted in Fig. 1a. , The FDTD grid is comprised of a uniform lattice of cubic grid cells ($\Delta = 2.5$ mm) with $dx=dy=dz=2.5$ mm was adopted. This grid resolution corresponds to 120 points per free-space wavelength at 1 GHz, and is therefore fine enough to accommodate accurate staircasing of the flared metal surfaces as well as the later inclusion of cell culture media. , along with a Courant stability factor of $S=0.5$. To model the experiments, a computational domain of $280 \times 280 \times 700$ cells was needed with a memory requirement (single precision) of about 2 GB. The GTEM walls and septum were modeled as Perfect Electrical Conductors (PECs) and staircased.

RESULTS: Figure 1a shows the FDTD-computed time-domain vertical electric fields recorded at three sampling points along the horizontal floor of the empty GTEM cell. These results illustrate that the pulse shape is preserved as the pulse propagates towards the load. (The amplitude, and thus the power density, decreases as the cross-sectional area of the GTEM cell increases.) There are only very slight distortions/fluctuations that are artifacts of the simulation shown as small fluctuations in the pulse tails. These artifacts were established to be the result of the staircase approximation of smooth tapered walls, particularly at the source end. Figure 1b compares the simulated and measured vertical electric field at a common observation point. The experimental waveform was measured using a Tektronix SCD 5000 transient digitizer and an asymptotic conical dipole D-dot sensor [4]. For the GTEM cell without media flasks, five points on the bottom of the GTEM cell were selected to sample the transient electric fields. The simulated electric field/FDTD-computed waveforms at the designated points agree well with the waveforms collected in measurements at all selected sample points. Ongoing computational studies of the GTEM cell loaded with T-25 flasks are being conducted to evaluate field distributions in space and time, as well as SAR distributions, inside the cell culture medium.

References:

This study was funded by ... Two of the authors (SCH, JHB) were supported in part by the US Department of Defense under its FY01 "RF Bioeffects" MURI program, through a consortium grant with Old Dominion University and managed by the Air Force Office of Scientific Research.

[1] T.E. Harrington, "GTEM Fields FDTD Modeling," IEEE International Symposium on Electromagnetic Compatibility, pp. 614 – 619, 1997.

[2] W.A. Radasky, K.S. Smith, D. Hansen, and D. Ristau, "Calculations and Measurements of Fast EM Pulses in the GTEM Cell," IEEE International Symposium on Electromagnetic Compatibility, pp. 52 – 57 1996.

[3] Allen Taflov and Susan C. Hagness, *Computational Electrodynamics: The Finite-Difference Time-Domain Method, 2nd ed.*, Norwood, MA: Artech House, 2000.

[4] J.-Z. Bao, "Picosecond domain electromagnetic pulse measurement in an exposure facility: An error compensation routine using deconvolution techniques," *Rev. Sci. Instrum.*, vVol. 68, No. 5, pp. 2221 – 2227, (1997).

This study was funded by the Air Force Office of Scientific Research (grant no. F49620-01-1-0349). Two of the authors (SCH, JHB) were supported in part by the US Department of Defense under its FY01 "RF Bioeffects" MURI program, through a consortium grant with Old Dominion University and managed by the Air Force Office of Scientific Research.

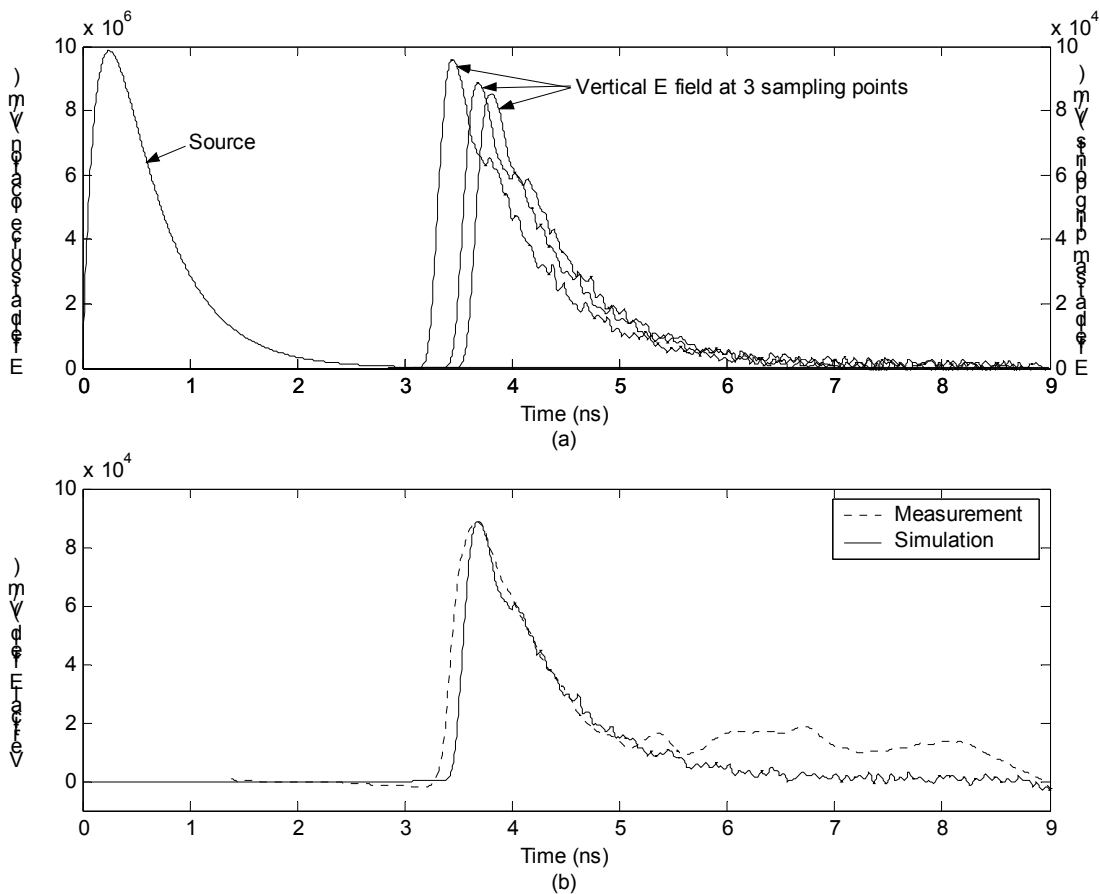


Figure 1: (a) Simulated UWB source waveform (far left) and radiated vertical electric fields computed along the horizontal floor of the GTEM cell. (b) Simulated and measured vertical electric field recorded at a common sampling point.

[2] T.E. Harrington, "GTEM Fields FDTD Modeling", IEEE International Symposium on Electromagnetic Compatibility, 18-22 Aug. 1997 pp. 614 – 619 (1997).

[3] W.A. Radasky, K.S. Smith, D. Hansen, and D. Ristau, "Calculations and Measurements of Fast EM Pulses in the GTEM Cell," IEEE International Symposium on Electromagnetic Compatibility, 19-23 Aug. 1996 pp. 52 – 57 (1996).

DEVELOPMENT OF NEW TRANSPARENCY GEL PHANTOM WITH CAPSULATE LIQUID CRYSTAL FOR VISUALIZATION OF THREE- DIMENSIONAL ELECTROMAGNETIC POWER ABSORPTION. Y. Suzuki*¹, M. Baba*¹, A. Ishii*¹, M. Taki¹, S. Watanabe². ¹Tokyo Metropolitan Univ, Tokyo 192-0397, Japan. ²Communication Res Lab, Tokyo 184-8795, Japan.

INTRODUCTION: Safety of radio frequency (RF) electromagnetic fields (EMF) is commonly discussed in terms of specific absorption rate (SAR). Phantoms are useful for the dosimetry on energy absorption of RF-EMF exposures. SAR is estimated from measurements of an increase in temperature within the phantom over a short period of time following the exposure. In the past study, a method for visualizing the three-dimensional (3D) distribution of temperature due to RM-EMF energy absorption was reported [1]. A difficulty of this method is that it can only visualize the temperature higher than the clouding point. We focused our interest on capsulate liquid crystal that has been used for visualization of temperature distribution within fluids [2].

OBJECTIVE: The objective of this study is to make a phantom containing capsulate liquid crystal so as to develop a method to visualize 3-D distribution of electromagnetic power absorption. We have investigated the suitable materials for transparency phantom and discussed for the method to adjust dielectric properties of the phantom.

METHODS: Micro-capsulated thermo-chromic liquid crystal (MTLC) is used for our experiments. Thermo-chromic liquid crystal is contained in the urea resin capsule. The diameter of the capsule is about 20 to 30 micrometer. The incident light into MTLC is needed for visualization. The wavelength of scattered light depends on the temperature of the capsulate liquid crystal. The wavelength becomes shorter with the increase of temperature. In other words, the scattered light changes in its color from red to purple with the increase of temperature. MTLC are suspended uniformly in the gel phantom.

The substrate material for the phantom should not be convective to measure SAR. Therefore, high-molecular gel constructed from “carrageenan”, which is extracted from seaweed and has high transparency, is used as the substrate of the phantom to prevent convection. The dielectric properties of the phantom are adjusted by mixing sucrose and KCl (potassium chloride).

RESULTS: Complex permittivity plots of the dielectric properties of phantoms that are made from carrageenan are shown in Fig.1. Values of complex permittivity are measured by the dielectric probe (Agilent 85070C). In this graph, horizontal axis and vertical axis indicate relative permittivity ($\epsilon'(\omega)$) and loss ($\epsilon''(\omega)$), respectively. Each marker shows the complex permittivity at 500[MHz], 900[MHz], 1.5[GHz], 1.95[GHz], and 2.45[GHz], respectively. Solid line which indicates muscle property is obtained by the parametric model of biological tissues [3]. As shown in Fig. 1, dielectric properties of the transparency phantom based on carrageenan can be controlled by varying the concentration of sucrose and KCl mixed in the phantom. We can adjust a value of complex permittivity of transparency phantom to that of muscle at 1.5[GHz].

We perform a preliminary exposure experiment using above-mentioned phantom. A dipole antenna is used to irradiate a phantom containing MTLC with RF-EMF at the frequency of 1.5GHz. The temperature distribution, which is indicated by scattering light from red to purple, on the plane lit up by the slit light is obtained clearly. The temperature distributions on other planes are also visualized by moving the slit light location. These observations imply the possibility of the 3-D visualization that is reconstructed by measured data at each plane.

CONCLUSIONS: We have proposed a new non-invasive method for visualizing the 3-D distribution of electromagnetic power absorption by using MTLC. The transparency phantom for this method is developed. The substrate material for the phantom is carrageenan. Values of complex permittivity for the phantom can be controlled by the concentration of sucrose and KCl mixed in it. The electromagnetic power absorption could be visualized by using the phantom. It suggests that this new method has capability to reconstruct the

3-D distribution of power absorption due to RF-EMF.

References:

- [1] M. Miyakawa, S. Hoshina, and Y. Kanai: "Visualization and 3-D measurement of local SAR using a gel phantom", Proc. 1998 IEEE EMC Symposium, Denver, Co., Vol. 2, pp. 751–756, 1998.
- [2] Y. B. Du and P. Tong: "Turbulent thermal convection in a cell with ordered rough boundaries", J. Fluid Mech., vol. 407, pp. 57–84, 2000.
- [3] S. Gabriel, R. W. Lau, and C. Gabriel: "The dielectric properties of biological tissues: III. Parametric models for the dielectric spectrum of tissues", Phys. Med. Biol., 41, pp. 2271–2293, 1996.

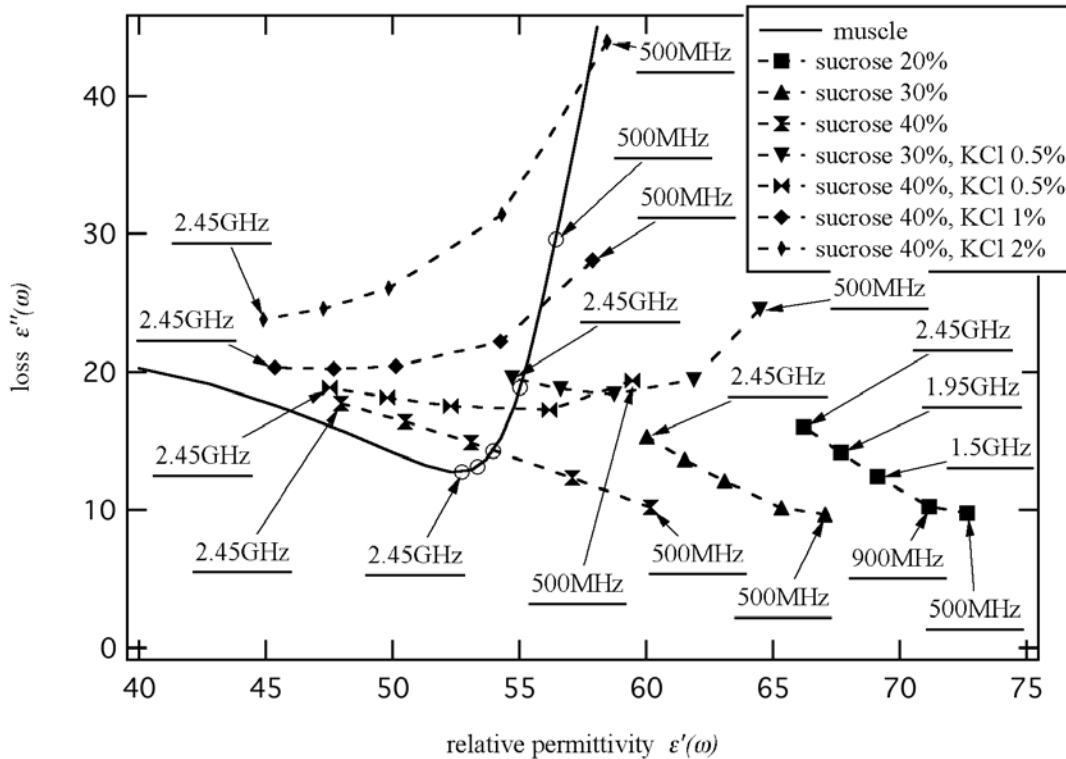


Figure 1: Complex permittivity plots of the dielectric properties for carrageenan phantoms.

6-6 STUDENT

DOSIMETRY OF RAT-HEAD SAR CAUSED BY A HIGH-PERFORMANCE g8h-SHAPED LOOP ANTENNA. H. Watanabe^{1,2*}, K. Wake¹, M. Hanazawa^{1*}, S. Watanabe¹, H. Masuda³, C. Ohkubo³, M. Taki⁴, Y. Yamanaka^{*1}, and T. Uno^{2*}, ¹Nat'l Inst of Information and Communications Tech, Tokyo 184-8795, Japan, ²Tokyo Univ of Agriculture and Tech, Tokyo 184-8588, Japan, ³Nat'l Inst of Pub Hlth, Tokyo 106-8638, Japan, ⁴Tokyo Metropolitan Univ, Tokyo 912-0397, Japan.

INTRODUCTION: Many in vivo studies on unknown health effects due to localized exposure to microwaves radiating from cellular phones have been reported. Most of the studies have been criticized due to insufficient localization of high SAR region in laboratory animals, e.g., rats and mice. Some new high-performance antennas have therefore been developed in order to improve the localization of high SAR region. Exposure setups including a small loop can realize localized exposure conditions (Chou, et al., *Bioelectromagnetics*, Vol.20, pp.75-92, 1998; Dulou, et al., *20th Annual Meeting of BEMS*, pp.152-153, 1998). It is however difficult to observe real-time biological changes, via “cranial-window” embedded in a rat’s head (Masuda, et al., *Microcirculation Annual*, pp.151-152, 2000), during exposure to cellular-phone signals by those antennas. We have therefore designed a new loop antenna which can provide real-time observation as well as highly-localized SAR distribution (Watanabe, et al., *6th International Congress of EBEA*, pp.147, 2003).

OBJECTIVE: In this presentation, we present the dosimetry of rat-head SAR caused by the new antenna, both numerically and experimentally.

METHOD AND MATERIAL: A high-performance X-ray CT equipment has been used in order to obtain high-resolution anatomical data of the cranial-window rat. From the CT data, we have developed a voxel rat model with 0.5-mm spatial resolution, as shown in Figure 1. Distribution and statistics of the rat SAR have been calculated with FDTD method. Homogeneous rat phantom with the same shape of the voxel model have also been developed. SAR distributions have been experimentally estimated with the thermography method.

RESULTS AND DISCUSSION: SAR distributions are shown in Figure 2. It is shown that high SAR region is localized around the top of the rat head, i.e., the target tissue of the “cranial-window observation”. The measure of the SAR localization, i.e., the ratio of target-tissue averaged SAR (TTA-SAR) to the whole-body averaged SAR (WBA-SAR), has been estimated to be over 60. This value is very effective in compared to at most about 20 for ordinary antennas. The comparison of the SAR distribution between the experiment and the calculation is shown in Figure 2. Good agreement between the experiment and the calculation implies that the results of our dosimetry have good accuracy.

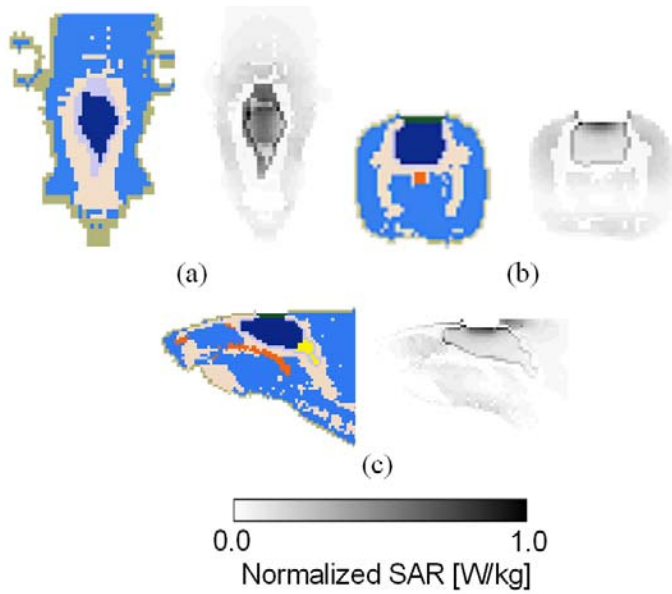


Figure 1: Calculated SAR distributions on the top surface of the brain (a), in the mid section of the brain normal to the sagittal axis (b), and in the sagittal section (c).

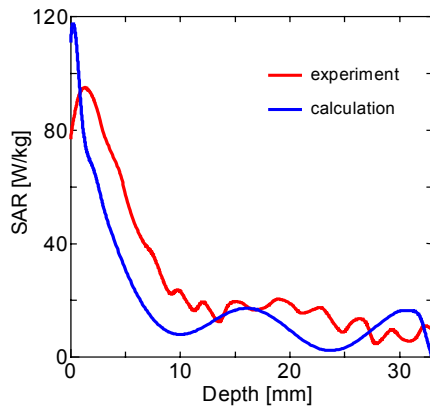


Figure 2: SAR distributions along the axis through the center of the brain from top surface of the brain to bottom of the head. SAR values are normalized as the antenna output power is 1 W.

LIGHT-DEPENDENT MAGNETIC FIELD INFLUENCE ON THE PERIODIC PEROXIDASE-OXIDASE OSCILLATOR. J.J.L. Carson and J. Walleczek. Bioelectromagnetics Laboratory, Department of Radiation Oncology, Stanford University Medical School, Stanford, California, USA 94305-5304.

OBJECTIVE: Under nonequilibrium conditions, the peroxidase-oxidase (PO) reaction generates dynamical behaviour that is qualitatively similar to oscillatory processes found in biological systems [1]. This property has led some investigators to implement the PO reaction as an in vitro model to study how magnetic fields might influence biological oscillators. It was observed that both the amplitude and periodicity of an oscillating PO reaction decreased when a static magnetic field was present [2]. Earlier experiments on the isolated peroxidase enzyme demonstrated that the rate of substrate consumption was field-dependent [3]. The earlier finding led many investigators to consider the enzyme itself as the field sensor in the PO reaction, however this hypothesis remained untested. During attempts to replicate the magnetic field influence on the PO reaction in our laboratory, we observed that suppression of oscillations was only observable when white light from the spectrometer and/or the laboratory environment was present. The objective of this work was to determine the illumination wavelength(s) at which the suppression effect was maximal so that the optically absorbing molecular species associated with magnetic field sensitivity in the PO reaction could be identified.

METHOD: Experiments were performed in a quartz cuvette temperature-controlled to $28.0 \pm 0.1^\circ\text{C}$ as described previously [4]. The cuvette was held between the poles of a water-cooled electromagnet, which was capable of producing uniform static fields up to 200 mT over the sample volume. PO oscillations were recorded using an O_2 -electrode. With this system we were able to observe stable oscillations for several hours as periodic variations in the concentration of dissolved oxygen.

RESULTS: Fig. 1 shows the response of a periodic PO oscillations to an 80-mT static magnetic field at different illumination wavelengths. Each point represents the change in average amplitude of dissolved oxygen during an exposure to a static magnetic field compared to intervals before and after exposure where the magnetic field was absent. Oscillations were affected by field only when the reaction mixture was illuminated by light of 600 nm to 700 nm with a maximal response near 650 nm.

DISCUSSION: The consistency of the wavelength dependence of the magnetic field effect with the absorbance spectrum of methylene blue (see solid line in Fig. 1) suggested that the magnetic field sensitivity of the PO reaction was dependent on the photoactivation of methylene blue. Methylene blue is a required component of the PO reaction and is known to oxidize NADH in a light-dependent manner [4]. Therefore, the mechanism of magnetic field action on the PO reaction may involve a reaction between methylene blue and NADH independent of reactions involving the peroxidase enzyme. Future work could examine methylene blue and NADH in the absence of the other PO components to determine if magnetosensitivity can be observed during illumination with light near 650 nm.

References.

[1] Scheeline, A., et al. (1997), *Chemical Reviews (Washington, D. C.)*, **97**, 739-756.

[2] Moller, A.C., A. Lunding, and L.F. Olsen (2000), *Physical Chemistry Chemical Physics*, **2**, 3443-3446.

[3] Taraban, M.B., et al. (1997), *Journal of the American Chemical Society*, **119**, 5768-5769.

[4] Carson, J.J.L. and J. Walleczek (2003), *Journal of Physical Chemistry B*, **107**, 8637-8642.

This work was supported by the US Department of Energy, the Fetzer Institute and the Canadian Institutes of Health Research.

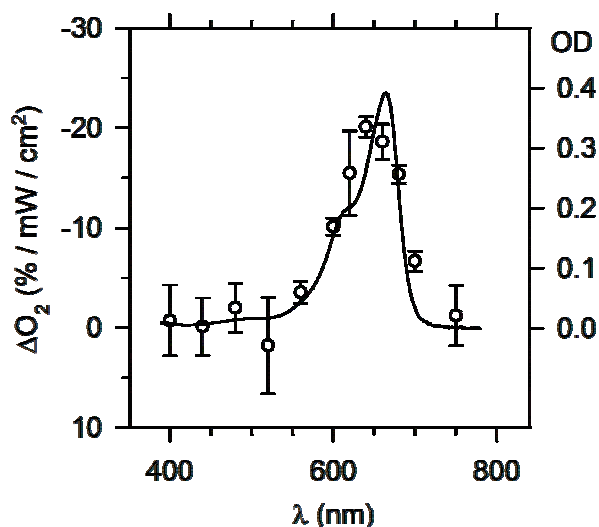


Figure 1. The dependence of periodic PO oscillations on an 80-mT static magnetic field during illumination at different wavelengths (λ). Symbols represent the relative change in O_2 -amplitude (ΔO_2) during an 80-mT static magnetic field exposure compared to oscillations observed in the absence of magnetic field (mean \pm s.e.m. from 3 independent experiments). During each experiment, reactants were illuminated continuously with filtered light from a xenon lamp ($\lambda \pm 5$ nm, 380 - 500 $\mu W/cm^2$). Each ΔO_2 was divided by the illumination intensity (in mW/cm^2) to normalize for small differences in illumination intensity between experiments due to adjustment limitations of the light source. The solid line shows the absorption spectrum of 4 - μM methylene blue (optical density axis on right).

6-8

EXPOSURE OF THE HUMAN HEAD TO 915 MHZ IRRADIATION: A THERMAL MODEL INCORPORATING BLOOD FLOW. D.A. Nelson¹, A.R. Curran², E.A. Marttila², E.T. Ng¹, J.M. Ziriak³, P.A. Mason⁴, W.D. Hurt⁴. ¹Michigan Technological University, Houghton, Michigan 49931; ²ThermoAnalytics, Inc., Calumet, Michigan 49913, USA; ³Naval Health Research Center Detachment, Brooks Air Force Base, Texas 78235, USA; ⁴Air Force Research Lab, Directed Energy Bioeffects Division, Brooks Air Force Base, Texas 78235, USA.

INTRODUCTION: Exposure to radio frequency (RF) fields of sufficient power density can significantly increase tissue temperatures [1]. Temperature increases are generally consistent with energy deposition. However, the rate of temperature increase may – in some cases – be affected by blood flow and other variables.

Exposures of the head at frequencies in the 900 MHz region are particularly relevant to mobile phone usage. The ability to accurately predict the magnitude of tissue heating effects has been limited by the lack of detailed models, with adequate spatial resolution, which incorporate known heat transfer and thermoregulatory mechanisms. Of particular interest is the role of blood flow, which can have a significant effect on brain temperature [2].

OBJECTIVE: The objective of this work is the development and validation of an anatomically realistic code, with high spatial resolution, capable of predicting transient tissue temperatures under given environmental conditions and RF exposure scenarios.

The thermal code is to exploit the simple structure of voxel-based descriptions to enable management of very large data sets associated with high-resolution models. Thermal loads from RF irradiation and the effects of physiological heat sources are to be included, as are environmental effects (ambient temperature, wind, and thermal radiation).

The code is to determine tissue temperatures resulting from exposure to 915 MHz fields – under a variety of orientations and power levels – under various blood flow scenarios: (i) zero blood flow, (ii) a basal flow rate, corresponding to blood flow in a resting, normothermic individual, and (iii) high blood flow, corresponding to maximal cardiac output and full vasodilation of the superficial vasculature.

METHODS: The model consists of (1) a raw file describing the "Brooks Man" head, with corresponding tissue properties (permittivity, thermal conductivity and diffusivity), and (2) a finite difference – time domain (FDTD) solver which predicts local specific absorption rate (SAR), and (3) a thermal code which solves a variation of the Pennes bio-heat equation [3] to determine tissue temperatures over time. Blood flow values are specified independently for each tissue type.

Within the thermal solver, spatial derivatives are discretized using second order finite difference expressions. The Crank-Nicholson scheme is applied for discretization in the time domain. The code utilizes the Message Passing Interface (MPI) to optionally run on multiple processors, allowing faster run-times with the larger data sets associated with high spatial resolution models.

The local SAR – as determined by the FDTD solver – is applied to each thermal node for a period of time set by the user. The primary thermal solver generates sets of three dimensional temperature files, of the same format as the SAR file, at specified simulation times.

RESULTS: The model has been used successfully to calculate tissue temperatures over time at a spatial resolution of 1 mm during simulated exposure at 915 MHz. Preliminary results show regions of maximal temperature increases are generally consistent with high SAR. Current efforts are devoted to parametric studies on the effects of blood flow and sensitivity of temperature calculations to variations in tissue thermal properties.

DISCUSSION: The zero blood flow case shows thermal patterns which are generally similar to the SAR patterns, suggesting thermal diffusion does not have a profound effect on tissue heating for those scenarios considered.

Future implementations of the thermal solver will incorporate full thermoregulatory feedback, including eccrine sweating and vasodilation of superficial tissues.

References.

CH Durney, H Massoudi, MF Iskander. Radiofrequency radiation dosimetry handbook, 4th ed. Brooks AFB, TX: USAF School of Aerospace Medicine, Aerospace Medical Division; 1986.

DA Nelson and SA Nunneley. Brain Temperature and Limits on Transcranial Cooling in Humans: Quantitative Modeling Results. *Eur J Appl Physiol Occup Physiol* 78:353-359; 1998.

HH Pennes. Analysis of tissue and arterial blood temperatures in the resting human forearm. *J Appl Physiol* 1:93-122; 1948.

This work was supported by the Small Business Innovation Research (SBIR) Program and administered through the Office of Naval Research (ONR). The Program Officer was CDR Stephen Ahlers of ONR and the Technical Monitor was John Ziriak of the Naval Health Research Center Detachment at Brooks Air Force Base.

Tutorial Session 1: HIGH-THROUGHPUT SCREENING
TECHNIQUES IN EMF RESEARCH
Chairs: Dariusz Leszczynski and Zheng-ping Xu

STUDENT

PROTEOMICS AND MASS SPECTROMETRY: TOOLS FOR GENOME-ERA BIOLOGY. T.J. Griffin. University of Minnesota, Department of Biochemistry, Molecular Biology and Biophysics, Minneapolis, Minnesota 55455, USA

The results generated from the Human Genome Project and other genome sequencing initiatives has revolutionized biology, catalyzing the emergence of new technologies that enable the systematic, quantitative analysis of genes and gene products. One of the most powerful of these emerging technologies has been the use of mass spectrometry to identify and also quantify expressed proteins in complex mixtures in a sensitive and rapid fashion. This technology has spawned the field of proteomics, with the stated goal of comprehensively characterizing protein products and their function. The combination of stable-isotope labeling of proteins and peptides, multidimensional separations, automated mass spectrometric analysis and automated sequence database searching has provided for a core methodology for large-scale identification and quantification of proteins contained in complex mixtures. This presentation will describe the state-of-the-art mass spectrometry-based technologies that have emerged to address a wide-array of biological problems that cut across the fields of biochemistry, molecular and cellular biology, and clinical research. Topics that will be discussed include:

- The analytical methodologies that collectively make up the current system for quantitative mass spectrometry-based proteomics
- The practical issues involved with using these methodologies, including experimental design and sample preparation
- The application of these tools to a wide-variety of biological problems, including large-scale analysis of protein expression, characterization of macromolecular complexes and interactions, and analysis of subcellular protein localization
- Future directions of the field

ANALYSIS OF GENE EXPRESSION IN EMF RESEARCH. C. Maercker, D. Remondini, R. Nylund, D. Leszczynski, K. Schlatterer, R. Fitzner, R. Tauber, S. Ivancsits, H. Rudiger, F. Bersani. RZPD German Resource Center For Genome Research. Heidelberg, Germany.

The method of whole-genome analyses on arrays have been established about six years ago and since then evolved to a promising standard procedure, which is applied in many laboratories all over the world. In the EU project REFLEX we wanted to find out together with eleven other groups, how far this technology fits into requirements for EMF research. One advantage of this high-throughput method is that it allows an unbiased view on the expression of all genes without pre-selection. Moreover, by analyzing the whole genome at the same time in a given cell by just one assay, gene-networks become visible. This is important, because e.g. heat shock genes can have many different functions, which are hard to discriminate by single gene assays like RT-PCR.

And indeed, the first results from in vitro studies on the Human Unigene RZPD-2 75k cDNA array are intriguing, because they show a new approach to the molecular effects of electromagnetic fields. ELF-EMF exposition of primary fibroblasts and a statistical analysis of the data gave indications for calcium signaling and other central pathways which might be involved in EMF effects. The increasing ribosome biogenesis in HL-60 leukemia cells after RF-EMF exposure was accompanied by expression of several heat shock

proteins. Therefore, heat shock genes might be involved, but the EMF response obviously is different from the heat shock response. A gene expression analysis of endothelial cells treated with RF-EMF revealed an regulation of cytoskeletal genes, and these results could be confirmed by protein data. However, the method also has its limitations. Different types of cells seem to behave very different after exposure to different fields. Therefore, we would need many repetitions of single experiments to get statistically significant data for all genes. Also RNA stability and post-translational modifications like phosphorylation of proteins cannot be investigated on the level of transcriptomics. This is the reason why we have started with pilot experiments on antibody chips. These arrays are able to specifically bind the different cellular proteins and are therefore a versatile tool for gene expression and phosphorylation studies. Although so far we only have preliminary data, we are convinced that these assays open a more detailed view on the proteome of a cell and are therefore a promising step towards functional genome analysis of EMF treated cells.

Our work is supported by the German Ministry of Science and Education (BMBF) and the Verum foundation.

PROTEIN MICROARRAY TECHNOLOGY – PRINCIPLES AND APPLICATIONS IN PROTEOMICS. D. Stoll, M.F. Templin, T.O. Joos. NMI Natural and Medical Sciences Institute at the University of Tuebingen, Markwiesenstr. 55, 72770 Reutlingen, Germany.

INTRODUCTION: DNA microarrays and sophisticated bioinformatics platforms allow scientists to take a global view into biological systems by generating mRNA expression profiles. The primary actors in biological systems depicting the overall cell status in the most direct way are proteins. Therefore methods that are able to display changes in the time or stimulus dependent expression at the protein level are valuable tools for the “discovery-science” since they are able to reveal biological effects on the molecular base.

In today's proteome era, the time is ready for protein microarrays to screen entire genomes for proteins that interact with particular factors, catalyse particular reactions, act as substrates for protein-modifying enzymes and/or as targets of immune responses. Therefore protein microarrays are useful tools for proteome analyses supplementing other technologies like e.g. 2DE-PAGE / mass spectrometry or liquid chromatography / mass spectrometry.

OBJECTIVES: The talk will give a brief introduction showing the advantages of microspot capture assays and the prerequisites to establish and perform such assays. The basic principles and application fields of planar microarray based systems and bead based flow cytometry approaches will be presented. Theoretical advantages, expectations and limitations of miniaturized multiplexed ligand binding assays will be discussed together with their huge potential for proteomic research and diagnostic purposes. Selected applications of protein microarray based assays will be presented.

2-DE/MS PROTEOMICS STUDIES – SOME PRACTICAL ASPECTS OF ANALYSIS. R. Nylund. Radiation and Nuclear Safety Authority, Helsinki, Finland.

Over the past years high-throughput screening techniques have become widely used in the several different research fields. Screening at the protein expression level is usually referred as proteomics. There are various ways to screen protein expression; one of the most common techniques is a combination of the two-dimensional gel electrophoresis (2DE) and mass spectrometry (MS). Proteins are separated by 2DE, usually by isoelectric point and molecular weight, and furthermore identified using MS. A building up a 2DE system for a specific application often requires optimization for enabling a generation of similar gels repeatedly. Repeatability is crucial for 2DE approach, since often several repeats are needed to be combined and compared against each others to obtain needed reliability. Therefore, the system needs to be

built up in such manner that the similar gels are reproduced and the combination of the gels is possible. The sample preparation is a key component for successful 2DE separation and the method may vary a lot depending on the sample nature. Finding a suitable focusing method, molecular weight separation method as well as a general sample loading amount requires also optimization. In total, the optimization of the system may take time from some weeks to months. However, after the system is on use, it is an efficient way to screen several proteins at the time and to get a general idea of the cellular level actions. Still during the analyses, it is needed also to remember the limitations of the technique. Typically staining method causes some limitations either in the detection sensitivity or in the linearity of the detection. Also protein separation from other proteins and the amount of protein is needed to be considered. 2DE pattern shows the general expression pattern, but the proteins itself are needed to be identified before finding the biological significance. This protein identification is usually done using MS. Several MS methods are used for protein identification, e.g. peptide fingerprinting and sequence tag analysis. The amount of protein has an influence on the method selection as well as on the reliability of the gained results. Common problems in MS studies are contaminants, which are in the sample, and also some non-natural protein modifications, e.g. caused by staining, may hinder the analysis. However, once in knowing hands, 2DE/MS methods provide a good overview of the general proteome appearance, in which unknown effects can be efficiently studied.

USE OF HIGH-THROUGHPUT SCREENING TECHNIQUES IN EMF RESEARCH. D. Leszczynski. Radiation and Nuclear Safety Authority, Helsinki, Finland.

In spite of years of research we are still facing an uncertainty whether low-energy EMF can induce any biological effects and whether such effects would be able to alter cell physiology and pose any risk of future health hazard. So far, the vast majority of research effort has been focused on the possibility of induction of cancer. However, the more and more of the available scientific evidence suggest that the risk of cancer induction by EMF might be either very low or even improbable. At the same time there continues discussion of whether EMF could induce some weak effects that, although would not induce any disease, however, they could induce effects detrimental to the quality of life causing such symptoms as sleep-disorders, headaches etc. The so far observed biological effects are uncertain as the biophysical mechanisms behind their occurrence are unknown. Thus far used research approach is too slow to determine all the possible effects of EMF.

The use of the high-throughput screening techniques (HTST) of proteomics and transcriptomics (“Discovery Science”) has been proposed as a useful approach to determine all possible biological targets of EMF on cellular level (Leszczynski et al. *Proteomics*, 4(2) 2004). However, there are certain limitations as well as advantages that need to be carefully considered:

- we have an uncertain effect – induction of biological response by EMF, and we have a new technology that has very many limitations and uncertainties of its own. Will the combination of the uncertainty of the biological effect and the uncertainty of the method, bring more uncertainty to the studies on biological effects of EMF? Or will it speed-up the discovery of new biological end-points? The answer is that, when cautiously used, the application of HTST offers a unique opportunity to rapidly determine which genes and proteins respond to EMF and then to focus all research resources on these known targets of EMF radiation.
- new telecommunication applications are continuously developing and new EMF frequencies and modulations will be continuously introduced. There is a need for a relatively simple screening test that would determine whether new EMF frequency or modulation will induce unpredicted/unexpected biological effects. Such rapid screening technique could be:
 - DNA chip/array with selected genes screening gene expression changes
 - protein array/chip with selected proteins – screening of protein expression changes
 - protein array/chip for screening of the changes in the activity of proteins (e.g. protein

phosphorylation)

→ the combination of the all above.

- how the data obtained with the use of HTST could help not only in finding biological effects of EMF but also in discovering of the biophysical mechanism behind the biological effects?

Therefore, we should consider:

- which of the presently available HTST are the most suitable for studying of the biological effects of EMF,
- is it possible to develop a standardized test for rapid screening of the future EMF frequencies in order to compare their effects with the effects of EMF frequencies being already in use? If the answer is yes, then:
 - what genes/proteins should be used for tests
 - how many different genes/proteins should be examined (not too many & not too few) should there be considered establishing a network of laboratories to perform standardized testing?

Reference

Leszczynski D, Nylund R, Joenväärä S, Reivinen J. (2004) Applicability of discovery science approach to determine biological effects of mobile phone radiation. *Proteomics*, 4 (issue #2, Feb. 2004), in press

ST-1

STUDY OF THE POTENTIAL LEUKEMOGENIC EFFECTS OF 50HZ MAGNETIC FIELDS AND THEIR HARMONICS IN A RAT LYMPHOBLASTIC LEUKEMIA. N. Bernard*¹, P. Chretien*², M-L. Tanguy*³, J. Lambrozo⁴, J-J Guillosson*¹, and J. Nafziger*¹. ¹Lab d'Hématologie Cellulaire et Moléculaire CNRS FRE 2444, Faculté de Pharmacie, 75006 Paris, France. ²Lab d'Immunologie – Hématologie, Hôpital Intercommunal, 94000 Créteil, France. ³Lab de Biostatistiques et informatique médicale GH Pitié-Salpêtrière, 750013 Paris France. ⁴ Service des Etudes Médicales, EDF-GDF, 75009 Paris, France.

INTRODUCTION: In 2002, IARC classified 50 Hz MFs as “possibly carcinogenic to humans”. Some epidemiologic studies have described a risk of leukemia for children living near power lines, whereas some have not. Because controversy persists, experimental animal models of leukemia are required to establish whether or not EMFs are potentially leukemogenic. We developed a rat model of chemically induced lymphoblastic leukemia, which is the most common leukemia among children. This leukemia model is the first one that permits to study the lymphoblastic leukemogenic process from the initiation to the progression. **OBJECTIVE:** We decided to expose our rat model to 50 Hz MFs and to their harmonics to examine their potential leukemogenic effects. Harmonics are EMF compounds that have never been studied in a large animal study before. We present here the final results of this experiment.

MATERIALS AND METHODS: Leukemia was chemically induced by N-butyl nitrosourea (BNU) at a dose of 6mg/day, 5days/week, for a period of 24 weeks in 3 month-old male WKAH/Hkm rats (SLC Inc Hamamatsu, Japan). 400 rats were divided in 5 groups: 1- BNU was administered to a 100 rats control group. 2- 100 rats were treated with BNU and exposed 18 hours a day to sinusoidal 50Hz MFs (100μT). 3- 100 rats were treated with BNU and exposed 18 hours a day to sinusoidal 50Hz MFs (100μT) with superimposed 3rd, 5th, and 7th harmonics. 4- a positive control group of 50 rats were treated with BNU plus PMA a promoting agent. 5- 50 cage-control had no treatment and no exposure. Sentinels were periodically analyzed during the entire process. The development of leukemia was followed by white blood cells counts, appearance of blasts in peripheral blood, and loss of body weight. Rats were sacrificed before death. Bone marrow cells were extracted. Bone marrow differential cell counts, cytochemistry and immunophenotyping were performed on cells to characterize the leukemia lineage.

RESULTS: 60% of leukemia were obtained in each group, 65% of those leukemia were B acute lymphoblastic leukemia. Survival time was 26 weeks which is long enough to follow leukemia development. The results showed no significant differences between the control group and the group exposed to 50 Hz MFs or to 50 Hz MFs plus harmonics, in terms of survival, total number of leukemia, and percentage of B cell ALL. No co-initiating or co-promoting effect of EMFs or harmonics could be detected in this experiment.

Electricité de France (EDF) and Réseau de Transport d'Electricité (RTE) have supported this work.

ST-2

THE PROTEIN EXPRESSION PROFILING OF MCF-7 CELLS INDUCED BY ELF MF EXPOSURE. Q.L. Zeng, H. Li*, D.Q. Lu*, H. Chiang, Z.P. Xu*. Bioelectromagnetics Laboratory, Zhejiang University School of Medicine, Hangzhou, Zhejiang, 310031 China.

BACKGROUND: Epidemiological studies have showed that ELF MF exposure could increase risk of breast cancer. Since then, a number of laboratory studies have been conducted in order to investigate how

ELF MF influenced mammary carcinogenesis and found ELF MF certainly exerted its effects on protein expression and / or function, however, some studies have failed to be replicated. The biological or health effects and mechanisms of ELF MF are still plausible. Obviously, focusing on the response of single gene or protein after EMF exposure in traditional research is limited for short of internal relation and difficult to describe the integrated effects of EMF exposure on biological system. Proteomics deals with the large-scale determination of genes and cellular function directly at the protein level at the same time. We are using this approach extensively to understand the biological effect of ELF MF exposure in order to discern rapidly any association between ELF MF and health hazards.

METHODS: Human breast cancer cells MCF-7 were exposed to 50 Hz 0.4 mT magnetic fields for 24 hr [1]. Whole cellular proteins were extracted and 200 μ g protein was subjected to 2-dimensional electrophoresis. 17 cm pH 3-10 linear IPG strips were selected in the first-dimension electrophoresis and the second-dimension electrophoresis were run in 12% uniform polyacrylamide gels. The silver stained images of the gel were analyzed with PDQuest analysis software 7.1. The results were analyzed on the overlay of nine repetition experiments. Some differentially expressed proteins were selected for identification using MALDI-TOF mass spectrometry.

RESULTS: There are approximately one thousand proteins detected using 2-D PAGE. Seven of them showed significant changes (at least 5-fold increase or decrease) after exposure to 0.4 mT MF for 24 hr. Thirty-three proteins disappeared and thirty-three proteins appeared in exposure group, comparing with sham-exposed group. Based on Mr and pI of all detected change spots, We searched the SWISS-PROT database and found that all of them fall in five categories: (a) cytosolic transport proteins; (b) regulators of certain protein phosphorylase; (c) ion channel (especially Ca^{2+} and K^{+}) proteins located on cell membrane and nuclear membrane; (d)-proteins associated with cancer genesis (p52K, and Zn-alpha 2-glycoprotein); (e) transcriptional coactivators.

Six proteins were identified. They were involved in cellular process, including connecting proteins of cytoskeleton, receptors of adenosine A2B, regulators of protein phosphorylase and cell cycle, proteins associated with cancer genesis. Other proteins are identifying by Tandem MS.

CONCLUSION: These data directly proved ELF MF exposure did alternate complex protein expression involved from signal transduction to cancer genesis. Further experiments using other cell biology methods are needed for validation.

Reference.

[1] Q.L.Zeng, H.Chiang, G.L.Hu, G.G.Mao, Y.T.Fu and D.Q.Lu. ELF magnetic fields induces internalization of Gap junction protein connexin 43 in Chinese hamster Lung cells. *Bioelectromagnetics*, 2003, 24(2):134-8

This research was supported by National Natural Science Foundation of China (No. 50137030, 30170792), Zhejiang Provincial Natural Science Foundation of China (No. 301524), Zhejiang Provincial Science and Technology key project of China(No. 021106135).

EM FIELD DETECTION IN A MYELINATED NERVE FIBER: A STOCHASTIC RESONANT BEHAVIOUR. M. Gianni*, F. Apollonio*, M. Liberti*, G. D'Inzeo. ICEmB at Department of Electronic Engineering, "La Sapienza" University of Rome, 00184 Rome, Italy.

OBJECTIVES: In this work the behaviour of a myelinated nerve fiber in the presence of an external electromagnetic (EM) field is investigated, in order to point out whether the main biophysical mechanisms that occur in the fiber are affected by extremely low frequency (ELF) fields. Stochastic resonance has been previously shown to occur in many non-linear systems including neuron models, where a noise-induced enhancement in the transduction of synaptic stimuli was observed [1]. Here an additive white gaussian noise is introduced in the fiber model to determine whether it exhibits stochastic resonance in the detection of an external EM field, which can be thought to be treated by the system as an input of the neuronal encoding process. The spatially distributed structure of the fiber also allows to study the field effect on action potential (AP) propagation.

METHODS: The spatial distribution of the nerve fiber is modelled following a multicompartimental approach [2], where every single compartment represents a node of Ranvier, described through an electric circuit constituted by a membrane capacitance and several ionic channels admittances modelled with both deterministic and stochastic dynamics. Axoplasmatic conductances between the nodes allow the action potential to propagate along the fiber with the typical features of the saltatory conduction. The fiber model structure is shown in Figure 1.

The model is set up to generate at the first node a 83 Hz self-supported firing [3], which then propagates along other 20 nodes of the fiber. White gaussian noise is added to the model as an input current, and an average over 100 realizations of noise seeds is made to obtain significant results.

According to previous studies [4, 5], EM field is introduced as a perturbation on the membrane voltage, with frequency in the range between 20 Hz and 120 Hz, far below the model corner frequency, calculated in 45kHz. The numerical solution is obtained approaching the large set of differential equations that represents the model through an adaptive step-size technique (Runge-Kutta).

RESULTS: At each node, when neither the field nor the noise are applied, the power spectrum of the membrane voltage shows a prominent peak at 83 Hz, related to the firing frequency. It was firstly pointed out that the introduction of the white noise determines a spreading of the power spectrum around 83 Hz, thus meaning that more variability is induced in the spikes time occurrences. Variance in the interspike interval (ISI) increases with noise amplitude as shown in Figure 2. Introducing the external field, a component at the field frequency appears in the output power spectrum, thus accounting for the information related to the field in the output spike sequence. Numerical simulations actually prove the existence of input noise intensities which optimize the output signal to noise ratio (SNR), which exhibits the typical shape of stochastic resonance (Figure 3). Field frequency and intensity where the system shows stochastic resonance are studied. Propagation of the spike sequence along the fiber is also considered, and results prove that propagation mechanism is robust over the introduction of both noise and external field.

CONCLUSIONS: Noise has already been shown to play a constructive role in neuronal sensory processing, but it is also important in the detection of an external EM field, which is enhanced for certain noise conditions, showing in a nerve fiber a stochastic resonant behaviour.

References

- [1] Liu F, Yu Y, Wang W : *Signal-to-noise ratio gain in neuronal systems*. Phys. Rev. E, Stat. Nonlin. Soft Matter Phys., May 2001; 63 (5 Pt 1):051912.
- [2] Mino H, Grill WM Jr : *Effects of stochastic sodium channels on extracellular excitation of myelinated nerve fibers*. IEEE Trans. Biomed. Eng., Jun 2002; 49 (6), pp. 527-32.
- [3] Koch C, Segev I : *Methods in Neuronal Modeling*, The MIT Press, Cambridge.
- [4] Tsong TY, Astumian RD : *Electroconformational coupling and the effects of static and dynamic EF on membrane transport*. Annu. Rev. Physiol. 1988; 80:1-56.

[5] Apollonio F, Liberti M, D'Inzeo G, Tarricone L : *Integrated models for the analysis of biological effects of EM fields used for mobile communications*. IEEE Transactions on Microwave Theory and Techniques, Nov 2000; 48 (11), pp. 2082-2093.

This work was supported by the European Union, V framework under the RAMP2001 Project.

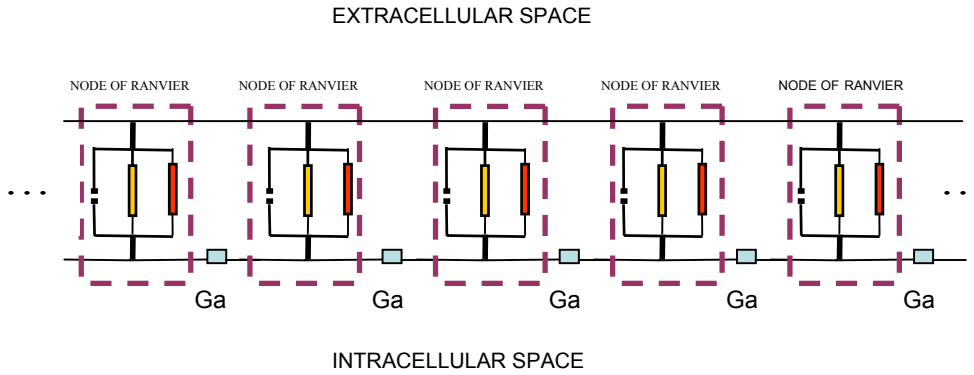


Figure 1. Sequence of compartments which represents the fiber model (multicompartmental approach).

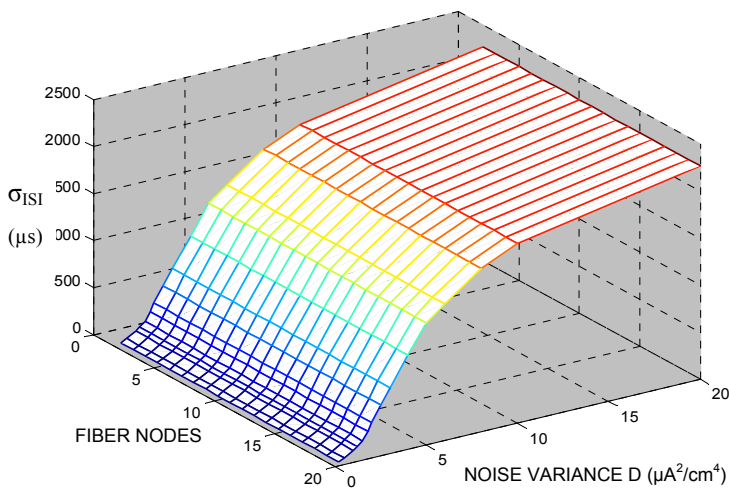


Figure 2. ISI standard deviation at the fiber nodes versus noise variance D: noise energy actually induces variability in the spike sequence.

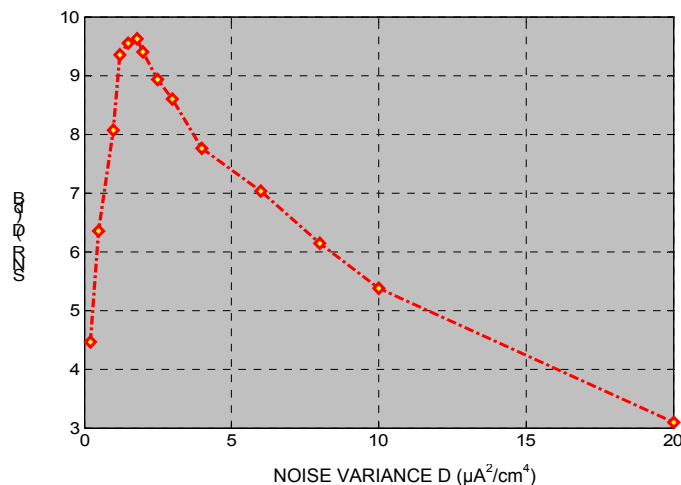


Figure 3.
Signal to noise ratio versus noise intensity in case of a 50 Hz external field with an induced membrane voltage of 250 μ V. SNR exhibits the typical shape of stochastic resonance, proving that there are noise intensities which enhance field detection.

ST-4

EGF RECEPTOR CLUSTERING AND RAS ACTIVATION WAS INDUCED BY 50Hz MF AND INHIBITED BY THE NOISE MF. W.J. Sun¹, H.Y. Fu², H. Chiang¹, Y.T. Fu¹ and D.Q. Lu¹.
¹Bioelectromagnetics Lab., ²First Affiliated Hospital, Zhejiang University School of Medicine, Hangzhou 310031, China.

OBJECTIVE: These are many evidences that ELF-MF exposure may activate signal transduction pathways. Our previous study also showed that 0.4 mT 50 Hz magnetic field (MF) could phosphorylate and activate the stress-activated protein kinase (SAPK) and P38 mitogen-activated protein (MAP) kinase (P38 MAPK) [1, 2]. However, the mechanism, especially the target site of MF interacting with cells, is still unclear. In the present study, we explored the effects of exposure cell to 50Hz MF on clustering of EGF receptors and the Ras activation, and investigated whether noise MF could interfere the effects caused by 50 Hz MF, as we found that the noise MF block the SAPK activation [3].

METHODS: Exposure System and Cell Treatment The uniform 50Hz sinusoidal MF was produced by three groups Helmholtz coils which located in the CO₂ incubator. The combined exposure system of 50 Hz sinusoidal and noise MF connects with different MF signals, one for 50 Hz sinusoidal MF and the other for noise signal. The noise signal was supplied by Litovitz Lab (USA). The MF signal was monitored with oscillograph. The cell in the experiment was divided into five groups: **a).** sham exposure, **b).** positive control (with EGF), **c).** 0.4mT 50 Hz MF exposure, **d).** 0.4mT noise MF exposure, and **e).** the combined MF exposure which 0.4 mT 50 Hz MF combined with 0.4 mT noise MF. CHL cells were cultured in RPMI-1640 medium at 37±0.5°C with 95% air and 5% CO₂. Before treated, all cells were cultured with serum-free medium for 12 hours. The positive control was treated with EGF for 15 min. Exposed cells were cultured in exposure system for various times with the same condition, and the MF was perpendicular to the dishes.

Confocal Microscope Analysis: Following different treatment, cells were rinsed, fixed, sealed, incubated with antibodies of receptors. Finally, the clustering of EGF receptors was analyzed with confocal microscope. Experiments were repeated more than three times.

Gst-RBD Expression: pGEX-2T plasmid which can express Gst-RBD (aa51-131 of Raf-1) fusion protein was cloned in BL21DE bacteria and induced with IPTG. The bacteria were sonicated on ice 6 times for 1 min. The lysate was aliquotted and stored at -80°C.

Ras Activation Measurement: Following different treatment, cells were lysed in RIPA buffer. The desired amount of crude Gst-RBD was thawed and incubated with glutathione-agarose beads at room temperature. The beads were isolated by centrifugation and washed three times with RIPA buffer. Gst-RBD, precoupled to glutathione-agarose beads in RIPA buffer, was added to cell lysates and incubated at 4°C. Beads were

collected by centrifugation, washed 3 times with RIPA buffer and resuspended in sample buffer. The protein samples were separated on a 12% SDS-polyacrylamide gel and subsequently transferred to NC membrane by Western blotting. Ras was detected using the corresponding antibody. The blot was developed with ECL.

RESULTS: The results of confocal microscope analysis showed that, like the EGF, 50 Hz MF at 0.4 mT obviously induced EGF receptors clustering after exposure for 5 min, while the noise MF with the same intensity didn't induce receptor clustering. When superposed of noise MF, the receptor clustering induced by 50Hz MF was inhibited. As the results of EGF receptors clustering, the Ras protein was activated by 50 Hz MF and inhibited by noise MF.

DISCUSSION and CONCLUSION: The receptor on the cell surface is one of important elements that receives the extracellular signals and transduces them into cells. Some ligands (such as EGF) binding to corresponding receptors induce the receptor clustering, and then activate the cellular signal transduction pathway. The results of the present study showed exposure to 0.4mT 50 Hz MF could induce the clustering of EGF receptors. It indicates that 50 Hz MF may interact with signal pathways normally used by growth factors. In order to investigate whether EGF receptor clustering induced by 50 Hz MF can transduce the biological signal into cell, Ras protein activation was serviced as biomarker. The result showed that 50 Hz MF also activated the Ras protein following the EGF receptor clustering. It suggests that the cellular membrane may be the initial sites for ELF-MF. ELF-MF may transfer and transduce its signal into cell via cell membrane receptor. However, the noise MF with the same intensity didn't induce the receptor clustering and Ras activation, and inhibited biological effects of the sinusoidal MF while combined with sinusoidal MF. Based on the present study, we concluded that the receptors on cell surface are the possible target sites that EMF acts on organism. We also confirmed the noise MF could interfere the biological effects of ELF-MF. But exactly how the 50 Hz MF lead to multimerization of cell surface receptor is not clear. Physical perturbation of the plasma membrane or a conformational change caused by 50 Hz MF may be the mechanism.

References:

1. W.J. Sun, H. Chiang, Y.D. Fu, Y.N. Yu, H.Y. Xie, and D.Q. Lu. Exposure to 50Hz Electromagnetic Fields Induces the Phosphorylation and activity of Stress-activated Protein kinase in Cultured Cells. *ELECTRO-AND MAGNETOBIOLOGY*, 2001, 20(3): 415-423.
2. W.J. Sun, Y.N. Yu, H.Chiang, Y.D. Fu, and D.Q. Lu. Exposure to Power-Frequency Magnetic Fields Can Induce Activation of P38 Mitogen-Activated Protein Kinase. *Chinese Journal of Industrial Hygiene and occupational Diseases*. 2002, 20(4): 252-255.
3. W.J. Sun, H.Chiang, Y.D. Fu, D.Q. Lu. and Z.P. Xu. Effects of Noise Magnetic Fields on the Enhancement of SAPK Phosphorylation Induced by 50 Hz Magnetic Fields. *Chinese Journal of Industrial Hygiene and occupational Diseases*. 2002, 20(4): 246-248

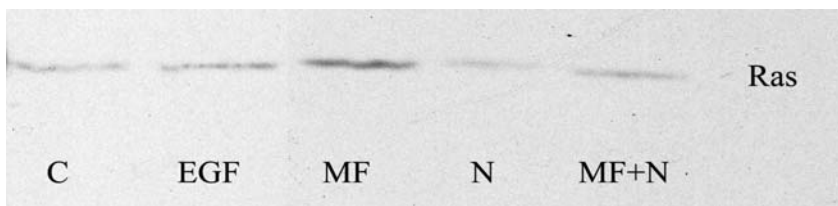


Fig.1. 50 Hz MF activated Ras protein. C, control; EGF, treated with EGF; MF, treated with 50Hz MF; N, treated with noise MF; MF+N, treated with combined MF

EVALUATION OF MICROWAVE FIELDS EFFECTS ON IONIC CHANNELS: AN EXPERIMENTAL STUDY WITH THE PATCH CLAMP TECHNIQUE. M. Pellegrino^{1*}, A. Paffi^{1*}, M. Liberti^{1*}, F. Apollonio^{1*}, G. D’Inzeo¹, M. Mazzanti^{2*}, ¹ ICEMB @ Department of Electronic Engineering, ² Dipartimento di Biologia Cellulare e dello Sviluppo, “La Sapienza”, University of Rome, 00184 Rome, Italy.

OBJECTIVES: At microscopic level, cellular membrane has been identified as the primary target of specific effects of electromagnetic (EM) fields on biological systems. Experimental studies [1] showed these effects on a particular class of proteins, the ionic channels, situated across the phospholipidic bilayer. The aim of this work is not only the analysis of possible interactions of this structure with the EM field, but also the achievement of a mathematical-theoretical model describing the channel’s behaviour and forecasting the experimental results. For this purpose, Markov process models seem to be possible candidate [2].

METHODS: We use the patch clamp technique to record single channel currents under microwave field exposure. In our experiments we employ dorsal root ganglion (DRG) cells of adult rat and embryonic chick ventricle cells. In order to obtain a controlled exposure, it has been realized an experimental set-up, which consists of the exposure [3] and the microwave signal generation [4] systems. The first one is a coplanar waveguide: it provides a well-known and uniform field, a simple accessibility to the exposed cells, a high efficiency in exposure and it is characterized by a very low interaction of the EM field with the electrodes of the patch clamp technique. The second one allows to select the frequency and power of a CW signal or simulate specific sources (i.e. modulated, GSM). In a first set of experimental recordings we exposed the cells to a CW at 900 MHz (SAR=2W/Kg). In this first approach a specific channel has been examined: the Sodium/Calcium cation channel; it is involved in neuronal cell behaviour [5]. The time domain data have been pre-elaborated also with a new version of a segmentation algorithm [6], which is more efficient than low pass filters to reduce only noise and not brief events.

RESULTS: First results show that the exposure to EM fields determines a decrease of channel’s open probability ($P_{\text{open}}(\text{PRE})=17\%$; Fig.1.a, $P_{\text{open}}(\text{EXP})=4.5\%$, Fig.1.b); this phenomenon is present after the exposure, too (POST in Tab. 1). Channel’s conductance, instead, is constant throughout the experiments and it is equal to 20 pS. With regard to dwell times, during the exposure we note a decrease of average open time and an increase of average closed time ($T_o(\text{PRE})=0.31$ ms; $T_o(\text{EXP})=0.22$ ms; $T_c(\text{PRE})=6.16$ ms; $T_c(\text{EXP})=18.12$ ms, Tab. 1); after the exposure, these values seem to go back to the initial ones (Tab. 1).

DISCUSSION: First single channel recordings on this channel underline a kind of effect on dwell times. In order to check these preliminary results and to complete our analysis we need other experimental traces. After data analysis and fitting of dwell time distributions, next step is the realization of a Markov model; in particular, we have to define number and type of states, and transition coefficients, which can be eventually modified with the simulation of the model. A new approach could be the use of “Hidden Markov Models” algorithms [7], by which model’s parameters can be directly calculated from the experimental recordings. These methods are characterized by a high computational intensity, but they are very efficient for obtaining good results even in presence of noisy data.

References.

- [1] G. D’Inzeo, P. Bernardi, F. Eusebi, F. Grassi, C. Tamburello, B.M. Zani, *Microwave effects on acetylcholine-induced channels in cultured chick myotubes*, Bioelectromagnetics, vol. 9, 1988, pp. 363-372.
- [2] *Single-Channel Recording*, edited by B. Sakmann and E. Neher, Plenum Press New York and London, 1995.
- [3] F. Duelli, M. Liberti, F. Apollonio, G. D’Inzeo, *Microwave exposure system for patch-clamp recording equipment*, EBEA 2003 Budapest, p.109.
- [4] S. Molfetta, F. Apollonio, M. Liberti, G. D’Inzeo, *Low cost exposure set-up for RF biological experiments*, Proc. of EBEA 2003 Budapest, p.132.

- [5] A. M. Swensen, B.P. Bean, *Ionic Mechanisms of Burst Firing in Dissociated Purkinje Neurons* Journal of Neuroscience, 2003, Oct 23 (29), pp. 9650-63.
- [6] A. Moghaddamjoo, *Automatic segmentation and classification of ionic-channel signals*, IEEE Trans. on Biomedical Engineering, vol. 38, 1991, pp. 149-155.
- [7] L. Venkataramanan, F. J. Sigworth, *Applying Hidden Markov Models Analysis of Single Ion Channel Activity*, Biophysical Journal, vol. 82, April 2002, pp. 1930-42.

This work was supported by European Union, V framework under the RAMP2001 Project.

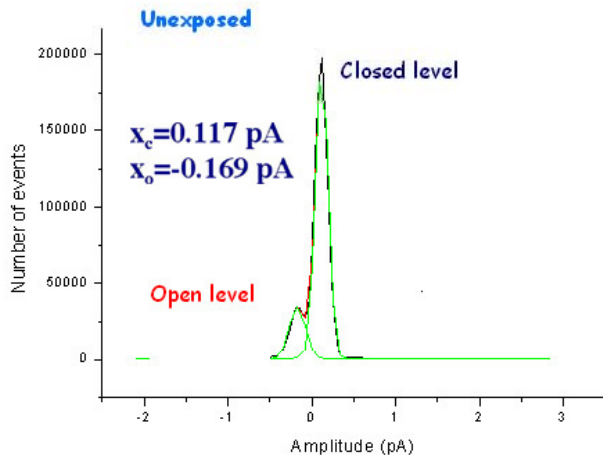


Figure 1.b. Na/Ca channel in DRG, exposed conditions, $f=900$ MHz, SAR= 2W/Kg, membrane potential= -10 mV, conductance \approx 20 pS, $P_{open}(EXP)=4.5\%$.

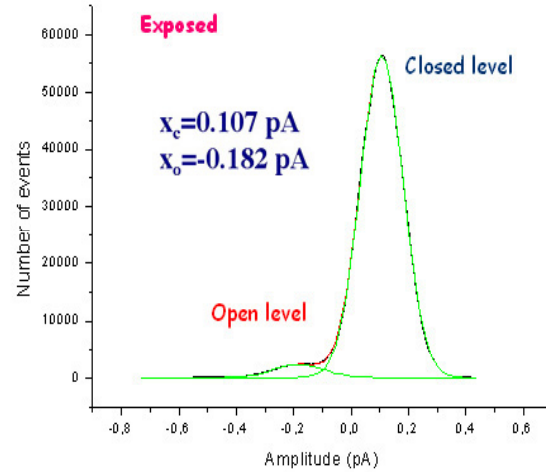


Figure 1.a. Na/Ca channel in DRG, unexposed conditions, membrane potential = -10 mV, conductance \approx 20 pS, $P_{open}(PRE)=17\%$.

Table 1

	Period	Bin width (ms)	A_1		t_1		A_2		t_2		R
			Mean value	Δ	Mean value	Δ	Mean value	Δ	Mean value	Δ	
T_c	PRE	0.5	1.2980	± 0.7030	6.1569	± 3.0300	62.734	± 3.560	0.6290	± 0.0374	0.91710
	EXP	0.5	38.8759	± 1.04626	18.1156	± 0.62753	—	—	—	—	0.90535
	POST	0.5	118.033	± 1.8615	10.9476	± 0.22801	—	—	—	—	0.97378
T_o	PRE	0.05	1102.95	± 51.3730	0.31476	± 0.00830	—	—	—	—	0.95382
	EXP	0.05	1802.77	± 58.2527	0.21581	± 0.00303	—	—	—	—	0.98771
	POST	0.05	3433.65	± 122.845	0.27296	± 0.00502	—	—	—	—	0.97988

Dwell times analysis of Na/Ca channel in PRE (unexposed), EXP (exposed at $f=900$ MHz, SAR=2 W/Kg) and POST (unexposed) conditions. The table contains the amplitude and the time constant (mean value and standard deviation) of decreasing exponential curves used to fit open time and closed time histograms [3].

THE STUDY ON HYPOTHALAMUS CELLS EXPOSED TO EMP. X. Cao¹, M. Zhao², D. Wang³.
¹Dept of Pathology, Lanzhou General Hospital, Lanzhou 730050, Gansu province, China; ²NIEHS/NIH, BIDG 101, MD F2-04, Res. Triangle Park, NC 27709, ³Beijing Inst of Radiation Medicine, Beijing 100850, China.²

The previous studies indicated that the internal secretion system is one of the most sensitive organs to EMP. To investigate the injury mechanisms on the cell and even on molecular level, the primary culture cells used are not only trying to get rid of the effects from complex factors, but also could focus on one kind of cells. The dynamic changes of the primary culture hypothalamus cells before and following EMP irradiating were observed, the aim is to explore the possible injury mechanisms of hypothalamus.

MATERIALS: MTT, PI, 5-DS(5-doxyyl-stearic acid)and CTPO (3-carbamoyl-2,2,5,5-tetramethyl-3-pyrroline-1-yloxy) and RNase were purchased from Sigma Co., DMEM, HS and FCS were purchased from Gibco Co., 6-well plates and 96-well plates were purchased from Costar Co.. LDH, AST, CHE, K⁺ Na⁺ test kits were from Beijing Zhongsheng Bio-technique Company. The electromagnetic pulse (EMP) simulator, which provides with electric field intensity 2×10^3 - 15×10^4 V/m, 20-ns rise time and 25-30 μ s pulse wide, was set up in the Beijing Institute of Radiation Medicine. BIO-RAD Model 550 Enzyme-link Immuno-test machine was purchased from Japanese BIO-RAD Co.. Bruker-ESP300 Electron Spin resonance (ESR) was purchased from German. BPCL-4 type, Ultra-Weak Chemiluminescence Analyzer (UWCA) was from Biophysical Institute of Chinese Science Academy. FACSCalibur Flow cytometer was from B-D Co. (USA). Radiance-2100 type laser scanning con-focal microscopy was purchased from American BIO-RAD Co., SPM-9500J3 type atom force microscopy (AFM) was from Japan (SHIMADZU, Japan).

METHODS: Wistar postnatal rats (within 24 hrs) are obtained from animal center, Beijing Institute of Radiation Medicine (China). The culture medium DMEM (Gibco) contains 10% fetal calf serum (heat inactivated), 100 unit/ml penicillin and 100 μ g/ml streptomycin.

The postnatal rats (within 24 hrs) were killed with aseptic manipulation. Separated the brain and meninges, take out the hypothalamus. Cut the hypothalamus into pieces in the iced PBS (0.01mol/L, 4°C). Digested the tissue by trypsin (0.25% w/v, in Ca²⁺ and Mg²⁺-free phosphate buffered saline, D-Hank's. pH7.2) at 37°C for 20min. The neurons were rinsed with culture medium DMEM (Gibco) contains 10% fetal calf serum and 10% horse serum (heat inactivated), suspended in PBS about 5×10^5 cell/ml. Seed the suspended cells into culture flask and 96-culture well with 6ml and 100 μ l/well separately. The cells were regularly cultured at 37°C in atmosphere containing 5% CO₂, 95% air and with a relative humidity of 98%.

MTT Measurements Cells were seeded in six 96-well culture plates at 10^4 cells/per well in 0.2 ml growth medium and incubated at 37°C for 24hrs, 1-6 columns were covered with double-layers tinfoil as control columns, then performed MTT stain at different time (0hr, 1hr, 6hr, 12hr, 24hr, 48hr) with BIO-ROD550 following exposing.

Examination of cell membrane fluidity Divided the collecting 2×10^7 cells into control and irradiating groups. The primary cultured cells spin labeled with 5-doxyyl stearic acids (5-DS), and irradiated by electromagnetic pulse (EMP) simulator for two minutes. By measuring the order parameter (S) and correlation time (tau) to examine the changes induced by EMP Following irradiating, Spin-label electron spin resonance (ESR) spectroscopy technique has been used to investigate the membrane fluidity changes of the cells. The test conditions: room temperature, CF=3470 Gs, SW=200 Gs, MF=25 kHz, MA=84S, P=10 MW.

Examination of the rate of consume oxygen Divided the collecting 2×10^7 cells into control and irradiating groups. Following irradiation, put the CTPO 50 μ l, 10mmol/L pyruvic acid 50 μ l, 10mmol/L α -ketoglutarate 50 μ l into 250 μ l PBS (pH7.4) and mixed them well, then transferred into quartz capillary in the sample chamber for ESR test. Test conditions: CF=3470 Gs, SW=1mT, MF=0.005mT, MA=0.128s, P=1 mW.

Ultra-Weak Chemiluminescence Analyzer (UWCA) was used to analyze the cells in the culture dishes.

Flow cytometer examination Cells were trypsinized and suspended in PBS about 10^6 cell/ml, washed with iced cold PBS and injected into cold (-20°C) 70% ethanol, which was kept overnight at 4°C . Cells were rinsed with PBS and stained with $50\mu\text{g/ml}$ PI PBS solution containing 0.1% triton-100, 0.1mM EDTA and 100U/ml RNase, incubated in the dark at room temperature for 30 minutes, then wash out PI with PBS, determined on flow cytometer (Facsclibure, Becton-Dickison, San Jose, CA) within 1 hour. All data were collected, stored and analyzed by Cellquest version 1.1.2 software (B-D).

The intracellular calcium examination Cells in the culture dishes were rinsed with PBS twice, added $10\mu\text{g/ml}$ fluo-3 probe 1ml, incubated in 37°C for 30 min, following irradiating, rinsed three times, and then tested by laser scanning con-focal microscopy, all data were analyzed by Laserssharp 4.0 software.

AFM examination. The cells were seeded on the 6-well plates with 4 coverslips each well and incubated at 37°C for the growing cells covered about 50% area of one coverslip. Following irradiation, the coverslips were fixed with 4% glutaraldehyde, then stick it on the sample stage, control the scan by SPM-online 2.45, data was analyzed by SPM-offline 2.2 software.

RESULTS: The effect of EMP on cells' activity The A_{570} value of MTT decreased immediately at 0hr, 1hr, 6hr following the cells being exposed, comparing with control ($P<0.01$). And recovery to the control level at 12 hr. (Fig.1)

The membrane fluidity changes induced by EMP The experimental results show that EMP can induce significant effects on the order parameter(S), correlation time (τ_c) of 5-DS spin label. The both values of S and τ_c are significant decreased which can be inferred that the membrane fluidity is increased. Following irradiation, The S value of EMP group is 0.6605, τ_c value is 3.0062×10^{-9} s, in control group the S value is 0.6782, τ_c is 5.6277×10^{-9} s. (Fig. 2)

Effect on the rate of consume oxygen in hypothalamus cells Fig. 3 is the control cells' ESR spectrum, showed that the rate of consume oxygen increased gradually. Fig.4 is the irradiated cells' ESR spectrum, the rate of consume oxygen increased greatly. Fig.5 is the K value chart showed the K value were increased compare with control groups.

Effect on the Ultra-Weak Chemiluminescence of hypothalamus exposed to EMP. Ultra-Weak Chemiluminescence Analyzer (UWCA) was used to analyze the cells in the culture dishes. The results showed that Ultra-Weak luminescence was inhibited, the light strength decreased from 4408 (control) to 2934. Fig.6-7

Apoptosis rate assay. The apoptosis ratio was determined by flow cytometer following exposure to EMP (Fig. 8 and Fig. 9). The highest ratio was 15.83% at 6 hr ($P<0.01$), then decreased gradually. Recovery at 12 hr.

The intracellular calcium concentration changes Fig. 10 showed that EMP exposure can affect the intracellular calcium concentration. Decreased to 30.64% comparing with control.

The membrane surface observed by SPM-9500J3 type atom force microscopy All data are showed in Fig.11-12. The results showed that membrane perforate with different size and shape ($273.21\text{nm} \times 330.10\text{nm} \times 13.57\text{nm}$).

CONCLUSION: EMP exposure could induce hypothalamus cells apoptosis, increase the membrane fluidity and the rate of consume oxygen, at same time decrease the oxidation metabolizing and chemical react rate. Also EMP could make calcium out the cell, infer that the membrane permeability is increased or perforated. AFM verified that EMP could induce cell membrane perforation directly.

[contact author for figures]

ST-7

AN EXTREMELY LOW FREQUENCY MAGNETIC FIELD ATTENUATES INSULIN SECRETION FROM THE INSULINOMA CELL LINE, RIN-m. T. Sakurai*, Y. Takashima*, S. Koyama*, and J. Miyakoshi. Department of Radiological Technology, School of Health Sciences, Faculty of Medical, Hirosaki University, Hirosaki, 035-8564, Japan.

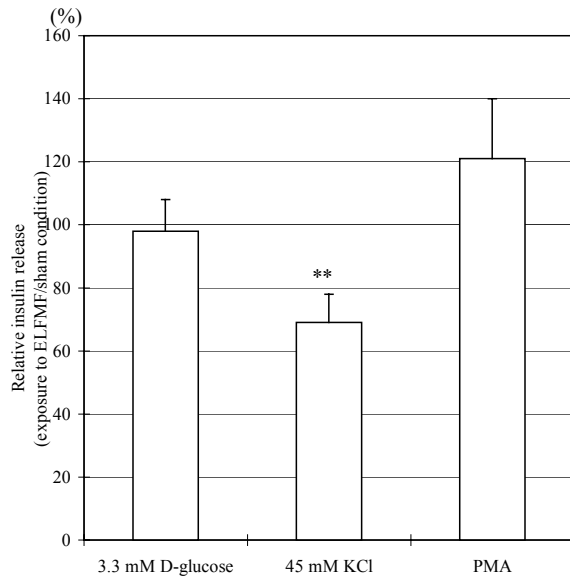
INTRODUCTION: Recently, human exposure to an extremely low frequency magnetic field (ELFMF) from various electrical appliances has increased significantly. Thus, the possible health effects of exposure to ELFMF have become a considerable public concern. On the other hand, occurrence of diabetes mellitus has increased progressively in recent years. Insufficient pancreatic islet function is the basis of various forms of diabetes. These two factors motivated us to investigate the effects of exposure to ELFMF on the function of insulin secreting cells.

OBJECTIVES: The objective of this study was to evaluate the effects of ELFMF on the function of insulin secreting cells.

METHODS: We stimulated RIN-m, an islet-derived insulinoma cell line, to secrete insulin under exposure to an ELFMF or under sham-exposure conditions for 1 h, and observed the effects using our established system for the exposure of cultured cells to an ELFMF (a sinusoidal vertical magnetic field at a frequency of 60 Hz and a magnetic density of 5 mT).

RESULTS: In the presence of a depolarizing concentration of potassium (45 mM KCl), exposure to ELFMF significantly attenuated insulin release from RIN-m cells, compared to sham-exposed cells (Figure 1). Treatment with nifedipine reduced the difference in insulin secretion between cells exposed to an ELFMF and sham-exposed cells. The expression of mRNA encoding synaptosomal associated protein of 25 kDa (SNAP-25) and synaptotagmin 1, which play a role in exocytosis in hormone secretion and influx of calcium ions, decreased with exposure to an ELFMF in the presence of 45 mM KCl. These results suggest that exposure to ELFMF attenuates insulin secretion from RIN-m cells by affecting calcium influx through calcium channels.

Figure 1. Insulin release from RIN-m cells under exposure to an extremely low frequency magnetic field (ELFMF) or under sham conditions. Insulin release was measured after 1 h incubation with 3.3 mM D-glucose, or 3.3 mM D-glucose plus 45 mM KCl, or 3.3 mM D-glucose plus 1 μ M phorbol-12-myristate-13-acetate (PMA). Data represent the mean \pm SE (3.3 mM D-glucose, n = 3; 45 mM KCl and PMA, n=5). The relative insulin release is expressed as the ratio of the insulin release under exposure to an ELFMF to under sham conditions. ** p < 0.01.



This study was supported in part by a Grant-in-Aid from the Research for the Future Program, Japan Society for the Promotion of Science.

ST-8

MODULATION-DEPENDENT EFFECT OF MICROWAVES ON PROTEIN EXPRESSION IN HUMAN ENDOTHELIAL CELL LINE EA.hy926. R. Nylund¹, T. Griffin^{2*}, C. Maercker³, J. Schuderer⁴, J. Reivinen^{1*}, N. Kuster⁴, R. Aebersold^{5*}, D. Leszczynski¹. ¹STUK – Radiation and Nuclear Safety Authority, 00880 Helsinki, Finland, ²Dept. of Biochemistry, Molecular Biology and Biophysics, Univ of Minnesota, Minneapolis, MN, USA, ³RZPD German Resource Center for Genome Research, Heidelberg, Germany, ⁴ETHZ, Zurich, Switzerland, ⁵Institute of Systems Biology, Seattle, WA, USA.

The aim of the study was to determine whether modulation of microwave radiation (RF-EMF, 1800 GSM signal) might induce different response in cells as compared with continuous wave (CW)-signal.

Semi-confluent cultures of human endothelial cell line EA.hy926 were exposed for 1 hour at 37 \pm 0.1 $^{\circ}$ C either to RF-modulated microwaves (RF-EMF; 1800 GSM mobile phone “talk”-signal of Kuster’s exposure system) or to continuous wave EMF (“CW”-signal of Kuster’s exposure system) at SAR of 2W/kg. Proteins were extracted from the cells immediately after the exposure and analyzed using cICAT method (peptides labelled with ligand containing C¹³ isotope) combined with liquid-phase chromatography and mass spectrometry. The used here method (cICAT) has an advantage over the 2-dimensional electrophoresis separation of proteins as it eliminates potential protein spot matching between two analysed samples and thus greatly increasing the accuracy of the result.

In total, 58 unique proteins (out of ca.1476 proteins present in the lysates) had increased expression but only in RF-exposed cells and not in the CW-exposed cells. These differentially expressed proteins were selected for identification by MS/MS analysis based upon the criteria that the measured abundance ratios (C¹³(0)/C¹³(9)) were either >1.7 or <0.60. The average abundance ratio for all detected cICAT reagent

labelled peptide pairs (n=1476) was 1.26 +/-0.38, indicating that the vast majority of the proteins within the two samples did not change in abundance. Several of the differentially expressed proteins were components of cytoskeleton (e.g. actin-like protein 2, cofilin, destrin, filamin A, myosin heavy chain, tubulin beta-2 chain).

Interestingly a number of the same proteins/genes came up using other analytical methods. Using cDNA expression arrays we have determined that also the expression of genes encoding various cytoskeletal proteins has been affected by RF-EMF exposure. Western blot analyses of the expression level of some cytoskeletal proteins (e.g. vimentin) have shown that RF-EMF exposure increases not only their expression level but also causes appearance of isoforms with altered molecular weight.

The obtained data confirm and support our previously published data showing the effect of RF-EMF on the organization of cytoskeleton and on the cell size and shape (Leszczynski et al., *Differentiation*, 70, 2002, 120-129; Leszczynski et al. *Proteomics*, 4 (2), 2004, in press). Thus, they confirm and provide further evidence for our hypothesis suggesting cytoskeletal effect of RF-EMF exposure, which hypothesis we have presented in the above mentioned publications.

In conclusion, our data suggest that RF-EMF exposure has an effect on cytoskeleton (expression of cytoskeletal proteins and structural organization of cytoskeleton). Furthermore, we suggest that the modulation of the microwave radiation might be the cause of the observed biological response. The notion that the modulation might be of importance for the induction of biological response might be of help for the determination of the still unknown biophysical mechanism behind the non-thermal effects of RF-EMF exposure.

ST-9

EFFECT OF PULSING ELECTROMAGNETIC FIELD STIMULATION ON OSTEOBLASTS AND HUMAN BONE MARROW DERIVED OSTEOCLASTS. C. Button*, B.S. Margulies*, J.A. Spadaro, T.A. Damron*, M.J. Allen*. Dept of Orthopedic Surgery, SUNY Upstate Medical Univ, Syracuse, NY 13210 USA.

INTRODUCTION: Pulsing electromagnetic fields (PEMF) have been used therapeutically to stimulate repair in fractures and fracture non-unions. PEMF has been shown to have positive effects on bone by stimulating either osteoblast proliferation or modulating osteoclastic resorption [1,2,3]. The effects on osteoblast proliferation by PEMF are significant for two reasons. First, changes in osteoblast proliferation impacts the number of bone cells available to make bone. Second, osteoblastic precursors are involved in osteoclastogenesis and changes in differentiation would affect the recruitment and formation of osteoclasts. Most observations previously have been made in confluent bone cell cultures where the cells would be slowing proliferation and increasing differentiation. The effect on actively dividing, pre-confluent osteoblasts, however, is not yet clearly understood.

OBJECTIVE: The objective of this work was to investigate the effect of PEMF treatment on osteoblast proliferation and differentiation in low-density cultures and on osteoclast formation in osteoblast/pre-osteoclast co-cultures.

METHODS: MC3T3-E1 mouse osteoblast-like cells were seeded at 1×10^3 cells/well in 4 well chamber slides to observe proliferation changes and 1×10^4 cells/well in 12 well plates to study changes in alkaline phosphatase (ALP) and caspase-3. Proliferation changes were measured using Cavalieri sampling and BrdU labeling. In the co-culture experiments, MC3 osteoblasts were seeded at 1×10^4 cells/well in 12 well plates 24 hours prior to the addition of 1×10^6 cells/well of primary human monocytes. The resultant monocyte derived multi-nucleate osteoclasts were counted using TRAP staining (Sigma). 1.5 Hz or 15 Hz PEMF or sham control stimulation was applied for 30 minutes a day at 37°C for the MC3 cells alone for 4 consecutive days while MC3/monocyte co-cultures were stimulated for 15 days (the approximate time needed for osteoclast formation to occur). The PEMF waveforms were similar to those used clinically and

composed respectively of short, asymmetric magnetic pulses repeated at 1.5 and 15 Hz, with peak amplitudes of 0.05 and 2 mT, and peak induced EMF bursts of 20 and 100 mV in an 8 mm 50 turn pick-up coil [4,5].

In a follow-on experiment, MC3T3 cells were seeded in 6-well plates at a low density, 1×10^4 cells/well, and also at a high density (confluency), 1×10^5 cells/well. Low density cells were allowed to grow for 24 hours and high density cells were grown for 5 days before their PEMF treatment. Each were treated with a single 30 minute PEMF stimulation. RANKL, OPG and ALP mRNA expression was measured by RT-PCR 24 hours later.

RESULTS: PEMF treatment for 4 days (30 minutes daily) decreased the number of MC3 cells by 26% and 25% in the 1.5 Hz and 15 Hz groups compared to the control (Fig 1). The percentage of BrdU labeled cells also decreased in the 1.5 Hz and 15 Hz groups compared to the control (Fig 2). However, PEMF treatment increased caspase-3 activity, by 25% and 38%, (Fig 3) as well as ALP activity, by 22% and 32%, (Fig 4) in the 1.5 Hz and 15 Hz groups compared to the control group. PEMF treatment of osteoclast cells for 15 days (30 minutes daily) decreased cell number by 19% and 39% in the 1.5 Hz and the 15 Hz groups compared to the control (Fig 5). RT-PCR did not detect mRNA expression of RANKL or ALP in the low density cells but showed mRNA expression of OPG which was increased in the 1.5 Hz and 15 Hz groups compared to control. In high density cells, mRNA expression of RANKL was not detected but mRNA expression of ALP and OPG was shown to increase in the 1.5 Hz and 15 Hz groups compared to the control.

CONCLUSIONS: These findings suggest that PEMF treatment inhibits proliferation of osteoblasts and induction of osteoclasts when cultured at low cell densities, in which the cells are actively dividing. In addition, the increase in ALP and caspase-3 suggest that there is an increase in osteoblast differentiation and an increase in apoptosis. RT-PCR results seem to confirm these findings by showing an increase in OPG expression in the low density group and with an increase in ALP and OPG expression in the high density group which also suggest an increase in osteoblast differentiation. These results appear opposite to what has been observed in confluent bone cell cultures.

References.

- [1] Brighton et al. (2001) J Bone Joint Surg Am 83-A:1514-24
- [2] Shankar et al. (1998) J Cell Physiol 176:537-44
- [3] Spadaro et al. (2002) Calcif Tissue Int 70:496-502
- [4] Pienkowski et al. (1992) J Orthop Res 10(2): 247-55
- [5] Zborowski et al. (2003) Ann Biomed Eng 31(2):195-206

This work was supported by the Department of Orthopedic Surgery at SUNY Upstate Medical University.

Osteoblast Cell Number

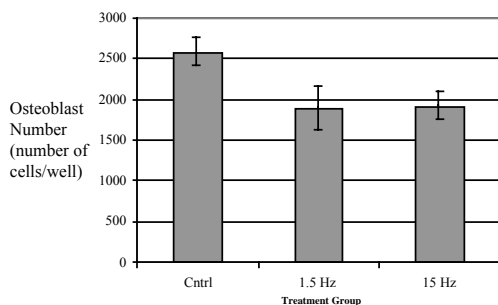


Figure 1. After 4 days of treatment (30 min daily), the number of MC3 cells decreased by 26% with 1.5 Hz and 25% with 15 Hz

Osteoclast Cell Number

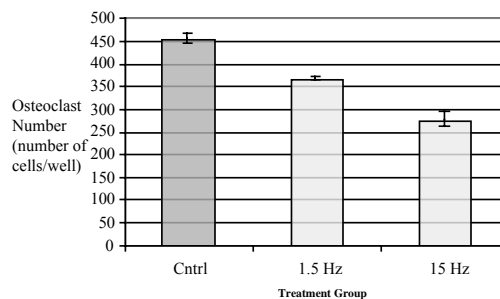


Figure 5. In co-cultures, after 15 days of treatment (30 min daily), the number of osteoclast cells decreased by 19% with 1.5 Hz and 39% with 15 Hz

Alkaline Phosphatase Expression

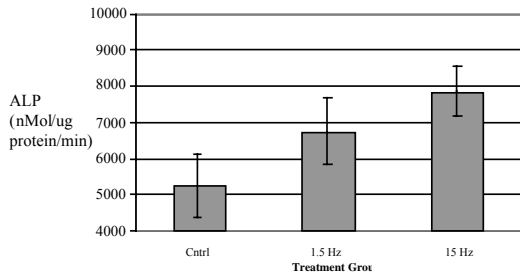


Figure 4. After 4 days of treatment (30 min daily), alkaline phosphatase activity increased by 22% with 1.5 Hz and 32% with 15 Hz

Osteoblast Proliferation BrdU Labeling

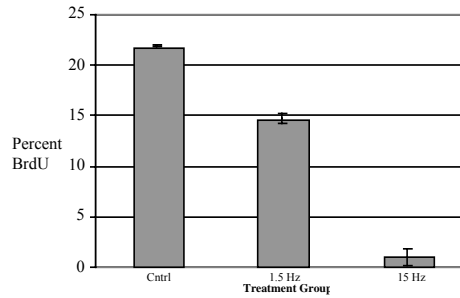


Figure 2. After 4 days of treatment (30 min daily), the percent of BrdU positive MC3 cells decreased compared to the control with only 14.10% in 1.5 Hz and 0.89% in 15 Hz groups

Caspase-3 Expression

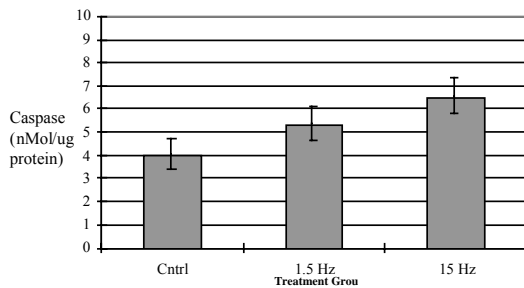


Figure 3. After 4 days of treatment (30 min daily), caspase-3 activity increased by 25% with 1.5 Hz and 38% with 15 Hz

ST-10

INSTRUMENTATION FOR ACCURATE MEASUREMENT OF NON-HOMOGENEOUS FIELD DISTRIBUTIONS. W. Oesch, N. Nikoloski, A. Kramer, N. Kuster. Foundation for Research on Information Technologies in Society (IT²IS), Swiss Federal Inst of Tech (ETH), Zurich, CH-8092 Zurich, Switzerland.

INTRODUCTION: In recent years the increasing number of GSM mobile phone base stations has resulted in public concern about potential adverse health effects due to electromagnetic radiation exposure. Measurements in apartments and offices have been increasingly requested by the public and community authorities. Most of the laboratories conducting such measurements use conventional antennas, which are calibrated under laboratory conditions, whereas the non-homogeneity of the field distribution in the apartments or offices is not known, nor is it known how the non-homogeneity should be weighted in the evaluation. Consequently, the measurement uncertainty of these evaluations can only be estimated and is subject to considerable controversy.

OBJECTIVES: The objective of this study is the design and development of a minimally disturbing measurement setup for the reliable, accurate measurement of non-homogeneous field distributions with high spatial resolution. The results will provide the scientific basis for the development of procedures for the assessment of exposure from base station radiation. Resulting measurement recommendations with minimized uncertainty will be transferred to standardization bodies.

METHODS: The minimally disturbing measurement concept employs miniature isotropic field probes with an integration volume of $< 0.1 \text{ cm}^3$. Combined with a motor-controlled high precision setup, these probes allow 3D scanning of fields with unique high spatial resolution. By using mainly dielectric materials

for the setup and by fiber-optic transmission of the electro-optically converted signal from the probe to the remote read out station, minimum disturbance of the measured fields is achieved.

The field data of an array of 8 probes is simultaneously acquired (with EASY4 from SPEAG, Switzerland) and saved in a format that it is importable in SEMCAD (SPEAG, Switzerland). This allows straightforward visualization and comparison with data from numerically evaluated scenarios.

RESULTS: We report on the design of a semi-automated measurement tower for 3D high-resolution mapping of inhomogeneous field distributions in a test room. It consists of two horizontal platforms, separated by one meter in height. Four miniaturized isotropic field probes (SPEAG, Switzerland) are fixed on each of the platforms. They can be lifted up by one meter, guaranteeing a total accessible height for the field measurement of $24 \text{ cm} < z < 200 \text{ cm}$. The vertical positioning is computer-controlled, while the horizontal (x,y)-positioning will be done manually moving the tower on a rail-guided system along the floor. The construction is designed to guarantee a positioning accuracy of the field probes of within a few millimeters. The measurement points lie on a 3D grid with 5 cm mesh distance ($\approx \lambda/6$ for 900 MHz). The project is being funded by the Swiss Research Foundation on Mobile Communication (Zurich, Switzerland) and TDC Switzerland AG.

ST-11

DEVELOPMENT OF MEASUREMENT PROCEDURE FOR COMPLIANCE TESTING OF WIRELESS DEVICES AT HIGHER FREQUENCIES (5 – 6 GHz). N. Nikoloski¹, A. Christ^{*1}, K. Schmid², D. Pokovic^{*2}, N. Kuster¹ ¹Foundation for Research on Information Technologies in Society (IT²IS), Swiss Federal Inst of Tech (ETH), Zurich, CH-8092 Zurich, Switzerland. ²SPEAG, Switzerland.

INTRODUCTION: Due to the rapid development of wireless technologies, new frequency bands in the microwave region operating at higher frequencies up to 6GHz have been opened up. Currently, these frequencies are mainly used for wireless local networks, but their range of application extends to health support systems or consumer electronics in general. Since these devices may operate in the immediate vicinity of the human body, it is required that they be tested for compliance with safety standards for electromagnetic radiation. Current compliance testing protocols only support a frequency range of up to 3GHz. Due to the strong field gradients at frequencies between 5 and 6GHz, these protocols cannot be applied directly, and the development of improved technologies and methods has become necessary. They must assert high accuracy and spatial resolution as well as fast SAR evaluation.

OBJECTIVES: The objective of this study was the development of new measurement procedures for the compliance testing of wireless devices with current safety limits for the frequency range between 5 and 6 GHz. This included the development of:

- head and body tissue simulating liquids for worst-case SAR assessment
- miniature E-field probes with increased spatial resolution
- an efficient SAR scanning procedure using a cube with a graded z-axis

METHODS: Dielectric parameters for head and body tissue simulating liquids were derived considering tissue layer distributions of different regions of the head and body. The thicknesses of the layers were varied in order to find the maximum absorption [1]. Tissue simulating liquid parameters were then chosen such that the worst-case SAR is reached in the phantom. Because of the strong field gradients, the reduced skin depth and the reduced transmitter dimensions, smaller probes are necessary to enable measurements closer to the phantom boundary and with higher spatial resolution. In order to determine the required resolution of the measurement grid, the SAR test functions defined in [2] were modified according to the high field gradients. Peak SAR, 1g and 10g average SAR were evaluated on different measurement grids with respect to interpolation and extrapolation accuracy as well as sensitivity to noise. The offset from the phantom boundary should not exceed 1.5mm. Furthermore, the necessary grid resolution of 3mm would

lead to more than 1000 points if applied on a measurement volume of $3 \times 3 \times 3 \text{ cm}^3$. Therefore, a fine mesh step is used only close to the phantom surface, and the step size is gradually increased when the probe is moved up. The results were carefully validated using the near-field scanner DASY4 equipped with the novel miniature E-field probes with increased spatial resolution which were developed within the study.

RESULTS: The worst-case tissue composition was evaluated for frequencies between 5 and 6GHz. Dielectric parameters could be determined for head and body tissue simulating liquids and corresponding recipes could be derived. The new high resolution probe has a tip diameter of 2.5mm and distance from probe tip to dipole sensors of 1mm. It can be operated at the required distance of 1.5mm from the phantom surface. The measurements on the different grids showed that the number of points can be limited by increasing the grid step in the z-direction without a negative impact on the accuracy.

References:

[1] Antonios Drossos, Veli Santomaa, and Niels Kuster, "The Dependence of Electromagnetic Energy Absorption upon Human Head Tissue Composition in the Frequency Range of 300-3000MHz", IEEE Transactions on Microwave Theory and Techniques, vol. 48, no. 11, pp. 1988-1995, November 2000.

[2] IEC 62209 "Procedure to measure the Specific Absorption Rate (SAR) for hand-held mobile wireless devices in the frequency range of 300 MHz to 3GHz", 2003.

Mobile Manufacturers Forum (B), MTT (J), SPEAG (CH), EUREKA SARYS BWP (CH)

ST-12

MILLIMETER WAVE INDUCED GENE EXPRESSION CHANGES IN HaCaT HUMAN KERATINOCYTES. Q. Chen, D.Q. Lu*, Z.P. Xu*, H. Chiang, Bioelectromagnetics Lab, Zhejiang Univ School of Med, Hangzhou 310031, China.

BACKGROUND and OBJECTIVE: Millimeter wave (MW) has been reported to produce a variety of bioeffects and millimeter wave therapy has been widely used for therapeutic purposes in some countries for more than 25 years. However, there are no clear mechanisms available to explain the biological effects elicited by MW exposure. In our previous experiments we found that 3.5 mW/cm^2 MW exposure could reverse GJIC suppression induced by TPA in HaCaT human keratinocytes. In order to explore the mechanisms of the biological effects induced by MW exposure, we conducted an in vitro study by using Genechip analysis, a high-through technology, to investigate gene expression pattern in response to MW exposure.

METHODS: HaCaT human keratinocytes were exposed to 3.5 mW/cm^2 MW at a frequency of 30.16 GHz[1]. After cells exposed or sham exposed to MW (30 min per day, for 4 days), total RNAs were isolated by Trizol method. Gene expression levels were quantified using an Affymetrix human genome U95 GeneChip and changes were determined by comparing data from MW-exposed cells to data from sham-exposed cells. For genes of interest, reverse-transcription polymerase chain reaction was performed to confirm the differential expression of these genes.

RESULTS: Comparison ranking analysis revealed that the expression of 18 genes increased by more than three-fold in response to MW stimulation. These genes may play a variety of important roles in cell growth and cell biochemical metabolism. Reverse-transcription polymerase chain reaction analysis confirmed the up-regulated genes are Human proteinase-activated receptor-2 (PAR-2) gene, Cartilage-associated protein (CASP) gene, Human microsomal stress 70 protein ATPase core (STCH) gene and ERGIC-53 gene (Fig.1).

CONCLUSIONS: The genechip technique was useful for investigation of the gene expression in response to MW exposure in HaCaT human keratinocytes. Our results indicate that millimeter wave could induce cellular differential gene expression and the biological consequence of gene expression changes is needed to be further explored.

Reference

1. Q.Chen, Q.L.Zeng, D.Q.Lu, H.Chiang. Millimeter wave exposure reverses TPA suppression of gap junction intercellular communication in HaCaT human keratinocytes. Bioelectromagnetics. 2004, 25(1): 1-

4.

This work was sponsored by National Natural Science Foundation of China (grant number: 39970189).

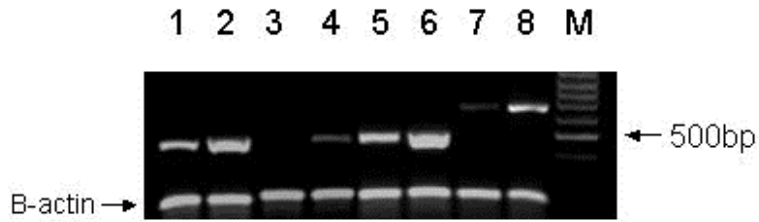


Fig.1. Semi-quantitative analysis of RNA expression by RT-PCR. The RT-PCR product obtained by using primers respectively specific to PAR-2, CASP, STCH and ERGIC-53 gene. Lane M, 100bp DNA ladder; lane 1, PAR-2 in control; lane2, PAR-2 in MW exposure; lane 3, CASP in control; lane 4, CASP in MW exposure; lane 5, ERGIC-53 in control; lane 6, ERGIC-53 in MW exposure. lane 7, STCH in control; lane 8, STCH in MW exposure.

LONG-TERM EFFECTS ON MELATONIN SYNTHESIS IN MALE RATS AFTER EXPOSURE TO A 1439 MHz TDMA ELECTROMAGNETIC FIELD. K. Hata ^{*1,2}, S. Ueno ², H. Yamaguchi ^{*1}, G. Tsurita ^{*1}, S. Watanabe ³, K. Wake ³, M. Taki ⁴, and H. Nagawa^{*1}. ¹Dept of Surgical Oncology, The Univ of Tokyo, Tokyo, 113-8655, Japan. ²Department of Biomedical Engineering, Graduate School of Med, The Univ of Tokyo, Tokyo, Japan. ³Communications Research Lab, Tokyo, Japan. ⁴Dept of Electrical Engineering, Graduate School of Engineering, Tokyo Metropolitan Univ, Tokyo, Japan.

INTRODUCTION: Melatonin is known to have lots of important biological effects including anti-cancer effect, anti-oxidant effect, and modulator effect of circadian rhythm. Low frequency electromagnetic field (EMF) was reported to influence melatonin synthesis [1,2]. We have reported that short-term high frequency EMF does not influence melatonin synthesis on rats [3]. The aim of this study was to investigate the long-term effects of exposure to a 1439 MHz Time Division Multiple Access (TDMA) EMF, as used in cellular phones in Japan, on melatonin synthesis in both male and female rats.

METHODS: Thirty-six male Sprague-Dawley rats were acclimatized to a 12 h light-dark cycle for at least two weeks. They were divided into three groups, the electromagnetic field, the sham, and the cage control groups. The EM group was exposed to a 1439 MHz TDMA field by a carousel type exposure system for 1 hour daily, for 4 weeks in the dark condition, the sham group was placed in the exposure system without TDMA exposure, and the cage control group was not placed in the exposure system. The average specific absorption rate of the brain was calculated as 7.5 W/kg. On the last exposure day, blood was collected and serum was frozen at -20 °C until assay. The melatonin and serotonin levels were measured by radioimmunoassay. These procedures were performed under a dim red light (less than 1 lux) until blood was collected.

RESULTS AND DISCUSSION: Neither melatonin nor serotonin level was altered with long-term TDMA exposure.

Reference.

[1] M. Kato, et al. (1993) Bioelectromagnetics 14: 97-106.

[2] L.J. Grotta, et al. (1994) Bioelectromagnetics 15: 427-37.

[3] K. Hata, et al. (2003) Bioelectromagnetics Society Annual Meeting.

We thank the members of the Committee to Promote Research on the Possible Biological Effects of Electromagnetic Fields in Ministry of Public Management, Home Affairs, Posts and Telecommunications in Japan.

SESSION 7: RF STUDIES
Chairs: Jim Lin and Andrei Pakhomov

7-1

AN OVERVIEW OF LOW-INTENSITY RADIOFREQUENCY/MICROWAVE RADIATION STUDIES RELEVANT TO WIRELESS COMMUNICATIONS AND DATA. C. Sage, Sage Associates, Santa Barbara, California, USA 93108.

This paper summarizes key scientific papers reporting bioeffects and potentially adverse health effects from low-intensity exposure to RF/MW radiation. In the effort to bring understandable scientific information on this subject to the public and decision-makers, this paper provides text summaries of significant articles and their relevant bioeffects, and also charts titled “Some Reported Bioeffects from Low-Intensity Radiofrequency and Microwave Radiation Exposure. The intent of this paper is to provide information for public discussion to guide decision-making about wireless communication devices and transmitting facilities; and a growing international commitment to reliance on wireless communication and data transmission.

The basis for decision-making about a relationship between electromagnetic fields radiofrequency and microwave radiation and adverse health effects at low intensity exposures rests on two key areas. The first is the “weight of the scientific evidence” pointing to a relationship between RF/MW and illness. The scientific evidence needs to be reported to decision-makers in a format that is concise, understandable and accurate. The second is definition of the basis on which the evidence is judged to be sufficient to take interim or permanent public health steps to limit public exposure. Whether the precautionary principle (prudent avoidance) or conclusive scientific evidence is judged to be the proper basis for action, this determination is fundamental to successful consensus on whether and when the scientific evidence is sufficient to take new actions. Given the potential for a very large world-wide public health impact if even a small health risk is present, interim public health actions should be proportionately triggered to the weight of scientific evidence with reported health effects at low-intensity exposure levels. New policies should be developed based on the weight of the evidence, rather than conclusive scientific evidence.

7-2

RF ENERGY ABSORPTION OVER BRIEF TIMES AND SMALL DISTANCES FOR MOLECULAR, CELLULAR, AND ANATOMICAL STRUCTURES. A.R. Sheppard¹, M.L. Swicord², Q. Balzano³. ¹Asher Sheppard Consulting, Redlands, CA 92373; ²Motorola Labs, Ft. Lauderdale, FL 33322; ³Annapolis, MD 21401 USA.

INTRODUCTION: Speculative mechanisms have been proposed for biophysical or biochemical effects occurring without significant temperature change (“non-thermal effects”), sometimes specific to pulse or amplitude modulation. Some concepts are: rapid effects that occur before heat can diffuse; SAR enhancements in small regions or those very close to a small RF source; higher localized SAR for nonuniform cell and tissue anatomical features; non-linear responses; localized vibrational modes of molecular subgroups, and resonant absorption by linear macromolecules. This paper offers a capsule summary of findings from recent research by several authors who have made numerical estimates for the magnitude of biophysical effects.

RESULTS: Heat diffuses so rapidly that hypothetical microscopic hot spots have exceptionally short lifetimes. For example, if the temperature of a sphere with the thermal properties of water and the size of a macromolecule (10^{-8} m) were instantly raised by 1 K, the temperature differential would be only $\approx 2 \cdot 10^{-8}$ K after 1 ns. For a sphere of cellular dimensions, 10^{-5} m, the same temperature insignificant

difference occurs within 1 ms (Foster 2002). Moreover, it is extremely difficult to heat small objects with RF energy. Absorption of 10 W/kg in a 1 μm sphere with the properties of water raises its equilibrium temperature by less than 10^{-8} K and even for a 1 cm sphere temperature would increase to less than 1 K (Foster 2002). Heat flow on the centimeter scale occurs with a time constant of hundreds of seconds, making it impossible to change temperature synchronously with pulse or amplitude modulation. The discontinuity in electric field strength at membrane surfaces suggests effects on the movements of mobile molecules in the region of strong electric field gradients, but the dynamical effects on drift velocity from RF fields within exposure standards are 100 to 1000 times too weak to influence chemical reaction rates (Barnes, Kwon 2003). Thermodynamic analysis shows that “almost elastic,” “photovibrational,” and “nonlinear” interactions between incident microwaves and the intrinsic electrical oscillators of biological material generate scattered RF fields that can be identified by unique frequency signatures (Balzano, Sheppard, 2003). Typical microwave energies are much too weak to trigger thermodynamical instability in a near-non-equilibrium biological system subject to nonlinear interactions, but this might occur with an extremely intense pulse (Balzano, Sheppard, 2003). As an example of exceptionally strong localized RF coupling, SAR of tissue within 2 to 3 mm of a short conductor carrying current at 900 MHz was enhanced up to 5-fold, but the local temperature change was less than ≈ 0.25 K (Balzano et al., 2004). External electric fields and SAR can be enhanced several times above tissue averages at anatomical structures such as an invaginated cell layer or near a cell gap, but at microwave frequencies the E-fields are orders of magnitude too small to cause significant changes in transmembrane potential (Gowrishankar, Weaver, 2003). Quantitative analyses and experimental data for myoglobin, a globular protein complex, and DNA, a linear macromolecule, indicate that the lowest modes for resonant absorption of RF energy are above 10^{11} Hz. Bulk vibrational modes involving a large molecule (or segment) are damped by water molecules, leaving only higher frequency modes associated with interhelical motion in DNA or iron movement in myoglobin (Prohofsky, in press).

CONCLUSION: A number of innovative models demonstrate circumstances where RF energy in tissues, cells, and molecules can be enhanced several-fold, but thermal diffusion precludes a significant increase in local temperature. Non-linear interactions and resonant absorption by molecular structures at frequencies below $\approx 10^{11}$ Hz are, like other nonthermal effects, highly unlikely.

References.

Balzano Q and Sheppard AR 2003. *Bioelectromagnetics* 24(7):473-482.

Balzano Q, Sheppard AR, Foster KR, Swicord ML, 2004. 26th meeting, The Bioelectromagnetics Society, Washington, DC, June.

Barnes F, Kwon Y 2003. P-191-B, 25th BEMS meeting, Maui.

Foster KR 2002. Presented at “Review of Progress in Research on Interaction Mechanisms for RF Energy and Biological Systems”, Rockville, MD, October.

Gowrishankar TR and Weaver JC 2003. *Proc Natl Acad Sci U S A* 100(6):3203-3208.

Prohofsky E (in press, 2004). RF absorption involving biological macromolecules. *Bioelectromagnetics*.

Research support by Motorola and Mobile Manufacturers Forum (ARS, QB).

7-3

A REVIEW OF IN VITRO AND ACUTE IN VIVO STUDIES DOES NOT PROVIDE SUPPORT FOR NON-THERMAL RF BIOLOGICAL EFFECTS. M.L. Swicord, J.J. Morrissey and J. Elder, Motorola Labs, 8000 W. Sunrise Blvd., Ft. Lauderdale, FL 33322 USA.

INTRODUCTION: Investigations of biological effects of RF exposure have been conducted for more than 50 years. The weight of evidence from three dozen long term animal studies indicates no adverse health effect from RF exposure at non-thermal levels. However, a number of in vitro studies do report changes in cell or bio-molecular function, and some acute in vivo studies also report effects at non-thermal levels. This presentation discusses whether the reported in vitro or acute in vivo effects constitute substantial

evidence of a biological response to RF exposure, or are statistical variations or artifactual reports.

DISCUSSION: There are more than 1300 peer reviewed publications in the RF database (see <http://www.who.int/peh-emf/research/database/en/>), of which more than 900 are in vitro or acute animal studies. This extensive literature can not be reviewed in this short presentation, but three areas of current interest [the blood brain barrier (BBB), gene expression and DNA damage] were selected for review as examples.

The weight of evidence of the 40 published BBB studies shows no effect of RF exposure unless thermal levels are reached. Some published studies do report effects at exposure levels that would not be expected to elevate the temperature, but attempts to confirm or replicate these studies were not successful. Oscar and Hawkins first reported effects but later determined that the changes were due to an artifact related to blood flow. The results of many investigators have confirmed that the permeability of the BBB can be affected by a significant increase in temperature caused by absorption of RF energy. Published reports of permeability changes in the BBB at SARs <4 W/kg have not been confirmed and no dose-rate response relationship is evident. There is at least one unpublished report of BBB effects (Abineau et al.) and at least two replication studies underway to address the work of Abineau et al. and Salford et al.

There are a number of studies (more than 70) indicating effects of RF exposure on gene and protein expression and activity. This area can be subdivided into effects on (1) expression of different cell cycle / early response genes known to change in response to chemicals, stress, and other insults (largely negative results), (2) studies of ODC, protein kinases and other enzymes (inconsistent results). (3) denaturation and/or polymerization of proteins (inconsistent results) and (4) stress proteins. The latter group has had two investigators with publications (Leszczynsk et al. and de Pomerai et al.) reporting effects. One investigator found that very low levels of RF exposure resulted in elevations in heat stress expression (hsp 27) in nematodes. The other investigator reported hsp 27 induction and phosphorylation changes in cell lines following RF exposure, but the increased expression required much higher SAR levels than in the nematode study. In contrast, other studies exposing different mouse and human cell lines to very high SAR levels under thermally controlled conditions have reported no induction in hsp gene or heat shock factor (HSF-1) expression levels.

There are at least 45 publications in the database addressing chromosomal or DNA alterations from RF exposure with several authors having multiple publications. Four authors reported effects with a fifth author (Maes et al.) first reporting effects but without confirmation in follow up studies. Subsequent studies have failed to support or confirm reported effects. Twenty additional authors have conducted studies showing either no effect or effects at thermal levels only. A review of the database on chromosomal and DNA alterations yielded no consistent finding or indication of RF effects other than thermal.

CONCLUSION: This review of the literature on the BBB, gene expression and chromosomal/DNA changes found no consistent evidence from both in vitro and acute in vivo studies for a reproducible effect of non-thermal RF exposure. The majority of the studies in these three areas reported no effect. Similar conclusions are reached for other endpoints.

7-4 STUDENT

PERSONAL DOSIMETER FOR RADIO FREQUENCY EXPOSURE ASSESSMENT. J. Wiart¹, F. Perrot², Y. Toutain², M.F. Wong¹ and C. Dale¹. ¹ France Telecom R and D, DMR/IIM, 38-40 rue du Général Leclerc, 92794 Issy-les-Moulineaux Cedex 9, France. ² Antennessa Hameau des Entreprises, 65 Place Nicolas Copernic, 29280 PLOUZANE, France.

There is a public concern about mobile telephone base stations. Previous reports (e.g. COST244 bis) or national measurement campaign (e.g. www.anfr.fr) have shown that the exposure to radio frequency (RF) electromagnetic field (EMF) is weak and well below the standard established by organisms such as ICNIRP and IEEE. Nevertheless there is a need to assess the RF exposure to EMF. The methods developed

to check the compliance to standards are not adequate to assess the RF exposure of a person during the day to day activity. A new approach was required to develop a Personal DosiMeter (PDM).

The aim of this study has been to analyse an isotropic, frequency selective and portable measurement system. The system has been designed to record, through probes allowing isotropic measurements, the RF exposure within specific frequency bands. The influence of the body has been analysed and a statistical method developed to estimate the main characteristics of the RF exposure.

Measurements have been carried out in parallel with this PDM and with a reference frequency selective measurement system used to check compliance to limits. Using these measurements, the accuracy of the statistical approach has been analysed.

This study will present the PDM and results of this analyse.

7-5 STUDENT

PILOT STUDY TO DETERMINE ENVIRONMENTAL FACTORS THAT INFLUENCE RF EXPOSURE FROM MOBILE PHONES. M. Shum*¹, A.R. Sheppard², M. Kelsh¹, N. Kuster³, J. Fröhlich³, M. McNeely*¹, N. Chan*¹. ¹Exponent, Inc., Menlo Park, CA, USA; ² Asher Sheppard Consulting, Redlands, CA, USA; ³ Foundation of Res on Information Tech in Society (IT'IS) Zurich, Switzerland.

INTRODUCTION: The characteristics of particular mobile phone technologies, environmental factors, and duration of phone use are significant influences on epidemiologically-relevant measures of RF exposure from mobile phones. This pilot study is the first phase of a larger study, also conducted in the “real world”, designed to assess the significance for handset exposures to RF energy of parameters such as handset design, network technology, base station density, terrain, time of day, and regional factors for selected network providers. “Designed experiment” methods will be used to examine handset power output as affected by the individual and joint effects of phone and external factors. SAR for a variety of handsets will be measured using a mobile phantom system and correlated with SAR and power control (PWC) data from GSM software-modified phones (SMPs) that record PWC settings commanded by the base station. The full study will collect sampling measurements in several environments under simulated usage conditions for a variety of cellular phones attached to four or more phantom heads with indwelling electric field probes for simultaneous SAR measurements. The SMP will be a reference phone included in each environment tested. This method will allow for estimated correlations between the SMP and other phones and between the GSM and other USA systems included in the study. The pilot study uses only SMPs operating on GSM networks as a first step designed to reduce the number of factors that will need to be varied and measured.

OBJECTIVE: To evaluate the relative influence of different environmental factors on PWC data from SMPs and to develop practical methods for data collection in the field.

METHODS: Trained technicians made numerous five-minute calls from a SMP to a landline phone throughout the day at various locations. Call scenarios were repeated three times to enable analyses for trends and to compare scenarios. Scenario parameters include:

- Time of day (to capture peaks during business and commute hours, midday, mid-afternoon, and early evening conditions)
- Different floors of commercial building
- Commercial/residential buildings
- Indoor and outdoor locations
- Talking versus not talking
- Using the handset against the head or handsfree
- Driving, walking
- Urban and rural environments

To the extent possible, parameters were evaluated individually, by holding other conditions “fixed” (e.g., evaluating time of day at a consistent). Conditions beyond our control, such as weather were recorded for future analysis.

RESULTS AND DISCUSSION: Statistical analysis of results from the pilot study data collection, which are currently underway, will be presented. These analyses will present effects on PWC means and ranges for the parameters listed above and rank-order influential environmental parameters. Based on this ranking, we will choose those most pertinent parameters for the main field study that will use phantom heads to measure SAR under similar environmental circumstances.

Technical Oversight: Radiation Biology Branch, Center for Devices and Radiological Health, U.S. Food & Drug Administration (FDA). **Research Funding:** Cellular Telephone and Internet Association (CTIA)

7-6

VISUALIZATION OF MILLIMETER WAVE EFFECTS ON MAMMALIAN SKIN. R. Blystone, R. Scholz, F. Catalan-Aguilar, J. Eggers¹, N. Millenbaugh², R. Sypniewska², J. Kalns³, J. Kiel¹, and P. Mason¹. Trinity Univ, Dept of Bio, San Antonio, TX 78212; ¹Directed Energy Bioeffects Div, Air Force Res Lab, Brooks City-Base TX 78235; ²General Dynamics Advanced Information Systems, San Antonio, TX 78235; ³Hyperion Biotechnology, San Antonio, TX 78235, USA.

INTRODUCTION: Millimeter wave (MMW) frequencies applied to whole animals initially deposit energy in the upper millimeter of skin. With increasing use of 35 and 94 Gigahertz (GHz) frequencies for commercial and military purposes, it is important to understand how the MMW energy influences the organism’s physiology and anatomy. Our research group is developing computer visualizations that demonstrate the interactions of MMW energy with the skin. Concurrently Stewart et al. are building mathematical models of skin heat flow using the same data sets.

OBJECTIVE: Most models of skin MMW interaction consider skin as a homogeneous slab. Our purpose is to develop a dimensional computer visualization of skin that shows how the stratified nature of skin, its follicular anatomy, and of the hair cycle can influence how MMW energy interacts with skin.

METHODS: Male Sprague-Dawley rats (350 to 400 g) were anesthetized with isoflurane and shaved on the left abdominal flank (approximately 10% of the body surface area). MMW exposures were made to the shaved area with 35 or 94 GHz at 75 mW/cm² for up to 75 minutes duration. Surface temperature as measured by infrared thermography increased to 44°C (35 GHz) and to 48.5°C (94 GHz). Subcutaneous temperature increased to 46°C (35 GHz) and 48°C (94 GHz). Body core temperature as measured colonically increased to 43°C for both frequencies. Skin samples were taken at different exposure time points, formalin processed, sectioned, and stained with hematoxylin and eosin. Digital images were recorded of the histology and pathology. Measurements of anatomical features were made using NIH-Image (public domain) and Adobe Photoshop software. Three-dimensional reconstructions and animations were made using POV-ray (public domain) and Macromedia Flash software. The animals involved in this study were procured, maintained, and used in accordance with the Federal Animal Welfare Act and the “Guide for the Care and Use of Laboratory Animals.”

RESULTS: Flank skin in sham-treated animals in the anagen stage of the hair cycle was 1793 ± 395 microns in thickness (including the cutaneous trunci muscle layer). Mean thickness of skin in telogen stages of the hair cycle was one-third less thick. The variation in thickness is due primarily to the loss of the subdermal fat during the hair cycle (324 ± 86 microns). Hair follicle depth and thickness vary greatly during the hair cycle with course hair bulbs having anagen diameters of 220 microns and fine hair bulbs at 120 microns. Fine hair follicles are primarily populated with either single or tripartite hairs. With skin anatomy varying so much during the approximate 30-day hair cycle in rats, energy distribution with exposure must vary as well. Previously we reported (BEMS-2003) how MMW exposure affected the various layers of the skin. Our computer visualizations will demonstrate how MMW induced changes interact with normal cyclic physiological and anatomical changes in rat skin.

This study was funded, in part, by the United States Air Force Office of Scientific Research.

SESSION 8: BIOPHYSICAL AND BIOLOGICAL DOSIMETRY I

Chairs: Frank Prato and Jim Weaver

8-1

GENOTOXICITY IN MICE EXPOSED TO MILLIMETER WAVES. Vijayalaxmi¹, M.K. Logani², A. Bhanushali², M.C. Ziskin². ¹Department of Radiation Oncology, University of Texas Health Science Center, San Antonio, TX 78229; ²Richard J Fox Center for Biomedical Physics, Temple University School of Medicine, Philadelphia, PA 19140.

INTRODUCTION: A multitude of beneficial uses of millimeter waves (MMW) in medicine have been described in the literature. MMW technologies are also increasingly used in traffic and military radar systems, wireless communication devices, etc. It was considered relevant to investigate the genotoxic potential of MMW exposure in experimental animals since such damage is very often linked to carcinogenesis.

OBJECTIVE: The objective of the investigation was to determine whether or not: (a) MMW wave exposure induces genotoxicity, and (b) MMW exposure will modify the genotoxic effects of cyclophosphamide (CP), a chemotherapeutic drug used in the treatment of various malignancies.

METHODS: MMW radiation was produced with a Russian-made YAV-1 generator and transmitted at 42.2 ± 0.2 GHz (7.1 mm). The peak SAR and peak incident power density were determined as 622.0 ± 100.0 W/kg and 31.0 ± 5.0 mW/cm², respectively. The experiment was conducted over a period of four days. A total of 48 male BALB/C mice were randomized to 6 groups of 8 animals each: (1) untreated controls, (2) exposed to MMW for 30 min/day, for 3 consecutive days, (3) sham-exposed as in group 2, (4) injected with CP (i.p. 15 mg/kg bw) on the second day of the experiment, (5) 30 min of MMW exposure on the first day, injected with CP (15 mg/kg bw) immediately after 30 min of MMW exposure on the second day, and 30 min of MMW exposure on the 3rd day, and (6) sham-exposures and CP treatment as in group 5. All mice were sacrificed at 24 hours following the last treatment. Peripheral blood and bone marrow smears were examined to determine the extent of genotoxicity which was assessed from incidence of micronuclei (MN) in polychromatic erythrocytes (PCEs).

RESULTS: The average frequencies of MN/2000 PCEs were 6.0 ± 1.6 in untreated mice, 5.1 ± 1.5 in MMW-exposed and 5.1 ± 1.3 in sham-exposed mice. In the bone marrow, the values were 9.1 ± 1.1 in untreated mice, 9.3 ± 1.6 in MMW-exposed and 9.1 ± 1.6 in sham-exposed mice. In contrast, mice which were injected with CP exhibited a significant increase in MN/2000 PCEs, 14.6 ± 2.7 in peripheral blood and 21.3 ± 3.9 in bone marrow cells ($p < 0.0001$). However, the values were not significantly different in mice which were additionally exposed to MMW (14.3 ± 2.8 in peripheral blood and 23.5 ± 2.3 in bone marrow) or sham-exposed mice (15.4 ± 3.0 in peripheral blood and 22.1 ± 2.5 in bone marrow cells).

CONCLUSION: There was no indication that MMW exposure was capable of inducing genotoxicity in both peripheral blood and bone marrow cells. Also, MMW exposure did not influence cyclophosphamide-induced MN in both tissues of mice.

8-2

GEOMAGNETIC FIELD AND LIGHT SENSITIVITY OF THE VISUAL SYSTEM – CHECKING THE MODEL-PREDICTIONS. F. Thoss and B. Bartsch*. Univ of Leipzig, Carl Ludwig Inst of Phys, D-04103 Leipzig, Germany.

BACKGROUND: In different experiments we could show that the human visual system is influenced by strength and direction of weak magnetic fields in the range of the geomagnetic field. On the basis of our

results we came to a formal model which is shown in fig. 1. In dependence on field strength and angle between viewing and field direction the light discrimination threshold is slightly changed.

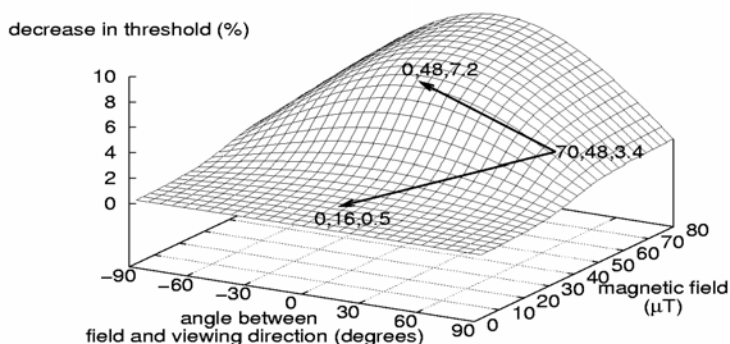


Figure 1: A formal model for the decrease of the visual threshold in comparison with the threshold in a field-free room. The points marked describe results of our former experiments (angle,field strength,threshold decrease).

OBJECTIVE: The objective of this paper was to test the predictions of the model. A relatively strong threshold decrease should result, if we compare the conditions: view against the full local geomagnetic field (angle: 0 degr., field: 48 μT) and view in zero field. The model predicts a threshold difference of 7.2 % for this case.

METHODS: The manipulation of the geomagnetic field was performed by means of two pairs of Helmholtz coils with a diameter of 1 m each. The heads of our subjects were positioned in the common centre of the coils. The discrimination threshold for a target with a diameter of 1 degr. on a screen with a background luminance of 3.2 cd/m^2 was determined for zero field condition and view against the full field of 48 μT . 33 test subjects took part in this experiment.

RESULTS: In comparison with the zero field condition viewing against the vector of the geomagnetic field resulted in a mean threshold decrease of 6.2 %. The paired t-test shows that this threshold difference is significant with $p < 0.0001$.

CONCLUSIONS: The results of our investigations show that an influence of weak magnetic fields on the visual process, supposed as one of the mechanisms underlying the compass orientation of animals, is verifiable for the man.

8-3

COMPARISON OF PEAK 1- AND 10-G SARS FOR PLASTIC "PINNA" SAM AND FOR ANATOMIC MODELS FOR EXPOSURE TO CELLULAR TELEPHONES AT 835 AND 1900 MHZ. O.P. Gandhi, G. Kang, and Q. Li*, Dept of Electrical and Computer Engineering, Univ of Utah, Salt Lake City, UT 84112, USA.

We have previously pointed out that a 2 mm thick plastic shell with 5-10 mm thick tapered plastic spacer as a surrogate of "pinna" – the so-called Specific Anthropomorphic Mannequin (SAM) Head Model proposed for SAR compliance testing both in the U.S. and Europe underestimates the peak 1- and 10-g SAR by up to a factor of two or more as compared to those obtained for anatomic models [1, 2]. Furthermore, with the

use of a relatively lossless plastic for "pinna", another handicap of the SAM Model is the total lack of knowledge of 1- or 10-g SAR in the pinna tissues required by all safety guidelines (present or proposed). In the past, we have explained this reduction in measured (or calculated) SAR for the SAM Model as due to an artificial physical separation of several millimeters (5-10 mm) of the radiating antenna from the lossy tissue-simulant media used for such models – an effect also observed for other shapes of the phantoms e.g. spheres and planar box phantoms [3].

To explain the considerably reduced SARs obtained for the SAM Model, the present study has focused on the visualization and a detailed examination of the peak SAR regions for 1- and 10-g SARs needed for compliance testing against IEEE and ICNIRP Safety Guidelines, respectively. Using the well-accepted FDTD numerical electromagnetic method, peak 1- and 10-g SARs are calculated for a typical cellular telephone handset for which either shorter or longer monopole antennas representative of today's telephones are assumed as the radiators. The head models used for the calculated SARs given in Tables 1 and 2 are (a) the digitized 1 mm resolution of SAM Model kindly provided by Brian Beard of U.S. FDA, (b) the tissue-classified 1 mm resolution "Visible Man" Model provided by U.S. Air Force, and (c) the 16-tissue Utah Anatomic Head Model for which the $2 \times 2 \times 3$ mm voxels are subdivided into $1 \times 1 \times 1$ mm voxels. Assumed for calculations are both the "cheek" and "15°-tilted" positions recommended in the IEEE and CENELEC standards, used in the U.S. and Europe, respectively.

As seen in Tables 1 and 2, the peak 1- and 10-g SARs for the SAM Model are considerably lower than those for anatomic models with lossy pinna and are, in fact, very similar to those obtained for the anatomic models where the pinna tissue is assumed to be lossless with $\epsilon_r = 2.56$ and $\sigma = 0$. Shown in Fig. 1 are the locations of the peak 1- and 10-g SAR regions marked by dark squares for the SAM Model and for two anatomic models for the "cheek" placement of the handset using a 20 mm long monopole antenna for which the calculated SARs are given in Table 2. Whereas the peak 1- and 10-g SAR regions, as expected, are at the base of the antenna (where the magnetic fields for these antennas are the strongest) and include the lossy pinna for the anatomic models, the highest SAR regions for the SAM Model are considerably lower (by about 2.5 cm) in the cheek region. This result is similar to that reported earlier in [4, 5] for plastic ear models. However, this region of the handset is associated with relatively weaker magnetic fields of the antenna which may well explain why the peak 1- and 10-g SARs for the plastic ear models such as SAM are considerably lower than those for the anatomic models at 835 MHz.

References

- [1] O. P. Gandhi and G. Kang, *Physics in Medicine & Biology*, 47, 1501-1518, 2002.
- [2] O. P. Gandhi and G. Kang, Abstract Book, 25th Annual Meeting of the Bioelectromagnetics Society, Maui, Hawaii, 48-49, 2003.
- [3] G. Kang and O. P. Gandhi, *Physics in Medicine & Biology*, 47, 4301-4313, 2002.
- [4] Q. Balzano, O. Garay, and T. J. Manning Jr., *IEEE Trans. Vehicular Technology*, 44(3), 390-403, 1995.
- [5] J. P. Oliver, C. K. Chou, and Q. Balzano, *Bioelectromagnetics*, 24(1), 66-69, 2003.

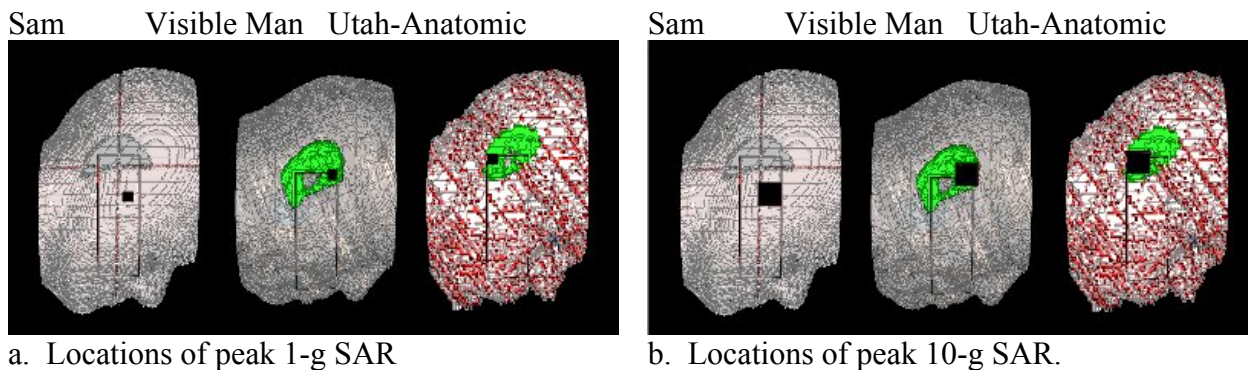


Fig. 1. Locations of the peak 1- and 10-g SAR regions (shown as dark squares) for the SAM Model and for two anatomic models for the "cheek" placement of the handset using a 20 mm long monopole antenna.

Whereas the peak 1- and 10-g SAR regions for the anatomic models include the lossy pinna, the highest SAR regions for the SAM Model are considerably lower (by about 2.5 cm) in the cheek region.

Table 1. Comparison of peak 1- and 10-g SARs obtained for the SAM Model and for two anatomic models of the human head for the "cheek" and "15°-tilted" positions of the 22×42×122 mm handsets with different antenna lengths. The SARs are normalized to a radiated power of 1 W at **1900 MHz**.

	Antenna Axial Length	Peak 1-g SAR (W/kg)				
		SAM Model	Visible Man Model (lossy pinna)	Utah Model (6 mm thick lossy pinna)	Visible Man Model (lossless* pinna)	Utah Model (6 mm thick lossless* pinna)
Cheek Position	20 mm monopole	9.05	34.49	33.49	21.08	9.52
	40 mm monopole	7.31	28.76	31.95	10.13	9.19
15°-tilted Position	20 mm monopole	13.24	25.37	43.10	5.61	9.81
	40 mm monopole	12.17	24.14	36.61	5.19	9.11
Peak 10-g SAR (W/kg)						
Cheek Position	20 mm monopole	5.22	13.80	10.48	6.74	4.59
	40 mm monopole	4.46	12.89	10.03	6.06	4.26
15°-tilted Position	20 mm monopole	7.84	12.89	12.93	3.19	4.86
	40 mm monopole	7.32	12.79	11.61	3.81	4.48

* All of the voxels associated with pinna for these anatomic models are assumed to be lossless with $\epsilon_r = 2.56$, $\sigma = 0$ S/m.

Table 2. Comparison of peak 1- and 10-g SARs obtained for the SAM Model and for two anatomic models of the human head for the "cheek" position of the 22×42×122 mm handsets with different antenna lengths. The SARs are normalized to a radiated power of 1 W at **835 MHz**.

	Antenna Axial Length	Peak 1-g SAR (W/kg)				
		SAM Model	Visible Man Model (lossy pinna)	Utah Model (6 mm thick lossy pinna)	Visible Man Model (lossless* pinna)	Utah Model (6 mm thick lossless* pinna)
Cheek Position	20 mm monopole	5.66	15.45	14.09	7.65	4.41
	80 mm monopole	5.52	13.74	13.39	7.43	4.22
Peak 10-g SAR (W/kg)						
Cheek Position	20 mm monopole	4.02	5.55	4.38	4.29	--
	80 mm monopole	3.93	5.49	4.22	4.22	--

* All of the voxels associated with pinna for these anatomic models are assumed to be lossless with $\epsilon_r = 2.56$, $\sigma = 0$ S/m.

8-4

OVERVIEW OF THE RADIOFREQUENCY DOSIMETRY RESEARCH BEING CONDUCTED BY THE U.S. AIR FORCE. P.A. Mason¹, J.M. Ziriya², M.R. Murphy¹, W.D. Hurt^{1*}, V.M. Swegle^{1*}, and J. D'Andrea². ¹ Air Force Res Lab, Human Effectiveness Directorate, Directed Energy Bioeffects Div, Brooks City-Base, TX, 78235-5147, USA, ²Naval Hlth Res Center Detachment Directed Energy Bioeffects Lab, Brooks Air Force Base, TX, USA.

Accurate dosimetry is a critical part of any scientific effort to assess the effects of electromagnetic fields (EMF) on biological systems. In addition, conducting high quality dosimetry and reporting detailed descriptions of the dosimetry are essential to permit precise replications of experiments by independent laboratories. Dosimetry includes the prediction and/or measurement of the incident and internal fields. These fields can be quite different, depending upon the characteristics of the object, including: size and shape, electrical properties, orientation with respect to the incident field, and the frequency of the incident field. The development of mathematical dosimetry modeling techniques and relatively powerful computer hardware has resulted in computer modeling as a principal tool in assessing the biological dose resulting from EMF exposure. Only with the use of realistic anatomical models and methods such as the finite difference time domain (FDTD) has the ability to estimate both whole body and localized specific absorption rate (SAR) values become possible. Laboratory research is aided by the FDTD analysis by indicating where localized SAR measurements should be made. The FDTD analyses show that whole body SAR values exhibit frequency-dependent resonances; as do individual organs and body sections (e.g., limbs, head).

The man dosimetry model developed by the U.S. Navy and Air Force was used in the present study to determine resonance frequencies as a function of: 1) object orientation with respect to the incident field and

2) use of whole body or partial body (e.g., head only) models. Comparison between whole-body model and the partial-body model produced substantial differences in localized SAR values. These differences are important to note since partial body simulations may be used to limit the computing resources required. Different results with whole- versus partial-body simulations would tend to limit the value of partial-body models and suggest that partial-body models must be employed with care.

Since validation of human dosimetry models is difficult or impossible with living human subjects, we have also developed animal dosimetry models that we compare to empirical animal data. Good agreement between the theoretical and empirical animal data provide support for the validity of the SAR values predicted in the man model. Validation of the computer models with empirical results and the subsequent refining of the models are essential in order to earn the confidence and credibility needed to use these models to establish or revise exposure standards.

8-5

EMF DOSIMETRY REQUIREMENTS FOR PHYSIOLOGICALLY SIGNIFICANT BIOEFFECTS: THIS ISN. A.A. Pilla and D. Muehsam, Dept of Biomedical Engineering, Columbia Univ and Dept of Orthopaedics, Mount Sinai School of Medicine, New York, NY, USA.

INTRODUCTION: Low intensity, non-thermal time-varying electromagnetic fields, PMF, over a very broad frequency range; static magnetic fields, SMF; ultrasound, US; and mechanical loading, SGP signals have proven clinical benefit when used as adjunctive therapy for a variety of musculoskeletal injuries. Clearly, each of these signals appears to have the capacity to achieve a physiologically meaningful bioeffect. Why should such seemingly different modalities be effective? Which parameters, or even which modality, should be used? This study discusses the common dosimetry parameters for molecular, cellular and tissue targets and the conditions for which both EMF and mechanical signals can produce meaningful therapeutic effects.

E-FIELD DOSIMETRY: Bioeffects from weak PMF signals are due primarily to the time-varying electric field, $E(t)$ induced from either an applied time-varying magnetic field, $B(t)$, or from streaming (electrokinetic) potentials from the US and SGP signals. This has been established experimentally for most of the clinical PMF and US devices in current use by simple orientation experiments which utilize the basic properties of Faraday's law of induction. Most EMF clinical devices induce a peak E of 1-10 mV/cm at the treatment site, but at widely differing frequencies. Clinical US signals also induce E in the mV/cm range due to the non-linear effects of the propagation of the pressure wave in tissue (microstreaming), with major frequency components below 1 kHz. Induced E in this case is a single repetitive pseudo-rectangular pulse with slow (millisecond) rise and fall times. Induced E from SGP is most often a slowly decaying exponential-type function having peak amplitudes in the mV/cm range and major frequency components centered below 1 kHz. The question then is whether $E(t)$ from US, SGP and EMF signals can be detected by a biological target in the presence of thermal noise. The cell array tissue model, which describes the dynamic electrical response of cells in real tissue configurations, allows thermal thresholds (SNR) to be evaluated for induced electric fields from any signal, and for any kinetics, including non-linear, in the target pathway. If the PMF, US or SGP signal produces sufficient amplitude in the frequency ranges exhibited by the time constant(s) of the target pathway, the signal is detected and a physiologically meaningful bioeffect may result. PMF or US signals can be configured very differently in the time domain and yet still induce sufficient amplitude at frequencies relevant to target kinetics to be detectable. This may or may not result in a physiologically meaningful bioeffect dependent upon the initial conditions of the target pathway, as discussed below.

B-FIELD DOSIMETRY: In contrast to PMF, US and SGP, SMF can be detected at input levels far below thermal noise in an ion binding pathway via Larmor precession of the already bound and thermally shielded ion-water complex. In addition to modulating the coherent oscillations of tightly bound oscillators, Larmor precession can also affect the thermally induced components of ions and ligands in oscillator potentials.

The thermal component oscillates at the fundamental frequency of the oscillator potential with amplitude increasing with time, ultimately resulting in ejection from the binding site after a bound lifetime determined by the magnitude of thermal forces. We have shown that both the coherent and thermal components of an ion at a binding site exhibit Larmor precession in the presence of an applied magnetic field. Thus, as the amplitude of the thermal component grows, the oscillator orientation still precesses at the Larmor frequency in the plane perpendicular to the applied magnetic field direction. Larmor precession converts the magnetic field amplitude into a frequency determined by the gyromagnetic ratio of the target. Each Larmor precession frequency determines the time to reach favored orientation(s) at the binding interface, which can modulate the rate constant for binding with a subsequent effect on the relevant biochemical cascade. The model predicts a threshold in the 0.1-1 μT range for magnetic field effects on the kinetics of ion binding in the presence of thermal noise for sufficiently long bound times. The biophysical link between PMF and SMF is the Larmor frequency since it couples to the same time constant(s) in the ion binding pathway as does the induced E from PMF signals.

MOLECULE/CELL/TISSUE TARGET DOSIMETRY: Clinical experience, particularly in bone and wound repair, as well as numerous in vitro studies, suggest the initial conditions of the EMF-sensitive target pathway determine whether a physiologically meaningful bioeffect can be achieved. Thus, normal bone tissue, which receives the same PMF dose as a fracture site, does not respond in a physiologically meaningful manner, whereas fracture repair is accelerated. Local peripheral blood flow is not affected by PMF or SMF in a healthy subject, but is increased when a musculoskeletal injury is present. Ca^{2+} binding to CaM is modulated by PMF or SMF only under depleted Ca^{2+} conditions. Dendritic outgrowth in a nerve regeneration model is modulated by PMF or SMF only in the presence of sub-saturation concentrations of NGF. We have interpreted this by showing that SNR calculations depend upon the electrical characteristics of the EMF-sensitive target which are substantially different when the target is at rest or reacting to a sudden change in its environment such as a fracture or other musculoskeletal injury. Thus, for an identical PMF or SMF stimulus, the impedance of the EMF sensitive pathway may alter sufficiently in the presence of an injury or pathology to enable a signal, which has otherwise been ignored (not detected) to be detected.

CONCLUSIONS: The analyses presented in this study strongly suggest, if ion/ligand binding with known kinetics is the EMF-sensitive target, PMF, SMF, US or SGP signals may be predictively configured to achieve adequate dosimetry for a physiologically meaningful bioeffect. This may explain why many of the PMF and US signal variants, as well as relatively weak static magnetic fields appear capable of producing meaningful clinical effects. The approach outlined here suggests a rationale for the use of programmed (vs target state) and/or combined modalities to achieve optimum therapeutic effect.

8-6 STUDENT

DETERMINATION OF THE CORRECTION FACTOR FOR OCCUPATIONAL ELECTROMAGNETIC EXPOSURE COMPLIANCE EVALUATION USING DIFFERENT HOMOGENEOUS PHANTOMS. W. Joseph and L. Martens. Dept of Information Technology, Ghent Univ, Sint-Pietersnieuwstraat 41, B-9000 Ghent, Belgium.

OBJECTIVE: To determine the safety compliance boundaries for occupational electromagnetic exposure of e.g., a GSM base station antenna, the Specific Absorption Rate (SAR [W/kg]) must be determined and be compared to the basic restrictions [1]. In practice, the SAR is experimentally determined in a homogeneous phantom. But because using a homogeneous phantom model may result in lower SAR values than for a heterogeneous and anatomically realistic model, the measured SAR must be multiplied by a correction number [2]. CENELEC proposes in standard [2] an arbitrary correction factor 2 for a rectangular box phantom. The objective of this paper is to define a frequency and phantom dependent correction factor (in contrary to CENELEC [2]) by determination of the whole-body SAR in an anatomically realistic model for plane-wave excitation and comparing it to the whole-body SAR in homogeneous phantoms.

METHODS: We investigate an electromagnetic plane-wave excitation for a homogeneous rectangular box

phantom, a homogeneous prolate spheroid phantom and a realistic heterogeneous model of a man. This model of the “Visible Human Project” has been developed at Brooks Air Force Base Laboratories. Figure 1 shows the three models. The size of the box phantom [2] has been chosen to correspond to the average trunk of an adult man. The dimensions of the spheroid correspond to those of an average man. For the box and spheroid phantom the dielectric parameters are those of muscle tissues for the investigated frequencies. We determine the whole-body SAR for the different phantoms for E-polarized (incident electric field parallel to the major axis of the spheroid or to the longest dimension of other phantoms) incident plane waves. For this polarization the highest SAR values will be obtained. This type of plane-wave excitation is thus a worst-case situation, necessary for the evaluation of safety compliance. We define the correction factor Σ as the ratio of the whole-body SAR in the human model and the whole-body SAR in the different phantoms. The whole-body SAR will deliver the most restrictive values for plane-wave excitation. For the determination of the SAR in the spheroid phantom we use a formula proposed by Durney et al [3]. For the rectangular box phantom we use an self developed model valid from 300 MHz on. For the heterogeneous model of a man developed at Brooks AFB we use FDTD simulations. The cell resolution of the model is $3 \times 3 \times 3 \text{ mm}^3$. This model can be used up to 1500 MHz.

RESULTS: First we investigate the different behaviour of the phantoms through the ratio $R = L_{\text{SAR}}/\text{whole-body SAR}$ if $S = L_S$, with the incident power density S equal to its reference level L_S at each frequency and with L_{SAR} the corresponding basic restriction for occupational exposure of the whole-body SAR [1] in the frequency range 10 MHz – 10 GHz (figure 2). For the whole frequency range R is greater than 1 for the three investigated models. Thus, the basic restriction is never exceeded for plane-wave excitation with a power density equal to the reference level. Therefore the power density will deliver more restrictive conditions than the SAR for plane-wave excitation. R reaches a minimum at 73 MHz because this is about the resonance frequency for a human body in free space. The realistic model of a human mostly delivers the highest SAR values (lowest R values), the box phantom is less restrictive than the spheroid phantom. Table 1 shows R and the correction factor $\Sigma = R_{\text{phantom}}/R_{\text{human}}$ for 73 and 950 MHz (typical GSM frequency). We consider also 73 MHz because the whole-body SAR will then be maximal. This table shows that the “arbitrary correction factor 2” of CENELEC [2] is not a good choice at 950 MHz. The factor should be about 3 at 950 MHz for the rectangular box phantom. Furthermore this factor is a function of the frequency and of the type of phantom. The spheroid phantom delivers almost equal SAR values at resonance.

CONCLUSIONS: We have presented a new correction factor for the determination of the SAR in a homogeneous phantom exposed e.g., by a GSM base station in occupational conditions. From our results the arbitrary factor 2 defined in the standard of CENELEC is not a good choice. The correction factor is frequency and phantom dependent and e.g., for the rectangular box phantom in the GSM band equal to 3 instead of 2.

References.

1. International Commission on Non-ionizing Radiation Protection, “Guidelines for limiting exposure to time-varying electric, magnetic, and electromagnetic fields (up 300 GHz),” *Health Physics*, Vol. 74, No. 4, pp. 494-522, 1998.
2. CENELEC EN50383, “Basic standard for the calculation and measurement of electromagnetic field strength and SAR related to human exposure from radio base stations and fixed terminal stations for wireless telecommunication systems (110 MHz – 40 GHz),” Sept. 2002.
3. C. H. Durney, M. F. Iskander, H. Massoudi and C. C. Johnson, “An Empirical formula for Broad-Band SAR Calculations of Prolate Spheroidal Models of Humans and Animals,” *IEEE Trans. Microwave Theory Tech.*, vol. MTT-27, No. 8, pp. 758 – 763, Aug. 1979.

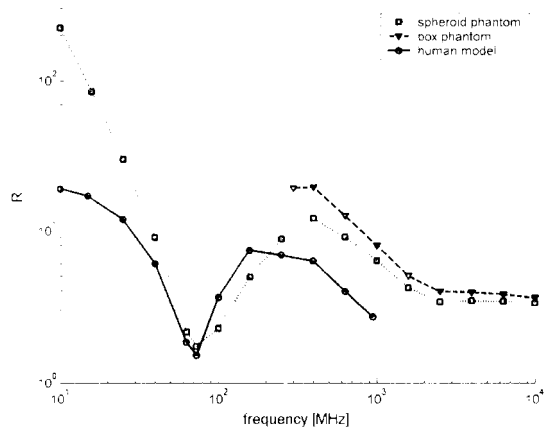
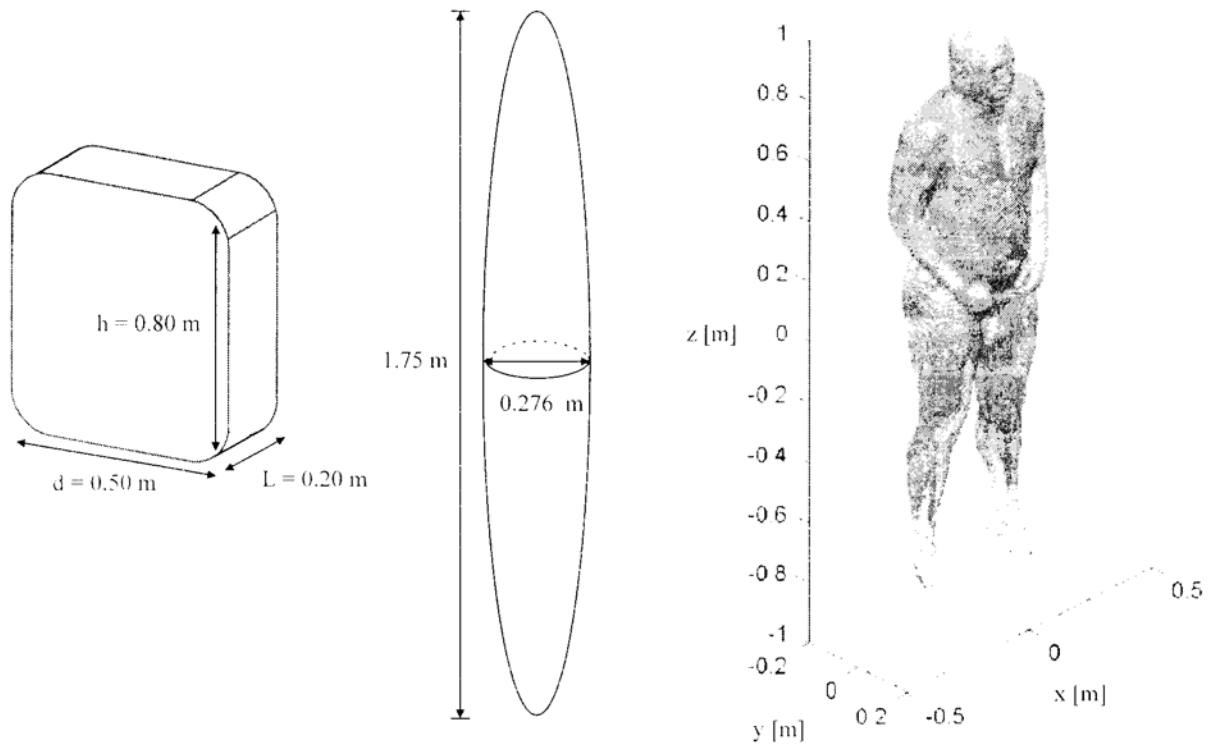


Figure 1: (a) The rectangular box phantom, (b) the prolate spheroid phantom and (c) the realistic model of a man.

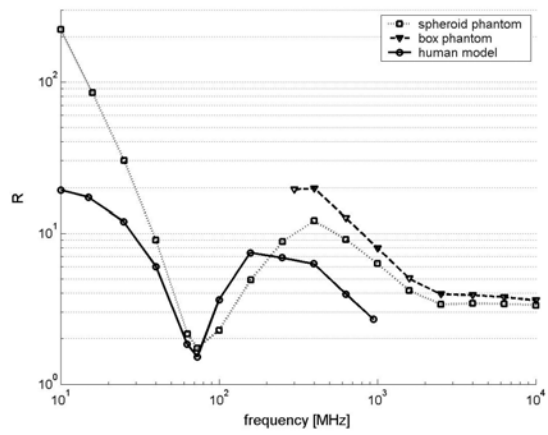


Figure 2: R for the three models as function of the frequency from 10 MHz to 10 GHz.

model	73 MHz		950 MHz	
	R	Σ	R	Σ
box	-	-	7.9	2.9
spheroid	1.7	1.1	6.7	2.5
human	1.5	-	2.7	-

Table 1: Comparison R and Σ at 73 and 950 MHz

SESSION 9: IN VITRO STUDIES
Chair: Abe Liboff and Betty Sisken

9-1

EFFECT OF HYDROGEN PEROXIDE ON JURKAT T CELLS AND ITS REGULATION BY LOW FREQUENCY EMFS. G. Nindl¹, W.X. Balcavage¹, C.J. Moulton*¹, L.R. Waite*², M.T. Johnson¹.

¹Center for Medical Education, Indiana Univ School of Med, Terre Haute, Indiana 47809, USA, ²Applied Biology and Biomedical Engineering, Rose-Hulman Inst of Tech, Terre Haute, IN 47803, USA.

INTRODUCTION: While hydrogen peroxide (H₂O₂) and other reactive oxygen species (ROS) have long been recognized to be deleterious to many cells, it has recently become clear that these small molecules also have an important, physiologically beneficial role as signaling molecules in certain cells such as T lymphocytes. Our laboratory is interested in applying biophysical methods such as non-invasive electromagnetic fields (EMFs) to regulate the activity of inflammatory T cells so as to ameliorate the effects of chronic and acute inflammation in human disease states. Understanding how to biophysically regulate the actions of H₂O₂ in T cells will lead to novel ways to treat inflammatory diseases.

OBJECTIVE: Our first aim is to determine if H₂O₂ can amplify the effects of signal transduction initiated through the T cell receptor (TCR) in Jurkat cells, our model of inflammatory T cells. Secondly, since TCRs contain amino acid sequences that seem to be important in antibody-catalyzed H₂O₂ production, we also aim to determine if TCRs produce H₂O₂ when activated with anti-CD3 and phorbol myristic acid (PMA). Finally, we aim to determine if EMFs can regulate the physiological effects that are H₂O₂-dependent.

METHODS: Jurkat E6.1, a human T lymphocyte cell line, was purchased from American Type Culture Collection. Cells were grown and activated with anti-CD3 and PMA as described in Nindl et al. (Biomed Sci Instrum 40, 2004). H₂O₂ was obtained from Sigma Chemical Co. (H-1005). The quantity of interleukin-2 (IL-2) secreted into culture medium (22 hr. after cell activation) was quantified using ELISA 88-7026-77 plates from eBioscience Inc. H₂O₂ was assayed electrochemically using an H₂O₂ electrode that we recently developed (Sharma et al., Biomed Sci Instrum, 39, 554, 2003). Electrochemical results were verified using the H₂O₂ indicator Amplex Red. H₂O₂-dependent Amplex Red color changes were quantitated and recorded using a Bio-Tek EL 808 plate reader. Apoptosis was monitored as described earlier (Nindl, et al., ISBN 960-86733-3-X, 167, 2002). In initial EMF experiments we employed an EMF Therapeutics Inc. field generator that produces a pulsed 15 mT, 120 pulses/sec. signal (Nindl et al., Marcel Dekker Inc., 25, 369, 2004). For later experiments, we developed a new field generator, which we describe in this presentation (see Results section below).

RESULTS AND DISCUSSION: To evaluate the biological effect of H₂O₂ we exposed activated Jurkat cells to 0 – 80 μM H₂O₂ and found that 50 ± 10 μM H₂O₂ promoted optimal IL-2 production, which was proportional to cell number. In contrast, in non-activated control cells H₂O₂ inhibited cell growth, induced apoptosis and had no effect on IL-2 production. These remarkable results show that in activated Jurkat cells, which are a model of inflammatory T cells, H₂O₂ enhances/stimulates the cellular consequences of cell activation at the TCR. In contrast, H₂O₂ has long been considered to be a cell toxin and in normal, proliferating (non-activated) Jurkat cells we found that H₂O₂ exhibits its anticipated toxic effects. In preliminary experiments it appears that EMFs downregulate IL-2 production of Jurkat cells.

Based on the amino acid sequence similarities between antibodies and the TCR we hypothesized that TCRs might catalytically produce H₂O₂, which could then act as an autocrine factor to regulate T cell activity. To investigate this possibility we developed a real-time H₂O₂ electrode monitoring-system capable of detecting 1 μM H₂O₂. Using CD3 antibody as catalyst we validated the H₂O₂ monitoring system by reproducing findings from Wentworth et al. (Science 293, 1806, 2001). In our experiments, we found H₂O₂ to be produced at a rate of about 30 nM/min/mM CD3 antibody. In preliminary experiments we observed that the rate of H₂O₂ catalyzed by CD3 antibody appears to be EMF-dependent. These accumulating *in vitro* data

promise to give insight into the mechanism of interaction between EMFs and biomolecules. Having demonstrated the utility of our H₂O₂ electrode, we employed the electrode to study H₂O₂ production by intact Jurkat cells and by a Jurkat cell membrane preparation enriched in TCRs. We found that the preparation enriched in TCRs actively catalyzes H₂O₂ production, indicating that H₂O₂ is a T cell autocrine factor. Since H₂O₂ catalysis by antibodies appears to be EMF-sensitive we hypothesize that EMFs will influence H₂O₂ production in these systems and regulate H₂O₂-dependent signal transduction in intact cells. In our preliminary experiments we used a therapeutic EMF generating device. To provide more flexibility in our EMF delivery capability we have constructed and characterized a new EMF generating system. The new system is integrated with our H₂O₂ monitoring system and it produces EMFs in excess of 10 mT at frequencies up to 20 kHz. The coil an inner diameter of 16.5 cm consists of 625 turns (cross section of 25 turns x 25 turns) of 16 gauge enamel wire. Using this system, we will determine if EMFs can influence signal transduction initiated by H₂O₂ in inflammatory T cells.

9-2

INFLUENCE OF DAMPS-835 OR EUROPEAN GSM-1800 SIGNALS ON ORNITHINE DECARBOXYLASE ACTIVITY IN L-929 MOUSE FIBROBLASTS AND SH-SY5Y HUMAN NEUROBLASTOMA CELLS. M. Taxile*, B. Billaudel, G. Ruffie*, E. Haro*, J. Schuderer¹, I. Lagroye and B. Veyret. Bioelectromagnetics Laboratory / UMR 5501, EPHE /PIOM-ENSCP, 33607-Pessac, France. I IT'IS Laboratories, Zeughausstrasse 43,8004

OBJECTIVES: Ornithine DeCarboxylase (ODC) plays a pivotal role in the synthesis of polyamines. It has been shown that ODC overexpression may be involved, not only in cell neoplastic transformation, but also in cancer cell invasiveness. The Litovitz group reported a temporary increase in ODC activity in L-929 fibroblasts after exposure to DAMPS-835 RFR (I). We are involved in a replication study (PERFORM-B) of the results published by this group and we extended this study to GSM-1800 signals.

METHODS: L-929 cells, cultured in DMEM, and SH-SY5H cells cultured in AMF-12 medium were plated at a density of 8x10⁵ cells/Petri dish. Following incubation for 20 h, the cells were blindly sham exposed or exposed inside waveguides (IT'IS, Zurich, Switzerland) to 50Hz modulated DAMPS-835 or to 217-Hz modulated GSM-1800 signals. Immediately after exposure, cells were suspended in cold PBS using a cell scraper and centrifuged twice at 500 g. The cell pellet from Petri dishes was stored at -80°C until assay in duplicate for ODC activity. Cell pellets were lysed and centrifuged. Aliquots of supernatant (100 ~l) were incubated for 1 h at 37°C with 2.22x10⁵ d.p.m. ¹⁴C-labeled L-ornithine. ¹⁴CO₂ generated by ODC was absorbed with hyamine hydroxide in a center well secured in a rubber septum-type stopper. The reaction was terminated by the injection of trichloroacetic acid through the rubber septum and incubation continued for 1 h. Radioactivity of ¹⁴CO₂ trapped in hyamine hydroxide was counted by liquid scintillation (Beckman-Coulter). The amount of protein of cell lysate was determined by the Bradford method. Total ODC activity was calculated as pmol ¹⁴CO₂ /h/mg protein. Sham-sham exposures allowed to check the absence of difference between both waveguides for the two set-up and consequently to compare exposed/sham ODC ratios using the univariate Student t test.

RESULTS: Using L-929 fibroblast cells, no significant modification of ODC activity was observed for all tested exposures to DAMPS-835 at SAR 2.5 W/kg; this ratio was not statistically different from unity (p = 0.783 at 2 hours (n = 5), p = 0.138 at 8 hours (n = 5), and p = 0.784 at 24 hours (n = 5)). During exposure to GSM-1800 at different SAR levels for 8 hours, this ratio was not statistically different from unity (p = 0.783 at 0.5 W/kg (n = 3), p = 0.138 for 1 W/kg (n = 5), and p = 0.784 for 2.5 W /kg (n = 5)). Under the experimental conditions used by the Litovitz group (L- 929 cells, 8 hours DAMPS-835 exposure at 2,5 W/kg) there was a 40% increase in ODC activity, but we observed no significant variation of ODC activity under the conditions described above. Complementary experiments for comparison between DAMPS-835 and GSM-1800 signals on ODC activity are currently in progress using another cellular type (SH-SY5H cells).

CONCLUSION: Exposure of L-929 cells to DAMPS-835 or GSM-1800 signals had no influence on ODC activity. This result does not agree with the previous observations of the Litovitz group using a Crawford cell exposure system(1), which were not confirmed in an other recent study (2). Results of complementary experiments using SH-SY5H cells will allow to settle this comparison of the potential effects on ODC activity of RFR emitted by mobile phones.

References.

(1) Penafiel *et al.*, 1997, *Bioelectromagnetics*, 18,132-141. (2) Desta *et al.*, 2003, *Radiation Research*, 160,488-491.

This work is supported by MMF and GSM association, the Aquitaine Council for Research and the CNRS.

CHANGES IN GENE EXPRESSION PROFILE OF MCF-7 CELL AFTER EXPOSURE TO ELF MFs. Z.P. Xu, G.D. Chen, Q.L. Zeng, D.Q. Lu, H. Chiang. Bioelectromagnetics Laboratory, Zhejiang University School of Medicine, Hangzhou 310031, China.

BACKGROUND: Health assessment of EMF exposure needs fully understanding of EMF-induced biological effects and then evaluating their possible health impacts on human. However, there are many knowledge gaps in reaching this goal and thus extensive researches need to be done. High-throughput screening techniques have been introduced into Bioelectromagnetics field and are expected to play a key role in elucidating all the possible effects of EMF exposure.

Epidemiological studies suggested that there is a possible link between breast cancer and ELF EMF exposure. However, the mechanism underlying the role of EMFs in promotion of carcinogenesis is plausible. Here we intended to explore the global effects of ELF MFs on gene transcriptions in breast cancer cell line MCF-7 cells by employing gene chip analysis.

OBJECTIVE: To investigate the global change of gene expression pattern induced by 50 Hz magnetic fields, and identify key EMF-responsive genes in this particular cells. Hopefully a working hypothesis will be formulated through bioinformatics analysis.

METHODS: MCF-7 cells were exposed to 50 Hz, 0.4 mT MFs [1], just below the occupational exposure limit of ICNIRP, for 24 h. Total RNAs were isolated by Trizol method and then purified by using QIAGEN's RNeasy mini Kit. Affymetrix Genome U133A gene chips were applied to detect the gene expression pattern following the manufacturer's instruction. The experiment was done in duplicates and data was analyzed by Affymetrix microarray suite version 5.0 (MAS 5.0) and Affymetrix Data Mining Tool 3.0 (DMT 3.0).

RESULT: MAS 5.0 software analysis showed that there were more than 1,000 differentially expressed genes. Among them, replication and coincidence analyses with DMT 3.0 software revealed 30 genes were affected by ELF MFs exposure with 100% consistency of differential calls in 4 pair-wise comparisons, including 6 down-regulated and 24 up-regulated genes which fell into 7 categories: 1. signal transduction related genes (intercellular and intracellular); 2. biochemical metabolism related gene; 3. transcription factor related genes; 4. extracellular matrix protein genes; 5. stress response related genes; 6. ion channel related genes; and 7. other function unknown genes. Also we found 80 genes with 75% consistency. Gene clustering analysis was carried out to predict the function-unknown responsive genes. A working hypothesis was constructed based on available information.

CONCLUSION: The result demonstrated that exposure to 50 Hz, 0.4 mT ELF MFs for 24 hours would induce cellular differential gene expression through multiple signal transduction pathways. 30 EMF-responsive genes were identified.

Reference.

[1] G.L. Hu, H. Chiang, Q.L. Zeng, and Y.D. FU. ELE Magnetic Field Inhibits Gap Junctional Intercellular Communication and Induces Hyperphosphorylation of Connexin43 in NIH3T3 Cells. *Bioelectromagnetics*, 2001, 22: 568-573.

This research was supported by National Natural Science Foundation of China (No. 50137030).

MYOSIN PHOSPHORYLATION IN GRADIENT MAGNETIC FIELDS. S. Engström, M.S. Markov*, M.J. McLean, R.R. Holcomb. Department of Neurology, 2100 Pierce Avenue, Vanderbilt Univ, Nashville, 37212 TN, USA. * Research International, Buffalo, NY, USA.

THE OBJECTIVE of this study was twofold: (1) To test a group of specific rejectable hypotheses designed to rule out some basic features of magnetotransduction in the myosin phosphorylation enzyme system. (2) To estimate response curves for at least a small range of parameter variations in the large space of possible combinations of field and gradients.

MATERIALS AND METHODS: A custom exposure device was constructed using two cylindrical NdFeB magnets (50 mm diameter, 25 mm tall; Figure 1). This allowed exposures with predictable field amplitude as well as perpendicular and parallel (to the local field vector) gradient components. In most of our exposures, the parallel gradient components were small in comparison to the perpendicular one. The myosin phosphorylation experiment was conducted as described previously [Engström et al., 2002].

RESULTS: Twelve null-hypothesis driven experimental conditions were repeated on 5 different days with highly consistent results in which the standard deviation divided by the mean (σ/μ) did not exceed 0.03, and in more than half of the experiments it was below 0.01. Figure 2 shows the evaluated parameter combinations. All exposed samples were significantly different from the control group ($\max p = 0.0005$ (for 10/11 comparisons $\log p < -6$), and many of the other pair-wise tests for which the exposures were chosen suggested emphatic rejections of the null hypotheses that: (a) The absolute magnitude is the only factor affecting the experimental outcome; (b) Perpendicular gradient strength is a single factor; (c) Perpendicular and parallel gradient components are interchangeable. However, an experiment designed to duplicate the field parameters with different device settings also showed a significant difference ($\log p < -8$).

Three series aimed at “scanning” the parameter ranges shown in Figure 3a were repeated twice with results consistent with the standard deviations observed in the first series of experiments. The corresponding response can be seen in Figures 3b-d.

DISCUSSION: Experiments designed to duplicate field conditions produced significantly different outcomes. This confounds the results of this study and it is important to understand why this might have happened. It should be borne in mind that the experimenter had information about field settings only, and with this type of device, that information is not very useful for second-guessing the field conditions for the experiment. That these experiments were so highly repeatable argues in our opinion for the possibility that there is something about this exposure that we do not characterize with our parameterization, but it is unclear at this point what the missing quantity is.

Reference.

Engström S, Markov MS, McLean MJ, Holcomb RR, Markov JM (2002) Effects of Non-Uniform Static Magnetic Fields on the Rate of Myosin Phosphorylation. *Bioelectromagnetics* 23:475-479.

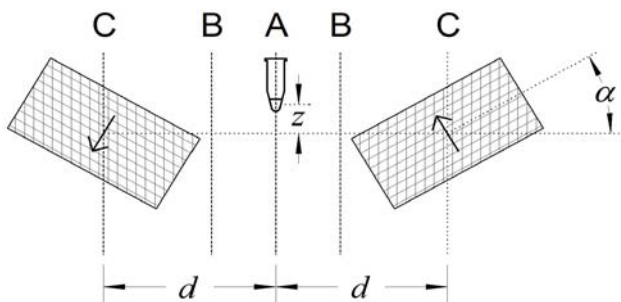


Figure 1: Schematic representation of the exposure device. Two magnets can be rotated (α) and translated (d) to generate different field exposures.

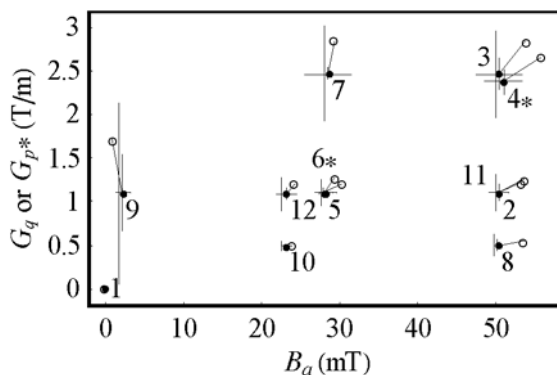


Figure 2: Exposure parameters considered for the first sequence of experiments. For the two cases indicated by (*) the ordinate shows parallel gradient components instead of the perpendicular component which is shown otherwise.

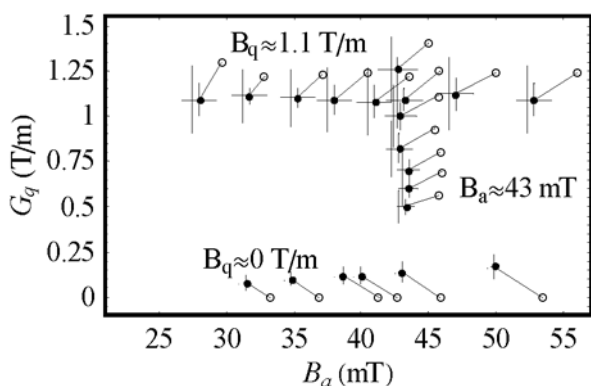


Figure 3a: Parameters for three field scans. The solid disks indicate the planned (calculated) parameters (with distribution spreads), the open circles show measured estimates of the fields.

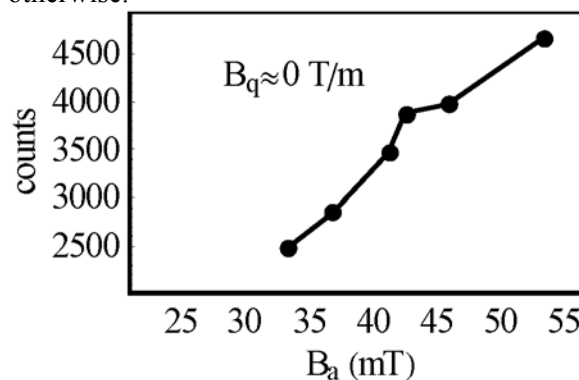


Figure 3b: Response in radioactive ATP uptake as a function of magnetic field amplitude for low gradients.

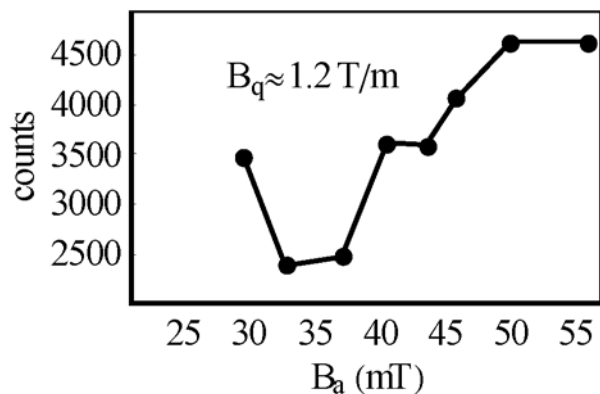


Figure 3c: Scan of field amplitude for a constant perpendicular gradient.

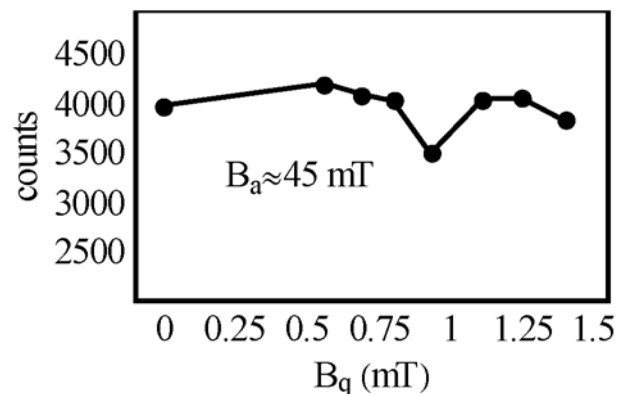


Figure 3d: Scan of perpendicular field gradient for constant field amplitudes near 50 mT.

ELECTROMAGNETIC FIELDS IN BIOMEDICINE: CYTOPROTECTION AND GENE THERAPY. R. Goodman¹, H. Lin², M. Blank³, Department of Pathology¹, Anatomy² and Physiology³, Columbia University 630 West 168 St, New York, NY 10032, USA.

INTRODUCTION. Electromagnetic (EM) fields as a tool for stimulation of biological effects offer many distinct advantages: bioelectromagnetic techniques are non-invasive, the fields can be easily directed, and they require low energy. The low thresholds at which EM fields stimulate biological processes, including the protective stress response, are below the level of perception, so they have the further advantage of not interfering with the subject. Here we describe two potential medical applications based on EM stimulation of the stress response and the use of EM field-responsive elements (EMREs) in genetic engineering .

EM fields stimulate gene expression. EM fields initiate gene expression, and the well-established stimulation of the stress response has now been found over a wide range of frequencies, including RF. Electromagnetic response elements (EMREs) in the promoters of genes are required for EM field interaction with DNA. A 900 base pair segment containing EMREs in the hsp70 promoter is needed for the response to EM fields. Removal of the segment eliminates the response, and transfection into a promoter construct renders the construct EM field-responsive (1).

EM field-induction of hsp70 for use in cardiac by-pass surgery. Induction of the stress protein hsp70 by electromagnetic (EM) fields is often used as an indication of the normal response of cells to biological hazards, but it should be emphasized that the same stress protein serves to protect against potential hazards. We have utilized the protective aspect of EM field induced stress proteins to develop two new beneficial medical tools (patents pending).

Elevating hsp70, usually through hyperthermia (high temperatures), protects the myocardium during reperfusion ischemic stress and helps prevent heart attack and stroke. Induction of increased hsp70 with EM fields eliminates patient discomfort associated with hyperthermia. EM fields are non-invasive, penetrate all cells, and have longer-lasting effects than hyperthermia. Within 30 minutes hsp70 levels are elevated at least 2-fold and remain elevated for more than 3 hours. Unlike hyperthermia, hsp70 levels can be augmented by restimulation for extended surgical procedures (2).

RESULTS OF CYTOPROTECTION STUDIES. The increase in hsp70 levels by EM fields *in vivo* and *in vitro* depends on the field strength. EM field-preconditioning produces a higher survival rate than thermal preconditioning in fertilized dipteran eggs and cultured rodent cardiomyocytes (1).

Beneficial use of EM fields for gene therapy. We have identified three nCTCTn EM field-responsive elements (EMRE) in the DNA sequences in the HSP70 promoter are EM field-responsive. Inactivating these sequences, by removal or mutation, renders reporter gene constructs unresponsive to EM fields. Inserting this sequence in an unresponsive reporter construct, renders the gene EM field-responsive (2). This innovation in gene therapy provides a non-invasive and precise technique for gene activation. For example, an exogenous insulin gene containing one or more EMREs introduced upstream of the gene, can be simply and safely regulated by the EM fields. The procedure can be made automatic with an EM field generating circuit activated by an implanted glucose sensor that responds immediately to changes in pre-set blood glucose levels.

References.

1. Carmody et al (2000) *J Cell Biochem* 79: 453-459.
2. Lin et al (2001) *J Cell Biochem* 192: 1622.

Support by Robert I Goodman Fund

EVALUATION OF MUTAGENICITY OF COMPLEX MAGNETIC FIELDS WITH STATIC AND TIME-VARYING COMPONENTS. M. Ikehata^{1*}, T. Nagai^{2*}, Y. Suzuki^{2*}, M. Taki² and T. Koana^{3*}.

¹Railway Technical Research Institute, Kokubunji, Tokyo 185-8540, Japan, ²Tokyo Metropolitan University, Hachioji, Tokyo 192-0397, Japan, ³Central Research Institute of Electric Power Industry, Komae, Tokyo 201-8511, Japan.

OBJECTIVE: In our environment, various types (e.g. frequency, field strength) of electric and magnetic fields (EMFs) exist and their distributions are complex. On the other hand, there are few reports on biological effects of such complex EMFs exposure. In this point, our project aims to construct a strategy for the safety evaluation on human health by exposure to complex EMFs. In this study, mutagenicity of complex EMFs, especially with static and power frequency components were examined by two independent mutation assay systems.

METHODS: For complex EMFs exposure, a Helmholtz coil was made and located at the center of superconducting magnet (JS-500, Toshiba, Japan). The Helmholtz coil is able to generate 50Hz, 1mT time-varying EMF under 5T static magnetic field. This exposure system was located in a constant temperature room and maintained exposure space at 37 ± 1 or 30 ± 0.5 °C. Induced current in the test plate which contains agar and nutrient compounds for complex exposure condition was estimated by impedance method. In addition, displacement of surface of agar plate by Lorentz force was estimated by numerical analysis. To investigate the mutagenicity, we employed two mutation assays. One is the bacterial mutation assay (Ames test). In this assay, *Salmonella typhimurium* TA98, TA100 and *Escherichia coli* WP2 *uvrA* was used. These bacterial cells were exposed to complex EMFs for 48 hours after plating onto glucose minimal media with trace of required amino acid (histidine and biotin for *S. typhimurium* strains and tryptophan for *E. coli* strain) at 37 ± 0.5 °C. Control cells were incubated in conventional incubator. After 48 hours of incubation, number of prototroph mutant colony appearing on each plate was scored. The other mutation assay is yeast mutation assay using *Saccharomyces cerevisiae* XD83. For detecting point mutation frequency on *lys 1-1*, harvested cells were mixed with molten soft agar (0.6 % Bacto-agar, 0.5 % NaCl) and were poured onto low lysine synthetic complete plate. For detecting gene conversion frequency on *ARG4* allele (between *arg 4-4* and *arg 4-17*), cell suspension was poured on to low arginine synthetic complete plate. At least 6 plates were made for both condition and randomly divided into two groups. One group was exposed to complex EMFs for 5 days at 30 ± 0.5 °C. The other group was incubated as control. Number of colonies on each plate was scored as reverse mutant and the mutation frequency was calculated.

RESULTS: It was observed that gene conversion/recombination on *ARG4* frequency in *S. cerevisiae* XD83 slightly increased by exposure to complex EMFs while point mutation frequency was not affected on *LYSI* allele. In bacteria, we observed no difference between exposed and control group on each point mutation in *S. typhimurium* and *E. coli*. These results are consistent with our previous study for strong static MFs [1,2], thus, we infer that the mutagenicity observed in this study caused by strong static magnetic field. However, it is interesting that the extent of mutagenicity is slight weaker than that by exposure to a 5T static MF alone. In future studies, different combination of field strength and frequency of complex EMFs will be investigated for estimation the effect of complex EMFs exposure in our environment. This work was supported in part by the Research Program from the Japan Railway Construction, Transport and Technology Agency.

References.

- [1] T. Koana, M. O. Okada, M. Ikehata and M. Nakagawa, Mut. Res., vol. 373, pp. 55-60, 1997.
- [2] M. Ikehata, Y. Suzuki, H. Shimizu, T. Koana and M. Nakagawa, Mut. Res., vol. 427, pp. 147-156, 1999.

IN VITRO EVIDENCE SUPPORTING THE EMF HYPERSENSITIVITY CLAIMS. D. Leszczynski.
STUK – Radiation and Nuclear Safety Authority, Helsinki, Finland.

Use of high-throughput screening techniques (HTST) of transcriptomics and proteomics is scientifically justified and necessary to determine the biological effects of mobile phone radiation (Leszczynski et al, *Proteomics* 4(2), 2004, in press). One of the controversial issues is the claim that there might be some sub-population of people who are hypersensitive to EMF. We have examined this problem using HTST methods of proteomics and transcriptomics.

We have previously shown (Leszczynski et al., *Differentiation*, 70, 2002, 120-129) that the exposure of human endothelial cell line EA.hy926 to simulated mobile phone radiation (900 or 1800 GSM) induces increase in phosphorylation of the stress response protein Hsp27. We have also observed that, as expected, Hsp27 translocates to nucleus where it is known to affect gene expression. Therefore, it was justified to assume that the RF-EMF-induced translocation of Hsp27 to the nucleus might affect gene expression that might, in turn, cause alteration in protein expression levels. Thus, examining the effects of RF-EMF on protein and gene expression using HTST methods was scientifically justified.

We have compared the response of two very closely related human endothelial cell lines: fast proliferating EA.hy926 and its slow proliferating variant EA.hy926v1 (derived by sub-cloning from the EA.hy926 cell line) to the 1-h exposure to 900 GSM simulated mobile phone signal at SAR of 2.4 W/kg and temperature controlled at $37\pm 0.3^{\circ}\text{C}$.

Using 2-dimensional electrophoresis to separate proteins and PDQuest software to analyse and compare protein spots we have determined what proteins respond to RF-EMF exposure. The protein expression pattern in ten replicates of sham samples was compared with the protein expression pattern in ten replicates of irradiated samples. The normalized spot volumes of the proteins from sham and exposed sample gels were statistically analysed using student t-test at the confidence level of 95%. The comparison of the shams of the two cell lines has shown that their normal protein expression patterns are very different, in spite of the closely related origin of both cell lines. Only approximately half of all of the protein spots could be matched confidently between the cell lines.

The RF-EMF-induced changes in protein expression differed dramatically between EA.hy926 and EA.hy926v1 cell lines. The comparison of the exposed and sham samples has shown several tens of protein spots with radiation-induced statistically significant change in expression levels (t-test $p < 0.05$). In EA.hy926 cell line there were ca. 38 of protein spots which expression was altered by the radiation exposure whereas in EA.hy926v1 cell line there were ca. 45. Most interestingly, the proteins that responded to the exposure in EA.hy926 cell line were different from the proteins that have responded in EA.hy926v1 cell line.

Using cDNA Expression Arrays we have determined that in response to RF-EMF a number of genes increased/declined their expression in both cell lines. Most strikingly, the genes that were up regulated in one of the cell lines were down-regulated or not affected in the other cell line.

In conclusion, it appears that different proteins and different genes responded to the RF-EMF exposure in both cell lines. This suggests that it is likely that the cell response might depend on the genotype and/or the phenotype of the cell. Thus, our evidence supports the notion that the phenomenon of EMF hypersensitivity might exist.

SESSION 10: INSTRUMENTATION and METHODOLOGY

Chair: Joe Bowman and Asher Sheppard

10-1

DESCRIPTION OF AN EXPOSURE SYSTEM USED IN A PROVOCATION STUDY TO MOBILE PHONE LIKE SIGNALS. J. Wilén, M. Sandström, A. Johansson*, O. Stensson* and K. Hansson Mild. National Inst for Working Life (NIWL), Umeå, Sweden.

INTRODUCTION: Previous provocation studies where symptoms and physiological responses have been studied in connection to exposure to radiofrequency fields (RF) have used ordinary mobile phones (MP), alternatively specially designed MP, as the exposure source. Huber et al (2000) have previously designed an exposure system where patch antennas have been used instead of an MP as the source of exposure. The advantages of this system are many, for instance better control of the exposure as well as the exposed area. We have in the same way designed an exposure system where we use an omni indoor antenna system. The antenna is chosen to give a homogenous exposure, not over the entire head, but in the area of the head where ordinary MP deposits the energy. The exposure system discussed here has been used in a provocation study, which will be presented separately at the conference.

OBJECTIVES: The aim of this presentation is to give a comprehensive description of the exposure system in a provocation study of subjects who reports MP related symptoms when they use mobile phones.

METHODS: The SAR distributions of ordinary MPs are quite dispersed. Some phone deposit most of the energy above the ear, while others deposit the energy below or on the ear (Wilén et al 2002). To obtain a more reproducible exposure we therefore used a modification of the system described by Huber et al (2000). A pair of omni indoor antennas was used and they were fed by an amplified mobile phone-like signal (890 MHz, pulsed with 217 Hz, DTX off) emitted from a test MP device where the output power could be set to a fix value. Both true exposure as well as sham exposure was considered (Figure 1). The SAR distribution was measured with the DASY 3 system, more details about the SAR measurements will be provided at the presentation.

RESULTS: The energy from the antennas is rather homogenous distributed over the entire area where ordinary MPs might deposit the energy. The presentation will include a detailed description of the exposure system including the SAR distribution from the antenna where the maximum SAR_{1g} value was 1 W/kg.

Reference.

Huber R et al. Neuroreport 2000,11:3321-3325.

Wilén J, Sandström M, Hansson Mild K. Bioelectromagnetics 2003; 24:152-159.

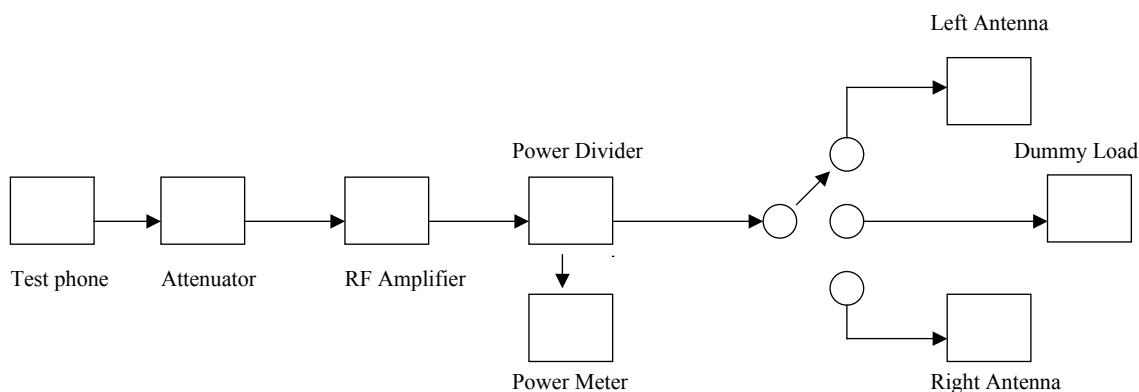


Figure 1. Schematic drawing of the exposure system.

This study was supported by the Swedish Council for Working Life and Social Research.

10-2

A SEMI-AUTOMATED IMAGE PROCESSING SYSTEM FOR EMF HUMAN MODELS. D.-S. Yoo, M.-H. Seo*¹, J.-H. Yun*, W.-Y. Choi*¹. Dept of Radio Science, Electronics and Telecommunications Res Inst (ETRI), Daejeon 305-350, KOREA, Dept of Electronics Engineering, Myongji Univ, Yongin 449-728, KOREA.

OBJECTIVE: The purpose of this study is to develop a semi-automated system for human image processing with which tissues or organs from human images can be segmented and classified by people who have basic knowledge of image processing. In addition, the proposed image processing system is independent on types of human tissues or images. In this paper, a new semi-automated image processing system with essential image processing functions for EMF human models is introduced.

INTRODUCTION: A high resolution human model is necessary in order to analyze EMF effects exposed on human body by telecommunication devices. The high resolution human model can be developed by segmenting human images such as magnetic resonance (MR) images and CT images. The segmented images can be reconstructed to 3D model with information of anatomical structures. However, it is almost impossible to develop a fully automatic program to segment every anatomical structures because of characteristics of the images. One of the simplest methods of segmentation is to manually classify anatomical structures by extracting features such as edges, landmark points and regions of similar grey level in the images [1]. However, manual contouring of structures is a difficult and time-consuming task. Errors arise from low tissue contrast, edge blurring caused by partial volume effects, image degradation due to artefacts and noise, slice selection, and poor coordination between eye and hand. Although automatic segmentation programs are available, all of them have restrictions dependence upon specific organs and image types. The limitation of the automatic program can be overcome by applying a semi-automatic approach which has advantages from manual and automatic method. In this study, a new semi-automated image processing system with essential image processing functions for EMF human models is introduced. In the following section, functions and user interface of the system is introduced.

USER INTERFACE AND FUNCTIONS: A new semi-automated image processing system (Human Analyzer) is developed using the C-language for operating in personal computers. Main functions in the Human Analyzer are as follows: Single and multi thresholding; Boolean operations; Histogram; Histogram equalization; Region growing; Mathematical morphology including Erosion, Dilation, Opening and Closing; Edge detections; Image contrast adjustment; Pen; Filling; Eraser; Color selection for tissue classification based on FCC classification; Reference images. The Human Analyzer was designed to adopt an intuitive menu method which helped users to use and understand the program easily (see Fig 1). The main control panel is an example of the intuitive menu method. All executive buttons for image processing functions were placed in the main control panel. After activating any buttons for processing, an independent control panel for the processing appeared. All images were displayed in an independent window. Color selection table was added to classify anatomical structures after segmentation. Based on the FCC tissue classification, 43 human tissues were selected for the color selection table.

CONCLUSIONS: A new semi-automated image processing system with essential image processing functions for EMF human models is introduced. In the proposed image processing system, anatomical structures in the images can be segmented and classified by people who have basic knowledge of image processing. In addition, the proposed image processing system is independent on types of human tissues or images.

Reference.

[1] Chung MS, Kim SY. (2000) *Yonsei Med. J.* 41: 299-303.

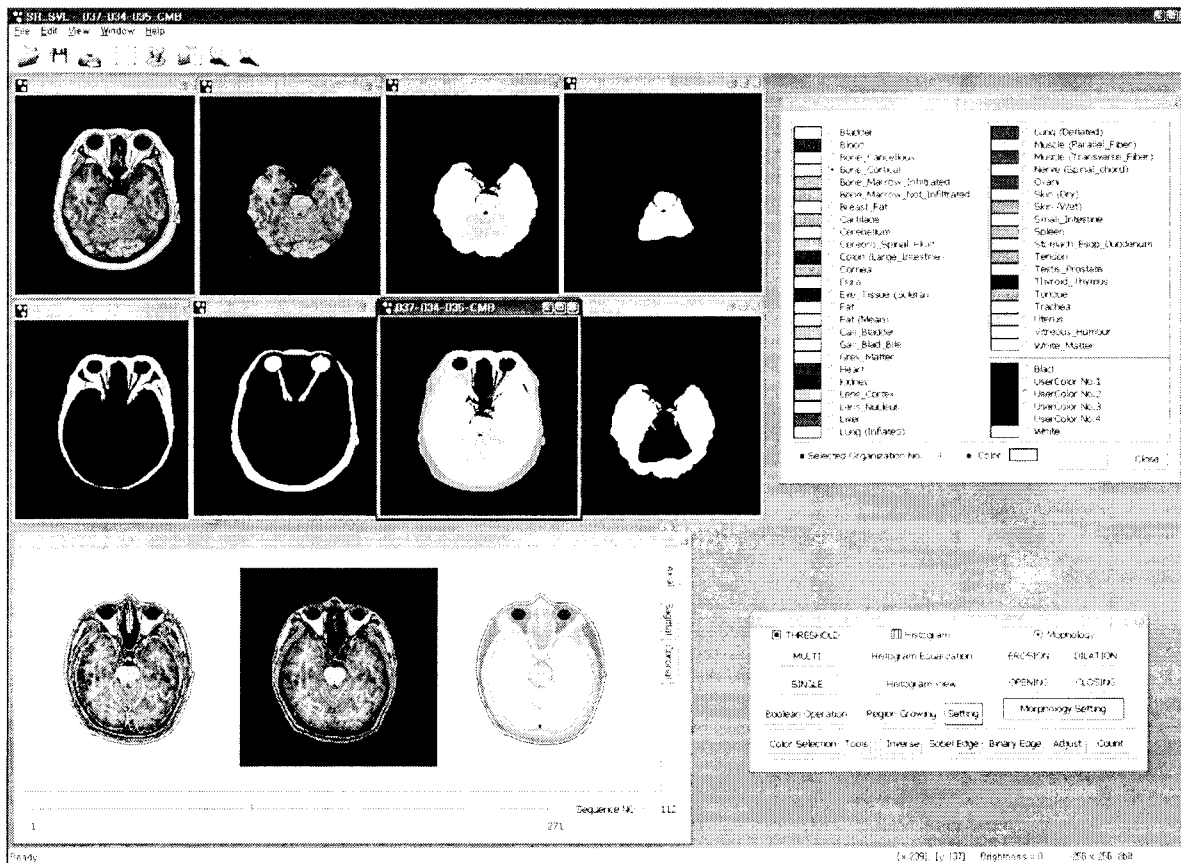


Figure 1: User interface of Human Analyzer

10-3

WHOLE BODY AVERAGED SAR: A MALE TO FEMALE NUMERICAL COMPARISON. L. Sandrini*#, A. Vaccari*, M. Mazzurana*, C. Malacarne*, R. Pontalti* and L. Cristoforetti*. Inst for the Scientific and Technological Res – Physics Chemistry Surface Division, 38050 Povo, Trento, Italy. #InterUniv Center "Interaction between Electromagnetic Fields and Biosystem" (ICeMEB), Genova, Italy.

INTRODUCTION: Numerical modeling involving sophisticated complex permittivity representations of the human body was developed in the last years [1-4] to provide useful tools for investigating the connection between an external E-field and the internal SAR (Specific Absorption Rate) distribution in the radiofrequency (RF) range. In the above mentioned papers the whole body averaged SAR is evaluated by using male models with the impinging E-field parallel to the standing body. Studies about female models are few and, in particular, a comprehensive comparison between male and female SAR distributions is still lacking. A second issue that affects numerical SAR evaluation by using FDTD technique is the spatial resolution. It is still rather poor because of the large number of cells required to completely embed the body. This number dramatically increases at higher frequencies for FDTD accuracy requirements and because the wavelength decreases inside the body by a factor of about $\epsilon^{-1/2}$.

OBJECTIVES: In this context the aims of this work are: first, to propose a female Dielectric Anatomical Model (fDAM); second, to compare the SAR distributions of male and female models from 0.1 to 2 GHz and third to apply a recent and robust FDTD subgridding algorithm, theoretically developed and discussed by the authors [5], that allows an abrupt mesh refinement by a factor of 7 inside the human body model.

METHODS: The same procedure used for the obtainment of the male Dielectric Anatomical Model

(mDAM) [4], was employed to develop the new fDAM. Briefly it can be summarized as follows: i) a set of 486 slices (thickness 2 mm for the head and 4 mm for the trunk and legs) were acquired with a MRI tomographer from a female volunteer (30 years old, 1.63 m tall, body weight of 47 kg) at two different repetition times (short 525 ms, long 2100 ms); ii) the ratio between the images at the two repetition times was performed to subtract out the spatial image nonuniformities; iii) the T1 value (longitudinal relaxation time) was correlated with the tissues water content; iv) by using the mixture theory the proper complex permittivity value was assigned voxel by voxel to the body tissues. With respect to the usual segmentation technique, the described procedure is faster and provides the advantage of taking into account the intrinsic variability of dielectric parameters even in the same tissue. The electric field and SAR distributions were computed by using the FDTD method at frequencies from 100 MHz to 2 GHz. The fDAM was grounded and exposed to a plane wave at the same conditions of mDAM. The new subgridding technique, here used for the first time for dosimetric purposes, is based on a low-pass filter implemented at the interfaces between the coarse and refined grids by means of spatial derivatives only [5].

RESULTS: Regarding the averaged total body SAR, a larger value at 120 MHz frequency with respect to 1000 MHz (about 85%) was found, as expected by resonance criteria. It is also interesting to compare the values of this quantity to those obtained for mDAM (34 years old, 1.73 m tall, body weight of 63 kg): it appears 20% and 48% higher for the female model at 120 MHz and 1000 MHz, respectively. It is probably due to: i) a different posture of the legs (slightly apart for the female, close together for the male), ii) the different height and iii) the presence of a thicker subcutaneous fat layer in fDAM, which slightly improves the matching between the impinging plane wave and the inner high water content tissues of the body. To better understand this last point, further investigations were performed on a muscle cylinder surrounded by a fat layer of given thickness. A maximum in the average SAR absorption appears for a thickness in the range $\lambda/4 - \lambda/2$ (in the fat).

CONCLUSIONS: The comparison of the results for male and female models shows differences in the whole body averaged SAR partially due to the different anatomical conformation and to the tissue content and location (e.g. subcutaneous fat). Furthermore, the recently proposed subgridding technique, able to achieve higher spatial resolution in the human body, was validated as a very powerful tool for numerical dosimetry purposes.

References:

- [1] Bernardi P, Cavagnaro M, Pisa S, Piuzzi E. (2002) *IEEE Trans.Biomed.Eng.* 50: 295-304
- [2] Dimbylow P J. (1997) *Phys.Med.Biol.* 42: 479-490
- [3] Tinniswood A D, Furse C M, Gandhi O P. (1998) *Phys.Med.Biol.* 43: 2361-2378
- [4] Mazzurana M, Sandrini L, Vaccari A, Malacarne C, Cristoforetti L, Pontalti R. (2003) *Phys.Med.Biol.* 48: 3157-3170
- [5] Vaccari A, Pontalti R, Malacarne C, Cristoforetti L. (2003) *Journal of Computational Physics*, in press
- [5] A . Vaccari A, R. Pontalti R, C. Malacarne C, L. Cristoforetti L, 2003 *Journal of Computational Physics*, in press, 2003,

This work was partly supported by the MIUR 5% Program (Italian Ministry for Education, University and Research).

10-4 STUDENT

A NOVEL INTEGRATION SYSTEM OF PULSED ELECTROMAGNETIC FIELDS STIMULATION WITH BIOREACTORS APPLIED TO BONE TISSUE ENGINEERING. M.T. Tsai, W.H. Chang, D.W. Wu*, and K.T. Chang. Bone Tissue Engineering Res Center, Dept of Biomedical Engineering, Chung-Yuan Christian Univ, Chung-Li, Tao-Yuan 32023 Taiwan.

INTRODUCTIONS: Bone defects, which result from tumors, diseases and infections, trauma, biochemical disorders, and abnormal skeletal development, pose a significant health problem [1]. Tissue engineering is a rapidly developing interdisciplinary field applying the principles of cell biology, molecular biology and biomimetic engineering to regenerate new tissues for replacement therapies in clinical contexts [2]. The core constituents of bone tissue engineering are osteogenic cells, biomaterials and growth factors. Despite growth factors have strong osteo-inductive activity, they are extremely expensive and controversy of safety. Pulsed electromagnetic fields (PEMF) stimulation has been proven that its effects on osteoporosis prevention and bone fracture healing in vivo [3-4]. PEMF is also effective on osteoblastic proliferation and bone defect healing in vitro. However, PEMF has not been considered as an alternative physical stimulation in bone tissue engineering. Consequently, PEMF might be a more potential perspective and approach applying to three-dimensional culture model in bone tissue engineering in the future.

OBJECTIVES: In this study, we attempt to integrate our well-developed pulsed electromagnetic fields (PEMF) stimulators with modified bioreactors and apply to bone tissue engineering for accelerating osteoblastic cells growth in vitro. The effects of PEMF with different intensities were investigated and compared on osteoblastic cells.

METHODS: Primary osteoblastic cells were acquired from calvariae of newborn Wistar rats in an aseptic procedure. Osteoblastic cells were isolated from calvariae with collagenase (300-400 units/ml) and grown to be confluence. After confluence, Trypsin-EDTA was used to release osteoblastic cells and resuspend in culture medium (DMEM+10% FBS+1% penicillin streptomycin) at a density of 8.3×10^3 cells/ μ l. 60 μ l of medium with cells were loaded into a three-dimensional poly(L-lactic-co-glycolic acid) (PLGA) scaffold with pore size ranging from 180-425 μ m. The diameter and height of a PLGA disc are 6 mm and 3 mm, respectively. Osteoblastic cells were located and seated into nine PLGA scaffolds for 6 hours and then placed in three glass tubes of a bioreactor filled with medium combined with PEMF stimulators. Scaffolds with cells were on the exposure of PEMF stimulation with specific parameters: single pulsed wave, pulse width of 300 μ s, extremely low frequency of 7.5 Hz, and induced electric fields intensities of 4 and 8 mV/cm. These matrices were divided into three groups: Control (matrices were not on the exposure of PEMF stimulation), PEMF-2 hr (matrices were on the exposure of PEMF stimulation for 2 hr/day), and PEMF-8 hr (matrices were on the exposure of PEMF stimulation for 8 hr/day). Each group was cultured in a modified bioreactor for 2 weeks. Culture medium and matrices of three groups were retrieved at each week for biochemical and histomorphological assays. ALP is an early marker of osteoblastic differentiation, and concentrations of glucose and lactate can reflect the metabolism of cells. H&E stain shows the distribution of cells in a scaffold.

RESULTS: The results of H&E stain showed the histomorphology of osteoblastic cells growing in PLGA scaffolds at different culture periods. Cells proliferated and filled of some pores obviously after 2-week culture. The ALP activity of PEMF-2 hr with 4 mV/cm was the highest at the 1st and 2nd week significantly (Fig. 1). PEMF-2 hr with 8 mV/cm also expressed the highest ALP level at the 2nd week (Fig. 4). The tendencies of glucose levels of three groups with different intensities decreased similarly (Fig. 2 and 5). However, lactate concentrations all increased at each time point (Fig. 3 and 6). The results revealed that the metabolism of osteoblastic cells cultured in PLGA scaffolds in modified bioreactors combined with PEMF system were stable and it indicated that cells were able to and suitable to live and grow in this integrated environment.

CONCLUSIONS: In this study, a novel integration system of PEMF stimulators combined with modified bioreactors was successfully set up, and the effect of PEMF was proved in bone tissue engineering in an osteoblastic culture model. PEMF with specific parameters in this integration system not only enhanced

osteoblastic differentiation in vitro, but also supplied a suitable condition for osteoblastic growth in bioreactors.

References:

Bruder SP and Fox BS, "Tissue Engineering of Bone," *Clinical Orthopaedics and Related Research*, 367 Suppl: S68-S83, 1999

Fleming JE Jr, Cornell CN, and Muschler GF, "Bone Cells and Matrices in Orthopedic Tissue Engineering," *Orthopedic Clinics of North America*, 31(3): 357-374, 2000

Cruess RL, Kan K, and Bassett CA, "The Effect of Pulsing Electromagnetic Fields on Bone Metabolism in Experimental Disuse Osteoporosis," *Clinical Orthopaedics and Related Research*, (173): 245-250, 1983

Bassett CA, "The Development and Application of Pulsed Electromagnetic Fields (PEMFs) for Ununited Fractures and Arthrodeses," *Orthopedic Clinics of North America*, 15(1): 61-87, 1984

This study was kindly supported by grant from the National Science Council (NSC 91-2213-E-033-031).

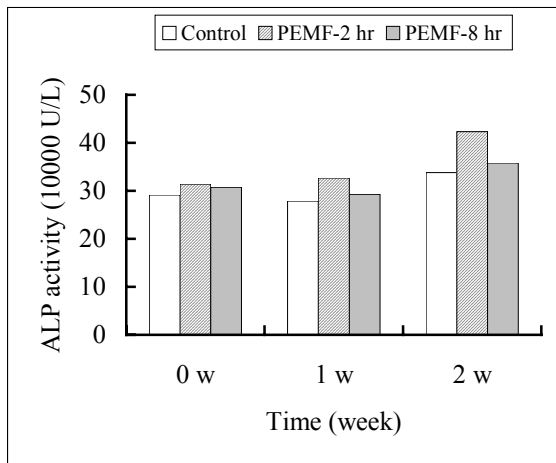


Figure 1. ALP activities of Control, PEMF-2 hr, and PEMF-8 hr at different time points with 4 mV/cm.

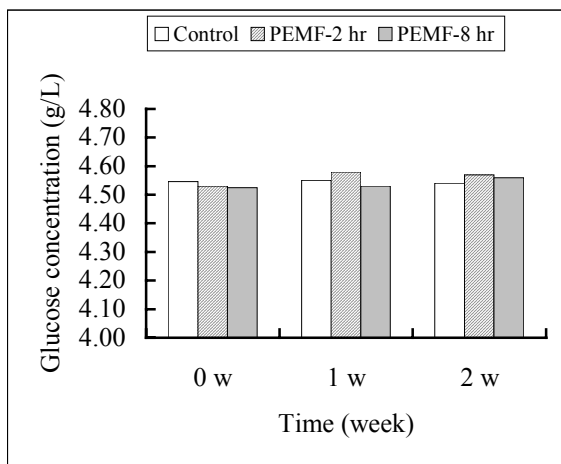


Figure 2. Glucose concentrations of Control, PEMF-2 hr, and PEMF-8 hr at different time points with 4 mV/cm.

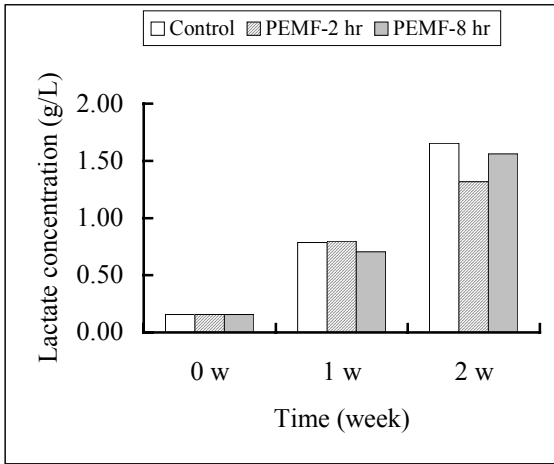


Figure 3. Lactate concentrations of Control, PEMF-2 hr, and PEMF-8 hr at different time points with 4 mV/cm.

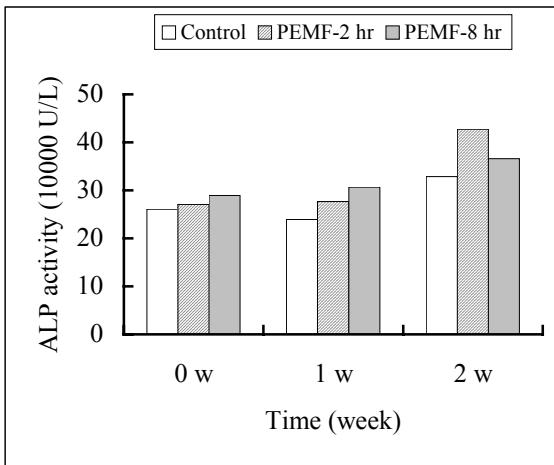


Figure 4. ALP activities of Control, PEMF-2 hr, and PEMF-8 hr at different time points with 8 mV/cm.

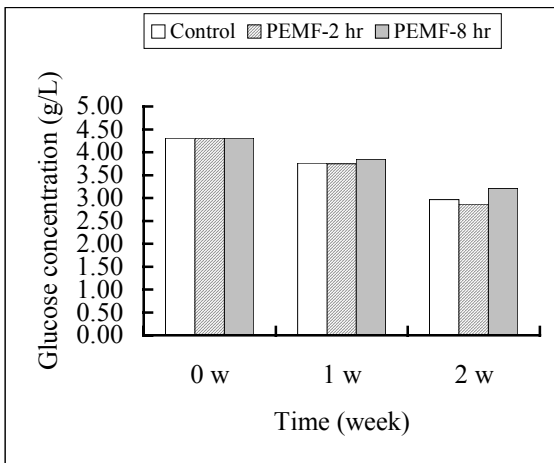


Figure 5. Glucose concentrations of Control, PEMF-2 hr, and PEMF-8 hr at different time points with 8 mV/cm.

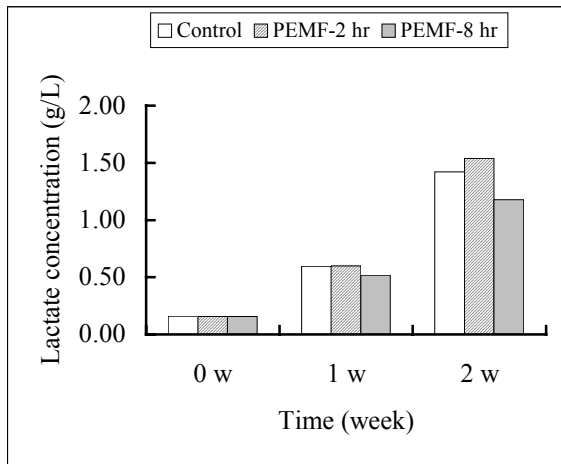


Figure 6. Lactate concentrations of Control, PEMF-2 hr, and PEMF-8 hr at different time points with 8 mV/cm.

10-5 STUDENT

EFFECTIVE EVALUATION OF HANDSET EXPOSURES IN DIFFERENT NETWORKS UNDER REAL-LIFE CONDITIONS. D. Spät*, J. Fröhlich*, N. Kuster, Foundation for Res on Information Technologies in Society (IT'IS), Swiss Federal Inst of Tech (ETH), CH-8092 Zurich, Switzerland.

INTRODUCTION: Most epidemiological studies on possible adverse health effects from mobile phone usage classify the exposure via the daily usage. Enhanced characterization of the exposure would allow for better classification of different user groups and therefore enhance the sensitivity towards a possible exposure-effect relation. Compliance data of mobile phones only deliver the maximum spatial peak SAR occurring in the user. The real-life head and brain exposure is much better characterized by the exposure pattern times the average output power. For the assessment of the average output power, the power control function of a mobile phone has to be recorded under real-life conditions. The characteristic of the power control function is highly dependent on the environment, base station density, network traffic, usage (stationary, walking, driving etc.) and the position of the phone at the head.

OBJECTIVE: The objective is to design a system for recording the power control (PWC) function of different handsets in different environments and under different usage conditions (stationary, moving). System requirements include:

- sampling rate: > 3000 samples/s (rise time < 0.1s)
- dynamic range: < 1mW/kg to 2W/kg
- linearity: < 0.2dB
- noise: < 1mW/kg
- temperature range: 10-40 °C (<< 1dB)
- humidity: 0 - 90%
- relative position accuracy (head/phone/probe): < 1mm
- battery and DC operated

METHOD: The design includes phantom heads containing field probes at the location of the ear. An additional mechanism allows the positioning of the handset in different ways including the predefined positions given in the standards on compliance testing of mobile phones (FCC, CENELEC). Up to four phantom heads, each holding two handsets, can be evaluated at a time. The system can be mounted on a trolley or put in a car simulating different ways of moving.

RESULTS: A prototype of the system and the corresponding measurement methodology were derived in order to record the exposure characteristics of different handsets all compared to a software-modified

phone delivering PWC settings. This allows the derivation of handset-specific differences with respect to power control, network provider, environment and positioning at the head. It also includes the ability to assess the differences of the power control between GSM and CDMA networks. It has proven to be an effective tool for the assessment of the exposure in epidemiological studies as well as the testing of the quality of handsets and of service providers.

The study was supported by the Cellular Telephone and Internet Association (CTIA) and Sunrise TDC.

10-6

AVERAGING METHODS FOR RELIABLE MEASUREMENTS OF THE ELECTROMAGNETIC FIELD STRENGTH IN THE VICINITY OF MOBILE COMMUNICATIONS BASE STATIONS.

P. Preiner, R. Überbacher, A. Kaczmarczyk, G. Neubauer*. Seibersdorf Research, Austria.

BACKGROUND: The area-wide maintenance of 4 GSM and 5 UMTS networks in Austria is warranted by about 17,000 mobile communication base stations. The radio frequency electromagnetic fields transmitted by the base stations are subject of public and private interests.

For the implementation of the protective measures of the European directive the European Committee has mandated international standardization institutions for creating harmonized standards. These standards should guarantee human public health protection in respect of electromagnetic field emission from mobile communication base stations. In the frame of the EUREKA project BASEXPO the exposure in the vicinity of mobile communication base stations taking into account emissions from other sources was evaluated using reliable methods. The ICNIRP (International Commission on Non-Ionizing Radiation Protection) guideline requires averaging procedures over a volume corresponding to the body of a human being, therefore the volume under investigation was approximately equal to this size.

OBJECTIVE: The investigations are dedicated to derive averaging methods which allow a representative statement about the field distribution using a limited number of measurement positions.

METHODOLOGY: The electromagnetic field strength in different indoor scenarios (7 story office building in Vienna [GTU – general typical urban], a 1 story office building in Seibersdorf [GRA – general rural area] and a lab building complex [GRA] in Seibersdorf) were examined in constricted volumes corresponding to the human body taking the spatial variation as well as the variation in time into account. A cube with an edge length of 90cm was chosen to fit the size of a human being with 7 times 7 examined positions in one layer, 7 layers in direction of the z-axis resulting in 343 examined positions. The distance between each examined position is 15cm. Measuring 343 positions takes a lot of time, therefore averaging procedures were created to reduce the effort of the measurement process. The reduction of examined positions was investigated by creating 1-, 2- and 3-dimensional templates consisting of only 3 to 12 examined positions. These templates were virtually moved through each measured cube delivering mean values which were then compared to the global mean of a cube. These comparisons should indicate how accurate each template is compared to the global mean.

RESULTS: Several templates, representing different averaging schemes, were applied to investigate the reliability in respect of the global mean value. Within all examined 1-dimensional templates a template including 3 vertical consecutive positions with a distance of 45cm between each other showed the lowest deviation from the global mean value. Out of all 2-dimensional templates, a template with 9 examined positions showed the lowest deviation from the global mean value and finally a 3-dimensional template consisting of a larger number of examined positions seemed to have the lowest deviation from the global mean. The result indicates that 2-dimensional geometrical figures might be better suited than three-dimensional templates. Line-combinations with bigger distances between the examined positions appear to be more suitable for delivering a more accurate mean value of the electromagnetic field strength compared to the global mean value. Geometrical figures with a small number of examined positions which comprises a bigger area might be better suited than figures with more examined positions comprising a small area.

CONCLUSION: Averaging methods are delivering deviations from the mean value of a template

compared to the global mean value in the range of 14.6% (Area with 8 positions) to 137.5% (Line with 3 positions). Depending on the desired accuracy such averaging methods seem to be a good approach for a low effort and reliable measurement methods.

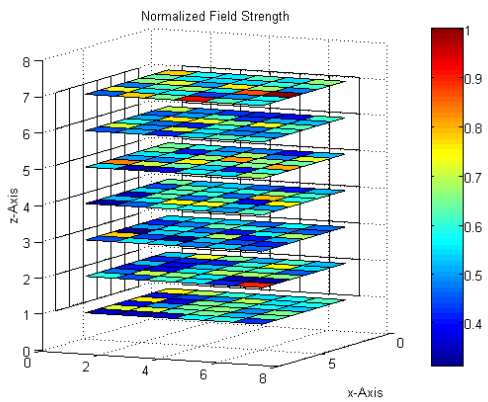


Figure 1: Normalized electromagnetic field distribution in a constricted volume (cube).

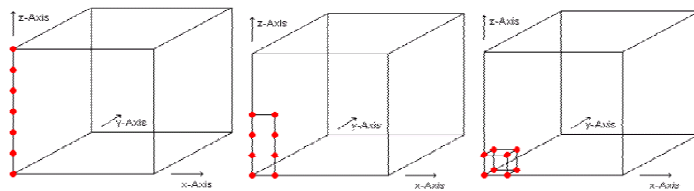


Figure 2: Examples for a 1-, 2- and a 3-dimensional template which were operated thru all examined volumes.

PLENARY SESSION III:
THZ SCIENCE AND ITS MEDICAL POTENTIAL
BIOFILMS, CLINICAL INFECTIONS AND A ROLE FOR EM
FIELD CONTROL
Chair: Bruce McLeod

**APPLICATIONS OF TERAHERTZ FREQUENCY RADIATION IN MEDICINE AND BIOLOGY:
A NEW TOOL FOR DIAGNOSIS, THERAPY AND ANALYSIS.** M. Chamberlain, University of
Durham, Medical Imaging, UK

Until recently the Terahertz region of the spectrum (generally taken to be: in frequency, 300GHz to 10THz; in wavelength, 1000 μm – 30 μm) has resisted attempts to harness its potential for application, largely because of the difficulty in providing a suitable source of radiation. Such sources as have hitherto been available are, usually: weak, bulky, expensive, and incoherent. Despite these concerns, there are many important reasons why the THz range is of intrinsic scientific interest and is rich in actual or potential applications. THz radiation is non-ionising, penetrates many visually opaque materials, suffers less Rayleigh scattering than infra-red, interacts strongly with water but passes through a few mm of biological tissue and a km of mist. Many material excitations lie in the THz range e.g. molecular rotations and librations, thus providing chemical “signatures”. It is noteworthy that a variety of important natural phenomena involve the THz frequency range. For example: the value of thermal energy ($K_{\text{B}}T$) at room temperature (300K) corresponds to approximately 6THz, so that biological processes might be regarded as THz phenomena. There are, therefore, powerful motivations for the development of systems for the generation, detection and manipulation of radiation at THz frequency.

Recent research has shown that: different tissues, and different tissues in various states of health and disease, affect the propagation and reflection of Terahertz radiation differently. The background to this remarkable sequence of observations will be discussed in the context of Terahertz images taken of soft and hard tissue. The origin of contrast in such images, and the significance of the various parametric representations that can be used to display information, will be outlined in this talk, as will some recent advances in instrumentation. The potential of medical Terahertz imaging and sensing will be compared to other modalities at this early stage of development. Finally, major concerns with the future development of Terahertz medical imaging, including safety issues, will be reviewed.

The basic building blocks of life show a characteristic spectra in the Terahertz frequency range due to the collective motion of large atom groups moving as rigidly bound subgroups, connected by weak hydrogen bonds of base pairs. This provides a sensitive tool to study the topology of biomolecules and, in particular, the conformational changes that are important in protein flexibility, and which can often be triggered by optical or other means. Furthermore, Terahertz frequency spectroscopy offers the distinct possibility that mutations in DNA can be investigated sensitively using a non-contact technique that may, one day, replace fluorescence probes. Progress in this general area will be reviewed, and the possibility of time-resolved studies of conformational changes will be discussed.

There have been many reports over the years that millimetre wave radiation can be used therapeutically. Some of the claims for this work have rested on rather insubstantial evidence, but often the (unsubstantiated) idea that biological systems might sustain coherent excitations has been invoked to provide some basis for these alleged observations. The Talk will therefore conclude with: a summary of the most recent investigations of the effects of Terahertz radiation on the efficiency of biological processes, such as enzyme activity; and of the experiments that need to be undertaken to test this intriguing hypothesis.

THE USE OF ULTRASOUND FOR BIOFILM STERILIZATION. W. Pitt, Brigham Young University, Chemical Engineering, 320 Clyde, Provo, UT 84602, USA.

Low frequency ultrasound (LFUS), having frequencies below 500 kHz, has not traditionally found timely application in medicine because of the difficulty in focusing and the lack of strong absorption (very little ultrasonic heating). However, since the mid 1990s there has been an increasing amount of research that has taken advantage of the low cavitation threshold of LFUS. While cavitation is often avoided in most diagnostic and therapeutic applications at higher frequency, LFUS often employs cavitation or its effects to accomplish a medical or biological goal. For example, LFUS has been employed to release drugs from polymeric carriers, and to render capillaries and cell walls more permeable to drugs. It is hypothesized that shear forces caused by oscillating bubbles create stresses on cell membranes or capillary walls, disorganizing the native structure and increasing the permeability toward drugs or drug carriers. For example, in our lab we have been able to sterilize biofilms with the combination of 70-kHz ultrasound and gentamicin; in other experiments we have reduced the growth of tumors in rats using 28-kHz ultrasound and anti-cancer drugs in polymeric carriers. Application of 20-kHz ultrasound above the inertial cavitation threshold renders normally impermeable skin more permeable toward large molecules such as insulin. While the above-mentioned technologies employ fairly low energy cavitation events, there are some medical procedures that use very high power densities with the goal of damaging tissue or structures by intense cavitation. Examples are ultrasound-assisted liposuction and shock-wave lithotripsy. There remain some challenges to the more widespread use of LFUS in medicine. These include the need for better focusing technology for spatial control, and the need for better understanding of the physics of cavitation in various tissues, such the threshold for inertial cavitation in the presence (or absence) of introduced gas bubble nuclei.

SESSION 11: BIOLOGICAL EFFECTS AND MEDICAL APPLICATIONS

Chair: Martin Blank and Mike McLean

11-1

BIOLOGICAL EFFECTS OF EMF, DO THEY EXIST AND WHAT MIGHT BE THEIR BIOPHYSICAL MECHANISM – A MOLECULAR BIOLOGISTS PERSPECTIVE. D. Leszczynski. STUK – Radiation and Nuclear Safety Authority, Helsinki, Finland.

There are ongoing many epidemiological and animal studies that are looking for health effects of EMF exposures. However, are these studies scientifically justified? There will never be any health hazard of EMF exposure without induction of biological effects. We need the proof of biological effect(s) induced by EMF exposure because only then the studies looking for potential health effects will be scientifically justified. However, at the present, we are still missing such reliable and replicable proof.

The early signs of cell response to any stress factor are changes in protein phosphorylation that include phosphorylation-induced activation of stress response proteins – the Hsp. Such responses, induced by EMF exposure on whole-proteome scale phosphorylation and expression of Hsp could relatively fast prove or disprove the ability of EMF to induce any biological responses. However there are published only two such whole-proteome studies of protein phosphorylation induced by EMF exposures (Pipkin et al. 1999; Leszczynski et al. 2002). Hopefully inclusion of this research topic into the revised research agenda of the WHO EMF Project will provide much needed boost for such studies.

Numerous studies have demonstrated that EMF exposure may induce some biological effects in living cells. However, because of the lack of known biophysical mechanism that would explain these effects, many put in question the existence of such biological responses. The major problem appears to be the very low level of energy deposited in living cell by EMF-emitting devices that meet the present international safety standards. This energy is far below the energy level needed to break chemical bonds or to change conformation of ready biological molecules. However, one needs to consider also that there might be effects that could alter conformation of proteins-in-making and their aggregation. Potential effect of EMF exposure on aggregation of bio-molecules and cells has been suggested in the report from the Mobile Manufacturers Forum organized Seminar in “Mechanisms for Interactions of Radiofrequency Energy with Biological Systems”, Washington DC, USA, May 22-23, 2001 (Swicord et al. 2001)

The working hypothesis will be proposed, that will suggest the biophysical mechanism behind the observed biological effects. This working hypothesis will account for the:

- Role of protein folding (amino acid sequence)
- Role of stress proteins
- Role of cellular protein crowding-phenomenon
- Role of protein networks- phenomenon

This working hypothesis will also suggest why the replicability of the EMF-induced biological effects appears to be so “difficult”.

References.

Pipkin JL, Hinson SG, Young JF, Rowland KL, Shaddock JG, Tolleson WH, Duffy PH, Casciana DA. (1999) Induction of stress proteins by electromagnetic fields in cultured HL-60 cells. *Bioelectromagnetics* 20: 347-357.

Leszczynski D, Joenväärä S, Reivinen J, Kuokka R. (2002) Non-thermal activation of hsp27/p38MAPK stress pathway by mobile phone radiation in human endothelial cells: Molecular mechanism for cancer- and blood-brain barrier-related effects. *Differentiation* 70: 120-129.

Swicord M, Lang S, Gollnick F. (2001) Mechanisms for Interactions of Radiofrequency Energy with Biological Systems: Principal Conclusions from a Seminar held in Washington, DC. Report available at:

11-2

VARIABLE EFFICACY OF A STATIC MAGNETIC FIELD AGAINST CHEMICALLY- AND GENETICALLY-INDUCED AUDIOGENIC SEIZURES (AGS) IN MICE. M.J. McLean, S. Engström, R.R. Holcomb, M. Zhang, Department of Neurology, 2100 Pierce Avenue, Vanderbilt University School of Medicine, Nashville, TN 37212, USA.

OBJECTIVE: To compare protective effects of a static magnetic field (SMF) consisting of a strong gradient component perpendicular to the local field vector against chemically-induced seizures and genetically-determined AGS in different mouse strains.

METHODS: Mice obtained from Charles River Laboratories, Wilmington, MA, including DBA/2 (“young”, 26-30 days old and susceptible to AGS; “old”, >48 days old, not susceptible to AGS) and ICR/CD-1 outbred mice. Animals were handled in accordance with standards of the National Institutes of Health and methods approved by the Vanderbilt University Institutional Animal Care and Use Committee. Magnetic field pretreatment was accomplished with a previously described water-cooled, static magnetic field (SMF) exposure device built with commercially available coils around four ferromagnetic cores in a square array. The coils were wired such that polarity alternated. A constant current power supply energized the coils. All mice were kept in perforated tubes prior to experiments. Different groups of mice were pretreated with sham or SMF exposure for 30 min before SMF exposure ($B=5.27$ mT, ∇B (perpendicular) = 0.24 T/m; values averaged over head volume). For acoustic stimulation, freely moving mice were observed in a closed chamber. A speaker in the lid delivered intermittent mixed-frequency sound at 120 decibels. Untreated AGS evolved from wild running (WR), to loss of righting (LOR), clonic jerks (CLO), tonic hindlimb extension (THE) and death (DEA).”Young” DBA/2 mice had AGS with acoustic stimulation only. Intraperitoneal (ip) injection of theophylline (75 mg/kg) induced AGS in “old” DBA/2 and wild-type mice. Occurrence of seizure stages in different groups of mice was compared.

RESULTS AND CONCLUSIONS: SMF pretreatment had different effects on AGS, depending on mouse strain (data normalized against concomitant sham controls): No seizures occurred in ~50% of “young” DBA/2 mice ($p<0.05$ to 0.01; seizures were unaffected in the rest. Against theophylline-induced AGS in “old” DBA/2 mice, SMF pretreatment reduced CLO (29%), THE and DEA (31%; $p=0.05$); other seizure manifestations were unaffected. SMF pretreatment produced no significant protection against theophylline-induced AGS in ICR/CD-1 mice. These findings suggest that strain- and age-dependent genetic factors modulate the response of AGS to pretreatment with SMF.

Supported by a research agreement between Holcomb Healthcare Services and Vanderbilt University.

11-3

INITIAL INTERACTIONS IN EM-STIMULATED BIOSYNTHESIS. M. Blank¹ and R. Goodman², Departments of Physiology¹ and Pathology², Columbia University, New York, New York 10032, USA.

An understanding of mechanism for EM field interaction with cells is essential for practical developments, such as medical applications and a scientific basis for safety standards. Central to progress in the two areas cited is explaining how EM fields initiate gene expression, specifically, the well established stimulation of the stress response found in ELF and RF ranges (1,2,3). Studies on a variety of systems indicate that the fields stimulate transcription by interacting with electrons in DNA, probably destabilizing the H-bonds holding the two DNA strands together (4). Several lines of evidence have led to this hypothesis:

· Consistently low thresholds at which EM fields stimulate many cellular processes indicate that the

processes require little energy (5,6). Such weak EM fields accelerate biochemical electron transfer reactions, e.g., cytochrome oxidase and the Belousov-Zhabotinski reaction (7,8).

- Electromagnetic response elements (EMREs) in the promoters of genes are needed for EM field interaction with DNA. A 900 base pair segment containing EMREs in the hsp70 promoter is needed for the response to EM fields (9). Removal of the segment eliminates the response, and transfection into a promoter construct renders the construct EM field responsive (10). The CTCT bases in EMREs have low electron affinity, indicating that electrons would be displaced relatively easily.
- EM field interaction with DNA can account for *in vivo* and *in vitro* biosynthesis by electric fields (11), with thresholds comparable to those observed in model systems (4).
- Frequency response in several biological systems suggests that EM fields require repetition and are most effective at frequencies that coincide with natural rhythms of the processes affected (12).

Potential medical applications, based on EM stimulation of the stress response and the use of EMREs in genetic engineering (9), take advantage of the fact that bioelectromagnetic techniques require little energy, are non-invasive and easily directed. In fact, the low thresholds at which EM fields stimulate biological processes, including the protective stress response, are orders of magnitude below suggested safety standards. The biological evidence demands a re-evaluation of safety criteria to include these 'non-thermal' responses.

References

- (1) Goodman, Blank (1998) *Cell Stress & Chaperones* 3:79-88.
- (2) dePomerai, Daniells, David, Allan, Duce, Mutwakil, Thomas, Sewell, Tattersall, Jones, Candido. *Nature* 405:417-418
- (3) Leszczynski, Joenvaara, Reivinen, Kuokka (2002) *Differentiation* 70:120-129.
- (4) Blank, Goodman (2004) *J Cell Physiol*, in press.
- (5) Blank, Goodman (2001) *J Cell Biochem* 81:689-692.
- (6) Goodman, Blank (2002) *J Cell Physiol* 192:16-22.
- (7) Blank, Soo (2001) *J Cell Biochem* 81:278-283.
- (8) Blank, Soo (2003) *Bioelectrochem* 61:93-97.
- (9) Lin, Blank, Goodman (1999) 75:170-176.
- (10) Lin, Blank, Rossol-Haseroth, Goodman (2001) *J Cell Biochem* 81:143-148.
- (11) Blank (1995) *Adv Chem* 250:143-153.
- (12) Blank, Soo (2001) *Bioelectrochem* 53:171-174.

SESSION 12: BIOPHYSICAL AND BIOLOGICAL
DOSIMETRY II

Chair: Junji Miyakoshi and Carl Blackman

12-1

EFFECTS OF ELECTROMAGNETIC STIMULATION ON PATIENTS RECOVERY AFTER ARTHROSCOPY SURGERY. S. Setti¹, C. Zorzi*², C. Dall'Oca*³, R. Cadossi¹. ¹Laboratorio di Biofisica Clinica, IGEA, 41012 Carpi (Mo), Italy; ²Ospedale "S. Cuore", 37024 Negrar (Vr), Italy; ³Ospedale "Borgo Roma", 37134 Verona, Italy.

INTRODUCTION. The degeneration of articular cartilage shows itself very frequently and gets progressively serious with age. Just only think that changes in cartilage surface appear only in 5% of the population younger than 25, while they are present in over 80% of people over 75(1). Our experimental studies *in vitro* and *in vivo* demonstrate that the treatment with ONE is able to prevent cartilaginous degeneration and to favour the healing of cartilaginous lesions treated with osteocondral grafts (2,3).

OBJECTIVE. The purpose of this randomised, prospective and double blind study was to evaluate the therapeutic effect of ONE on cartilaginous lesions of the knee, Outerbridge degree I, II, III, IV, diagnosed and treated in arthroscopy.

MATERIALS AND METHODS. Between May 2002 and September 2003 patients have been recruited at "S. Cuore" Hospital in Negrar, Verona, who presented pain symptomatology at knee. The same patients have been treated by arthroscopy with condroabrasion and/or perforations. The patients have been randomised in 4 homogenous groups separate from each other for the seriousness of the cartilaginous lesion according to Outerbridge degree. All patients received the ONE stimulator: half were active and half were placebo. The treatment with ONE started within 7 days since arthroscopy and continued for 90 days, 6 hours per day. The patients were submitted to clinical evaluation at 0, 45 and 90 days since the beginning of stimulation. The clinical evaluation of pain was carried out by means of the Visual Analogue Scale-VAS by Scott and Huskisson. The clinical evaluation about health was carried out by means of the KOOS test (Knee Injury and Osteoarthritis Outcome Score) used to monitor the effects of a treatment (pharmacological, surgical and rehabilitative) on the knee. This includes the evaluation of articular rigidity and functional limitations. The questionnaire maximum score is 100, corresponding to optimal health. It was also evaluated the need of using NSAD. The data were processed following the Stepwise logistical model.

RESULTS. 32 (16 M- 16 F) patients were evaluated, 17 patients belonging to the active group and 15 to the placebo one. The average stimulation time for the two groups was 4.5 hours per day. The KOOS test highlighted that, even starting at time zero from the same value ($p=n.s.$), the KOOS values at 45 and 90 days are higher in the active group, the difference is significant at 90 days ($p<0.05$). The percentage of patients who had taken anti-inflammatory drugs and underwent the treatment with active stimulator is 29%, compared to 82% of the patients belonging to placebo group ($p<0.004$).

CONCLUSIONS. The treatment with ONE has shown to be effective in recovering patients after treatment in arthroscopy, favouring a fast and complete healing and reducing the use of NSAD. Our studies show that the treatment with ONE has a positive effect on articular cartilage and on its repair, and its efficacy will have to be challenged in clinical studies involving the repair of large cartilage defect with chondrocyte transplantation.

References.

- 1) Buckwalter JA, et al.: Articular cartilage: degeneration and osteoarthritis, repair, regeneration, and transplantation. Instr Course Lect. 1998,47:487-504.
- 2) De Mattei M, et al.: Effects of electromagnetic fields on proteoglycan metabolism of bovine articular cartilage explants. Connective Tissue Research 2003,44(3-4):154-9

3) Benazzo F, et al.: Biological effects of pulsed electromagnetic fields in the integration of osteochondral grafts in a animal model. 2nd European Congress Of Sport Traumatology- Monaco, 2003.

12-2

WHOLE BODY AVERAGE SAR COMPUTED IN A CHILD BODY AT FREQUENCIES FROM 1 GHZ TO 6 GHZ. G. Bit-Babik, A. Faraone, C.K. Chou, M. Swicord. Motorola Florida Research Labs, Fort Lauderdale, FL. 33322. USA.

INTRODUCTION: The present study was performed to calculate the whole body (WB) average SAR for a child model exposed to RF energy at frequencies from 1 GHz to 6 GHz. The IEEE C95.1-1999 *Standard for Safety Levels with Respect to Human Exposure to Radio Frequency Electromagnetic Fields from 3 kHz to 300 GHz* and *International Commission on Non-Ionizing Radiation Protection (ICNIRP)* define the basic restrictions on exposure level in terms of *specific absorption rate (SAR)* averaged over the body and the spatial peak locally averaged SAR. Maximum permissible exposure (MPE) levels in the IEEE standard and reference levels in the ICNIRP are derived to ensure that the basic restrictions are met for frequencies between 100 kHz and 6 GHz (IEEE) or 10 GHz (ICNIRP). The MPE levels were derived from prolate spheroids in the 1980's. Mason et al. (2000) and Dimbylow (2002) have shown that in inhomogeneous adult models the WB SAR levels are higher than those calculated for spheroids. Dimbylow (2002) also showed that in a scaled child model the WB SAR could be higher than permitted using the existing MPEs.

OBJECTIVES: The goal of this work was to estimate the whole body average SAR for a 1-year old child model exposed to a plane wave at frequencies from 1 GHz to 6 GHz.

METHODS: To verify the results of Dimbylow (2002), this study was conducted first for E-field parallel to the body axis. According to the RF dosimetry handbook, WB SAR in 1 year old child spheroid model exposed to H polarization plane wave are higher than those of E-polarization at frequencies above 1 GHz. Therefore, WB SAR of H polarization was also calculated. A scaled 5 mm resolution heterogeneous model of a human body with 23 different tissues (Brooks Visible Man) was used for this study. Scaling was performed by changing the voxel size to produce two child models with mass of 8 kg and 10 kg with the height of 56 cm or 75 cm respectively to study the effects of different body size. The scaled voxel sizes were (2.5 x 2.5 x 1.6) mm and (2 x 2 x 2.5) mm respectively.

RESULTS: The whole body average SAR was computed for 1-year old child model at frequencies from 1 GHz to 6 GHz for plane wave exposure. In general there is a good agreement with the results up to 3 GHz published by Dimbylow except for about 30% lower SAR values in the 2 GHz frequency region. H polarization SAR is slightly higher than E polarization. These results are presented in the form of plane wave power densities required to produce WB average SAR limits in the body.

CONCLUSIONS: The computed WB average SAR results show that the present maximum permissible exposure levels at frequencies from 2 to 6 GHz are not consistent with basic-restriction limit imposed on WB average SAR by the existing IEEE RF safety standard.

References.

Mason, P.A.; Hurt, W.D.; Walters, T.J.; D'Andrea, J.A.; Gajsek, P.; Ryan, K.L.; Nelson, D.A.; Smith, K.I.; Ziriak, J.M. "Effects of frequency, permittivity, and voxel size on predicted specific absorption rate values in biological tissue during electromagnetic-field exposure." IEEE Trans. on Microwave Theory and Techniques, Vol. 48, No 11, 2000, pp. 2050-2058.

P.J. Dimbylow, "Fine resolution calculations of SAR in the human body for frequencies up to 3 GHz." Physics in medicine and Biology, No. 47, pp2835-2846, 2002.

DETERMINATION OF LOW FREQUENCY MEASUREMENT CAPABILITY OF AGILENT 85070C DIELECTRIC PROBE KIT. M. Ballen*, M. Kanda*, M. Douglas*, C.K. Chou. Motorola Labs, Corporate EME Research Lab, Fort Lauderdale, FL. 33322. USA.

OBJECTIVE: This study evaluates the low frequency capability of the open ended coaxial probe beyond the manufacturer's specifications.

METHOD: A common method to measure the dielectric parameters of tissue-equivalent liquids is the open ended coaxial probe. This method is easy to use and allows for frequency sweeping across a broad range. The widely available Agilent 85070C Dielectric probe kit has a stated operating frequency of 200 MHz to 20 GHz [1]. For measurement of tissue-equivalent liquids below 200 MHz, a similar method is desired. To demonstrate the low frequency accuracy of Agilent's open-ended coax probe method, measurements of three lossy liquids (0.1 M saline, Di-ethylene glycol butyl ether (DGBE)-based solution, and diacetin-based solution) were performed and compared with intrinsic measurements of a slotted line. The length of the slotted line is approximately 0.9 m that is sufficient to minimize reflections at frequencies of interest. 0.1M saline was chosen because the dielectric characteristics have been published. The DGBE and diacetin solutions are recipes predicted to have dielectric parameters similar to those of tissue-equivalent liquids at 75 MHz using the method found in [2]. The diacetin solution is composed of 55.7% water, 43% diacetin, 1.2% salt, and 0.1% bactericide. The DGBE solution is composed of 56.6% water, 42% DGBE, and 1.4% salt.

RESULTS: The accuracy of the Agilent 85070C for 0.1 M saline is shown in Tables 1 and 2. Measurement data at 23 ± 1 °C are compared with results of equations by Chris Davis derived from [3] and results using a capacitive technique at 25°C reported in [4]. The results are in close agreement across the frequency range of 75 – 3000 MHz, considering the differences in methods and environmental conditions. The DGBE-based and diacetin-based solutions also showed agreement between the two methods (within 10%) for both permittivity and conductivity from 75 to 300 MHz as shown on Tables 3 and 4. Below 75 MHz, the results show good agreement for the conductivity, but there is substantial deviation between the two methods for permittivity of the diacetin-based solution.

CONCLUSION: In this study, low frequency dielectric measurement accuracy of the HP open-ended coaxial probe was shown using comparison to published results and measurements using a slotted line. The results give confidence in the use of the Agilent 85070C for tissue-equivalent liquids over an increased frequency range. Further investigation will include additional dielectric measurement methods to determine if the low-end frequency cutoff can be extended below 75 MHz.

References:

- [1] Agilent, "Agilent 850702D Dielectric Probe Kit: Product Overview," available at <http://cp.literature.agilent.com/litweb/pdf/5968-5330E.pdf>
- [2] M. Kanda, M. Ballen, S. Salins, C-K. Chou. "Tissue Simulation Prediction (TSP)," *Bioelectromagnetics Society Annual Meeting*, St. Paul, MN, June 10-14, 2001
- [3] A. Stogryn, "Equations for Calculating the Dielectric Constant of Saline Water (Correspondence)," *IEEE Trans. MTT*, MTT-19, 733-736, Aug. 1971.
- [4] A. von Hippel, *Dielectric Materials and Applications*, MIT Press: Cambridge, MA, 1954.

Table 1: Measured conductivity of 0.1 M saline solution using the Agilent 85070C and slotted line, as compared with reference data from Arthur von Hippel [4] and Chris Davis.

f (MHz)	85070C	Slotted line	von Hippel	Davis
75	0.97	1.02		0.98
300	0.99	1.04	0.99	0.998
837	1.15	1.18		1.129
1000	1.22	1.26		1.193
3000	3.133	2.95	3.02	2.86

Table 2: Measured permittivity of 0.1 M saline solution using the Agilent 85070C and slotted line, as compared with reference data from Arthur von Hippel [4] and Chris Davis.

f (MHz)	85070C	Slotted line	von Hippel	Davis
75	80.8	77.9		76.95
300	78.48	79	76	76.93
837	77.6	77.76		76.81
1000	77.43	77.56		76.75
3000	75.15	76.5	75.5	75.15

Table 3: Measured dielectric parameters using the two methods for diacetin-based solution.

f (MHz)	Conductivity (S/m)		Relative Permittivity	
	85070C	Slotted line	85070C	Slotted line
30	0.85	0.85	63.9	50.5
40	0.86	0.87	60.7	50.1
50	0.86	0.87	58.9	50.5
60	0.86	0.87	56.7	50.6
70	0.86	0.87	56	50.8
80	0.86	0.86	55.4	51.1
100	0.87	0.86	54.7	50.8
150	0.88	0.87	54	50.7
300	0.94	0.93	52.1	49.5

Table 4: Measured dielectric parameters using the two methods for DGBE-based solution.

f (MHz)	Conductivity (S/m)		Relative Permittivity	
	85070C	Slotted line	85070C	Slotted line
30	0.72	0.75	57.7	63
40	0.73	0.74	56.2	60.7
50	0.73	0.75	56.6	58.1
60	0.73	0.75	53.7	56.7
70	0.73	0.75	54.6	55.7
80	0.73	0.77	54.1	54.5
100	0.74	0.77	53.3	53.9
150	0.75	0.79	52.8	52.7
300	0.83	0.86	50.5	50.3

LONG-TERM MONITORING OF STATIC ELECTRIC FIELD AND SPACE CHARGE NEAR AC TRANSMISSION LINES. W.H. Bailey¹, T.D. Bracken², R.S. Senior^{2*} ¹Exponent™, New York, New York, 10170 USA, ²T. Dan Bracken, Inc., Portland, Oregon, 97202 USA.

BACKGROUND: A vertical static electric field and space charge consisting of electrically charged air molecules (air ions) and aerosols are part of the ambient electrical environment. Corona on an alternating current (AC) transmission line generates air ions of both polarities. The conductors capture most of the ions but a small fraction of the ions are carried away by wind and attach to aerosols that over time can result in a net unipolar space charge in excess of ambient values. Fluctuations in the density of the space charge as it passes overhead produce changes in the static electric field that can be detected at ground level. Historically, this phenomena has been observed near high-voltage conductors as far back as 1927 (Carroll & Lusignan, 1927). Recent short-term measurements of static electric fields greater than 100 V/m (typical background level of static electric field) around AC transmission lines in the United Kingdom have been reported and interpreted as evidence for elevated concentrations of space charge at ground level (Fews et al, 1999; 2002). Computed values of excess ion concentrations downwind of these lines were at least 3000 ions/cm³ and 6000 ions/cm³, respectively. From these data Fews et al. hypothesize that the resulting additional charge on fine aerosols may be sufficient to increase the deposition of aerosols in the respiratory tract and enhance the toxic effects of inhaled ambient pollutants in the air.

OBJECTIVE: To analyze previous (1990-1992) long-term measurements of static fields, air ions, and meteorological parameters made at the edges of rights-of-way of two 230-kV transmission lines (North site) and a single 345-kV line (South site) in New Hampshire, USA (Bracken, 1993). These data were collected for other purposes, but provide the basis for characterizing short and long-term levels of static fields and ions and the influence of wind near operating transmission lines.

METHODS: Measurements of static electric fields (measured with field mills), ion concentrations (measured with ion conductivity meters and assuming mobilities of 1.2×10^{-4} and 1.5×10^{-4} m/s² for positive and negative ions, respectively), and wind speed/direction (cup anemometer/wind vane) were taken on each side of the ac lines at two sites. Many factors (conductor surface condition, temperature, humidity, wind) that affect corona activity and ion production are highly variable. Therefore the parameters associated with corona-generated space charge, like those for audible noise and radio interference, were described by statistical distributions of long-term measurements.

RESULTS: Measurements of electrical and meteorological parameters collected during more than ~5000 hours over more than two years were analyzed. Upwind and downwind values at the NE station at the North site are shown for static field (Figure 1), for static field versus wind speed (Figure 2), and for positive ion concentration (Figure 3). Generally, the no-wind and upwind measurement distributions were very similar over about 98% of their respective sample populations (1-99th percentiles). Downwind distributions deviated from these distributions over about 30% (70-99th percentiles) representing an increase in positive field. Only downwind field values above the 75th percentile in a wind interval were elevated above upwind values at the North Site; no such elevation was seen at the South Site.

CONCLUSIONS: As expected, corona activity produced localized downwind enhancement of ambient atmospheric field levels and ion concentrations. These data are generally consistent with short-term survey measurements reported as far back as 1927. However, this first report of measurements taken over a long period of time reveals that the magnitudes of the downwind values exceed the range of upwind values for only a small percentage of the time under most conditions. Maximum (99th percentile) upwind (ambient) fields were exceeded less than 2% of the time during downwind conditions at the NW and SE stations, less than 11% of the time at the NE station and less than 22% of the time at the SW station. The fields at the SW station were very low; less than 0.6 kV/m for all winds. Downwind positive ion concentrations exceeded the maximum range (99th percentile) of upwind levels for 20% or less of the downwind time at a station, and even less for negative ions. Based on this study, AC transmission lines appear to have a minor impact on potential long-term exposure to space charge outside the right-of-way. Measured ion densities

are much lower than those modeled by Fewes et al. at similar levels of static field.

References:

Bracken T.D. 1993. Program to monitor electric and magnetic fields and ions before and after energization of a ± 450 kV HVDC transmission line in New Hampshire. Fourth annual (and final) report: For the period January, 1992 - October, 1992. Portland: T. Dan Bracken, Inc., Portland, OR.

Carroll JS, Lusignan JT. 1927. The space charge that surrounds a conductor in corona. Trans. Amer. Inst. Elect. Eng. Dec:1350-1357.

Fewes AP, Henshaw DL, Wilding RJ, Keitch, PA. 1999. Corona ions from power lines and increased exposure to pollutant aerosols. Int. J. Radiat. Biol. 75:1523-1531.

Fewes AP, Walding RJ, Keitch PA, Holden NK, Henshaw DL. 2002. Modification of atmospheric DC fields by space charge from high-voltage power lines. Atm. Res. 63:271-289.

This research was supported by EPRI under contract EP-PID#00435.

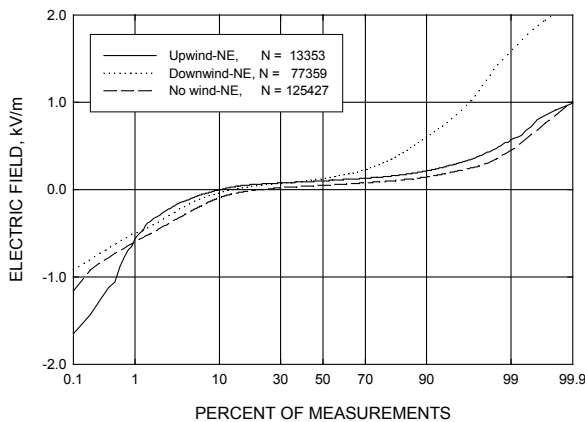


Fig. 1. Cumulative distribution of electric-field measurements by wind condition – North Site-NE Station

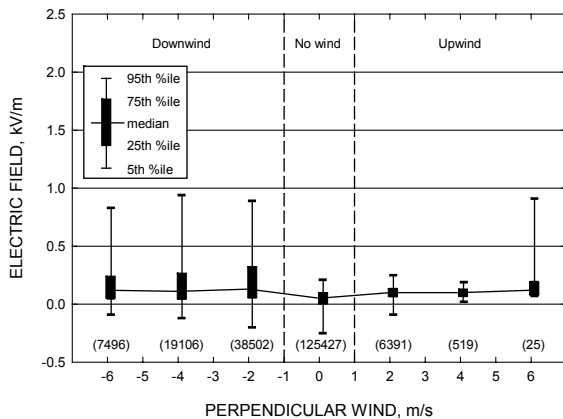


Fig. 2. Electric field versus wind speed by North Site – NE Station

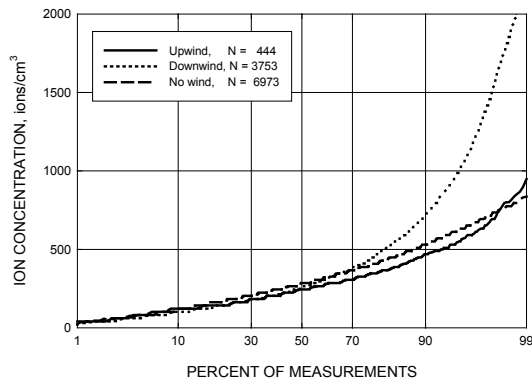


Fig. 3. Cumulative distribution of positive ion concentration measurements at the North Site by polarity and by wind condition: NE Station – positive ions

12-5

FIELD AND TEMPERATURE GRADIENTS IN TISSUES NEAR RESONANT SHORT WIRES. Q. Balzano¹, A.R. Sheppard², K.R. Foster³, M.L. Swicord⁴, ¹Annapolis, Maryland 21401; ²Asher Sheppard Consulting, Redlands, CA 92373; ³Dept of Bioengineering, U. PA, Philadelphia, PA 19104; ⁴Motorola Labs, Ft. Lauderdale, FL 33322 USA.

INTRODUCTION: The largest electromagnetic field and temperature gradients in tissue can be expected near wires of small cross-section carrying large RF currents and charges. These RF sources are quite different from resonant antennas, such as straight or helical wires, and strip-lines, for which the sections with large RF currents and charges are separated by about one-quarter wavelength. In contrast, we consider a thin, short (1/30-1/15 wavelength) conductor with sharp bends at both ends (Fig. 1). The wire supports both high charges and uniform currents along its short length so that it becomes a concentrated source of intense electromagnetic energy. A radiator like this may occur on a mobile phone circuit board if a short linear section of an electrically-small resonant loop is inductively excited. RF current is limited only by the loop's radiation resistance, $\ll 1 \Omega$, not by the feed line characteristic impedance (normally $\sim 50 \Omega$). We calculate SAR (specific absorption rate) in a flat tissue-equivalent slab with high water content placed within a few millimeters of the short wire and therefore tightly coupled to the RF electric and magnetic fields along its entire length.

METHODS: Electromagnetic fields from a short wire were computed using a novel expansion in the coordinate orthogonal to the wire axis. Unlike FDTD analyses, this allowed SAR determinations for arbitrarily small tissue volumes (e.g., a $10 \mu\text{m}$ cube). RF current amplitude on the wire is determined from an average SAR specified for a macroscopic volume (1 cm^3) much greater than the regions of interest. Computations were performed at 900 MHz for a wire 1 cm long, 0.04 cm dia., placed 0.2 cm from a flat tissue-equivalent dielectric slab. Steady state temperature profiles were calculated using a two-dimensional finite element program (PDEase, Macsyma, Inc.) assuming that the irradiated medium had thermal properties similar to those of soft tissue and ignoring convective cooling by blood flow. As an upper-limit approximation, SAR along the wire was assumed to be the same as at its midpoint.

RESULTS: Fig. 2 shows that in the first $50 \mu\text{m}$ layer within the slab (0.2 cm from the wire) and near the wire's midpoint ($z = 0$), the peak SAR values were 5 times higher than the volume-averaged reference SAR of 1.6 mW/cm^3 averaged over 1 cm^3 ($\approx 1 \text{ g}$). SAR decayed linearly with distance from the axis of the wire until $\rho \approx 0.5 \text{ cm}$, a depth about one-half the length of the wire. SAR then decayed $\propto \rho^{-2}$ (inverse square law) until $\rho \approx L$. Exponential decay typical of far field exposure began at a tissue depth approximately 1.5-2 times the wire's length. SAR was attenuated to 0.1 times SAR_{peak} within the first 0.5-0.6 cm of tissue. The SAR distribution (Fig. 2) established the thermal potential for the temperature gradient evaluation.

Calculated temperatures beneath the center of the wire ($z = 0$) for a two-dimensional analysis of planar slabs of a homogeneous tissue-equivalent region (Fig. 3) indicated a maximum increase of approximately 0.25K for the extreme conditions assumed.

CONCLUSION: The method used is useful for calculations in small volumes where high local SAR and corresponding local temperature increases can occur in tissues very close to RF sources with high electromagnetic energy density. Results indicate significantly increased SAR in very small regions. Nonetheless, local temperature increases were less than $\approx 0.25\text{K}$ despite omitting consideration of blood flow and overestimating SAR as a constant along the wire.

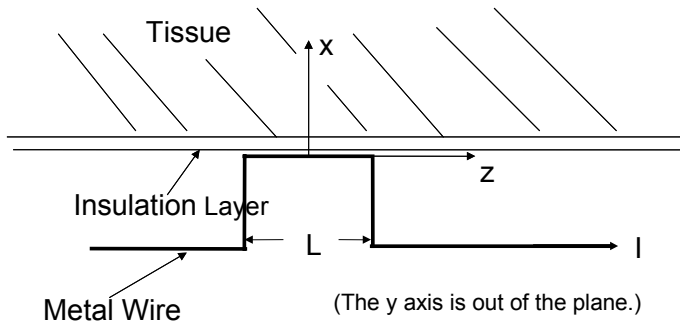


Figure 1. Short wire of length L , carrying current I , near tissue slab.

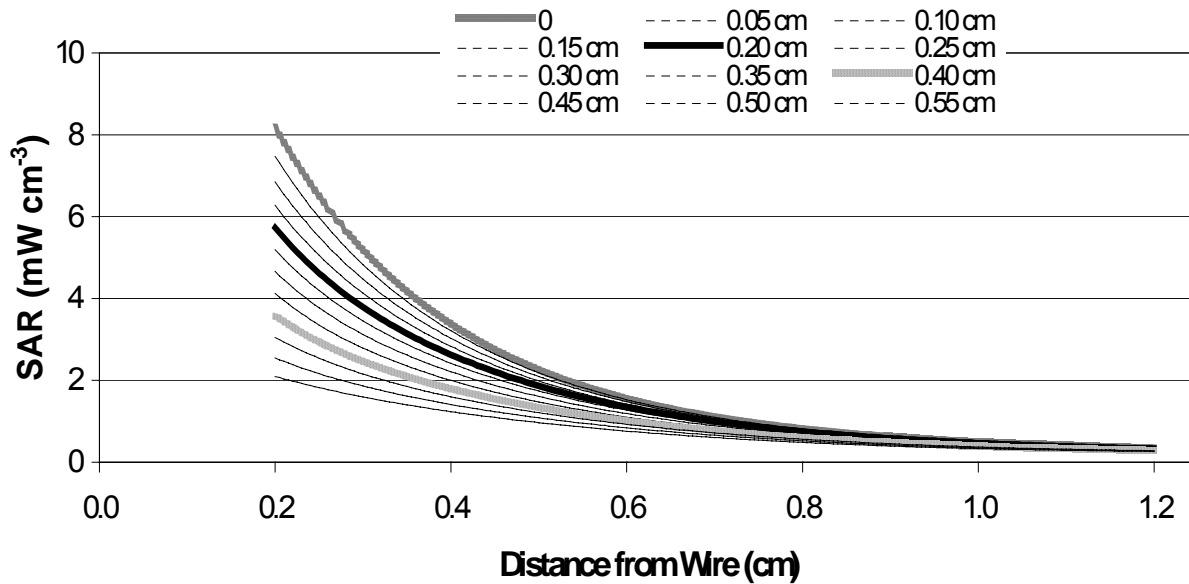


Figure 2. SAR vs depth in a dielectric slab ($\epsilon = 54\epsilon_0$, $\sigma = 1.3 \text{ Sm}^{-1}$) for distances $z = 0$ to 0.55cm from the center of a wire of length $L = 1$ cm carrying 17 mA at 900 MHz.

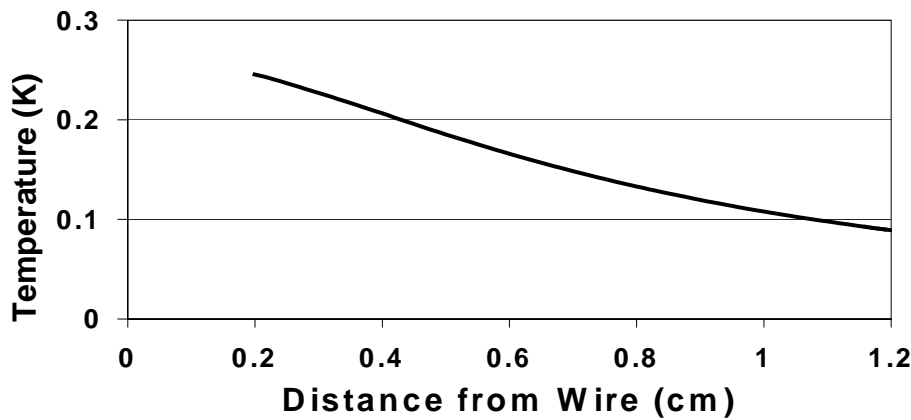


Figure 3. Steady-state temperature increase in tissue (K) at $z = 0$ vs. depth (cm) for worst-case assumptions (see text). The first 0.2 cm corresponds to a layer of insulation (e.g., plastic case) beneath the wire and distances greater than 0.2 cm correspond to tissue.

Research supported by Motorola (QB, ARS) and the Mobile Manufacturers Forum (KRF).

12-6

ACCURATE COMPLIANCE ZONE CALCULATIONS AROUND BASE STATION ANTENNAS USING FULL BODY SAR PROFILING. F.J.C. Meyer, M.J. van Wyk*, M. Bingle*, EM Software and Systems-S.A., EMSS Blding, 32 Techno Ave, Technopark, Stellenbosch, 7599, South Africa.

OBJECTIVES: Spatial-peak and whole-body-averaged SAR assessment in the human body in close proximity to base station antennas is of importance for the assessment of **occupational** compliance to international exposure guidelines and standards. Our goal is to accurately calculate, using numerical simulation techniques, the three-dimensional (3D) SAR profile around a typical base station antenna used in GSM networks for the purpose of comparing this to basic restrictions. This would yield a realistic and accurate occupational exposure compliance zone around a base station antenna. In a previous paper we investigated the level of detail that needs to be included in the numerical models, and in particular, the base station antenna [1]. In this presentation we focus on the human phantom model and compliance zone results obtained.

METHOD: A hybrid Finite Element Method (FEM) / Method of Moments (MoM) has been implemented. The main advantage of the hybrid FEM/MoM compared to the popular FDTD technique is the efficiency with which the large free space region around the base station antenna can be modeled. Numerical experiments were performed to quantify the effect of the shape and size of the phantom on SAR. Further investigations were done on a homogeneous vs heterogeneous phantom to ensure conservative but realistic SAR profiling. A SAM-like full body homogeneous phantom was subsequently selected and used for all SAR calculations. SAR profiling requires FEM/MoM solutions for the human phantom at numerous positions on a 3D grid around the antenna. A total of $9 \times 9 \times 9$ (or 729) different positions were required, which can be reduced to 405 due to the symmetry of the antenna. It was further required to rotate the phantom resulting in another 16 solutions at each position. In total 6480 solutions were required for a complete 3D SAR profile. The efficiency of the FEM/MoM technique [2] enables SAR calculations for the human phantom at all these positions within a realistic time frame.

RESULTS: Positioning of the human phantom (translation and rotation) around the base station antenna and SAR extraction were automated. For the positions close to the antenna, the human phantom has a significant influence on the feed network, and thus on the active power at the antenna elements. This was taken into account and adjusted for in the antenna models as discussed in [1]. SAR results were processed for all positions and compared to the whole-body-averaged as well as 10g spatial-peak **basic restriction**

guidelines. This yields a realistic 3D compliance zone around the base station antenna, which can be compared to the often used but more conservative and unnecessarily restrictive compliance zone based on reference levels.

CONCLUSIONS: The investigation showed that the hybrid FEM/MoM technique can be used for accurate SAR calculations around a GSM base station antenna. These SAR results can then be used to calculate *accurate and realistic* compliance zones around such an antenna.

[1] F.J.C Meyer and M.J van Wyk, “*SAR Profiling of GSM Base Station Antennas for Comparison to Basic Restriction Exposure Guidelines*,” Proceedings of the 6th International Congress of the European Bioelectromagnetics Association, Budapest, Hungary, 13-15 November 2003.

[2] F.J.C Meyer, D.B Davidson, U Jakobus and M.A Stuchly, “Human Exposure Assessment in the Near Field of GSM Base-Station Antennas Using a Hybrid Finite Element / Method of Moments Technique,” IEEE Transactions on Biomedical Engineering, Vol. 50 No. 2, page 224-233, February 2003.

12-7

IMPROVED NUMERICAL MODEL FOR EXPOSURE TO PULSED MAGNETIC FIELD FROM A MOBILE PHONE. A.-P. Sihvonen, K. Jokela. STUK - Finnish Radiation and Nuclear Safety Authority. Helsinki, FIN-00881 Helsinki, Finland.

INTRODUCTION AND OBJECTIVES: Pulsed battery currents generate pulsed magnetic fields and currents in the head of the user of a digital mobile phone.

In the previous work [1] a simplified model, based on a simple current loop and spherical head model and analytical quasi-static calculations, was used for the estimation of current density. The simplified model is based on the vector potential representation of the field produced by the pulsed current in a circuit loop. The induced current was calculated from the simple presentation of analytic vector potential by assuming zero scalar potential.

The current pulses were measured using a current transformer wound over the battery wires of the phone, the current loop (diam. 6 cm) was tangential to the brain simulating sphere, and the distance from the sphere was assumed to be 2 cm. The broadband exposure was assessed by employing the multiple frequency rule and the weighted peak approach [2], both recommended by ICNIRP [3].

In the new work dosimetry was improved by using a realistic heterogeneous head model and actual measured magnetic field of a mobile phone.

METHODS: The numerical code was based on the Finite Integration Technique (FIT) which has not, to our knowledge, previously been used for dosimetric calculations [4]. The measurement was performed with a miniature one dimensional coil probe (1cm², 100 turn), preamplifier and a PICO-212 oscilloscope connected to a PC computer. The coil was attached to the DASY4 (Schmid & Partner Engineering AG, Switzerland) dosimetric test system as a dummy probe. The field was measured in three orthogonal directions and the components were synchronized using a fixed trigger coil beneath the phone. The measured field is used as a source term for the FIT calculation of the induced currents within a realistic head model. Finally, the weighted peak value was determined from the computed current density waveforms.

RESULTS: Preliminary estimations indicate that with the realistic model the current ratios are considerably less than with the case of the simplified model where the exposure ratios varied from 0.05 to 0.14. The exact results will be presented in the meeting. The realistic model gives lower exposures because the size of the equivalent current loop is smaller and the distance of the loop from the brain larger than conservatively assumed for the simplified model.

CONCLUSIONS: The exposure caused by the pulsed magnetic fields in the vicinity of mobile phones does not exceed the present exposure limits.

References.:

[1] Jokela, K., Puranen, L., and Sihvonen, A.-P. Pulsed magnetic field exposure from digital GSM mobile

phones. Health Physics; In press.

[2] Jokela, K. Restricting exposure to pulsed and broadband magnetic fields. Health Phys. 79:373- 388.

[3] ICNIRP, International Commission on Non-Ionizing Radiation. Guidance on determining compliance of exposure to pulsed and complex non-sinusoidal waveforms below 100 kHz with ICNIRP guidelines. Health Phys 84: 383–387; 2003.

[4] Weiland, T. A discretization method for the solution of Maxwell's equation for six-component fields. Electron. Commun. AEU 31:116–120; 1977.

12-8

ANALYSIS OF THE POSSIBILITY FOR WORKERS TO TOUCH PANEL BASE STATION ANTENNAS FROM BEHIND AT 900 MHZ, 1800 MHZ AND 2100 MHZ. C. Dale, V. Dronne, O. Colas, J. Wiart. France Telecom R and D, DMR/IIM, 38-40 rue du Général Leclerc, 92794 Issy-les-Moulineaux Cedex 9, France.

INTRODUCTION: ICNIRP guidelines have been established to protect public and workers from the exposure to electromagnetic fields. On the other hand, it may be useful, in an operating network, to be able to perform some maintenance operations without being obliged to cut off base station input power. Antennas used in GSM/UMTS networks are often directional antennas consisting of radiating elements in front of a metallic panel, leading to a backward radiated field very weak. So it was of interest to know if touching the antenna from behind was possible with respect to ICNIRP guidelines

OBJECTIVES: The aim of this study is to analyse the local and whole body SAR of a worker touching the antenna from behind or the side. This estimation has been carried out through simulations and measurements, using a generic approach, to be able to take into account, as far as possible, *any* panel antenna.

METHODS: Simulations are performed using the FDTD method, very useful to take into account strong inhomogeneities. The body model considered is the Visible Man 3D volume made available by Brooks Air Force. The human model is considered either homogeneous or heterogeneous, and a flattening of the phantom has been performed to fit to the antenna back-panel. Simulations have been performed on one stage antennas, and then on a two stage antenna to look at the behaviour of increasing the height of the antenna. Measurements have also been carried out according to CENELEC EN50383 standard, with the flat phantom and the homogeneous liquids defined in the standard.

RESULTS: In a first step, the antenna model has been validated between measurements and simulations. Then, the measurement liquid has been validated through simulations in a homogeneous and heterogeneous phantom. Analysing the tissue depths repartitions encountered in Visible Man, a validation of the homogeneous liquid has also been done using multiplayer analytic formulas. Then, measurement and simulations have been performed and analysed at 900 MHz, 1800 MHz and 2100 MHz. A two-stages antenna has been simulations to see the impact on local and whole body SAR. As expected, with a two-stages antennas, the whole body SAR is almost the same whereas the local SAR is divided by two. The results could then be extrapolated to any antenna height. To conclude, with classical panel antennas (over 1.3 m), and classical input power of antennas (below 40 W per band for tri-band antennas), it is possible to touch the back or the side of antennas for workers. The contact is possible if the hand or body part, stays behind the metallic back-panel.

This study was supported by Orange France.

POSTERS

BIOELECTROMAGNETICS: JOURNAL UPDATE. B. Greenebaum, Dept. of Physics, University of Wisconsin-Parkside, Kenosha, Wisconsin 53141-2000, USA.

Comparative statistics for 2003 and prior years concerning manuscripts received and accepted, geographical and subject matter distribution, and review times will be presented at the meeting. Preliminary indications are that 138 manuscripts were received in 2003, somewhat fewer than the 155 received in 2002 (excluding the 13 papers designated for the special issue containing “white papers” on RF effects) and substantially above the 114 received in 2001. Preliminary figures show that submissions from outside North America (mostly Europe and Japan) were about 64% of the total, about the same as in 2002. The number of RF papers (54) was about equal to the ELF ones (59), each comprising about 40% of the total, while DC fields dropped from about 10% to about 5% of the total, the remainder of the submissions concerning relatively low frequency pulsed fields and other subjects. By the meeting abstract deadline, reliable numbers for the decrease in the backlog at the publisher or for changes in the typical length of the review cycle were not available. These will be presented at the meeting.

Dr. Ann Henderson has resigned as one of the Associate Editors, due to the press of other duties. The Editor in Chief is grateful to her and the other Associate Editors for their efforts; and all of the editors thank him and the many members of the Society and other scientists who acted as reviewers for the journal, as well as the authors for their submissions. Her replacement is scheduled to be confirmed at the February, 2004, meeting of the Society’s Directors, after the deadline for abstracts.

P-A-1

EFFECTIVE EVALUATION OF HANDSET EXPOSURES IN DIFFERENT NETWORKS UNDER REAL-LIFE CONDITIONS. D. Spät, J. Fröhlich, N. Kuster, Foundation for Research on Information Technologies in Society (IT²S), Swiss Federal Inst of Tech (ETH), CH-8092 Zurich, Switzerland.

INTRODUCTION: Most epidemiological studies on possible adverse health effects from mobile phone usage classify the exposure via the daily usage. Enhanced characterization of the exposure would allow for better classification of different user groups and therefore enhance the sensitivity towards a possible exposure-effect relation. Compliance data of mobile phones only deliver the maximum spatial peak SAR occurring in the user. The real-life head and brain exposure is much better characterized by the exposure pattern times the average output power. For the assessment of the average output power, the power control function of a mobile phone has to be recorded under real-life conditions. The characteristic of the power control function is highly dependent on the environment, base station density, network traffic, usage (stationary, walking, driving etc.) and the position of the phone at the head.

OBJECTIVE: The objective is to design a system for recording the power control (PWC) function of different handsets in different environments and under different usage conditions (stationary, moving). System requirements include:

- sampling rate: > 3000 samples/s (rise time < 0.1s)
- dynamic range: < 1mW/kg to 2W/kg
- linearity: < 0.2dB
- noise: < 1mW/kg
- temperature range: 10-40 °C (<< 1dB)
- humidity: 0 - 90%
- relative position accuracy (head/phone/probe): < 1mm
- battery and DC operated

METHOD: The design includes phantom heads containing field probes at the location of the ear. An additional mechanism allows the positioning of the handset in different ways including the predefined positions given in the standards on compliance testing of mobile phones (FCC, CENELEC). Up to four phantom heads, each holding two handsets, can be evaluated at a time. The system can be mounted on a trolley or put in a car simulating different ways of moving.

RESULTS: A prototype of the system and the corresponding measurement methodology were derived in order to record the exposure characteristics of different handsets all compared to a software-modified phone delivering PWC settings. This allows the derivation of handset-specific differences with respect to power control, network provider, environment and positioning at the head. It also includes the ability to assess the differences of the power control between GSM and CDMA networks. It has proven to be an effective tool for the assessment of the exposure in epidemiological studies as well as the testing of the quality of handsets and of service providers.

The study was supported by the Cellular Telephone and Internet Association (CTIA) and Sunrise TDC.

SHIELDING CHARACTERISTICS OF HIGH CONDUCTIVITY OR HIGH PERMEABILITY MATERIALS ON ELF MAGNETIC FIELDS GENERATED FROM SINGLE OR THREE PHASE AC LINE. S.W. Min, K.H. Song, S.H. Myung¹. Division of Information Tech Engineering, Soonchunhyang Univ, Asan, Chungnam, 336-745, Korea, ¹Electrical Power Research Laboratory, Korea Electrotechnology Research Inst, Seongju-dong, Changwon-city, Kyongnam, 641-120, Korea.

INTRODUCTION: Shielding methods on ELF magnetic fields may include the use of induced currents, modification of magnetic field flux patterns using high permeability and/or high conductivity materials, and others. The magnetic shielding properties of enclosures can be utilized to reduce the magnetic field of current carrying conductors. In this paper, to get a more practical understanding of shielding phenomena, we investigate the magnetic field reduction by means of 3 dimensional numerical analysis and experiments.

OBJECTIVES: Evaluate factors such as materials, shape, thickness of enclosure, and arrangement of current carrying conductors in view of the magnetic field reduction.

METHODS: We measured magnetic field flux density outside the shield enclosure by using a full scale experimental setup and compared them with calculation results which 3 dimensional boundary element method (BEM) was applied to. We adjusted 1.5m single-phase and three-phase 60Hz current sources to generate 10 μ T and 50 μ T at 10cm far from enclosure when shield is not applied. Shielding effect in case of 1 phase and 3 phase straight triangular and horizontal configurations was investigated by enclosing all three conductors with one common shield. Silicon steel, iron, and permalloy are considered as magnetic shield materials, and copper are as conductive shield. Permeability of silicon steel and iron is assumed as 2000 and 8000 at 10 μ T respectively. Resistivity of copper and iron is assumed as 1.724 micro ohm-cm and 47 micro ohm-cm respectively. Finite cylindrical and box shells are studied with changing size. Thickness of shield also varies from 0.9mm to 5mm. To check the shield effects, reduction rate = $(B_o - B_i) / B_o \times 100$ [%] is applied, where B_o means magnetic flux density without shield and B_i is magnetic flux density with shield.

RESULTS: Cylindrical shield could not reduce flux density more than box shield in both cases of magnetic metal and nonmagnetic metal. Iron under 10 μ T of 1 phase could reduce flux density about 20[%] more than silicon steel, but both of them under 50 μ T has a similar reduction rate of 10[%]. The 3 phase horizontal model gave the highest reduction rate and the 1mm thickness iron under 10 μ T of 3 phase lines did the lowest.

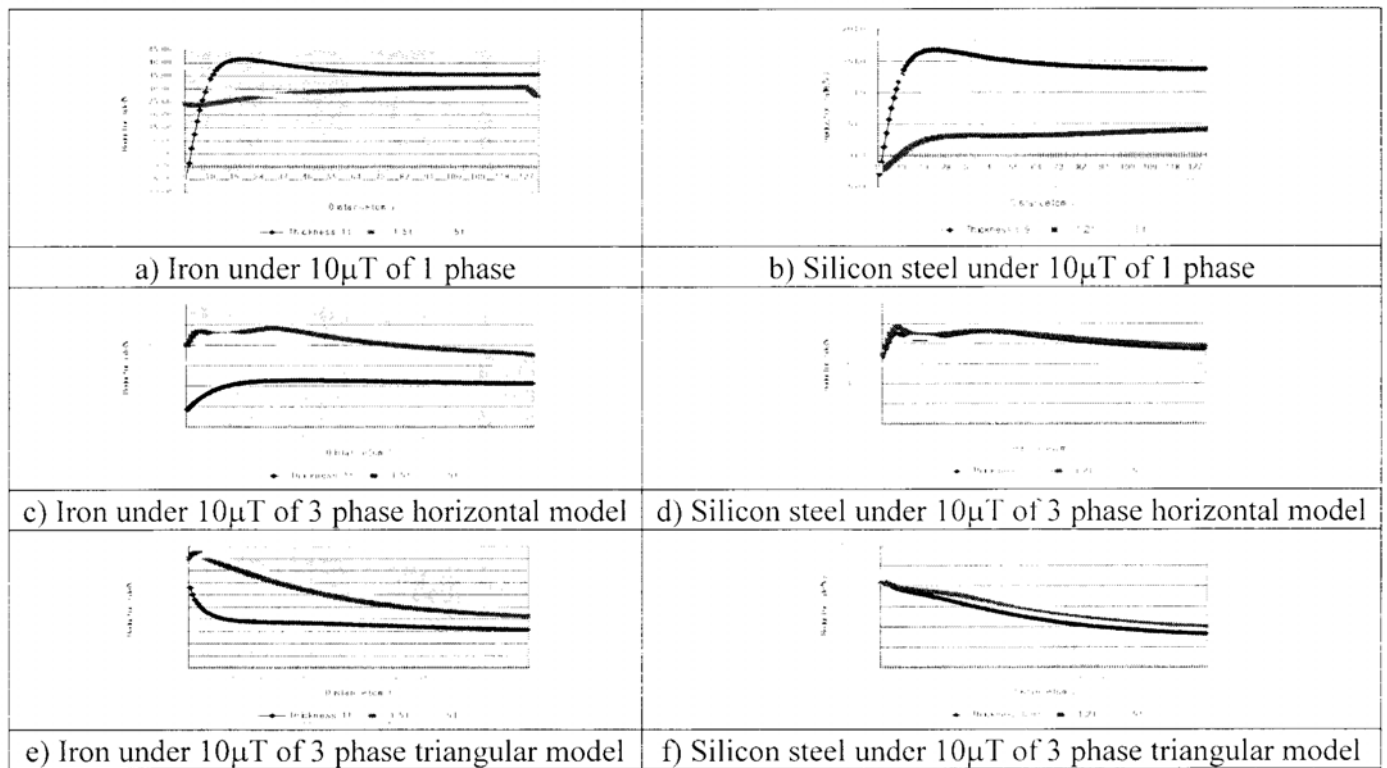


Figure 1: Shielding characteristics of iron and silicon steel with variations of current source arrangement

P-C-3 RELOCATED - DISPLAYED IN INVITRO STUDIES-CELLULAR BETWEEN P-A-55 AND P-B-56, FOUND ON PAGE 60-61

P-A-4

AN EVALUATION OF POTENTIAL GPRS 900/1800 MHZ AND WCDMA 1900 MHZ INTERFERENCE TO MEDICAL DEVICES. R.J. McKenzie¹, S. Iskra¹, B.W. Thomas¹ and J. Rowley², ¹Telstra Research Laboratories, Clayton, Victoria, 3168, Australia; ²GSM Association, Deasgrange Co., Dublin, Ireland.

OBJECTIVE: The aim of this work was to assess the potential for interference from GPRS (General Packet Radio Service) 900/1800 MHz and wideband CDMA (WCDMA - frequency division duplex (FDD) mode) 1900 MHz handsets to medical devices.

BACKGROUND: The proliferation of mobile communication and wireless devices into sensitive environments such as hospitals has raised questions about the adverse effect of electromagnetic interference (EMI) to medical equipment and its potential impact on patient care. This study builds on EMI work already performed at this and other laboratories [1-3] and examines the potential EMI impact of newer mobile technologies such as GPRS and WCDMA on the performance of medical devices. In addition to GPRS and WCDMA FDD-mode fields, test fields characteristic of GSM 900/1800 MHz handsets were used to provide a basis for a comparative analysis and serve as a benchmark against which the interference impact of GPRS and WCDMA can be assessed relative to the well established and globally adopted GSM technology.

METHOD: The study was conducted on a range of medical equipment including cardiac defibrillators,

monitors, ventilators, pumps, humidifiers, and pulse oximeters. The test protocol was based on ANSI C63.18-1997 [4] for estimating radiated electromagnetic immunity of medical devices to radio transmitters such as mobile telephones. A balanced half wave dipole was used as a substitute for an actual handset. The nominal peak/average transmit power levels were: 2 W/250 mW for GSM 900 MHz, 2 W/500 mW for two timeslot GPRS 900 MHz, 1 W/125 mW for GSM 1800 MHz, 1 W/250 mW for two timeslot GPRS 1800 MHz and 125 mW for WCDMA 1900 MHz. For GSM and GPRS, the carrier was GMSK modulated (pseudo-random data) and for WCDMA, symbol rates of 15, 960 and 6 channels of 960 kilo-symbols per second were used. In addition, signal fading was simulated using fast power control (1dB steps at 1500 Hz, frequency of fading dips 100 Hz, carrier peak envelope power +11.5 dB) and implemented for WCDMA in order to gauge its potential EMI impact. The medical devices were subjected to vertically and horizontally polarised fields and the resulting performance degradation was noted with the worst-case interference result being recorded.

RESULTS: The data revealed that many medical devices exhibited no interference effects even when the dipole was brought to within 1 cm of the device. This is consistent with the observations of other studies [1-3] that found a significant proportion of devices were unaffected by mobile phones, even when the phone was transmitting at maximum power and in close proximity to the devices. Signals at 900 MHz were more prone to causing interference than those at the higher frequencies of 1800/1900 MHz. Similarly, the study reported in [3] showed that even at the same test field strength, higher frequency signals (eg., 1800/1900 MHz) were less likely to cause interference than those at the lower frequency of 900 MHz. The EMI threat from two timeslot GPRS is similar to GSM at the same frequency. The application of fast power control to the WCDMA signal causes additional amplitude modulation of the RF carrier and an increase in peak envelope power resulting in an increased EMI threat. The results suggest that WCDMA is unlikely to be a significant interference threat when compared to 900/1800 MHz GSM or GPRS. Its interference threat is similar to 1800 MHz GSM or GPRS (two timeslots) but increases under fast fading conditions.

References:

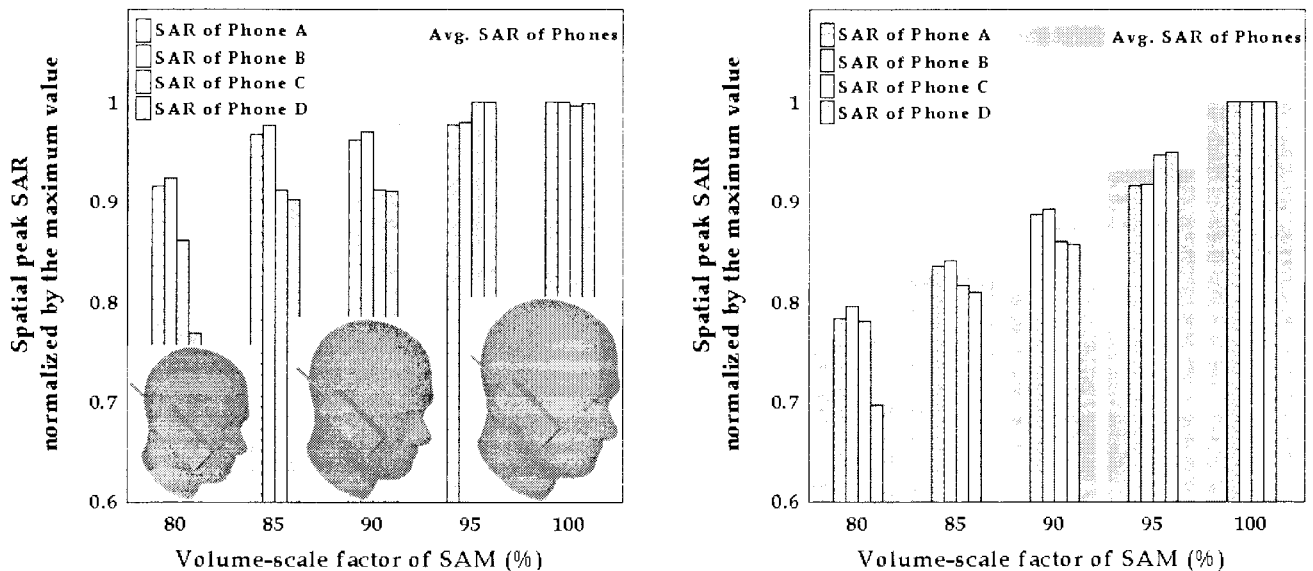
1. Medical Devices Agency, Electromagnetic Compatibility of Medical Devices with Mobile Communications, MDA; London, Devices Bulletin DB 9702, March 1997
2. Morrissey J. J, Swicord M. and Balzano Q., Characterisation of electromagnetic Interference of Medical Devices in the Hospital Due to Cell Phones, Health Physics, 82 no. 1, Jan. 2002.
3. S. Iskra, R. McKenzie and Z. Pleasants, Characterising the Electromagnetic Interference of Medical Equipment to GSM 900/1800 MHz and CDMA 800 MHz Mobile Telephones, Engineering and Physical Sciences in Medicine (EPSM) Conference, Rotorua, New Zealand 10th-14th November 2002
4. ANSI C63.18-1997, Recommended practice for an on-site, ad hoc test method for estimating radiated electromagnetic immunity of medical devices to specific RF transmitters.

P-B-5

THE CORRELATION BETWEEN HEAD SIZE AND SARS FOR HANDSET EXPOSURES AT 835 MHZ. A.K. Lee¹, H.D. Choi¹, J.H. Yun¹, J.I. Choi¹, and J.K. Pack². ¹Radio Technology Group, Electronics and Telecommunications Research Institute, 161 Gajong-Dong, Yusong-Gu, Daejeon, 305-350, KOREA, ²Dept. of Radio Science & Engineering, Chungnam National University, 220, Gung-Dong, Yusong-Gu, Daejeon, 305-764, Korea.

OBJECTIVE: SARs (specific absorption rates) in volume-scaled head models for handset exposures have been simulated using FDTD (finite difference time domain) technique in order to find out the relation among SAR, human head size and radiation characteristics of handset.

INTRODUCTION: The correlation of human head size and SAR characteristics for handset exposure had been studied using an anatomical model and a simple homogeneous model. In [1] and [2], the higher local SAR had been shown in the smaller head but radiation characteristics of the phone touched on the head had



not been considered. The radiation power level from a phone with a user plays an important role in the SAR level in the user's head. It is closely connected with the user's head size, the EM environment, and the distance and direction from a corresponding base station. In order to analyze the effects of head sizes on SAR, this paper considers radiation power, and the accepted power by the antenna of a phone as well as SARs in head models.

METHODS: The voxel model of the SAM (specific anthropomorphic mannequin) was scaled by volume to five different sizes with the size being 80, 85, 90, 95, and 100 %. Four phones with different combination in antenna length, antenna position, body size and body material were used. Then the touch position for each scaled head model was implemented carefully. The uniform grid size of $1 \times 1 \times 1 \text{ mm}^3$ was used in all the cases.

RESULTS AND DISCUSSION: The spatial peak SARs in the above five head models exposed to each phone model were calculated and then were normalized by the maximum value of them. Avg. SAR of phones in Figure 1 means the averaged spatial peak SAR of four phones. From the figure, it is found that that mostly lower peak SAR is produced in a smaller head derived from the original SAM phantom. This trend is similar to those in [1] and [2].

- (a) For the constant antenna-accepted power (b) For the constant radiation power
 Figure 1: Comparison of spatial peak SARs in head models of different sizes.

References.

[1] A.K. Lee and J.K. Pack, "Effect of head size for cellular telephone exposure on EM absorption," IEICE Trans. On Commun., vol.E85-B, no. 3, pp 698-701, Mar. 2002.
 [2] A.K. Lee, H.D. Choi, H.S. Lee, and J.K. Pack, "Human head size and SAR characteristics for handset exposure," ETRI Jour. vol. 24, no. 2, pp 176-179, Apr. 2002.

P-C-6

UMTS SIGNAL CHARACTERIZATION FOR SAR COMPLIANCE TESTS OF CELLULAR PHONES. A. Schiavoni, M. Francavilla, D. Forigo, TILAB, via Guglielmo Reiss Romoli 274, 10148, Torino, Italy.

INTRODUCTION: SAR qualification of UMTS cellular phones does not differ from other mode of phone’s operation (GSM, TACS, AMPS, CDMA) except for the value of the Crest Factor (CF) used to describe the typology of signal to be detected by the electric field probe inside the human head like phantom. The time behavior of the signal emitted by the cellular phone is described in terms of CF defined as the ratio between the peak power and the average power; as an example for TACS mode of operation the value of CF is 1 and it is 8.3 for GSM mode.

OBJECTIVES: The goal of the poster is the determination of the CF value for a UMTS signal and to discuss its value in terms of the period where the peak power is evaluated. Furthermore some considerations regarding the possibility to consider the UMTS as a tone, for SAR measurement purposes, are discussed.

METHODS: The CF of a general time varying signal, defined in the time interval [0,T], is given by:

$$CF = \frac{P_p}{P_m} = \frac{\text{Max} \left[\frac{1}{\tau} \int_t^{t+\tau} p(t) dt \right]_{\forall 0 \leq \tau \leq T-\tau}}{\frac{1}{T} \int_0^T p(t) dt} = \frac{\text{Max} \left[\frac{1}{n} \sum_{k=s}^{s+n} p(k) \right]_{\forall 1 \leq s \leq N-n}}{\frac{1}{N} \sum_{k=1}^N p(k)}$$

where $\tau \ll T$ is a whatever sub interval in which the signal is defined. In the second part of the previous formula, it is described the evaluation of the CF for a signal sampled in the time. The time behavior and the frequency spectrum of a UMTS signal is shown in figure 1. The UMTS signal in the time domain has been sampled with a sampling frequency multiple of the Chip Rate F_c . The CF has been determined as a function of the sampling frequency and of the number of shifted samples from $t=0$.

RESULTS AND CONCLUSIONS: Figure 2 shows the CF as a function of the over sampling frequency and of the shift from the beginning of the time evolution of the signal. As can be noted the CF value rapidly converge to the value 1.08 indicating that the, for SAR measurement purpose, the UMTS signal can be well assimilated to an equivalent tone with associated all the power contained in the spectrum of the real UMTS signal. In fact, as shown in Figure 3, it can be noted that there is not difference in the SAR space distribution measured inside the anatomical head phantom considered in the international standards, for the same mock-up phone radiating a UMTS signal and equivalent tone at the same central frequency.

This work has been fully supported by TIM – Telecom Italia Mobile.

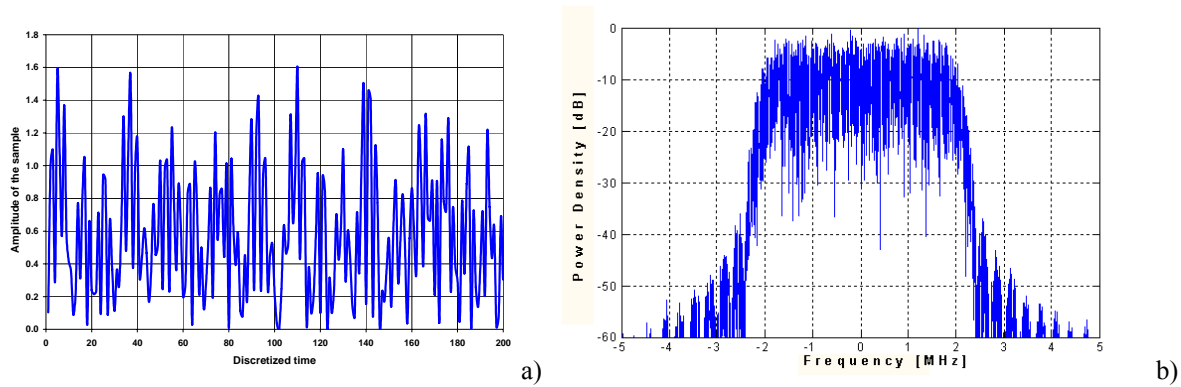


Figure 1: a) A UMTS signal in the time; b) Spectrum of a UMTS signal

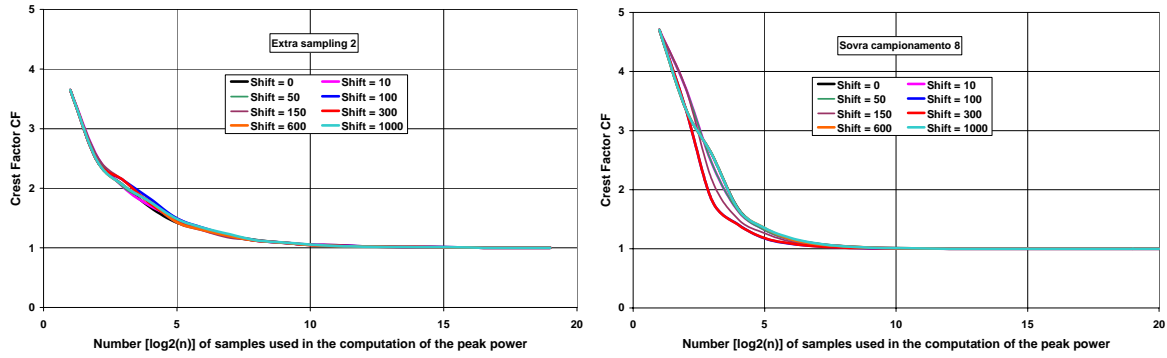


Figure 2: Crest factor as function of the over sampling rate and shift from $t=0$.

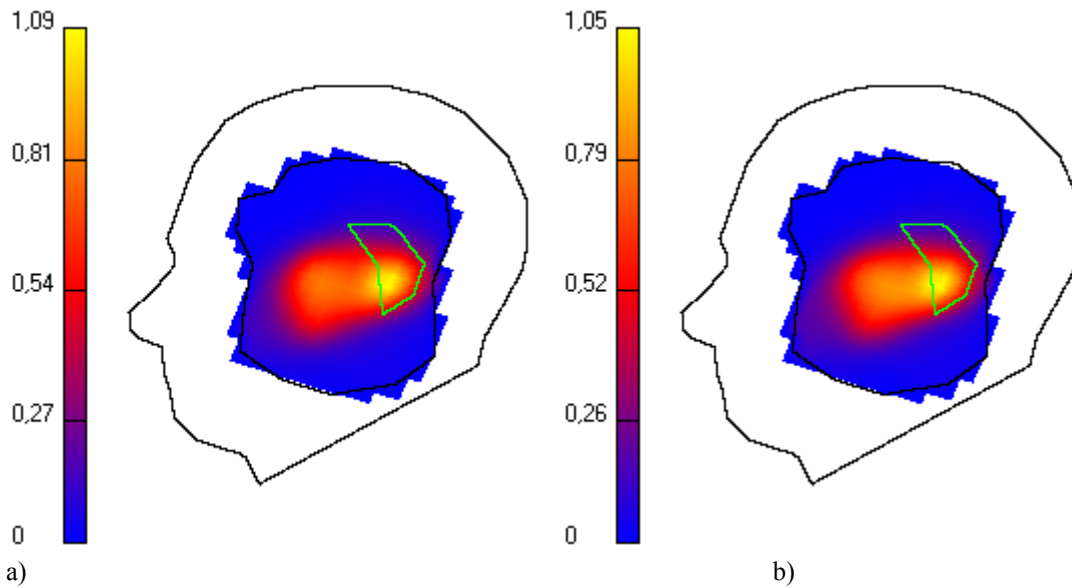


Figure 3: SAR distribution inside the head phantom: a) UMTS signal; b) Sinusoidal signal.

P-A-7

2 GHz-EXPOSURE OF NON-RESTRAINED AKR/J MICE IN A SLIGHTLY OVER-MODED RADIAL WAVEGUIDE. A.K. Bitz¹, J. Streckert¹, A.M. Sommer², A. Lerchl², and V.W. Hansen^{1,1},¹Chair of Electromagnetic Theory, University of Wuppertal, D-42097 Wuppertal, Germany, ²School of Engineering and Science, International University Bremen, D-28759 Bremen, Germany.

In order to accomplish whole body exposure of a large number of non-restrained animals, one approach is to design exposure setups based on radial waveguides. Inside the waveguide the animals are kept in cages which are arranged at a constant distance from a radiating antenna in the centre, thus uniform exposure of the cages can be achieved. Another advantage is that the radial waveguide is an electromagnetic shielded system, on that score no costly shielding of any laboratory is necessary. The height of the waveguide is preferably chosen smaller than half a wavelength [1]. Thereby, single-mode operation of the TEM-mode is possible and a homogeneous field distribution inside every cage can be guaranteed. For the exposure of small rodents at frequencies around 900 MHz this condition is easily fulfilled.

If, however, the exposure is performed at higher frequencies, the animals' size as compared to the wavelength increases, and especially for long-term experiments, when more space for the free movement of the animals is required, waveguides with a height larger than half a wavelength are needed. As a result, higher order modes are able to propagate in addition to the TEM-wave. These modes have inhomogeneous field distributions in the waveguide's cross-section. Furthermore, the simultaneous propagation of several modes leads to interference effects and thus to an unstable exposure field.

In the present project 160 non-restrained mice are exposed to a UMTS signal [2] at 2 GHz. The above mentioned drawbacks have been avoided by adopting modified radial waveguide exposure devices. The two implemented waveguides (one for exposure, one for sham-exposure) both carry up to 24 plastic cages measuring 425 mm x 265 mm x 70 mm (L x W x H) each of them housing 6 – 7 mice. Therefore the sizes of the radial waveguides amount to 4 m in diameter and 8 cm plate distance. Obviously, such height of the waveguides, which exceeds half a wavelength by a factor of approx. 1.1, would in principle allow for the propagation of at least 1 higher order mode, i.e. the waveguides are slightly overmoded.

In order to produce a well defined field distribution, regardless, the cage region is excited only by the fundamental TEM-mode in a first step, i.e. for small radii the plate distance is kept below 6 cm and for larger radii the height is increased to the required value of 8 cm. Since it is still possible that the additional modes are excited by the field scattered from the mice, metal rip structures are attached to the upper and lower plate between adjacent cages in order to shift the cut off frequencies of these unwanted modes to higher values, so that they cannot propagate at the exposure frequency. The optimum size of the rips is determined by numerically solving the eigenvalue problem of the modified waveguide. It yields that a maximum attenuation of the higher order modes is reached for specific heights and widths of the rips. Therewith, it is shown that the unwanted modes can be forced to become evanescent and thus a stable field distribution is achievable. Moreover, the rip structure does not alter the propagation constant of the TEM-mode, and the perturbation of the field distribution of the fundamental mode is negligible within the cage volume.

References:

- [1] V. W. Hansen, A. K. Bitz, J. R. Streckert, RF Exposure of Biological Systems in Radial Waveguides, IEEE Trans. EMC, Vol. 41, 487-493, 1999.
- [2] Ndoumbè Mbonjo Mbonjo, H., Streckert, J., Bitz, A., Hansen, V., Glasmachers, A., Gencol, S., Rozic, D., A generic UMTS test signal for RF bio-electromagnetic studies. Accepted for publication in Bioelectromagnetics, December 2003.

This study was part of a project supported by the Bundesamt für Strahlenschutz, St. Sch 4399: "In vivo-Experimente unter Exposition mit hochfrequenten elektromagnetischen Feldern der Mobilfunkkommunikation. B Kanzerogenese".

P-B-8

DETERMINATION OF THE SPATIAL-PEAK SAR IN HUMAN MODELS FROM A HYBRID FEM/MOM SOLUTION. M. Bingle, F.J.C. Meyer, EM Software and Systems-S.A., EMSS Building, 32 Techno Avenue, Technopark, Stellenbosch, 7599, South Africa.

OBJECTIVES: Spatial-peak and whole-body-averaged SAR assessment in the human body in close proximity to base station antennas or wireless communication devices is important for the evaluation of compliance to international exposure guidelines and standards. Our goal is an automated, spatial-peak SAR extraction algorithm to accurately and efficiently calculate, using numerical simulation techniques, the spatial-peak SAR of a 1-g or 10-g cubic tissue volume, following the guidelines in the standards [1], [2].

METHOD: The spatial-peak SAR is defined as the maximum averaged SAR of a 1 g or 10 g volume of tissue in the shape of a cube. A hybrid Finite Element Method (FEM) / Method of Moments (MoM) formulation has been implemented and is used to solve numerical dosimetry problems [3]. The mass-averaged SAR of a cube is computed from the hybrid FEM/MoM solution for the electric fields in the dielectric body. The 3D integrals to perform the averaging (including the mass, volume fraction of tissue, and average SAR) are computed numerically. For complex, heterogeneous models, the cube dimension at a given location is determined through an adaptive procedure to obtain the specified mass. The numerical integration is performed by repeated one-dimensional quadrature, using an extended trapezium rule to a specified accuracy. An advantage of the FEM/MoM solution is that the field at any location in the FEM region (typically the human model) is known analytically. This allows efficient, adaptive near-field sampling and renders evaluation of the 3D integrals relatively fast. Since models may become large, the search for the location of the spatial-peak SAR cannot be conducted indiscriminately. In dosimetry applications, the spatial-peak SAR should usually be in the vicinity of the source, and close to the surface of the dielectric body. However, internal hot spots may also occur. Localised SAR values and voxel-average SAR is used as indicators for the location of spatial-peak SAR. Special attention is paid to SAR values at interfaces between tissue and non-tissue materials. In search of the spatial-peak SAR, a 1-g or 10-g cube is scanned along dielectric boundaries. Along these boundaries the cubes are positioned by the *method of the tangential face* [1], in order to fully include the region of (most-likely) highest localised SAR in the averaging volume. Results from the interface scan, and localised SAR values interior to dielectric regions are used as starting positions for a search algorithm based on the downhill simplex method to obtain the location and value of the spatial-peak SAR of a 1-g or 10-g cube. A restriction is placed on the volume fraction of non-tissue content included in the cubic volume.

RESULTS: In order to validate the computation of the mass-averaged SAR of a cube from the hybrid FEM/MoM solution, results have been obtained for a sphere-dipole benchmark configuration (Figure 1, dimensions are in mm). It consists of a $\lambda/2$ -dipole antenna (y -directed) below a semi-spherical glass bowl, filled with a lossy dielectric material. The operating frequency is 900 MHz. The results are presented for a total radiated power of 1 W, and a mass density of $\rho = 1000$ W/kg for the dielectric. The 10-g spatial-average SAR distribution along the symmetry axis (z -axis) is compared in Figure 2 to published results [4], obtained with the FDTD method. The 10-g spatial-peak SAR for two positions of the dipole antenna are shown in the table. For both, the cube is tangential to the surface of the lossy dielectric.

CONCLUSIONS: An automated search algorithm has been developed to obtain the 1-g or 10-g spatial-peak SAR of cubic tissue from a FEM model and hybrid FEM/MoM solution. We will extend the algorithm to numerical simulations using the full MoM (either the surface or the volume equivalence principle).

References.

[1] CENELEC, "Basic Standard for the Measurement of Specific Absorption Rate Related to Human Exposure to Electromagnetic Fields from Mobile Phones (300 MHz-3 GHz)," Tech. Rep. EN 50 361, July 2001.

[2] IEEE Standards Coordinating Committee 34, Subcommittee 2, "*Draft* Recommended Practice for Determining the Spatial-Peak Specific Absorption Rate (SAR) Associated with the Use of Wireless

Handsets—Computational Techniques,” Tech. Rep. IEEE P1529/D0.0, IEEE SCC34/SC-2, 2002.

[3] F.J.C Meyer, D.B Davidson, U Jakobus and M.A Stuchly, “Human Exposure Assessment in the Near Field of GSM Base-Station Antennas Using a Hybrid Finite Element/Method of Moments Technique,” IEEE Transactions on Biomedical Engineering, vol. 50, no. 2, pp. 224-233, February 2003.

[4] N Stevens and L Martens, “Comparison of Averaging Procedures for SAR Distributions at 900 and 1800 MHz,” *IEEE Trans. Microwave Theory Tech.*, November 2000.

Dipole Centre ($h=5$ mm)	10-g peak SAR (W/kg)	Cube position x, y, z (mm)	Cube size (mm)	Non-tissue fraction
Centred	9.65	0.01 -1.61 -107.05	21.8	3.4%
Offset by 74.5 mm	2.7	-0.41 43.91 -97.92	21.9	4.8%

Figure 1

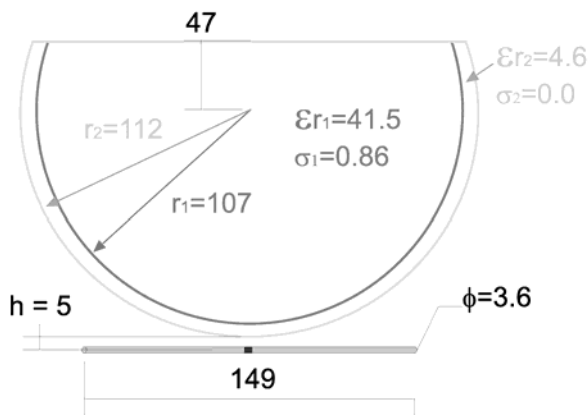
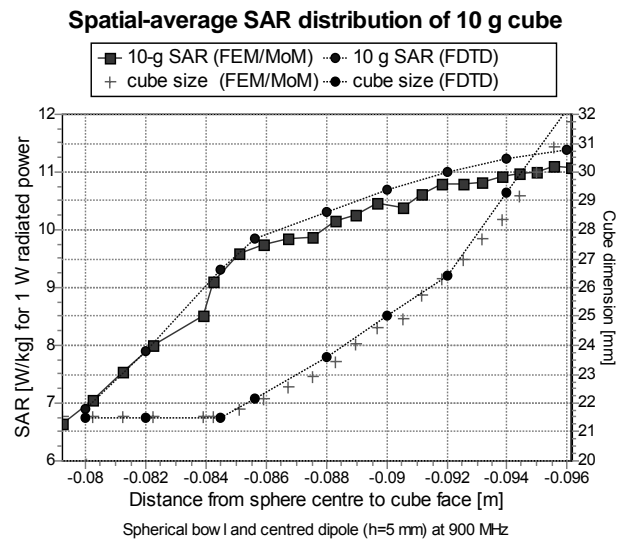


Figure 2



P-C-9

EXPOSURE ANALYSIS IN TERM OF LOCAL AND WHOLE BODY SAR IN A RAYLEIGH (INDOOR) ENVIRONMENT AT 900 MHZ, 1800 MHZ AND 2100 MHZ. C. Dale, J. Wiart. France Telecom R&D, DMR/IIM, 38-40 rue du Général Leclerc, 92794 Issy-les-Moulineaux Cedex 9, France.

INTRODUCTION: In order to protect public and workers from electromagnetic fields, exposure limits have been defined in terms of basic restrictions and reference levels by organisms such as ICNIRP and IEEE. Basic restrictions represent the real exposure of the body whereas reference levels established with maximum coupling conditions are sufficient conditions to guaranty the respect of basic restrictions. Exposure analysis are often realised by considering one incident source, would it be in the far field or the near field. The reality of the exposure conditions in indoor is often a superposition of multiple sources from multiple directions.

OBJECTIVES: The aim of this study is to analyse the indoor exposure condition in terms of local and whole body SAR. The second objective is to analyse the behaviour of the environmental field with the presence of the body. The plane wave case is considered as a reference exposure condition since it is very often used.

METHODS: The exposure analyse is carried out using FDTD excited by given incident field distributions though a Huygens box. Two body models are analysed. On one side, an ellipsoid is used to represent a simple shape of human body to be able to carry out statistics easily. On the other side, a numerical heterogeneous 3D model is used to analyse the exposure. The Rayleigh distributions are built by adding multiple plane waves (either specific or randomly), first using a vertical polarisation, and then using a random polarisation. 10g-SAR-averaging is performed according to IEEE requirements on simulations.

RESULTS: First, the structure of a Rayleigh distribution field is analysed in free space and then with the presence of the body. Then, the local SAR and whole body SAR are compared to the spatial average field which is *the* reproducible value that can be measured on site. We conclude by comparing these results to a plane wave exposure condition to see which one gives the highest exposure (local or whole body) regarding exposure guidelines.

P-A-10

NEW EXPOSURE SYSTEM FOR HUMAN STUDIES ON EFFECTS OF RADIO FREQUENCIES ON BRAIN FUNCTIONS. G. Schmid¹, M. Kundi², H. Molla-Djafari³. ¹ARC Seibersdorf research GmbH, A-2444 Seibersdorf, Austria, ²Institute of Environmental Health, Medical University of Vienna, A-1090 Vienna, Austria, ³Austrian Workers Compensation Board (AUVA), A-1200 Vienna, Austria.

OBJECTIVES: Several studies on human volunteers concerning possible effects of radio frequencies (RF) on brain functions were conducted in recent years. Within most of this studies a diversity of different cognitive parameters as well as the EEG of the subjects were investigated in double blinded crossover trials of RF exposure from modern mobile communication devices. So far no consistent picture is emerging from these studies and some of the results are not unequivocal. One reason for this fact might be the difficulty to precisely control exposure of the subjects, which is a crucial issue. Most of the setups used so far for exposing the subjects' head showed considerable inter-individual as well as intra-individual variations in the specific absorption rate (SAR) in the brain considering sources of variation as for example different head sizes and shapes and movements of the head during exposure. In order to minimize these problems we developed a new head exposure system for hands free exposure of subjects introducing only a minimum of restriction and inconvenience for the subjects and at the same time reducing variations in the actual exposure of the brain.

MATERIALS AND METHODS: The newly developed exposure system (head set) consists of two patch antennas (one for each hemisphere of the brain) mounted on a carrier unit which can be worn by the

subjects like glasses (Fig.1). The carrier unit (made of low loss material) is adjustable for different head sizes and ensures reproducible and constant position of the antennas with respect to the head. In contrast to many other setups used so far the headset described here provides a certain distance between the test subjects' head and the antennas (adjustable between 65 mm and 100 mm in discrete steps). This is advantageous compared to exposure systems having the antennas extremely close to the head, with respect to SAR variations caused by small unavoidable variations in the relative position between head and antenna (e.g. due to different head shape and/or size). Each of the robust patch antennas (dimensions for a 900 MHz exposure system: 132 mm x 135 mm x 10 mm) are consisting of a backplane and a resonant patch (both of 0.1 mm copper foil) with a synthetic foam material (10 mm thickness, $\epsilon_r \approx 1.5$, $\sigma \leq 10^{-4} \text{S/m}$) in between. Feeding of the antenna (patch) is accomplished via a commercial SMA connector from the back. Due to the directional antenna pattern the setup provides high power efficiency. Depending on the exact antenna position, e.g. at 900 MHz only 0.8 W antenna feed point power is required for achieving 1 W/kg spatial peak SAR (1g average) in the brain cortex at an antenna-head distance of 65 mm. In order to reduce the weight to be carried by the subject the entire headset (including the feeding cables) is suspended from the ceiling using a counterbalanced suspension system (Fig. 2), which provides a maximum of freedom regarding head movements while at the same time keeping the relative position between head and antennas constant.

RESULTS: The developed exposure system enables well defined and reproducible exposure of the human head by minimizing inter-individual as well as intra-individual variations of SAR.



Fig. 1: Test subject wearing the headset

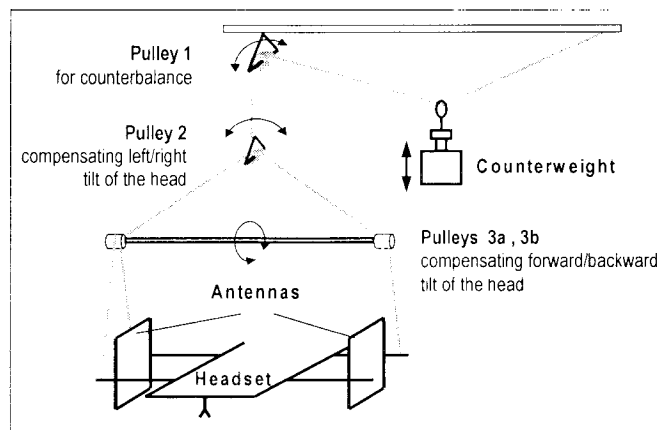


Fig. 2: Schematic of the suspension system

This work is part of a project funded by the Austrian Workers Compensation Board (Allgemeine Unfallversicherungsanstalt, AUVA).

P-B-11
STUDENT

COMPARISON OF VOLUMES USED FOR AVERAGING OF LOCAL SAR. G. Vermeeren, L. Martens; Department of Information Technology, Ghent University, Ghent 9000, Belgium.

INTRODUCTION: Standards for compliance testing of hand-held mobile communication devices, such as [1], describe various cubical averaging schemes to obtain the spatial peak 1 g or 10 g mass averaged SAR. These cubical averaging schemes originate from the cubical FDTD-grid. A spherical averaging scheme is more appropriate from the viewpoint of the diffusion of the heat in tissue.

OBJECTIVE: Evaluation of the cubical averaging schemes [1] as opposed to the irregular coherent volume with maximum averaged SAR [2] and a new spherical averaging scheme.

METHOD: In the spherical averaging method of Figure 1, one chooses the centre of a sphere on the phantom surface and extends the radius r of the sphere until the part of the sphere inside the phantom encloses a volume of 1 g or 10 g mass. Three analytical functions representing the possible range of SAR distributions caused by a hand-held are defined in [2]:

$$f_1(x, y, z) = A \exp\left(-\frac{z}{2a}\right) \cos^2\left(\frac{\pi}{2} \frac{\sqrt{x'^2 + y'^2}}{5a}\right)$$

$$f_2(x, y, z) = A \exp\left(-\frac{z}{a}\right) \frac{a^2}{a^2 + x'^2} \left(3 - \exp\left(-\frac{2z}{a}\right)\right) \cos^2\left(\frac{\pi}{2} \frac{y'}{3a}\right)$$

$$f_3(x, y, z) = A \frac{a^2}{\frac{a^2}{4} + x'^2 + y'^2} \left(\exp\left(-\frac{2z}{a}\right) + \frac{a^2}{2(a + 2z)^2}\right)$$

with

$$A = 20 \text{ mm} \quad a = 1 \text{ W/kg} \quad x' = x + d \text{ mm} \quad y' = y + d \text{ mm}$$

d = a lateral shift of the SAR distribution

These functions are used to evaluate the spherical (S), irregular coherent volume (I) and the cubical averaging schemes (method of the tangential face (T), method of averaging (A), extrude method of averaging (E)). The test-functions are originally developed for a flat phantom surface, but can be adapted to a smooth curved phantom surface according to [2]. Two phantom surfaces are considered: a flat phantom surface and a curved phantom surface with a hyperbolic variation along one direction.

RESULTS: Standards, as [1], mention that the cube of averaging needs to be rotated to find the maximum averaged SAR inside the cube. The irregular coherent volume averaging scheme always returns the maximum value of the mass averaged SAR that occurs locally in the phantom (Figure 3 to Figure 6). Spherical averaging gives a higher value for local averaged SAR compared to cubical averaging. It is well known that in a homogenous tissue the highest SAR values occur at the surface of the phantom. The larger the number of averaging points close to the surface of the phantom, the higher the value of the 1 g or 10 g averaged SAR. This also explains the slightly higher 1 g and 10 g averaged SAR for the cubical averaging scheme A in the case of a curved phantom surface (Figure 6). Figure 3 to 6 draws the 1 g and 10 g averaged SAR as a function of the averaging scheme (cubical, spherical and irregular coherent volume) for the three analytical test-functions. The steep gradient of test-function f_3 results in a large variation between 1 g and 10 g averaged SAR, whereas the flat distribution of test-function f_1 results in nearly equal values for 1 g and 10 g averaged SAR. Thus, the 1 g averaged SAR is obvious more stringent in case of steep SAR distributions, which will typically occur for RF-sources radiating at higher frequencies.

CONCLUSION: The use of a spherical averaging scheme is preferred because of: 1) the rotation symmetry of a sphere (in the case of cubical averaging the cube needs to be rotated to find the maximum averaged SAR over the cube). 2) spherical averaging delivers values that agree very well with the maximally obtainable values produced by the averaging using the irregular coherent volume. The cubical averaging underestimates the maximum value by approximately 20 % in case of the steep test-function f_3 . 3) the use of a spherical averaging scheme excludes the variation of the averaged SAR caused by the availability of different averaging schemes (the cubical schemes T, A and E).

References:

- [1] CENELEC EN50361, "Basic Standard for the measurement of Specific Absorption Rate related to human exposure to electromagnetic fields from mobile phones (300 MHz – 3 GHz)", 2001.
- [2] IEC TC106/61/CDV, "Procedure to measure the Specific Absorption Rate (SAR) in the frequency range of 300 MHz to 3 GHz – Part 1: hand-held mobile wireless communication devices, 2004.

[3] N. Stevens and L. Martens, "Comparison of averaging procedures for SAR distributions at 900 MHz and 1800 MHz", IEEE Trans. Microwave Theory Tech., vol. 48, pp. 2180-2184, Nov. 2000.

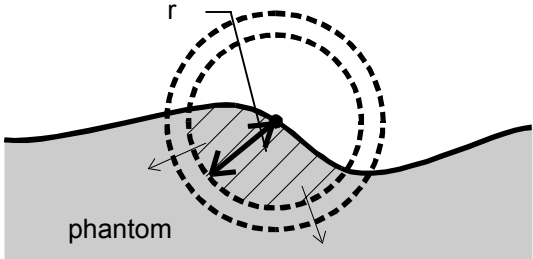


Figure 1: Spherical averaging method.

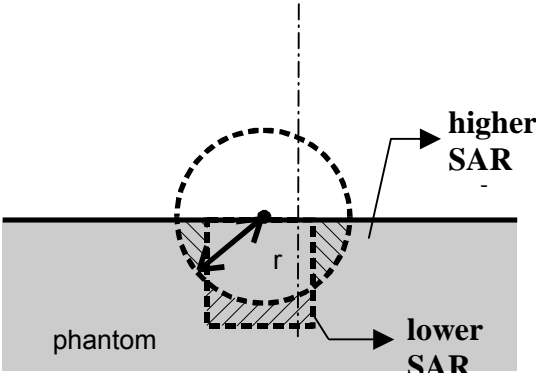


Figure 2: Spherical averaging versus cubical averaging.

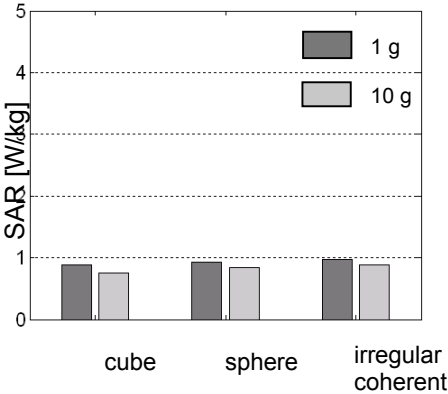


Figure 3: The 1 g and 10 g averaged SAR for a flat phantom surface and test-function f_1 .

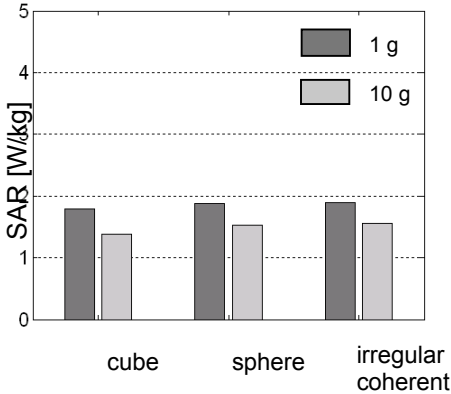


Figure 4: The 1 g and 10 g averaged SAR for a flat phantom surface and test-function f_2 .

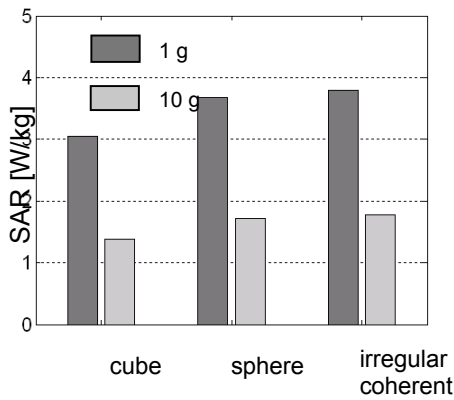


Figure 5: The 1 g and 10 g averaged SAR for a flat phantom surface and test-function f_3 .

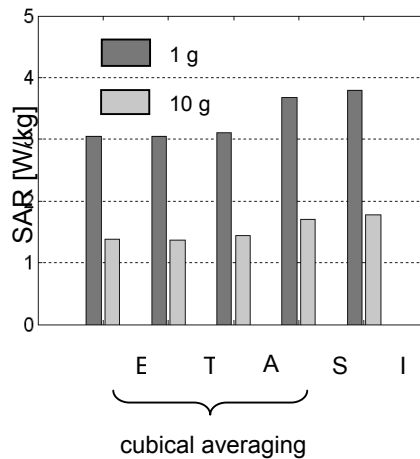


Figure 6: The 1 g and 10 g averaged SAR for a hyperbolic phantom surface and test-function f_3 .

P-C-12 WITHDRAWN

P-A-13

DIELECTRIC MEASUREMENT OF MICROSOMES BY THE TRANSMISSION METHOD USING A COAXIAL LINE. H. Ebara¹, K. Tani², M. Sekijima³, T. Onishi¹, S. Uebayashi¹, and O. Hashimoto². ¹NTT DoCoMo, Inc., 3-5 Hikari-no-oka, Yokosuka-shi, Kanagawa, 239-8536, Japan. ²Aoyama Gakuin University, 5-10-1 Fuchinobe, Sagamihara-shi, Kanagawa, 229-8558, Japan. ³Mitsubishi Chemical Safety Institute Ltd., 14 Sunayama, Hasaki-machi, Kashima-gun, Ibaraki, 314-0255, Japan.

INTRODUCTION: Several studies on the interaction between electromagnetic (EM) fields and biological tissues were conducted in the radio frequency range. Knowing the dielectric properties of cell components is important in the evaluation of EM fields at a microscopic level. Although a wide range of dielectric measurements at a low frequency have been performed, the dielectric properties of each cell component in the microwave and millimeter wave frequencies have not been thoroughly studied. Further detailed investigation is required to clarify the dielectric properties of each cell component. The necessity of microdosimetry research at the cellular or subcellular level is listed in the World Health Organization (WHO) research agenda [1].

OBJECTIVE: The objective of this study is to estimate the complex permittivity of a membrane as one of the cell components by the transmission method using a coaxial line at microwave frequencies.

MATERIALS AND METHODS: Microsomes are intracellular membrane fragments derived from the endoplasmic reticulum. In this study, rat liver microsomes were selected as a sample for the dielectric measurement of a biological membrane. The microsomes were prepared by ultra-centrifugation from rat liver homogenate in buffer. The prepared samples are in five different microsome volume ratios (0.0, 4.9, 10.0, 24.9, and 51.5%). The transmission method with a coaxial line was used to measure the complex permittivity of the membrane as shown in Figure 1. The coaxial line has the inside diameter of 0.87 mm and the outside diameter of 2.00 mm. A characteristic of this coaxial line is that the required sample volume for the measurement is very small. When the coaxial line, which is $L = 20$ mm long, was used for the measurement, the required volume of the sample was approximately 0.05 ml. The samples in different volume ratios of the microsomes were filled in the coaxial line. The transmission coefficient (S_{21}) was

measured using the Vector Network Analyzer for frequencies from 0.5 GHz to 6.0 GHz. The equivalent permittivity of the mixtures was measured at different volume ratios of the microsomes using the procedures described above. The complex permittivity of the 100-percent ratio of the microsomes was estimated by extrapolation from the measured equivalent permittivity.

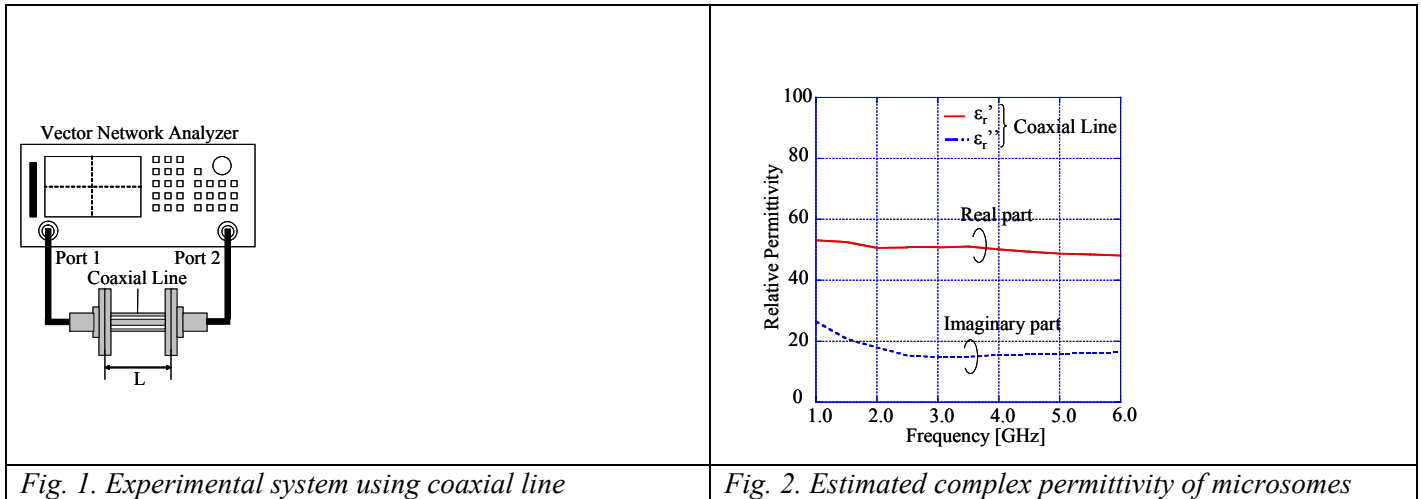


Fig. 1. Experimental system using coaxial line

Fig. 2. Estimated complex permittivity of microsomes

RESULTS AND DISCUSSION: Figure 2 shows the estimated complex permittivity of the 100-percent ratio of the microsomes by extrapolation from the measured equivalent permittivity at different volume ratios. These results are fairly consistent with those in [2] in which the complex dielectric constants of human erythrocyte suspensions were determined with the open-ended coaxial probe technique. In their study, the whole cell human erythrocyte suspensions were perceived as a cell membrane. The complex permittivity was around 50 in the real part and 15 in the imaginary part in the frequency range from 1.0 GHz to 6.0 GHz. The estimated complex permittivity of the microsomes as shown in Figure 2 might include effects due to moisture and impurities. These influences are an issue to be addressed in the future.

References.

[1] <http://www.who.int/peh-emf/research/rf03/en/>

[2] J. Bao, C.C. Davis, M.L. Swicord. (1994): *Biophysical Journal*, Vol.66, pp.2173-2180.

P-B-14

DESIGN AND FABRICATION OF LOCAL-EXPOSURE SYSTEMS FOR *IN VIVO* STUDY ON MOBILE FREQUENCY BANDS. H.J. Doh¹, J.K. Park¹. ¹Dept. of Radio Science & Engineering, Chungnam National University, 220 Gung-dong, Yuseong-gu, Daejeon 305-764, Korea.

OBJECTIVE: Due to the rapid growth of mobile communication users, many studies have been performed and currently ongoing on the biological effects of mobile-phone EMF exposure. We have developed local exposure systems for long-term animal experiments at Cellular and PCS frequency band (Cellular: 848.5 MHz, PCS: 1762.5 MHz). Key results are presented in this paper.

METHODS: We developed carousel-type exposure systems. The exposure system consists of real CDMA signal source module, trays, antennas, and chamber for shielding. The chamber was designed to expose 4 trays that are stacked on the supporters inside chamber. Each tray contains 10 acrylic-tube restrainers, and thus 40 mice can be exposed at the same time. In this type of chamber, minimizing a stress on mice is very important. So we carefully designed the environmental condition like an illumination, ventilation, and noise inside chamber. To supply fresh air, two-fold ventilation scheme is used, one for the chamber using fans, and the other through restrainers using blowers. Proper illumination is also provided by fluorescent lamps. The design goal of luminance is 150 ~ 300 lux. The sound noise should also be low enough. It is less than

50 dB. The chamber is made of aluminium, the external size of which being 745 mm x 1060 mm x 1980 mm and we used an absorber foam inside the chamber with the thickness of 4.5 inch (AEL 4.5, AEMI. Inc.), which can reduce reflections from the wall at least -20 dB in the each operating frequency band. The carousel-type restrainers are chosen for head-mainly exposure. EMF signal are supplied the center of each tray by the sleeve dipole antennas, which were supplied by Motorola. The restrainers are tilt upwards about 3 ° for mice filth excretion. Proximal acrylic wings that makes angles of 50 ° with the tube's sagittal (shape of the arrow) plane, are attached to the tips of restrainers. Each tray has a pipe to fix the antenna and to afford ventilation through the restrainers. At the design stage, we simulated the E-field inside the chamber using FDTD (Finite Difference Time Domain) method. The FDTD method was also used to compute SAR (specific absorption rate) inside a mouse. The size of a mouse we simulated is 8 cm in length, 3.5 cm in height, and 3.5 cm in width. The mouse was modelled with 25 tissues, referring to the model of U.S Air Force Research Laboratory. SAR inside a mouse heads was measured using flouoptic temperature probes (model 790, Luxtron Corp.). The probe was inserted into the head of an exposed mouse using a plastic catheter, and the probe was located at 3 locations in the head of a mouse or a brain equivalent solid phantom. The SAR distribution inside mice and solid phantoms were also measured using IR camera (IRIS-5000, Medicare Co. Ltd.).

RESULTS AND DISCUSSIONS: At PCS frequency band the FDTD-simulated brain-averaged SAR value for mouse cadaver is 5.3 W/kg/W. The measurement result showed an excellent agreement. The FDTD simulation result for brain-averaged SAR value at cellular frequency band is 0.33 W/kg/W for mouse cadaver, which was in a good agreement with measurement result. These exposure systems are currently used for animal experiments.

References.

“A compact shielded exposure system for the simultaneous long-term UHF irradiation of forty small mammals: I. Electromagnetic and environmental design”, Eduardo G. Moros et al. *Bioelectromagnetics* vol. 19, 459-468, 1998.

“A compact shielded exposure system for the simultaneous long-term UHF irradiation of forty small mammals: II. Dosimetry”, Eduardo G. Moros et al. *Bioelectromagnetics* vol. 20, 81-93, 1999.

“Dosimetry in mice exposed to 1.6 GHz microwaves in a carrousel irradiator”, Mays Swicord et al, *Bioelectromagnetics* vol. 20, 42-47, 1999.

“The SAR Evaluation Method by a Combination of Thermo-graphic Experiments and Biological Tissue-Equivalent Phantoms”, Yoshinobu Okano et al. *IEEE Transactions on Microwave Theory and Techniques*, vol. 48, No. 11

This research was supported by the EMERC(ElectroMagnetic Environment Research Center) in Chungnam National University, one of IT Research Centers.

P-C-15

THE DETERMINATION OF CENTRAL MICROWAVE OPERATING FREQUENCY IN THE SOURCE OF MICROWAVE-INDUCED THERMOACOUSTIC TOMOGRAPHY. J. Yan*, SH.Z. Wu*, BEM Lab., Institute of Electrical Engineering, Chinese Academy of Sciences, 100080, Beijing, P.R.China.

OBJECTIVES: The optimization design of pulse microwave source is a key problem in the design of microwave-induced thermoacoustic tomography. This paper discussed the determination of central microwave operating frequency. As for which frequency to be chosen as the inducing source, the following factors should be considered: (1) Penetration depth in the biological tissue; (2) Microwave absorption rate in this frequency band; (3) The volume and the weight of the microwave-induced source.

ANALYSIS AND CONCLUSION: (1) Operating frequency and penetration depth in the biological tissue: When the biological tissue is radiated by the microwave pulses, its absorption characters are closely

related to its electrical parameters (relative dielectric constant ϵ_r and electrical conductivity σ), which are determined by tissue type and operating frequency. Meanwhile, the relationship between microwave energy attenuation along with the spread distance and the penetration depth in biological tissues presents as exponent attenuation relationship. For human body, its penetration depth can be expressed approximately

as $\delta = \frac{1}{\alpha} = \frac{1}{\omega} \sqrt{\frac{\mu\epsilon}{2} \left[\sqrt{1 + \left(\frac{\sigma}{\omega\epsilon}\right)^2} - 1 \right]}$. It can be seen the higher the electrical parameters and the operating

frequency, the less the penetration depth. Moreover, in this frequency scope, the electrical parameters change so little that the influence of chromatic dispersion in biological tissue is negligible.

(2) Microwave operating frequency and the absorption rate of biological tissues: In the bioelectromagnetic dosimetry, distribution specific absorption rates $SAR(\bar{r})$ means the electromagnetic power absorbed by average unit mass tissue in the adjacent area of point r . If the frequency of incidence wave is too low, the ability of electromagnetic power absorption in biological tissue is poor and it cannot induce the thermoacoustic wave effectively. If the frequency is too high, the electromagnetic power that passed the skin and absorbed by the coelomic tissue will decrease when the penetration depth decrease. Then thermoacoustic wave also cannot be induced effectively.

Since $SAR(\bar{r})$ is the normalized value to the mass, the energy absorbed by the tissue is: $W = \rho_r \times SAR(\bar{r}) \times t$. Generally the quality of heat converted from absorbed energy is expressed as $Q=0.24W(\text{cal})$ ($1J=0.24\text{cal}$.) In the microwave hyperthermia system, affected part of patient's body is heated to the special temperature ($41.5-43^\circ C$), cancer cells of the body will be killed and normal cells won't be affected. Usually $45-47^\circ C$ is thought as the highest temperature under the endurance limitation of human body exposed to the microwave radiation because during the converting process from the radiation energy to the quality of heat, a part of the energy is loss with flowing blood and the converting efficiency isn't 100%. Then the upper limitation of operating frequency can be worked out according to above conversion relationship. Considering all above thoughts and calculation, the frequency band is 100-1000 MHz.

When the frequency is given, both penetration depth and absorption ability in biological tissue are not easy to be satisfied simultaneously. Consequently, if choose the high operating frequency, the penetration depth is low and most power will be collected on the skin. Then the power proportion that passed the skin and entered the coelome tissues will decrease. Moreover, if the penetration ability is strong, the absorption ability of this tissue must be poor. As a result, the higher the microwave frequency, the lower the penetration depth. Balancing penetration and absorption, the operating frequency band of 300-1000MHz is considered more reasonable after calculation and analysis. The basic imaging requirements of muscle and fat tissues exposed to microwave are satisfied in this frequency band and the absorption capability of microwave power in human tissues is stronger in this frequency band than in others.

(3) Microwave frequency and the volume and mass of the stimulation source: As viewed from engineering, low frequency will result in excessively high cost, large volume and weight. Considering technique difficulties during the process of realization, the central operating frequency is set in 1GHz. This frequency not only satisfy both the demand of penetration depth and absorption rate, but also make the system volume and cost easy to be realized in engineering.

P-A-16

FACTORS AFFECTING OUTPUT POWER (AND RADIOFREQUENCY EXPOSURE) OF GSM MOBILE PHONES. L.S. Erdreich, M.D. Van Kerkhove, M. McNeely, Exponent, Inc., New York, NY 10170, USA.

OBJECTIVE: The purpose of the study is to identify which behavioral and situational factors affect power output of GSM phones (US technologies) in order to develop exposure metrics for future epidemiology studies. Software-modified phones (SMP) that record radiofrequency (RF) power output of

mobile phones are used to monitor potential variations in individual RF exposure.

BACKGROUND: Epidemiology studies and most human laboratory studies cannot directly measure the specific absorption rate (SAR), the dosimetric measure of individual exposure. Long-term epidemiology studies have previously assessed exposure by reported user minutes, or years as a subscriber. However, data on duration are subject to flaws if ascertained by phone records or by recall. More important, however, is that the duration of use does not capture variations in the level of RF exposure. The predominant contribution to exposure intensity is the output power, which varies with the phone design, user position, user anatomical characteristics, transmission technology, and environmental and network characteristics. Data do not exist to rank the precise or the relative importance of each; however, based on engineering concepts, Balzano (1999) estimated that most networks would vary the RF power of cell phones over a 100-fold range of intensity while variation in RF exposure based on anatomical differences between persons is no more than two fold. The network power control depends on the network technology and the phone traffic in a geographic area in a given time period. We will examine how behavioral and situational factors correlate with power output.

METHODS: The study population consists of cell phone users in different geographic areas in the US, who will be asked to switch their subscriber identity module (SIM) card into the SMP phone and fill out a logbook recording characteristic variables for each call. A questionnaire will be used to assess position of phone use and demographic characteristics of users, including body size. Because all the SMP phones are the same, the effect of phone design and antenna geometry is kept constant. To date, base station density can only be estimated indirectly, based on market penetration of GSM, or numbers of users in area. We will assess the relation of total minutes of use to total RF power output (a surrogate for exposure), and how power output varies with use, location and environment. We explored the power output of calls made under different conditions to evaluate variability and calculate better sample size estimates.

RESULTS: Preliminary data indicate differences in power output from calls made from different locations within the same geographic region, and calls made from different geographic regions (e.g., rural vs. urban). Within a region, these comparisons show differences in power output between calls made under different conditions, e.g., calls made from a higher floor vs. lower floor (Figure 1), and calls made from inside a home vs. while driving (Figure 2). The cumulative power output from calls made on an elevated floor of a building in an urban setting was 44 watts compared with 12.1 watts from calls made on a lower floor for the same call duration. These data represent work in progress.

This research is sponsored by the Cellular Telecommunications & Internet Association (CTIA) under a Collaborative Research and Development Agreement (CRADA) with the US Food and Drug Administration (FDA).

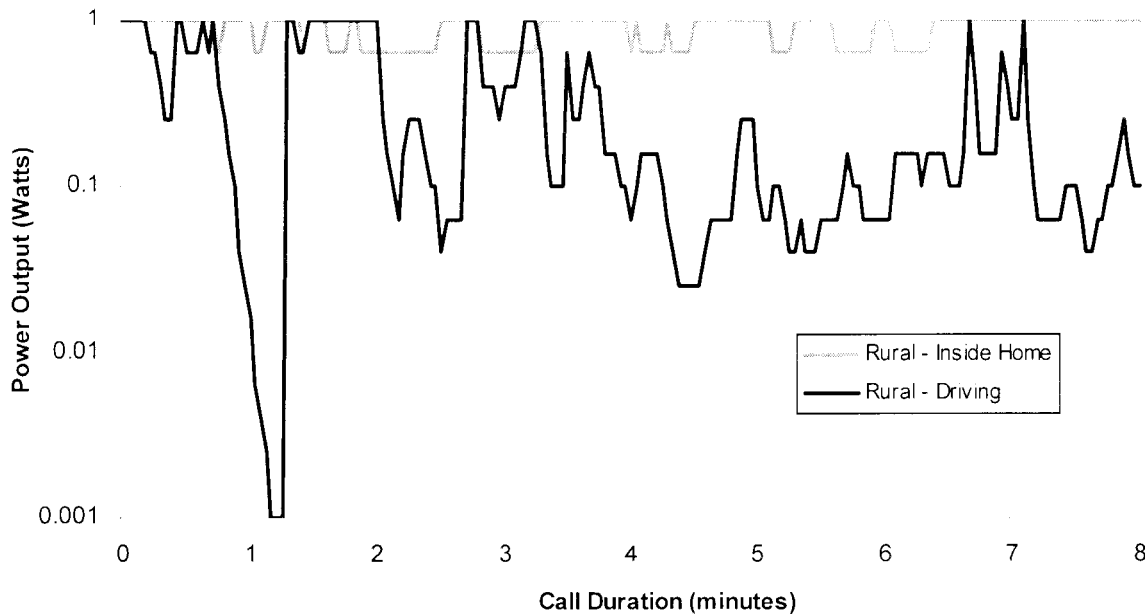


Figure 1. Example of variation in power output between calls made on different floors of a building in an urban environment

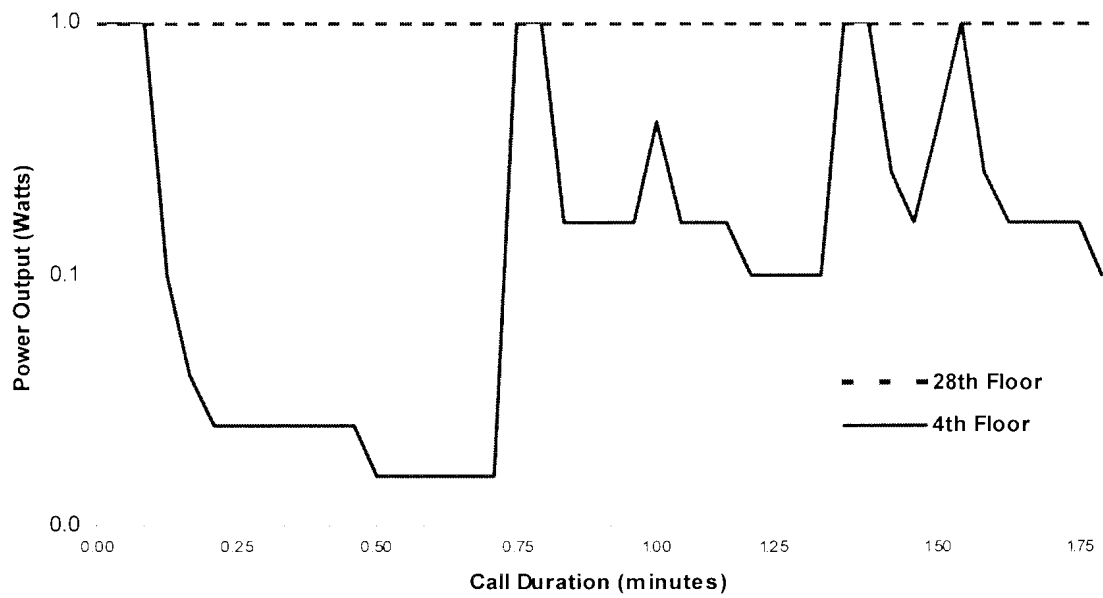


Figure 2. Example of variation in power output between call made inside a rural, residential building vs. while driving in rural area

P-B-17

TEM CELL SETUP FOR STUDIES ON THE BIOLOGICAL EFFECTS OF THE RADIO-FREQUENCY EXPOSURE ON THE NERVOUS CELLS SYSTEM. L. Arduino¹, F. Apollonio², G.A. Lovisolò¹, S. Mancini¹, R. Pinto¹. ¹Section of Toxicology and Biomedical Sciences, CR ENEA, Roma, Italy; ²Dept. of Electronic Engineering, "La Sapienza" University, Roma, Italy.

INTRODUCTION: According the main guidelines about the design and the realisation of exposure systems for high quality experiments in the field of the studies of biological effects of EM fields, a new complete exposure system has been realised. For the EM field generation a TEM cell [1,2,3,4] has been chosen and according the needs of the biological protocol, a suitable, very small TEM cell operating at the frequencies of mobile phones has been designed.

OBJECTIVES: Aim of this work was the design and the characterisation of a small TEM cell to be placed inside a standard incubator and allowing to radiate *multiwells* dishes.

MATERIALS AND METHODS: It is well known that cells require all the incubation conditions, so the system has been designed taking into account that - it should be small enough to be placed inside a standard incubator - to allow the incubator atmosphere reaching the cells, it should be provided by holes and grids and, at the same time, shielded to avoid interferences with the incubator electronics.

As first, a suitable TEM cell has been designed according the electromagnetic constraints. The cell has been designed with a squared cross section and thin inner conductor in order to obtain a large volume with uniform field for placing different kind of dishes. After the definition of the cell main dimensions, the complete system (cell and multiwells) has been numerically analysed by mean of a numerical code (CST Microwave Studio): optimised values has been defined for the length, for the tapered sections and for the dishes position versus the reflection coefficient and the efficiency. The model is showed in Fig.1 with the resulting SAR distribution inside the wells.

RESULTS: Different exposure modalities versus homogeneity and efficiency have been evaluated. Because of the target of the experimental study was constituted by nervous cells particular attention to the SAR distribution on the well bottom cells layer has been payed. A good level of homogeneity is evidenced for the SAR distribution at the bottom of the wells when the power is supplied from the bottom of the TEM cell. Significant differences have been observed between the couple of wells close to the inner conductor (w_I) and the one close to the outer (w_O), but not between groups (Fig. 1): at least 12 wells at the same dose level are always available.

CONCLUSIONS: The exposure protocol requires two exposure systems in order to obtain sham and exposed samples at the same time. An incubator with two TEM cells inside will be used, as showed in figure 2. Each cell has been provided by a large door and, to allow efficient air circulation, two opposite grid and two external fans have been connected to each one. To realise experimental blind conditions the entire system has been designed, including MW generation chain and control system (hardware card and specific software): double blind procedure is allowed by using an encrypting code, which blinds the linkages between doses and exposure systems (the TEM cells). This information can be decrypted only at the end of experiment.

References

- [1] M. Crawford. Generation of standard EM fields using TEM transmission cells. IEEE Transact 16:189-195, 1974.
- [2] M. Burkhardt, K. Pokovic, M. Gnos, T. Schmid, N. Kuster. Numerical and experimental dosimetry of Petri dish exposure setup. Bioelectromagnetics 17:483-493, 1996.
- [3] L. Martens, JV Hese, DD. Zutter, CD Wagter, L. Malmgren, B. Persson, L. Salford. Simulation of the effect of inhomogeneities in TEM trasmission cells using the FDTD-method. IEEE Transactions of Electromagnetic Compatibility, vol.34, n.3, 1992.

[4] A.W. Guy, C.K. Chou, and J.A. McDougall. A Quarter Century of *In Vitro* Research: A New Look at Exposure Methods. *Bioelectromagnetics* 20:21–39, 1999.

P-C-18

INFLUENCE OF CUBE ORIENTATION ON PEAK SPATIAL-AVERAGED SAR. M.G. Douglas, C.K. Chou. Motorola Florida Research Laboratories, Ft. Lauderdale, Florida, 33322, USA.

OBJECTIVES: This study examines the sensitivity of orientation on the peak spatial-averaged SAR in a 1-gram or 10-gram cube tilted relative to the phantom surface.

METHODS: In the process of creating international SAR measurement standards (e.g., [1]), questions were raised as to how the peak spatial-averaged SAR is affected by the orientation of the averaging volume (a 1-gram or 10-gram “tissue volume in the shape of a cube” [2]). It is important to use an averaging volume that is as close as practical to a cubical shape. This is easily achieved when measuring in flat phantoms (Fig. 1a). In curved phantoms, such as head phantoms, the shape can deviate from that of a cube in at least two ways. First, due to the fact that the peak SAR is typically located at the phantom surface, the front face of the cube should be distorted in order to conform to the phantom surface and ensure that the peak SAR is captured (Fig. 2a). The back face is typically distorted in the same way to ensure the correct averaging mass. The side faces are ideally parallel to the direction normal to the phantom surface at the center of the cube (\hat{n} in Fig. 2). Second, system limitations during measurement (probe positioning, phantom sagging, phantom shape tolerances, etc.) can cause the side faces of the averaging volume to be oriented at an angle θ away from \hat{n} (Fig. 2b). In flat phantoms alone, θ can be as much as 5° due to

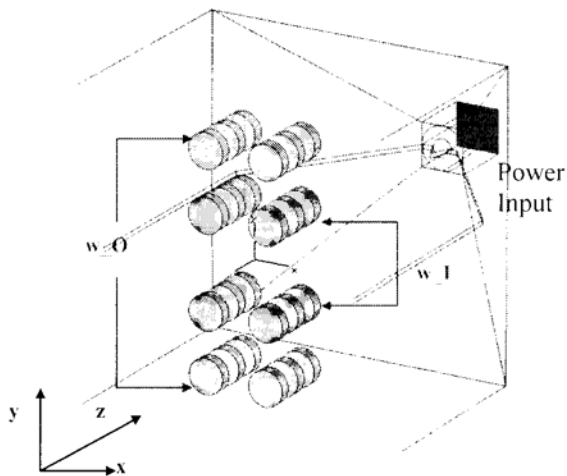


Fig. 1 – SAR distribution in numerical model of the system (CST code).

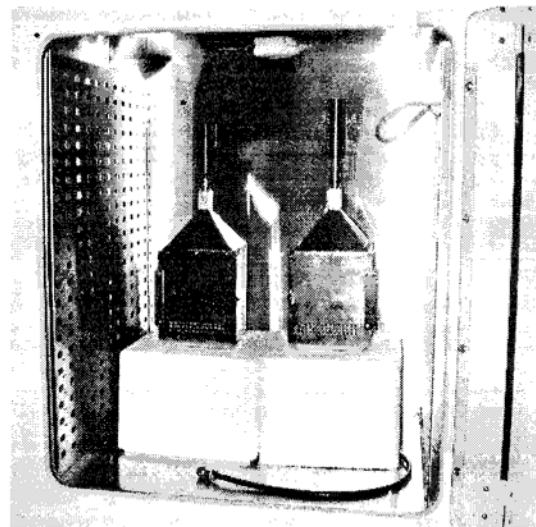


Fig. 2 – The two TEM cells in the incubator: power is supplied from bottom and the upper port is connected to the matched load through a cable.

sagging within the specifications of [1]. It is therefore important to define a reasonable tolerance of the cubical shape of the averaging volume. In particular, an upper limit on θ should be established based on its effects on the peak spatial-averaged SAR. Analytical and experimental studies are performed here to understand these effects.

RESULTS: For the analytical study, the three reference SAR distributions in [1] were used. For the case where $\theta = 0^\circ$, the distributions were sampled on a 3D grid with 1 mm resolution that is oriented normally to a flat surface (Fig. 1a). The peak spatial-averaged SAR values were calculated. The peak spatial-averaged SAR values were also calculated on a re-interpolated grid that is at an angle $\theta = 10^\circ$ from normal (Fig. 1b).

The height of the re-oriented averaging volume is slightly less than that of the normally-oriented volume (by a factor of $\cos \theta$) to simulate how typical SAR measurement systems would perform the measurement. The base length is therefore longer (by $1/\cos \theta$) to ensure the correct averaging volume. The deviation in SAR results between these two cases is then found. Results show a maximum SAR deviation of 0.3% and 0.4% for SAR_{1g} and SAR_{10g} , respectively. The experimental study used 264 SAR measurements from 55 different products. The transmit frequencies of these products range from 150 to 2450 MHz. The 264 measurements include 146 measured on a SAM head phantom [1] and 118 measured on a flat body phantom. Data were re-interpolated onto grids at angles of $\theta = 3^\circ, 5^\circ$ and 10° . Due to the fact that the measured data can be highly asymmetric, the re-interpolated grids were rotated by $\phi = 0, 30^\circ, 60^\circ, \dots, 360^\circ$ at each angle θ and the worst-case SAR deviation from $\theta = 0^\circ$ was found. Results are shown in Table 1. The mean of the worst-case deviations of the 264 measurements is within 0.5% for all angles studied. The maximum worst-case deviation at $\theta = 10^\circ$ is 1.0% and 2.6% for SAR_{1g} and SAR_{10g} , respectively. A histogram of the SAR deviations is shown in Fig. 4 for SAR_{10g} at $\theta = 10^\circ$. The root-mean-squared deviation was found to be within 0.7% for all cases studied. This has a negligible effect on measurement uncertainty (e.g., a 12% uncertainty would increase to 12.02%).

CONCLUSIONS: The results of this study show that a tolerance in the cube orientation of up to 10° has a small effect on SAR measurement uncertainty. A tolerance on the cube orientation is needed to account for limitations in the SAR measurement system. We recommend that this tilted cube tolerance be included in the IEEE and IEC standards.

References.

- [1] IEEE, "IEEE Recommended Practice for Determining the Peak Spatial-Average Specific Absorption Rate (SAR) in the Human Head from Wireless Communications Devices: Measurement Techniques," IEEE Standard 1528, 2003.
- [2] IEEE, "IEEE Standard for Safety Levels with Respect to Human Exposure to Radio Frequency Electromagnetic Fields, 3 kHz to 300 GHz," IEEE Standard C95.1, 1999.

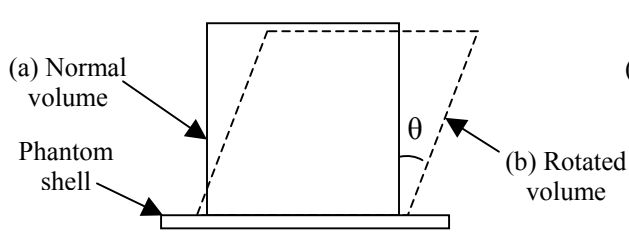


Fig. 1: Averaging volumes used for analytical and experimental studies.

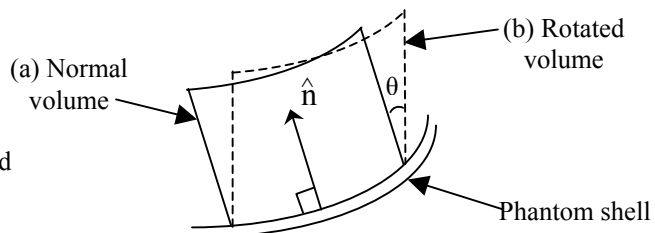


Fig. 2: Averaging volumes used in a curved phantom.

θ	SAR_{1g}		SAR_{10g}	
	Mean	Max	Mean	Max
0°	0	0	0	0
3°	0.0%	0.2%	0.0%	1.1%
5°	0.1%	0.4%	0.2%	0.8%
10°	0.5%	1.0%	0.5%	2.6%

Table 1: Percent deviation in SAR due to re-orientation of averaging volumes for experimental study.

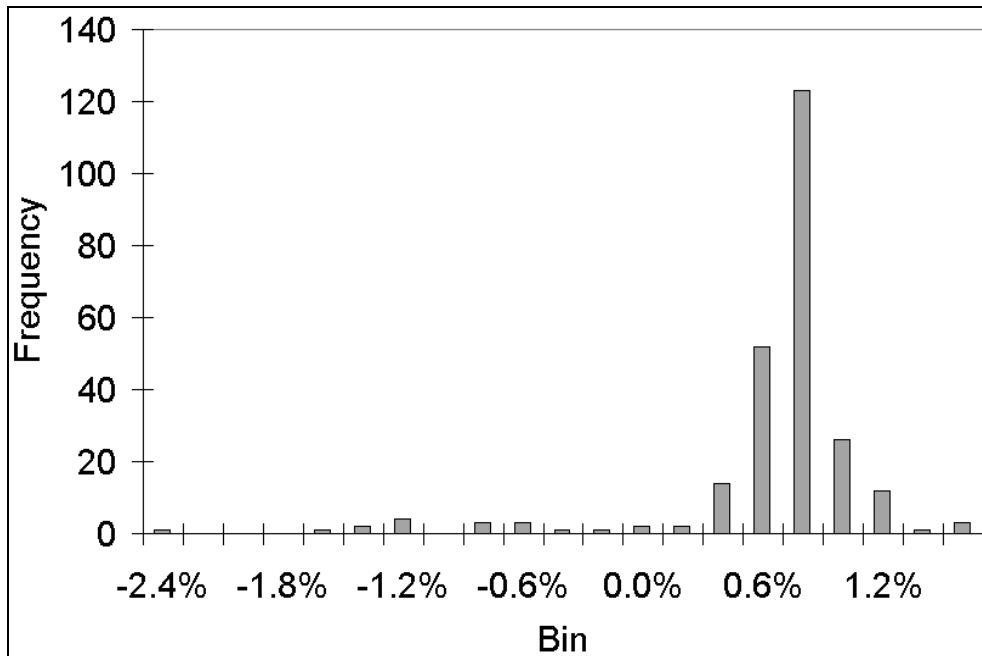


Fig. 4: Histogram of maximum deviation in SAR_{10g} of the 264 SAR measurements for $\theta = 10^\circ$.

P-A-19

SAR MEASUREMENTS AT MULTIPLE FREQUENCIES USING A SINGLE TISSUE-EQUIVALENT LIQUID. M.G. Douglas, M. Kanda, C.K. Chou. Motorola Florida Research Laboratories, Ft. Lauderdale, Florida, 33322, USA.

OBJECTIVES: Rather than using different tissue-equivalent liquids for each frequency band as per international SAR measurement standards (e.g., [1]), a single tissue-equivalent liquid is used. Errors are examined and corrections are applied to study the usefulness of this approach.

METHODS: For the measurement of SAR from wireless handsets, a standard head phantom is filled with a liquid whose homogeneous dielectric properties match those of human tissues in a conservative sense [2]. Unfortunately, the dielectric properties of typical phantom liquids vary differently with frequency than those of human tissues. Therefore, in order to match the values of [2] as closely as possible, different liquid recipes are used at different frequency bands. It is expensive to make and maintain multiple phantom liquids. At higher frequencies (above 2 GHz) it can also be difficult to find stable and accurate recipes using safe and inexpensive ingredients. An alternative approach is proposed where a single phantom liquid is used at all frequencies. The chosen liquid uses safe, inexpensive ingredients (water, sugar, salt, cellulose and a preservative, as per the 900 MHz recipe in [1]). The dielectric properties of this liquid are compared with the target values of [1] from 300 – 2500 MHz in Fig. 1. At frequency bands other than the band covering 900 MHz, corrections are used to adjust the measured SAR to that using the target dielectric parameters in [1]. There are two questions with this approach. One is whether the antenna impedance of the wireless handset is sensitive to changes in the dielectric parameters of the phantom liquid. If so, the relationships between the SAR values using the single liquid vs. multiple target liquids will be confounded by the handset-dependent change in antenna impedance. The second question is whether the SAR correction will be accurate given the dependence of spatial-averaged SAR on penetration depth, which is handset dependent. Both of these questions need careful study.

RESULTS: To address the first question, two investigations were carried out. First, the plane wave transmission coefficient at the air-liquid boundary was calculated (assuming no phantom shell) both for the single liquid and the target dielectric parameters (Fig. 2). The agreement between the two is within 5% at all frequencies studied, indicating that the power transferred to the phantom and the phantom average SAR

are similar for these two cases. This result agrees with [3]. This is notable given that the conductivity and permittivity differ by as much as 50% and 25%, respectively, for the two cases. Second, 1900 MHz dipole antennas under a flat phantom were simulated in FDTD for the two cases (Table 1). Results are compared between the dielectric parameters of the targets at 1900 MHz and the 900 MHz liquid at 1900 MHz. Three different distances between the dipole antenna feed point and the liquid are shown. It is seen that the dipole antenna impedance ($Z = R + jX$) and efficiency (η) and the phantom average SAR (SAR_{av}) are very close for the two cases at all three distances. This indicates that the antenna impedance is not sensitive to the choice of dielectric parameters for this condition. Results for other antennas and test conditions are also needed. To address the second question, a previously-reported study on 264 SAR measurements from over 30 handsets [4] showed that despite a large range of measured penetration depths found (range of $\pm 25\%$ from the mean value), the mass-averaged SAR could be accurately estimated from area scan data (errors within $\pm 2\%$ and $\pm 7\%$ for SAR_{1g} and SAR_{10g}) with only an estimate of the penetration depth. This shows that an accurate SAR correction for this approach is possible.

CONCLUSIONS: Investigations thus far give encouraging results that using a single tissue-equivalent liquid together with post-processing corrections can provide an accurate estimate of the SAR for the case where standardized target dielectric parameters are used. Experimental studies on handsets will be necessary to validate this approach.

Reference:

- [1] IEEE, "IEEE Recommended Practice for Determining the Peak Spatial-Average Specific Absorption Rate (SAR) in the Human Head from Wireless Communications Devices: Measurement Techniques," IEEE Standard 1528, 2003.
- [2] A. Drossos, V. Santomaa, N. Kuster, "The dependence of electromagnetic energy absorption upon human head tissue composition in the frequency range of 300-3000 MHz," *IEEE Trans. Microwave Theory Tech.*, vol. 48, no. 11, pp 1988 – 1995, Nov. 2000.
- [3] P. Gajsek, W.D. Hurt, J.M. Ziriak and P.A. Mason, "Parametric dependence of SAR on permittivity values in a man model," *IEEE Trans. Biomed. Eng.*, vol. 48, no. 10, pp. 1169 – 1177, Oct. 2001.
- [4] M. G. Douglas, M. Y. Kanda, and C-K. Chou, "Post-processing errors in peak spatial-average SAR measurements of wireless handsets," in *25th Ann. Meeting of the Bioelectromagnetics Soc*, Wailea Maui, June 2003, pp. 370–371.

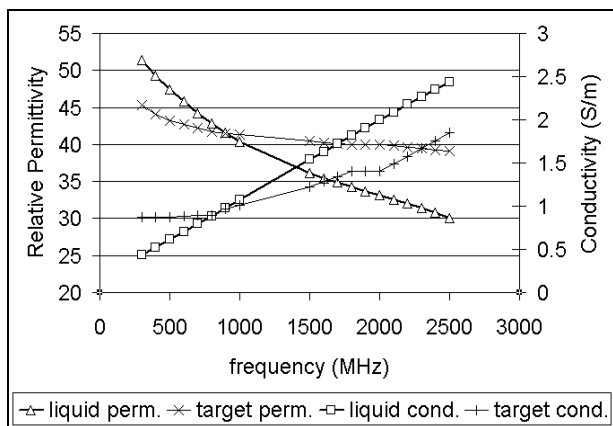


Fig. 1: Permittivity and conductivity of 900 MHz tissue-simulating liquid vs target values of [1] from 300 – 2500 MHz.

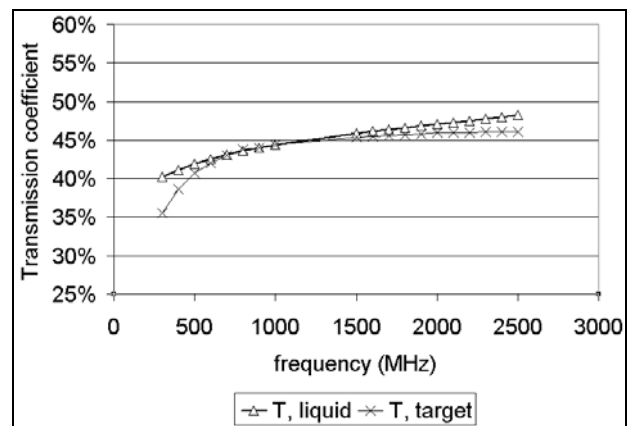


Fig. 2: Transmission coefficient at air-liquid interface for two sets of dielectric parameters of Fig. 1

	5 mm distance			10 mm distance			15 mm distance		
	Target	Liquid	Diff.	Target	Liquid	Diff.	Target	Liquid	Diff.
SAR_{1g}	45.7	53.7	18%	25.9	29.9	15%	12.8	14.9	17%
SAR_{10g}	21.7	22.9	5.4%	13.9	14.3	2.9%	7.4	7.6	3.2%
SAR_{av}	1.4	1.3	3.9%	1.0	1.0	4.4%	0.7	0.7	4.0%
$R (\Omega)$	73.6	73.8	0.3%	58.8	60.5	2.9%	67.6	69.7	3.2%
$X (\Omega)$	83.1	88.8	6.8%	106.0	109.0	2.9%	126.8	128.4	1.3%
η	9%	10%	1%	30%	32%	1%	53%	54%	1%

Table 1: FDTD simulations of 1900 MHz dipole antenna under a flat phantom for three distances of the dipole feed point to the air-liquid interface (phantom shell was not simulated). At each distance, the target dielectric parameters of [1] and the 1900 MHz dielectric parameters of the 900 MHz liquid (from Fig. 1) are compared. The model resolution is 1.25 mm in all directions. The width and length of the phantom are greater than $0.4 \lambda_0$ and $0.6 \lambda_0$, respectively, as per [1]. The depth of the phantom liquid is greater than three penetration depths. Results show that for the peak 1-gram averaged SAR (SAR_{1g}), the difference between the two cases is consistent across all three distances. The same is true for the peak 10-gram averaged SAR (SAR_{10g}).

P-B-20

INVESTIGATION OF APPROACHES FOR FAST SAR TESTING OF MOBILE PHONES. M. Siegbahn, T. Persson, C. Törnevik, Ericsson Research, Ericsson AB, SE-164 80 Stockholm, Sweden.

INTRODUCTION: The procedure of SAR measurements of mobile phones involves several phone test positions and test frequencies normally requiring a substantial amount of laboratory time for a complete test. A fast SAR testing methodology would be beneficial in many cases, such as during phone prototype development or for testing purposes in phone production. The ideal approach would be to use a near-field sensor measuring just a few field values from which the corresponding maximum mass averaged SAR for the phone is estimated.

OBJECTIVES: In this study laboratory measurements on a large sample of phones of the same model have been conducted for evaluating the approaches of either estimating the head phantom mass averaged SAR from the squared maximum free-space H-field [1], or from the maximum point SAR determined in a coarse surface scan [2].

METHODS: Measurements of SAR and H-fields were conducted on 100 randomly selected units of the Ericsson mobile telephone model R380world for the 900 MHz and 1900 MHz GSM bands. The measurements were carried out with the Schmid & Partner Engineering AG near-field scanner DASY3. Maximum surface scan SAR and mass averaged SAR were measured in a head phantom for all the units. Planar H-field scans were conducted in free-space 14 mm above the keypad of each phone for finding the maximum H-field value. The grid resolution used in the SAR and H-field measurements was 10 mm. To evaluate the relation between the maximum mass averaged SAR and the squared maximum H-field as well as the maximum surface scan SAR, the correlation coefficients were calculated.

RESULTS. Figure 1 (left) shows the 10g mass averaged SAR versus the squared maximum free-space H-field at 900 MHz for the tested R380world units. The measurement data has a quite linear appearance and the correlation coefficient is 0.87. In Figure 1 (right) the 10g mass averaged SAR versus the maximum surface scan SAR is shown. The measurement points adapt well to a straight line and the correlation coefficient is here 0.98.

CONCLUSIONS: Two possible approaches for fast estimation of head phantom mass averaged SAR have been evaluated with the measurement data for 100 units of the Ericsson R380world phone model. An approach based on the excellent correlation between the mass averaged SAR and the maximum surface scan SAR seems to offer the best accuracy. However, a method based on H-field measurements in free-

space could also be feasible.

References.

- [1] N. Kuster, Q. Balzano, "Energy Absorption Mechanism by Biological Bodies in the Near Field of Dipole Antennas above 300 MHz", IEEE Transactions on Vehicular Technology, Vol. 41, No. 1, February 1992.
- [2] M.Y. Kanda, M. Ballen, M.G. Douglas, A.V. Gessner, CK Chou, "Fast SAR determination of gram-averaged SAR from 2-D coarse scans", Proceedings of the 25th BEMS Annual Meeting June 2003.

(Unable to extract figure from PDF file)

Figure 1: The 10g averaged SAR versus the maximum squared H-field for the 100 GSM phones (left). The 10g averaged SAR versus the local maximum SAR for the tested phones (right).

P-C-21

STUDENT

CALCULATIONS OF INDUCED CURRENT DENSITIES FOR HUMANS BY MAGNETIC FIELDS FROM EAS COUNTERTOP ACTIVATION/ DEACTIVATION DEVICES USING FERRO-MAGNETIC CORES. Q. Li, O.P. Gandhi, and G. Kang, Department of Electrical and Computer Engineering, University of Utah, Salt Lake City, Utah 84112, USA.

We have previously reported on the use of the impedance method to calculate induced current densities for a 2 mm resolution anatomic model of the human body for the non-uniform magnetic fields of a pass-through electronic article surveillance (EAS) system as well as for a typical air core magnetic desktop system for activation/deactivation of tags at the point of checkouts [1]. Using Biot-Savart's law, the spatially non-uniform magnetic fields were calculated for the pass-through region for the first EAS system and for the space in front of the countertop system for activation/deactivation of tags. The vector magnetic fields thus obtained were used to calculate the induced electric fields and current densities for various tissues in the 2 mm resolution anatomically-based Utah Model of the human body placed in the pass-through EAS system or in front of the countertop activation/deactivation system for positions and spacings suggested in the European Standard EN50357 [2]. The induced current densities for any 1 cm² cross sectional area of the CNS tissues e.g. the brain and the spinal cord were compared against the basic restrictions proposed by the ICNIRP Safety Guidelines [3].

Increasingly, ferromagnetic cores are being used to create the highly-concentrated time-varying magnetic fields for countertop activation/deactivation devices. This creates a necessity to model the shaped high reluctance path/s provided by the ferromagnetic core and any proximal magnetic shields that may be used to reduce the leakage magnetic fields experienced by the human in front of such a device. Because of the duality of magnetic and electric circuits, electrical conductors shaped like the ferromagnetic core and any proximal shields may be used to calculate the leakage electric fields and thus leakage magnetic fields of the countertop activation/deactivation device for the space occupied by a human operating such a device.

We have used this magnetic circuit/electric circuit equivalence approach to calculate the leakage magnetic fields of a typical ferromagnetic core using tapered pole pieces. As expected, the magnetic fields drop off extremely rapidly for increasing distance from the front narrow gap between the pole pieces of the ferromagnetic applicator. However, the magnetic fields and their variations along central horizontal and vertical axes at distances of 30, 45, and 60 centimeters from the ferromagnetic applicators are in excellent agreement (within $\pm 5\%$) of those measured for a typical ferromagnetic applicator. A distance of 30 cm from the front plane of the human model is suggested in [2] for compliance testing of such countertop EAS systems. Hence, the distances of 30, 45, and 60 cm taken for comparison with the measured data correspond to the front plane, the central plane, and the back plane of the anatomic human model to be placed in front of the assumed ferromagnetic core EAS system.

For an assumed EAS system frequency of 60 Hz, the induced electric fields and current densities are

calculated using the well-published impedance method for each of the voxels of dimensions $1.974 \times 1.974 \times 1.93$ mm for the 31-tissue Utah Model of the human model [1, 4, 5]. As recommended in [2], the electrical conductivities assumed for the various tissues are taken from [6] except for the heart for which we have taken a weighted average of the conductivities of heart muscle and blood rather than for just the heart muscle given at the website. The maximum 1 cm^2 area-averaged current densities thus calculated for the CNS tissues i.e. the brain and the spinal cord are compared with the basic restriction of 2 mA/m^2 given in the ICNIRP Guidelines [2] for the assumed EAS frequency of 60 Hz.

References

- [1] O. P. Gandhi and G. Kang, "Calculation of Induced Current Densities for Humans by Magnetic Fields from Electronic Article Surveillance Devices," *Physics in Medicine & Biology*, Vol. 46, pp. 2759-2771, 2001.
- [2] European Standard EN50357, "Evaluation of Human Exposure to Electromagnetic Fields from Devices Used in Electronic Article Surveillance (EAS), Radiofrequency Identification (RFID) and Similar Applications," CENELEC Central Secretariat: rue de Stassart 35, B-1050, Brussels, Belgium, October 2001.
- [3] ICNIRP (International Commission on Non-Ionizing Radiation Protection), "Guidelines for Limiting Exposure to Time-Varying Electric, Magnetic, and Electromagnetic Fields," *Health Physics*, Vol. 74(4), pp. 494-522, April 1998.
- [4] O. P. Gandhi, G. Kang, D. Wu, and G. Lazzi, "Currents Induced in Anatomic Model of the Human for Uniform and Nonuniform Power Frequency Magnetic Fields," *Bioelectromagnetics*, Vol. 22(2), pp. 112-121, February 2001.
- [5] G. Kang and O. P. Gandhi, "Comparison of Various Safety Guidelines for Electronic Article Surveillance Devices with Pulsed Magnetic Fields," *IEEE Transactions on Biomedical Engineering*, Vol. 50(1), pp. 107-113, 2003.
- [6] <http://safeemf.iroe.fi.cnr.it/tissprop/>

P-A-22

AN IN VITRO STUDY IN THE FRAMEWORK OF CTIA- FDA PROJECT: DESIGN AND DOSIMETRY OF A FOUR CHANNEL SET UP OPERATING AT 900 MHZ. R. Pinto¹, L. Ardoino¹, V. Lopresto¹, C. Marino¹, S. Mancini¹, M. Sarti², M.R. Scarfi², and G.A. Lovisolo¹. ¹ICEmB at ENEA, Section of Toxicology and Biomedical Sciences, Roma, Italy; ²ICEmB at CNR-IREA, Napoli, Italy.

BACKGROUND: In the framework of the CTIA funded research on wireless phone safety, the Italian Interuniversity Center on Interaction between Electromagnetic Fields and Biosystems (ICEmB) is involved in the study of micronucleus induction following 24 hours exposure of human peripheral blood lymphocytes to 900 MHz, GSM signal, RF radiation.

OBJECTIVE: Design a complete set up (exposure system, power supply, control and storage of parameters) both for simultaneous blinded exposure at four SAR levels and for experiments performed to evaluate the role of temperature increase (from 35 to 42°C) by using either conventional heating and radiofrequency at two different peak SAR values.

MATERIAL AND METHODS: The exposure system is constituted by four Wire Patch Cells (WPC) [1] hosted inside two standard CO₂ incubators (two WPCs for each incubator), surrounded by RF absorbing panels positioned inside a Faraday cage in order to avoid Electromagnetic Compatibility problems. The dosimetry and the optimization of the exposure system has been carried out [2] by experimental measurements (E-field measurements and SAR evaluations by temperature measurements) and numerical codes (XFDTD and CST Microwave Studio). An appropriate system has been realized for maintaining and monitoring the samples temperature in the WPC during the exposure in order to avoid undesired temperature increase due to EM power dissipation in the biological medium. A four RF channel system, fully computer controlled, has been designed in order to allow us to blindly expose the biological samples

The microwave signal generation system is constituted by four GSM signal generators and four MW amplifiers. A control and acquisition system for the different parameters (amplifier gain, direct and reflected powers) is constituted by a hardware control card (WPCController) communicating with PC by the TCP-IP communication protocol, in order to maintain and store exposure conditions during the experiments. A specific software was developed (using LabVIEW 6.1) to have a friendly user-system interface, even useable by non expert staff. Biological and exposure data are stored in a database (Microsoft Access 97) by this software in real time. The experimental double blind conditions are allowed by using an encrypting code, which blinds the linkages between doses and exposure systems (WPCs). This information can be decrypted only at the end of experiment and only by the project responsible. Monitored exposure data (such as net power) are stored in the database too, directly during time of exposure. The access to database from file system is protected by a password in order to maintain denied the access to row data.

CONCLUSION: Detailed experimental and numerical analysis of WPC has been performed. At the moment the RF exposures are in progress in both labs.

References.

- [1] Laval L, Leveque Ph, Jecko B. A new *in vitro* exposure device for the mobile frequency of 900 MHz. *Bioelectromagnetics*, 21: 255-263, 2000
- [2] Lovisolò GA, Asta D, Ciammetti L, Mancini S, Marino C, Pinto R, and D'Inzeo G, Proceedings of Millenium International Workshop on Biological Effects of Electromagnetic Field. eds. P. Kostarakis and P. Stavroulakisp, Crete, p. 527-532, 2000.

P-B-23 MOVED TO SESSION 3-4.

P-C-24

VARIATION OF SAR VALUES MEASURED BY COMMERCIAL MEASUREMENT SYSTEMS COMPATIBLE TO INTERNATIONAL STANDARDS. S. Watanabe¹, Y. Miyota², K. Satoh², and Y. Yamanaka¹, ¹National Institute of Information and Communications Technology, Tokyo 184-8795, Japan, ²NTT Advance Technology Co., Tokyo 180-0012, Japan.

INTRODUCTION: Maximum local SAR in a human head during use of a cellular phone has been estimated by using several commercial SAR measurement systems. While specifications for the SAR measurement systems have recently been standardized, a few commercial SAR measurement systems compatible to the standards are now available. It is not unclear whether the different standard-compatible SAR measurement systems can provide measured value within the reasonable deviation, about 30 % as typical expanded uncertainty, reported in one standard (IEEE Std. P1528).

OBJECTIVE: We have therefore performed to measure head SAR by different SAR measurement systems compatible to the standards and compared SAR distributions and maximum local SAR values between those systems.

METHOD AND MATERIAL: We used three commercially available SAR measurement systems, i.e., DASY3 (SPEAG Inc.), DASY4 (SPEAG Inc.), and SARA2 (IndexSAR). A bath-type SAM phantom and upright-type one were used for DASY3 and DASY4 and for SARA2, respectively. The electrical properties of the phantom liquid were maintained within 5% from the target values for each measurement. Six types of cellular phones for 800-MHz PDC, 1500-MHz PDC, or 2000-MHz W-CDMA were tested.

RESULTS AND DISCUSSION: Some of the measured SAR distributions are shown in Figures 1 and 2. It is shown that similar SAR distributions were obtained by the three measurement systems. The maximum local SARs were then compared between the measurement systems. We have found that the deviation of the maximum local SAR values is small, typically within 10%, when the peak SAR appears around the ear reference point (ERP) as shown in Figure 1, and that, on the other hand, the deviation can becomes larger than 20% when the peak SAR appears around lower part as shown in Figure 2. This discrepancy may be

due to the different angle of incidence of the SAR probes, which was one of the major controversy topics in standardization. In most cases, however, the deviation of the maximum local SAR values was within the typical expanded uncertainties (about 30%).

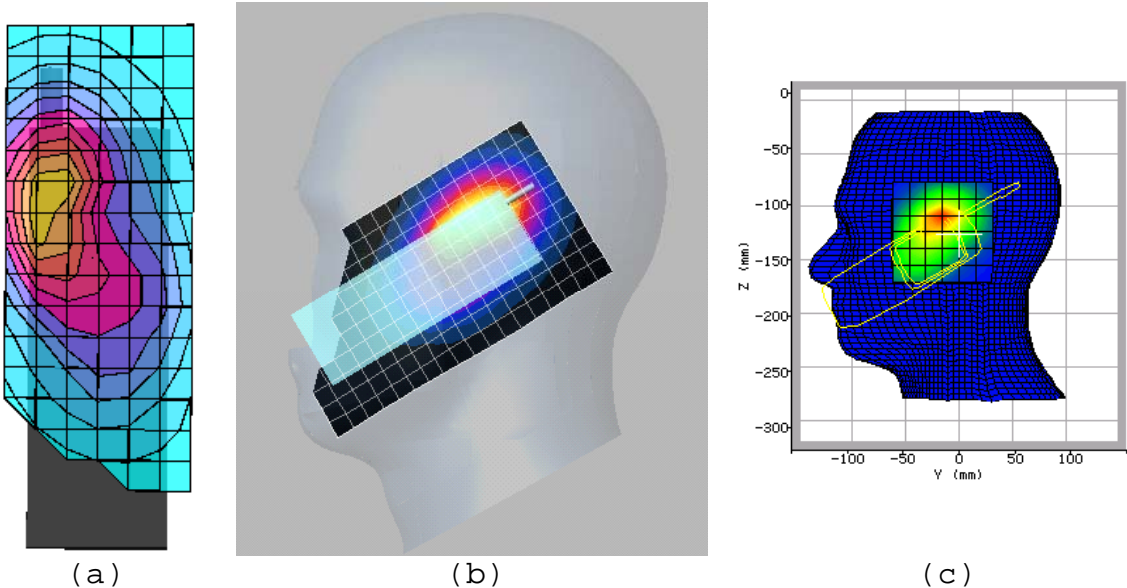


Figure 1: SAR distributions on the surface of SAM phantom, measured by DASY3 (a), DASY4 (b), and SARA2 (c), with the same condition; cellular phone, position, and frequency.

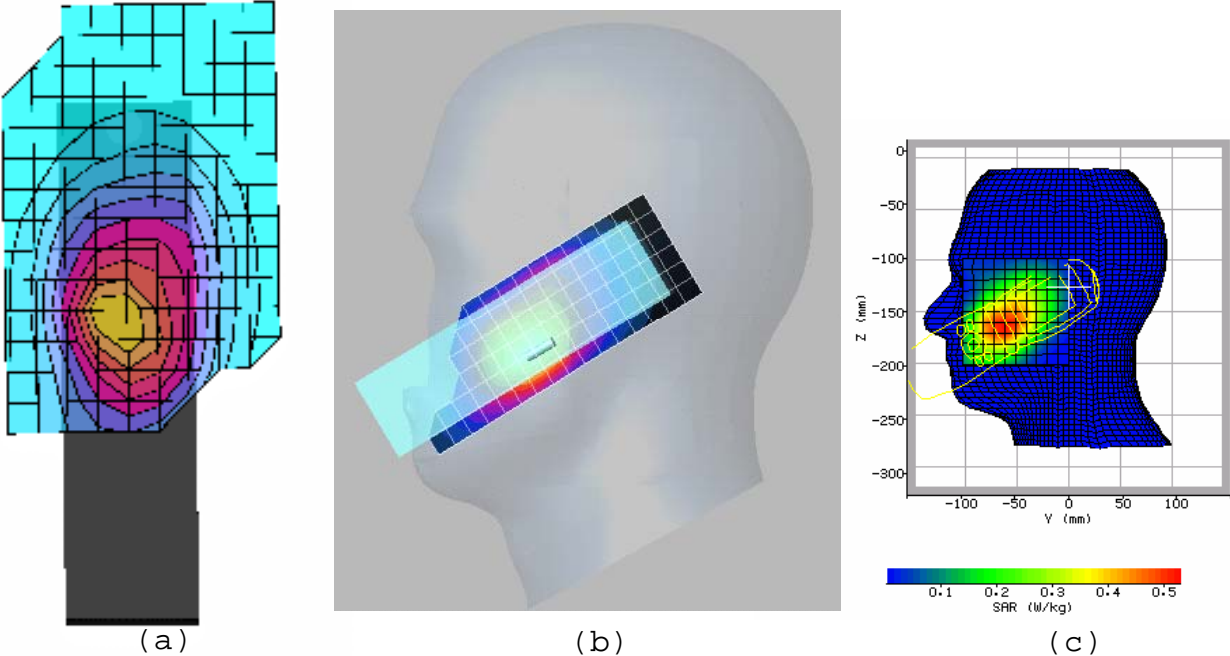


Figure 2: SAR distributions. Except the cellular phone type, the conditions are the same as Figure 1.

EMPIRICAL DOSIMETRY IN SUPPORT OF 220 MHZ WHOLE BODY RF EXPOSURE IN HUMAN VOLUNTEERS. S.J. Allen¹, E.R. Adair², K.S. Mylacraine¹. ¹General Dynamics, Brooks City Base, TX 78235, ²US Air Force Research Laboratory HEDR, Brooks City-Base, TX 78235, USA.

BACKGROUND: Eleanor Adair at the John B. Pierce Foundation initiated a series of human exposures to radiofrequency RF energy in 1995. The purpose of these experiments was to study the basic physiological thermoregulatory responses of human volunteers. Four studies were completed at 450 and 2450 MHz. The study using 2450 MHz was basically a superficial exposure, having a penetration depth of 2.3 cm. The thermoregulatory studies were continued at 100 MHz, the resonance frequency for a seated human. To fill in the gap between 100 and 450 MHz, this study was performed at 220 MHz.

OBJECTIVE: It is imperative that the exposure conditions for human volunteers be defined as accurately as possible. An orderly measurement protocol was followed to achieve accurate exposure criteria.

METHODOLOGY: Several detailed experiments were performed to define the RF fields to which human subjects were to be exposed. The experimental protocol called for a series of measurements starting with the simplest measurement of instrument drift and proceeding to detail field maps and SAR measurements. Beam centerline scans were made at 180 to 280 cm from the radiating dipole antenna. Field maps were made with 1000 Watts of transmitter output, using NBS dipole and loop antennas, over an 80 cm horizontal by 100 cm vertical plane at 200, 225, and 250 cm from the radiating dipole. These data were input into Microsoft Excel to generate a field impedance map. Excel was also used to average the E-field over the back of the area exposed using the 225 cm field map. SAR was measured using the “green man”, a human-shaped plastic bag filled with tissue equivalent material. Measurements were taken at 156 points inside the phantom. All measurements were repeated and the two results averaged. From these data the whole body SAR was calculated for the 220 MHz exposure conditions. To assure consistent exposures, NBS loop antenna measurements were taken before and at 5-minute intervals during all exposures. Transmitter forward and reverse powers, as well as plate current, were also read at 5 minute intervals.

RESULTS: Minor deviations from $1/R^2$ (+/- 7% over the region of interest) indicate some scattering off the back wall of the chamber. E and H-field maps were relatively uniform and the field impedance map indicated impedances within 20% of the impedance of free space (377 Ohm) over the exposure area. The average normalized incident power density over the back exposure area was 0.0116 mW/cm²/W +/- 4%. The normalized whole body SAR was 0.046 W/kg/mW/cm² for the first run and 0.044 W/kg/mW/cm² for the second run showing excellent repeatability. The pre-exposure H-field measurements repeated within 4% minimum to maximum. The transmitter plate current stayed constant within 1% minimum to maximum. The transmitter forward power changed less than 1% and the H-fields measured during the human exposures varied by +/- 6% due to the interaction of the subject with the field. All these measurements indicate excellent control of the exposure conditions.

CONCLUSION: All measurements made to define and control human exposures to 220 MHz fields were well behaved. The field and SAR measurements were all repeated within experimental accuracy and exposures of 6 human subjects were controlled within +/- 1% over the 45-minute exposure time. Dosimetry required to evaluate human response to 220 MHz and to evaluate the applicability to safety standards was successfully accomplished.

This work was funded by the U.S. Air Force and U.S. Navy. The views, opinions, and/or findings contained in this report are those of the authors and should not be construed as official Department of the Air Force, Department of the Navy, Department of Defense, or U.S. government position, policy, or decision unless so designated by other documentation. Trade names of materials and/or products of commercial or nongovernmental organizations are cited as needed for precision. These citations do not constitute official endorsement or approval of the use of such commercial materials and/or products. Approved for public release; distribution unlimited.

THE INFLUENCE OF A PHANTOM SHELL ON SAR MEASUREMENT IN HIGHER FREQUENCY RANGE (3-6 GHz). T. Onishi¹, R. Ishido², K. Saito², S. Uebayashi¹, and K. Ito². ¹NTT DoCoMo, Inc., Kanagawa 239-8536, Japan, ²Chiba University, Chiba 263-8522, Japan.

INTRODUCTION: The thickness and electrical properties of the phantom shell were previously defined in some Specific Absorption Rate (SAR) measurement standards for 300 MHz to 3 GHz with respect to mobile phones such as in [1]. Another SAR measurement procedure, for which the frequency range is expanded to 30 MHz to 6 GHz, is being developed by the International Electrotechnical Commission (IEC) [2]. The thickness and electrical properties of the shell are defined such that they do not affect the SAR, i.e., 2 mm ±0.2mm, relative permittivity (ϵ_r) ≤ 5, and loss tangent ($\tan\delta$) ≤ 0.05. However it is anticipated that the influence of the phantom shell will increase at higher frequencies.

OBJECTIVE: The objective of this study is to show to what degree the phantom shell affects the SAR measurement in the higher frequency range of 3-6 GHz.

METHODS: The following frequencies are employed: 0.9, 2.0, 3.8 and 5.2 GHz. Figure 1 shows the model used in this study, which comprises a phantom, a shell, and a dipole antenna. The dimensions of the phantom satisfy the recommended values in [2]. Distance "d" is defined as the distance between the center of the dipole and the surface of the phantom. The electrical properties of the phantom are given in Table I. The Finite- Difference Time-Domain (FD-TD) method is employed. Additionally, a measurement is taken using the solid phantom and the thermographic method. The difference in the SARs between that with and that without the shell is defined as the equation below. Namely, if the SAR with the shell is greater than that without the shell, difference (Δ) will be a positive value. It should be noted that all SARs are normalized to the antenna feed-point current.

$$\Delta = (\text{SAR}_{\text{with}} - \text{SAR}_{\text{without}}) / \text{SAR}_{\text{without}} \times 100[\%]$$

RESULTS: Figure 2 shows the calculated results using the FD-TD method pertaining to the relationship with the relative permittivity of the shell ($d = 10$ mm, $\tan\delta = 0$). The initial measured results are also plotted in this figure. The results indicate that the phantom shell affects the SAR measurement. The SAR with the shell is higher compared to that without the shell if the frequency is higher. The maximum difference between the SAR with and that without the shell exceeds 30% at 5.2 GHz. This value depends on not only the frequency, but also the relative permittivity of the shell. Further study on reducing the phantom shell effect as well as more detailed experiments are necessary in the higher 3 - 6 GHz frequency range.

References.

[1] IEC TC106 PT62209, "Procedure to measure the specific absorption rate (SAR) in the frequency range of 300MHz to 3GHz. – Part 1: hand-held mobile wireless communication devices," Committee draft for voting 106/61/CDV, Aug 1, 2003.

[2] IEC TC106 PT62209, "Evaluation of human exposure to radio frequency fields from handheld and body-mounted wireless communications devices in the frequency range of 30 MHz to 6 GHz: human models, instrumentation, and procedures," Draft ver. 0.7, 2003.

Table I Electrical properties of a phantom

Frequency [GHz]	ϵ_r	σ [S/m]
0.9	41.50	0.97
	40.00	1.40
3.8	37.59	3.22
5.2	35.99	4.66

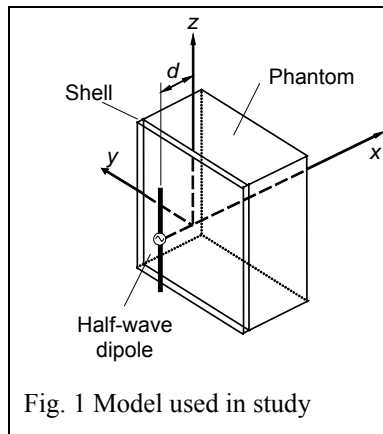


Fig. 1 Model used in study

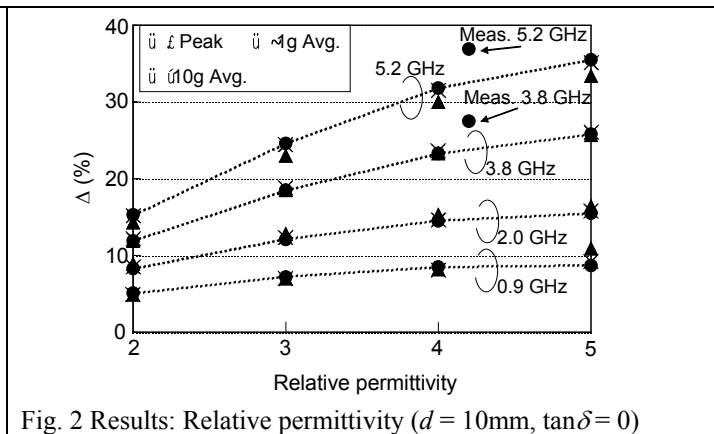


Fig. 2 Results: Relative permittivity ($d = 10\text{mm}$, $\tan\delta = 0$)

P-C-27 WITHDRAWN

P-A-28

COMPARISON OF PERSONAL EXPOSURE TO MAGNETIC FIELDS ON CHILDREN IN PRIMARY SCHOOLS NEARBY AND AWAY FROM HIGH VOLTAGE POWER LINE. Y.S. Kim, Y.J. Hyun, Y.S. Cho, S.C. Hong, and J.H. Cho. Institute of Environmental and Industrial Medicine, College of Medicine, Hanyang University, Seoul, 133-791, Korea.

INTRODUCTION: Arguments of relationship between health effects of school children an extremely low frequency (ELF) electromagnetic fields (EMF) become increasingly of considerable interesting during the past decade in Korea. Since no data on actual level of exposure to magnetic fields in the 27 Korean primary schools nearby high voltage power overhead transmission lines to date, the present study is to compare personal exposure level of MF between school children exposed and not-exposed to power line.

OBJECTIVE: This study was to compare 24 hr personal exposure levels of 60 Hz magnetic fields on children in primary schools between nearby and far away high voltage power lines and to characterize their exposure levels using their time activity pattern.

METHODS: The study was carried out for 53 children aged 12 in a primary school near power lines and 55 children in a primary school away from power lines in the Seoul suburbs during February-October 2003. Twenty-four hour personal exposure measurements to 60 Hz magnetic fields were recorded using EMDEX II and EMDEX Lite (Enertech, Co., Ltd.) carried by the study subjects during at home, school and the other place. Children wore a small satchel in which personal exposure instrument in leather and a diary of activities (activity list) for the period of registration by 20 minutes of time intervals. A diary recording their time activity pattern was used to classify the location of the child as at home, at school, at educational institute, at PC game room, and at all other places. After each period of measurement, the data stored in each meter was downloaded into a microcomputer for data management.

RESULTS: The 24 hr personal exposure levels of children studying in a school away from the power lines were 0.16 μT (arithmetic mean) highly represented by exposure level at home (awake: 0.11 μT ; sleep: 0.14 μT because of high correlations between 24 hr personal exposure and measurement at home ($r = 0.95$, $p < 0.001$) and highly time spent at home (57% of 24 hr). Among other micro-environment, children spent about 23% of 24 hr at school, in which exposure level at ground was 0.16 μT higher than exposure level at class room (0.06 μT), whereas MF exposure levels in most of children of other studies in many kind of educational institutes were 0.23 μT and they spent about 8% of 24 hr. Our interim study result shows fairly high correlations between 24 hr personal exposure and measurement at home; correlation coefficients varied between 0.91 and 0.95. In addition, this results suggests that the 24 hr personal exposure of 60 Hz magnetic fields far away from the power lines may be related with the level of exposure at home and the

level of exposure at home may be representative of 24 hr personal exposure of school children. Since the mean 24 hr personal exposure of children in a school nearby power line are now analyzing at this time, more detailed results will be discussed at the meeting.

This research work was supported by ECO2 Research Grant No. 2002-022-1400020 from the Korea Ministry of Environment.

P-B-29 WITHDRAWN

P-C-30

CELLULAR TELEPHONE USE AMONG PRIMARY SCHOOL CHILDREN IN GERMANY. E. Böhler, J. Schüz., Institute for Medical Biostatistics, Epidemiology and Informatics (IMBEI), University of Mainz, D-55101, Mainz, Germany.

OBJECTIVE: There is some concern about potential health risks of cellular telephone use to children. Heads of children might absorb electromagnetic energy of cellular telephones to a higher extent because their anatomy differs from adult heads.^{1 2}

METHODS: We carried out a cross sectional study among children in their fourth elementary school year to explore their use of new technologies. Whereas 9 (0.5%) children were 8 years old, 942 (48.8%) children were 9 years old, 854 (44.2%) were 10 years old, 112 (5.5%) were 11 years old and 14 (0.7%) were 12 years old.

The data collection was performed using a standardized questionnaire which was especially designed for children. The survey was accomplished during school-time within the class. In addition to interviewing the children we also asked the teachers in the respective classes, about the number of children in class and their appraisal of attention of the class. We also asked how many foreign children, how many children with insufficient knowledge of the German language and how many children from socially deprived families were in the class.

Setting: The study was carried out in Mainz. The study-collective was composed of all 28 primary schools in Mainz and a random sample of nine further primary schools located in the near surroundings of the municipal area.

Participants: Altogether 1933 children from 34 primary schools took part in the survey (participation rate of 87.8%). A total of 110 children did not attend school the day we conducted the interview, only 4 children refused to participate. The remaining nonparticipants are due to the refusal of 3 schools.

RESULTS: Roughly a third of all children (N= 671, 34.7%) reported to own a cellular telephone. Overall, 119 (6.2%) of the children used a cellular telephone at least once per day, 123 (6.4%) used it several times per week and 876 (45.6%) children used it only once in a while, respectively 805 (41.9%) children never used a cellular telephone. The habit of making phone calls with a cellular telephone depends on having an own cellular telephone. Among all cellular telephone users, 53.0% (N=593) owned a cellular telephone, the others used phones of their parents or siblings. There was an increase in owning cellular telephone with age, more TV and computer consumption and going to bed late. Children with siblings had a lower chance of having an own cellular telephone (OR 0.60 95%-CI 0.44-0.76). There was no association with gender.

Children who go to school by bus (OR 1.51 95%-CI 1.04-2.20) or are taken to school by car (OR 1.99 95%-CI 1.35-2.91) had a higher chance to have an own cellular telephone compared to those who walk to school. The ownership of cellular telephones is more common in classes with more foreigners and with more socially deprived children.

CONCLUSIONS: This study points out that the ownership of a cellular telephone and also the use of it are not rare among children in the fourth grade of primary school. Moreover, the time spent watching TV or playing computer games is considerable. A number of factors was related to the child's ownership of a cellular telephone, including age, having siblings or not, activities during leisure time, and social status. We cannot reach a general statement about the association between low social status and ownership of a cellular phone, because we could not ascertain these data on an individual level. So, the cellular telephone could be a status symbol or be used for security reasons. It is still an unclarified issue whether children should be advised to use a cellular telephone only in emergency situations, to avoid adverse health effects from exposure to radiofrequency radiation.

The project was supported by the university of Mainz.

References.

1. Gandhi OP. Electromagnetic fields: human safety issues. *Annu Rev Biomed Eng* 2002; 4:211-34
2. Schönborn F, Burkhardt M, Kuster N. Differences in energy absorption between heads of adults and children in the near field sources. *Health Phys* 1998; 74: 160-8

P-A-31

SARs NEEDED TO SUPPRESS SARS—AND OTHER EPIDEMICS. H. Wachtel, Department of Electrical and Computer Engineering and of Neuroscience, University of Colorado, Boulder, Colorado 80309-0425, USA.

OBJECTIVE: To develop a technology for RF/MW induced prophylactic hyperthermia for use in suppressing the spread of contagious diseases.

RATIONALE: Elevation of body temperature (fever) is one of the human body's most effective ways of combating infectious diseases. Unfortunately, in the case of many highly contagious infections such as SARS (Severe Acute Respiratory Syndrome), transmission of the disease can occur during the early stages of incubation—well before symptoms, including fever, appear. We suggest that if a relatively safe and effective means of producing prophylactic hyperthermia could be deployed in thousands of high risk subjects prior to their contagious period the spread rate of an epidemic could be significantly reduced.

APPROACH: There are several means of artificially elevating body temperature in a relatively safe manner such as; by administering pyrogenic agents, by cooling the hypothalamic "thermostat" of the body and by warming large blocks of body tissue slowly and evenly. In particular, RF energy can be used to produce whole body hyperthermia if the hypothalamus is kept relatively cool. Absorption of RF energy below the surface can also allow deep tissue warming without causing excessive discomfort due to skin heating. We estimate that an average Specific Absorption Rate (SAR) of 10 watts/kg could produce a body temperature rise of 4°C ("pseudo fever") in about an hour if heat dissipation were kept to a minimum. This relatively slow rate of RF induced temperature rise should also allow for thermal equilibration throughout the body and thus avoid the buildup of "hot spots" even if SAR levels were not uniform. After the initial warming this pseudo fever could be maintained (for several hours to several days) with much lower SAR levels or even by non-RF absorption means—if physiological heat dissipation mechanisms were suppressed. This can be achieved by insulation, by hypothalamic cooling and, if need be, by administering pyrogens.

RF "exposure chambers" for individual patients should be designed to expose all parts of the body except for the head, This would allow for hypothalamic cooling while also minimizing the particular risk of exposing eyes, ears and brain tissue to RF heating. To be practical for "anti epidemic" usage, such chambers must be highly portable, fairly inexpensive, easily sterilized (or disposable), and allow for a reasonably comfortable position for the patient. Our conceptual design, which could achieve all of these requirements takes the form of a large, inflatable, metal foil-lined, "sleeping bag" which could fold up into a small volume weighting only a few pounds—and could be cheap enough to be disposable after each patient's use. Such chambers could be energized by ordinary magnetron devices having an output in the range of one kW. These could be similar to those produced for microwave ovens (although longer RF wavelengths would be optimal). If mass produced, the cost of the disposable chambers along with the reusable RF sources should bring the cost per patient down to under \$100 and allow for treatment of thousands of "high contagion risk" subjects over the course of just a few days.

SIGNIFICANCE: If not checked early on, outbreaks of epidemics such as SARS, smallpox, various forms of "flu" and "biological warfare" contagion grow exponentially. Early intervention that is even partially successful could reduce contagious spread to the point where subsequent treatments can "snuff out" a looming epidemic. We believe that prophylactic hyperthermia induced in selected groups of subjects likely to be contagious could provide such an early intervention and that RF heating could be an effective and relatively safe means of producing it. Obviously, the risk- to -benefit ratios of such an approach need to be studied very carefully before deployment. However, in the situation of a looming epidemic the issue

of "safe and efficacious" treatment would have to be applied much differently than, say, for winning FDA approval as an individual patient therapy. Perhaps most importantly these days, this approach could be particularly helpful in suppressing "bioterrorism-initiated" epidemics wherein previously unknown pathogens might be used to initiate contagious diseases for which there is no specific vaccination or medical treatment regime available.

P-B-32

DESIGN OF A PROSPECTIVE COHORT STUDY: AIRWAVE HEALTH MONITORING FOR ASSESSMENT OF POSSIBLE HEALTH RISKS ASSOCIATED WITH TETRA. P. Elliott, D. Neasham, M. Little, N. Khan, A. Burgess, A. Heard. Department of Epidemiology and Public Health, Faculty of Medicine, Imperial College London, Norfolk Place, London, W2 1PG, United Kingdom.

BACKGROUND: The UK Home Office has recently commissioned Imperial College to conduct a research programme on "Airwave Health Monitoring" [www.police-health.org.uk]. Airwave, the new digital communications system for the police service in England, Wales and Scotland, is based on Terrestrial Trunked Radio (TETRA) technology and operates in the frequency range between 380 and 400 MHz. The aim of the Airwave Health Monitoring program is to investigate any possible health impact of the use of Airwave on the health of police officers and staff. The program addresses needs raised in the recent report by the National Radiological Protection Board's Advisory Group on Non-ionizing Radiation (AGNIR), in particular that "microwave radiation from mobile phones (including TETRA) might carry a risk of cancer that becomes manifest many years after first exposure or that relates to intense exposure over several years" [AGNIR 2001]. Previous studies have been limited both by study size and by assessment and duration of exposure to radiofrequency (RF) radiation, and as such have been unable to provide estimates of any long-term health risk.

OBJECTIVES: The main part of the current proposal (*module 1*) describes a prospective long-term cohort study of Airwave use that includes the current cohort of ca.130,000 police personnel in England, Wales and Scotland. Airwave data from each police participant will be collected prospectively from monthly downloads of relevant parameters from the Airwave O2 database, giving unprecedented information on Airwave exposure at individual level. Health outcome data will be assessed by linking information on individual participants to national records on mortality and cancer incidence, and from sickness and pension records, with the option of obtaining data on health symptoms from a questionnaire distributed after 5 years.

In the pilot phase of the study (*module 2*) we will also test the feasibility of collecting baseline health data, including height, weight, blood pressure, ECG, a health questionnaire, and collection for long-term storage of blood and urine samples (which could be accessed for analysis of biochemical and genetic factors on the basis of a "nested case control" design).

The final part of the research programme (*module 3*) is an electroencephalogram (EEG) and cognitive study to examine short-term health effects (such as cognitive performance) in relation to Airwave use.

METHODOLOGY: *Module 1* – A long-term health monitoring study (duration: 15 years) among ca.130,000 police officers to flag for mortality and cancer incidence using registry data at the Office for National Statistics (ONS) (England and Wales) and Information and Statistics Division (ISD) of the Scottish Health Service in Scotland, as well as sickness and pension records. This study will commence in 2005. *Module 2* – A pilot phase (duration: 1 year) among selected police forces currently using Airwave O2. This study component started in January, 2004. *Module 3* – An electroencephalogram (EEG) and cognitive study (duration: ca.2.5 years) based on Airwave exposure (high vs low) and symptoms (symptomatic vs asymptomatic) in three samples of police officers (50 in each) recruited from the initial pilot project. This study component will commence after the pilot phase.

BENEFITS OF THE STUDY: The Airwave Health Monitoring Study will provide long-term epidemiological monitoring of the health of the police force with respect to Airwave exposure, and ability

to monitor both cancer and non-cancer outcomes. The follow-up period of ca.15 years will provide sufficient power to detect elevations in risk of between 15-20% for all cancer and all cause mortality, as well as epidemiological appraisal of the causes of police sickness/absence from work/early retirements in relation to Airwave exposure and other factors.

This study is being supported by the UK Home Office.

References:

- [1] AGNIR. *Possible Health Effects from Terrestrial Trunked Radio (TETRA)*. Report of the Advisory Group on Non-ionising Radiation. (2001) NRPB Documents Vol 12, No.2, NRPB, Chilton, Didcot, UK.
- [2] IEGMP. *Mobile Phones and Health* (2000). Independent Expert Group on Mobile Phones. ISBN 0-85951-450-1.

P-C-33**MICROARRAY GENE EXPRESSION PROFILING OF A HUMAN GLIOBLASTOMA CELL LINE EXPOSED *IN VITRO* TO 1.9 GHZ PULSE-MODULATED RADIOFREQUENCY FIELDS.**

S.S. Qutob, P.V. Bellier, C.L. Yauk¹, G.R. Douglas¹, G. Gajda, P. Lymyre, E. Lemay, A. Thansandote, and J.P. McNamee. Consumer and Clinical Radiation Protection Bureau, Health Canada, 775 Brookfield Rd., Ottawa, Ontario, Canada K1A 1C1, ¹Mutagenesis Section, Environmental Health Sciences Bureau, Health Canada, Environmental Health Centre, Tunney's Pasture, Ottawa, Ontario, K1A 0L2, Canada.

INTRODUCTION: To date, there is no conclusive evidence that exposure of humans to non-thermal radiofrequency (RF) fields results in any adverse health effect. However, it is unclear whether such exposure may cause subtle non-detrimental changes in gene expression of exposed tissue. We have previously designed and optimized a unique, water-cooled, *in vitro* RF exposure system capable of maintaining exposed cell cultures at a constant temperature ($37 \pm 0.5^\circ\text{C}$), thereby eliminating thermal effects as a confounding variable.

OBJECTIVES: The objective of this study is to evaluate the effect of non-thermal 1.9 GHz pulse-modulated (50 Hz, 1/3 duty cycle) RF field exposure on genome-wide gene expression in a human glioblastoma cell line in an attempt to identify genomic response to RF field exposure.

METHODS: A human glioblastoma cell line (U87MG) will be exposed *in vitro* for 4 hours to a 1.9 GHz pulse modulated RF field using a series of six circularly polarized, cylindrical waveguides and then incubated at 37°C for an additional 6 hours to allow for transcription to occur. Mean specific absorption rates (SAR) of 0, 0.1, 1, 10 W/kg will be used and the temperature within the cell cultures will be monitored and maintained at $37.0 \pm 0.5^\circ\text{C}$ throughout the exposure period. Concurrent negative- and positive- (heat) controls (43°C for 1 hour) will be run for each of five independent experiments and incubated for a further 6 hours at 37°C , similar to the RF-exposed sample. Total RNA will be isolated from all samples and subjected to amplification and fluorescent labeling with Agilent's Fluorescent Linear Amplification Kit. Statistical noise in basal gene expression patterns amongst experimental controls will be evaluated by comparing untreated control RNA from each experiment to a large pool of reference RNA collected prior to all of the experiments. Following this, labeled cRNA of control and exposed samples will be hybridized to Agilent's Human 1A Oligonucleotide Microarray containing 17,000 characterized genes. Reciprocal labelling will also be performed for each sample (see figure 1 for the experiment design). Microarray slides will be scanned using ScanArray Express (Packard BioScience, Meriden CT, USA) and the resulting 16-bit grayscale image files for each channel, will be quantified with Image 5.5 (Biodiscoveries, Inc., El Segundo, CA, USA) to determine pixel intensities and statistically analyzed in comparison to non-RF exposed controls using the array analysis program GeneSpring 6.0 from Silicon Genetics (Redwood City, CA, USA). \log_2 ratios representing expression values for experimental versus control samples with a mean log ratio of at least 1 or -1 will be considered significant. Q-PCR analysis will also be performed to verify genes identified by the microarray.

RESULTS: Experiments are currently underway and the results may provide novel information on the possible genomic effects of non-thermal pulsed RF field exposure and thereby assist in future mechanism-based experiments and in the development of exposure standards.

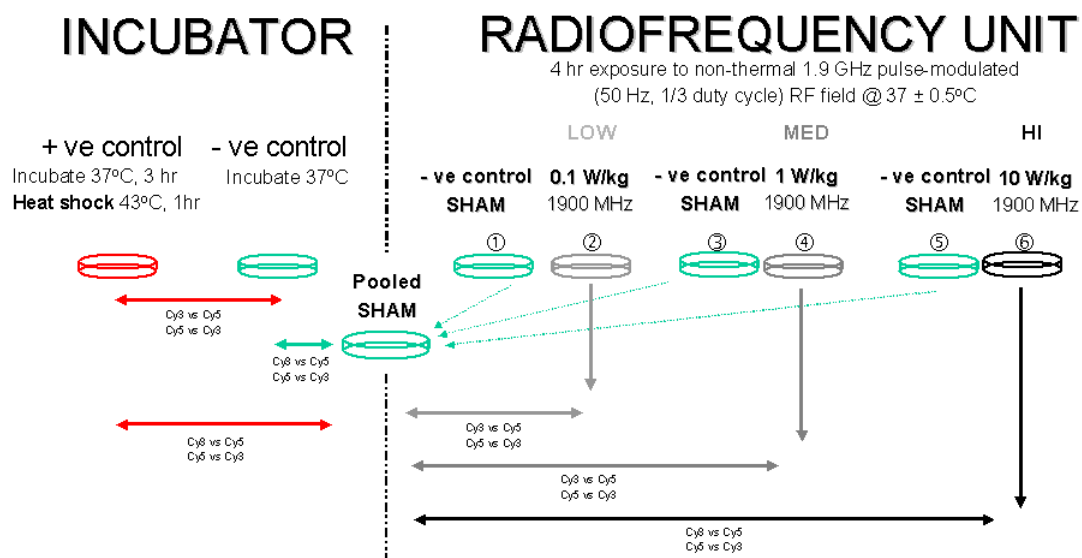


Figure 1: A schematic illustrating the experimental design. All heat and RF exposed samples will be compared to the pooled total RNA sham controls. Circled numbers represent, water-cooled, cell culture dishes taken from the individual waveguides.

HIGH THROUGHPUT SCREENING – PROTEOMICS

P-A-34

EFFECT OF CW AND W-CDMA MODULATED SIGNALS AT 2-GHZ BAND MICROWAVES ON GENOME-WIDE EXPRESSION PROFILING IN HUMAN CELL LINES. M. Sekijima¹, H. Takeda¹, K. Yasunaga¹, T. Nojima² and J. Miyakoshi³. ¹Mitsubishi Chemical Safety Institute Ltd., Kashima-Gun, Ibaraki 314-0255, Japan, ²Hokkaido University, Sapporo, Hokkaido 060-8628, Japan ³Hirosaki University, Hirosaki, Aomori 036-8563, Japan.

OBJECTIVE: The aim of the present study was to investigate the changes in the gene expression profile of three human cell lines, A172 (glioblastoma), H4 (neuroglioma), and IMR-90 (normal fibroblasts from fetal lung) following exposure to 2.1425GHz CW and/or W-CDMA radio frequency fields at two field levels. Firstly, to confirm the gene expression profile of the human cell lines exposed to microwaves at SAR of 80 mW/kg, which corresponds to the limit of whole-body average SAR for general public exposure defined as a basic restriction on the ICNIRP guidelines [1]. Secondly, to investigate if continuous wave (CW) and MT-2000 (W-CDMA) modulated signal radio frequency fields affect the changes in the gene expression profile to different extents.

MATERIALS AND METHODS: We used the *in vitro* exposure system with a horn antenna and dielectric lens in an anechoic chamber, which was developed by NTT DoCoMo [2]. Microarray hybridization was performed using the Affymetrix GeneChip[®] Human Genome U133A & B Array using protocols described by Affymetrix, Inc. Data was analyzed using SiliconGenetics GeneSpring[®] 6.0 software. Genes were considered to be differentially expressed if (i) expression changed by at least 2-fold in two to four independent experiments performed with multiple RNA samples, (ii) the mRNAs were assigned at least one “present” detection call by the Affymetrix software in both experiments and (iii) the change in gene expression was in the same direction (“increased” or “decreased”) in both experiments.

RESULTS AND CONCLUSIONS: During the incubation phase, each cell was exposed at SAR of 80 and 250 mW/kg with both CW and W-CDMA electromagnetic fields at 2.1425GHz for up to 96 hrs. The

temperatures were at $37.0 \pm 0.5^\circ\text{C}$ in both the CW and W-CDMA experiments. Each assay corresponded to the repetition of the same culture conditions in 16 dishes per cell line and that it could be reproduced repeatedly two to four times. No difference of cell morphological phenomenon was detected when the exposure took place during the period of incubation. No significant effects were detected between the sham and exposed cell growth ratio, viability after exposure in both the CW and W-CDMA. Using the Affymetrix GeneChip® system, only a very small (<1%) number of available genes (ca 10,000) were altered in their expression in each experiments. In contrast, the change of gene expression profile in human cells exposed to heat shock at 39 or 41°C was significantly different from RF-radiation- and sham-exposed cells. It is considered that a mild heat shock for human cells had been exposed to heat (39°C, 72hr), since it does not affect the viability of these cells but strongly induces Hsps, including Hsp27 and Hsp72, as well as relating stress proteins. Our results confirm that long-term and low-level exposures to CW and W-CDMA 2.1425 GHz microwave did not affect the gene expression profile at the limit of whole-body average SAR levels on the basis of ICNIRP guidelines. In a future plan, we will evaluate whether or not there are biological effects of exposure to microwave at high-level SAR radiations on the gene expression profile in human cell lines.

References.

[1] ICNIRP, "Guidelines for limiting exposure to time-varying electric, magnetic, and electromagnetic fields (up to 300GHz)," *Health Phys.*, 74, 494-522, 1998.

[2] Uebayashi et al., (2003) "Large-scale in vitro experiment system for low-level long-term irradiation by 2-GHz mobile radio base-stations: System design and its performance. 26th BEMS annual meeting, Maui, Hawaii, p19

This work was supported by NTT DoCoMo Inc.

P-B-35

STUDENT

THE PROTEIN EXPRESSION PROFILING OF MCF-7 CELLS INDUCED BY ELF MF EXPOSURE. Q.L. Zeng, H. Li, D.Q. Lu, H. Chiang, Z.P. Xu. Bioelectromagnetics Laboratory, Zhejiang University School of Medicine, Hangzhou, Zhejiang, 310031 China.

BACKGROUND: Epidemiological studies have showed that ELF MF exposure could increase risk of breast cancer. Since then, a number of laboratory studies have been conducted in order to investigate how ELF MF influenced mammary carcinogenesis and found ELF MF certainly exerted its effects on protein expression and / or function, however, some studies have failed to be replicated. The biological or health effects and mechanisms of ELF MF are still plausible. Obviously, focusing on the response of single gene or protein after EMF exposure in traditional research is limited for short of internal relation and difficult to describe the integrated effects of EMF exposure on biological system. Proteomics deals with the large-scale determination of genes and cellular function directly at the protein level at the same time. We are using this approach extensively to understand the biological effect of ELF MF exposure in order to discern rapidly any association between ELF MF and health hazards.

METHODS: Human breast cancer cells MCF-7 were exposed to 50 Hz 0.4 mT magnetic fields for 24 hr [1]. Whole cellular proteins were extracted and 200µg protein was subjected to 2-dimensional electrophoresis. 17 cm pH 3-10 linear IPG strips were selected in the first-dimension electrophoresis and the second-dimension electrophoresis were run in 12% uniform polyacrylamide gels. The silver stained images of the gel were analyzed with PDQuest analysis software 7.1. The results were analyzed on the overlay of nine repetition experiments. Some differentially expressed proteins were selected for identification using MALDI-TOF mass spectrometry.

RESULTS: There are approximately one thousand proteins detected using 2-D PAGE. Seven of them showed significant changes (at least 5-fold increase or decrease) after exposure to 0.4 mT MF for 24 hr. Thirty-three proteins disappeared and thirty-three proteins appeared in exposure group, comparing with

sham-exposed group. Based on Mr and pI of all detected change spots, We searched the SWISS-PROT database and found that all of them fall in five categories: (a) cytosolic transport proteins; (b) regulators of certain protein phosphorylase; (c) ion channel (especially Ca²⁺ and K⁺) proteins located on cell membrane and nuclear membrane; (d) proteins associated with cancer genesis (p52K, and Zn²⁺ alpha 2 glycoprotein); (e) transcriptional coactivators.

Six proteins were identified. They were involved in cellular process, including connecting proteins of cytoskeleton, receptors of adenosine A2B, regulators of protein phosphorylase and cell cycle, proteins associated with cancer genesis. Other proteins are identifying by Tandem MS.

CONCLUSION: These data directly proved ELF MF exposure did alternate complex protein expression involved from signal transduction to cancer genesis. Further experiments using other cell biology methods are needed for validation.

Reference.

[1] Q.L.Zeng, H.Chiang, G.L.Hu, G.G.Mao, Y.T.Fu and D.Q.Lu. ELF magnetic fields induces internalization of Gap junction protein connexin 43 in Chinese hamster Lung cells. *Bioelectromagnetics*, 2003, 24(2):134-8

This research was supported by National Natural Science Foundation of China (No. 50137030, 30170792) Zhejiang Provincial Natural Science Foundation of China No. 301524 Zhejiang Provincial Science and Technology key project of China No. 021106135

P-C-36

INTEGRATED APPROACH TO MILLIMETER WAVE BIOMARKER DISCOVERY. N.J. Millenbaugh^{2,3}, R. Sypniewska^{2,3}, J.E. Kalns⁴, P.A. Mason², J.S. Eggers², R.V. Blystone⁵ and J.L. Kiel¹.
¹Biosciences and Protection Division, Air Force Research Lab, Brooks City-Base, TX, 78235, USA,
²Directed Energy Bioeffects Division, Air Force Research Lab, Brooks City-Base, TX, 78235, USA,
³General Dynamics, San Antonio, TX, 78235, USA, ⁴Hyperion Biotechnology, San Antonio, TX, 78235, USA, ⁵Dept of Biology, Trinity Univ, San Antonio, TX, 78212, USA.

INTRODUCTION: High-throughput screening techniques can be extremely efficient in identifying targets for subsequent evaluation of biological significance. Our laboratory has adopted a novel, integrated approach to application of these survey technologies to pull together key data from multiple assays to gain a broader insight into the biological effects of millimeter waves (MMW) and to cross validate data from individual experiments and techniques. The main goals of our investigations are to identify compounds in biofluids that could be used as diagnostic biomarkers of overexposure and to characterize the biochemical pathways involved in response to MMW. This global and integrated design of our studies should allow elucidation of how MMW-induced changes in individual tissues and cell types within tissues may be linked.

METHODS: Male Sprague-Dawley rats were anesthetized with isoflurane and either sham-exposed or exposed to 35-GHz MMW at 75 mW/cm² or environmental heat at 42°C (EH). For MMW and EH exposures, instrument settings were selected so that the rates of increase of colonic temperatures would be similar. Colonic and skin surface temperatures were measured using a thermistor probe or infrared camera, respectively. The endpoint of exposures was a colonic temperature of 41 or 42°C, which corresponded to end skin surface temperatures of 40.7 to 43.4°C. Following exposure, rats were allowed to recover and breath, plasma, and tissue samples were collected at 6 or 24 hr post-exposure. Assay techniques employed include gene microarray analysis of skin, lung, and liver tissues, proteomic analysis of plasma and internal organs, chromatographic screening of marker compounds released in the breath, histological analysis of skin, and bioassay analysis of active mediators in plasma.

RESULTS: Thus far, screening of samples has shown that the plasma protein profiles for MMW and EH exposures are different indicating the presence of possible unique markers of MMW overexposure. Identification of these proteins is currently underway and we have identified an increase in creatine kinase and carbonic anhydrase III, which have been linked to muscle turnover. This result correlates with

preliminary histopathology results of exposed skin which shows the most severe changes in the deeper region of skin containing the panniculus muscle. Analysis also revealed increases in levels of the acute phase proteins α -1-acid glycoprotein, alpha and beta chains of clusterin, apolipoprotein B, and prothaptoglobin. Increases in levels of acute phase proteins indicate stimulation of a non-specific and protective systemic response to MMW and involvement of the liver.

CONCLUSIONS: Continued comparisons of data from the global screening technologies will permit us to compile information from multiple assays to correlate changes occurring at the site of exposure, mediators released into plasma, and subsequent responses in the internal organs. Improved fundamental understanding of the response of tissues to millimeter wave radiation from application of this integrated design of investigations will contribute to further development of health and safety standards for protection of personnel, clinical diagnostics, and targets for therapeutic interventions. Research was funded, in part, by the Air Force Office of Scientific Research.

HIGH THROUGHPUT SCREENING – TRANSCRIPTOMICS

P-A-37

STUDENT

PRELIMINARY PROTEOMIC EVIDENCE OF 1.8 GHz MOBILE PHONE SIGNAL-INDUCED CELLULAR REACTION IN VITRO. Q.L. Zeng, Y. Weng, H. Li, D.Q. Lu, H. Chiang, Z.P. Xu. Bioelectromagnetics Lab, Zhejiang Univ School of Medicine, Hangzhou, Zhejiang, 310031 China.

BACKGROUND: Several epidemiological studies have reported that there might be an association between mobile phone use and human cancers. To confirm this association and to elucidate the internal mechanism of action, extensive laboratory studies have been performing to investigate the biological consequences and to assess health risks of mobile phone signal radiation. However, so far the data are contradictory and no conclusion could be made based on current knowledge. Traditional approach in exploring biological effects of RF radiation is to select biological mediators (such as single gene or protein) and determined the changes. Here we employed high-throughput proteomic technology to measure thousands of proteins simultaneously in response to RF exposure. It may be one of the most powerful tools in understanding of mechanisms of mobile phone radiation.

OBJECTIVE: The objective of this study is to investigate protein expression changes of MCF-7 cells induced by 1.8GHz mobile phone radiation.

METHODS: 1. RF Radiation system. The setup was designed based on a waveguide from IT'IS. RF signal-generator produce 1.8G simulation-mobile signal modulated by rectangular pulses with a repetition frequency of 217 Hz. PC calculates the correspond SAR (0.1-4W/kg) and completes the whole feedback control of cell-exposure system. The temperature difference between sham- and EMF-exposed cultures never exceeded 0.05°C.

2. Cell culture and proteomics analysis. Human breast cancer cells MCF-7 were exposed to 1.8GHz GSM 217Hz signal (5 minutes on and 10 minutes off) at an average SAR of 2W/kg for 24 hrs. Whole cellular proteins were extracted and two dimension electrophoresis was performed in the first-dimension electrophoresis using 17cm pH 4-7 linear IPG strips and in the second-dimension electrophoresis using 12% uniform polyacrylamide gels. The silver stained images of the gel were analyzed with PDQuest analysis software 7.1. The results were analyzed on the overlay of three repetition experiments.

RESULTS: Approximately one thousand and one hundred protein spots were detected. Compared to sham exposure, only four proteins were appeared and seven proteins disappeared after exposure to 1.8GHz RF. There are about seven protein were significantly affected by RF exposure (at least 5 folds increase or decrease). Based on Mr and pI of all detected change spots, We searched the SWISS-PROT database and found that all of them fall in six categories: (a) cytosolic transport proteins; (b) regulators of some protein phosphorylase; (c) ion channel proteins; (d) proteins associated with cancer genesis; (e) some

transcriptional coactivator; (f) heat shock proteins. These results are similar with that of ELF MF exposure except the heat shock proteins.

CONCLUSION: These preliminary data showed 1.8GHz mobile phone signal induced complex protein expression changes. Further studies are underway to identify these proteins.

This research was supported by National Natural Science Foundation of China (No. 50137030, 30170792)[] Zhejiang Provincial Natural Science Foundation of China[] No. 301524[] [] Zhejiang Provincial Science and Technology key project of China[] No. 021106135[] []

P-B-38**EFFECT OF CONTINUOUS OR INTERMITTENT EXPOSURE TO ELECTROMAGNETIC FIELDS EMITTED BY MOBILE PHONES ON CARDIOVASCULAR SYSTEM.**

A. Bortkiewicz¹, E. Gadzicka¹, W. Szymczak². ¹Nofer Institute of Occupational Medicine, Department of Work Physiology and Ergonomics, 90-950 Lodz, Poland. ²Nofer Institute of Occupational Medicine, Department of Environmental Epidemiology, 90-950 Lodz, Poland.

OBJECTIVE: The increasing use of mobile phones has caused a growing interest in the possible health effects of electromagnetic fields, which they produce. The EMF source is held very close to the user's head, and it is quite likely that, by acting directly on the brain, EMF may affect the regulation of many physiological functions. Some theoretical data suggest that the use of mobile phones may be harmful to human health. Neither the animal experiments nor human studies have brought a conclusive answer to the question whether the electromagnetic fields emitted by mobile phones may harmfully affect living organisms. Some experimental data have pointed to an increase in arterial blood pressure in the exposed subjects; EEG changes during the awake and sleep hours, and changes in the cognitive functions. These findings require further research. Therefore, we had undertaken a study on the effect of mobile phone EMFs on heart rate and blood pressure.

METHODS: All participants were volunteers, and they were qualified for the experiment on their prior agreement. Before the start of the experiment, all procedures were fully explained to each participant. The protocol was approved by the Regional Research Ethics Committee. 10 young, healthy male individuals, aged 19-29, were examined three times: on a day without exposure (control day), with continuous exposure (60 min. exposure when using 900 MHz mobile phone), with intermittent exposure (4x15 min "on" and 15 min "off"). The subjects did not know which day was the exposure and which the control day. There was at least one-week interval between the tests. The subjects entered the laboratory at 6 p.m. From 7 p.m. to 9 p.m. they were subjected to a real or sham exposure. Since it was necessary to eliminate the influence of possible stress caused by a conversation on the physiological parameters, the use of the phone involved only keeping the subject's head close to the receiver mounted on a stand. After exposure, the subjects rested for some time and then they slept until 7 a.m. During the experiment, the heart rate (HR) was monitored and the systolic and diastolic blood pressure (BPS, BPD) was recorded every 5 minutes. The data were analysed using Wilcoxon matched-pairs signed-ranks test performed for each subject and for the whole group separately for the individual periods of the experiment. We compared heart rate and blood pressure separately for 3 periods: during exposure, after the exposure (21.00-midnight), night hours (midnight - 7.00).

SUMMARY: Our analysis of arterial blood pressure (ABP) and heart rate (HR) in the subjects has revealed great intra-individual differences, but an attempt to explain those differences would go far beyond the scope of this paper, therefore it will be presented only the changes characteristic for the whole group.

During continuous exposure, the mean level of BPS was significantly lower than on the non-exposed day (110.7 ± 11.6 vs. 115.1 ± 10.6). No significant changes were noted in the BPD (66.4 ± 10.4 vs. 67.8 ± 11.5) and HR (70.1 ± 10.4 vs. 73.7 ± 25.1). No statistically significant differences were recorded within two hours after exposure cessation (110.8 ± 11.8 vs. 107.2 ± 11.0) and during the night hours (100.6 ± 14.7 vs. 100.7 ± 13.9). Higher systolic blood pressure during intermittent exposure (113.9 ± 13.8 vs. 111.4 ± 10.8), after its cessation (110.1 ± 12.2 vs. 107.2 ± 11.0) and at night hours that followed (104.5 ± 19.9 vs. 100.7 ± 13.9) was noted. The differences were approaching the limit of statistical significance. The value of the diastolic blood pressure during intermittent exposure was insignificantly higher than that recorded during the same time on the no-exposure day (69.8 ± 10.7 vs. 67.4 ± 10.8). During the night following intermittent exposure, BPD was higher by ca. 4 mm Hg than on the control day ($p=0.0092$). No significant changes were noted in HR on the day

with intermittent exposure compared to the control day (68.2 ± 16.1 vs. 71.7 ± 25.3).

CONCLUSIONS: Results of our study show that exposure to mobile phone EMF may affect physiological functions of human organism. The systemic response depends on individual characteristics, but predominantly on exposure type (continuous or intermittent). More intense response observed after the intermittent exposure may point to EMF stimulating effect (with prolonged exposure, an adaptation to the agent takes place; the adaptation is not possible when the exposure is intermittent and short lasting). Further research is required to verify that conclusion.

Considering health effects of mobile phone EMF exposure, it is worth noting that the changes of arterial blood pressure (diastolic in particular) after the exposure, both intermittent and continuous, occurred at night, many hours after exposure cessation.

These changes could be related to lowered nocturnal melatonin secretion observed after exposure, reported in our previous paper.

P-C-39

STUDENT

EFFECTS OF MOBILE PHONE-LIKE RF EXPOSURE ON SUBJECTIVE SYMPTOMS AND PHYSIOLOGICAL RESPONSES. A. Johansson¹, J. Wilén¹, M. Sandström¹, E. Lyskov², N. Kaledzic², O. Stensson¹ and K. Hansson Mild¹. ¹National Institute for Working Life (NIWL), Umeå, Sweden. ²Centre for Musculoskeletal Research, Gävle, Sweden.

INTRODUCTION: We have previously shown in a cross-sectional study among 7800 mobile phone users that about 13 percent reported at least one symptom in connection with their mobile phone (MP) use. Warmth sensations on and around the ear, burning sensations in the skin and headaches were the most commonly reported symptoms. This group of people reports the same type of symptom as people claiming sensitivity to electromagnetic fields in general, but the MP sensitive group do not in general connect their symptoms to other electrical appliances, and there might be reason to believe that these two groups are not similar with respect to origin of the symptoms.

OBJECTIVES: The overall aim of the present provocation study is to detect whether a relation exists between mobile phone-like RF exposure and subjective symptoms among MP sensitive people. Also, to examine possible effects of exposure on base line autonomic system data (such as heart rate, blood flow, electrodermal activity, respiration rate), Critical Flicker Fusion Threshold (CFFT), short-term memory and reaction time. This presentation will focus on the exposure system and some of the results from the physiological examination. **METHODS:** 20 subjects reporting MP sensitivity and 20 controls, matched with respect to age and gender, were recruited. Personal characteristics of the subjects and the nature of the symptoms related to MP use were collected by means of a questionnaire delivered to the subjects before the experiment. The test procedure was performed in an electromagnetically shielded exposure chamber and lasted two hours. The experiment was performed twice, in true exposure and sham condition, respectively. During the experiments the physiological parameters mentioned above were recorded continuously. To achieve a homogeneously distributed specific absorption rate of 1 W/ kg over the entire exposure area, an indoor Omni Antenna fed by an amplified GSM signal from a 900 MHz mobile phone was used as exposure source. After an initial resting period of 10 minutes, tests of the CFFT, short-term memory and reaction time were performed before the start of the 30-minute exposure/sham period. After the experiment a follow-up questionnaire was delivered to the subjects to investigate the appearance of symptoms during the exposure.

RESULTS: The presentation will include a description of the exposure system and the test protocol as well as some preliminary results of the physiological examination.

This study was supported by the Swedish Council for Working Life and Social Research (FAS).

RADIO FREQUENCY RADIATION EFFECTS ON HUMAN LEUKOCYTES IN VITRO. A. Aly, E. Zhou, K. Rathnabharathi, and F.S. Barnes. Department of Electrical Engineering, University of Colorado, Boulder, Colorado, USA.

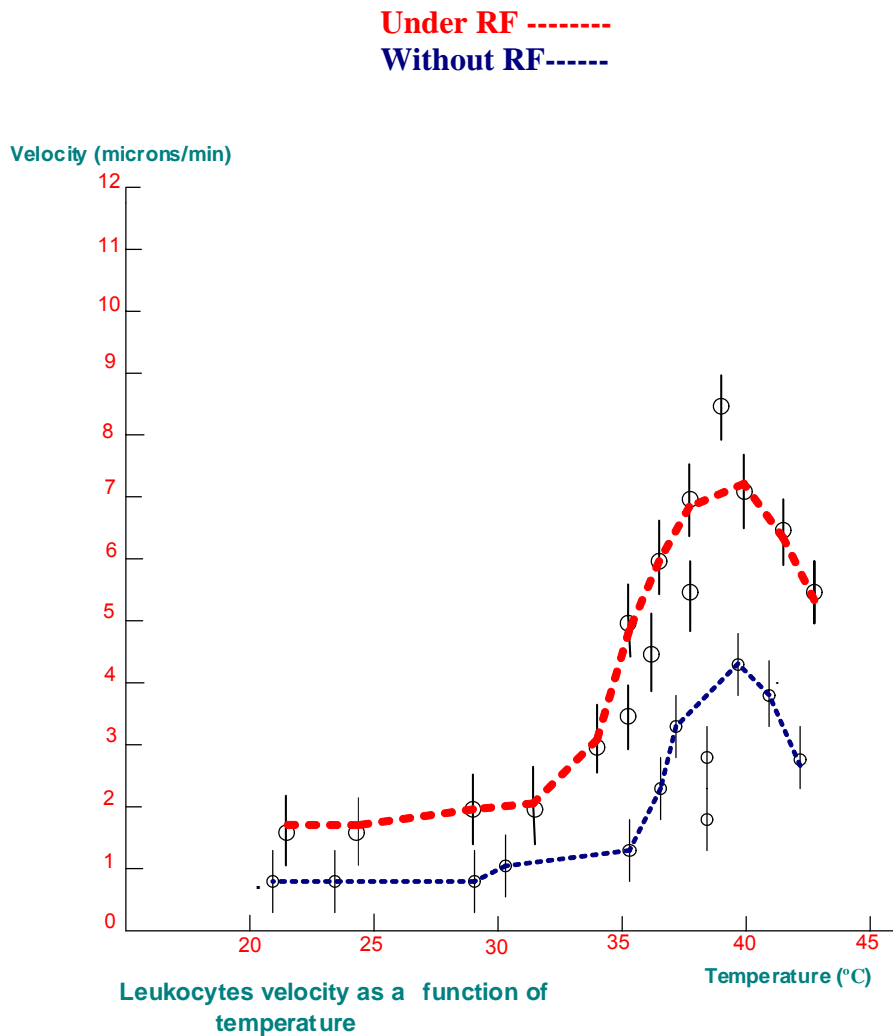
INTRODUCTION: The focus on the health effect of mobile phones has increased in recent years. The public concern has increased about the possible interaction between the radio frequency electromagnetic radiation and the biological effects on human tissues, particularly the brain and the human immune system. Evidence has been reported about the possible health effects such as; brain tumor, blood-brain barrier (BBB) permeability function, sleep problems, cognitive function, DNA damage, immunity system function, stress reaction, and increased incidence rate of traffic accidents due to using mobile phone during driving. Leukocytes (WBC) playing essential roll in our human immune system. It is the body defense against invading bacteria, viruses, fungi, and parasites. Leukocytes attack the invading organisms (pathogens), by identifying them, attaching, destroying them, and take them out of the blood, and continuously produce antibodies against that organism to the rest of the body life.

OBJECTIVE: The aim of this paper is to study the effects of mobile phones radio frequency radiation on the immune system by investigate the activity and behavior of human leukocytes (white blood cells) upon exposure to radio frequency fields in vitro by using microscopic techniques. This is done by investigating the ability of leukocytes to track cyclic-Amp concentration gradients, and changes in cells activity.

METHODES: We used blood from healthy adult donors. The leukocytes were extracted from the boundary between the plasma and red blood cells after centrifuging and placed on a microscope slide upon which a one-dimensional concentration gradient of C-AMP is established. These slides are held at constant temperature of about 38oC. The effects of applying radio frequency electromagnetic fields (for approximately 15 min) on leukocyte cells from digital cellular phone and a 990MHz signal generator are observed. The effects of the exposure to radio frequency radiation on the ability of the leukocytes to track concentration gradients are compared with the unexposed cells as a function of temperature.

RESULTS: Our experimental results to date shows significant change in leukocytes behavior upon the application of RF fields, including more rapid changes in shape, [cells shrinking, expanding, and rolling]. The leukocytes tracking speed increases rapidly upon raising temperature between 35°C and \approx 40oC, peaks and decreased after 40°C. Under the exposure to RF radiation, the leukocytes movement speed will rise by about an additional 50%. See Figure 1. Significant changes in leukocytes movement direction also occur. The movement direction is observed to be perpendicular to the chemotactic direction that is toward increasing concentrations of C-Amp and random movements are suppressed. We observed the same results using mobile phone and signal generator.

Figure (1).



P-B-41

STUDENT

HUMAN ELECTROENCEPHALOGRAM RECORDED DURING PULSED (200 μ T) MAGNETIC FIELD EXPOSURE. C.M. Cook, A.W. Thomas and F.S. Prato. Lawson Health Research Institute, St. Joseph's Health Centre and Dept. of Medical Biophysics, University of Western Ontario, London, Ontario, N6A 4V2, Canada.

BACKGROUND: A recent number of reports suggest that exposure to extremely low frequency magnetic fields (ELF MFs) may affect human brain electrical activity as measured by electroencephalography (EEG), specifically within the alpha frequency (8-13 Hz) [1,2]. We have recently determined that exposure to a pulsed ELF MF affects the human EEG, notably the occipital alpha activity (8-13 Hz) [3] and have also developed a method of recording EEG during exposure [4]. This present study constitutes a partial replication of our previous experiments, with the only procedure change occurring in the 'refractory period' between magnetic field pulses. In previous experiments, this period was 1200 ms. In the current experiment it is expanded (5000 ms) to allow for collection of segments (4096 ms) of EEG data between pulse trains.

OBJECTIVE: Assess any effects of pulsed magnetic field on the EEG during the exposure. Previous experiments have demonstrated an effect after brief (<60min) exposures [1]. We are hypothesizing that the effect upon the alpha frequency will occur within the first 5 min of magnetic field exposure.

METHODOLOGY: Normal subjects (n=20, gender matched) were randomly assigned to receive both a 15 min. MF and sham exposure across two sessions separated by approximately one week. Subjects were placed within 3 orthogonal, nested square Helmholtz coils with the uniform magnetic field volume centred at the head level. In a 30 min. experimental session, subjects were exposed to both an ambient sham and a pulsed ELF MF (< 500 μ T, 0-500 Hz). EEG was recorded using a commercial electrode cap (*Quik-Cap*, Neuroscan labs, Sterling, VA) from 14 scalp locations (F3, F4, Fz, C3, C4, Cz, Pz, P3, P4 O2, O3, Oz, CPz, FCz) during both sham and MF exposure conditions. Data acquisition was performed with a Neurodata Acquisition System (Model 12, Astro-Med, Inc., West Warwick, RI) and processed using Scan 4.3 (Neuroscan labs, Sterling, VA). 98 artifact-free EEG segments were selected between magnetic field pulses and subjected to Fourier transformed to examine the theta (4-7 Hz), alpha (8-13 Hz) and beta (14-30 Hz) frequency bands.

RESULTS: Analysis of variance (ANOVA) revealed that beta activity was significantly higher in the 1st min after a 15 min magnetic field exposure over the frontal electrodes (F3, Fz, F4) [$F_{1,16}=4.66$; $p=0.046$, $\eta^2=0.226$] and theta activity was also marginally higher over the frontal electrodes [$F_{1,16}=4.35$; $p=0.053$, $\eta^2=0.214$]. Theta activity was later found to be significantly higher over the frontal electrodes [$F_{1,16}=4.94$; $p=0.042$, $\eta^2=0.235$] and alpha activity was also marginally higher over the frontal region [$F_{1,16}=4.07$; $p=0.06$, $\eta^2=0.203$] approximately 7 min. post-MF compared to sham. The higher occipital alpha activity noted in our previous expt. [3] was not noted. Analysis of the EEG recorded *during* MF exposure is ongoing and will be presented in full.

CONCLUSION: The present experiment did not replicate the findings of earlier work, suggesting that the modification of the pulse train using 5000 ms refractory periods may affect the EEG in a way that that renders our current results inconsistent with previous literature [1,3]. Our working hypothesis does not seem to be supported by the current data.

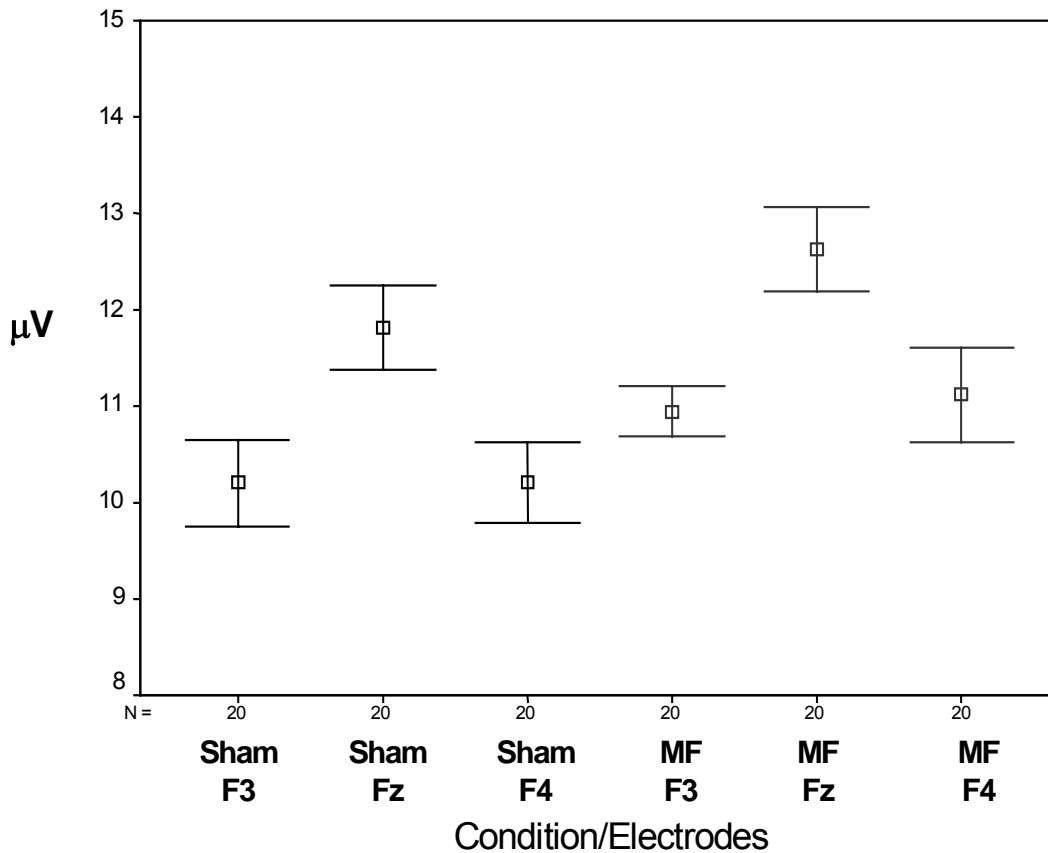


Figure 1: A significant main effect for magnetic field exposure [$F_{1,16}=4.94$; $p=0.042$, $\eta^2=0.235$] with

significantly higher frontal theta activity (4-7 Hz) after pulsed magnetic field exposure compared to sham exposure. This effect was noted approximately 7 minutes post-MF. Error bars represent standard error of the mean.

References.

- [1] Cook CM, Thomas AW, Prato FS (2002) *Bioelectromagnetics* 23(2):144-57.
- [2] Hamblin DL, Wood AW. (2001) *Int J Radiat Biol.* 2002 Aug;78(8):659-69.
- [3] Cook CM, Thomas AW, Prato FS *Bioelectromagnetics* (in press).
- [4] Cook CM et al. *25th Annual Meeting of the Bioelectromagnetics Society, Maui Hawaii, USA, June 22-27 2003*, 271.

This study was funded by Canadian Institutes of Health Research (CIHR) St. Joseph's Health Care (SJHC - London) Foundation; Lawson Health Research Institute; the Department of Nuclear Medicine & MR, SJHC; Natural Sciences and Engineering Research Council of Canada (NSERC); and National Research Council (NRC); Canada Foundation for Innovation (CFI); and the Ontario Innovation Trust (OIT).

P-C-42

EFFECT OF OCCUPATIONAL EXPOSURE TO VHF-UHF ELECTROMAGNETIC FIELDS (EMF) ON BLOOD PRESSURE. E. Gadzicka¹, A. Bortkiewicz¹, M. Zmyslony². ¹Nofer Institute of Occupational Medicine, Department of Work Physiology and Ergonomics, 90-950 Lodz, Poland. ²Nofer Institute of Occupational Medicine, Department of Physical Hazards, 90-950 Lodz, Poland.

OBJECTIVE: Nowadays, the TV and radio programmes are broadcast mainly via VHF (30-300 MHz) and UHF (0.3-3.0 GHz) band waves. The dynamic growth in the number of TV and radio programmes entails a rapid increase in the number of broadcast stations and their workers. The findings suggest that exposure to radio frequency EMF may cause an increase of blood pressure. However, no clinical studies have been performed on workers occupationally exposed to this EMF range. In view of the above, we made an attempt at assessing the effects of EMF exposure on arterial blood pressure in workers at radio and TV broadcasting station exposed to EMF of the VHF-UHF wave bands.

METHODS: The examinations were carried out in 71 workers of broadcasting stations (BS), aged 45±9.4 years, and with the period of employment 19.1±8.8 years, as the exposed group. They were divided into two subgroups that differed only with respect to exposure level. The stations selected for the study operated at frequencies ranging from 66 MHz to 727 MHz. The controls were 42 workers of radio link stations (RLS), aged 40.7±9.2, with the period of employment 12.9±4.0 years. They were free from EMF exposure. The workers had the following performed: an interview including cardiological and family history, general medical examination with office blood pressure measurement, ambulatory blood pressure monitoring (ABP) recorded during everyday professional and other activities using Oxford Medilog ABP System; this had to be properly coordinated with the subjects' working cycle. The measurements were carried out automatically, every half hour during daily activities and every hour during sleep.

Our assessment of exposure was based on the spectrum analysis of EMF, at UHF-VHF wave bands, emitted at a typical broadcasting station, and on the technical specifications of the apparatus installed there. To assess individual exposure to EMF, the following parameters were determined separately for VHF, UHF and VHF+UHF: maximum value of the electric field strength (E_{max}), mean value of E (E_{mean}) and lifetime dose of E (E_{dose}). Lifetime dose was calculated for each worker from the history of his employment and timetable of his jobs.

The data from the medical examinations and interviews indicate that the exposed group did not differ significantly with respect to the level of physical fitness, dietary intake or the smoking habit. They differed only in alcohol intake (which was higher in the control group). Its possible influence on the study results was eliminated by the statistical methods. The differences between the groups were analysed using: chi-square test, t-Student test, non-parametric Mann-Whitney test, Fisher test, and logistic regression model.

SUMMARY: In spite that the exposure was within the relevant standards, the risk of increased blood

pressure and disturbed blood pressure regulation in the examined workers was elevated. The observed disturbances may be characterised as follows: in all test periods the systolic and diastolic blood pressure was elevated vs. control, the percentage of people with elevated pressure during ABP test in the exposed groups was significantly higher ($p=0.0011$) than in the control (70% vs. 23%), in 53% exposed workers with normal arterial blood pressure during the single measurement, ABP test revealed elevated blood pressure values, the percentage of people without the nocturnal systolic and/or diastolic blood pressure drop was statistically significantly higher ($p=0.008$) in the exposed groups (52%, vs. 23%). The risk of elevated arterial blood pressure was significantly higher ($OR=8.6$). The disturbances of blood pressure were dependent on EMF exposure: the risk of disturbed arterial blood pressure increased with higher lifetime dose in the UHF, VHF, UHF+VHF ranges ($OR=2.6$, $OR=2.3$, $OR=2.3$, respectively), and also with higher E_{mean} in the UHF and VHF ranges ($OR=2.3$, $OR=2.5$, respectively), the risk of disturbed arterial blood pressure regulation (no nocturnal blood pressure drop) significantly increased with higher lifetime dose in the UHF range ($OR=2.6$), and also with growing E_{mean} in the VHF range ($OR=2.1$).

CONCLUSIONS: The risk of elevated arterial blood pressure and disturbed blood pressure control in the exposed group was significantly higher. The risk of elevated arterial blood pressure values and disturbed blood pressure control significantly increased with growing lifetime dose of E (E_{dose}) and mean value of E (E_{mean}).

The lifetime dose of E (E_{dose}) and the mean value of E (E_{mean}) seem to essentially affect the changes in the functions of the circulatory system and, therefore, they should be taken into account during the hygienic assessment of worker exposures. Prospective studies would be necessary to explain the prognostic value of this finding.

P-A-43

STUDENT

A PULSED 2.45 GHZ EXPOSURE SYSTEM FOR BIOLOGICAL STUDIES. H.L. Gerber¹, A Bassi¹, C.Q. Zhou¹, S. Lee², S.M. Wang³, C.C. Tseng¹. ¹Purdue University Calumet, Hammond, Indiana 46323, USA; ²Department of Medicine, University of Chicago, Chicago, Illinois 60637, USA; ³ENH Research Institute, Northwestern University, Evanston, Illinois 60201, USA.

INTRODUCTION: Biological studies that require a small amount of cells in culture such as gene expression, enzyme studies, DNA fragmentation, etc. can use the exposure system described here. Typically, the cells density can be in the neighborhood of $10^6/ml$, which can be housed in a T25 flask that fits easily into a WR 340 waveguide. The waveguide functions as an environmental chamber allowing for a cell response over an extended period.

OBJECTIVES: 1) To provide a reproducible environment for cell suspensions. 2) To provide a high enough electric field that is likely to produce a cell responses; specifically for screening gene expression as an initial study. 3) To keep the time-average SAR level at or below 10 W/kg. 4) To analyze the electric field distribution and its dependence on electrical and physical parameters.

METHODS: For a gene expression study, human HL-60 cells were grown in RPMI + 10% FBS and placed in a T25 flask. The flask contained 10 ml of medium and 10^7 cells and placed in the center of the WR 340 waveguide. The ridges on the bottom surface of the flask were ground down so that the flask's surface was in direct contact with the bottom surface of the waveguide whose temperature was controlled by means of an external plastic water channel and temperature controlled circulator. The cells were allowed to stabilize for 30 minutes at 37 °C and settle down to the bottom of the flask to form a monolayer before applying radio frequency power. The absorbed power in the flask was measured with three power meters for 2 h and 6 h exposures and adjusted for 10 W/kg. The system was analyzed with a finite element program using measured properties of the medium. The electrical field distribution was determined taking into account the amount of suspension in the flask and its proximity to the bottom of the waveguide. An identical flask with suspension was placed in an identical waveguide under identical conditions as a control.

RESULTS: For the gene expression study, 168 transcripts (genes) were found to be affected by the RF system after a 2 h exposure. The area-averaged pulsed electric field at the monolayer was calculated to be 90 V/m for a pulse power of 3 W and a duty cycle of 7.7 %. The electric field is polarized perpendicular to the bottom surface of the guide and its magnitude is higher than that at middle depth. The calculated area-average-time-average SAR at the cell monolayer was 7 kW/kg. The electric field is dependent on the permittivity and conductivity of the medium, the depth of the medium, the electrical parameters and thickness of the plastic making up the flask, and the air-gap between the top surface of the waveguide and medium.

CONCLUSIONS: The system is useful for determining reproducible non-thermal conditions for producing alterations in cells that form a monolayer. The electrical field at the monolayer can be controlled and is higher than the average value throughout the medium. Studies on the effect on cells could be undertaken using narrower and higher pulsed electric fields or smaller pulsed electric fields to correlate electric field with cell response.

This research is supported by an AFOSR DOD MURI grant.

P-B-44

USE CELLULAR AND CORDLESS TELEPHONES AND THE ASSOCIATION WITH BRAIN TUMORS IN DIFFERENT AGE GROUPS. L. Hardell^{1,2}, K. Hansson Mild^{1,3}. ¹Department of Natural Sciences, Örebro University, SE-701 82 Örebro, Sweden. ²Department of Oncology, University Hospital, SE-701 85 Örebro, Sweden. ³National Institute for Working Life, SE-907 13 Umeå, Sweden.

We included in a case-control study on brain tumours and mobile and cordless telephones 1 617 patients aged 20-80 years of both sexes diagnosed during January 1, 1997 – June 30, 2000. They were alive at the study time and had histopathology verified brain tumour. One matched control was selected from the Swedish Population Register to each case. Exposure was assessed by a questionnaire that was answered by 1 429 (88%) cases and 1 470 (91%) controls. In total use of analogue cellular telephones gave an increased risk with odds ratio (OR)=1.3, 95% confidence interval (CI)=1.04-1.6, whereas digital and cordless phones did not overall increase the risk significantly. Ipsilateral use (same side as tumour localisation) yielded for analogue phones OR=1.7, 95% CI=1.2-2.3, digital phones OR=1.3, 95% CI=1.02-1.8 and cordless phones OR=1.2, 95% CI=0.9-1.6. The analysis for different age groups showed the highest risk in the age group 20-29 years with OR=5.91, 95% CI=0.63-55 for ipsilateral use of analogue phones. With >5-year latency period the highest risks were found in the age group 20-29 years for analogue phones; OR=8.17, 95% CI=0.94-71, and cordless phones; OR=4.30, 95% CI=1.22-15, whereas no consistent pattern was found for digital phones. When the analyses was done for the age at the start of use of mobile phones the OR was increased for those under age of 20 for all types of phones. Taken together for those < 20 regardless of which phone they had used the OR were for 1 year latency 1.60, 95% CI 0.69-3.73, 5 year latency 2.60, 95%CI 0.79-8.57. However, the number in these groups are low and continued studies are needed with special regard to this age group.

P-C-45

STUDENT

THE 2.45 GHZ RADIO FREQUENCY FIELDS ALTER HUMAN GENE EXPRESSION. S. Lee¹, C.C. Tseng², J. Chen¹, M. Sun¹, H.L. Gerber², C.Q. Zhou², D.S. Johnson², K. Dunbar², S.M. Wang³.
¹Department of Medicine, University of Chicago, Chicago, Illinois 60637, USA; ²Purdue University Calumet, Hammond, Indiana 46323, USA; ³ENH Research Institute, Northwestern University, Evanston, Illinois 60201, USA.

INTRODUCTION: Previous inconclusive studies on the effects of radio frequency (RF) fields were focused on limited number of genes, which may or may not be affected by the fields. Considering the tens of thousands genes in a cell, there may yet exist the possibility that gene expression is affected by RF. The rapid development of genome sciences provides new opportunities to address the issue of potential biological effects of RF fields. By analyzing the genes at the genome level without pre-selection, the genes affected by RF may be identified.

OBJECTIVES: 1) To determine if there is any change of gene expression in a human cell line exposed to 2.45 GHz RF fields. 2) To identify and classify the affected genes (if any) according to their functional categories.

METHODS: HL-60 human promyeloblast cell line was grown in RPMI 1640 medium + 10% fetal bovine serum (FBS) in an incubator at 37°C with 5% CO₂. Prior to RF exposure, 10 x 10⁶ cells in a volume of 10 ml were transferred to a 25 ml culture flask, of which a small hole was made at the center of the upper surface to accommodate a thermal probe for monitoring the temperature (37.1 ± 0.2°C) during the exposure period. The flask was placed at the center of the waveguide and exposed to the RF field at 2.45 GHz for 2 h. SAGE (Serial analysis of gene expression) method was used for the analysis of gene expression in cells with and without RF treatment. The SAGE procedure involves 1) RNA isolation, 2) cDNA synthesis, 3) digestion of cDNAs with *Nla*III and collection of 3' portion of cDNAs, 4) linker ligation to the 3' cDNAs, 5) digestion of linker-ligated 3' cDNAs with *Bsm*FI, 6) purification of 51 bp fragments from the digested 3' cDNAs, 7) ligation of the 51 bp fragments to make 102 bp ditags, 8) PCR amplification of 102 bp fragments and digestion of the fragments with *Nla*III, 9) purification of 26 bp SAGE ditags and concatemerization of 26 bp SAGE ditags, 10) cloning of concatemers into pZero vector, 11) colony PCR, 12) sequencing of PCR products, 13) extraction of SAGE tags with SAGE 2000 software, and 14) data analysis.

RESULTS: A total of 106,122 SAGE tags was collected. From these tags, 27,588 unique SAGE tags are identified with quantitative information for each tag. Comparison of the data between the control and the RF exposed cells results in the identification of 168 transcripts with statistical difference between the control and the exposed cells (P<0.05, over 4-fold differences). Of these 168 transcripts, 23 (13%) are novel transcripts that do not exist in current databases, thus representing potential novel genes. The remaining 155 (87%) are from known genes with different functions including aerobic respiration, apoptosis, adhesion, cell cycle, cell differentiation chromatin structure, cytoskeleton, lipid biosynthesis, metabolism, mitosis, mRNA splicing, inflammatory mediator, protein synthesis and degradation, signal transduction, transcription regulation, and transport. Interestingly, the expression of classical stress-response genes (e.g., heat shock genes) was not affected by the RF treatment, indicating that the altered gene expression was not related to thermal effects.

CONCLUSIONS: Our study shows that the 2.45 GHz radio frequency fields can alter gene expression in human cells. The genes responding to the RF fields include the ones with wide biological functions and the ones whose functions are currently unknown.

This research is supported by an AFOSR DOD MURI grant.

P-A-46

INVESTIGATION INTO THE EFFECTS OF MILITARILY RELEVANT RADIO FREQUENCY EXPOSURE ON COGNITION. S.C. Bowditch, L.O. Evans, M. Fricker, R.I. Grose, S.J. Holden, R.H. Inns, R. Lane, L. Richards, S.J. Smith. Defence Science Technology Laboratory (Dstl), Porton Down, Salisbury, Wiltshire, SP4 0JQ, UK. J. A. Groeger, Surrey University, Guildford, Surrey, GU2 7XH, UK.

BACKGROUND: Previous research conducted in the civilian domain has indicated that exposure to certain types of radio frequency (RF), at levels within existing guidelines, can have subtle effects on human performance. Specifically, reaction time (RT) has been shown to decrease on a variety of computer based cognitive tasks requiring memory and attention.

OBJECTIVE: The aim of current studies is to investigate whether similar cognitive effects can be demonstrated during controlled exposure to RF emitted by military communication equipment.

METHODOLOGY: Critical review and comparison of previously published studies revealed methodological inconsistencies in both RF exposure (source, location and duration) and cognitive assessment techniques. Therefore, it was considered essential to develop a clear conceptual / theoretical framework on which to base the cognitive performance assessment. An extended and refined battery of cognitive tasks has been developed to enable the investigation and partition of previously reported effects. The battery includes a combination of attention, memory and reaction time tasks and lasts approximately 1.5 hours. 60 right-handed male volunteers participate in three test conditions: HF exposure, VHF exposure and a sham control condition. Test days are conducted under double blind conditions in a free space environment. Additional measures include ability, personality and subjective evaluations of mood, workload and symptom occurrence.

This work was funded by the Human Sciences Domain of the UK Ministry of Defence Scientific Research Programme.

P-B-47

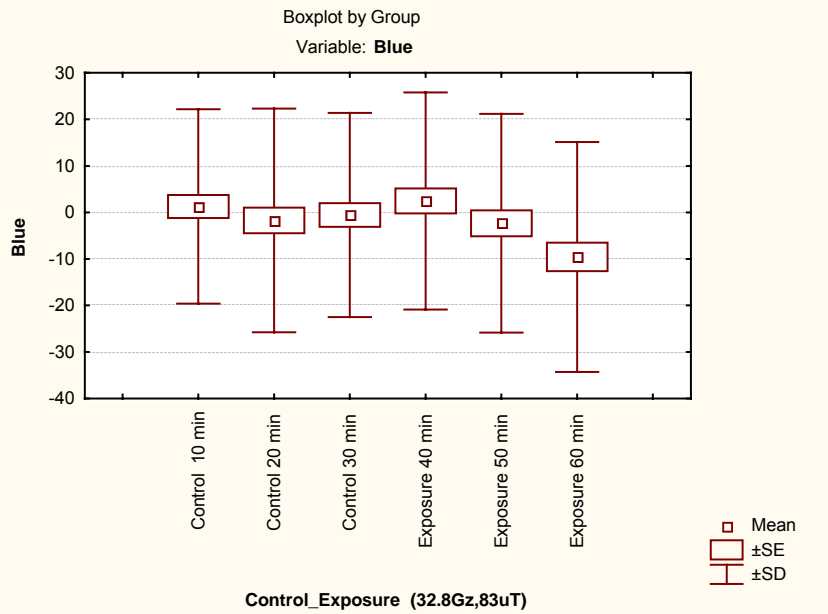
PSYCHOPHYSIOLOGICAL REACTIONS IN HUMAN TO ELF MAGNETIC FIELDS. V.N. Binhi, S.V. Kapranov, V.A. Milyaev, R.M. Sarimov. General Physics Institute of the Russian Academy of Sciences, Moscow 119991, Russian Federation.

INTRODUCTION: Electromagnetic field effects on psychophysiological processes in humans were repeatedly described in literature (Cook et al. Bioelectromagnetics, 23:144, 2002). Most of published articles reported just minimal effects or even no effect at all. An important point is that experiments in those works were performed mainly with the only set of MF or EMF frequency and intensity. At the same time, the frequency and power “windows” are sometimes observed in biological responses to EMFs. Therefore, researches into the spectral properties of the EMF biological effects are a topical task. They could help to find effective parameters of the electromagnetic exposures and to better understand the nature of MF effects on the cognitive reactions in human.

OBJECTIVES: To measure the frequency and power spectra of the effect of ELF magnetic fields on the color memory in humans.

METHODS: The Helmholtz system was used to expose human beings to ELF MFs. It consisted of four coils 1 m in diameter. All coils were set at 50 cm distance from each other, collinear to the geomagnetic field vector. The static MF in the center of the system was equal to 41.5 μ T. In the preliminary set of experiments, 0.5-hour sham exposure was followed by 0.5-hour actual exposure to the ac MF. Its amplitude equaled 83 μ T. The MF frequency 32.8 Hz was chosen to fit the characteristic (cyclotron) frequency of Cations in the above static MF. During both the sham and the actual exposures, a volunteer was subjected to a special psychophysiological computerized test. The original software was developed for this test that measured the color memory in human. In the test, two colored images (squares) were shown to the

examinee in series. The first image of a uniform monochromatic color (one of 16M possible colors) was displayed in 1 s. The second image, a continuous spectrum of colors, which included the color of the first image, was displayed in 3 s. The examinee should have found and click a color in a spectrum, which was that of an initial image. The result, a digitized difference between colors of the first image and that pointed at the second image, featured the color memory ability of the examinee.



RESULTS: Ten control experiments without exposure and two experiments with the MF exposure of examinees were carried out. The results of the latter experiment are shown in the figure. We analyzed the measured color difference in the RGB basis. There was found statistically insignificant tendency to darken G and B components, the Kruskal-Wallis test for B being $p = 0.165$. In this experiment, a significant difference in reaction time (the time needed to point a memorized color in the spectrum) has been found: $T_{\text{control}} = 2.37$ s, $T_{\text{exposure}} = 2.25$ s ($p < 0.001$ t-test). In the control set of experiments, the tendency of G and B darkening, as well as any reduction in the reaction time were not found.

CONCLUSION: Preliminary results do not exclude the possibility to register frequency and amplitude spectra of the ELF MF effect on the cognitive processes in human beings.

P-C-48

DESIGN OF FOLDER-TYPE MOBILE PHONE WITH LOW SAR IN HUMAN HEAD. Y.H. Choi¹, N. Kim¹, J.D. Park², H.T. Oh³, ¹Radio and Communication Lab, Chungbuk Nat'l University, Cheongju, 361-763, Korea., ²ETRI, Taejon 305-350, Korea., ³Radio Research Laboratory, Seoul 140-848, Korea.

OBJECTIVE: The increasing use of mobile phone has caused public concern about possible radiation hazard. In this research, folder-type mobile phone that has dual antenna was designed to reduce SAR on the human head. The antenna characteristics in variety of design parameters of double-semi-disc MPA are analyzed. In addition, 1g peak average SAR is calculated.

METHODS: In order to design the antenna and the phone, SAMCAD(SPEAG Co., based upon FDTD) was used. The resonance frequency was tuned for PCS and IMT-2000. Double-semi-disc MPA was adopted in order to improve the narrow band and the structure was deformed into the folded radiation patches to minimize the size (as shown in Fig.1(a)). The resonant frequency was tuned to 2.0 GHz for PCS and IMT-2000 band. Antenna was composed of two semi-disc patches, ground plate, shorting strip and feeding wire. In this simulation, bandwidth, resonant frequencies radiation patterns were calculated. 1g

peak averaged SAR values were also calculated and compared with those of conventional folder-type mobile phone.

RESULTS: The simulated and measured return losses of an antenna are as follows. The simulated bandwidth of double semi disc MPA are based on 10dB is about 25%(1.76~2.26GHz). The measured bandwidths are about 31%(1.74~2.36 GHz) (as shown in Fig.1(b)). For normalized output to 1W(conduction power at the feeding point), the 1g peak averaged SAR caused by double-semi-disc MPA on folder type handset are 0.781[W/kg]. This value is lower than monopole antenna, 1.206[W/kg] (as shown in Fig.2).

DISCUSSION: We suggested a double-semi-disc MPA to folder-type mobile phone. We obtain the broadband property and the radiation pattern of the monopole antennas is symmetrical, that of double-semi-disc MPA is asymmetrical and the SAR caused by double-semi-disc MPA is less than that by the monopole antenna.

References.

1. Y. J. Wang and C. K. Lee, "Compact semi-disc microstrip patch antenna with improved bandwidth," in Proc. *Antenna Technol. Appl. Electromag. Symp.*, pp. 239-242, July 2000.
2. J.D. Park, B.C. Kim, H.D. Choi, and N. Kim, "Design of folder-type mobile phone for SAR Reduction," BEMS Abstracts for the Bioelectromagnetics Society Annual Meeting, pp. 388-389, June 2003

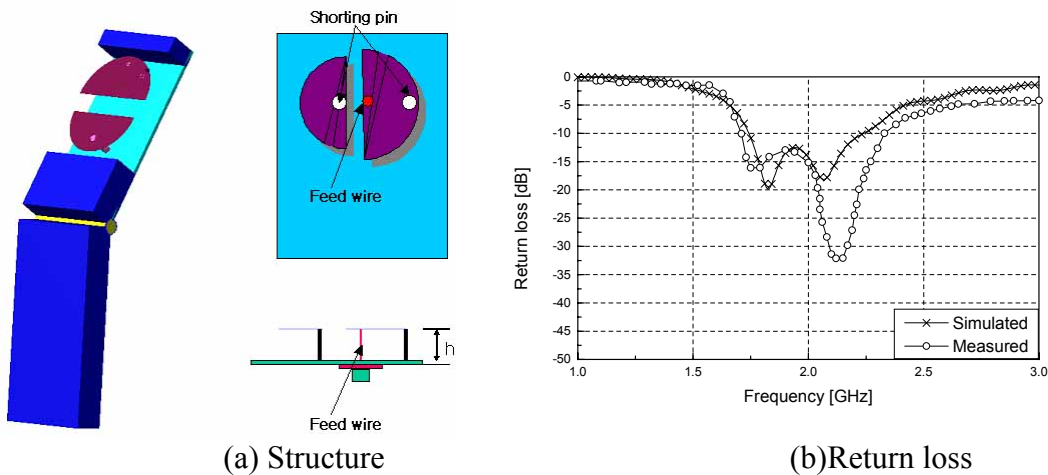


Fig. 1. The structure and return loss of double-semi-disc MPA.

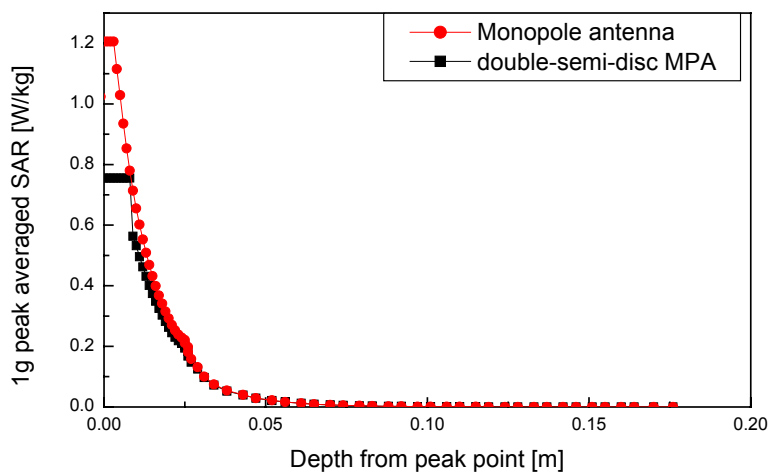


Fig. 2. Variation of peak SAR according to the depth of human

P-A-49

SAMPLE KOREAN'S OCCUPATIONAL AND RESI-DENTIAL EXPOSURES TO ELF MAGNETIC FIELD OVER A 24-HOUR PERIOD. K.H. Yang, M.N. Ju, S.H. Myung. Electrical Environment & Transmission Group, Electric Power Research Lab., Korea Electrotechnology Research Institute (KERI), Changwon, Gyeongnam 641-120, Korea.

BACKGROUND: There is a growing concern over the possibility of the exposure to power line frequency EMF (electric and magnetic field), called the 4th environmental pollution. This type of exposure has been affecting the people's health and its hazard has been growing worse. The report published by Wertheimer and Leeper in 1979 triggered deep concern in science and medical communities over the possibility that the EMF from power lines and other source might be affecting the health of exposed individuals.[1] EMF problem is much severe social issue in Korea also. This is the first-ever unique personal MF (magnetic field) exposure survey done in Korea.

OBJECTIVE: Characterize personal MF exposure of sample Koreans in general living environment.

METHODOLOGY: The participants for the survey on MF exposure were randomly selected, by occupation. The survey was conducted as follows; a participant wears a MF meter for about 25 ~ 28 hours and the data is stored in the meter. MF values are recorded every 4 seconds. The personal MF exposure meter used for this survey is EMDEX-LITE made by Enertech Consultants, Inc., USA. Participants are asked to record their activities so that MF exposure can be evaluated for a 24-hour period. The personal MF exposure survey started in July 2001. Up to now, 409 respondents in eight different jobs have been surveyed. The statistics of the 24-hour exposure data are our major concern in this survey. The survey also provided the opportunity to analyze exposures corresponding to different types of activities. It was analyzed in separate periods of time corresponding to the following activities: entire 24-hour period, in bed, at work and by occupations. Therefore, the database is going to be established to analyze the present status of personal magnetic field exposure and safety.

RESULTS: The 24-hour average MF exposure of sample Koreans is about 1.3mG; 11.8% of the participants are exposed to over 2mG, while 5.9% are exposed to more than 4mG. Approximately 25% of the participants are exposed to over 3mG for 2 hours, while 7% is exposed to more than 10mG for 1 hour. The average MF exposure in bed is 0.99mG and 21.8% of the participants are exposed to over 1mG in bed. The share of participants exposed to over 2mG reaches 9.8%. Also, approximately 20% is exposed to over 1mG for 3 hours while 10% is exposed to more than 3mG for 20 minutes. As the MF exposure during working hours only was surveyed, the average MF was 1.62mG. The percentage of participants who were exposed to over 2mG reaches 12.9%, while 4% showed more than 5mG of exposure level. In addition, about 15% of the participants were exposed to over 3mG for about 1 hour, and about 5% were exposed even more than 10mG for about 20 minutes. Table 1 shows the distribution of 24-hour average MF exposures according to occupations.

CONCLUSION: There was found no much effect of gender, age and the types of houses on the 24-hour average MF. However it was shown that living close to a power line can increase resident's overall exposure to MF. As for electricians and the hospital workers who operate special medical facilities, some of them were exposed to 100~230mG of MF continuously at their service-area. We can also conclude that the overall MF environment of Korean bedroom is good as the MF exposure in bed is below 1mG, which is quite low in general. In the next step, some occupations with high exposure will be surveyed in 2005-2006. Finally, an exposure database will be able to be established to assess the status of personal MF exposure and public safety in Korea.

REFERENCES

[1] Wertheimer N, Leeper E, 1979. Electrical wiring configurations and childhood cancer, Am J Epidemiol 109:273-284.

Table 1: Distribution of 24-hour Average MF Exposures of Sample Koreans by Occupations

Occupation	Max.	L5%	L50%	Min.	
Office Worker	6.06	2.24	0.55	0.05	
Factory Worker	18.14	7.84	0.79	0.32	
House -wife	Without Job	1.64	1.42	0.60	0.16
	With Job	6.06	5.01	0.63	0.16
Student	5.47	2.95	0.67	0.12	
Warehouse Worker	5.42	2.46	0.87	0.17	
Hospital Worker	10.76	3.71	1.00	0.30	
Restaurant Worker	6.34	4.51	0.84	0.26	
Electric Railway & Train operator	3.18	2.23	1.27	0.60	
Total	18.14	4.34	0.81	0.05	

P-B-50

STUDENT

A DOUBLE-BLIND, RANDOMIZED ANALYSIS OF EXPOSURE TO A SPECIFIC PULSED EXTREMELY LOW FREQUENCY MAGNETIC FIELD ON PAIN RATINGS IN FIBROMYALGIA PATIENTS. N.M. Shupak^{1,3}, W.R. Nielson^{2*}, L. Keenlside^{3*}, G.B. Rollman^{4*}, F.S. Prato^{1,3}, A.W. Thomas^{1,3}. ¹Dept of Med Biophysics, Univ of Western Ontario; ²Dept of Med, Div of Rheumatology, Univ of Western Ontario; ³Lawson Hlth Res Inst and Dept of Nuclear Med & MR, St. Joseph's Health Care (London), London, ON, Canada, N6A 4V2; ⁴Dept of Psych, Univ of Western Ontario; London, ON, Canada.

INTRODUCTION: One of the most reproducible effects of extremely low frequency (ELF) magnetic field (MF) exposure has been the effect on opioid-related behaviors. It has been shown that a specific pulsed ELF MF induces analgesia in snails, rodents, and healthy human volunteers. In a double-blinded and randomized study, we investigated the effects of 30-minute MF exposure ($\leq 400 \mu\text{T}$; $< 1 \text{ kHz}$) on pain ratings in fibromyalgia patients.

OBJECTIVE: Determine the effects of exposure to a specific pulsed extremely low frequency magnetic field on pain ratings in fibromyalgia patients. Investigate effects of exposure on self-report anxiety ratings, as well as physiological measures including heart rate and muscle tension.

METHODOLOGY: Female patients ($N=18$; mean age = 51.28 years) received either the MF or sham exposure treatment. Magnetic field exposure was provided via a portable headset programmed to deliver a maximum of $\pm 200 \mu\text{T}$ to the deep brain to a maximum of $\pm 400 \mu\text{T}$ to the outer cortex. The magnetic field had a frequency ranging from 0 to 1 kHz. Patients completed the McGill Pain Questionnaire (MPQ) and pain and anxiety visual analog scales (VAS) before and after a 30-minute (MF or sham) exposure period. Muscle tension and heart rate were recorded throughout the experiment to assess possible physiological correlates of MF exposure.

RESULTS: A repeated measures analysis revealed a significant overall pre-post effect for the MPQ Pain Rating Index (Total), $F(1,15) = 16.16$, $p < 0.01$, $\eta^2 = 0.519$, power = 0.963. The MF group, $F(1,8) = 17.60$, $p < 0.01$, $\eta^2 = 0.688$, power = 0.955, but not the sham group, $F(1,7) = 3.98$, $p = 0.09$, $\eta^2 = 0.362$, power = 0.406 showed a decrease in the PRI. Similar findings were found for the sensory, affective, and emotional components of pain as measured by the MPQ; comparable findings existed for the VAS pain ratings. Patients in the MF group also had significantly reduced variability in heart rate post-exposure relative to patients in the sham group. A significant condition by time interaction existed for the minute immediately following the 30-minute exposure, $F(1,15) = 8.137$, $p < 0.05$, $\eta^2 = 0.352$, power = 0.760.

CONCLUSION: Results confirm past findings that exposure to a specific pulsed MF has a pain-reducing effect. The significantly lower pain ratings following MF, but not sham exposure, indicate the potential clinical use of MF exposure for reducing pain in patients with fibromyalgia. Given the lack of effective treatments for fibromyalgia, future research should investigate the efficacy of MF exposure for pain relief

in this population.

This study was supported in part by the Canadian Institutes of Health Research (F.S.P), the Natural Science and Engineering Research Council (N.M.S.), Lawson Health Research Institute (A.W.T.), FrAlex Therapeutics Inc. (A.W.T.), the Ontario Research and Development Challenge Fund (A.W.T.), the Canadian Foundation for Innovation (F.S.P.), Ontario Innovation Trust (A.W.T., F.S.P.), and St. Joseph's Health Care Foundation (A.W.T.).

P-C-51

PULSING ELECTROMAGNETIC FIELDS SUCCESSFULLY TREAT NEUROMUSCULAR INJURIES AND DISORDERS. F. Sivo and A.A. Pilla, Department of Biomedical Engineering, Columbia University and Department of Orthopaedics, Mount Sinai School of Medicine, New York, NY, USA.

INTRODUCTION: Low intensity, non-thermal, time-varying electromagnetic fields, PMF have been extensively employed with success for tissue healing, pain, and various musculoskeletal disorders. We have discovered that PMF can also be configured to be remarkably successful when used to address neuromuscular disorders which involve abnormal skeletal muscle tonicity and motor function. These syndromes often lead to structural instability, inflammation, and chronic pain of the associated joints and soft tissues. This study describes a new PMF signal and its application to several patients presenting neuromuscular disorders of both upper and lower extremity musculature. These syndromes are easily diagnosed and tested using the standard orthopedic grading assessment for muscle range of motion against gravity and manual resistance.

METHODS: The PMF waveform was configured using the cell array tissue model which describes the dynamic electrical response of cells in real tissue configurations and allows thermal thresholds (SNR) to be evaluated for induced electric fields from any signal, and for any kinetics, including non-linear, in the target pathway. The signal employed was configured assuming a Ca/CaM target and consisted of a 30msec burst of 10usec pulses repeating at 1/sec. Peak induced electric field was 5mV/cm at a 2cm radius. The experimental device consisted of a pair of 6 or 9 cm diameter circular coils driven by a portable battery operated signal generator. The signal was applied on the skin over the belly of the treated muscle targeting the muscle motor end plate and its spindle apparatus. The durations of PMF exposure in clinic ranged from 10 sec to 15 min dependent upon the complexity of the neuromuscular disorder. Patients requiring further treatment were instructed on coil placement and requested to self-treat for 5 min 3X daily. Patients were selected by their inability to perform normal movements of joints with both pain and non-pain perception, within their full physiologic range of motion, and by the demonstration of a grade two or three muscle contractile weakness upon standard orthopedic physical assessment and manual muscle testing (Grade 1 = weakest, Grade 5 = strongest). Patients with lower motor neuron disorders, demonstrated by a decreased response to deep tendon reflex testing, were included in this study. Patients with upper motor neuron pathology were excluded from these studies. Patients were identically assessed pre, during and post PMF treatment using standard orthopedic grading assessment.

RESULTS: Patients presenting with Grade 2 functional assessment for motor strength typically demonstrated one level of improvement within minutes after PMF treatment. Of this group, approx 90% had moderate pain perception both at rest and with active joint movement, and approx 10% had minimal to absent pain prior to treatment. After treatment, approx 70% of this group experienced 50% or more pain reduction upon active movement which diminished to minimal or absent pain over the course of several days to several weeks in all movement and non-movement parameters. Overall, 10% required re-application of the PMF on a daily basis to local areas of pain directly over the associated joint. These patients are currently under treatment. Patients presenting with Grade 3 functional assessment for motor strength demonstrated up to two levels of improvement within minutes of PMF treatment. Of this group, approx 50% reported pain only upon active movement of the involved joint, 10% reported pain at rest and with active movement and 40% experienced no pain. Of those patients who experienced no pain from the onset of treatment, approx 90% improved to Grade 5 and approx 10% to Grade 4, within minutes of PMF application. The latter group improved to Grade 5 after one week of daily treatment. Of the Grade 3 group originally reporting pain at rest or with active joint movement, approx 80% improved to Grade 5 after several daily applications and reported their pain decreased more than 75%, and approx 20% improved to

Grade 4 with a moderate decrease in pain. These patients required re-application on a daily basis directly to the involved joint and are currently under treatment.

DISCUSSION AND CONCLUSIONS: The results of this preliminary study suggest neuromuscular disorders can be rapidly improved or corrected with short exposure to this new PMF modality. These corrections persist well after the PMF signal is removed, in some cases for as long as several months. The mechanism of PMF action in this study is not yet known. It is interesting to speculate that this PMF signal may function via Ca^+ binding/release at Ca/CaM, which is associated with neurotransmitter release in the synaptic cleft at the neuromuscular (motor) end plate. This signal may also function via an affect upon the intrafusal fibers of the muscle spindle organ through gamma motor neuronal systems and/or via Ca^+ mobilization in the stretch sensitive ion channels of spindle sensory receptor membranes. Either pathway could influence local and centrally modulated feedback systems which govern muscle tone and contractile strength. The timing of neurotransmitter release at the neuromuscular synaptic cleft, relative to the feedback component of the muscle spindle's reference signal, may also be a factor. Aberrant neuronal firing patterns which result in end organ dysfunction may cause, or can be a result of, abnormal Ca^+ binding/release oscillations associated with that neuron's intracellular signaling system, its membrane receptor channels, and/or synaptic cleft channels. Therefore, under physical conditions which suggest abnormal neuromuscular activity, in conjunction with clinically measurable muscle/lower motor dysfunction, the PMF signals employed in this study may act to reset an aberrant Ca^+ binding/release oscillation(s) at the molecular level of the targeted neuromuscular junction and/or intrafusal fiber system, thereby altering the tonicity and contraction force of the associated innervated muscle. Localized binding/release events of Ca^+ /Troponin at the sarcoplasmic reticulum may also be a factor in the context of our physical findings relative to force of muscle contraction. These promising results strongly suggest a novel and important clinical application of PMF therapy in the treatment of neuromuscular disorders.

P-A-52

STUDENT

OPTIMIZATION OF CURRENT DISTRIBUTION IN TRANSCRANIAL MAGNETIC STIMULATION AS AN ALTERNATIVE TO ELECTROCONVULSIVE THERAPY. M. Sekino, S. Ueno. Department of Biomedical Engineering, Graduate School of Medicine, University of Tokyo, 7-3-1 Hongo, Bunkyo-ku, Tokyo 113-0033, Japan.

INTRODUCTION: In electroconvulsive therapy (ECT), application of electric current to the brain has produced an improvement of depression under a commonly used voltage (100 V) and an electrode position (a pair of electrodes attached to the tempora). Though transcranial magnetic stimulation (TMS) has been used for treatments of depression in numerous studies, these trials have not necessarily given beneficial results. An appropriate approach for the initial attempt of TMS therapy is to find a stimulus condition which gives a similar current distribution in the brain to ECT. In this study, current distributions in TMS were calculated under various conditions and compared with the current distribution in ECT to find an optimum condition of TMS.

METHODS: We used a human head model developed by the Brooks Air Force Laboratory. Numerical solutions were obtained using a computer program based on the finite element method. The figure-eight coils used for the TMS model consisted of a pair of circular coils with diameters of 50 mm, 75 mm, and 100 mm. Pulsed electric currents were applied to the coils with intensities ranged from 0 to 300 kA Turn. To investigate dependence of eddy current distributions on the coil position, the coil was rotated around the head with an angle θ from the vertex toward the forehead. The difference in current distributions between ECT and TMS was evaluated using a performance function, $F = (1/V_0)[\int (|j_E| - |j_T|)^2 dV]$, where V_0 is the volume of the brain, j_E and j_T are the current densities in ECT and TMS, respectively. Because this function increases with the difference in current distributions between ECT and TMS, the optimum condition of TMS gives a minimum value of the function.

RESULTS AND DISCUSSION: The minimum value of F decreased with an increase of the coil angle θ . At larger coil angles, the coil approached to the electrode positions in ECT, and generated currents in the forehead. The minimum value of F decreased with an increase in the coil diameter. This was because eddy currents induced by larger coils distributed in larger and deeper areas. In the case of a 100 mm coil at $\theta = 60^\circ$, the performance function had a minimum value of $53 \text{ A}^2/\text{m}^4$ at a coil current of 87 kA which corresponded to a magnetic flux density of 1.1 T. The coil current giving a minimum value of F decreased with an increase in the coil diameter. This was because large coils produced higher current densities in the side of the brain. In conclusion, a coil position on the forehead and the use of a large coil gave better results. These results provide useful information for choosing stimulus conditions in therapeutic applications of TMS.

P-B-53

STUDENT

THE EFFECT OF REPETITIVE MAGNETIC STIMULATION ON THE TUMOR DEVELOPMENT. S. Yamaguchi, M. Ogiue-Ikeda, M. Sekino, and S. Ueno; Dept of Biomedical Engineering, Graduate School of Medicine, Univ of Tokyo. 7-3-1 Hongo, Bunkyo-ku, Tokyo, 113-0033, Japan.

INTRODUCTION: Biomagnetic stimulation is a method for stimulating tissues non-invasively. Recently the effects of magnetic stimulation on the living system became to be clear in the brain, especially in the hippocampus [1]. However, the effects on other tissues, especially on tumors, have not been clarified yet. In this study, we investigated the effect of the magnetic stimulation on tumor developing processes *in vitro* and *in vivo*.

OBJECTIVES: To clarify the effect of magnetically induced eddy current on cancer cells, we examined the effect of magnetic stimulation on B16-BL6 melanoma cells. Secondly, we examined the effect of repetitive magnetic stimulation on tumor development processes using animal models.

MATERIALS and METHODS: <*In vitro* study> Murine melanoma-derived B16-BL6 melanoma cells (provided by Cell Resource Center for Biomedical Research, Tohoku University, 3.0×10^5 cells/dish) were exposed to repetitive pulsed magnetic stimulation of 0.75 T, 25 pulses/sec at the stimulus conditions of 1000 pulses, 2000 pulses, 3000 pulses, and 1000 pulses/day for 3 days 3000 pulses in total. MTT assay was performed to evaluate the cell viability. <*In vivo* study> Group1 (Stimulated group) B16-BL6 cells were subcutaneously injected into flanks of C57BL/6J mice. From the next day of the injection, repetitive pulsed magnetic stimulation (0.75 T, 25 pulses/sec, 1000 pulses/day) was applied to the mice for series of 16 days. The estimated eddy currents induced in tumor area were $2.31 - 4.61 \text{ A}/\text{m}^2$. Group2 (Sham group): mice were also placed in the holder and exposed to the sham stimulation. Group3 (Control): mice were not placed in the holder, and not exposed to the noise produced during the stimulation. On the day 17, all mice were sacrificed and tumor weights were measured. Statistical analysis was carried out by analysis of variance (ANOVA). Results were expressed as mean \pm S.D.

RESULTS AND DISCUSSIONS: Magnetically induced eddy currents did not induce acute damages such as cells death and accumulative damages on B16-BL6 cells, suggesting that magnetically induced eddy currents have no direct effect on cancer cells and cell proliferative activities. The tumor weights (mean \pm S.D) of group 1, 2 and 3 were $1.16 \pm 0.48 \text{ g}$ (n=18), $1.35 \pm 0.16 \text{ g}$ (n=18), and $1.91 \pm 0.16 \text{ g}$ (n=23), respectively. The tumor weight of stimulated group was 86 % of that of the sham group, and 60 % of that of the control group. There was no significant difference of the tumor weight between the stimulated group and the sham group. This result suggests that repetitive transcutaneous magnetic stimulations in this condition have no upregulative effect on tumor growth. In conclusion, magnetically induced eddy currents have no effect on cancer cells and proliferative activation, and the transcutaneous magnetic stimulation of 0.75 T at 25 pulses/sec causes no upregulation tumor growing processes.

References.

[1] M. Ogiue-Ikeda, S. Kawato and S. Ueno, *Brain Res.*, vol. 993, pp. 222 – 226, 2003.

P-C-54

MAGNETIC FIELD THERAPY OF PAIN. M. Markov. Research International, Buffalo, USA.

The increasing interest in the clinical application of magnetic/electromagnetic fields for pain control is discussed. This paper will review the magnetic field therapy which provides non-invasive, safe and easy to apply methods is used to directly treat the site of injury, the source of pain and inflammation. The second half of 1990's marked an increasing interest in the USA toward the use of permanent magnets fields for pain relief. This interest was stimulated mainly by the large commercial marketing of permanent magnets which triggered the interest of the general public. The use of permanent magnets appears to compliment the set of EMF based methods already in use for treatment of problems related to musculoskeletal apparatus. The modality most often employed in the USA for "treatment of pain and edema in superficial soft tissues" (as labeled by FDA) is 27.12 MHz pulse radiofrequency signal. PRF magnetic fields have been applied for the reduction of post-traumatic and post-operative pain and edema in soft tissues, wound healing, burn treatment, ankle sprains, hand injuries, migraine, chronic pelvic pain, neck pain, and whiplash injuries and nerve regeneration. In parallel with improvement after the injury, a reduction in the pain of 35% for patients having migraine, accompanied by a significant reduction of occurrence of headaches had been reported. Neck pain decreases from 7.0 to 4.0 after 3 weeks of daily treatment with PRF and to 2.0 after 6 weeks of treatment. For the whiplash injuries VAS pain scores decreased from 6.75 to 3.75 after 2 weeks, to 2.5 after 4 weeks and to 1.5 after 12 weeks of daily treatment with PRF. A 50% reduction in use of pain medication was also reported in whiplash patients as result of EMF treatment.

Low frequency sine waves and low frequency pulsed EMF have been used for treatment of pain associated with rotator cuff tendinitis, multiple sclerosis, carpal tunnel syndrome, and periathritis. An improvement was observed in 93% of patents suffering carpal tunnel pain, and 83% in rotator cuff tendinitis. Using ellipsoidal coil with 14x21inches diameters to deliver 120 pps semi-sinewave TEMF we successfully treated chronic low back pain and achieved 22-34% reduction in pain in the post treatment period as compared with baseline period. It was shown that TEMF of 15 mT was more effective than 10 mT or 20 mT. It was also reported that 65% of the patient who received daily treatment over 8 weeks for rotator cuff tendinitis were pain-free at the end of the study, as well as 70% of the multiple sclerosis patients which received 15 treatment with low frequency sine wave EMF reported a reduction in spasticity, improvement of bladder control and improvement in endurance.

In a recent paper published in "Bioelectromagnetic medicine" A. Colbert reviewed 25 recent papers on application of magnetic fields from permanent magnets for pain control. Reduction of pain in post-polio patients (up to 76%), fibromyalgia (up to 32%), peripheral neuropathy (up to 33%), and postsurgical wounds (37-65%), as well as diabetic neuropathy were reported to emphasize the potential use of magnetic fields for pain relief. One possible mechanism to be discussed is linked to magnetic field influence on inflammation processes.

P-A-55

EVALUATION OF DNA DAMAGE ON HUMAN FIBROBLASTS FOLLOWING EXPOSURE TO 50 Hz ELECTROMAGNETIC FIELDS: A REPLICATION STUDY. A. Sannino¹, O. Zeni¹, M. Romanò¹, P. Mesirca², F. Bersani², M.R. Scarfi¹. ¹ICEmB at CNR- Institute for Electromagnetic Sensing of Environment (IREA), via Diocleziano, 328, 80124, Napoli, Italy, ²ICEmB at Dept. of Physics, University of Bologna, Viale Berti Pichat 6/2, 40126, Bologna, Italy.

INTRODUCTION: Most of the literature devoted to the evaluation of the effects of Extremely Low Frequency Electromagnetic Fields on mammalian cell cultures failed to find induction of genotoxic effects. Recently, Rüdiger and coworkers reported induction of DNA damage, assessed applying the Neutral and Alkaline Comet Assay, following intermittent exposures to 50 Hz EMFs at different experimental conditions (cell type, intermittent cycles duration, exposure duration). The highest effect was found in human fibroblasts following an intermittence of 5 min field-on/10 min field-off. This very interesting finding deserve attention and must be confirmed.

OBJECTIVES: Aim of this study was to replicate the results published by Ivancsits et al. (1) on the induction of genotoxic effects in human fibroblasts following intermittent exposures to 50 Hz EMFs for 24 hours. For this purpose, the same cells and the same exposure system have been employed.

METHODS: Cultured human fibroblasts, kindly provided by Dr. Ivancsits, were cultured in Dulbecco's modified Eagle's medium (DMEM) containing 10% fetal calf serum, 20 mM Hepes buffer, 2mM L-glutamine, 100IU/ml penicillin and 100 µg/ml streptomycin at 37°C in a humidified atmosphere of 5% CO₂. 24 hours before the experiments, cells were seeded into 35 mm Petri dishes (50000 cells/3 ml complete medium). Intermittent exposures at 50 Hz (1 mT field intensity) were carried out using two coil systems, provided by IT'IS-foundation (Zurich, Switzerland). The decision of which coil system becomes exposed or sham was performed randomly by the PC, in order to have a blind condition. The exposure file will be decoded following the completion of slides scoring. The two systems were hosted in the same commercial CO₂ incubator. Following 24 hours intermittent exposure, cultures were processed for the comet assay, as described in details in (1). One thousand cells from each sample/experiment were analyzed by a computerized Image Analysis System (Delta Sistemi, Roma, Italy) and results were expressed as mean value ± SE of Comet tail factor %. The tail moment was also evaluated.

RESULTS: At the moment, 3 independent experiments have been carried out and the analysis of the results is in progress. Further experiments are planned and will be completed in a short time.

Reference.

[1] Ivancsits S, Diem E, Pilger A, Rüdiger W, Jahn O. (2002) Induction of DNA strand breaks by intermittent exposure to extremely-low-frequency electromagnetic fields in human diploid fibroblasts. *Mutation Research* 519: 1-13.

P-C-3

EFFECT OF GSM-900 EXPOSURE ON HSP27 EXPRESSION IN EA-HY926 ENDOTHELIAL CELLS. F. Poullietier de Gannes, I. Lagroye, S. Sanchez, B. Billaudel, B. Veyret. PIOM/Bioelectromagnetics lab, ENSCPB/ EPHE, Univ of Bordeaux, Pessac, France.

INTRODUCTION: In 2002, the Finnish group of D. Leszczynski published a paper reporting that exposure to GSM-900 at 2.0 W/kg significantly affected protein expression of Hsp27 and p38MAPK as well as the phosphorylation status of numerous largely-unidentified proteins in the human endothelial cell line EA.hy926 (Leszczynski et al., 2002). Based on the known functions of Hsp27 and on recent results (Leszczynski, 2003), the authors postulated that mobile-phone exposure could cause an increase in blood-

brain-barrier permeability through stabilisation of stress fibers. In our laboratory, we had shown that exposure to GSM-900 microwaves did not induce the expression of some of the heat shock proteins in brain cells (Poullietier de Gannes et al., 2003).

As part of a collaborative effort with D. Leszczynski within the European Reflex programme, we attempted a replication of these results obtained on Hsp27 expression using immunofluorescence techniques, image analysis and ELISA. Two EA.hy926 cell lines were tested: one was a generous gift from D. Leszczynski, the other one from Dr. Cora-Jean S. Edgell who first developed the cell line and gave permission to use these cells in Bordeaux.

METHODS: *EA.hy926* (a gift from D. Leszczynski, STUK, Helsinki, Finland). Cells were grown in Dulbecco's MEM supplemented with 1% penicillin- streptomycin, 2% L-glutamine (200 mM), HAT-supplement and 10% Fetal Calf Serum (FCS).

EA.hy926 (a gift from Dr. Cora-Jean S. Edgell, North Carolina University at Chapel Hill, NC, USA). Cells were grown in Dulbecco's MEM supplemented with 1% penicillin- streptomycin, 2% L-glutamine (200 mM) and 10% FCS.

Cells were removed from culture flasks with trypsin, washed and seeded on glass coverslips at a density of 1.2×10^6 cells/35-mm-diameter petri dishes. After overnight culture, *EA.hy926* cells were sham-exposed or exposed to RF radiation (RFR) for one hour at 2.0 W/kg in a wire-patch antenna.

At the end of RFR- or sham-exposure, the cells were fixed in PBS-paraformaldehyde (3.7%) for immunocytochemistry. Anti-Hsp27 antibodies were obtained from Stressgen® (Tebu, France). The first antibody was revealed using a FITC-labelled antibody. Coverslips were mounted on slides with Mowiol® before microscopy observation, and fluorescence analysis was performed using the Aphelion® image software (n = 5).

Hsp27 ELISA kit (Stressgen®) was used as indicated by the manufacturer to quantify hsp27 in cell lysates immediately or 5 h after sham or RFR exposures (n=4).

Positive controls for heat shock proteins induction were performed by exposing each *EA.hy926* cell lines at 42°C for 20 min or 1 hour.

All experiments were performed in a blind manner (coded samples).

RESULTS AND DISCUSSION: Fluorescence analysis of Hsp27 expression in both *EA-hy926* cell lines revealed no significant difference between sham-or exposed cells. ELISA allowed us to determine precisely whether RFR were able to induce changes in Hsp27 expression. With this method, even if the trend was toward an increase in Hsp27 expression (only with the *EA-hy926* given by Dr D. *Leszczynski* after 1-hour exposure), the differences were not statistically significant. We were thus unable to confirm previous data on Hsp27 expression in endothelial cell lines.

References.

Leszczynski, D. (2003). Use of Discovery science-approach to elucidate bioeffects of electromagnetic fields, 25th BEMS meeting, june 2003, Hawaii, 104.

Leszczynski, D., Joenväärä, S., Reivinen, J., and Kuokka, R. (2002). Non-thermal activation of hsp27/p38MAPK stress pathway by mobile phone radiation in human endothelial cells: Molecular mechanism for cancer-and blood-brain barrier-related effects, *Differentiation* 70, 120-129.

Poullietier de Gannes, F., Sanchez, S., Lagroye, I., Haro, E., Dulou, P., Billaudel, B., and Veyret, B. (2003). In vitro and vivo studies of the effects of GSM-900 microwave exposure on heat shock proteins in the brain and skin, 25th BEMS Meeting, june 2003, 18.

ELECTRICAL PULSE-INDUCED CHANGES IN HL-60 DIELECTRIC PROPERTIES. A.L. Garner¹, J. Yang, N. Chen, J. Kolb, K.C. Loftin, R.J. Swanson, S. Beebe, R.P. Joshi, K.H. Schoenbach. Center for Bioelectrics, Old Dominion University, Norfolk, Virginia, 23510, USA. ¹ Department of Nuclear Engineering and Radiological Sciences, University of Michigan, Ann Arbor, Michigan, 48109, USA.

BACKGROUND: Microsecond- duration pulsed electric fields (PEF's) above a certain voltage cause electroporation [1], or increased permeability of the cell membrane due to pore formation, while submicrosecond pulses induce intracellular effects [2]. Models developed to describe and interpret these effects often depend on the electrical properties of the cells, which are altered by the PEF [3]. We determined the complex permittivity of a cell suspension using time domain dielectric spectroscopy (TDDS) [4], which measures the reflection of a 250 mV, 5 μ s square pulse from a the cell suspension to determine the complex permittivity of the cell suspension. We used a cell two-shell model of the cell to obtain the conductivity and permittivity of the cell membrane, cytoplasm, nuclear envelope, and nucleoplasm from the complex permittivity.

OBJECTIVE: The objective of this study Our objective was to determine how 50 μ s and 10 ns pulses of the same energy density alter the electrical properties of HL-60 cells (a human leukemia cell line), particularly that of the cell membrane, as a function of time after the pulse.

METHODS: We washed cultured HL-60 cells once with Ca²⁺ and Mg²⁺-free phosphate buffered saline (PBS) without Ca²⁺ and Mg²⁺ and once with a buffer consisting of 229 mM sucrose, 16 mM glucose, 1 μ M CaCl₂, and 5 mM Na₂HPO₄ in double distilled water [5]. We adjusted the cells to a cell concentration of to 5% (6 x 10⁶ cells/100, or 6 million cells in 100 μ l of solution), for optimal operation of the TDDS system [4,5]. We used a A MOSFET-modulated, capacitive discharge to generated 50 μ s pulses with a 30 ns rise time. We used a A Blumlein generator, limited by an employed self-discharging spark gap with SF₆ fill gas, to generate produced 10 ns pulses with 1 to 2 ns rise times. The electric fields generated by the two pulses (1.1 kV/cm for the 50 μ s pulse, and 78 kV/cm for the 10 ns pulse) were set such that the electrical energy densities in the suspension were identical (5.5 J/cm³). After pulse application, TDDS measurements were conducted for the pulsed sample and an unpulsed control samples over time.

RESULTS: The 50 μ s pulses caused a rise in suspension conductivity within ten seconds after the pulse post-pulse, while 10 ns pulses caused a rise in suspension conductivity after a with one to two minutes post-pulse delay. The 50 μ s pulse caused a much more significant initial rise in membrane and suspension conductivity than a 10 ns pulse of the same energy. For both pulse lengths, the suspension conductivity stayed at a high level for approximately 40forty minutes. After this time forty minutes, the membrane resistivity not only recovered, but increased beyond its resting state level. . Raising the electric field to 2 kV/cm and 140 kV/cm for the 50 μ s and 10 ns pulses, respectively, frequently led to increased membrane permeability a loss of membrane integrity and followed by a gradual recovery about thirty to forty minutes after pulse application, as indicated by changes in trypan blue uptake [6].

CONCLUSION: Observations such as instant poration for long pulses and delay for 10 ns pulses are consistent with other experimental observations [7]. These results indicate that while membrane opening poration is a primary effect for long pulses and a secondary effect for ultrashort pulses; h. However, the time to membrane recovery is on the same time scale for both pulse durations. The resistivity overshoot indicates a reduction in membrane permeability in both cases, possibly due to pulse-induced conformational changes.

References

- [1] Tien, H. T. and A. Ottova A. (2003) *IEEE Trans. Diel. Elec. Insul.* 10: 717-727.
- [2] Schoenbach, K. H., S. J. Beebe SJ, and E. S. Buescher ES. (2001) *Bioelectromagnetics.* 22: 440-448.
- [3] Joshi, R. P., Hu Q.Q. Hu, and K. H. Schoenbach KH. (2003) *IEEE Trans. Diel. Elec. Insul.* 10: 778-787.

- [4] Feldman, Y., I. Ermolina, I, and Y. Hayashi Y. (2003) *IEEE Trans. Diel. Elec. Insul.* 1. 10: 728-753.
- [5] Polevaya, Y., I. Ermolina I, M. Schlesinger M, B-Z. Ginzburg B-Z, and Y. Feldman, Y. (1999) *Biochim. Biophys. Acta.* 1419: 257-271.
- [6] Velizarov, S., M. Reitz, M, B. Gluck, B, and H. Berg, H. (1998) *Bioelectrochem. Bioenerg.* 47: 89-96.
- [7] Beebe, S. J., P. M. Fox PM, L. J. Rec LJ, E. L. Willis EL, and K. H. Schoenbach KH. (2003) *FASEB J.* 17: 1493-1495.

This study was funded by an AFOSR DOD MURI grant on “Subcellular Response to Narrow Band and Wide Band Radio Frequency Radiation,” administered by Old Dominion University, and by an AFOSR grant on bioinspired concepts.

P-C-57

EVALUATION OF GENOTOXIC EFFECTS IN HUMAN PERIPHERAL BLOOD LYMPHOCYTES FOLLOWING RF EXPOSURES AT BOTH GSM 1800 AND UMTS 1950 SIGNALS. O. Zeni¹, A. Schiavoni², A. Perrotta¹, D. Forigo², M.R. Scarfi¹. ¹CNR- Institute for Electromagnetic Sensing of Environment (IREA), via Diocleziano, 328, 80124, Napoli, Italy, ²TILAB, via G. Reiss Romoli 274, 10148, Torino, Italy.

INTRODUCTION: Many in vitro studies have been published on the possible genotoxic effects of electromagnetic field (EMF) exposure at frequencies from mobile communication systems. They mainly refer to frequencies in the range 900-1800 MHz, but the results are far to be conclusive. Moreover none of them refers to the new wireless technology of UMTS signal.

OBJECTIVES: The objective of this study is to investigate the genotoxic effects in human peripheral blood lymphocytes (HPBL) following exposure to 1800 MHz GSM and 1950 MHz UMTS signals. For this purpose, micronucleus (MN) frequency and cell cycle kinetics have been investigated following intermittent exposures.

METHODS: On the whole, blood samples coming from 9 healthy subjects, have been employed to set up both exposed and sham exposed cultures, according to the routine method for lymphocyte cultures [1]. Diluted HPBLs were maintained for 24 h in absence of mitogen (Go phase) and then cultured for 72 hours. Positive controls were also provided by treating cultures with mitomycin-C (MMC, 0.033 µg/ml final concentration). Exposures were performed in a TEM cell IFI CC110SEXX hosted in an incubator, opportunely equipped to maintain constant the temperature, supplied by a feeding and controlling line to get well defined exposure conditions. Sham exposures were performed in a completely equivalent exposure set-up, except for the presence of the radiofrequency power, and hosted inside the same incubator in the same time as the real exposure set-up. Computational dosimetry has been used to establish the exposure conditions of the cell cultures.

Intermittent (6' RF on, 2h RF off) exposures were conducted at Specific Absorption Rates (SAR) of 0.4 W/Kg and 2.2 W/Kg for GSM and UMTS, respectively. Three different exposure conditions were used, in order to apply RF in different phases of cell cycle:

- intermittent exposures of unstimulated lymphocyte cultures (Go phase) for 24 h before PHA stimulation – indicated as exposure condition 1;
- intermittent exposures of unstimulated lymphocyte cultures (Go phase) for 24 h followed by 44 h of exposure after PHA stimulation – indicated as exposure condition 2;
- intermittent exposures during the 44 h after PHA stimulation – indicated as exposure condition 3.

For each subject, four cultures have been considered; the first (indicated with RF in figures 1 and 2) is the culture exposed to the radiofrequency pattern as described in the previous list; the second one (indicated with SH in figures 1 and 2) is the same culture exposed in the same environmental conditions except for the radiofrequency, the third one (indicated with MMC in figure 1 and 2) is the culture treated with MMC, the fourth one (indicated with C in figure 1 and 2) is the control culture untreated and unexposed.

RESULTS AND CONCLUSIONS: By analyzing MN induction in 1000 binucleated cells and cell

proliferation in 500 cells, no statistically significant difference (two tailed paired Student *t* test) has been detected in exposed cultures with respect to sham exposed ones, when 1800 MHz GSM and 1950 MHz UMTS signals were employed. Moreover, no difference has been detected depending on the phase of cell cycle in which RF was applied. On the contrary, as expected, MMC treatment in all cases has induced a statistically significant increase in MN induction with respect to untreated cultures, without affecting cell proliferation. Results obtained in terms of MN frequency are reported in figure 1 and 2 for GSM and UMTS respectively. In conclusion, these findings extend our previous results on 900 MHz GSM signal [2], and represent a pilot study for the evaluation of biological effects related to the new wireless technology of UMTS signal, since, at our knowledge, there are no data in the available literature.

References

- [1] Scarfi. MR, Lioi MB, Zeni O, Della Noce M, Franceschi C, Bersani F. (1999) *Health Physics* 76: 244-250.
- [2] Zeni O, Schiavoni A, Sannino A, Antolini A, Forigo D, Bersani F, Scarfi MR. (2003) *Radiation Research* 160: 152-158.

This work has been fully supported by TIM – Telecom Italia Mobile

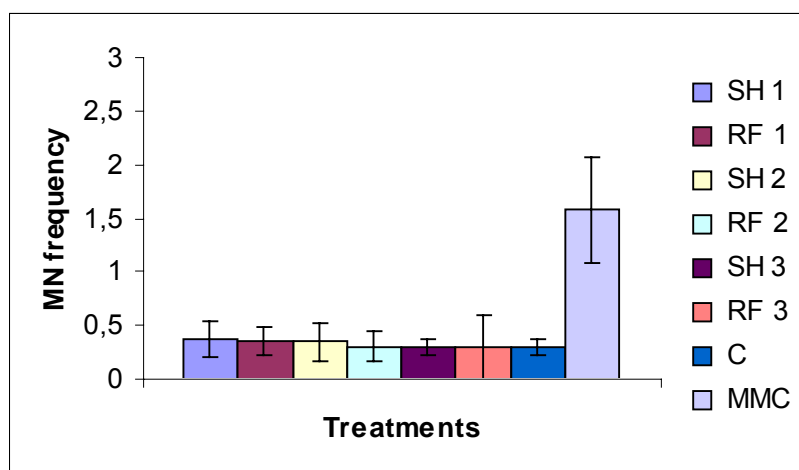


Figure 1: MN frequency in HPBL following intermittent exposure to 1800 MHz GSM signal. Data are presented as mean \pm SD of the 4 subjects examined; RF 1-3 stand for Radiofrequency exposures in the different exposure conditions, described in the text; SH 1-3 stand for sham exposures; C stands for control; MMC stands for positive control.

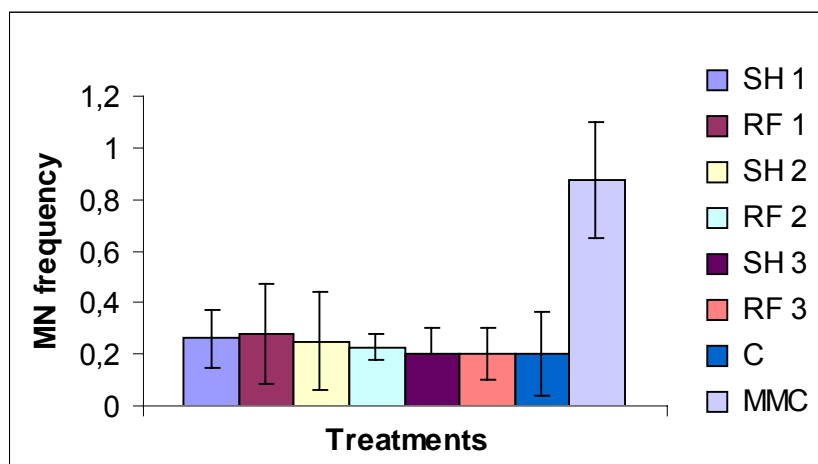


Figure 2: MN frequency in HPBL following intermittent exposure to 1950 MHz UMTS signal. Data are presented as mean \pm SD of the 5 subjects examined. RF 1-3 stand for Radiofrequency exposures in the different exposure conditions, described in the text; SH 1-3 stand for sham exposures; C stands for control;

MMC stands for positive control.

P-A-58

STUDENT

THE EFFECT OF EXTREMELY HIGH POWER PULSES (EHPP) - TREATED WATER ON BARLEY SEEDS' DRY WEIGHT KINETICS DURING THEIR AWAKENING. A.M. Amyan, S.N. Ayrapetyan. UNESCO Chair-Life Sciences International Center, 31 Acharyan st. Yerevan, 375040 Armenia.

INTRODUCTION: It was shown that dry weigh (d.w.) and wet weight (w.w.) kinetics of barley seeds during their awakening can be modulated by preliminary treatment of aqua bathing solution by low frequency electromagnetic fields (LF EMF) [1]. Seeds d.w. and w.w. dynamics gives information on the osmotic properties of seeds, dissolvent of water soluble components of seeds and water binding in them, as well as metabolic-dependent cell hydration, root formation and germination. At the same time by resent study at our laboratory it was shown that at room temperature specific electrical conductivity (SEC) of distilled water (DW) exposed to EHPP was higher comparing to the control one [2]. These data allow us to suggest that EHPP-induced water structure changes could serve the mechanism, through which the possible specific (non-thermal) biological effect of EHPP is realized.

OBJECTIVE: To estimate the physiological meaning of EHPP-induced water structure changes on seeds germination potential, the comparative study of preliminary EHPP-treated and heat-treated distilled water (DW) on seeds d.w. and w.w. kinetics during their awakening process (72 hours incubation) was performed.

METHODS: The seeds of spring barley (sort- Nutans 115, Gramineae family, class Monocotyledoneae, forms fibrous root system, cleistogamous) were used. The distilled water was obtained using the device-DE-4-2M (Russian production, State Standard 64-1-721-91). Fresh distilled water (DW) was frozen at -1°C during 1 hour after which was defrost at room temperature (18°C). The water was poured out into three identical glass test tubes for control, heat-treated and EHPP-treated DW. DW was treated by EHPP (MIG 9.3 generator Russian production) during 15 minutes (Peak SAR = 180 kW/g. , $1\ \mu\text{sec} = 9.3\ \text{GHz}$). The equivalent heating of the second sample was performed in water bath, after which 5ml of DW was added to each Petri's dishes (vol.~45-50 ml.), containing 20 seeds and this moment was considered as a starting time of seeds incubation. Before and after DW treatment its SEC was measure by special conductometer (Production of Institute of Radiophysics and Electronics of Armenian NAS). To exclude the side effect of light and to create the natural conditions for seeds, the experiments were performed in dark conditions (at 18°C). The determination of w.w. and d.w. was carried out separately for each seed. Seeds d.w. was determined by 24 hours seeds heating at thermostat (at 104°C).

RESULTS: At 18°C SEC of DW before and after 15 min. heat- and EHPP-treatment were 145×10^{-3} sim., 73×10^{-3} and 97×10^{-3} , correspondingly. DW exposure to EHPP leads to temperature increase to 35°C . The results of studying the time-dependence of changes of d.w in process of seed swelling in non-treated (control), heat- and EHPP-treated DW are presented on Fig 1. As it can be seen from these data, in case of heat- and EHPP-treated DW the rate of d.w. decrease was slower than in control one. However, this process in EHPP-treated DW was much slower than in heat-treated medium. It is interesting to note that these differences between d.w. kinetics were more pronounced after 2 hours of seeds incubation. As it can be seen on presented figure, during 48-72 hours incubation, when the process of seeds germination was activated, the decrease of d.w. of seeds incubated in heat-treated DW was more significant comparing to the control one, meanwhile it must be noted that in EHPP-treated DW this decrease was more pronounced than in case of heat-treated DW.

DISCUSSION: The obtained data on EHPP-treated DW depressing effect in period of 2-48 hours incubation and accelerating effect in period of 48-72 hours incubation on time-dependant decrease of seeds d.w. comparing to heat-treated and non-treated DW could serve as strong evidence on the existence of specific effect of EHPP on seeds awaking which is realized through EHPP-induced structural changes of

bathing water.

References.

[1] Amyan A.M., Ayrapetyan S.N. (2003). Effect of Water treated by LF EMF, SMF and MV on Barley Seeds Hydration. Bioelectromagnetics (in press)

[2] Hayrapetyan H.V., Avanesyan A.S., Ayrapetyan S.N. On specific effect of extremely high power pulses on physical properties of water. Abstract presented to BEMS 26th Annual meeting.

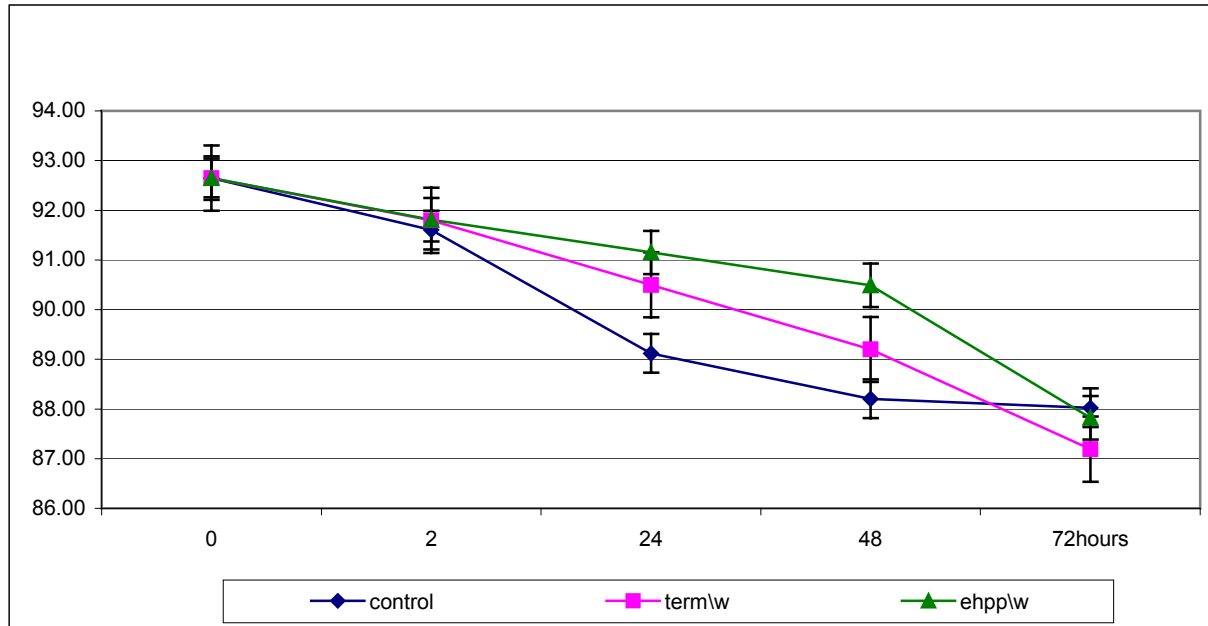


Figure 1. The time-dependant changes of dry weight of barley seeds, incubated in non-treated (control), heat-treated and EHPP- treated DW.

This study was founded by European Office of Aerospace Research and Development (EOARD) through ISTC A-803 Partner project.

P-B-59

STUDENT

THE EFFECT OF EXTREMELY HIGH POWER PULSES (EHPP) –TREATED PHYSIOLOGICAL SOLUTION ON ACH-INDUCED CURRENT IN SNAIL NEURONAL MEMBRANE. A.Sh. Hunanyan, S.N. Ayrapetyan. UNESCO Chair-Life Sciences International Center, 31 Acharyan st. Yerevan, 375040 Armenia.

INTRODUCTION: At present the existence of specific (non-thermal) biological effects of RF-EMF still remains discussable. However, by resent study at our laboratory it was shown that at room temperature specific electrical conductivity (SEC) of distilled water (DW) exposed to EHPP was higher comparing to the control one [1]. On the basis of these data it was suggested that EHPP- induced structural changes of physiological solution (PS) could modulate neuromembrane chemosensitivity. To check this hypothesis the effect of preliminary EHPP-treated PS on Ach-induced current in snail neuronal membrane was studied.

OBJECTIVE: The comparative study of the effect of preliminary EHPP-treated and heat-treated PS at room temperature on Ach-induced current in snail neuronal membrane in voltage clump experiment was performed.

METHODS: PS was frozen at -1°C during 1 hour after which was defrost at room temperature ($20-21^{\circ}\text{C}$). After temperature stabilization (after 1 hour) PS was divided into two samples (Vol: 5ml): control and

experiment. Experimental sample was exposed to EHPP source (MIG 9.3 generator, Russian production) during 15 minutes (Peak SAR = 220 kW/g., 1 μ sec = 9.3 GHz). EHPP exposure leads to temperature increase to 50,5 $^{\circ}$ C. The equivalent heating of control sample was performed in water bath.

The experiments were carried out on giant neurons from the right parietal ganglion of *Helix pomatia*. To record the Ach-induced current through the neuronal membrane, the usual Voltage-Clamp method combining with Digidata acquisition system (Axon Instruments) connected to personal computer was used. PS contains (in mM): NaCl-80, KCl-4, CaCl₂-7, MgCl₂-13, Tris-HCl (pH 7.8)-10, glucose-10.

RESULTS: Previously it was shown, that Ach-responses of *Helix* neurons can be distinguished according their pharmacological properties and ionic nature: A-type neuron responses are depressed by Na-K pump inhibition and they are generated by the increase of membrane permeability for Cl and Na ions. While B-type responses are due to increase of K and Na ions membrane permeability and they are pump-insensitive. PS preliminary treated by EHPP in A-type neurons has non-reversible depressing effect on amplitude of Ach-induced current. The typical record of EHPP-treated PS-induced depressing effect on Ach response at room temperature is presented on Figure 1a. The B-type neurons in normal PS have Ach-induced response with constant amplitude (interval between Ach applications-5 min). The RP1neurons having bursting peacemaker activity have B-type Ach responses, which are depressed in K-free solution (Fig. 1b). As it can be seen on Fig. 1b, there are spontaneous miniature responses which were also depressed in K-free solution. EHPP-treated PS has depressing effect on Ach-induced current, while the amplitude of miniature potential was not depressed (Fig. 1c).

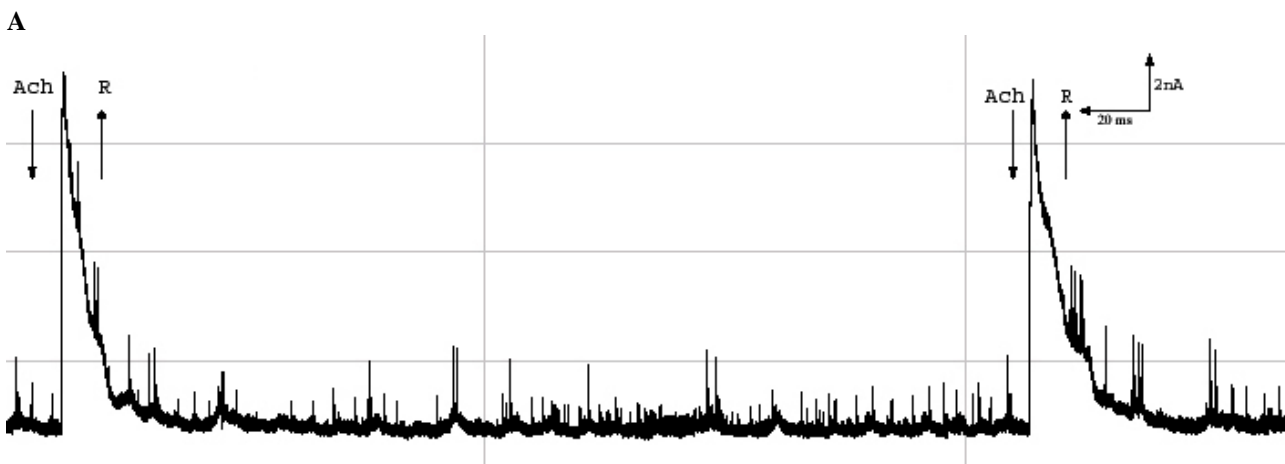
0.5 hour of perfusion by normal PS did not recover the initial level of Ach-induced current (before the application of EHPP-treated PS) (Fig. 1d). However the miniature responses were not significantly affected by EHPP-treated PS. These different sensitivities of Ach responses and spontaneous synaptic responses to EHPP-treated PS seems extremely interesting and can be the subject for special investigation. Preliminary heat-treated PS has no significant effect on Ach-induced current and amplitude of miniature potential.

DISCUSSION: The obtained data on existence of depressing effect of preliminary EHPP-treated PS on amplitude of Ach-induced current in A-type neurons and the absence of such effect in heat-treated PS allow us to suggest that EHPP-treated PS has specific (non-thermal) effect on Ach-induced current in snail neuronal membrane. The membrane mechanism of damaging effect of EHPP-treated PS is a subject for current investigation.

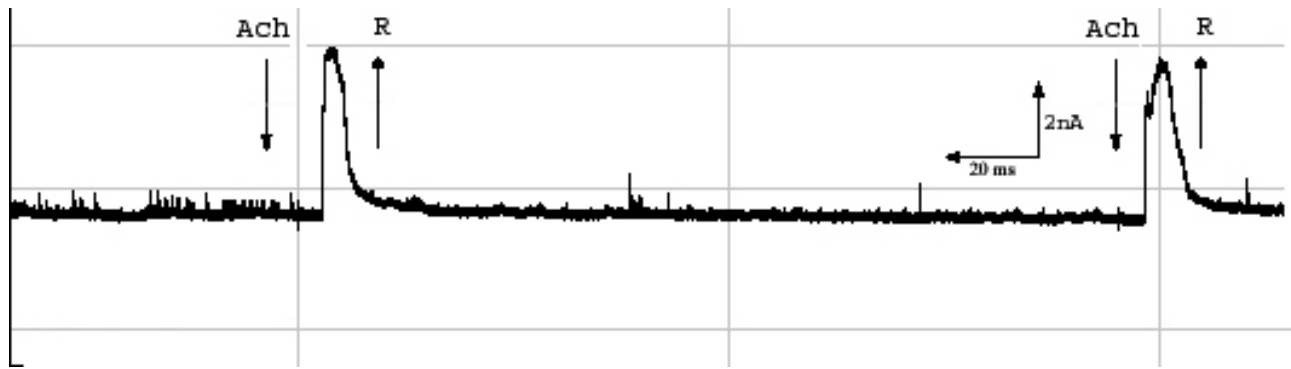
References.

[1] Hayrapetyan H.V., Avanesyan A.S., Ayrapetyan S.N. On specific effect of extremely high power pulses on physical properties of water. Abstract presented to BEMS 26th Annual meeting

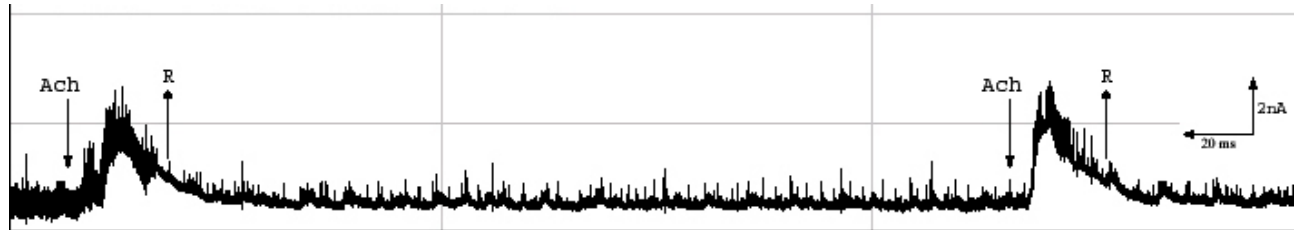
Fig. 1 The effect of 15 min. EHPP treated PS on Ach-induced current through the membrane of *Helix* neuron in voltage clamp conditions. Resting potential was equal to holding (clamping) potential (53 mV). A- in normal PS, B- in K-free PS, C-in PS 15 min. pretreated by EHPP, D-after 30 min. washing in normal PS.



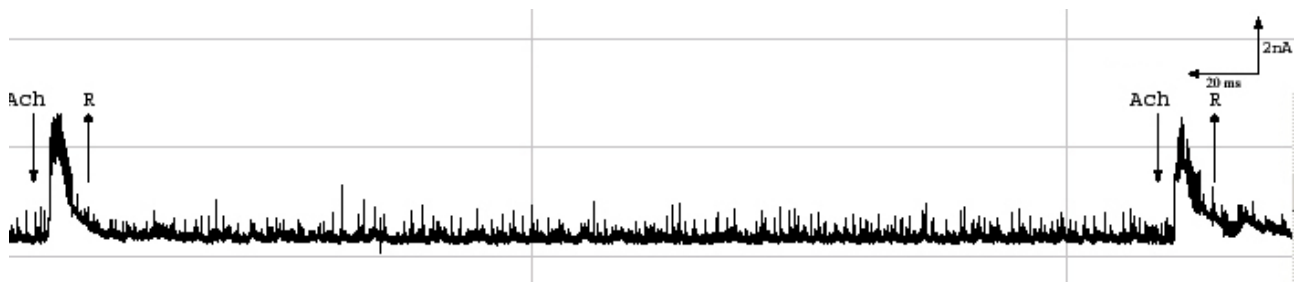
B.



C.



D.



This study was funded by European Office of Aerospace Research and Development (EOARD) through ISTC A-803 Partner project.

P-C-60

ELEVATION OF GENOMIC INSTABILITY FOLLOWING EXPOSURE OF CELLS TO THz RADIATION. A. Korenstein-Ilan¹, A. Barbul¹, A. Eliran², A. Gover², and R. Korenstein¹. ¹Dept of Physiology and Pharmacology, and ²Department of Electrical Engineering-Physical Electronics, Tel-Aviv University, 69978 Tel-Aviv, Israel.

INTRODUCTION: Recent technological break-through in electromagnetic radiation sources, components and devices, in the THz region (which spans the spectral interval between the microwave- and the infrared regions of the electromagnetic spectrum) has triggered new applications in the field of material science, biology and biomedicine.

OBJECTIVE: In order to examine the safety of being exposed to THz radiation we have studied genetic and epigenetic changes induced in human lymphocytes following exposure to radiation at 100GHz.

METHODS: The exposure to CW 100GHz radiation was carried out in a specially designed exposure system, maintaining a temperature of 37°C. Since the penetration depth of radiation at 100GHz into a water suspension of lymphocytes is very short (~0.13 mm), the lymphocyte cells lying, due to gravity, at the bottom of the culture flasks were illuminated from the bottom. The power density of the 100GHz radiation at the bottom of the flask was 0.05mW/cm² (where the international guidelines limit exposure to a value of 1mW/cm² for the general population and to 5mW/cm² for occupational exposure). Lymphocytes isolated from peripheral blood were irradiated for 1,2 and 24 hours and were harvested by common cytogenetic procedures 69 to 72 hours after the onset of exposure. The genetic and epigenetic markers for genomic instability were the increase of the levels of aneuploidy and replication synchrony, respectively. These parameters were evaluated by interphase FISH based cytogenetics. We scanned slides of nuclei, derived from the exposed and appropriate control cultures, hybridized with probes specific for the centromeric regions of chromosomes 11 (orange labeled; Vysis, USA) and 17 (green labeled; Vysis, USA) using the Metafer platform for semi-automatic interphase FISH scoring. Cells were scored automatically; the gallery was then manually corrected by two independent technicians. Between 800 and 1100 cells were scored from each culture. The Metafer platform automatically presents the results obtained for the levels of chromosomal gains and losses for each locus plus a correlation between the two loci. The subset of cells which had two hybridization signals for both signals, were manually analyzed for the pattern of replication of 600 cells.

RESULTS: The exposure of lymphocytes to THz radiation induced increase in both replication asynchrony and aneuploidy after two hours and 24 hours of exposure, but no effect was observed after one hour radiation. The aneuploidy level, in the exposed cultures, increased by 37% for centromere of chromosome 17 (CEN17) and by 50% for centromere of chromosome 11 (CEN11) compared to the control cultures. The level of aneuploidy observed in the control cultures was 9.4±2.5% and 7.2±2.5% for CEN17 and CEN11, respectively. After two hours of exposure the levels of aneuploidy levels increased to 12.8±3.7% and 9.5±2.9%, respectively ($p < 10^{-3}$). These levels increased slightly more after 24 hours of exposure to 13.1±3.6% and 11.8±2.5%, respectively ($p < 10^{-2}$). When analyzing the frequency of asynchronous replication in these cultures we observed an even more pronounced effect. While two hours of exposure led to an increase of about 56% in the frequency of asynchronous replication of each of the two loci tested, 24 hours of exposure led to a 108% and 71 % increase for CEN17 and CEN11, respectively. The levels of asynchronous replication in the control cultures were 14.7±3.3% and 14.4±3.5% for CEN17 and CEN11, respectively. After exposure these levels reached 24.7±5.3% after two hours and 28.5±4.7% after 24 hours for CEN17 ($p < 10^{-5}$). For CEN11, after two hours of exposure asynchronous replication was observed in 22.4±4.9% of cells and was 24.6±5.0% after 24 hours of exposure ($p < 10^{-4}$).

DISCUSSION: Both genotoxic and epigenetic effects are induced in lymphocytes following exposure to CW 100 GHz radiation of 0.05 mW/cm² when exposure period exceeds one hour. The induced effects seem to saturate already for short exposures and occur at power density much lower than those set by the international guidelines for exposure limits.

This study was supported by the European Commission (Contract QLK4-CT2000-00129).

P-A-61

Presented as ST-6

P-B-62

STUDENT

TWO SIMILAR EMF SIGNALS ELICIT DIFFERENT EFFECTS ON NEURITE OUTGROWTH OF SPINAL CORD EXPLANTS *IN VITRO*. A. Chan¹, J. Smith¹, M.S. Markov² and B.F. Siskin¹.

¹Center for Biomedical Engineering and Dept Anatomy and Neurobiology, University of Kentucky, Lexington, Kentucky, 40506-0070, United States. ²Research International, Buffalo, New York 14221 USA.

INTRODUCTION: It has been previously reported that one of two similar (by amplitude and wave-shape) EMF signals has been found to stimulate neurite outgrowth in dorsal root ganglia (DRG) *in vitro* (Siskin et al, 2002). DRG are part of the peripheral nervous system and quite capable of regenerating their processes. It appears that a study designed to determine whether spinal cord segments, which do not regenerate well, would also respond in the same way to these two signals was a logical next step, since there is now active interest in promoting regeneration of spinal cord using physical modalities.

METHODS: 9-10 day old chick embryo spinal cord was sliced into approximately 100 µm thick pieces and 4-6 pieces set onto five cooled 60 mm Falcon culture dishes containing a layer of Matrigel (Collaborative Res., Bedford, MA) diluted 1:3 with Neurobasal Medium (Gibco, N.Y.). Then the dishes were placed in a 37 °C incubator for 2 hrs. to "gel" the Matrigel and trap the tissue in it. Equal portions of Neurobasal Medium containing B27 (Gibco) and penicillin and streptomycin, and Dulbecco Medium containing fetal calf serum and antibiotics were added to each dish. The dishes were exposed for 15 min/day for 5 days or not exposed (no magnetic field) for the same time period to electromagnetic fields generated by animal model TEMF-005 generating system (EMF Therapeutics, Inc., Chattanooga TN). The signal consists of 120 pps fully rectified semi-sine wave. The rectified semi-sine wave maximums with magnetic flux density of 15 mT were separated by 4 µs (Signal 2) or 8 µs (Signal 1) DC components which are the result of changes in the device impedance due to the presence of different components in the electrical circuit. This schedule was repeated 4-5 times. The explants were fixed in 4 % formalin after 6 days in culture. Color photographs of all explants were taken at 3 and 6 days incubation *in vitro*. To quantify neurite growth emanating from spinal cord neurons, the length of the neurites (mm) from the original slice to their farthest point was measured, each neurite specified as a count. Statistical analyses were performed using ANOVA followed by Tukey-Kramer Multiple Comparison.

RESULTS AND DISCUSSION: In dishes treated with signal 1 TEMF, there was no difference in the number of neurites or neurite length in control vs TEMF explants at 3 days incubation, but there was a significant decrease (p=.05) in the average length of neurites at 6 days of incubation. In explants exposed to signal 2 TEMF, there was a significant increase in the number of neurites (p=.012) at 3 days, but not at 6 days. Neurite length was unaffected by signal 2 TEMF at either 3 or 6 days. Therefore, it appears that a central nervous system model reacts to these two signals in a like fashion. Both the DRG and spinal cord models react more negatively to signal 1 while they react in a neutral or positive way to signal 2. These differences in bioresponses to two similar signals are of interest to those involved with the role of EMF in neurobiological research.

P-C-63

MAGNETIC FIELD INFLUENCE ON NGF-STIMULATED NEURITE OUTGROWTH IN PC-12 CELLS: EFFECT OF PAINT FUMES. C.F. Blackman¹, D.E. House², S.G. Benane³, A. Ubeda⁴, M.A. Trillo⁴. ¹National Health and Environmental Effects Research Laboratory, EPA, Research Triangle Park, North Carolina 27711 USA, ²Durham, NC, ³Wendell, NC, ⁴Dept. Investigacion, Hospital Ramon y Cajal, 28034 Madrid, Spain.

OBJECTIVE: Examine the influence of a painted mu-metal magnetic-shielding box in incubators on the magnetic-field (MF)-induced neurite outgrowth response in PC-12 cells. The box shields the cells and the MF generating coils from MF generated external to the box. The work reported here focuses on the influence of fumes, generated from paint coating the surfaces of the box, on the cell response.

METHODS: We used an assay of neurite outgrowth (NO) from NGF-stimulated, primed PC-12 cells to explore the effects of 23 hours of exposure to magnetic fields (Blackman et al., 1994). The cells were exposed to a 45 Hz ac vertical magnetic field over the flux density range of 132 - 347 mGrms [13.2-34.7 microT]. The Bac was parallel to a dc field of 366 mG [36.6 microT], with a perpendicular dc field < 2 mG [0.2 microT]. These MF exposure conditions are predicted by the IPR model to produce the maximal reduction in NO under resonance conditions for Mg/Mn and H. Exposures were performed under four conditions: 1) with the painted mu-metal box as received, 2) after the box had been heated to 121 degrees C for 3 hours, 3) after the box had been heated for an additional 15 hours, and 4) after the paint has been stripped from the box.

RESULTS: The experimental results using the painted box as it was delivered did not show the expected U-shaped inhibitory response function over the ac MF flux density tested. There was no discernable NO pattern. After the painted box was heated for 3 hours and the experiment repeated, a slight 'U' shaped response was observed but the amount of change in NO was dramatically attenuated compared to what was observed in the absence of the box. After the box was heated for 15 more hours, the cell response was closer to the expected one, but still sufficiently attenuated to require rejection of the painted box. The results obtained with the box after the paint had been stripped, were essentially identical to the response observed with no box present.

DISCUSSION: These results demonstrate external factors capable of confounding NO responses to MF. In this case, outgassing chemical components from paint ("fresh" paint smell was clearly detectable), were clearly implicated in aberrant cell responses to MF. It should be noted that there was no effect of the paint on the ability of NGF to stimulate NO in cells not exposed to MF. Although the implications of this result were not pursued, this incident should be a warning for scientists using exposure apparatus that may contain vapors from manufacturing process, e.g., glue drying, to be alert to potential confounders in their experiments that could lead to alternative results.

Authors receiving EPA support (CFB, SGB, DEH), DOE support (CFB, SGB), IAG# DE-AI01-89CE34024 and DE-AI01-94CE34007, and Spanish support (AU, MAT) by Fondo de Investigacion Sanitaria (BAE 92/5044 and BAE 92/5045). This abstract does not necessarily reflect the policy of EPA or other support organizations.

P-A-64**STUDENT**

MEMBRANE EFFECTS OF PULSED HIGH POWER RADIOFREQUENCY RADIATION IN MAMMALIAN CELLS. D.W. Jordan, R.M. Gilgenbach, M.D. Uhler, A.L. Garner, L. Gates, Y.Y. Lau. Dept of Nuclear Engineering and Radiological Sciences and Mental Health Research Inst, Univ of Michigan Medical School, Ann Arbor, MI, 48109, USA.

INTRODUCTION: Electroporation is a common technique in biological research and has promise for therapeutic applications including chemotherapy enhancement and gene therapy [1,2]. The University of

Michigan has performed a series of experiments to determine the effectiveness of radiofrequency (RF) electric fields for electroporation, since these fields can be propagated in a waveguide or antenna.

OBJECTIVES AND METHODS: To compare the electroporation response of electrically excitable and non-excitable cells, two cell lines were used, the N1E-115 murine neuroblastoma and the COS-1 African green monkey kidney fibroblast. Cells were electroporated in a phosphate-buffered sucrose suspension in cuvettes. Four electric field modalities were used; each exposure consisted of a train of five pulses at 1 s intervals. 1 ms square pulses were used for comparison to the RF-modulated fields. 2 ms bursts of unipolar RF at 25 kHz, bipolar RF at 20 kHz, and bipolar RF at 13.56 MHz were used to observe the frequency dependence of the electroporation response. Applied electric fields ranged from 0 - 2.0 kV/cm. Membrane permeabilization was observed by using fluorescence microscopy to measure DAPI uptake in cells. Cell killing (lysis) was measured using trypan blue exclusion at 15 minutes after exposure. Experiments are currently underway to determine the response of cells to ultrawideband (UWB) RF pulses with sub-nanosecond risetime and 60 ns pulse width, up to maximum applied field strength of ≤ 100 kV/cm.

RESULTS: Electroporation and cell killing by DC pulses and unipolar RF pulses were consistent with Chang's earlier results [3]. For field strengths up to 2 kV/cm, 2 ms unipolar RF bursts produced both less killing and less permeabilization than 1 ms DC pulses. The reduced killing of the RF bursts resulted in higher electroporation yields for these exposures at some electric field strengths. For bipolar RF bursts (no DC offset), 2 ms bursts had no measurable effect on cell killing or permeabilization at field strengths up to 1.5 kV/cm. Neither the 20 kHz nor the 13.56 MHz bipolar RF exposures caused any measurable permeabilization of the cell membrane.

This work is supported by the Air Force Office of Scientific Research.

References.

[1] Selby M, Goldbeck C, Pertile T, Walsh R, Ulmer J. (2000) *J. Biotechnology* 83:147-152.

[2] Pucihar G, Mir LM, Miklavcic D. (2002) *Bioelectrochem.* 57:167-172.

[3] Chang DC, Chassy BM, Saunders JA, Sowers AE. (1992) *Guide to Electroporation and Electrofusion*. New York, New York: Academic Press.

P-B-65

DESIGN AND FABRICATION OF LOCAL-EXPOSURE SYSTEMS FOR *IN VIVO* STUDY ON MOBILE FREQUENCY BANDS. H.J. Doh¹, J.K. Pack¹. ¹Dept. of Radio Science & Engineering, Chungnam National University, 220 Gung-dong, Yuseong-gu, Daejeon 305-764, Korea.

OBJECTIVE: Due to the rapid growth of mobile communication users, many studies have been performed and currently ongoing on the biological effects of mobile-phone EMF exposure. We have developed local exposure systems for long-term animal experiments at Cellular and PCS frequency band (Cellular: 848.5 MHz, PCS: 1762.5 MHz). Key results are presented in this paper.

METHODS: We developed carousel-type exposure systems. The exposure system consists of real CDMA signal source module, trays, antennas, and chamber for shielding. The chamber was designed to expose 4 trays that are stacked on the supporters inside chamber. Each tray contains 10 acrylic-tube restrainers, and thus 40 mice can be exposed at the same time. In this type of chamber, minimizing a stress on mice is very important. So we carefully designed the environmental condition like an illumination, ventilation, and noise inside chamber. To supply fresh air, two-fold ventilation scheme is used, one for the chamber using fans, and the other through restrainers using blowers. Proper illumination is also provided by fluorescent lamps. The design goal of luminance is 150 ~ 300 lux. The sound noise should also be low enough. It is less than 50 dB. The chamber is made of aluminium, the external size of which being 745 mm x 1060 mm x 1980 mm and we used an absorber foam inside the chamber with the thickness of 4.5 inch (AEL 4.5, AEMI. Inc.), which can reduce reflections from the wall at least -20 dB in the each operating frequency band. The carousel-type restrainers are chosen for head-mainly exposure. EMF signal are supplied the center of each tray by the sleeve dipole antennas, which were supplied by Motorola. The restrainers are tilt upwards about 3 ° for mice filth excretion. Proximal acrylic wings that makes angles of 50 ° with the tube's sagittal (shape of the arrow) plane, are attached to the tips of restrainers. Each tray has a pipe to fix the antenna and to afford ventilation through the restrainers. At the design stage, we simulated the E-field inside the chamber using FDTD (Finite Difference Time Domain) method. The FDTD method was also used to compute SAR (specific absorption rate) inside a mouse. The size of a mouse we simulated is 8 cm in length, 3.5 cm in height, and 3.5 cm in width. The mouse was modelled with 25 tissues, referring to the model of U.S Air Force Research Laboratory. SAR inside a mouse heads was measured using flouroptic temperature probes (model 790, Luxtron Corp.). The probe was inserted into the head of an exposed mouse using a plastic catheter, and the probe was located at 3 locations in the head of a mouse or a brain equivalent solid phantom. The SAR distribution inside mice and solid phantoms were also measured using IR camera (IRIS-5000, Medicare Co. Ltd.).

RESULTS AND DISCUSSIONS: At PCS frequency band the FDTD-simulated brain-averaged SAR value for mouse cadaver is 5.3 W/kg/W. The measurement result showed an excellent agreement. The FDTD simulation result for brain-averaged SAR value at cellular frequency band is 0.33 W/kg/W for mouse cadaver, which was in a good agreement with measurement result. These exposure systems are currently used for animal experiments.

References

- “A compact shielded exposure system for the simultaneous long-term UHF irradiation of forty small mammals: I. Electromagnetic and environmental design”, Eduardo G. Moros et al. *Bioelectromagnetics* vol. 19, 459-468, 1998.
- “A compact shielded exposure system for the simultaneous long-term UHF irradiation of forty small mammals: II. Dosimetry”, Eduardo G. Moros et al. *Bioelectromagnetics* vol. 20, 81-93, 1999.
- “Dosimetry in mice exposed to 1.6 GHz microwaves in a carrousel irradiator”, Mays Swicord et al, *Bioelectromagnetics* vol. 20, 42-47, 1999.
- “The SAR Evaluation Method by a Combination of Thermo-graphic Experiments and Biological Tissue-Equivalent Phantoms”, Yoshinobu Okano et al. *IEEE Transactions on Microwave Theory and Techniques*, vol. 48, No. 11

This research was supported by the EMERC(ElectroMagnetic Environment Research Center) in Chungnam National University, one of IT Research Centers.

P-C-66

EXPOSURE TO ELF MAGNETIC FIELD TUNED TO Zn INHIBITS GROWTH OF CANCER

CELLS. E. Markova^{1, 2}, R. Sarimov^{1, 3}, F. Johansson¹, D. Jenssen¹, G. Selivanova⁴, I. Belyaev^{1,3},
¹Department of Genetics, Microbiology and Toxicology, Stockholm University, Stockholm, Sweden;
²Department of Molecular Genetics, Cancer Research Institute, Bratislava, Slovak Republic; ³Department
of Biophysics, Radiation Physics and Ecology, Moscow Engineering Physics Institute, Russia; ⁴Cancer
Centrum Karolinska, Karolinska Institutet, Stockholm, Sweden.

INTRODUCTION: Effects of weak magnetic fields of extremely low frequency (ELF) on cell proliferation have been described and both inhibition and stimulation has been observed dependent on cell type and exposure conditions [1]. According to some models, ELF affects cells through influence on specific ions if parameters of exposure (frequency, alternating and static magnetic fields) are tuned to these ions [2, 3]. About 50% of all cancers have mutations in p53. Recent data have indicated that small molecules such as PRIMA-1 restored the tumor suppression function of mutant p53 presumably by restoring its conformation [4]. Since the presence of Zn ion in the DNA binding domain of p53 is important for its conformation and functional activity [5], we investigated whether modulation of Zn by ELF can reactivate the growth suppression function of mutant p53.

OBJECTIVE: Here, the effects of ELF tuned to Zn were investigated on growth of cancer cells with different status of p53.

MATERIALS AND METHODS: Cancer cells HeLa (cervix cancer, p53+/+), Saos-2 and Saos-2-His-273 (osteosarcoma, p53-/- and p53 His-273 mutant, respectively), H1299tTA and H1299tTA-His175 (lung carcinoma, p53-/- and p53 His-175 mutant) and normal human fibroblasts VH-10 were used. Cells were seeded at appropriate concentrations in the 96-well plates and cell growth was assessed with the DRAG test [6]. Conditions of exposure were calculated for the first harmonic of Zn as based either on the magnetic parametric resonance (MPR) model by Lednev [3] or the ion parametric resonance (IPR) model by Blanchard and Blackman [2]. Exposure was 48-96 h. Vertical static magnetic field was 43 μ T, collinear alternating field was 20 Hz at the amplitudes of 38.7 μ T or 77.4 μ T (IPR or MPR, respectively), and horizontal static magnetic field was zeroed. Treatment of cells with PRIMA-1 and γ -rays was used as a control. Most data did not fulfill the normal distribution as analyzed using Kolmogorov-Smirnov test. Therefore, the data were compared by Mann-Whitney U-test or Kruskal-Wallis test.

RESULTS: Growth inhibition was observed in cells after exposure to ELF according to the IPR model. Inhibition of HeLa, VH-10, and Saos-2-His-273 cells was statistically significant, $p=0.0003$, 0.02 , and 0.006 , respectively. No ELF effects under conditions according to the MPR model were seen. PRIMA-1, 20 or 50 μ M, inhibited growth of all cell lines with stronger effect in mutant p53-carrying cell lines. The effects of γ -rays, 1-10 Gy, were relatively weak as compared to PRIMA-1.

CONCLUSIONS: ELF under conditions of exposure tuned to Zn according to the IPR model inhibited the growth of normal and cancer cells. No clear relationship of the observed growth inhibition to p53 status has been found. Further experiments using complementary techniques are required in order to test whether mutant p53 reactivation by ELF is feasible.

The Swedish Council for Working Life and Social Research and the Swedish Radiation Protection Authority supported these studies.

References

- [1] G. Olsson, I. Y. Belyaev, T. Helleday, and M. Harms-Ringdahl, "ELF magnetic field affects proliferation of SPD8/V79 Chinese hamster cells but does not interact with intrachromosomal recombination," *Mutat Res*, vol. 493, pp. 55-66, 2001.

- [2] J. P. Blanchard and C. F. Blackman, "Clarification and application of an ion parametric resonance model for magnetic field interactions with biological systems," *Bioelectromagnetics*, vol. 15, pp. 217-38, 1994.
- [3] V. V. Lednev, "Bioeffects of weak static and alternating magnetic fields," *Biofizika*, vol. 41, pp. 224-32, 1996 (in Russian).
- [4] V. J. Bykov, N. Issaeva, A. Shilov, M. Hultcrantz, E. Pugacheva, P. Chumakov, J. Bergman, K. G. Wiman, and G. Selivanova, "Restoration of the tumor suppressor function to mutant p53 by a low-molecular-weight compound," *Nat Med*, vol. 8, pp. 282-8, 2002.
- [5] C. Meplan, M. J. Richard, and P. Hainaut, "Metalloregulation of the tumor suppressor protein p53: zinc mediates the renaturation of p53 after exposure to metal chelators in vitro and in intact cells," *Oncogene*, vol. 19, pp. 5227-36, 2000.
- [6] T. Helleday, F. Johansson, and D. Jenssen, "The DRAG test: an assay for detection of genotoxic damage," *Altern Lab Anim*, vol. 29, pp. 233-41, 2001.

P-A-67

RADIOFREQUENCY ELECTROMAGNETIC FIELDS (1800 MHZ) INDUCE ELEVATED PRODUCTION OF REACTIVE OXYGEN SPECIES IN HUMAN PROMYELOCYTIC HL-60 CELLS. R. Fitzner¹, R. Gminski¹, K. Schlatterer¹, R. Tauber²,¹Dept. Clinical Chemistry and Pathobiochemistry, ²Charité - University Medicine Berlin, Campus Benjamin Franklin, Hindenburgdamm 30, D - 12200 Berlin, Germany.

OBJECTIVES: We observed that radiofrequency electromagnetic fields (RF-EMF, 1800 MHz, continuous wave, SAR 1.3 W/kg, 24 h exposure) caused DNA damage in human promyelocytic HL-60 cells with single-cell gel electrophoresis (SCGE) assay and induced micronuclei with cytokinesis-block micronucleus (MN) assay. Aim of this study is to explore whether these genotoxic effects are associated with elevated production of reactive oxygen species (ROS).

METHODS: Human HL-60 cells (ATCC, Rockville, MD, USA) were cultured in RPMI 1640 medium supplemented with 10% fetal bovine serum, penicillin G (50 IU/ml) and streptomycin (50 µg/ml). The cell line was maintained in logarithmic growth phase at 37°C in a 5% CO₂ atmosphere. Cells were exposed or were sham-exposed in waveguides connected with a highly standardized RF generator system provided by Prof. Kuster (ITIS, ETH Zurich, Switzerland).

For monitoring oxidative DNA damage, with 8-oxoguanine as the major oxidative DNA product, the fluorometric OxyDNA Assay Kit from Calbiochem (Calbiochem-Novabiochem GmbH, Bad Soden, Germany) was used. The assay utilizes oxyDNA-FITC conjugate to stain 8-oxoguanine residues on oxidative damaged DNA. Finally, cells were resuspended in FACS buffer and were analyzed by flow cytometry (FACSCalibur, Becton Dickinson). For measuring intracellular ROS levels, the cells were incubated in growth medium containing 5 µmol/L dihydrorhodamine 123 (DHR123). The fluorescence intensity of rhodamine123, which was the product of cellular oxidation of DHR123, was detected by flow cytometry with a Becton Dickinson FACSCalibur.

RESULTS: The presence of oxidized DNA was indicated for the RF-exposed cells by a significant augmentation of the FL-1 fluorescence intensity in comparison to sham-exposed cells. RF-field exposure of HL-60 cells induced an increase of oxidative DNA damage of $21.65 \pm 2.0\%$ (N=4) compared to sham-exposed cells.

Cellular production of ROS was determined by measuring the rhodamine fluorescence of HL-60 cells. In RF-field exposed cells the fluorescence intensity showed a significant increase of $17.8 \pm 9.7\%$ (N=3) in comparison to sham-exposed cells. The treatment of cells in an incubator with 100 µmol/L H₂O₂, as a positive control, resulted in an increase of fluorescence intensity of $31.9 \pm 12.4\%$ (N=3) in comparison to sham-exposed cells. These enhanced fluorescence intensities reflect an elevated production of intracellular ROS as an effect of RF-field exposure and H₂O₂ treatment of HL-60 cells, respectively.

CONCLUSIONS: The genotoxic effects of RF-field exposure (1800 MHz, continuous wave, SAR 1.3 W/kg, 24 h) in HL-60 cells seems to be at least partly associated with an elevated intracellular generation of reactive oxygen species and the presence of oxidized DNA.

P-B-68

STUDENT

EFFECTS OF LOW AND HIGH STATIC MAGNETIC FIELD ON MAMMALIAN CELLS. H. Yuan, G.S. Schneiderman, Y. Haik, C.J. Chen. Center for Nanomagnetism and Biotechnology, Florida State University, Tallahassee, Florida, USA 32310.

INTRODUCTION: There are several reports investigating the effects of high static magnetic field on mammalian cells in vitro. Some results indicate that there is no effect after exposure. Some reports suggest that magnetic field could slow down cell growth. In this study, we exposed animal and human cell lines to static magnetic field from 0.2 T to 12 T and studied the effects at cellular and sub-cellular levels. Iodine-125-IudR Labeling technique allows us to investigate the kinetics of cell death by continuous monitoring the release of ¹²⁵IudR from cell, rather than simply counting dead cells periodically.

OBJECTIVE: The objective of this study was to investigate the low (up to 0.5 T) and high (up to 12 T) static magnetic field effects on mammalian cells. Under different magnetic flux density and exposure pattern, comparisons were made between treated cells and control cells about kinetics of cell death, cell survival rate, cell growth at cellular level and DNA synthesis at sub-cellular level.

METHODS: A human hepatocellular carcinoma cell line HepG2 and Chinese hamster ovary (CHO-K1) were purchased from ATCC (Manassas, VA). HepG2 was grown in Minimum essential medium (Eagle) supplemented with 2 mM L-glutamine, 10% FBS, 0.01 mg/ml Gentamicin. CHO was grown in McCoy's 5A medium modified to contain 1.5 mM L-glutamine, 10% FBS, 0.01 mg/ml Penicillin. All cells were grown at 37 °C in a humidified 5% CO₂/95% air atmosphere, tissue culture incubator. Cells were re-cultured from the frozen vials in the cell bank after two months' culture. Low and high static magnetic field were applied in the experiments. Neodymium Iron Boron magnets provide up to 0.5 T magnetic field. High resolution NMR magnet system provides homogeneous 12 T magnetic field. Temperature, humidity and pH were controlled to keep the same as controlled group during the exposure. Cells were incubated and labeled by the incorporation of Iodine-125-IudR into DNA. ¹²⁵IudR release assay was used to measure the effect of magnetic field on kinetics of cell death. ¹²⁵IudR incorporation assay was used to investigate the effect of magnetic field on DNA synthesis. The colony-forming assay developed by Puck and Marcus (1956) was used to study the magnetic field effect on in vitro survival of cells.

RESULTS: Some preliminary results have been made from effects of low magnetic fields. Effects of high magnetic field need be further confirmed. Statistical significance was calculated with the t test for control and magnetic treated samples. 24 hours' low magnetic field exposure brought a slightly difference on DNA synthesis (p=0.09). While longer exposure reduced the difference (p=0.95). There are no significant effects of low magnetic field on CHO cell survival rate and cell death kinetics. The effects of high magnetic field on cells need to be further confirmed.

This study is supported by Florida State University Research Foundation.

Effect of 0.5 T magnetic field on IUdR incorporation after 24 hour and 64 hour

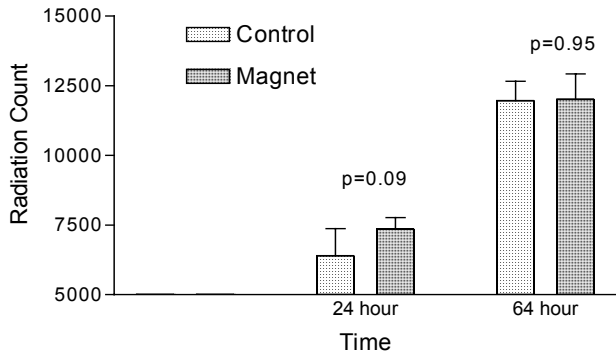


Fig. 1 Effect of 0.5 T magnetic field on DNA synthesis of HepG2 cell.

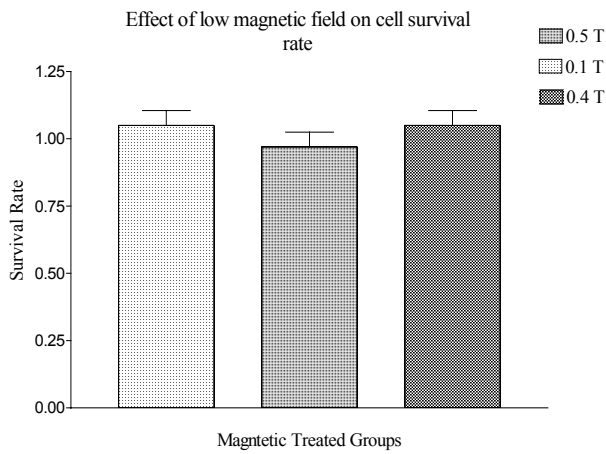


Fig. 2 Effect of low magnetic fields on CHO cell survival rate.

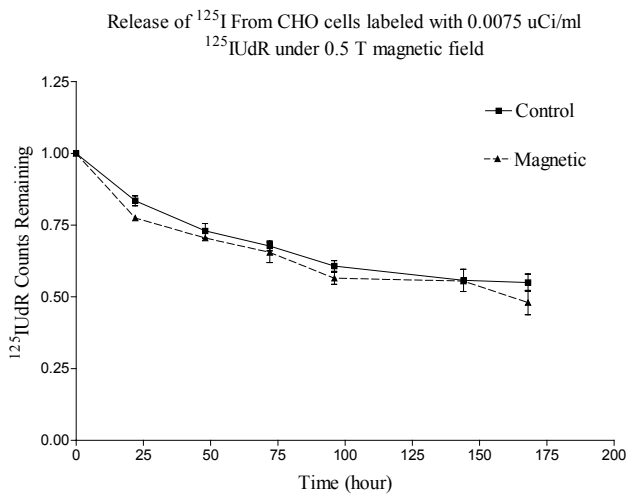


Fig. 3 Release of ^{125}I from CHO cells labeled with $0.0075 \text{ uCi/ml } ^{125}\text{IUdR}$ under 0.5 T magnetic field.

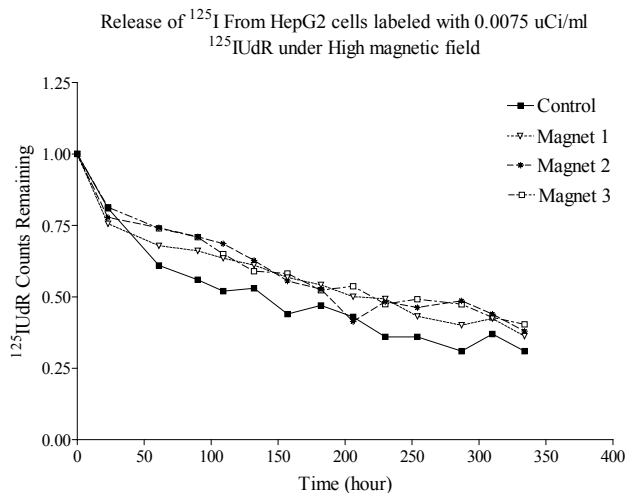


Fig. 4 Release of ^{125}I from HepG2 cells labeled with 0.0075uCi/ml $^{125}\text{IUdR}$ under High magnetic Field. Magnet 1: Homogenous 12 T; Magnet 2: Gradient 11.5 T; Magnet 3: Gradient 8 T

P-C-69

STATIC MAGNETIC FIELD WITH A STRONG MAGNETIC FIELD GRADIENT INDUCES C-JUN EXPRESSION IN HL-60 CELLS. H. Hirose^{1,2}, T. Nakahara³, Q.-M. Zhang¹, S. Yonei¹, J. Miyakoshi³. ¹Lab of Radiation Biology, Graduate School of Science, Kyoto Univ, Sakyo, Kyoto 606-8502, Japan. ²Applied Biology Div, Kashima Lab, Mitsubishi Chemical Safety Institute Ltd., Kashima, Ibaraki 314-0255, Japan. ³Dept of Radiological Tech, School of Health Sciences, Faculty of Medicine, Hirosaki Univ, Hirosaki, 036-8564, Japan.

INTRODUCTION: It has been reported that electromagnetic fields (EMFs) can affect gene expression [1]. However, no clear positive results on the induction of gene expression have been presented to date [2]. On the other hand, meanwhile, some studies have reported the biological effects of following exposure to the strong static magnetic fields (SMFs) of the order of one Tesla (T) [3]. Therefore, it is supposed believed that the clear biological changes of gene expression may be detected on the gene expression by the following exposure to the strong SMFs.

OBJECTIVE: In this study, we investigated the effects of 6 and 10 tesla (T) SMFs on the expression of proto-oncogenes using western blot methods. We used a SMF exposure system, which can expose cells to 10 T is the 6 T with is a strong magnetic field gradient (41.7 T/m) and 10 T of the highest magnetic flux density with little or no magnetic field gradient.

METHODS: The exposure system for a strong SMF has previously been described elsewhere previously [4]. We used the human promyelocytic HL-60 cells [5] in the experiment, because we could detect these basal levels of gene expressions in these cells, without additional induction stimuli. HL-60 cells were exposed to the 6 T or 10 T SMF for 1, 2, 4, 8, 24, 36, 48 and 72 hours. For western blot analysis, total cell lysates containing 20µg protein were separated by 10% SDS-PAGE and transferred onto nitrocellulose membrane. Immunoblots were developed with the using ECL enhanced chemiluminescence reagents. The amount levels of immunoreactive proteins was were quantified using ATTO Image Analysis Software after scanning with ATTO CoolSaver.

RESULTS AND DISCUSSION: The amount of c-Jun expression in HL-60 cells increased following 24 - 72 hours exposure to 6 T SMF with 41.7 T/m. However, no remarkable differences were detected in the levels of c-Jun expression ratio at any of the periods of exposure to 10 T with little or no magnetic field gradient for c-Myc and c-Fos and . And then, c-Jun expression did not change in HL-60 cells following exposure to 6 T SMF without a magnetic field gradient. These results suggest that the increase in c-Jun

expression depends on the presence of a strong magnetic field gradient but not necessarily the magnitude of magnetic flux density. On the contrary on non-treated increased twice for a The increase in phosphorylation of c-Jun was detected at 24 to 72 hours following exposure to 6 T SMF with 41.7 T/m. The phosphorylation and transcriptional activation of c-jun oncogene are stimulated by c-Jun amino terminal kinase (JNK), a distant member of the mitogen-activated protein kinase (MAPK) superfamily [6]. We attempted to detect changes in the levels of JNK and JNK phosphorylation between the 6 T SMF-exposed HL-60 cells and sham-exposed cells. However, no changes in JNK and JNK phosphorylation were demonstrable. because HL-60 cells exposed to either 6 or 10 T SMF for periods of 1 - 48 hours did not exhibit remarkable differences in levels of c-Fos and c-Myc expression, as compared to sham-exposed cells. These results suggest that 10 T SMF does not alter the expression of c-jun, c-fos, and c-myc proto-oncogenes, while a strong magnetic force may induce c-Jun expression in HL-60 cells. This work was supported in part by a Grant-in-Aid from the Research for the Future Program, Japanese Society for the Promotion Science.

References.

- [1] Goodman R., Blank M. *Cell Stress & Chaperones* 3, 79-88, 1998
- [2] Owen RD. *Radiat. Res.* 150, 23-30, 1998
- [3] Hirose H., Nakahara T., Miyakoshi J. *J. Neurosci. Lett.* 338, 88-90, 2003
- [4] Nakahara T., Yaguchi H., Yoshida M., Miyakoshi J., *Radiology* 224, 817-822, 2002
- [5] Collins SJ., Gallo RC., Gallagher RE. *Nature* 270, 347-349, 1977
- [6] Pulverer BJ., Kyriakis JM., Avruch J., Nikolakaki E., et al. *Nature* 353, 670-674, 1991

P-A-70**EFFECTS OF ELF MAGNETIC FIELDS ON SIGNALS FOR DIFFERENTIATION OF CULTURED OSTEOBLASTIC CELLS BY MULTISPECTRAL IMAGING SYSTEM.**

H. Yamaguchi¹, K. Hosokawa², H. Shichijo³, M. Kitamura², A. Soda², T. Ikehara², Y. Kinouchi³, K. Yoshizaki², H. Miyamoto², K. Aizawa⁴. ¹Dept of Environmental Physiology, Faculty of Human Life Sciences, Tokushima Bunri Univ, Tokushima 770-8514, Japan, ²Dept of Molecular and Cellular Physiology, School of Medicine, ³Dept of Electrical & Electronic Engineering, Faculty of Engineering, The Univ of Tokushima 770-8503, Japan, ⁴Dept of Physiology, Tokyo Medical College, Tokyo 160-8402, Japan.

OBJECTIVE: The objective of this study is to examine the physiological effects of exposure to ELF magnetic fields on regulation of differentiation in cultured osteoblast-like cells(MC3T3-E1). We have obtained a few preliminary results that a treatment with some regulators of differentiation and a exposure to ELF magnetic fields for these cells resulted in same effects on the acceleration of differentiation. In this study, we tried a variety of approaches to reveal more about the effects of exposure to the ELF magnetic fields.

MATERIALS and METHODS: Osteoblast-like cells(MC3T3-E1) were cultured with alpha-modified minimum essential medium (H. Miyamoto et al., 1976) supplemented by 10% fetal bovine serum in plastic culture dish of 35 mm in diameter. The culture dishes were placed in two special incubators to keep the temperature of the cultures constant (37.0C). Sinusoidal(60Hz) magnetic fields were produced by two coils and their rms values were about 3.0 mT. Induced current density in the medium about 10 mA/m² in average. Duration of exposing to magnetic fields was 72 hours for 3 days cultures, respectively. Cultures were maintained to grow with or without 10 mM beta-glycerophosphate and Vitamin C of 50 ug/ml as inducer of differentiation. And then, IGF(20 ng/ml) and NGF(2 ng/ml) were add to fairly differentiated cells. Intracellular alkaline phosphatase(ALP) activities as the indicator of the differentiation of these osteoblasts in vitro were measured by calorimetric assay kit(WAKO Ltd, Japan). Collagen and non-collagen protein contents in the cultures were measured microscopically by multispectral imaging method.

RESULTS and DISCUSSION: In exposure to ELF magnetic fields for 3 days, both collagen and non-collagen protein contents increased with exposure time in the cells at peripheral regions of culture dish than that at central regions of same dish. The treatment of IGF increased in collagen contents at the peripheral cells for 17 days culture. But the additive effects of the exposure and IGF treatment were not observed. ALP activity was increase significantly by the exposure alone or by combined with NGF treatment. These results indicate that the mechanisms of differentiation related to IGF and NGF in the osteoblasts were altered by the magnetic fields of extremely low frequency.

ON SPECIFIC EFFECT OF EXTREMELY HIGH POWER PULSES ON PHYSICAL PROPERTIES OF WATER. H.V. Hayrapetyan¹, R.H. Simonyan¹, A.S. Avanesyan², S.N. Ayrapetyan¹.¹UNESCO Chair-Life Sciences International Center, 31 Acharyan St., Yerevan, 375040 Armenia,²Biophysical Department of Artsakh State University, Nagorni Karabagh Republic.

INTRODUCTION: At present the existence of specific (non-thermal) biological effects of RF EMF still remains discussable. As water is the main medium, where the measure part of biochemical reactions of different metabolic cascades of cell and organism take place, it is obvious that even non-significant alterations of physico-chemical properties of water can dramatically change the cell metabolic activity. Previously it was shown that ELF EMF-induced water structure changes actively modulated metabolic activity of cell [1,2,3,4]. On the basis of these data it was suggested that EMF-induced water structure changes could play important role in realisation of biological effect of ELF EMF [1,2,3,4,5]. However, the effect of RF EMF on water structure remains unclear, although it is well known that because water molecules are polar, i.e. they have positively and negatively charged ends; they vibrate when subjected to microwave energy, causing considerable friction between molecules.

Therefore, it is suggested that extra high power pulses (EHPP) causes water structure changes, which could have adequate biological effect on cells.

OBJECTIVES: The purpose of the present work is to check the above-mentioned hypothesis, for which the effect of EHPP on Specific Electrical Conductivity (SEC), thermal capacity and thermal anomaly of water and water solution were studied.

METHODS: Fresh distilled water (DW) was frozen at -1°C during 1 hour after which was defrost at room temperature ($20-21^{\circ}\text{C}$). After temperature stabilization (after 1 hour) it was divided into two samples (Vol: 10ml): control and experiment. Experimental sample was preliminary exposed to EHPP source (MIG 9.3 generator Russian production, Peak SAR = 220 kW/g., 1 μsec = 9.3 GHz). In all experiments the equivalent heating of control sample was performed in water bath. EHPP exposure leads to temperature increase to $50,5^{\circ}\text{C}$. The continuous temperature measurements of both samples were performed by extra sensitive thermometer (correctness of $+0,2^{\circ}\text{C}$ at $0,01^{\circ}\text{C}$ sensitivity). (Production of Institute of Radiophysics and Electronics of Armenian NAS.). Water SEC was measured by special conductometer (Production of Institute of Radiophysics and Electronics of Armenian NAS). The data on simultaneous measurements of temperature and conductivity were transferred through Digidata acquisition system (Axon Instruments) to personal computer.

RESULTS: As it can be seen on Fig. 1 (A,B) the time-dependant decrease of temperature of EHPP-treated DW was significantly faster than in control one, heated in water bath and SEC of DW exposed to EHPP was higher comparing to the control.

DISCUSSION: Presented date clearly demonstrate that heat-treated and EHPP-treated DW at the same temperature has different physical parameters. It is obvious that this EHPP-induced tracing effect on water structure could underlay in the ground of specific (non-thermal) biological effect of EHPP.

References.

[1] Klasen V.I. (1982) Magnetizing of water systems. M. Chemistry. 296 p.

[2] Lednev W. (1991) Possible mechanisms for the influence of weak magnetic fields on biological systems. Bioelectromagnetics 12:71-76.

[3] Ayrapetyan S.N, Avanesian A.S, Avetisian T, Majinian S. (1994a) Physiological effects of magnetic fields may be mediated through actions on the state of calcium ions in solution. In Carpenter D, Ayrapetyan SN (eds): Biological Effects of Electrical and Magnetic Fields, Vol. 1 Academic Press, pp 181-192.

[4] Ayrapetyan S.N, Grigorian CV, Avanesian AS. (1994b). On mechanism of action of magnetic field on the electrical conductivity of water solutions and some properties of Helix neurons. Bioelectromagnetics 15:133-142.

[5] Ayrapetyan S.N (2003) The metabolic nature of biological effect of Low Frequency Electromagnetic Fields on Membrane Excitability. Abstract book of BEMS 25th Annual Meeting, Maui, Hawaii, (P-120-C) p. 300.

This study was founded by European Office of Aerospace Research and Development (EOARD) through ISTC A-803 Partner project.

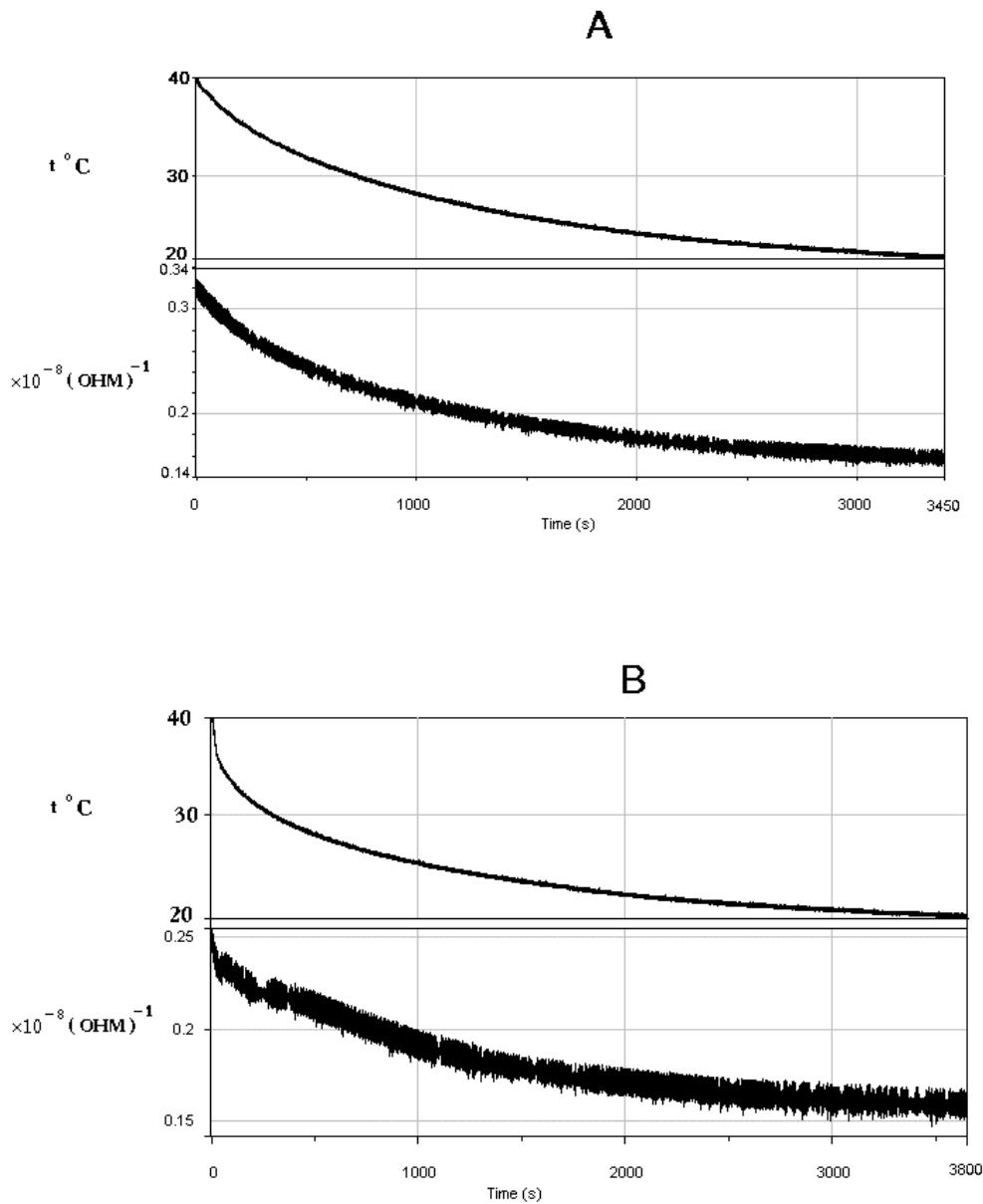


Figure 1. The time-dependant decrease of temperature and Specific Electrical Conductivity changes of non-treated (A) and EHPP-treated (B) DW.

MICROWAVES OF MOBILE PHONES AFFECT HUMAN LYMPHOCYTES FROM NORMAL AND HYPERSENSITIVE SUBJECTS DEPENDENT ON FREQUENCY. I. Belyaev^{1,2}, L. Hillert^{3,4}, E. Markova^{1,5}, R. Sarimov^{1,2}, L. Malmgren⁶, B. Persson⁶, M. Harms-Ringdahl¹. ¹Dept of Genetics, Microbiology and Toxicology, Stockholm Univ, Stockholm, Sweden; ²Dept of Biophysics, Radiation Physics and Ecology, Moscow Engineering Physics Inst, Russia; ³Occupational and Env Hlth, Stockholm County Council, Stockholm, Sweden; ⁴Dept of Pub Health Sci, Div of Occupational Med, Karolinska Institutet, Stockholm, Sweden; ⁵Dept of Molecular Genetics, Cancer Res Inst, Bratislava, Slovak Republic; ⁶Dept of Radiation Physics, Lund Univ Hospital, Lund, Sweden.

INTRODUCTION: It was shown that biological effects of non-thermal microwaves (MWs) occur dependent on biological variables and physical parameters including frequency [1-6]. Stress response and induction of DNA double-strand breaks (DSBs) was observed under specific conditions of exposure to MWs [7, 8]. The effects of non-thermal MWs that are used in wireless communication are in the focus of public concern. However, dependence of such effects on frequency has not been studied.

OBJECTIVE: Here, we investigated whether MWs of Global System for Mobile Communication (GSM) at various frequencies induce stress response or DSBs in human lymphocytes. Heat shock and treatment with camptothecin (CPT) and γ -rays were used as positive controls.

MATERIALS AND METHODS: Effects of MWs were studied at different frequencies in the range of 895-915 MHz in experiments with lymphocytes from 19 healthy persons and 12 persons who reported hypersensitivity to electromagnetic fields. Exposure, 0.5-2 h, was performed in a transverse electromagnetic transmission line cell using a GSM test-mobile phone, all standard modulations included, output power level, 2 W. Changes in chromatin conformation, which are indicative of stress response and DNA damage, were measured by the method of anomalous viscosity time dependencies [2]. 53BP1 and γ -H2AX foci that colocalize with DSBs were analyzed by immunofluorescence confocal laser microscopy *in situ*. Most data did not fulfill the normal distribution and were compared by non-parametric tests.

RESULTS: 0.5-h exposure to MWs resulted in statistically significant condensation of chromatin. Stronger effects of MWs were found following 1- and 2-h exposure to MWs. Dependent on donor, condensation or decondensation of chromatin was found in response to GSM exposure. While condensation of chromatin was observed under conditions of mild heat shock, chromatin decondensation was induced both by severe heat shock and DNA damage induced by CPT or γ -rays. 1- and 2-h exposure at 915 MHz induced statistically significant decrease in 53BP1 and γ -H2AX foci. In contrast, exposure to 905 MHz induced either decrease or increase in 53BP1 and γ -H2AX foci suggesting induction of either mild stress response or DSBs, respectively, dependent on donor. Based on pooled data, the effects of MWs at 905 and 915 MHz on foci were statistically significantly different. No significant differences in effects between groups of healthy and hypersensitive subjects were observed.

CONCLUSIONS: GSM microwaves from a mobile phone affect DSB-co-localizing 53BP1 and γ -H2AX foci and chromatin conformation in human lymphocytes. These effects suggest induction of stress response and/or DNA damage. Effects of MWs differ at various GSM frequencies and vary between donors.

The Swedish Council for Working Life and Social Research, the Swedish Authority for Radiation Protection supported these studies.

References

[1] W. R. Adey, "Cell and molecular biology associated with radiation fields of mobile telephones," in *Review of Radio Science, 1996-1999*, W.R. Stone and S. Ueno, eds. Oxford University Press, 1999, pp. 845-872.

[2] I. Y. Belyaev, V. S. Shcheglov, E. D. Alipov, and V. D. Ushakov, "Non-thermal effects of extremely high frequency microwaves on chromatin conformation in cells in vitro: dependence on physical, physiological and genetic factors," *IEEE Transactions on Microwave Theory and Techniques*, vol. 48, pp.

2172-2179, 2000.

[3] V. N. Binhi, *Magnetobiology: Underlying Physical Problems*. San Diego: Academic Press, 2002.

[4] G. d'Ambrosio, R. Massa, M. R. Scarfi, and O. Zeni, "Cytogenetic damage in human lymphocytes following GMSK phase modulated microwave exposure," *Bioelectromagnetics*, vol. 23, pp. 7-13, 2002.

[5] C. F. Blackman, L. S. Kinney, D. E. House, and W. T. Joines, "Multiple power-density windows and their possible origin," *Bioelectromagnetics*, vol. 10, pp. 115-28, 1989.

[6] B. R. R. Persson, L. G. Salford, and A. Brun, "Blood-Brain Barrier permeability in rats exposed to electromagnetic fields used in wireless communication," *Wireless Networks*, vol. 3, pp. 455-461, 1997.

[7] H. Lai and N. P. Singh, "Melatonin and a spin-trap compound block radiofrequency electromagnetic radiation-induced DNA strand breaks in rat brain cells," *Bioelectromagnetics*, vol. 18, pp. 446-454, 1997.

[8] D. de Pomerai, C. Daniells, H. David, J. Allan, I. Duce, M. Mutwakil, D. Thomas, P. Sewell, J. Tattersall, D. Jones, and P. Candido, "Non-thermal heat-shock response to microwaves," *Nature*, vol. 405, pp. 417-418, 2000.

P-A-73

EFFECTS OF EXPOSURE TO 1950 MHz RADIO-FREQUENCY FIELD ON EXPRESSION OF HSP 27 AND HSP 70 IN HUMAN GLIOMA MO54 CELLS. J. Miyakoshi¹, Y. Takashima¹, G-R. Ding¹, H. Hirose², S. Koyama³.¹Department of Radiological Technology, School of Health Sciences, Faculty of Medicine, Hirosaki University, 66-1 Hon-cho, Hirosaki, 036-8564, Japan, ²Graduate School of Science and ³Graduate School of Human and Environmental Studies, Kyoto University, Yoshida-Konoe-cho, Sakyo-Ku, Kyoto 606-8501, Japan.

INTRODUCTION: In recent years, with the rapid introduction of mobile telecommunication devices, the possible health effects, in particular brain tumor, due to exposure to radio-frequency (RF) field from mobile phones have become a public concern. Since heat shock response is a universal fundamental mechanism necessary for cell survival under a variety of unfavorable conditions, we examined the expression level of heat shock proteins (Hsp27 and Hsp70) as well as cell proliferation in Human glioma MO54 cells after RF fields exposure.

METHODOLOGY: MO54 cells were cultured in Dulbecco's modified Eagle's medium supplemented with 10 % fetal bovine serum. RF fields were generated by REFLEX 1950 (Switzerland). The setup consists of two single-mode resonator cavities for 1.8 GHz, which are based on the R18 waveguide placed in an ordinary incubator. Exponentially growing cells were cultured in 35 mm dishes (3×10^5 cells/dish) and were moved to dish holders in two waveguides (one for sham, the other for exposure). Cells were sham-exposed or exposed to 1950 MHz continuous-wave for 1 or 2h. Specific absorption rates (SARs) were 1, 2 and 10 W/kg. None of the exposures produced a rise in temperature more than 0.1°C. For the experiment of cell growth, cell number was counted at 0, 1, 2, 3, and 4 days after exposure. Expression of Hsp27 and Hsp70 was determined by western blotting. The cellLytic™ mammalian cell lysis/Extraction reagent (Sigma) was used for protein extraction. The antibodies used in this experiment were as follows: anti-Hsp27 goat polyclonal antibody (Santa Cruz Biotechnology), anti-Hsp70 mouse monoclonal antibody (StressGen Biotechnologies Corp), anti-β-actin mouse monoclonal antibody (Sigma), anti-goat IgG horseradish peroxidase (Santa Cruz Biotechnology), and anti-mouse IgG horseradish peroxidase (Amersham-Pharmacia Biotech). The blot was visualized with an ECL kit (Amersham-Pharmacia Biotech). Densitometric analysis was performed using ATTO Image Analysis Software. The experiment was repeated three times. Data were normalized as Hsp/β-actin. Statistical analyses were performed by Student *t* test. $p \leq 0.05$ was considered to be statistically significant.

RESULTS AND CONCLUSION: Sham-exposed and RF-exposed cells demonstrated a same growth pattern up to 4 days after RF exposure. RF exposure at both 2 and 10 W/kg could not affect the cell growth. Cell number increased exponentially up to 4 days after RF exposure. In addition, there were no significant

difference in protein expression of Hsp27 and Hsp70 between sham-exposed and RF-exposed cells at 1W/kg, 2W/kg or 10 W/kg for 1 and 2 h. However, exposure to RF at 10W/kg for 1 and 2h decreased the phosphorylated Hsp27 protein significantly. In mammalian cells, Hsp synthesis is induced not only by hyperthermia, but can be triggered by a wide variety of toxic conditions. Induction of Hsp synthesis can result in stress tolerance and cytoprotection against stress-induced molecular damage. In the present study, we examined that whether 1950 MHz RF exposure could activate stress response, especially expression of Hsp27 and Hsp70, in MO54 cells. Our results suggest that 1950 MHz RF field has no effect on Hsp27 and Hsp70 expression as well as cell proliferation, while it may inhibit the phosphorylation of Hsp27 in MO54 cells.

This study is supported, in part, by the Grant from NTT DoCoMo, Inc. and by the Grant-in-Aid from the Research for the Future Program, Japan Society for the Promotion of Science.

P-B-74

STUDENT

LOW FREQUENCY AC AND DC ELECTRIC FIELD EFFECTS ON WHITE BLOOD CELL MOBILITY. K.N. Rathnabharathi, A. Aly, R. Zhou, F.S. Barnes. Department of Electrical and Computer Engineering, University of Colorado, Boulder, CO 80302, USA.

INTRODUCTION: This research project is an experimental study on the effects of external electric field exposure on the mobility of human white blood cells, (mainly polymorph nuclear leucocytes). The basis for this project came from the results of several research studies done in the 80's, which showed that children living in close proximity to power lines were at a higher risk of developing childhood cancer and other immune related problems. With this research we expect to determine to what extent exposure to such fields could affect white blood cells and thus overall immune responses.

OBJECTIVE: The primary objective of this research is to determine the effects of DC and 60Hz AC electric fields on the mobility of white blood cells and also on their ability to track a chemotactic gradient. Observations were made based on the polarity, intensity, and distribution of the applied electric fields at temperatures ranging from 36°C to 40°C

METHOD: Using the "Stripe Source Diffusion Technique" and Cyclic-AMP (Adenosine3', 5'-monophosphate) as the chemoattractant, well-defined chemotactic fields are created on microscope slides. To create such a chemotactic (concentration) gradient, a stripe of the chemo-attractant is drawn on one side of a microscope slide, and then the cover slip containing the blood sample is slowly slid over it, the C-AMP in the stripe re-dissolves in the sample creating the gradient. Initially experiments were performed without any exposure at a set temperature (usually 38°C), and then again with exposure to either AC or DC electric fields (with field strengths ranging from 6 to 20V/mm) at the same temperature, the results of the two cases were compared to find the electric field effects. With the experiments performed so far, the electric fields (both AC and DC) were applied parallel to the concentration gradient. In the case of the DC field, it was applied so that its direction is opposite to the direction of the gradient.

RESULTS: So far we've observed that the white blood cell mobility degrades with exposure to electric fields compared to the mobility without any exposure. This phenomenon is true for both DC and AC electric fields. It was also observed that the mobility of the cells increase exponentially with the increase of the electric field strength. The main difference between the DC and AC electric field results is that the exponential increase in the speed of the cell exposed to the AC field is much more steeper than the exponential rise in the speed of the cells with the DC field. This result is shown below in figure 1. An interesting observation we made was that in the case of the DC electric field exposure, when the direction of the field was reversed, the direction of the cell movement also reversed. However, this result was not always reproducible.

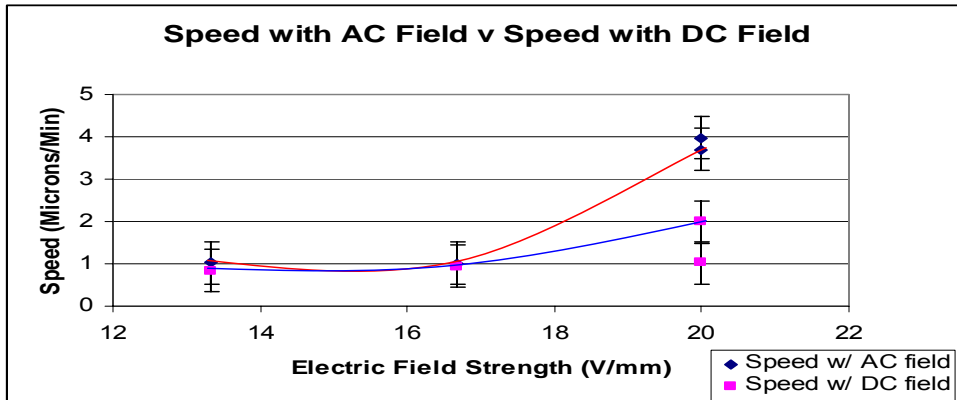


Figure 1: Difference between AC and DC electric Field Effects on WBCs.

CONCLUSION: This research is still in its preliminary stage, there are so many unknown variables that need to be understood and controlled in order to get more accurate results. More experiments are expected to be performed with frequencies other than 60 Hz, different electric field directions, strengths and orientations before definite conclusions can be reached.

P-C-75

NEURONAL OUTGROWTH OF PC-12 CELLS AFTER COMBINED TREATMENT WITH NERVE GROWTH FACTOR AND A MAGNETIC FIELD: INFLUENCE OF THE INDUCED ELECTRIC FIELD STRENGTH. J. Schimmelpfeng, K.-F. Weibezahn and H. Dertinger. Forschungszentrum Karlsruhe, Institute for Medical Engineering and Biophysics, POB 3640, D-76021 Karlsruhe, Germany.

BACKGROUND AND OBJECTIVES: Magnetic field stimulation may offer a non-invasive way to promote and align nerve regeneration. Dorsal root ganglia explant cultures exposed to a pulsed magnetic field grew parallel to the induced electric field (~ 250 $\mu\text{V/m}$) and exhibited enhancement of neurite length (Macias et al., 2000). Feria-Velasco et al. (1998) reported neuronal differentiation of chromaffin cells in vitro induced by extremely low frequency magnetic fields of 700 μT magnetic flux density or by nerve growth factor. Starting point of our experiments were the investigations of Blackman and co-workers (1993) with PC-12 cells treated with NGF and 50 Hz power line frequency fields below 10 μT magnetic flux density, corresponding to 0-50 $\mu\text{V/m}$ induced electric field strength. We were interested in a possible enhancement of neuronal outgrowth at higher figures of flux density and induced field strength.

MATERIALS AND METHODS: PC-12 cells were incubated for 2-6 days under sub-optimal concentration of NGF (5 ng/ml) and treated 8 hours each night with a 50 Hz sinusoidal magnetic field of 100 μT modified according to Aaron et al. (2000). Exposure was carried out in an open Helmholtz configuration with the magnetic field perpendicular to the culture dishes. Organ culture dishes were used, where the strength of the induced electric field ranged from 0-135 and from 251-400 $\mu\text{V/m}$ in the inner and outer compartment, respectively. Neuronal differentiation was quantified by means of the neurite outgrowth assay, with microscopical quantification of the number of cells forming neurites during treatment.

RESULTS AND CONCLUSIONS: On the average, magnetic field treatment at 100 μT did not change NGF-induced neurite outgrowth to a statistically significant extend. However, a slight tendency towards a decreased neuronal outgrowth was noted in the outer compartment of the organ culture dish. This tendency was also found in a preliminary experiment, where, in order to search for a possible induction of differentiation markers, the expression of neurofilament-L and β -actin mRNA was investigated by means of RT-PCR. These results suggest, that further increasing the induced field strength by using either higher flux densities, and/or more sophisticated wave forms, might be necessary to cause the neuronal response of

PC-12 cells, seen in the experiments by Feria-Velasco et al. (1998) or Macias et al. (2000) in other cell systems. In view of possible therapeutic applications of magnetic fields, which are, for example, discussed in the context of psycho-neuronal disorders, further experiments are warranted.

References.

Aaron RK, Ciombor DM, Keeping H, Wang S, Capuano A, Polk C. *Bioelectromagnetics* 1999; 20(7): 453-458. Erratum in *Bioelectromagnetics* 2000; 21(1): 73.

Blackman CF, Benane SG, House DE. *FASEB J.* 1993; 7: 801-806.

Feria-Velasco A, Castillo-Medina S, Verdugo-Diaz L, Castellanos E, Orozco-Suarez S, Sanchez-Gomez C, Drucker-Colin R. *J. Neuroscience Research* 1998; 53: 569-582.

Macias MY, Battocletti JH, Sutton CH, Pintar FA, Maiman DJ. *Bioelectromagnetics* 2000; 21: 272-286.

P-A-76

LOW-FREQUENCY ELECTROMAGNETIC FIELD AS A TOOL TO TRIGGER PLURIPOTENT HUMAN STEM CELLS DIFFERENTIATION. A. Lisi¹, M. Ledda¹, A.M. Patti², A. Vulcano², S. Rieti¹, E. Rosola¹ and S. Grimaldi¹. ¹Istituto di Neurobiologia e Medicina Molecolare C.N.R. Rome Italy. ²Dipartimento di Scienze di Sanità Pubblica G. Sanarelli Università "La Sapienza" Rome, Italy.

OBJECTIVE: In this study we report experiments which evaluate whether applying extremely low frequency electromagnetic field (ELF-MF 50Hz 1mT) may influence proliferation and differentiation on mesenchymal human cells of bone marrow.

In literature is well described that this cells are able to differentiate to osteoblast following treatment with chemical agents such as dexamethasone.

Regulation of osteoblast differentiation its an important phenomena that must occur to mantain the continuous supply of mature osteoblast needed for bone growth, remodelling, and in particular for bone repair.

METHODS: Culture and differentiation of mesenchymal stem cells. Height- ten ml of bone marrow, obtained from iliac crest, was mixed with one volume of phosphate-buffered saline and nucleated cell fraction was enriched for mesenchymal stem cells by density-gradient centrifugation over Lympholyte-H cushion. The cells at the medium- Lympholyte-H interface were collected, washed three times with culture medium and seeded into culture flask. Confluent monolayers of adherent cells were obtained about one week after the start of cell division. Subcultivation was performed by replating at 6×10^3 cells per cm^2 flasks. To promote osteogenic differentiation cells were stimulated during subpassages by cultivation in standard medium supplemented with 100nM dexamethasone or by exposure to extremely low frequency electromagnetic field (50Hz 1mT) under controlled condition. The constant electro-magnetic field of 1mT at 50 Hz was generated in a solenoid.

RESULTS: Exposure to low frequency electromagnetic field for 5 days resulted in a change in plasma membrane morphology and this modification were also accompanied by a rearrangement in actin filaments as showed by confocal microscopy analysis after cells labeling with FITC-phalloidin.

In particular, mesenchymal cells exposed to the field showed the same actin organization found in the same cells after treatment with dexamethasone. The differentiating effect of dexamethasone were potentiate by exposure to the field.

Indirect immunofluorescence assay of osteopontin, a marker of osteoblast differentiation showed an increase in osteopontin positive cells after treatment with electromagnetic field.

In conclusion our finding demonstrated that exposure to ELF can act as a differentiating agent on mesenchymal human cells outline the importance of low frequency electro-magnetic field as a therapeutical agent suggesting a possible use of ELF as support in medicine for different pathologies therapy.

A PROJECT IN THE FRAMEWORK OF THE “CAMPANIA EU-REGION CENTER OF COMPETENCE ON INFORMATION AND COMMUNICATION TECHNOLOGIES” RELATED TO THE EVALUATION OF CANCER RELATED ENDPOINTS IN MAMMALIAN CELLS FOLLOWING *IN VITRO* EXPOSURES TO UMTS RADIOFREQUENCY SIGNAL. M. Calabrese¹, G. Castello⁴, G. d’Ambrosio¹, F. Izzo⁴, G.F.Grossi², R. Massa¹, M. Napolitano⁴, G. Petraglia¹, A. Sannino³, M. Sarti³, P. Scampoli², M.R. Scarfi³, O. Zeni³. ¹Università di Napoli Federico II - DIET - Via Claudio, 80125 Napoli, Italy, ²Università di Napoli Federico II -DSF- Monte S.Angelo, 80126, Napoli, Italy, ³CNR-IREA – Via Diocleziano 328 , 80124, Napoli, Italy, ⁴INSCT-Pascale-Via M.Semmola, 80131, Napoli, Italy.

INTRODUCTION: Very few data are available in the literature, concerning the influence on living material of electromagnetic field exposure related to the 3G mobile communication system (UMTS) and to other new wireless technologies. In the framework of the research programs on Information and Communication Technologies funded by the Campania EU-Region, four different research groups in this region have joined in a three-year project, for evaluating some cancer related biological effects in mammalian cells following in vitro exposure to UMTS signal.

OBJECTIVES: Some selected cellular processes related to genotoxic and non-genotoxic carcinogenesis will be studied on adequately chosen cell models, in order to obtain information on the role of UMTS exposure in such carcinogenesis processes.

METHODS: Genotoxic effects will be evaluated in human peripheral blood lymphocytes, since they are genetically stable and easy to obtain; moreover the experimental procedures are well standardized. In particular, direct DNA damage will be investigated in unstimulated lymphocytes, by applying the alkaline comet assay, and in PHA stimulated lymphocytes, by applying the cytokinesis block micronucleus assay and the chromosomal aberration assay. Moreover, the DNA repair efficiency will be also studied, by treating human lymphocytes with ionizing radiation before radiofrequency (RF) exposure by means of the chromosomal aberrations technique. Non-genotoxic effects related to carcinogenesis will be investigated by evaluating reactive oxygen species formation and induction of apoptosis in two different cell lines: Jurkat (human lymphoblastoid cells) and NIH-3T3 (murine fibroblasts). As long as the field applicator system is concerned, a basic feature of the program is the strict control and unification of the exposure conditions. To this end 3 ml samples in 34 mm diameter Petri dishes were chosen for all the experiments, and careful dosimetric evaluations performed in the past year, will allow the in vitro exposures to be exactly defined in terms of average SAR, SAR relative dispersion (less than 30%), carrier frequency (1.95 GHz) and modulation parameters. Waveguide based exposure (and sham-exposure) chambers will be used, provided with a temperature control system.

RESULTS: The applicator design (of the waveguide type) was performed, and the dosimetric requirements were already met. The major expected result in the next two years is to obtain information on the possible role of UMTS-RF exposure in carcinogenesis processes. It must be stressed that the proposed experimental protocol will allow us crossed comparisons, by applying the same technique on different cell types and different techniques on the same cell type. Of special value, in our opinion, is that three different, independent biological laboratories (DSF of Univ. of Naples, IREA of CNR, and INSCT Pascale) will work on common biological targets, under unified exposure conditions controlled by a microwave laboratory (DIET of Univ. of Naples).

This project is supported by the “Center of Competence on Information and Communication Technologies” of the Regione Campania, Italy.

THE SPECIFIC EFFECT OF EXTREMELY HIGH POWER PULSES (EHPP)- TREATED PHYSIO-LOGICAL SOLUTION ON CELL VOLUME OF SNAIL NEURON. M.G. Khachatryan, S.N. Ayrapetyan. UNESCO Chair-Life Sciences International Center, 31 Acharyan st. Yerevan, 375040 Armenia.

INTRODACTION: The existence of possible non-thermal biological effect of MW still remains discussable. Recent studies at our laboratory were shown that EHPP-induced heat treatment of water and water solution caused specific effect on their physico-chemical properties [1]. Earlier it was shown that neuronal volume is controlled by cell metabolic activity and it is extra sensitive to weak environmental factors having chemical and physical nature. Therefore, it was suggested that cell volume could be convenient experimental model for studying the biological effect of factor-induced changes of physico-chemical properties of cell bathing medium.

OBJECTIVE: The objectives of the present work is the comparative study of EHPP-treated and water bath heat-treated physiological solution (PS) on volume of isolated single neurons.

METHODS: The neurons were isolated from *Helix pomatia* nerve ganglia by special micro-scissors and needles under the binocular microscope. Isolated neurons were incubated in special experimental glass micro-chamber containing PS. This chamber was placed under the microscope (MB-14, Russian production) with digital video camera (Sony). This chamber can be continuously perused by non-treated (control), preliminary heat-treated and EHPP-treated PS. PS was treated by EHPP (MIG 9.3 generator Russian production) during 15 minutes (Peak SAR = 180 kW/g., 1 μ sec = 9.3 GHz) in Petri's dishes (vol.~45-50 ml.). After EHPP exposure PS temperature rose from 18 °C to 26 °C. The equivalent heating of the second sample was performed in water bath. After PS treatment the temperature of both of the samples was returned back to 18 °C and only after it they were used for perfusion of neuronal bath medium.

RESULTS: The effect of heat and EHPP-treated PS on cell volume was studied on 35 neurons. Preliminary heat-treated PS has no significant effect on cell volume, while EHPP-treated PS has the following results: cell volume of 15 neurons was increased, in 6 neurons it was decreased, in 5 neurons it had biphasic (shrinkage-swelling) effect and 9 neurons has no significant volume changes. On figure 1 is presented a picture of the same neuron in normal PS (A), after 2 min. (B) and 5 min. (C) incubation in preliminary EHPP-treated PS. As it can be seen from these data cell volume changes were accompanied by changes of axon diameter in opposite manner, i.e. cell soma increase was accompanied by axon diameter decrease.

DISCUSSION: Preliminary EHPP-treated PS-induced cell volume changes and its insensitivity to adequate heat-treated PS can be considered as evidence on the existence of EHPP specific (non-thermal) effect on cell volume, which is realized through EHPP-induced specific structural changes of perused PS. Non-adequate effect of EHPP effect on cell volume can be explained either by initial functional state of neurons or different sensitivity of metabolic cascade of individual neurons to EHPP-induced PS structural changes. From literature data on electrophysiological experiments it is well known that mollusk neurons have non-adequate (membrane hyper-polarizing and depolarizing) responses to different physical and chemical factors. Therefore, these non-adequate responses of cell volume are not unexpected data. However, for final conclusion on the existence of EHPP specific effect on cell volume it is necessary to carry out more detailed investigation of cell volume in combination with other methods giving information on its metabolic activity.

Reference.

[1] Hayrapetyan H.V., Avanesyan A.S., Ayrapetyan S.N. On specific effect of extremely high power pulses on physical properties of water. Abstract presented to BEMS 26th Annual meeting

This study was founded by European Office of Aerospace Research and Development (EOARD) through ISTC A-803 Partner project.

P-A-79

STUDENT

1800 MHZ RF-EMF DO NOT INDUCE FREE RADICAL PRODUCTION IN DIFFERENT IMMUNE RELEVANT CELLS. M. Lantow and M. Simkó. University of Rostock, Institute of Cell Biology and Biosystems Technology, Division of Environmental Physiology, Albert Einstein Str.3, D-18059 Rostock, Germany.

OBJECTIVES AND INTRODUCTION: The goal of our study was to investigate the cell activating capacity of radiofrequency (RF) radiation (1800 MHz) to produce free radicals using different cell systems, and various exposure, and co-exposure conditions.

METHODS: Human Mono Mac 6 cells, human K562 cells, and primary murine bone marrow-derived macrophages were used to examine the free radical release after exposure to RF-EMF, 1 μ M TPA, 1 μ g/ml LPS or to co-exposure conditions. Cells were exposed to 1800 MHz RF-EMF (IT'IS, Zurich, Switzerland) or to chemicals in parallel to sham and to incubator conditions as controls, as well as to heat (40°C) for 45 min. For RF-EMF exposure different signals (continuous wave, GSM Basic, DTX Only, and GSM Talk) and SAR values (0.5, 1.0, 1.5, 2.0 W/Kg) were applied. Super oxide radicals were determined by colorimetric measurement of the reduction of NBT to formazan at 550 nm optical density. ROS formation was detected by flow cytometric analysis using the DHR assay. Data were compared to sham and/or to control values and the statistical analysis was performed by the student's t-test on the $p < 0.05$ level.

RESULT AND CONCLUSION: Heat (40°C) and TPA treatment induced a significant increase in super oxide and in ROS production in all investigated cells when compared to sham and to incubator conditions. However, there were no significant differences found in free radical production after exposure to any RF EMF condition and no additional effects were detected after co-exposure to RF-EMF+TPA or RF-EMF+LPS as well.

Our results show that none of the used exposure and co-exposure conditions, signals and SAR values of 1800 MHz RF-EMF has any cell activating potential regarding free radical production in the cells investigated.

This work is supported by the Federal Office for Radiation Protection, Salzgitter, Germany.

P-B-80

STUDENT

THE ATOM FORCE MICROSCOPY STUDY ON THE HIPPOCAMPUS NEURON MEMBRANE PERFORATE INDUCED BY EMP. M. Zhao¹, X. Cao², D. Wang³, S. Zhang³, J. Liu³. ¹NIEHS/NIH, BIDG 101, MD F2-04, Res. Triangle Park, NC 27709, ²Department of Pathology, Lanzhou General Hospital, Lanzhou 730050, Gansu province, China; ³Beijing Institute of Radiation Medicine, Beijing 100850, China.

OBJECTIVE: Using the atomic force microscopy (AFM) to observe the membrane surface changes of rat's hippocampus primary culture neurons irradiated by EMP, and to explore possible injured mechanism of EMP to neuron membrane.

METHODS: Hippocampus neurons from postnatal rats(24 hours) were isolated by dissection microscope, the concentration of the dilution neurons was 1 \times 10⁶/ml, then the cells were cultured in 6-well culture plates. About 14 days later, the cells were irradiated by high field strength 5 EMP (electromagnetic pulse simulator which provides 5 pulses/min with a high electric field intensity 60 KV/m, 20-ns rise time and 30 μ s pulse wide) within 2 minutes. The exposed cells were fixed immediately following irradiation and scanned by AFM (SPM-9500J3, SHIMADZU).

RESULTS: The results showed that there is membrane perforate with different size and shape (Fig. 2, 3, 4) (281.56nm \times 89.90nm \times 17.76.57nm).

CONCLUSION: EMP could injury the neurons' membrane of hippocampus, and the membrane may be the target position of EMP.

P-C-81

STUDENT

THE EFFECT OF EXTREMELY HIGH POWER PULSES- TREATED WORT ON GROWTH AND DEVELOPMENT OF YEASTS. N.S. Baghdasaryan, S.N. Ayrapetyan. UNESCO Chair-Life Sciences International Center, 31 Acharyan st.Yerevan, 375040 Armenia.

INTRODACTION: The existence of possible non-thermal biological effect of MW still remains discussable. Recent studies at our laboratory were shown that EHPP-induced heat treatment of water and water solution caused different effect on their physico-chemical properties than similar heat-treatment one [1]. Such differences were demonstrated by studding their biological effect on plant seeds germination potential and neuronal cell volume [2,3]. However, EHPP-induced non-thermal effect on other biological objects could be the subject for future investigations.

OBJECTIVE: The objectives of the present work was to study the effect of adequate heat and EHPP-induced wort treatment on growth and development of yeasts.

METHODS: During the experiments three samples of wort were used: control (non-treated), heat-treated and EHPP-treated. Experimental sample (tube vol: 5ml) was exposed to EHPP (MIG 9.3 generator Russian production), (Peak SAR = 180 kW/g., 1 μ sec = 9.3 GHz) during 10 min in sterile conditions. The equivalent heating of the second sample was performed in water bath. The temperature of the experimental samples was returned back to the initial room temperature (18 $^{\circ}$ C) in water bath during 30min. Than in each samples 300 μ l leaven yeast- containing medium (*Saccharomyces cerevisiae*, strain L-41), grown one day before the experiment, was add. Immediately after sowing to check the equal dilution of yeasts the optical transmission factor (τ) of samples was measured by spectrometer (SF-48 Russian production) $\lambda=540$ nm. All three groups (each contains 10 samples) were incubated in thermostat at 30 $^{\circ}$ C during 24 hours. After which their optical transmission factor was measure again.

RESULTS: Heat and EHPP-treatment of yeast-free nutrient medium did not produce any significant changes of its optical transmission factors. Therefore the differences between optical transmission factors in yeast-containing medium in control and experiments are due to the differences in intensities of yeasts growth. Data presented on Figure 1 clearly show that yeast growth in heat-treated mediums was depressed comparing to the control (non-treated), while there is no differences between EHPP-induced heat-treated and water bath-heat treated mediums.

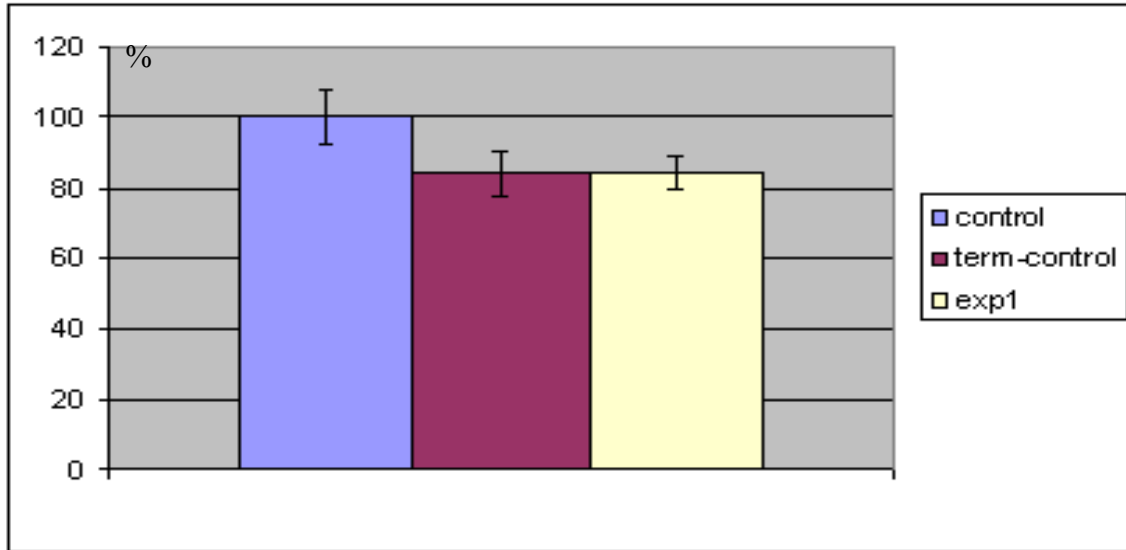
DISCUSSION: The obtained data show the absence of specific (non-thermal) effect of EHPP on yeast growth, while its existence was demonstrated on water and water solutions [1], plant seeds germination [2] and neuronal volumes [3]. The absence of specific effect of EHPP on yeast growth can be explained either by insensitivity of investigated yeasts to specific effect of EHPP, or by absence of this effect on nutrient medium depending on its own physico-chemical properties. The nature of the disagreement of mentioned experimental data will be the subject for future investigations.

References

- [1] Hayrapetyan H.V., Simonyan R.H., Avanesyan A.S., Ayrapetyan S.N. On specific effect of extremely high power pulses on physical properties of water. Abstract presented to BEMS 26th Annual meeting.
- [2] Amyan A.M., Ayrapetyan S.N. The effect of extremely high power pulses-treated water on barley seeds' dry weight kinetics during their awakening. Abstract presented to BEMS 26th Annual meeting.
- [3] Khachatryan M.S. , Ayrapetyan S.N. THE specific effect of extremely high power pulses (EHPP)-treated physiological solution on cell volume of snail neuron. Abstract presented to BEMS 26th Annual meeting.

Figure 1. The effect of heat-treated and EHPP-treated nutrient medium (wort) on yeast growth, comparing

to control (100%).



This study was funded by European Office of Aerospace Research and Development (EOARD) through ISTC A-803 Partner project.

P-A-82

LOW FREQUENCY AC AND DC MAGNETIC FIELD EFFECTS ON WHITE BLOOD CELL MOBILITY. R. Zhou, K. Rathnabharathi, A. Aly, F.S. Barnes. Department of Electrical and Computer Engineering, University of Colorado, Boulder, Colorado, 80309, USA.

BACKGROUND: As we know, electric and magnetic field (EMF) exposures are complex and exist in the home and workplace as a result of all types of electrical equipment and building wiring as well as a result of nearby power lines. Some researches have indicated that exposure to DC and extremely low frequency (ELF) AC magnetic fields (MFs) involves a potential risk to human health, and there exists association with chronic leukemia among electrical power plant workers and between childhood leukemia and MFs emitted by power distribution line. One hypothesis is that these fields affect the immune system and white blood cells (WBCs) play important roles in the body's immune system. All five kinds of them participate in defense of the body against infections and other foreign materials, and it is an easy way to track WBCs' movement along a chemo-attractant gradient on a microscope slide.

OBJECTIVE: Use microscopic techniques to study the effects of low frequency AC and DC magnetic fields on the ability of individual white blood cells (WBCs) from human donors to track concentration gradients of chemo-attractants. Further to determine the effects of changes in frequency and exposure amplitudes on these cells.

METHODOLOGY: Draw about 2ml~4ml blood from different volunteers, centrifuge blood collection tube so as to separate white blood cells from red blood cells. Then use stripe source diffusion technology to make microscopic slide where the concentration and concentration gradient of the chemo-attractant can be calculated. The slide is then placed in a microscope where the temperature is fixed between 37.5°C ~ 39°C. Apply different DC and AC magnetic fields on the slide, and then observe white blood cell's movement.

RESULTS: Our preliminary results indicate low frequency AC magnetic fields with intensities in the range of several tens μT at 60Hz can decrease the average white blood cells velocity. Conversely a DC magnetic fields of several tens μT at 60Hz will increase the average white blood cells velocity. In some cases, both DC and AC magnetic fields have a little influence on white blood cells' moving direction. The activity

level of the donor, infections, other history, and variability from cell to cell and donor to donor can effect the results so that consistent reproduce results are hard to obtain.

P-B-83

STUDENT

EFFECTS OF HIGH FREQUENCY ELECTRO-MAGNETIC FIELDS ON MICRONUCLEUS FORMATION IN CHO-K1 CELLS. S. Koyama^{1,2}, T. Sakurai¹, T. Nakahara¹, K. Wake³, M. Taki⁴, Y. Isozumi² and J. Miyakoshi¹. ¹Dept of Radiological Tech, School of Hlth Sciences, Faculty of Medicine, Hirosaki Univ; ²Dept of Molecular Environment of Life and Nature, Graduate School of Human and Environmental Studies, Kyoto Univ; ³EMC Research Group, Communications Research Lab, Independent Administrative Inst; ⁴Dept of Electrical Engineering, Graduate School of Engineering, Tokyo Metropolitan Univ., Hachioji-shi , Tokyo 192-0397, Japan.

OBJECTIVE: To investigate the effects of high frequency electromagnetic fields (HFEMFs), we assessed the frequency of micronucleus (MN) formation induced by chromosomal breakage or inhibition of spindles during cell division in Chinese hamster ovary (CHO)-K1 cells, using the cytokinesis block micronucleus method.

METHODOLOGY: The MN frequency in cells in the inner, middle and outer wells of an annular culture plate was counted for the following four conditions: 1) CHO-K1 cells were exposed to a HFEMF for 18 hours at average specific absorption rates (SARs) of 13, 39 and 50W/kg with input power 7.8W, and were compared with a sham-exposed control; 2) The cells were also exposed to a HFEMF at SARs of 78 and 100W/kg with input power 13W, and were compared with a sham-exposed control; 3) The cells were treated with bleomycin alone or with bleomycin followed by exposure to a HFEMF for 18 hours at SARs of 25, 78 and 100W/kg, and were compared with a bleomycin-treated positive control. The cells treated with bleomycin alone were compared with sham-exposed control; and 4) As a high temperature control, CHO-K1 cells were incubated at 39°C for 18 hours.

RESULTS: In study 1), the MN frequency of cells exposed to a HFEMF at a SAR of up to 50W/kg was not different to that in sham-exposed cells. In study 2), there were statistically significant increases in the MN frequencies of cells in the middle and outer wells of the annular culture plate caused by exposure to a HFEMF at 100 and 78W/kg respectively. In study 3), the MN frequencies of cells in the middle (100W/kg) and outer wells (78W/kg) of the annular culture plate were statistically higher than that caused by bleomycin treatment alone. In study 4), there was a statistically significant increase of MN frequency in the cells treated by heat at 39°C.

CONCLUSIONS: Cells exposed to a HFEMF at a SAR of 78W/kg and higher form MN more frequently than sham-exposed cells, while exposure to a HFEMF up to 50W/kg does not induce MN formation. In addition, a HFEMF at SAR of 78W/kg and higher may potentiate MN formation induced by bleomycin treatment.

This work is supported in part by a Grant-in-aid from the Research for the Future Program of the Japan Society for the Promotion of Science.

P-C-84

CELL BATHING SOLUTION AS TARGET FOR SPECIFIC BIOLOGICAL EFFECT OF MICROWAVES. S.N. Ayrapetyan. UNESCO Chair-Life Sciences International Center, 31 Acharyan St. Yerevan, 375040 Armenia.

At present the existence of specific (non-thermal) biological effect of microwaves still remains discussable and it serves as subject for intensive investigations. The fact that extremely high power pulses (EHPP) can certainly produce thermal effect makes it technically difficult to discriminate its possible specific effect in experiments. As the most probable pathways through which the possible specific effect of EHPP could be realized is the modulation of cell metabolic activity (enzymatic cascades), according to the Arrhenius' equation, predicting that temperature-dependence of chemical reaction rate must be much higher than the energy activation (E_a)-dependence one, which is main target for non-thermal effect of EHPP. Therefore, there is high possibility that in the presence of EHPP thermal effect to record its specific effect on cells is experimentally difficult. Thus, the comparative study of the trace effect of EHPP and adequate heating effect on living systems will make possible to separate non-thermal and thermal biological effects of EHPP. Although, water is the main medium, where the measure part of biochemical reactions of different metabolic cascades of cell and organism take place, our knowledge on the biological effect of microwave-induced water structure changes is rather weak. Because of water molecules are polar and they vibrate when subjected to microwave energy, causing considerable friction between molecules it is suggesting that EHPP-induced water structure changes must be different from traditional heated one and such differences could underlay in the ground of generation of non-thermal effect of EHPP.

At our laboratory comparative study of the effect of preliminary heat- and EHPP-induced treatment of water and water solution on its physical properties (specific electrical conductivity, thermal capacity, thermal anomaly properties), and the effect of treated water on plant seeds germination potential, yeast growth, cell volume, neuromembrane chemo-sensitivity and snail isolated heart contractility was performed. Water and water solution were preliminary exposed to EHPP source (MIG 9.3 generator Russian production, Peak SAR = 220 kW/g., 1 μ sec = 9.3 GHz). In all experiments the equivalent heating of control sample was performed in water bath.

The both EHPP and heat-treatment-induced increase of SEC of water and water solution was not recovered fully after returning back its temperature to the initial level. This trace effect for EHPP was higher in about 15 –20 % than in heat-treated one. These differences depend on concentration of CO_2 in water and water solution. The rates of spontaneous temperature recovery after heating was significantly different than it was in case of EHPP-induced treatment. Preliminary EHPP- and heat-treated water and water solution have different effects on plant seeds germination potential, cell volume of *Helix* neurons, chemo sensitivity of neuronal membrane, contractility of snail isolated heart, however, the significant differences between the effect of heat and EHPP-treated nutrient medium on yeast growth did not observed, although, the preliminary treatment of nutrient medium in both cases has significant depressing effect on yeast growth comparing to the non-treated one.

On the basis of obtained data it is suggested that EHPP-induced water structural changes in result of its molecule vibration can serve as one of the main pathway through which the specific (non-thermal) biological effect of EHPP is realized.

This study was founded by European Office of Aerospace Research and Development (EOARD) through ISTC A-803 Partner project.

P-A-85

DIVALENT CATION ENTRY INTO HUMAN POLYMORPHONUCLEAR LEUKOCYTES (PMN) FOLLOWING SUBMICROSECOND, INTENSE PULSED ELECTRIC FIELD (sm/i-PEF) APPLICATIONS DOES NOT OCCUR VIA CALCIUM STORES-OPERATED CATION ENTRY CHANNELS. E.S. Buescher, R.R. Smith and K.H. Schoenbach. Center for Pediatric Research, Eastern Virginia Medical School/Children's Hospital of The King's Daughters and Center for Bioelectrics, Old Dominion University, Norfolk, Virginia, USA.

Human polymorphonuclear leukocytes (PMN) are highly functional, terminally differentiated cells in which rapid alterations in intracellular free Ca^{++} concentration ($[\text{Ca}^{++}]_i$) are required for their functional activity. PMN do not have surface membrane potential-gated Ca^{++} channels. Modulation of $[\text{Ca}^{++}]_i$ occurs via release of Ca^{++} from intracellular stores, followed by opening of surface membrane divalent cation channels called Ca^{++} Stores-Operated Channels (CSOC) that mediate Ca^{++} influx. Single sm/i-PEF applications (60 ns, 60 kV/cm) to PMN result in rapid rises in $[\text{Ca}^{++}]_i$ that are reduced by >90% by chelation of extracellular Ca^{++} - indicating that influx of extracellular Ca^{++} is the predominant mechanism for the rise in $[\text{Ca}^{++}]_i$. To determine whether this rise in $[\text{Ca}^{++}]_i$ occurred via CSOC, we compared influx of different divalent cations/cation combinations into Fluo3 (a fluorescent Ca^{++} -binding probe) loaded PMN either following a single sm/i-PEF application, or after addition of cation/cation combinations to PMN whose CSOC were open (CSOC-PMN) due to intracellular Ca^{++} stores depletion. Effects of sm/i-PEF applications were assessed by use of a microscope-based pulser system with continuous fluorescence imaging and image analysis to quantitate divalent cation influx. Divalent cation influx via CSOC was assessed using a spectrofluorometer. In CSOC PMN, addition of 20 mM CaCl_2 resulted in a fluorescence rise of 20 ± 3 (n=3) units, while in the presence of 20 mM $\text{CaCl}_2 + 5$ mM NiCl_2 , (NiCl_2 is an inhibitor of PMN CSOC function), the rise was only 8 ± 3 (n=3). In contrast, the intracellular fluorescence of sm/i-PEF treated PMN (PEF-PMN) in 20 mM CaCl_2 buffer rose 108 ± 12 (n=3) units, and this rise was unaffected by suspension of cells in 20 mM $\text{CaCl}_2 + 5$ mM NiCl_2 buffer: 105 ± 12 (n=3) units. Additional studies using $\text{MnCl}_2 \pm \text{NiCl}_2$, $\text{MgCl}_2 \pm \text{NiCl}_2$ and $\text{BaCl}_2 \pm \text{NiCl}_2$ conditions, all showed that patterns of divalent cation influx were distinctly different in PEF-PMN vs. CSOC-PMN. When 300 ns, 60 kV/cm pulse applications were examined (a pulse condition in which approximately 50-60% of the rise in $[\text{Ca}^{++}]_i$ is due to release of Ca^{++} from intracellular stores - and *should* trigger some CSOC function), PEF-PMN vs. CSOC-PMN responses also showed distinctly different patterns of intracellular fluorescence. When PMN were treated with 0.25% butanol or 100 mg/mL pentoxifylline (membrane fluidizing treatments), no significant effect on the magnitude of sm/i-PEF-triggered rises in $[\text{Ca}^{++}]_i$ was observed. We conclude that sm/i-PEF applications to human PMN result in divalent cation influx via mechanisms other than straight forward CSOC functioning, and that the mechanism(s) is not significantly altered by increasing membrane fluidity.

These studies were supported in part through a Virginia Commonwealth Health Research Board Grant entitled "Nanosecond High Voltage Pulsed Electric Field Effects on Cell Structure and Function" and an AFOSR/DOD MURI grant "Subcellular responses to Narrowband and Wideband Radiofrequency Radiation".

P-B-86

CELLULAR RESPONSE OF HELA CELLS EXPOSED TO REPEATED 10 NANOSECOND, HIGH ELECTRIC FIELD PULSES. T.D. Whitehead, R. Higashikubo, and J.L. Roti Roti, Radiation Oncology Department, Radiation and Cancer Biology Division, Washington University School of Medicine, St. Louis, Missouri 63108 USA.

INTRODUCTION: SURRF (Subcellular Response to Narrow Band and Wide Band Radio Frequency Radiation) is a Multidisciplinary University Research Initiative (MURI) program to investigate non-thermal

sub-cellular responses to narrowband and wideband radiofrequency radiation, with frequency distribution, power, and exposure time as variable parameters. The results from these studies may lead to development of sensitive detectors based on RF-induced changes in gene or protein expression, diagnostic, and possibly therapeutic, techniques (<http://www.odu.edu/engr/coet/surrf/>).

OBJECTIVE: This presentation reports on the cellular response of HeLa cells exposed repeatedly to 10 nanosecond pulses of 80 and 150 kV/cm nominal field strengths.

METHOD: HeLa cells in exponential growth were trypsinized then concentrated to $1.2\text{-}3.6 \times 10^6$ cells/ml suspension. An aliquot of the cell suspension was placed in a standard electroporation cuvette (0.2 or 0.4 cm) and then placed in the 10 ns, high voltage pulse generator (J. Kolb, S. Kono & K.H. Schoenbach, Center for Bioelectrics, Old Dominion University). The cells were exposed to varying number of electric field pulses spaced about 2.5 seconds apart. The number of pulses ranged from 0 to 900. Following treatment the cell suspension was diluted and the cells plated for a clonogenic survival curve study, a growth curve study, or both. Experiments were also performed to assess apoptosis using a flow cytometric annexin V FTPC/PI staining kit.

RESULTS: There exists a threshold below which the number of pulses has no measurable impact on clonogenic survival. Beyond the threshold values, however, the decrease in clonogenic survival is dose dependent. The threshold magnitude (~ 100 for 150 kV/cm and ~ 200 kV/cm for 80 kV/cm) and the descent of the survival vs. pulses curves are both functions of field strength (see Figure 1). The curves of Figures 1 suggest that a fraction of the cells may be resistant to this method of cell kill. This resistance is more evident in the 150 kV/cm survival curve where the survival appears to level at approximately 5%. This observation is under further study. For 80 kV/cm field strength, the number of pulses had no affect on the exponential growth kinetics (i.e. the exponential growth rate constant), however, because of initial cell death the onset of exponential growth was delayed compared to controls. Following 500 pulses of 80 kV/cm field strength, the cells examined immediately after treatment had an annexin V population significantly greater than the control. Within 1hr of treatment, however, the annexin V positive and PI positive population distributions were basically identical to control.

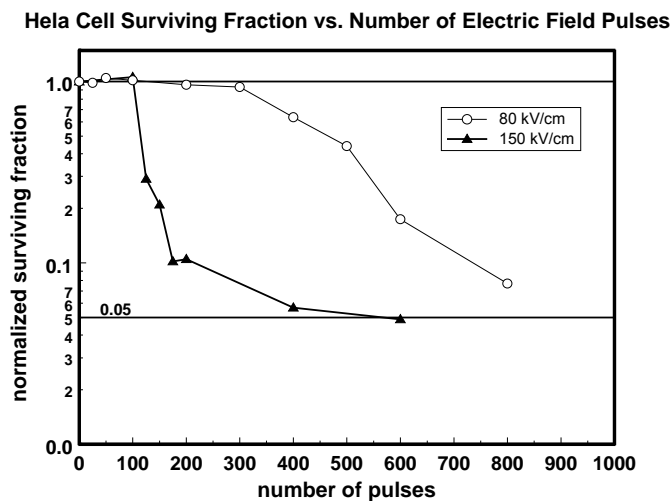


Figure 1. Clonogenic surviving fraction of HeLa cells vs. number of high energy 10 ns pulses.

P-C-87

REAL-TIME IMAGING OF HL-60 CELLS EXPOSED TO NANOSECOND PULSED ELECTRIC FIELDS. W. Frey^{1,2}, M. Artemiou¹, J. Kolb¹, N. Chen¹, S.J. Beebe³, K.H. Schoenbach¹, ¹Old Dominion University, Center for Bioelectrics, Norfolk, VA 23510; ²Forschungszentrum Karlsruhe GmbH, D-76021, Karlsruhe, Germany; ³Eastern Virginia Medical School, Norfolk, VA 23510, USA.

INTRODUCTION: When exposing cells to nanosecond pulsed electric fields, the classical electroporation theory, which only considers a poration of the outer cell membrane, is not sufficient to explain the observed effects, such as apoptosis followed by caspase activation and DNA fragmentation [1]. A possible explanation would be intercellular membrane charging and subsequent pore formation, which is already supported by experiments [2] and by the results of modeling [3]. In order to study the primary effects of ultrashort electrical pulses on biological cells such as membrane charging and instant changes in the morphology of the cell, diagnostic methods with a temporal resolution in the nanosecond range are required.

OBJECTIVES: The objective was to develop an optical diagnostic system which allows us to measure changes in membrane potentials and morphology of cells in response to ultrashort electrical pulses of high electric fields (up to 100 kV/cm). The system was to be designed for a temporal resolution on the same order as the electrical pulse, i.e. nanoseconds.

METHODOLOGY: An Olympus IX71 inverted fluorescence microscope was used to study the response in the morphology of HL-60 cells to ultrashort, intense electrical pulses. The cell suspension was placed in a 100 μm gap between two stainless steel electrodes. The electric field pulse was provided by a 50 Ω Blumlein pulse generator switched by a fast HV-MOSFET. The cells were exposed to 300 ns long pulses. Instead of using a fast camera, the required temporal resolution was achieved by illuminating the cells with a high-intensity, broad-emission-spectrum flashlamp (Nanolamp, Xenon Corporation). The duration of the light pulse was 12 ns FWHM. The time of illumination was varied during the 300 ns pulse. In this case the images were recorded by a high-resolution CCD-camera (Retiga 1300).

RESULTS: When exposing HL-60 cells to a 300 ns long, 80 kV/cm strong pulse, the initially circular shaped cells were elongated in the direction of the electric field. The average longitudinal change was 4.5% when the cells were immersed into a low conductivity (1 mS/cm) suspension. At least 10 seconds after pulse application, the membrane of the elongated cells was ruptured. In a suspension of higher conductivity (16 mS/cm), the longitudinal elongation is less than 0.5% and cell membrane rupture was not observed.

DISCUSSION: The elongation of cells in the electric field consists of two phases. A rapid phase, exhibiting elongation time constants below 1 μs , is due to the smoothing and stretching of thermal membrane undulations. After smoothing the membrane surface, additional elongation of the cell is due to an increase of membrane surface caused by electroporation [4]. The time constant for the second elongation process for HL-60 cells is estimated to be several 100 μs . At a pulse duration of 300 ns, cell elongation is consequently assumed to be due to a fast smoothing process, rather than electroporation. One possible explanation for an increased effect at lower buffer conductivity might be a loss of cytoplasm when the HL-60 cells are suspended in a low conductivity buffer medium. This might increase the initial outer membrane undulations resulting in a larger longitudinal change after pulse application.

References:

- [1] Beebe SJ, White J, Blackmore PF, Deng Y, Somers K, Schoenbach KH (2003) *DNA and Cell Biology* 22(12): 785-796.
- [2] Deng J, Schoenbach KH, Buescher ES, Beebe SJ (2003) *Biophysical Journal* 84(4): 2709-2714.
- [3] Schoenbach KH, Buescher ES, Beebe SJ (2001) *Bioelectromagnetics* 22: 440.
- [4] Kakorin S, Liese T, Neumann E (2003) *J. Phys. Chem. B* (107): 10243-10251.

This study was funded by an AFOSR DOD MURI grant on "Subcellular Response to Narrow Band and Wide Band Radio Frequency Radiation", administered by Old Dominion University.

P-A-88

EFFECTS OF ELF PULSED MAGNETIC FIELDS ON THE PROLIFERATION OF MC3T3-E1 CELLS. X.L. Huo, W. Yang, T. Song. Bioelectromagnetic Lab, Institute of Electrical Engineering, Chinese Academy of Sciences, Beijing 100080, China.

OBJECTIVE: Many investigations have been carried out that electromagnetic stimulation can be used successfully to treat a wide range of bone disorders, such as delayed and nonunion fractures, fresh fracture healing and so on. Otherwise, the clinical success contrasts with many negative reports on the effects of electromagnetic stimulation on the cellular proliferation, differentiation, and bone formation in vitro. The electromagnetic fields of 16Hz have been demonstrated by several studies as a “frequency window” which can regulate the release of Ca^{2+} of cells. Thus, we choose 16Hz pulsed magnetic fields to study the effects of magnetic fields on the proliferation of Mouse Osteoblastic Cell Line- MC3T3-E1 cells.

METHODS: **1.ELF exposure system:** The exposure system of pulsed magnetic fields consisted of a pulsed power and two solenoid coils placed in two incubators. Each solenoid coil was composed of two parallel-wise coils and the current of the pulsed power could be injected into the parallel-wise coil individually. If the current directions of the two parallel-wise coils were same the solenoid coil could produce the effective fields. Otherwise, if the current directions of the two parallel-wise coils were reverse the solenoid coil had no effective fields. A switch was used to control the current directions and to choose control or sham solenoid coils randomly. By the structure of the exposure system, double blind experiments could be performed and the temperature of the incubator could be controlled easily because the two solenoid coils (control and sham) had the same quantity of heat. The frequency of the system could be changed from 5 to 200 Hz and the effective magnetic field density could be tuned from 0 to 6mT. The solenoid inner diameter was 20cm. A frequency of 16Hz and a magnetic flux density of 1.55mT were used in our experiments. **2.Cell culture:** MC3T3-E1 cells were cultured at 37°C in an atmosphere of 5%CO₂ incubator in α MEM, supplemented with 10% fetal bovine serum and 2μM L-glutamine. **3.Assay:** MTS method was used to determine the cell proliferation rate and the flow cytometry was applied to analyse the change of cell cycle. **4. Statistical analysis:** Data analysis was performed by Student’s *t*-test with a criterion level of $\alpha=0.05$.

RESULTS: The cell suspensions were added to the wells of a 96-well culture plate (2×10^4 cells/ml for MTS method assay) or culture dish (2.5×10^5 for flow cytometry assay). After 24h of incubation at 37°C, 5%CO₂, the cells were treated under the pulsed magnetic fields for another 24h. The cell proliferation was determined by MTS method and the change of cell cycle was determined by flow cytometry assay. The results showed that there were no significant differences between the sham and the exposure on the cell proliferation and the change cell cycle on exposure to 16 Hz pulsed magnetic fields by *t*-test ($P>0.05$).

CONCLUSIONS: In this study, no significant effects were observed the on cell proliferation and the change of cell cycle on exposure to 16Hz, 1.55mT pulsed magnetic fields. Many investigations revealed that the release of intracellular calcium responding to the modulation frequency is a ‘window’ effect, with a largest response occurring around the frequency of 16Hz. However, it was not testified as such under our experiment conditions. Other investigations regarding the effects of 16Hz, 1.55mT magnetic fields on MC3T3-E1 cells will be attempted for further progresses in the future.

XiaoLin Huo: Bioelectromagnetic Lab, Institute of Electrical Engineering, Chinese Academy of Sciences, Beijing 100080, China Tel: 86-10-62552364. Fax: 86-10-62558093. E-mail: huoxl@mail.iee.ac.cn

P-B-89

STUDENT

MAGNETICALLY ALIGNED COLLAGEN GUIDES AXON ELONGATION. Y. Eguchi and S. Ueno. Department of Biomedical Engineering, Graduate School of Medicine, University of Tokyo, 7-3-1 Hongo, Bunkyo-ku, Tokyo, 113-0033 Japan.

OBJECTIVE: Recently strong magnetic field of tesla order can orient extracellular matrix such as collagen[1] and fiblin [2], and adherent cells such as osteoblasts and Schwann cells[3]. The control of orientation of biological materials may be useful in medical and tissue engineering. There is a common consensus that longitudinal alignment of extracellular matrix improve axon regeneration, otherwise known as contact guidance[4,5,6]. We investigated axon elongation from chick embryo dorsal root ganglia (DRG) cultured on the magnetically aligned collagen after strong magnetic field exposure.

METHODS: We used horizontal-type superconducting magnet, which produced 4.7 T and 8 T at its center to align collagen gels perpendicular to the magnetic field during self-assembly of collagen fibrils from molecules. We dissected dorsal root ganglia (DRG) from 10-day old chick embryos, and cultured DRGs on type- α collagen gel after strong magnetic field exposure (4.7 T, 8.0 T) for 2 h or without magnetic field (0 T). We measured length of axon elongation on the first and third day of culturing.

RESULTS: The length of axon elongation in aligned collagen was longer than that in unaligned collagen on third day of culturing magnetic field exposure. The tendency of axon to elongate along the aligned collagen fibers were observed after prolonged culturing. The tendency became greater with an increase in magnetic field strength (Figure 1).

DISCUSSION: These results showed that magnetically aligned collagen provided a scaffold for neurons on which to grow and it directs the axon growth as contact guidance. Magnetically aligned collagen is useful in techniques in nerve regeneration in tissue engineering and regenerative medicine.

References

- [1] Torbet J, Ronziere MC : Magnetic alignment of collagen during self-assembly. *Biochem J* 219(3) :1057-1059, 1984.
- [2] Torbet J, Freyssinet JM, Hudryclergeon G : Oriented fibrin gels formed by polymerization in strong magnetic-fields. *Nature* 289(5793) : 91-93, 1981.
- [3] Eguchi Y, O-Ikeda M, Ueno S : Control of orientation of rat Schwann cells using an 8-T static magnetic field. *Neurosci. Lett.* 351 : 130-132, 2003.
- [4] Williams L : Exogenous Fibrin Matrix Precursors Stimulate the Temporal Progress of Nerve Regeneration Within a Silicone Chamber. *Neurochem Res* 12(10) : 851-860, 1987.
- [5] Ceballos D, Navarro X, Dubey N, et al. : Magnetically aligned collagen gel filling a collagen nerve guide improves peripheral nerve regeneration. *Exp Neurol* 158 (2) : 290-300, 1999.
- [6] Dubey N, Letourneau PC, Tranquillo RT : Guided neurite elongation and Schwann cell invasion into magnetically aligned collagen in simulated peripheral nerve regeneration. *Exp Neurol* 158(2) : 338-350, 1999.

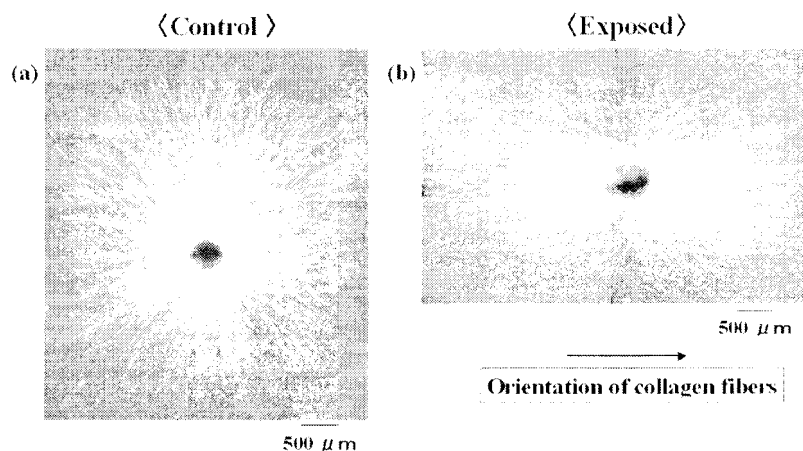


Figure 1: Elongation of DRG cultured on the collagen gel after 3 days of culturing. (a) Control group (without magnetic field exposure). (b) Exposed group (8T magnetic field exposure).

P-C-90

DNA DAMAGE IN HUMAN CELL LINES AFTER 24H IN VITRO EXPOSURE TO W-CDMA MODULATED SIGNALS AT 2-GHZ BAND MICROWAVES. Y. Komatsubara¹, M. Sekijima¹, H. Takeda¹, N. Sakuma¹, T. Nojima², and J. Miyakoshi³. ¹Mitsubishi Chemical Safety Institute Ltd., Kashima-Gun, Ibaraki 314-0255, Japan, ²Hokkaido University, Sapporo, Hokkaido 060-8628, Japan ³Hirosaki University, Hirosaki, Aomori 036-8563, Japan.

OBJECTIVE: We tested the hypothesis that modulated radiofrequency (RF) fields may act as a mutagen. Firstly, to confirm the response of the human cell lines exposed to microwaves at SAR of 80 mW/kg, which corresponds to the limit of the whole-body average SAR for general public exposure defined as the basic restriction in the ICNIRP guidelines [1]. Secondly, to investigate if continuous wave (CW) and W-CDMA modulated signal RF fields affect genotoxicity to different extents.

MATERIALS AND METHODS: We used the *in vitro* exposure system with a horn antenna and dielectric lens in an anechoic chamber, which was developed by NTT DoCoMo [2]. Two human cell lines, A172 (glioblastoma) and IMR-90 (normal fibroblasts from fetal lung) were used, and the cells were exposed in plastic 35 mm petri dishes at 15 dishes (five replicate culture each; sham, expose and positive control) per cell line. The alkaline single cell gel electrophoresis (SCG) assay was performed on log-phase cultures for period 2 or 24 h exposure at 80, 250, and 800 mW/kg SAR. Concurrent negative (sham) and positive (methyl methane sulfonate; 20 μg/mL MMS) control cultures were run for each experiment. Comets were visualized by ethidium bromide staining (10 μg/mL) and were analyzed by Komet 5 imaging system (Kinetic Imaging LTD.) at least 100 comets from each of five replicate cultures. DNA damage was quantified immediately after RF-field exposures using three parameters (tail moment, comet length and tail length) for each comet.

RESULTS AND CONCLUSIONS: During the incubation phase, each cell was exposed at 37.0±0.5°C, for 2 or 24h at average SAR of 80, 250, and 800 mW/kg with W-CDMA or CW electromagnetic fields at 2.1425GHz. No differences in either cell morphological phenomenon or in cell cycle profile were detected when the exposure took place during the period of incubation. When compared to the sham-treated controls, no evidence of increased primary DNA damage was detected by any parameter for any of the RF-field-exposed cultures by the alkaline comet assay. In contrast, the response of human cells exposed to MMS was significantly different from RF-radiation- and sham-exposed cells. Thus, under the experimental conditions tested, there is no evidence for induction of DNA single-strand breaks and alkali-labile lesions in human cultured cell lines exposed to W-CDMA and CW 2.1425 GHz microwave radiation. Our results confirm that low-level exposures did not act as a genotoxicant at up to 800 mW/kg SAR. In a future plan,

we will evaluate whether or not there are biological effects of exposure to microwave at high-level SAR radiations on the genotoxicity and the gene expression profile using DNA microarray in human cell lines.

References

[1] ICNIRP, "Guidelines for limiting exposure to time-varying electric, magnetic, and electromagnetic fields (up to 300GHz)," *Health Phys.*, 74, 494-522, 1998.

[2] Uebayashi et al., (2003) "Large-scale in vitro experiment system for low-level long-term irradiation by 2-GHz mobile radio base-stations: System design and its performance. 26th BEMS annual meeting, Maui, Hawaii, p19

This work was supported by NTT DoCoMo Inc.

P-A-91

EFFECTS OF HIGH-FREQUENCY ELECTRO-MAGNETIC FIELDS ON CELL GROWTH, CELL SURVIVAL AND CELL CYCLE DISTRIBUTION. Y. Takashima¹, H. Hirose², S. Koyama³, Y. Suzuki⁴, M. Taki⁴, J. Miyakoshi¹. ¹Faculty of Medicine, Hirosaki University, ²Graduate School of Science, Kyoto University, ³Graduate School of Human and Environmental Studies, Kyoto University, ⁴Graduate School of Engineering, Tokyo Metropolitan University, ¹66-1 Hon-cho, Hirosaki, 036-8564 Aomori, Japan.

INTRODUCTION: Use of high-frequency electromagnetic fields (HFEMFs) is increasing in various areas, including radio communication in the use of mobile phones. Therefore, it is important to examine the biological effects of HFEMFs on cells, and here we have examined cell proliferation following exposure to a wide range of specific absorption rates (SARs). Furthermore, to determine whether non-thermal effects of electromagnetic fields influence cell proliferation at SAR levels at which thermal effects are present, we compared the effects of continuous exposure and intermittent exposure at high SARs.

METHODS: A high frequency electromagnetic field exposure unit operating at a frequency of 2.45GHz was used to ensure exposure of the cells at high SAR. Chinese-hamster ovary cells or human malignant glioma cells were cultured in conventional media, and cells showing exponential growth were then cultured in exposure dishes and were HFEMF-exposed or sham-exposed for 2 h.

RESULTS AND CONCLUSIONS: When cells were exposed continuously at SARs up to 100 W/kg, the growth rate, survival and cell cycle distribution were not affected [Figure 1]. At 200 W/kg, the cell growth rate was suppressed and cell survival decreased [Figure 1]. However, when CHO-K1 cells were exposed intermittently at 1500 W/kg_{pk} (100W/kg_{mean}), no significant differences were observed between these conditions and continuous wave exposure at 100 W/kg. Exposure to the HFEMF results in heating of the medium, and the thermal effect depends on the mean SAR. Hence, these results suggest that the proliferation disorder is caused by the thermal effect.

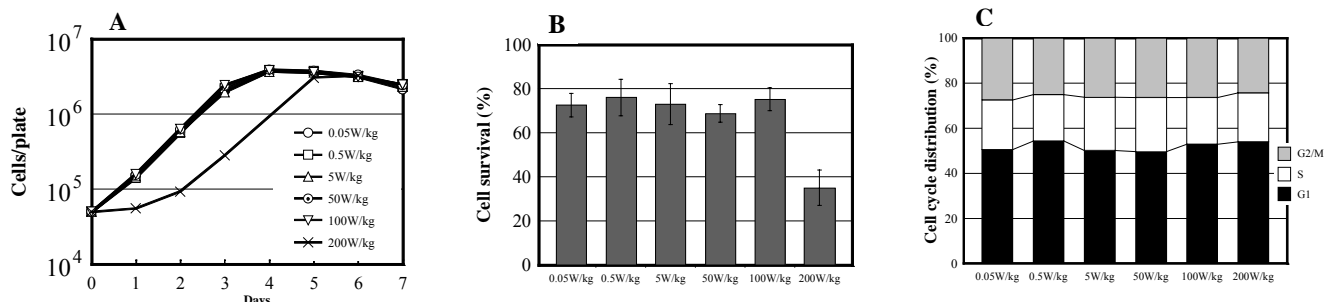


Fig. 1. Effects of 2.45GHz electromagnetic fields on (A) cell growth, (B) cell survival and (C) cell cycle distribution.

This study was financially supported by the committee to Promote Research on the Possible Biological Effects of Electromagnetic Fields, Ministry of Public Management, Home Affairs, Posts and telecommunications, Japan.

P-B-92

MUTAGENIC EFFECTS OF HIGH-FREQUENCY ELECTROMAGNETIC FIELDS USING A BACTERIAL MUTATION ASSAY. Y. Takashima¹, Y. Suzuki², M. Taki², J. Miyakoshi¹. ¹Faculty of Medicine, Hirosaki University, ²Graduate School of Engineering, Tokyo Metropolitan University, ¹66-1 Hon-cho, Hirosaki 036-8564 Aomori Japan.

BACKGROUND: The use of high-frequency electromagnetic fields (HFEMFs) is increasing in various areas, including radio communication in the use of mobile phones, making it important to examine the biological effects of HFEMFs. The bacterial mutation assay (Ames test) developed by Ames et al [1] is widely used to screen the mutagenicity of chemicals and environmental contaminants. This test is also useful for evaluation and comparison of the possible mutagenic effects of exposure to electromagnetic fields, and in this study the bacterial mutation assay was used to determine the mutagenicity of HFEMF exposure.

OBJECTIVE: To determine the possible relationship between mutagenicity and HFEMF exposure using the bacterial mutation assay.

METHODS: *Salmonella typhimurium* TA98, TA100, TA1535 and TA1537, and *Escherichia coli* WP2 *uvrA* were used, and experiments were carried out using the preincubation method [1]. A high frequency electromagnetic field exposure unit operating at a frequency of 2.45GHz was used to ensure exposure of the cells at high specific absorption rate (SAR). A cell suspension in phosphate buffer was preincubated for 30 min in 2.45GHz electromagnetic fields up to 200 W/kg or in a sham space. Cell suspensions were plated onto minimal glucose agar plates and incubated at 37 °C in a conventional incubator for 48 hr. Revertant colonies were then scored. Each experiment was run in triplicate and conducted at least three times with a positive control.

RESULTS: There was no significant difference in the number of revertant colonies between cells exposed at 200 W/kg and sham-exposed cells [Figure 1]. Similar results were observed for 5, 10, 50 and 100 W/kg exposures. Hence, these results suggest that HFEMF exposure up to 200 W/kg does not induce reverse mutation in any of the tested strains.

Reference.

[1] N. Ames, J. McCann and E. Yamasaki, Methods for detecting carcinogens and mutagens with the Salmonella/mammalian-microsome mutagenicity test, Mutation Res. 31, 347 (1975).

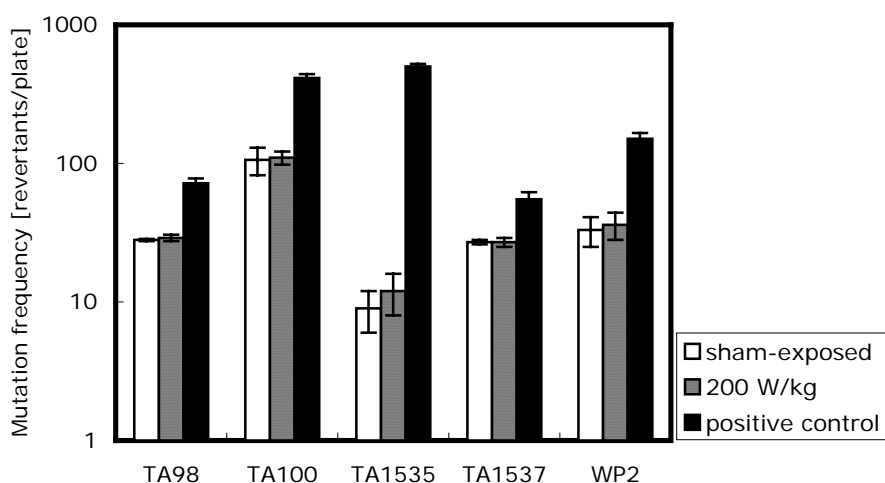


Fig. 1 Results of a mutagenicity test for a 200 W/kg high-frequency electromagnetic field. Data are given as mean +/- standard deviation of at least three independent tests with triplicate plates.

This study was financially supported by the committee to Promote Research on the Possible Biological

Effects of Electromagnetic Fields, Ministry of Public Management, Home Affairs, Posts and telecommunications, Japan.

P-C-93

STUDENT

HSP70 REGULATION IN HUMAN CELLS AFTER EXPOSURE TO 50 HZ MAGNETIC FIELDS.

A.C. Mannerling¹, S. Hannemann², M. Simkó², K. Hansson Mild^{1,3}, M.O. Mattsson¹. ¹Cell Biology Laboratory, Department of Natural Sciences, Örebro University, SE-701 82 Örebro, Sweden. ²Division for Environmental Physiology, Institute for Cell Biology and Biosystems Technology, University of Rostock, D-18059 Rostock, Germany, ³National Institute for Working Life, SE-907 13 Umeå, Sweden.

OBJECTIVE: The objectives of this study have been to: 1. make certain that 50 Hz magnetic field (MF) exposure can induce expression of the stress response gene hsp70 on the protein level. 2. Ascertain that any findings are possible to independently replicate in two separate laboratories.

INTRODUCTION: The stress response gene hsp70 can be induced by many different external factors, including temperature stress, various chemicals, oxidative stress, heavy metals, ionizing radiation etc. It has further been suggested that ELF MF exposure can act as a stressor which promotes hsp70 expression, although this has been contradicted by several studies with negative outcome. The biological relevance of any induction of hsp70 is difficult to forecast. However, an increased hsp70 level is often associated with stress protection on the cellular level, which could indicate a general stress effect by ELF MF if the exposure causes induction of the gene. To test this assumption, ELF exposure was performed on several human cell lines.

METHODS: Several human cell lines were used in this study and cultured according to standard procedures. Exposure to 50 Hz sinusoidal MF (various flux densities, horizontal or vertical polarization) was performed in cell culture incubators equipped with Helmholtz coils for one hour followed by different post-exposure incubation times (0-24 hours). As a positive control, heat shock was employed (42°C). The possible induction of hsp70 was semi-quantitatively investigated by immunoblotting. Furthermore, a quantitative determination of hsp70 was done by flow cytometric analysis. All experiments were performed in the presence of the local geomagnetic field and under controlled temperature conditions.

SUMMARY AND CONCLUSION: Induction of hsp70 expression on the protein level is obtained after exposure to vertical 50 Hz MF, 0.1 or 0.2 mT, whereas this effect is less obvious after horizontal exposure. This possible dependency of polarization, as well as flux density and exposure time is presently further investigated.

P-A-94

DEPENDENCE OF THE SPIN-SPIN RELAXATION TIME OF COLLAGEN GELS ON COLLAGEN FIBER DIRECTIONS. M. Takeuchi, M. Sekino, and S. Ueno, Dept of Biomedical Engineering, Graduate School of Medicine, Univ of Tokyo, 7-3-1 Hongo, Bunkyo-ku, Tokyo 113-0033, Japan.

OBJECTIVES: Many studies have reported that the spin-spin relaxation time (T_2) of protons in water molecules is affected by bonding interactions between water molecules and surrounding macromolecules. However, it is largely unknown how directionality in macromolecular structures affects T_2 relaxation times. In a previous study, we investigated the effect of directionality in the fiber structures on T_2 relaxation. As a model of a macromolecule with directional fiber structures, we measured the T_2 relaxation times of fibrin gels [1]. In this study, magnetically oriented collagen gel was used as a model of a macromolecule with directional fiber structures. To investigate the magic angle effect, we measured the T_2 relaxation times of collagen gels with different collagen fiber directions.

MATERIALS AND METHODS: All experiments were performed using a 4.7 T, 60cm bore magnetic resonance imaging (MRI) system with a quadrature radio frequency coil operated at 200 MHz for ^1H resonance. Cylindrical tubes with a 13 mm diameter were filled with a collagen solution (3.0 mg/ml) and collagen gels. Collagen gels were polymerized from the collagen solution in 120 minutes. We prepared two collagen gels that were polymerized with and without 4.7 T magnetic fields. The T_2 relaxation time was measured by the Carr-Purcell-Meiboom-Gill (CPMG) sequence. A 90° pulse was applied at $t=0$ ms, followed by a train of 180° pulses at 1 ms intervals. Spin echo signals were acquired at $t = 256, 512, \dots, 4096$ ms. The T_2 relaxation time was obtained by fitting the relaxation curve $S(t) = S(0) \exp(-t/T_2)$ to a series of peaks in echo signals. The temperature in the bore was 15 degrees Celsius.

RESULTS AND DISCUSSION: At an angle of 90 degrees to the main magnetic field, water molecules in the collagen gel with magnetically oriented fibers had the relaxation time $T_2 = 1.39$ s. At an angle of 55 degrees (magic angle) to the main magnetic fields, water molecules in the collagen gel had the relaxation time $T_2 = 1.55$ s. Orientation of the collagen fibers to the magic angle caused a decrease in the T_2 relaxation rate. Peto et al. extracted a collagen sample from the pig Achilles tendon with fibers oriented to one direction, and measured the T_2 relaxation time of protons in water molecules [2]. The samples had water content of about 60 %. At collagen fiber directions of 55° and 90° from the main magnetic field, the collagen samples exhibited four components in T_2 relaxation for each direction: 2.8, 10.6, 25.5, 89.6 ms for 55° , and 2.4, 9.3, 24.7, 90.5 ms for 90° . Henkelman et al. conducted a similar measurement for the beef Achilles tendon [3]. The T_2 relaxation times in the cases with 55° and 90° to the main magnetic field were 23 ± 2 ms and 17 ± 2 ms, respectively. Our result is consistent with the previously reported results on the point that a collagen sample at 55° orientation had a longer T_2 relaxation time compared to a collagen sample at 90° orientation. However, the T_2 relaxation times of our sample are long compared to the previous studies. This difference is attributable to the low collagen concentration in our sample because a decrease in interactions between collagen and water causes a decrease in the T_2 relaxation rate. Furthermore, in the samples of previously reported experiments, various macromolecules other than collagen may affect T_2 relaxation of water molecules.

References.

[1] Takeuchi M, Sekino M, Yamaguchi K, Iriguchi N, and Ueno S. "Multicomponent proton spin-spin relaxation of fibrin gels with magnetically oriented and randomly oriented fibrin fiber structures," J Appl Phys 2003; 93:6736-6738.

[2] Peto S, Gillis P, Henri VP. Structure and dynamics of water in tendon from NMR relaxation measurements. Biophys J 1990;57:71-84.

[3] Henkelman RM, Stanisz GJ, Kim JK, Bronskill MJ. Anisotropy of NMR Properties of Tissues. Magn

P-B-95

MODIFICATIONS IN CELL CYCLE KINETICS AND IN EXPRESSION OF G1 PHASE-REGULATING PROTEINS IN HUMAN AMNIOTIC CELLS AFTER EXPOSURE TO 50 HZ ELECTROMAGNETIC FIELDS AND IONIZING RADIATION. M. Simkó¹, S. Hannemann¹ and S. Lange². ¹University of Rostock, Institute of Cell Biology and Biosystems Technology, Division of Environmental Physiology, D-18059 Rostock, Germany, ²Research Centre Rossendorf, Institute of Bioinorganic and Radiopharmaceutical Chemistry, D-01328 Dresden, Germany.

OBJECTIVES AND INTRODUCTION: Since development of cancer is associated with deregulated cell growth and we previously observed a MF-induced decrease in DNA synthesis (Lange et al. 2002, *Radiat Environ Biophys.* 41:131-137.), this study aims to document the influence of 50 Hz, 1 mT magnetic fields (MF), with or without initial γ -ionizing radiation (IR), on the following cell proliferation-relevant parameters in human amniotic fluid cells: cell cycle distribution, expression of the G₁- and G₁/S-phase-regulating proteins such as Cdk4, Cdk2, cyclin D1, cyclin E, p21^{CIP1}, and p16^{INK4a}, and kinase activity.

METHODS: Human amniotic fluid cells were exposed to 50 Hz MF at 1 mT for different time periods (0-30 h). In the co-exposure experiments IR (2 Gy-8 Gy) was applied prior to MF. For S-phase analysis the BrdU assay and for cell cycle distribution flow cytometry was used. Whole cell lysates and immunoprecipitates were separated by SDS-PAGE and subjected to immunoblotting and subsequently using ECL. Bands of several G₁-phase (Cdk4, cyclin D1 and p16^{INK4a}) and G₁/S-phase specific proteins (Cdk2, cyclin E) as well as p21^{CIP1} and p53 were quantified by optical scanning in a Fluor-S-MultiImager. Data were compared to control and to IR values; differences were considered as statistically significant on the $p < 0.01$ level. Data of the flow cytometric measurements were assessed by the Student's t-test, whereas for statistical analysis of the immunoblotting experiments, the Wilcoxon matched pairs signed rank test was carried out. The quantified raw data of band intensities of whole cell lysates were analysed after correction for α -tubulin as an internal standard. Due to the absence of α -tubulin in the immunoprecipitates the quantification of Cdk4-associated proteins was done without this correction.

RESULT AND CONCLUSION: A significant decrease in the rate of BrdU incorporation could be observed after exposure to MF during the entire time period (0-30h). Investigations of expression patterns of G₁-phase proteins showed a significant alterations in the expression of cyclin D1, p21^{CIP1}, and p16^{INK4a} after exposure to MF and/or IR, respectively, whereas only a slight diminution of Cdk4 kinase activity was noticed. The expression of cyclin D1 is slightly decreased after MF exposure. The protein level of p21^{CIP1} was increased in MF exposed cultures followed by a decrease after longer exposure time periods. No changes in the expression level of p53 could be observed. IR induced a G₁ delay as well as a dose-dependent G₂ arrest, whereas no discernible changes in cell cycle kinetics were observed due to MF exposure by using flow cytometry. Combined exposure to MF/IR affected neither cell cycle distribution nor protein expression or kinase activity additionally or synergistically.

This work was supported by the Federal Office for Radiation Protection, Salzgitter, Germany.

P-C-96

STUDENT

REAL-TIME STUDY OF ACCUMULATION EFFECTS OF ELECTRIC FIELDS UPON MEMBRANE TRANSPORT IN SINGLE LIVING CELLS. Q. Wan¹ X.N. Xu¹, J. Kolb² and K.H. Schoenbach². ¹Department of Chemistry & Biochemistry; ²Dept of Electrical and Computer Engineering; Old Dominion Univ, Norfolk, VA 23529, USA.

INTRODUCTION: Timing of cellular membrane transports can be used to control the cellular pathways and the cellular function in living cells. It is well known that electric fields can be used to change the cellular membrane transport. However, it still remains unclear whether accumulation of electric fields can be used to tune the membrane transport of sub-cellular compartments. In addition, it is still unknown whether the living cells can recover from critical electric field strengths or will suffer post electric field stresses. Moreover, it remains essentially unknown whether one can selectively eradicate the unwanted cells while remain the desired cells unharmed by tuning and timing of electric fields. These are crucial questions to be addressed in order to advance our understanding of the cellular and subcellular functions upon the electric fields and to employ electric fields for therapy.

OBJECTIVES: The goal of this study is to address some of these questions, such as, whether accumulation of electric fields can be used to tune the membrane transport of sub-cellular compartments, and whether one can selectively eradicate the unwanted cells while remain the desired cells unharmed by tuning and timing of electric fields. The outcome of this work will advance our understanding of the effects of electric fields on membrane transport. The possible applications include the selective eradication of specific cells and cellular pathways.

METHODS: We have developed the microfabricated electrochemical cells and interfaced these electrochemical systems with our real-time single nanoparticle and single living cell imaging station, and a nanosecond (ns) pulser system. This unique unification allows the narrowband ns high electric fields at 100-1000 KV/cm to be applied in situ while real-time monitoring of the change of membrane transport at the cellular and subcellular level. Furthermore, high-speed imaging system permits us to precisely control the timing and frequency of the ns pluses that we apply to the living cells.

RESULTS: The results have demonstrated that the cellular and subcellular membrane transports are highly dependent upon the number and frequency of electric pluses, showing the promise of tuning of cellular and subcellular membrane transport by controlling the number of pulses and timing of pulses. In addition, it appears that the viability of cells is highly dependent upon their exposure to the frequency (number) of pulses. This opens up the new opportunity to selectively control the viability of specific cells by tuning the number of pulses. The experimental approach, updated research results and prospective applications will be discussed in detail.

This work is supported by an AFOSR/DOD MURI grant on Subcellular Responses to Narrowband and Wideband Radiofrequency Radiation, administered through Old Dominion University

COMBINED EFFECTS OF ELF ELECTROMAGNETIC FIELDS AND X-RAYS ON MUTATION IN pTN89 PLASMIDS. S. Koyama^{1, 2}, H. Hirose³, T. Nakahara¹, G-R Ding¹, Y. Isozumi² and J. Miyakoshi¹. ¹Department of Radiological Technology, School of Health Sciences, Faculty of Medicine, Hirosaki University; ²Department of Molecular Environment of Life and Nature, Graduate School of Human and Environmental Studies, Kyoto University; ³Laboratory of Radiation Biology, Graduate School of Science, Kyoto University, Japan.

INTRODUCTION: Previously, we reported that exposure to power-line frequency magnetic fields increased chromatid-type chromosomal aberrations in mouse m5S cells, and that exposure to a 5 mT ELF MF might induce mutations and enhance X-ray-induced mutations. In addition, we observed that exposure to a 400 mT ELF MF for 2 h increased X-ray-induced mutations in human melanoma MeWo cells, and that exposure to strong magnetic fields at power frequency potentiated X-ray-induced DNA strand breaks in MO54 cells. Then we suggested that ELF MFs might enhance DNA damage after X-ray irradiation

OBJECTIVE: We detected mutations that occurred in the *supF* gene carried by pTN89 plasmids in *Escherichia coli* (*E. coli*) to examine the effects of extremely low frequency magnetic fields (ELF MFs) and/or X-rays to the plasmids. This *E. coli* system was developed by Obata *et al* [1].

METHODOLOGY: The plasmids were subjected to sham exposure or exposed to an ELF MF (5 mT), with or without X-ray irradiation (10 Gy). For the combined treatments, exposure to the ELF MF was done immediately before or after X-ray irradiation.

RESULTS: The mutation frequency were 9.40×10^{-6} for X-rays alone, 1.58×10^{-5} for an ELF MF followed by X-rays, and 3.64×10^{-5} for X-rays followed by an ELF MF. Increased mutation frequency was not detected following exposure to a magnetic field alone, or after sham exposure. The mutation frequency for X-rays followed by an ELF MF was statistically significant compared to the other treatments. Sequence analysis of the *supF* mutant plasmids revealed that base substitutions were dominant on exposure to X-rays alone and X-rays plus an ELF MF. Deletions were detected in only the combined treatments with X-rays and an ELF MF, but not with X-rays alone.

CONCLUSIONS: We could not detect direct effects of ELF MFs on DNA, but exposure to ELF MFs immediately before or after X-ray irradiation may enhance the mutations.

Reference.

[1] F. Obata, T. Nunoshiba, T. Hashimoto-Gotoh and K. Yamamoto. (1998) *Journal of Radiation Research* 39: 263-70.

This work was supported in part by a Grant-in-aid from the Research for the Future Program of the Japan Society for the Promotion of Science.

P-B-98

RADICAL SCAVENGING ACTIVATION PROCESSES OF XANTHOPHYLLS IN BIOMEMBRANE. H. Nakagawa¹, S. Ueno², H. Kotani², M. Murakami¹, H. Abe. ¹Laboratory of Marine Biochemistry, Graduate School of Agricultural and Life Sciences, The University of Tokyo, Bunkyo-ku Tokyo 113-8657, Japan; ²Department of Biomedical Engineering, Graduate School of Medicine, The University of Tokyo, Bunkyo-ku, Tokyo 113-0033, Japan.

OBJECTIVE: We previously reported that the intramembranous canthaxanthin could be also important for the additional functions discovered for xanthophylls in the membrane, namely not only the singlet oxygen quencher but also the radical scavenging function of xanthophylls [1]. In the present study, we have investigated the effect of these compounds on the structure and the fluidity of model membranes by ¹³C-nuclear magnetic resonance (¹³C-NMR) technique.

METHODS: MLV (multilamellar vesicles) were prepared by adding D₂O (2.0 mL) to the dry phospholipid (150 mg) and mechanical shaking. The MLV solutions were treated for 2-4 h in a cooled bath-type sonicator. The SUV (small unilamellar vesicles) solutions were then centrifuged and passed through a Millipore filter (0.2 μm) to remove large liposomes. Mixed SUV were prepared by first co-dissolving both components in CHCl₃. The lipid-to-xanthophyll molar ratio used was 5 : 1. The SUV vesicle preparations for ¹³C-NMR (relaxation times *T*₁) were placed into conventional 5 mm NMR tubes and ¹³C*T*₁ values were obtained with a JEOL JNM A-600 (600.05 MHz) spectrometer operating at 150.8 MHz in the pulse inversion recovery Fourier transform (IRFT) mode employing (180°- *t* - 90°) pulse sequence. In all these experiments a pulse width of 9.6 μs (90°) and 19.2 μs (180°) and pulse delay of 3.6 s were used at a temperature of 27 °C or 50 °C. In addition, there were no major differences in proton noise-decoupled ¹³C spectra obtained before and after the IRFT experiments.

RESULTS AND DISCUSSION: ¹³C*T*₁ relaxation times for the PC carbons generally reflect the membrane fluidity. The increase in the fluidity of the PC bilayer is especially evidenced by a large increase (100-250 %) in the relaxation times of the bilayer upon addition of β-carotene. In particular, great increases for C=C bonds are observed in ¹³C*T*₁ for β-carotene of the model membrane. While the ¹³C*T*₁ of the hydrocarbon chain carbons in the presence of astaxanthin is slightly reduced (5-20 %), the reductions in motional freedom are observed in almost all the chain carbons. In the case of canthaxanthin-incorporated PC vesicles, increases in ¹³C*T*₁ for the hydrocarbon chain carbons were relatively small and not reduced. This result indicates a major difference between the behaviour of astaxanthin and that of canthaxanthin.

Reference.

[1] H. Nakagawa, M. Murakami, H. Abe, S. Ueno, "Anti-radical and Molecular Aspects of the Interaction of Xanthophylls with the Phospholipid Bilayer." 25th Annual Meeting of the Bioelectromagnetics Society, Wailea, Maui, Hawaii, 2003. P375

P-C-99

NUCLEAR CHANGES AFTER ULTRASHORT ELECTRIC PULSES. N. Chen, J. Kolb, J. Yang, W. Frey, R.J. Swanson, K.C. Loftin, S.J. Beebe. R.P. Joshi, K.H. Schoenbach. Center for Bioelectrics, Old Dominion University, Norfolk, Virginia 23510, USA.

INTRODUCTION: An electrical model for living cells predicts that an electric pulse with a duration less than the plasma membrane charging time will increase the probability of electric field interactions with intracellular organelles. While previous imaging studies with ultrashort pulses have demonstrated intracellular effects on granules in human eosinophils with pulse durations greater than 60 ns [1,2], we examine the consequence of applying 10 ns and 60 ns pulses on the nuclei of HL-60 cells using real time, nanosecond imaging. Analyzing the response of nuclei in real-time will elucidate how ultrashort pulsed

electric fields (PEF) alter cell survival and stimulate DNA damage [3]. This could advance new applications in gene therapy. The two nuclear stains used were acridine orange (AO) which easily crosses the cell and nuclear membranes of living cells, and propidium iodide (PI) which is excluded by the cell membrane under normal growth conditions.

OBJECTIVES: Our objective is to record and analyze nuclear and cell-membrane responses to 10 ns pulses in HL-60 cells to confirm or disprove the hypothesis that ultrashort pulses selectively effect intracellular structures more than cell membranes.

METHODS: Using confocal microscopy, temporal and spatial resolution of 10 ns pulse-induced poration of the nuclear membrane and other nuclear changes were measured by recording intra-nuclear fluorescence of HL-60 cells upon intercalation of AO and PI into the DNA. Both the AO stain/HL-60 cell- and the PI stain/HL-60 cell solutions were exposed to a 10 ns, 65 kV/cm pulse or a 60 ns, 26 kV/cm pulse thereby generating pulses of the same energy density. Comparisons were made between pulse data with both 10- and 60 ns durations on plasma membrane and nucleus. **RESULTS:** A PEF of 10 ns did not porate the plasma membrane but targeted the nucleus while a 60 ns PEF of approximately the same energy density caused delayed poration of the plasma membrane and delayed nuclear changes. A 10 ns pulse (65 kV/cm field amplitude) of HL-60 cells stained with AO produced an exponential decrease in AO fluorescence intensity inside the nucleus with an approximate 3-minute time constant. A 60 ns pulse (26 kV/cm field amplitude) delayed the onset of the fluorescence decay by approximately 10 minutes before following the same fluorescence decay pattern as the 10 ns-pulsed cells. In the presence of PI, HL-60 cells failed to porate the plasma membrane with 10 ns, 65 kV/cm pulses. After 60 ns, 26 kV/cm pulses, PI uptake was observed with a post-pulse mean delay time of almost 20 minutes.

CONCLUSIONS: Ultrashort pulses of 10 ns duration (shorter charging time constant than the plasma membrane) changed cell nuclei properties. One target of the ultrashort pulses could be the nuclear membrane, which probably led to conformational changes of membrane proteins allowing poration and relatively slow decrease in fluorescence. If nuclear membrane poration occurred, the fluorescence reduction could be a result of (1) stained DNA exiting the nucleus or (2) AO exiting the nucleus. Another target was possibly the nuclear DNA molecules which could cause a fluorescent-decreasing change in stain intercalation. Nuclear membrane changes after nanosecond PEFs that cause increased permeability to macromolecules, e.g. DNA, introduces potential technology to induce and control nuclear membrane processes that were, until now, only available for use on the plasma membrane by electroporation with PEFs of multi-microsecond pulse durations.

References

- [1] Schoenbach KH, Beebe SJ, and Buescher ES. (2001) *Bioelectromagnetics*. 22:440-448.
- [2] Deng J, Schoenbach KH, Buescher ES, Hair PS, Fox PM, and Beebe SJ. (2003) *Biophys J*. 84:2709-2714. Buescher ES and Schoenbach KH, (2003) *IEEE Trans. Dielectrics and Electrical Insulation* 10:788-794.
- [3] Stacey M, Stickley J, Fox P, Statler V, Schoenbach KH, Beebe SJ, Buescher S. (2003) *Mutation Research*. 542:65-75

This study was funded by an AFOSR DOD MURI grant on "Subcellular Response to Narrow Band and Wide Band Radio Frequency Radiation," administered by Old Dominion University.

EFFECT OF STRONG MAGNETIC FIELD ON CHONDROGENIC DIFFERENTIATION OF ATDC5 CELLS. Y. Eguchi, S. Ueno. Department of Biomedical Engineering , Graduate School of Medicine, University of Tokyo, 7-3-1 Hongo, Bunkyo-ku, Tokyo, 113-0033 Japan.

OBJECTIVE: Strong static magnetic field (SMF) of tesla order can stimulate differentiation and extracellular matrix synthesis of osteoblasts in vitro and also stimulate bone formation in vivo[1]. In this study, we investigate the effects of a SMF (8T) on chondrogenic differentiation of mouse embryonic cell line ATDC5 as a model of chondrogenesis in the enchondral bone development[2].

METHODS: We used horizontal-type superconducting magnet (bore: diameter = 100 mm, length = 700 mm, temperature = 37°C), which produced 8 T at its center. Mouse embryonic ATDC5 cells were provided by RIKEN Cell Bank (Tsukuba, Japan)[2,3]. ATDC5 cells were cultured in a DME/F12 medium containing 5% FBS, and 10 µg/ml bovine insulin, 10 µg/ml human transferrin, and 3×10^{-8} M sodium selenite. The cells were seeded in 20 ml closed flasks with a cell density of 2.0×10^4 cells/cm². On day 3, the flasks were positioned at the center of the magnet and exposed to 8 T magnetic fields for 3 days. In other groups, cells were exposed to 200ng/ml bone morphogenetic protein-2(BMP-2) for 3 days. Control group were kept in same conditions without SMF and BMP exposure. Then, the flasks were transferred to a 37°C incubator. Cell number and chondrogenesis of ATDC5 cells were observed microscopically.

RESULTS: Undifferentiated ATDC5 cells rapidly proliferated and ceased growing at confluence with monolayer on day 3. In the presence of 10 µg/ml insulin, cells gradually proliferated and formed cartilage nodules via the cellular condensation until about day 21 (early phase differentiation). Although 8T SMF exposure did not affect cell number, it promoted differentiation of ATDC5 cells to change undifferentiated cells into round chondrocytic cells all over the culture within 3 days of SMF exposure (Figure 1). Similarly BMP-2 also induced differentiation of ATDC5 cells [3].

DISCUSSION: In this study we showed that SMF exposure can stimulate differentiation of chondrogenic precursor cells as well as growth factor such as BMP-2. This physical technique has a potential clinical uses such as tissue engineering of articular cartilage for cartilage repair. Further studies are needed to investigate the mechanisms by which SMF exposure stimulate chondrogenic differentiation.

References.

- 1 Kotani K, Iwasaka M, Ueno S, et al. : Strong static magnetic field stimulates bone formation to a definite orientation in vitro and in vivo. *J bone Miner Res* 17 : 1814-1821, 2002.
- 2 Shukunami C, Shigeno C, Atumi T, et al. : Chondrogenic differentiation of clonal mouse embryonic cell line ATDC5 in vitro. Differentiation –dependent gene expression of parathyroid hormone (PTH)/PTH-related peptide receptor. *J Cell Biol* 133 : 457-468, 1996.
- 3 Shukunami C. Ohta Y. Sakuda M. Hiraki Y. : Sequential progression of the differentiation program by bone morphogenetic protein-2 in chondrogenic cell line ATDC5. *ExpCell Res* 24:1-11, 1998

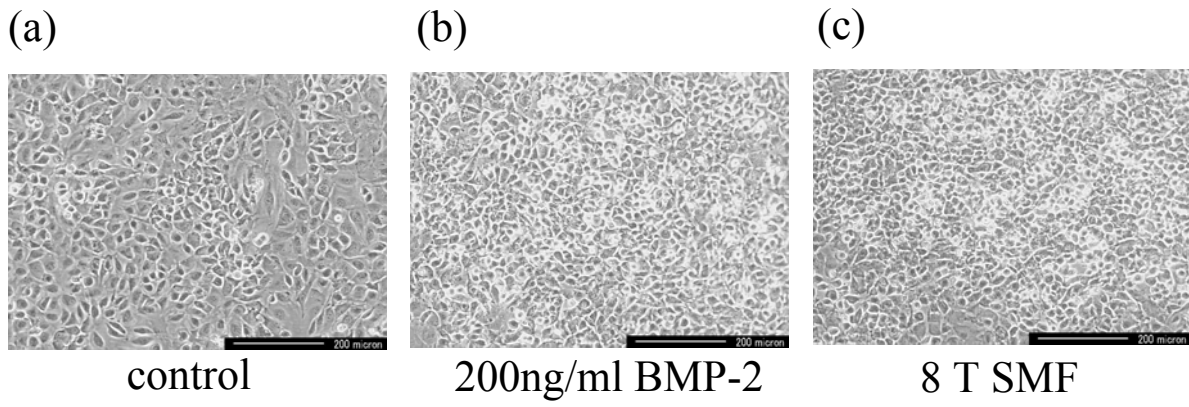


Figure 1: Effects of 8T SMF and BMP-2 on differentiation of ATDC5 cells. Cells were grown to a confluency in DME/F12 medium containing 5% FBS and 10 $\mu\text{g/ml}$ insulin for 3 days. Cells were incubated in the absence (a) or presence of BMP-2 (b) or 8 T SMF exposure (c) for additional 48 h. Bar:200 μm .

P-B-101

STUDENT

IN VITRO 1800 MHZ RADIOFREQUENCY EXPOSURE DOES NOT AFFECT HUMAN THYMOCYTE DIFFERENTIATION. M. Capri¹, E. Bianchi¹, S. Carosella¹, C. Lanzarini¹, L. Ugolini¹, G. Gargiulo², J. Schuderer³, N. Kuster³, P. Mesirca⁴, C. Franceschi¹ and F. Bersani⁴. ¹Department of Experimental Pathology, Section of Immunology, University of Bologna, 40126 Bologna, Italy; ²S. Orsola-Malpighi Hospital, 40126 Bologna, Italy; ³Foundation for Research on Information Technologies in Society IT'IS, Zurich, Switzerland; ⁴Department of Physics, University of Bologna, 40126 Bologna, Italy.

OBJECTIVE: Within the frame of the European Reflex Project, Bologna's group studied the possible effects of radiofrequency (RF) on thymocyte differentiation in human thymus organ cultures (HTOC). Fragments of thymus (waste tissue taken from paediatric cardio-surgery) from 9 baby donors (age from 5 days to 8 months) were exposed to 1800 MHz DTX modulated RF (1.3 W/Kg SAR) and thymocytes were analysed for the following biological parameters: 1) viability; 2) apoptosis; 3) phenotypical differentiation.

METHODS: The exposure system, provided by Prof. Kuster's team, consist of two wave guides placed inside a CO₂ incubator (atmosphere at 37 °C) and connected to a generator, an amplifier and a PC by which is randomly determined the operating wave guide, so that all the experiments were performed in blind. The exposure time was 10 min ON and 20 min OFF for 24 h. Biological parameters were evaluated by flow cytometry techniques, using a FACScalibur cytometer (Becton Dickinson), before exposure and after 48 h of HTOC (24 h of exposure plus 24 h of recovery). Viability was evaluated by propidium iodide (PI) incorporation; apoptosis was analyzed using Annexin-V/PI staining and phenotypical differentiation was assessed by analysing the following membrane markers: CD3, CD4, CD8, $\alpha\beta$ TCR (T cell receptor), $\gamma\delta$ TCR, CD71 (transferrin receptor on proliferating cells) and CD16 (receptor for IgG).

RESULTS: HTOC were performed in order to assess *in vitro* apoptotic phenomena due to negative selection and phenotypical differentiation, which usually occurs *in vivo* inside the thymus. Data obtained clearly indicated that no significant difference was found between sham and field-exposed thymocytes related to all the endpoints analysed. Thus, we can state that 1800 MHz DTX modulated RF exposure is not able to interfere with thymic function, in conditions very near to what happens *in vivo*. Given the importance of a right thymocyte differentiation for mature T lymphocyte production and human immune system functionality, these negative results can be considered for further evaluations related to possible human health risk.

This study was fully supported by REFLEX project (5th Framework Programme of the European Union) "Risk Evaluation of Potential Environmental Hazards From Low Energy Electromagnetic Field (EMFs) eXposure Using Sensitive *in vitro* Methods"

CHARACTERISTICS OF A 10 NANOSECOND BLUMLEIN GENERATOR FOR CELL SUSPENSION STUDIES. H.L. Gerber¹, J. Kolb², Q. Zhou¹, A. Bassi¹, K.H. Schoenbach². ¹Purdue University Calumet, Hammond, Indiana 46323, USA; ²Old Dominion University, Norfolk, Virginia 23510, USA.

BACKGROUND: Ultra-short electrical pulses have been used for studying possible interactions between electric fields and cell substructures. Some topics include the effects of electromagnetic fields on gene expression, apoptosis, electroporation, and DNA fragmentation. The instrumentation of short pulses is difficult to determine because of the high frequency and high power interference generated by the pulser. Of interest is the ability to determine a more accurate representation of voltage, energy, and frequency components that are applied to a cell suspension.

OBJECTIVES: The main objective is to shield a high-speed digital oscilloscope for analyzing the voltage waveforms for frequency and energy content. In addition, it is desired to provide a simplified model for predicting voltage and energy as a function of load parameters for investigators.

METHODS: Voltage waveforms are evaluated for peak electric field, energy content, and frequency distribution. A simplified model of the pulse generator is presented for determining peak electric field and energy. A model of the thermal response to the pulsed energy content is also presented. Several measurement techniques are used for determining electrical parameters of cell suspensions.

RESULTS: Typical waveforms and their analysis as a function of electrical parameters are presented (see Fig.1 below). Ninety percent of the total energy content is at frequencies below 60 MHz.

References.

- [1] K. Schoenbach et al., Intracellular effect of ultrashort electrical pulses. *Bioelectromagnetics* 22:440-448 (2001)
- [2] R. Joshi and K. Schoenbach, Electroporation dynamics in ultrafast biological cells subjected to ultrafast electrical pulses: a numerical simulation study. *Phys Rev E* 62:1025-1033 (2000)
- [3] Tseng et al., Effects of nanosecond pulsed electric fields on human gene expression. *Trans. 22nd SPRBM meeting* 22:8-9 (2004)

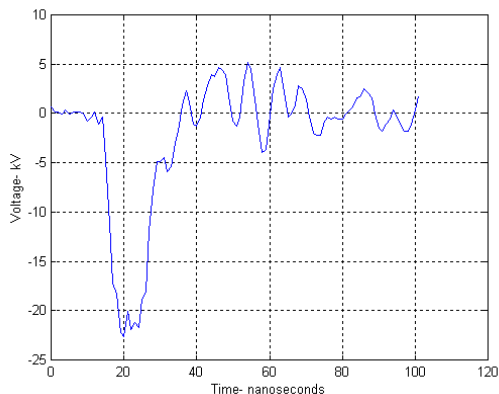


Fig. 1 Typical High Voltage Waveform with 1 mm Cuvette

This research is supported by two AFOSR DOD MURI grants.

P-A-103

EFFECT OF EXPOSURE TO RADIO FREQUENCY ELECTROMAGNETIC FIELDS ON CYTOKINE-INDUCED NITRIC OXIDE PRODUCTION IN ORGAN CULTURED RAT AORTA.

H. Masuda^{1,2}, F. Poulletier de Gannes¹, S. Sanchez¹, E. Haro¹, I. Lagroye¹, B. Billaudel¹ and B. Veyret¹.
¹PIOM Laboratory CNRS-ENSCP, University of Bordeaux, 33607, Pessac-France. ²Department of Environmental Health, National Institute of Public Health, Tokyo 108-8638, Japan.

OBJECTIVES: Nitric oxide (NO) plays an important role in vascular physiology. Although several research groups have investigated the effects of radiofrequency radiation (RFR) on biological systems producing NO, there is today little information about the effects of RFR on NO and blood vessels. The aim of present study was thus to examine whether RFR affect a NO-inducible system which is related to septic shock and vascular inflammatory lesions.

METHODS: To evaluate changes in the system of inducible NO production, we measured the production of nitrite, a metabolite of NO, in organ-cultured rat aorta. The aortic rings isolated from Wistar rats were incubated in culture medium with or without tumor necrosis factor- α (TNF- α , 10 ng/ml) at 37°C under 95% air and 5% CO₂. The Petri dishes were divided into two groups, Sham-exposed group and RFR-exposed group. All 8 exposed Petri dishes were placed in a wire-patch antenna (GSM-900 MHz) installed in a CO₂ incubator, and were simultaneously exposed to RFR at an average SAR of 2 W/kg. We incubated the aortic rings under two kinds of RFR exposure protocols: 1) 48-hr exposure to RFR with TNF- α application, or 2) 24-hr pre-exposure to RFR before a 48-hr application of TNF- α .

RESULTS: Treatment with TNF- α increased nitrite accumulation in culture medium in a time-dependent manner for 48 hrs. At the end of the incubation of aorta with TNF- α for 48 hrs, immunohistological analysis showed a strong positive immunoreaction to inducible form of nitric oxide synthase (iNOS) in the smooth muscle layer of the aorta, but not in the aorta incubated without TNF- α . Besides, the increase in nitrite accumulation was inhibited by aminoguanidine, a specific inhibitor of iNOS. In the aorta exposed to RFR for 48 hrs, there was no difference in the level of nitrite accumulation between sham- and RFR-exposed groups. Pre-exposure to RFR for 24 hrs had no influence on the time-dependent increase in nitrite accumulation induced by TNF- α .

CONCLUSIONS: Application of TNF- α induced nitrite production accompanied by the expression of iNOS protein in cultured rat aorta. Exposure to RFR, however, had no effect on the inducible nitrite production under the present conditions. These results suggest that RFR does not affect the system of inducible NO production in rat aorta in the presence cytokine.

P-B-104

STUDENT

THE EMP INFLUENCED THE EXPRESSION OF BAX, P53 AND BCL-2 IN THE HIPPOCAMPUS, CEREBELLUM AND CEREBRAL CORTEX.

X. Qian¹, M. Zhao¹, X. Cao², D. Wang³, X. Cui³, J. Liu³, ¹NIEHS/NIH, BIDG 101, MD F2-04, Res. Triangle Park, NC 27709, ²Department of Pathology, Lanzhou General Hospital, Lanzhou 730050, Gansu Province, China; ³Beijing Institute of Radiation Medicine, Beijing 100850, China.²

OBJECTIVE: With primary observing the expression changes of Bax, P53 and Bcl-2 in the hippocampus, cerebellum and cerebral cortex after the rats were irradiated by EMP, to explore the possible brain injury mechanism.

METHODS: 80 Wistar rats(40 males and 40 females) were divided into irradiated groups and control

group. A high field strength EMP simulator, which provides 2.5 pulses/min with a high electric field intensity 60 KV/m, 20-nsec rise time and 25 μ s pulse wide being used in this study. Irradiated groups were irradiated by high field strength 5 EMP(electromagnetic pulse, EMP) within 2 minutes respectively, no treatment to control group, then the rats were killed at 1h, 6h, 12h,24h and 48h separately. Immunohistochemical method was used to investigate the expression of Bax, P53 and Bcl-2 in the hippocampus, cerebellum and cerebral cortex and stereological analysis for positive cells at 12h time point after irradiating were performed by CMTAS- II image analysis system at a magnification 400. *All data was analyzed by SPSS8.0 software.*

RESULTS: The decreasing expression of Bcl-2 were showed in the hippocampus, cerebellum and cerebral cortex at as early as 6h, the strongest expression were at 12h. There were increasing expression of Bax and P53 in the different brain areas, especially in hippocampus and cerebral cortex at 12h.

CONCLUSION: It is inferred that EMP promoted apoptosis in the hippocampus, cerebellum and cerebral cortex after the rats were irradiated by EMP, and Bax, P53 and Bcl-2 are supposed to play an important role in the injury of rats brain. The hippocampus and cerebral cortex are more sensitive to the EMP than the cerebellum, it is probably related with the non-thermal effects.

P-C-105

STUDENT

INDUCTION OF SECONDARY METABOLISM BY PULSED ELECTRIC FIELD IN SUSPENSION CULTURES OF *TAXUS CHINENSIS*. H. Ye, L.L. Huang, S.D. Chen¹, Key Laboratory of Optical and Magnetic Resonance Spectroscopy, East China Normal University, 3663 North Zhongshan Road, Shanghai 200062, China.

The effects of pulsed electric field (PEF) on the growth and secondary metabolite accumulation by plant cell cultures were studied. Suspension cultures of *Taxus chinensis* in different cell growth phases were exposed to a PEF (50Hz, 10⁵v/cm) for various periods of time. A significant increase in intracellular accumulation of taxuyunnanin C (Tc), a bioactive secondary metabolite, was observed by exposing the cells in early exponential growth phase to a 30-min PEF. The Tc content (*i.e.* the specific production based on dry cell weight) increased by 30% after exposure to PEF, without loss of biomass compared with that of the control. Combination of PEF with sucrose feeding showed a synergistic effect on the improvement in the secondary metabolite accumulation. Production of reactive oxygen species (ROS), extracellular Tc and phenolics was all enhanced with PEF treatment, which suggests that PEF induced the defense response of plant cells and may also have altered cell membrane permeability. The work indicates that PEF is a promising new abiotic elicitor for stimulating secondary metabolite biosynthesis in plant cell cultures.

P-A-106

EFFECT OF EXPOSURE TO STATIC MAGNETIC FIELDS ON ENDOTOXIN-INDUCED NITRIC OXIDE PRODUCTION IN ORGAN CULTURED RAT AORTA. T. Kishimoto^{1,2}, H. Masuda¹, A. Ushiyama¹, S. Hirota¹ and C. Ohkubo¹. ¹Department of Environmental Health, National Institute of Public Health, Tokyo 108-8638, Japan. ²Department of Science, Pip Tokyo Co., Ltd., Tokyo 101-8528, Japan.

OBJECTIVES: Nitric oxide (NO), which was reported its production may be modified by magnetic fields, plays an important role in vascular physiology. In addition, several findings about the physiological effects of static magnetic fields (SMF) on blood vessel were recently reported. The aim of the present study was to investigate whether SMF affect on inducible NO producing system which closely relates to the pathogenesis of septic shock and several vascular inflammatory lesions.

METHODS: To evaluate the changes in inducible NO producing system, we measured the production of

nitrite, a metabolite of NO, in organ cultured rat aorta. Aortic rings isolated from Wistar rats were incubated in culture medium with or without lipopolysaccharide (LPS, 5ng/ml) at 37°C under 95% air and 5% CO₂. Each petri dish for organ culture was placed on a discal permanent magnet (SMF group) or a dummy magnet (sham group). Magnetic flux density of aortic rings in the petri dish was 80mT. To find the effects of SMF exposure, we incubated the aortic rings under two kinds of SMF exposure conditions, 1) 48 hrs exposure to SMF with or without LPS application, 2) 72 hrs exposure to SMF that was included 24 hrs exposure to SMF alone before 48 hrs exposure to SMF with LPS application.

RESULTS: Application of LPS increased the nitrite accumulation in culture medium with time-dependent manner for 48 hrs. At the end of the incubation of aorta with LPS for 48 hrs, the immunohistological analysis recognized a strong positive immunoreaction to inducible form of nitric oxide synthase (iNOS) in smooth muscle layer of the aorta, but it did not recognized in the aorta incubated without LPS. Besides, the increase in nitrite accumulation was inhibited by aminoguanidine, a specific inhibitor of iNOS. In the aorta exposed to SMF for 48 hrs, there was no difference in the level of nitrite accumulation between sham and SMF group. During SMF exposure for 72 hrs, the time-dependent increase in nitrite accumulation in SMF group was similar to that in Sham group.

CONCLUSIONS: Application of LPS induced nitrite production accompanied by an expression of iNOS protein in cultured rat aorta. The exposure to SMF, however, had no effect on the inducible nitrite production under present conditions. These results suggest that SMF dose not affect inducible NO producing system in rat aorta under endotoxic conditions.

P-B-107

NITRATION PATHWAYS ACTIVATED IN MACROPHAGE CELLS TREATED WITH PLASMA FROM 35GHZ MMW EXPOSED RATS. R. Sypniewska³, J. Kiel¹, N. Millenbaugh³, J. Kalns⁴, R. Blystone⁴, P. Mason², C. Cerna⁴, B. Brott⁴, M. Tarango³, H. Coppage⁵, N. Pedrick⁵, J. Tan⁵, F. Witzmann⁵. ¹Air Force Research Laboratory, Biosciences and Protection Division, Brooks City-Base, TX, ²Air Force Research Laboratory, Directed Energy Bioeffects Division, Brooks City-Base, TX, ³General Dynamics Advanced Information Systems, San Antonio, TX, ⁴Trinity University, Department of Biology, San Antonio, TX, ⁵Dept. of Cellular & Integrative Physiology, Indiana University School of Medicine, Indianapolis IN, USA.

OBJECTIVES: Determine nitrated protein expression in cells stimulated by plasma of rats exposed to following prolonged exposure (up to 45 min) of rats to prolonged 35 GHz (75 mW/cm² for up to 45 min) and elucidation of their direct or indirect influence on the signaling pathways of cells affected by the plasma.

INTRODUCTION: Our previous study indicated that prolonged long term (1hr) overexposure of rats to millimeter waves to 35 GHz MMW can lead to release of several acute phase proteins into the plasma several acute phase proteins (Radiation Research mMeeting, August, 2003). Based on the identity of those proteins, it has been hypothesized that a non specific protective and systemic response was activated. One of the fast responder cell types to circulating mediators are ubiquitous macrophages. Those cells can be stimulated and relay information pass the message through nitration, phosphorylation, or other modifications of signaling cellular proteins.

Our current interest is in the nitrated proteins of MMW exposed rat plasma itself and their influence on the signaling pathways of cells affected by the flow of the plasma. Preliminary experiments revealed that rat macrophage cells CRL-2192 cultivated with plasma from 35 GHz- exposed animals had changed morphology. To further characterize this phenomenon, the present experiment was designed to which will detect changes in nitrated proteins in theof reporter rat macrophage cell line CRL-2192.

METHODS: Male Sprague-Dawley rats (350-400 g) were anesthetized with 5% isoflourane and either sham-exposed or exposed to 35-GHz MMW at 75mW/cm² or environmental heat at 41-42°C throughout the exposure period. The MMW rats were exposed over the left, shaved, lateral flank area. The body

surface temperature was recorded using infrared thermography and showed an increase to 41-42°C. Following exposure, rats were allowed to recover and plasma samples were collected at 24 hr post-exposure. Plasma from 35-GHz exposed rats exposed to 35 GHz, heat exposed, (42 degree C) and sham-exposed animals was added to the cultures of the CRL 2192 rat macrophage cell line for 24 hr stimulation. Subsequently cells were harvested, and their protein lysates were separated on 2-D gels, followed by transfer to PVDF membranes on which only nitrated proteins were visualized by Western Blot protocol.

RESULTS: The 2-D gel image analysis revealed the differential expression of 53 proteins (cControl vs. MMW, $P < 0.005$) in 35 GHz. Nitrated proteins and differentially expressed proteins were cut from the gels and identified by peptide mass fingerprinting. This accomplishment provides the very first information about the activation of the nitrated pathways by the mediators present in the plasma of 35 GHz exposed animals. In addition, 34 proteins whose nitration pattern expression was altered by interferon gamma (positive control) were also subjected to peptide mass fingerprinting. Results indicate that the activation of the cells by interferon gamma is different than by mediators in the plasma.

CONCLUSION: Pattern of nitrated proteins from the positive control (LPS and interferon gamma) is different than from CRL 2192 rat macrophage stimulated with plasma from 35 GHz overexposed rat or Sham or EH control. Results from this study will answer the question, showed that if prolonged exposure of rats 35 GHz overexposure in rat model can lead to the release of stimulating mediators in plasma increasing the presence of nitrated proteins as plasma components activating the nitration pathways in macrophages. Specific identification of those nitrated proteins (53 spots) can help in elucidation of the nitration pathways associated with prolonged 35 GHz exposure.

This research was funded, in part, by the Air Force Office of Scientific Research.

P-C-108

METHOD FOR ESTIMATION OF STIMULATING POINTS BASED ON STRUCTURE OF CORTEX IN TRANSCRANIAL MAGNETIC STIMULATION. O. Hiwaki. Faculty of Information Sciences, Hiroshima City University, 731-3194 Hiroshima, Japan.

INTRODUCTION: Transcranial magnetic stimulation (TMS) is a non-invasive and painless method to map regions of the cortex. Exact estimation of stimulating points is much important to evaluate cortical functions such as cortical motor output maps. However, most studies using TMS did not take the individual cortical anatomy and property of nerve excitation into account; thereby the estimated stimulating points could not be trustworthy.

OBJECTIVE: This study proposed a novel method to provide exact estimation of stimulating points of the cortex in TMS.

METHODS: This method is based on the cortical anatomy and excitation property of nerve fiber. All apical dendrites of pyramidal cells are oriented perpendicular to the surface of the cortex. Furthermore, the theoretical model shows that induced electric fields parallel to a nerve fiber elicit nerve excitation optimally at the endpoint of the nerve fiber. Therefore, the points on the cortical surface with the maximal value of the induce electric field perpendicular to the surface can be estimated as the stimulating points in TMS. The components of the induced electric fields perpendicular to the cortical surface were calculated using magnetic resonance imaging (MRI) of the brain. We conducted TMS mapping of the motor cortex to confirm the reliability of this method.

RESULTS: Motor evoked potentials of the higher extremity to TMS of the contralateral hemisphere were measured. Cortical representation of the motor area was obtained by the proposed method. The points innervating each muscle were distinguished in the motor area.

P-A-109

WITHDRAWN

P-B-110

STUDENT

ESTIMATION OF THE MUSCLE FIBER DIAMETER BASED ON DIFFUSION MAGNETIC RESONANCE IMAGING. T. Saotome^{1,2}, M. Sekino¹, F. Etou², S. Ueno¹. ¹Department of Biomedical Engineering, Graduate School of Medicine, University of Tokyo, ²Department of Rehabilitation Medicine, Graduate School of Medicine, University of Tokyo, 113-0033, Japan.

INTRODUCTION: A prolonged bed rest due to diseases or traumatic injuries causes weakness and atrophy of skeletal muscles. Rehabilitation aims at recovery of extensibility and endurance of muscles by trainings. The manual muscle test (MMT) is a simple and widely used method for evaluating the effect of the training. However, the MMT does not provide a completely objective criterion. In this study, we propose a method for estimating the muscle fiber diameter based on diffusion magnetic resonance imaging (MRI). This method has a potential application in quantitative and objective evaluations of the atrophy and the recovery process of skeletal muscles.

MATERIALS AND METHODS: A normal male Wistar rat (350 g) was anesthetized by inhalation of diethyl ether and a subsequent intraperitoneal injection of urethane (1.5 g/kg). Measurements were performed using a 4.7 T MRI system. The stimulated echo acquisition mode (STEAM) [1] sequence was used to obtain signals from a 4×4×4 mm³ voxel located on the gastrocnemius muscle. Diffusion signal

attenuations were measured with q gradients up to $q (= \gamma\delta g/2\pi) = 84 \text{ mm}^{-1}$, where γ is the gyromagnetic ratio of ^1H , g and δ are intensity and pulse duration of the q gradient. The q gradient was applied in the six directions shown in figure 1. The diffusion coefficient D of water in the muscle fibers was estimated from the diffusion signal attenuation in the direction parallel to the muscle fibers using an equation $E(q) = \exp\{-4\pi^2 q^2 D(\Delta - \delta/3)\}$ [2]. The muscle fiber diameter was estimated by fitting an equation derived by Tanner et al. [3] to the diffusion signal attenuation in the direction perpendicular to the muscle fibers.

RESULTS AND DISCUSSION: Figure 2 shows diffusion signal attenuations measured with the six q gradient directions. The signal attenuations exhibited a high anisotropy because diffusion of water was restricted in the direction perpendicular to the muscle fibers due to membrane structures. The fastest attenuation was observed in the case that the q gradient was applied in the direction parallel to the muscle fibers. Figure 3 shows the signal attenuation and a fitted curve for this q gradient direction. In this direction, the signal attenuation depends only on the diffusion coefficient of water because diffusion of water is not restricted by the membrane structures. An estimate of the diffusion coefficient of water was $1.9 \times 10^{-3} \text{ mm}^2/\text{s}$. Figure 4 shows the signal attenuation measured with the q gradient direction perpendicular to the muscle fibers and a fitted curve. The signal attenuation with this q gradient direction reflects both the diffusion coefficient of water and membrane structures. The muscle fiber diameter was estimated as $15 \mu\text{m}$ using the Tanner's equation. This method is non-invasive, and useful for quantitatively evaluating atrophy and recovery process of muscles.

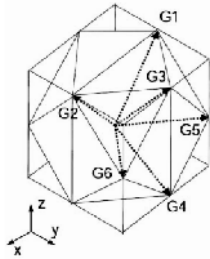


Figure1: Directions of q gradients.

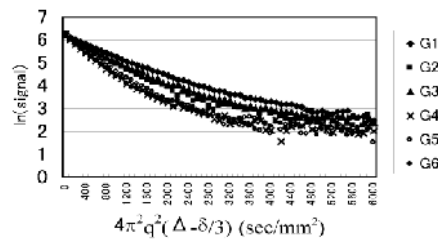


Figure2: Diffusion signal attenuations of the rat gastrocnemius muscle for the six directions of q gradients.

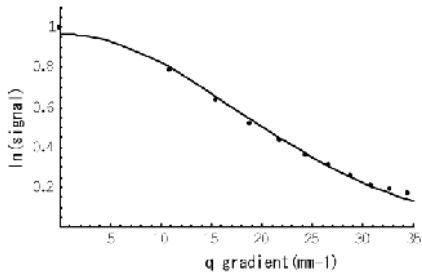


Figure3
Signal attenuations and fitted curves for the q gradient directions parallel (Figure 3) and perpendicular (figure 4) to the muscle fibers.

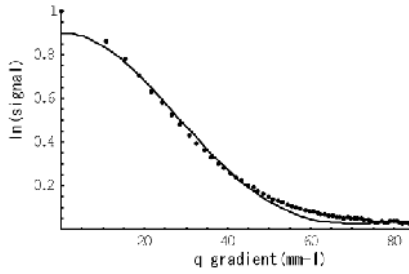


Figure4

References.

- [1] K. D. Merboldt, D. Horstmann, W. Hanicke, H. Bruhn, and J. Frahm, *Magn. Reson. Med.* 29, 125 (1993).
- [2] E. O. Stejskal and J. E. Tanner, *J. Chem. Phys.* 42, 288 (1965).
- [3] J. E. Tanner and E. O. Stejskal, *J. Chem. Phys.* 49, 1768 (1968).

INSTRUMENTATION AND METHODOLOGY

P-C-111

ELECTROPHYSIOLOGICAL PROPERTIES OF HIPPOCAMPAL SLICES FROM MICE EXPOSED TO 900MHz GSM FIELDS. A.J. Smith, P.K. Harrison, G. Underwood and J.E.H. Tattersall. Biomedical Sciences Department, Dstl Porton Down, Salisbury, Wiltshire SP4 0JQ, UK.

OBJECTIVE: Previous studies have suggested that *in vitro* exposure to 700MHz radiofrequency (RF) fields can affect both evoked and spontaneous electrical activity in rat hippocampal slices, an effect which lasted beyond the end of the exposure period (Tattersall et al, 2001). The aim of the present study was to determine whether *in vivo* exposure of mice to 900MHz fields results in electrophysiological changes in brain tissue, using sensitive *in vitro* techniques. This work forms part of a larger study in which effects of the exposure on behaviour and gene expression are also being studied.

METHODS: Adult male C57BL mice (25-30g) were restrained in Perspex “rockets” and exposed to unmodulated 900MHz or 900MHz GSM fields (36 W.kg^{-1}) for 1 hour using a head-only loop antenna system. Sham-exposed control mice were treated in the same way, but the RF signal was not switched on. Immediately following exposure, the mice were anaesthetised with halothane and decapitated, and parasagittal slices of brain tissue (400 μm thick) containing the hippocampus were prepared. The slices were maintained at $32.0 \pm 0.1^\circ\text{C}$ and perfused with artificial cerebrospinal fluid. Extracellular field potentials were recorded in CA1 stratum pyramidale using glass microelectrodes filled with 2M NaCl. Responses were evoked every 30s by a concentric bipolar stainless steel stimulating electrode placed in stratum radiatum. Constant current pulses (70 μs duration) were delivered at increasing intensities to characterise stimulus-response relationships for the field excitatory postsynaptic potential (fEPSP) and population spike (PS). These were also used to derive the E-S relationship between the fEPSP and PS. A paired-pulse protocol (two stimuli separated by 25ms) was used to characterise facilitation and inhibition of field potentials. Finally, the ability of the slice to express long term potentiation (LTP) was determined using theta burst stimulation 5 trains of 4 pulses at 100Hz separated by 200ms, repeated twice with an interburst interval of 10s (Morgan and Teyler, 2001). LTP was evaluated by the change in fEPSP and PS 1h after theta burst stimulation and by the change in the E-S relationship. The investigators recording and analysing the slice data were blind to the exposure conditions for each animal.

RESULTS: No significant differences in any of the parameters measured were found between slices from sham exposed animals and those from animal exposed to 900MHz fields. The statistical power of the study was estimated as 90% to detect, for example, a change of 70 μA in EPSP or PS threshold and a change of 44% in EPSP or PS LTP.

DISCUSSION: The lack of any significant changes in hippocampal electrophysiology following exposure to 900MHz fields is consistent with the absence of behavioural effects in mice exposed to the same fields in an identical system (Bottomley et al, Bioelectromagnetics Society Abstracts 2004). Future experiments will examine the effects of exposure to TETRA (400MHz) and UMTS (2200MHz) signals on these parameters, as well as the effects of repeated exposures.

The work was supported by the Mobile Telecommunications and Health Research Programme but the views expressed are those of the authors.

References

- Morgan, S. L. and Teyler T. J.. Electrical stimuli patterned after the theta-rhythm induce multiple forms of LTP. *J. Neurophysiol.* 86: 1289–1296, 2001.
- Tattersall J. E. H., Scott I. R., Wood S. J., Nettell J. J., Bevir M. K., Wang Z., Somasiri N. P., and Chen X. Effects of low intensity radiofrequency electromagnetic fields on electrical activity in rat hippocampal slices. *Brain Res.* 904: 43-53, 2001.

P-A-112

EFFECTS OF CONTINUOUS WHOLE-BODY EXPOSURE TO 50 Hz ELECTROMAGNETIC FIELDS WITH TRANSIENT MAGNETIC FIELDS IN MICE WITH BRAIN TUMOR.

A. Ushiyama¹, Y. Suzuki², H. Masuda¹, S. Hirota¹, M. Taki², C. Ohkubo¹. ¹Department of Environmental Health, National Institute of Public Health, Tokyo, Japan. ²Department of Electrical Engineering, Tokyo Metropolitan University, Tokyo, Japan.

OBJECTIVE: The goal of this study was to explore subchronic effects of whole body exposure to ELF-EMF with transient magnetic fields on implanted brain tumor growth and tumor microcirculation within a mouse cranial window (CW). To evaluate the exposure effects of 50Hz EMF with transient magnetic fields *in vivo*, we quantified the growth of implanted brain tumor and microcirculatory parameters of brain tumor tissue including vessel permeability.

METHODS: We employed a mouse CW technique, allowing for the chronic observation of cerebral microcirculation, and a brain tumor implantation model using the CW. Male SCID (severe combined immuno-deficiency) mice were used in this study. One week after CW installation, the window was opened and a small piece of human glioma U87 tissue grown in a source mouse was implanted into the center of the CW. Then, mice were divided into two groups: exposure and sham groups. In the exposure group, mice were subchronically exposed to a combination of 50 Hz EMF at 3.0 mT (rms) with repetitive transient magnetic fields (1 burst/s, 7.4 kHz waves with duration of 50 msec and peak magnet density of 162 μ T) for 16 days (15 hours/day: 7 p.m. to 10 a.m.) following tumor implantation. During and after the exposure, we measured the size of tumor, microcirculatory parameters of angiogenic vessels in the growing tumor by real-time confocal microscopy, and vascular permeability of rhodamine-labeled albumin using a photon counting system.

RESULTS: Although tumor size increased markedly following implantation, tumor growth did not show any significant difference between the exposure group and control group. Tumor angiogenesis was also induced inside and around the tumor tissue, however, ELF-EMF with transient magnetic fields did not affect any of the microcirculatory parameters of these angiogenic vessels, that is, vascular density, mean diameter and numbers of branched vessels.

CONCLUSIONS: We have shown that no possible pathophysiological effect in the brain tumor microcirculation was induced by the subchronic and combined exposure of 50 Hz (3 mT) and transient magnetic fields. The growth rate of implanted brain tumor tissue was also unaffected by the present exposure conditions.

P-B-113

NO EFFECT FROM 900 MHZ ELECTROMAGNETIC FIELDS ON THE SPONTANEOUS DEVELOPMENT OF LYMPHOMA IN FEMALE AKR/J MICE.

A.M. Sommer¹, A. Bitz², J. Streckert², V. Hansen², A. Lerchl¹, ¹School of Engineering and Science, International University Bremen, D-28759 Bremen, ²Chair of Electromagnetic Theory, University of Wuppertal, D-42097 Wuppertal, Germany.

BACKGROUND: Several reports indicate that non-thermal electromagnetic radiation, such as that from mobile phones and base stations, may be carcinogenic [1,2]. However, the overall literature is not consistent [3]. Therefore, it was investigated experimentally whether GSM-like electromagnetic fields affect lymphoma development in a mouse strain which is viremic from birth and spontaneously develops thymic lymphoblastic lymphoma within one year.

OBJECTIVE: Experimental investigation to determine whether 900 MHz electromagnetic field exposure influences lymphoma induction in a mouse strain that is genetically predisposed to this disease.

METHODS: 48 groups of 6-7 unrestrained female akr/j mice were sham-exposed or exposed (n = 160

animals) by use of a radial waveguide setup [4] to gsm-like 900 mhz electromagnetic fields for 24 hours per day, 7 days per week. Average whole body sar was 0.4 w/kg. Animals were visually checked daily for signs of a developing disease and were weighed and palpated weekly to detect swollen lymph nodes. Starting at the age of 6 months, blood samples were taken monthly from the tail to perform differential leucocyte counts. Animals with signs of disease or with an age of about 42 weeks were sacrificed and a gross necropsy was performed.

RESULTS: There was no effect of electromagnetic field exposure with average whole body SAR values of 0.4 W/Kg on body weight gain or survival rate, and lymphoma incidence did not differ between exposed and sham-exposed animals.

CONCLUSION: These data do not support the hypothesis that exposure to 900 MHz electromagnetic fields is a significant risk factor for developing lymphoma in a genetically predisposed mouse species.

References.

- [1] Mashevich M, Folkman D, Kesar A, Barbul A, Korenstein R, Jerby E, Avivi L (2003) Exposure of human peripheral blood lymphocytes to electromagnetic fields associated with cellular phones leads to chromosomal instability. *Bioelectromagnetics* 24(2):82-90.
- [2] Repacholi MH, Basten A, Gebiski V, Noonan D, Finnie J, Harris AW (1997) Lymphomas in E μ -Pim 1 transgenic mice exposed to pulsed 900 MHz electromagnetic fields. *Radiat Res* 147(5):631-40.
- [3] IEGMP (2000) *Mobile phones and health. Report of an independent expert group on mobile phones.* UK Minister of Public Health. National Radio Protection Board, Chilton, Oxon: www.iegmp.org.uk.
- [4] Streckert, J., Bitz, A., Hansen, V., Buschmann, J., High SAR exposure of 24 rats at 900 MHz: problems of temperature limits and uniform field distribution, Millenium Workshop on Biological Effects of Electromagnetic Fields, Heraklion, Greece, October 2000, 185-195.

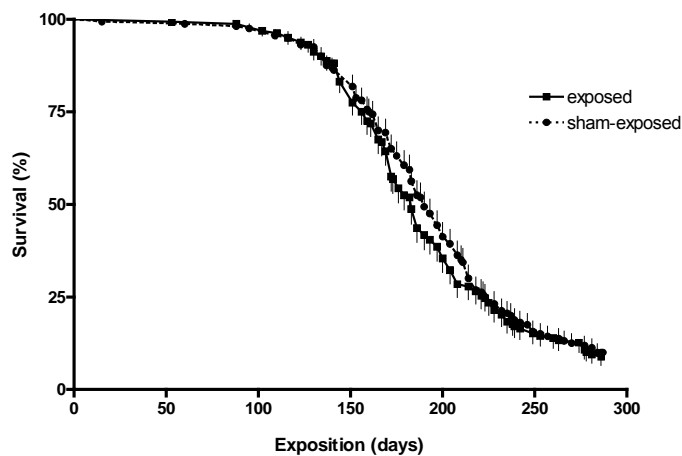


Figure 1: No significant differences in the survival proportion were seen between exposed and sham-exposed female AKR/J mice at average whole body specific absorption rates of 0.4 W/Kg. Data are given as % of 160 animals \pm standard error of the mean.

This study was part of a project supported by the Bundesamt für Strahlenschutz, St. Sch 4315: “Wirkung chronischer Exposition mit einem athermisch wirkenden GSM-Mobilfunksignal auf die Entwicklung spontaner lymphatischer Leukämie bei frei beweglichen weiblichen Mäusen des AKR/J-Stammes”.

P-C-114

EFFECTS OF HEAD-ONLY EXPOSURE TO RADIOFREQUENCY FIELDS ON LEARNED BEHAVIOUR IN MICE. A.L. Bottomley, R. Bartram, R.P. Blackwell, R.G.E. Haylock and Z.J. Sienkiewicz, National Radiological Protection Board, Chilton, Didcot, Oxfordshire, OX11 0RQ, UK.

OBJECTIVE: This work investigates the possibility that head-only exposure to radiofrequency (RF) fields associated with mobile telephones can induce changes in brain physiology and function. The specific objective is to seek evidence of RF-induced changes on learned behaviour in mice.

METHODS: Adult, male C57BL/6J mice were habituated to restraint as required for exposure in a head-only loop antenna system. These animals were subsequently trained in seven sessions to locate a submerged escape platform in a Morris water maze. After the last training session, animals were randomly allocated to a treatment group and then tested in a probe trial during which the escape platform was removed. Treatment consisted of 60 min exposure to either 400, 900 or 2200 MHz unmodulated or modulated fields at specific energy absorption rates (SARs) ranging from 0 to 36 Wkg⁻¹. SAR values were determined using finite-difference time-domain techniques and measurements on mouse cadavers with fibre optic thermometers. A further group of naïve animals were trained solely in the watermaze and used as cage controls. During acquisition of the task, latency to reach the platform, swim pattern and swim speed were analyzed for each treatment group. Percentage of time in the quadrant that had contained the platform, and relative frequency of visits to the platform location were also scored during the probe trial. All experiments were performed blind.

RESULTS: Using model fitting techniques to analyze the results, no significant field-dependent effects were found on the indices of performance examined during the probe trial. Animals from all treatments spent more time in the quadrant where the platform was located during acquisition, and visited the relative platform location with increased frequency, suggesting that there was no impairment in spatial memory. The cage control group, however, was less able to locate the platform during the acquisition trials, less active in the pool, and did not spend as high a percentage of time in the platform quadrant during the probe trial. This impaired ability of the cage controls may be associated with the reduced handling of the animals before the onset of the acquisition trials.

DISCUSSION: The results of this work provide an initial assessment of the effects of TETRA-, GSM- and 3G-type signals on learned behaviour in mice. No detrimental effects were observed on the animals' ability to perform a water maze task. Continuation of the work will examine if repeated exposure to 900 MHz impairs the animals acquisition of this task.

The work was supported by the Mobile Telecommunications and Health Research Programme but the views expressed are those of the authors.

P-A-115

ARE THERE ANY HEALTH CONSEQUENCES OF CHRONIC EXPOSURE TO GSM- OR UMTS-FIELDS? RESEARCH PROJECT ON EVENTUAL COGNITIVE, IMMUNOLOGICAL, AND BLOOD-BRAIN-BARRIER EFFECTS IN THREE GENERATIONS OF RATS. M. Bornhausen¹, S. Okorn¹, M. Stangassinger¹, M. Erhard², M. Stohrer¹, J. Detlefsen³, S. Schelkshorn³, J. Eberle⁵, O. Petrowicz⁴. ¹Institutes of Animal Physiology and ²Animal Welfare, Faculty of Veterinary Medicine, Ludwig-Maximilians-University Muenchen; ³Institute of High-Frequency Engineering HFS, Department of Electrical Engineering and Information Technology, ⁴Institute of Experimental Oncology, Faculty of Medicine, and ⁵Council of the Technical University Muenchen, Germany.

In response to a research initiative of the German Federal Office of Radiation Protection (BfS) on alleged effects of chronic exposure to electromagnetic fields (EMFs) of mobile communication, an interdisciplinary cooperation between several institutes of the Ludwig-Maximilians-University (LMU) and the Technical University of Munich (TUM) has obtained a research contract with the following outlines: Three consecutive generations (F0, F1, F2) of Wistar rats will be continuously exposed within the framework of a

double-blind study to either GSM- or UMTS-EMFs in HF-exposure chambers (80x80x200 cm³) provided by T-Systems Nova GmbH. In a first experiment, the SAR values for GSM- and UMTS-exposure will be identical to those of human exposure levels (0.4 W/kg). Regarding the particular sensitivity and vulnerability of the central nervous system during development, our experiment focuses on the assessment of eventual cognitive or learning ability deficits in chronically and prenatally exposed rats. For that purpose the rats of the three generations will be confronted with a sequence of 9 different operant-behavior performance tests (differential reinforcement of high or low rate and combinations) with increasing learning demand (3 DRH, 3 DRL, 3 COM). Test sessions are run automatically during night. Test performance (lever presses, food reinforcements, test efficiency) of each animal is stored and related to the occurrence of test-specific inter-response interval (IRI) pattern. Part of our experiment thus replicates previous work published in *Bioelectromagnetics* 21:566-574, 2000 where a prenatal EMF exposure (17.5-75 mW/kg SAR) did not induce any changes of operant-behavior performance relative to controls. In order to minimize inter-individual variability among the members of a test group and to enhance statistical power, all subjects of this experiment, however, will be preselected by appropriate measures of IRI dynamics. Resulting test groups, thus, will represent subjects showing a better performance than the group mean. Our experiment will include the assessment of conventional parameters of health and reproduction including developmental landmarks in dams and their offspring. Additional experiments are being prepared to detect eventual EMF-induced changes of biochemical reactions to stress, immunological responses, and those of the blood-brain-barrier in litter mates. Experimental protocols will respect the OECD-issued GLP rules.

P-B-116

STUDENT

THE POSSIBLE INFLUENCE OF MICROWAVES ON LEUCOCYTES: AN IN VIVO METHOD.

D. Adang^{1,2}, M.A. VanderVorst¹, ¹Catholic University Louvain, Emic Division, 1348 Louvain-la-Neuve, Belgium, ²ACOS Well Being, Epidemiology Division, 1120 Neder-over-Heembeek, Belgium.

INTRODUCTION: The lack of scientific consensus regarding the athermal long-term effects of microwaves forced the World Health Organisation to state that more scientific research is needed on this issue [1]. Very few people are exposed to thermally significant levels of microwaves. The big majority of exposures occur at levels at which weak-field interactions would be the only possible source of any adverse health response. There is a major deficiency in the understanding of the effects of pulsed fields in which very high peak power densities occur, separated by periods of zero power. Data to assess human health hazard in terms of pulse peak power, repetition frequency, pulse width and carrier frequency are needed in view of the widening application of systems using modulated signals like cellular phones and radar systems, involving both occupational and general population exposures. Today, the general use of radar systems for navigation, together with the extension of radio communication links and satellite communication into the microwave frequency range, has meant a wider need for engineers and physicians to investigate the possible harmful effects of microwaves on the human body. It is of a vast importance to assess the range of microwave effects in relationship to the human health. An increased or decreased presence of a biological parameter does not necessarily indicate any pathological process, but may be a useful index for biological dosimetry of microwave exposure.

OBJECTIVES: The objective of the present study consists in verifying on an animal model the cellular alterations and possible biological modifications due to microwave exposure (1 GHz and 10 GHz), using both continuous and pulsed waves. In a first time, this study focuses on physiological changes of selected blood and hormonal parameters. Besides, different parts of the immune system – lymphocytes, monocytes, granulocytes – are used as a biological indicator for its good functioning.

MATERIAL AND METHODS: A possible causal link between radar radiation and the physiological and cellular changes is checked by an experimental study. The *Wistar albino* rat is used as a model. To reduce

as much as possible the stress factor, we have chosen for a new element in our research, namely a collective exposure in an exposure unit, suitable for 30 rats, instead of an individual exposure where the rat is caged in a small waveguide. The different groups of rats are exposed to microwaves at 1 GHz and 10 GHz, continuous and pulsed mode at an average power density of respectively $200 \mu\text{W}/\text{cm}^2$ and $500 \mu\text{W}/\text{cm}^2$. In order to determine the possible biological long-term effects of microwaves, we selected a series of tests based on the following parameters: blood cells, stress-induced hormones (adrenocorticotrophic hormone (ACTH) and corticosterone) and cytokines (interleukine (IL) I, IL VI, tumor necrosis factor a (TNF a)). Enzyme-linked immunosorbent assays (ELISA) are used to quantify those hormones in the blood plasma. Food and water intake are recorded too. Daily observations of the rats' behaviour are part of the protocol. The first series of experiments run at a frequency of 1 GHz. At the end of the third month, three animals of each group are sacrificed and are object to histopathology. To identify the rats during the whole experiment (one year) in general and during blood sampling in particular, an unmistakable method to distinguish one rat from another has been thought out. The ear of the rat is pierced following a formerly established pattern of figures.

RESULTS: The first definitive results are expected in the summer of 2004.

References

Repacholi, M., Low-level exposure to radiofrequency electromagnetic fields: health effects and research needs. *Bioelectromagnetics*, **19** (1), pp.1-19, 1998.

P-C-117

STUDENT

MAINLY-HEAD EXPOSURE SYSTEM FOR BEHAVIORAL STUDIES WITH A SMALL NUMBER OF MICE AT 900 MHZ. S.J. Eom, J. Fröhlich, N. Nikoloski, N. Kuster. Foundation for Research on Information Technologies in Society (IT'IS), Swiss Federal Institute of Technology (ETH), Zurich, Switzerland.

INTRODUCTION: PERFORM-B is a two-year project that addresses replications of *in vitro* and *in vivo* studies that were recommended by the WHO agenda. One of these studies [1] reported reduced task performance of rats after exposure to pulsed 2.45 GHz fields. In addition to the replication (same exposure and species), the project foresees equivalent experiments at GSM exposures with mice and rats.

OBJECTIVE: The object of this study was to develop an exposure setup for mainly-head exposure of mice.

The requirements for the setup have been set as follows:

- 1.) Simultaneous exposure of two animals, stable and reproducible exposure, easy handling and cleaning, usage of non-toxic materials;
- 2.) Three different exposure levels (average brain SAR: approx. 0.1, 0.6 and 3 W/kg), exposure as uniform as possible in the brain, flexible modulation scheme;
- 3.) The exposure units shall be software controlled to enable double-blinded exposures;
- 4.) All the relevant parameters, such as sensor H-field, temperature and the ventilation status, shall be continuously monitored during the experiment.

METHODS: The evaluation and optimization of the setup was performed using the advanced FDTD simulation platform SEMCAD, including its thermal solver extension for the numerical assessment of the thermal load. The results were verified using the near-field scanner DASY4 equipped with the latest probe technology. The SAR assessment with a temperature method was performed with a highly resistive thermistor probe.

RESULTS: The 900 MHz rectangular waveguide was adopted for mono-mode excitation (TE₁₀) and symmetric exposure of two mice. The locations of the animals were determined to obtain the highest uniform exposure condition and absorption in the brain. For stable and reproducible results of mouse movements with higher efficiency, the H-field plane (wide wall) was chosen for mouse insertion. Good

performance of the mainly-head exposure setup was achieved when the numerical mouse model was located at a distance of 112.5 mm from the shortcut with an insertion depth of 34 mm from the inner metal surface of the waveguide. An airflow system supplies the necessary oxygen to the mice. The exposure is controlled using a calibrated H-field sensor located at the maximum H-field on the inner plane of the shortcut. For this case the relationship between the H-field at the sensor and whole-body SAR was validated using the experimental temperature method. The stopper for restraining the mouse or liquid dummy consists of electrically lossless material. The simulation results were experimentally validated by comparing the field distribution to the whole-body SAR in phantoms filled with muscle simulating liquid at 900 MHz. The numerical dosimetry was conducted with two high-resolution anatomical mouse models of 25g and represents the arrangement for the clinical experiments. The organ, head and whole-body SAR were determined, as well as the corresponding uncertainties. For the numerical analysis, the brain, head, and whole-body showed the specific absorption rates of 3.2 W/kg, 2 W/kg and 1 W/kg on the H-field of 1 A/m at the monitoring sensor, respectively. The thermal load of the animals and the phantoms was numerically assessed and verified experimentally using a high resistive thermistor probe.

Reference.

[1] Lai H, Horita A, Guy AW, Microwave irradiation affects radial-arm maze performance in the rat., *Bioelectromagnetics* 15:95-104, 1994.

The study was supported by the Mobile Manufacturers Forum(MMF) and the GSM Association(GSMA).

P-A-118

PHYSIOLOGICAL ROLE OF BLOOD FLOW ON ELEVATED SKIN TEMPERATURE INDUCED BY RF ELECTROMAGNETIC WAVES IRRADIATION IN RABBITS.

F. Jia, A. Ushiyama, H. Masuda, L.L. Traikov, C. Ohkubo. Department of Environmental Health, National Institute of Public Health, 4-6-1 Sirokanedai, Minato-ku, Tokyo 108-8638, Japan.

OBJECTIVE: RF electromagnetic wave energy emitted from the antenna of a mobile phone is partly absorbed by human skin surface, especially by the head. The blood flow plays an important role for regulating body temperature including skin tissue. The objective of this study is (1) to test whether the local SAR 2W/kg, the partial-body absorption guideline value of Ministry of Public Management, Home Affairs, Posts and Telecommunications of Japan, could induce any temperature changes in living tissue; (2) to investigate how blood flow can modify the elevated skin temperature due to RF electromagnetic wave energy absorption.

METHOD: Rabbits having a rabbit ear chamber (REC) which enable to observe and evaluate cutaneous microcirculatory events including vasomotion by use of intra-vital microscopy were used. Japanese domestic white rabbits (Tokyo Jikken Dohbutsu Inc., Tokyo, Japan) of adult male weighing 2.5-4.0 kg were used for the experiment. The rabbits were housed in cages equipped with an automatic water-cleaning system. They were given free access to laboratory chow (RM4, Funabashi Nohjoh Inc., Chiba, Japan) and tap water *ad libitum*. The breeding house was automatically adjusted to 12 hour light/dark cycle, temperature at $21.5 \pm 0.5^\circ\text{C}$ with $50 \pm 5\%$ R.H. During exposure to microwaves, rabbit was kept prone in an acrylic cylindrical drum, his eyes were covered with an eye mask to prevent an emotional stress, and the fur of ears was shaved for the measurement of precise temperature of skin surface. Prior to the experimental procedure, rabbits were accommodated in the acrylic cylindrical drum kept at an anechoic shield chamber more than 5 times during one-week time. Before start of irradiation of microwaves, almost 30 minutes were given to stabilize the emotion of rabbits. REC was surgically implanted, and 6 weeks later regenerated subcutaneous tissue with a thickness of about 50 micron in which cutaneous microvasculature including arterioles, capillaries, venules and microlymphatics were clearly observed by microscope. Average exposure intensities to rabbit ear were controlled as SAR 0W/kg, 2W/kg, and 30W/kg, respectively. An anechoic chamber (Tokin EMC Engineering Inc., Kawazaki-shi, Japan) equipped with a fan ventilation system whose ventilation rate was $2.0 \text{ m}^3/\text{min}$ was used for the exposure experiment for maintaining

chamber temperature constant. For the dosimetry, we used a jelly phantom (Wireless Laboratories, NTT DoCoMo Inc., Japan) and surgically isolated rabbit ear. The composition of the jelly phantom (weight%) was TX150 8.5%, powder polyethylene 15.2%, 0.9% of NaCl, and 75.4% of pure water, and the specific heat of phantom was 3600J/kg□. Microwave, 1,500MHz electromagnetic near-field which in near the frequency band for PDC system (1429-1453MHz), was emitted from RF electromagnetic wave generating system (Anritsu MG 3660A Digital Modulation Signal Generator, Japan and A1020-4040-R RF Power Amplifier, Wireless Laboratories, NTT DoCoMo Inc., Japan). A microscope (specially made by Olympus Optical Co., Ltd. Tokyo, Japan), equipped with a special long working distance object lens (M Plan Apo, Mitsutoyo, Inc. Tokyo, Japan), was used for the observation of microvascular dynamics in REC. The object stage of the microscope was specially made from acrylic board. A loop dipole antenna (Wireless Laboratories, NTT DoCoMo Inc., Japan) with an internal diameter of 42mm was embedded into the acrylic stage. A piece of foamed polystyrene board with a thickness of 20mm was placed upon the antenna, and rabbit ear was fixed flat on the surface of this board with double-sided adhesive tape. Vasomotion, spontaneous rhythmic oscillation of calibers in arterioles within REC were recorded by the CCD video camera system (CV-2000, KEYENCE Corp. Tokyo, Japan), and were analyzed with image shearing monitor (Instrumentation for Physiology & Medicine Inc., San Diego, California 92119). Erythrocyte flow was measured with high-speed CCD video camera system (FASTCAM-Net 500/1000/Max, Photron Ltd). The surface temperature of rabbit ear and phantom was measured with thermal video system (TVS-700, Nippon Avionics Co., Ltd. Tokyo, Japan). Time serial infrared image data from the thermal video system were analyzed using software (PE Professional, Nippon Avionics Co., Ltd. Tokyo, Japan). Changes in temperature and vasomotion were continually measured during 20 minutes exposure and 10 minutes recovery time. All data were collected very 5 minutes and compared among exposure intensities under with/without blood flow. No blood flow conditions were designed by occlusion of proximal part of the central artery of ear with soft rubber. Statistical analysis was evaluated by Kruskal Wallis test and Mann-Whitney test. All experimental procedures are adapted to ethic guidelines for animal experiment at National Institute of Public Health.

RESULT: Under no blood flow conditions, the local microwave irradiation at SAR 2W/kg and 30W/kg showed statistically significant increases in surface temperatures of rabbit ears compared with control conditions (0W/kg). However, under the physiological conditions with blood flow, microwave irradiation at SAR 2W/kg showed neither temperature increase nor difference from control conditions. The extent of skin temperature elevation due to microwave exposure at 30W/kg was also significantly reduced. Analysis of vasomotion is under going.

CONCLUSION: Present results showed that under physiological conditions accompanying normal blood circulation, blood flow could modify and reduce skin temperature elevation induced by RF electromagnetic wave irradiation. And no skin temperature elevation was recognized due to local exposure to 1,500 MHz microwave at SAR 2.0 W/kg under normal conditions.

This study is financially supported by NTT DoCoMo Inc., Japan. Authors express great appreciation to Drs. Uebayashi, Ohnishi, Yamaguchi and Nakamatsu for their useful suggestions and their kind cooperation.

P-B-119

SUPPRESSION OF PLASMA NOREPINEPHRINE DEPLETION IN RESERPINE-INDUCED HYPOTENSIVE WISTAR-KYOTO RATS EXPOSED TO 25 mT STATIC MAGNETIC FIELD. H. Okano^{1,2}, H. Masuda¹, C. Ohkubo¹. ¹Department of Environmental Health, National Institute of Public Health, Tokyo 108-8638, Japan. ²Department of Science, Pip Tokyo Co., Tokyo 101-8528, Japan.

OBJECTIVE: Characterizing the physiological effects of static magnetic fields (SMF) on blood pressure (BP) in both hypertension and hypotension remains an important area of research. Previously we found that whole-body exposure to SMF at magnetic flux density of **10.0 mT** (*B*_{max}) for 2–9 weeks suppressed and retarded BP elevation in stroke-resistant spontaneously hypertensive rats (SHR) by eliciting antipressor effects [1]. In addition, we have demonstrated that both local and whole-body exposures to SMF (1.0 mT [*B*_{max}] or 5.5 mT [*B*_{max}], for 30 min) modify the hypertensive and hemodynamic responses to a nitric oxide (NO) synthase inhibitor (L-NAME) and an adrenergic neurotransmitter (norepinephrine), by reducing BP in unanesthetized rabbits [2,3]. SMF in the mT range mediates hypotension, by antagonizing biochemical action, thereby inducing homeostatic effects, for example, by suppressing vasodilation and hypotension induced by an L-type voltage-gated Ca²⁺ channel blocker, nicardipine [2]. However, the effect of SMF on hypotension in reserpine-treated animals has not yet been investigated, and the mechanism by which SMF might inhibit the hypotensive actions of reserpine is still unknown. This study examines the hypothesis that SMF may influence catecholamine dynamics in reserpine-induced hypotensive Wistar Kyoto rats (WKY) and suppress reduced BP. Specifically, this investigation was designed to evaluate mT intensities and spatial gradients of SMF on WKY, and to elucidate how SMF influences cardiovascular parameters and catecholamine-related biological pathways and responses.

METHODS: Seven week-old male rats were exposed to two different ranges of SMF intensities, 3.0–10.0 mT (*B*_{max}) or 7.5–25.0 mT (*B*_{max}) for 12 weeks. The SMF exposure device (L, 41 cm; H, 16 cm; W, 29.6 cm, PIP Fujimoto Co., Ltd., Osaka, Japan) was composed of a pair of rectangular magnetic plates (L, 41 cm; H, 16 cm; D, 0.6 cm or 1 cm) as described elsewhere [1]. The magnetic plates (L, 41 cm; H, 16 cm; D, 0.6 cm or 1 cm) were attached to both outer walls of a rat cage (cage space L, 38 cm; H, 16 cm; W, 24 cm). Each magnetic plate was made of an alloy of strontium-ferrite (SrFe₁₂O₁₉). Six experimental groups of 10 animals each were examined: 1) sham exposure with intraperitoneal (ip) saline injection (control); 2) 3.0–10.0 mT SMF exposure with ip saline injection (10 mT); 3) 7.5–25.0 mT SMF exposure with ip saline injection (25 mT); 4) no exposure with ip reserpine injection (RES); 5) 10 mT SMF exposure with ip reserpine injection (10 mT+RES); 6) 25 mT SMF exposure with ip reserpine injection (25 mT+RES). Reserpine (RES, 5.0 mg/kg) was administered intraperitoneally three times a week for 12 weeks, and then 18 h after each injection, arterial BP, heart rate, skin blood flow, plasma nitric oxide metabolites (NO_x=nitrate/nitrite), plasma catecholamine levels and body weight were monitored. The action of reserpine significantly decreased systolic BP and reduced plasma norepinephrine (NE) at 18 h in the RES group compared with the age-matched control group.

RESULTS: Exposure to SMF at 25.0 mT (*B*_{max}), but not 10.0 mT (*B*_{max}), for 2–12 weeks significantly prevented the decrease of BP in the 25 mT+RES group compared with the RES alone group. Furthermore, exposure to 25.0 mT (*B*_{max}) suppressed NE reduction and thereby inhibited the hypotensive action of reserpine. The NE levels for the 25 mT+RES group (0.13 ± 0.02 ng/ml, mean ± SEM) were significantly higher compared with for the RES group (0.08 ± 0.01 ng/ml) at 5 weeks (Fig. 1). However, there were no significant differences in any of the physiological parameters (eg, NE and NO_x levels) measured between the two SMF alone groups (10 mT and 25 mT) and control group.

CONCLUSION: SMF in the range of 7.5–25.0 mT, but not 3.0–10.0 mT, for 2–12 weeks significantly prevented the reduction of BP in reserpine-induced hypotensive rats compared with unexposed (sham-exposed) reserpine-treated rats. The antihypotensive effects of SMF on reserpine-induced hypotensive

animals were related to the inhibition of NE depletion. These results suggest that SMF with spatial gradients may suppress reserpine-induced hypotension by modulating NE pathways and responses.

References

- [1] Okano H, Ohkubo C. (2003b) *Bioelectromagnetics* 24:403–412.
- [2] Okano H, Ohkubo C. (2001) *Bioelectromagnetics* 22:408–418.
- [3] Okano H, Ohkubo C. (2003a) *Bioelectromagnetics* 24:139–147.

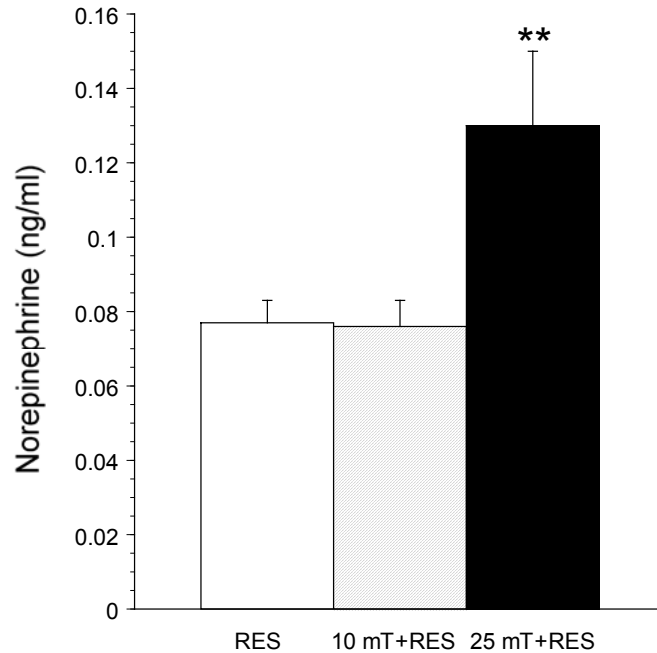


Fig. 1: Plasma concentrations of norepinephrine, with or without exposure to SMF (10 and 25 mT), at the experimental period of 5 weeks in reserpine (RES)-treated groups of WKY (12 weeks old). The vertical bars indicate mean \pm SEM. **, $P < 0.01$ for differences between 25 mT + RES and RES groups. Differences were compared between groups using the Kruskal-Wallis test followed by the Wilcoxon rank-sum test for pairwise comparisons.

P-C-120

STATIC MAGNETIC FIELDS ENHANCE THE HYPOTENSIVE EFFECT OF A CALCIUM CHANNEL BLOCKER IN SPONTANEOUSLY HYPERTENSIVE RATS. H. Okano^{1,2}, H. Masuda¹, S. Hirota¹, C. Ohkubo¹. ¹Department of Environmental Health, National Institute of Public Health, Tokyo 108-8638, Japan. ²Department of Science, Pip Tokyo Co., Tokyo 101-8528, Japan.

OBJECTIVE: Characterizing the physiological effects of static magnetic fields (SMF) on blood pressure (BP) in both hypertension and hypotension remains an important area of research. Previously we found that whole-body exposure to SMF at magnetic flux density of **10.0 mT** (Bmax) for 2–9 weeks suppressed and retarded BP elevation in stroke-resistant spontaneously hypertensive rats (SHR) by eliciting antipressor effects [1]. In addition, we have demonstrated that both local and whole-body exposures to SMF (1.0 mT [Bmax] or 5.5 mT [Bmax], for 30 min) modify the hypertensive and hemodynamic responses to a nitric oxide (NO) synthase inhibitor (L-NAME) and an adrenergic neurotransmitter (norepinephrine), by reducing BP in unanesthetized rabbits [2,3]. SMF in the mT range mediates hypotension, by antagonizing biochemical action, thereby inducing homeostatic effects, for example, by suppressing vasodilation and

hypotension induced by an L-type voltage-gated Ca^{2+} channel blocker, nicardipine [2]. Furthermore, effects of artificial SMF and natural geomagnetic field (GMF) on carotid sinus baroreceptor together with another L-type Ca^{2+} channel blocker, verapamil were investigated in conscious rabbits and consequently verapamil blocked the SMF and GMF effects on baroreflex sensitivity [4]. However, therapeutic application of SMF to carotid sinus baroreceptor along with nicardipine has not yet been studied in SHR. This study examines the hypothesis that SMF may influence Ca^{2+} dynamics in nicardipine-induced hypotensive SHR and modulate reduced BP. Specifically, this investigation was designed to evaluate mT intensities and spatial gradients of SMF on SHR, and to elucidate how SMF influences cardiovascular parameters and Ca^{2+} -related biological pathways and responses.

METHODS: Five week-old male rats were exposed to a SMF at 180 mT (Bmax) for 14 weeks. Four experimental groups were examined: 1) sham exposure with intraperitoneal (ip) saline injection (control); 2) 180 mT SMF exposure with ip saline injection (180 mT); 3) sham exposure with ip nicardipine injection (NIC); 4) 180 mT SMF exposure with ip nicardipine injection (180 mT+NIC). For SMF exposure, a cylindrical permanent magnet (SmFeN, 4.4 mm in diameter, 2.2 mm in depth, and 90 mg in weight, PIP Elekiban X, PIP Fujimoto Co., Ltd., Osaka, Japan) was implanted in the vicinity adjacent to the left carotid sinus baroreceptor of each rat. The nearest distances from the edge of the magnet to the left carotid sinus baroreceptor were 2–3 mm. With the aid of a gaussmeter (Model 4048, Bell Technologies, Orland, FL), the measured intensities were 7–8 mT in the left carotid sinus baroreceptor, < 1 mT in the right baroreceptor, and ~0.05 mT in the aortic arch baroreceptor and heart, which intensity was almost the same as the background intensity of the geomagnetic field at our laboratory. For sham exposure, a dummy magnet was implanted in the same position of each rat to compare the effect. Nicardipine (NIC, 2 mg/kg) was administered intraperitoneally three times a week for 14 weeks, and then 15 min after each injection, arterial BP, heart rate, skin blood flow, plasma nitric oxide metabolites (NO_x =nitrate/nitrite), plasma catecholamine levels and body weight were monitored. The action of nicardipine significantly decreased BP, increased heart rate, skin blood flow and blood velocity, and elevated plasma norepinephrine at 15 min in the NIC group compared with the age-matched control group.

RESULTS: Local exposure to 180 mT alone significantly suppressed and retarded the development of hypertension. Furthermore, exposure to 180 mT along with NIC treatment significantly enhanced the decrease of mean BP compared with the NIC treatment alone. However, except BP, SMF did not induce any significant effects in any of the physiological parameters (eg, NO_x and catecholamine levels). These differences were not significant between the two groups: 180 mT vs. control; 180 mT+NIC vs. NIC. Neither adverse physiological systemic symptoms nor local toxicity associated with magnetic materials were observed in any of rats locally implanted magnets or dummy magnets adjacent to the carotid sinus baroreceptor.

CONCLUSION: Local application of SMF to carotid sinus baroreceptor suppressed and delayed the elevation of BP in SHR. The SMF acted synergically with nicardipine-induced hypotension. These results suggest that SMF may enhance nicardipine-induced hypotension by more effectively antagonizing the Ca^{2+} influx through the Ca^{2+} channels compared with the NIC treatment alone.

References.

- [1] Okano H, Ohkubo C. (2003b) *Bioelectromagnetics* 24:403–412.
- [2] Okano H, Ohkubo C. (2001) *Bioelectromagnetics* 22:408–418.
- [3] Okano H, Ohkubo C. (2003a) *Bioelectromagnetics* 24:139–147.
- [4] Gmitrov J, Ohkubo C. (2002) *Bioelectromagnetics* 23:531–541.

EFFECTS OF MOBILE PHONE RADIATION ON CELL PROLIFERATION, APOPTOSIS AND STRESS RESPONSE IN C57BL/6 MICE. J.-S. Lee^{1,3}, T.-Q. Huang^{1,2}, Y.-C. Chung⁴, J.-K. Park⁵, J.-J. Jang⁶, J.-S. Seo^{1,2}. ¹ILCHUN Molecular Medicine Institute MRC, Seoul National Univ College of Medicine, Seoul 110-799, Korea, ²Dept of Biochemistry and Molecular Biology, Seoul National Univ College of Medicine, Seoul 110-799, ³BK21 Human Life Science, Seoul National Univ College of Medicine, Seoul 110-799, ⁴Dept of Information & Communication, Seokyeong Univ, Seoul 136-704, ⁵Dept of Radio Sciences & Engineering, Chungnam National Univ, Daejeon 305-764, ⁶Dept of Pathology, Seoul National Univ College of Medicine, Seoul 110-799, Korea.

Biological effects of mobile phone radiation were examined in C57BL/6 mice. Eight-week-old mice were exposed twice daily for 45 min exposure, with a 15 min interval between exposures, 5 days a week for 10 weeks. Whole-body average specific absorption rate (SAR) applied was either 2.4 W/kg at 849 MHz or 12.2 W/kg at 1,763 MHz radiofrequency (RF) fields. Major tissues were histopathologically analyzed, and immunocytochemically evaluated for cell proliferative activity. Apoptosis was investigated by TdT-mediated dUTP nick-end labeling (TUNEL) assay. No difference was observed in the histopathological analysis between sham- and RF-exposed mice. No evidence of increased proliferative and apoptotic activities were detected. Recently, mobile phone is one of the major sources of radiofrequency (RF) electromagnetic field (EMF) radiation in our environment. Even it is important to determine whether RF-EMF elicits a stress response, controversy still remains. To answer this issue, we investigated the expression levels of heat shock proteins (HSPs) in RF-exposed mice. Phosphorylation of the stress-activated kinases was also examined to determine if kinase-activating pathway was involved in RF field-induced stress response. The levels of HSP90, HSP70, and HSP25 showed no obvious changes by the RF exposure. RF exposure did not affect the phosphorylation status of the major stress-activated kinases, ERK1/2, JNK1/2, or p38 MAPK. Taken together, these results indicate that RF radiation causes no significant effect on cell proliferation, apoptosis, and stress response under our exposure conditions in C57BL/6 mice.

P-B-122**SUBCHRONIC EXPOSURE OF *hsp70.1*-DEFICIENT MICE TO MOBILE PHONE RADIATION.**

J.-S. Lee^{1,3}, T.-Q. Huang^{1,2}, J.-J. Lee¹, J.-K. Pack⁴, J.-J. Jang⁵, J.-S. Seo^{1,2}.¹ILCHUN Molecular Medicine Institute MRC, Seoul National University College of Medicine, Seoul 110-799, ²Department of Biochemistry and Molecular Biology, Seoul National University College of Medicine, Seoul 110-799, ³BK21 Human Life Science, Seoul National University College of Medicine, Seoul 110-799, ⁴Department of Radio Sciences & Engineering, Chungnam National University, Daejeon 305-764, ⁵Department of Pathology, Seoul National University College of Medicine, Seoul 110-799, Korea. Heat shock proteins (HSPs) are highly conserved proteins in all organisms. They are well known chaperone molecules and are of central importance in the repair of misfolded or denatured proteins. Of the HSPs, HSP70 is induced most to play a cytoprotective role under stressful conditions. Recently, HSP70 was reported to be an important anti-apoptotic molecule. To elucidate the *in vivo* function of HSP70 in detail, we generated *hsp70.1*-deficient mice. The renal tissues and embryonic fibroblasts of these mice are more vulnerable to hyperosmotic stress (EMBO Rep. 3, 857-861, 2002). Nonthermal RF energy has been suggested to be an environmental stressor. Since *hsp70.1* deficient mice express HSP70 at much lower levels than wild type mice, we exposed *hsp70.1* deficient mice to RF fields to determine whether they have any significant biological effect. Eight-week-old *hsp70.1* deficient mice were exposed twice daily for 45 min, with a 15 min interval, 5 days a week for 10 weeks. Whole-body average specific absorption rate was 0.4 W/kg for fields of both 849 MHz and 1763 MHz. The tissues of sham-exposed and RF-exposed mice were histopathologically analyzed, and immunocytochemically evaluated for cell proliferative activity and apoptosis. No difference was evident in cell proliferation and apoptosis in RF-exposed mice. Neither levels of HSPs, HSP90, HSP70, or HSP27, nor the activities of mitogen-activated protein kinases were changed. In conclusion, *hsp70.1* deficient mice did not show any significant changes due to exposure of 849 or 1,763 MHz RF fields in terms of cell proliferation or stress response.

P-C-123**WEIGHT GAIN IN MICE EXPOSED TO POWER FREQUENCY MAGNETIC FIELDS IS ASSOCIATED WITH INCREASED FAT MASS.**

J.T. Babbitt^{1,4}, S.S. Murray^{2,5}, L. Kheifets³, T.J. Hahn^{1,5}. ¹Geriatric Research, Educational and Clinical Center, V.A. Medical Center West Los Angeles, Los Angeles, California 90073, ²Sepulveda Ambulatory Care Center, North Hills, California 91343, ³Department of Epidemiology, and ⁴Department of Community Health Sciences, School of Public Health, and ⁵Department of Medicine, University of Los Angeles, Los Angeles, California 90095, USA.

OBJECTIVE: Our previous study determined that chronic lifetime exposure of female C57BL/6 mice to a residential power frequency magnetic field (MF) produced small but extremely significant increases in body weight [1]. To elucidate the nature of this weight increase, dual energy x-ray absorptiometry (DEXA) was used to determine the bone density, lean tissue mass, and fat mass of exposed and unexposed mice from the original study [2].

METHODOLOGY: Formalin preserved carcasses from the terminal sacrifice, representing the 1.4mT circularly polarized MF exposure group (n = 23) and ambient (0.13 μ T) MF exposure group (n = 23), were selected by a random numbers procedure. Residual formalin was absorbed prior to scanning. Carcasses were scanned three times, with repositioning between scans, using the Lunar PIXImus densitometer (Lunar Corp., Madison, WI). Heads and tails were excluded from the analysis. Data are expressed as mean \pm SD for all groups. Mean values were compared between groups using the unpaired t-test. Within each group the relationship of body compartment values to individual body weights and body weight difference from baseline values was determined by Pearson correlation. Significance was considered at two-tailed P values \leq 0.05.

RESULTS: Exposed mice had slightly higher mean values for bone mineral density (BMD), bone mineral content (BMC), lean mass, fat mass and per cent fat than unexposed mice, although these differences were

not significant (Table 1). Correlation coefficients of individual body weights and body weight difference from baseline values with individual fat mass values and percent fat were significant for both exposed and unexposed mice (Table 2). However, these relationships were more strongly correlated and extremely significant among exposed mice compared to unexposed mice.

CONCLUSIONS: Although MF exposure appears to weakly stimulate growth in all body compartments, the strong association between body weight and fat parameters suggests a likely role for increased fat mass as a determinant of greater body weight gain during 29 months of MF exposure.

References:

Babbitt JT, Kharazi AI, Taylor JMG, Bonds CB, Zhuang D, Mirell SG, Frumkin E, Hahn TJ. "Increased body weight in C57BL/6 female mice after exposure to ionizing radiation or 60 Hz magnetic fields." *Int. J. Radiat. Biol* 2001, 77(8):875-882.

Babbitt JT, Kharazi AI, Taylor JMG, Bonds CB, Mirell SG, Frumkin E, Zhuang D, Hahn TJ. "Hematopoietic neoplasia in C57BL/6 mice exposed to split-dose ionizing radiation and circularly polarized 60Hz magnetic fields." *Carcinogenesis* 2000, 21:1379-1389.

Table 1. DEXA determined mean values (std.dev.) for bone mass, lean tissue mass, and fat mass of female C57BL/6 mice exposed either to 1.4 mT or ambient 60 Hz magnetic fields for 29 months.

Exposure group	BMD (gm/cm ² x100)	BMC (gm x 100)	Bone area (cm ²)	Lean Mass (gm)	Fat Mass (gm)	Fat%
1.4 mT n = 23	3.83 (0.57)	3.25 (0.75)	8.42 (1.22)	5.80 (0.98)	9.58 (2.36)	61.6 (7.9)
ambient n = 23	3.69 (0.55)	3.13 (0.83)	8.46 (1.36)	5.74 (1.09)	9.35 (2.0)	61.5 (8.3)

Table 2. Correlation coefficients for the association of fat and percent fat measured by DEXA with actual body weight (wt) and weight difference from baseline (wtdif) of female C57BL/6 mice exposed either to 1.4 mT or ambient 60 Hz magnetic fields for 29 months.

Exposure Group	r(wtdif/fat)	r(wtdif/%fat)	r(wt/fat)	r(wt/%fat)
1.4 mT n = 23	0.8321 P < 0.0001	0.7064 P < 0.0002	0.8682 P < 0.0001	0.7352 P < 0.0001
Ambient n = 23	0.4984 P = 0.015	0.4267 P = 0.042	0.5117 P = 0.012	0.3822 P = 0.072

MECHANISMS OF INTERACTION – PHYSICAL TRANSDUCTION

P-A-124

THE EFFECT OF 3 EMF SIGNALS ON NERVE REGENERATION IN A SCIATIC NERVE CRUSH INJURY MODEL. J.L. Walker^{1,2}, J.M. Smith¹, P. Resig⁴, E. Herbst⁴, B.F. Sisken^{1,3}. ¹Univ. of Kentucky Wenner-Gren Center for Biomedical Engineering, ²Univ. of Kentucky, Division of Orthop. Surg. and Shriners Hospitals for Children and ³Univ. of Kentucky Dept. of Anatomy and Neurobiology, Lexington Kentucky 40536 USA, ⁴Herbst Research, Inc., Edgewater New Jersey 07020 USA.

OBJECTIVE: Electromagnetic fields have been demonstrated to enhance mammalian nerve regeneration in both *in vitro* and *in vivo* experiments. (Sisken et al 1989, Walker et al 1994) The sciatic nerve crush injury model is a well-established animal model for the study of regeneration following axotomy. The EMF signals studied in this report were chosen because of their enhancement of neurite outgrowth *in vitro* (Herbst et al 2002). The purpose of this study is to evaluate effects of this signal on nerve regeneration in a rat crush injury model, using three different signal amplitudes.

METHODS: This research was approved by the IACUC of the University of Kentucky. All rats were anesthetized using intraperitoneal injections of xylazine and ketamine. Under sterile conditions, the right sciatic nerve was exposed and crushed with a modified needle holder, just distal to its branch to the gemelli. The wound was closed with 2-0 and 4-0 absorbable sutures. The animals were then assigned to sham EMF treatment or to treatment with various electromagnetic fields produced inside of a solenoid. The animals were restrained in plastic restrainers and their whole bodies were exposed to sham or active EMF's for 4 hours/day for 5 days. 9 groups of 8 rats were operated upon (total of 72 rats) and assignments consisted of 2 sham controls plus 2 rats in each of the 3 EMF treatment groups. One rat in each group did not complete the study leaving an n=17 rats in each of sham and 3 experimental groups for analysis.

EMF treatments were applied using 96 turn solenoid with inside diameter of 5.5 inch. The EMF treatment signals had the same waveform but different magnetic flux density B peak values, defined by controlling the current in the coil. Peak magnetic fields were 3.00 mT, 0.30 mT, and 0.03 mT respectively. The signal was a ramp with: repetition rate=2 Hz; rise time=1.0 msec; and fall time=0.3 msec.

Walking function was assessed at 10, 17, 19, 22, 24, 26, 31, and 43 days after injury using video image analysis of 1-5 toe spread distances comparing each animals injured to uninjured hindlimb. These parameters were measured from videotapes of the plantar aspects of the rats' feet while they walked across a narrow frosted Plexiglas walkway. The tapes were reviewed to select runs where the walking speed was smooth, without hesitation, and images were clear. We obtained 2 to 10 pairs of footprints for the toe spread, measured from the outside edge of the 1st to the 5th toes using QuantIm software and compared consecutive right and left steps. Mean responses were compared using a linear mixed model having fixed effects due to treatment, day post surgery, and the interaction between treatment and day and random effects due to surgical group, animals nested with group and treatment, and measurement error.

RESULTS AND CONCLUSIONS: There was no statistical difference in recovery of toe spread function between the EMF treatment groups compared to sham. There was no difference in recovery between the surgical date groups. As expected, there was greater recovery of function on each successive day from surgery for all rats. This same experimental model has been successfully used in our lab in similar experiments to demonstrate *in vivo* enhancement of nerve regeneration using pulsed EMF generated in a different coil system (Walker et al,1994). Procedural deviations from these previous experiments include: use of an image analysis system to measure the rat footprints, though we have found this to be comparable to our previous method, xylazine+ketamine anesthetics which were clinically safer than the pentobarbital used previously, modification of the needle holder crush technique which still produced the expected functional loss and recovery pattern, and a more sophisticated statistical model which is felt to be more appropriate than the 3 way repeated measures ANOVA. This current field was applied in a different room which may have different ambient fields. The coils were of solenoid rather than Helmholtz design which

effects the direction of the field and the a 20 msec pulse waveform we used in 1994 was a square wave as opposed to the ramp waveform tested in the experiments reported here.

References:

Sisken: *Brain Res* 485:309, 1989, Walker: *Exp Neurol* 125:302, 1994, Herbst: *BEMS Abstr* pg 10, 2002.

Supported in part by NIH Grant R44NS33033 to Herbst Research Inc.

P-B-125

STUDENT

PULSED EXTREMELY LOW FREQUENCY MAGNETIC FIELD INDUCTION OF HEAT SHOCK PROTEINS. J.A. Robertson^{1,2}, Y. Bureau¹, F.S. Prato^{1,2}, A.W. Thomas^{1,2}. ¹Bioelectromagnetics, Lawson Health Research Institute, St. Joseph's Health Care, 268 Grosvenor St. London, ON, Canada, N6A 4V2, ²Dept. of Medical Biophysics, University of Western Ontario, London, ON, Canada.

INTRODUCTION: Heat shock proteins (HSPs), in particular the 70 kDa family, have been shown to protect tissue from damage following ischemia-reperfusion injuries, such as those suffered during a heart attack [1]. The use of HSPs as a treatment avenue is in part limited by the ability to induce their production, as traditional methods such as hyperthermia and ischemic preconditioning themselves damage the tissue they are meant to protect. Magnetic fields have been shown to induce HSPs in cell cultures and chick embryos [2,3], which is highly promising, as they don't produce gross damage. We will extend this work to a mouse model, as well as investigating pulsed magnetic fields.

OBJECTIVE: To determine whether HSP production can be induced by ELF magnetic fields in a mouse model, and whether the induction is pulse-form or tissue dependent.

METHODS: Swiss CD-1 mice approx. 45 days old were exposed to a $\pm 200 \mu\text{T}$ magnetic field with either a 60 Hz sinusoidal or a complex pulsed waveform [4] delivered by a set of square Helmholtz coils (1.2 m); or to a sham (coils deactivated) condition. The ambient geomagnetic field of approx. 55 μT was not shielded or cancelled. Mice were exposed for 30 or 60 minutes, with a rest time of 0, 30 or 90 minutes prior to sacrifice and tissue extraction. Heat stress produced via a heat lamp while under anesthesia was used as a positive control (40 °C for 30 or 60 minutes). Tissues (hearts, livers, and brains) were frozen in liquid nitrogen and stored at -80°C until Western blots were performed. Blots were stained with HSP25 and HSP70 antibodies (SPA-801 and SPA-812, respectively, from Stressgen, Victoria, BC).

RESULTS: To date, hearts from 18 mice have been analyzed. While there is no significant difference between the HSP70 levels for the different pulse types applied, there is a tendency for HSP70 levels to increase from 60 Hz magnetic field exposure compared to the pulsed complex waveform. There was also no significant difference between HSP25 levels for different exposure groups, but there was a significant correlation between HSP25 levels and the global Ap index obtained from the British Geological Survey ($p < .001$, $r = .798$). A weaker correlation was also found for HSP70 levels ($p < .05$, $r = .540$). Positive control heat stressed mice ($n = 2$) were excluded from the correlation analysis.

CONCLUSION: While there is not yet enough data collected to support or disprove the idea that magnetic fields can influence heat shock protein production in a mammalian model, correlation with the Ap index indicates that perhaps HSP levels are sensitive to the magnetic environment of the animal.

This study was funded (in part) by FrAlex Therapeutics Inc.; St. Joseph's Health Care (London) Foundation; the Lawson Health Research Institute Internal Research Fund; the Department of Diagnostic Imaging, SJHC; Natural Sciences and Engineering Research Council of Canada (NSERC); Canadian Institutes of Health Research (CIHR); National Research Council (NRC); the Ontario Research and Development Challenge Fund (ORDCF), Canada Foundation for Innovation (CFI); and the Ontario Innovation Trust (OIT).

References.

1. Suzuki, K., *et al.* Journal of Clinical Investigations. 1997; 99:1645-165.
2. Carmody, S. *et al.* Journal of Cellular Biochemistry. 2000; 79:453-459.

3. Shallom, J.M. *et al.* Journal of Cellular Biochemistry. 2002; 86:490-496.
4. US patent #6,234,953; Thomas *et al.* Neuroscience Letters. 1997;222(2):107-10.

P-C-126

EFFECT OF 50 HZ MAGNETIC FIELDS ON THE 5-HT_{1B} SEROTONINERGIC RECEPTOR: A REPLICATION STUDY. J.M. Espinosa, E. Haro, I. Lagroye, B Veyret. PIOM/Bioelectromagnetics lab, ENSCPB/EPHE, University of Bordeaux, Pessac, France.

Some epidemiological studies have reported associations between extremely low frequency (ELF) magnetic fields (50-60 Hz) and sleep quality, anxiety, or depression. These physiological functions or pathologies are closely controlled by the serotonergic central system. Among the serotonin (5-HT) receptor family, the 5-HT_{1B} receptors are presynaptic receptors located on serotonergic as well as on other axon terminals, where they regulate the release of the corresponding neurotransmitter. The 5-HT_{1B} receptor is a 7-transmembrane-region receptor and is negatively coupled with the adenylate cyclase through G-proteins. As a consequence, it exerts an inhibiting control of the serotonergic activity by decreasing the release of 5-HT. Massot *et al.* (2000) showed a specific and reversible desensitization of the 5-HT_{1B} receptor induced by a 50-Hz magnetic-field exposure. The authors demonstrated that this desensitization could be observed on three different levels after an exposure at 2 mT: (1) a decrease in the receptor affinity for the [3H]5-HT in CHO-transfected cells and rat brain membrane preparations was observed above 0.6 mT; (2) a decrease in the second messenger [32P]cAMP synthesis inhibition was observed on CHO-transfected cells; (3) a decrease of the inhibition of the release of [3H]5-HT by synaptosomes was measured. We undertook a partial replication of the work of Massot *et al.* and used the same exposure system and performed binding experiments on rat brain membrane preparations. The exposures lasted for 1 hour and we tested magnetic flux densities up to 2 mT. The data will be presented at the meeting. Further investigations will include *in vivo* experiments.

P-A-127

EXPOSURE OF EXTREMELY LOW FREQUENCY ELECTROMAGNETIC FIELDS IMPROVES SOCIAL RECOGNITION IN RATS. L. Verdugo-Díaz, G. Reyes-Guerrero¹, D. Elías-Viñas², A. Domínguez-González¹, M. Vázquez¹ and R. Guevara-Guzmán¹. ¹Departamento de Fisiología, Facultad de Medicina, UNAM, México D.F. 04510, ²Departamento de Ingeniería Eléctrica, Sección de Bioingeniería, CINVESTAV, IPN, México, D. F., 07360, México.

Studies focused on the alterations on learning and memory by the exposure to extremely low frequency electromagnetic fields (ELF EMF) had use an assortment of field intensities, exposure conditions, animal models and behavioral tasks. Results of electromagnetic fields exposure on spatial learning performance are not conclusive. A number of studies have shown that the ELF-EMF may increase or decrease memory functions in rodents. The aim of this study was to determinate the effect of ELF-EMF stimulation on social recognition of rats. Adult male Wistar rats (240g) were exposed to a vertical sinusoidal 60Hz magnetic field at 1mT. Stimulation was applied with a pair of circular Helmholtz coils located above and below of a plastic cage, separated 30 cm. Daily stimulation was applied for two hours in the morning during 9 days. The sham-stimulated animals were maintained an equal period of time inside exposure chamber with coils turned off. Magnetic fields ambient background levels were <0.04 mT. Two days previous to the experiment and just before the test, each subject was habituated to the test cage for 4 minutes. Then, each adult rat was presented with a juvenile conspecific for 4 min on two occasions, separated by inter-exposure interval. The intervals between the initial and the test trails were 30, 150, 300 and 24 hours. The interactions during the initial and the re-exposure were videotaped and later scored (contacts made by the adult over the juvenile) by a computing program previously tested by trained observers. Locomotor's activity was measured. Results obtained showed that sham and ELF EMF-exposed animals are a social recognition behavior similar at inter-exposure intervals of 30 and 150 minutes. At 300 minutes of interval, only EMF-exposed rats continue to recognize the juvenile conspecific. When the interval between encounters to the same juveniles was 24 hours, neither group of rats remembers the conspecific. Locomotor's activity was not affected by exposure to ELF EMF. Our results showed an improved of social recognition memory by the exposure to ELF-EMF of 1 mT during two hours for nine days of adult male Wistar rats. These data indicate, for the first time, that ELF EMF improved social recognition memory in rats, however we do not know the mechanisms by ELF EMF exercises their effects. This study was supported by DGAPA: IN-202302-2 to LVD.

P-B-128

Presented as ST-1

P-C-129

CHANGES IN INFRADIAN ACTIVITY OF PHYSIOLOGICAL PROCESSES IN RATS EXPOSED TO LOW INTENSITY, ULTRA-HIGH OR ULTRA-LOW FREQUENCY ELECTROMAGNETIC RADIATION. N.A. Temuryants, V.S. Martynyuk, O.B. Moskovchuk, E.N. Chuyan, V.A. Minko, E.I. Nagaeva, I.A. Brusil. V.I. Vernadskiy Tavrida National University, 4 Prospekt Vernadskogo, Simferopol, 95007, Ukraine.

INTRODUCTION: Due to the growing appreciation of the important role epiphysis is thought to play in the mediation of magnetobiological processes, a very special role is given to research directed at the influence of electromagnetic radiation of various frequencies, characterized by different penetrating abilities, on the rhythm of physiological processes.

OBJECTIVE: To establish physiological systems responsible for modulation of EMF effects.

METHODS: 10 parameters of neutrophile functional activity have been studied in rats exposed to low intensity electromagnetic radiation (EMR) in the ultra-high frequency range (42 gigaHz, 0.1 mWatt/cm²) and in the ultra-low range (8 Hz, 5mTl).

RESULTS: It was found that in all studied parameters 8Hz EMR caused considerable changes in the amplitude and phase of the infradian rhythms in all periods of spectra. Ultra-high frequency EMR was found to affect amplitude and phase characteristics only in some parameters and only in certain periods. It was also shown that in desynchronosis induced by hypodynamic conditions both low intensity electromagnetic factors normalize infradian rhythmicity of the physiological processes. The ultra-low frequency EMR is more efficient in correcting desynchronosis.

CONCLUSION: Ultra-low frequency EMR can penetrate tissues and, apparently, does change the functional state of the epiphysis – one of the natural pace makers – which leads to considerable changes in the parameters of infradian rhythmicity. Ultra-low frequency EMR is absorbed by the skin, which, according to the multi-ocillator theory of biorhythms, contains peripheral occilators that are controlled by the centrally located pacemakers. Any changes in their status translate into slight deviations in the rhythmic processes. Therefore, effects of EMR may be modulated by the main regulator of the biological rhythmicity – melatonin. It is secreted in not only the epiphysis, but also in numerous neuro-endocrine cells that are capable of autofluctuation.

P-A-130

EFFECTS OF GSM-RELATED ELECTROMAGNETIC FIELDS ON COCHLEAR OUTER HAIR CELLS IN SPRAGUE-DAWLEY RATS. P. Galloni¹, A. Brazzale², M. Parazzini², M. Piscitelli¹, P. Ravazzani², C. Marino¹, ¹Toxicology and Biomedical Sciences Unit, Enea Casaccia, Via Anguillarese 301, 00060 Rome, Italy; ² Biomedical Engineering Institute, CNR, Piazza Leonardo da Vinci 32, 20133 Milan, Italy.

INTRODUCTION: the auditory system is a target of possible effects of mobile phones derived electromagnetic fields (EMF). The purpose of this study was to evaluate the possible changes of cochlea's outer hair cells (OHC) functionality in rats exposed to EMF at the typical frequencies of GSM mobile phones (900 and 1800 MHz). The OHC functionality was investigated by Distortion Product Otoacoustic Emissions (DPOAE) that are known as indicator of the cochlea status: they are present in all healthy cochleae of humans and many species of animals, whereas they are not generally observed or are greatly reduced in ears with mild to profound hearing loss. DPOAE can therefore provide indirect information on the inner auditory system functionality.

MATERIALS AND METHODS: according to results of previous pilot studies, some changes have been operated in the experimental protocol regarding exposure time and Specific Absorption Rate (SAR). A preliminary study on morphology of cochlea cells' has been also performed. A population of 48 rats (16 each group) was subjected to a localized exposure (close to the right ear), simulating the use of a cellular phone, by 3 different sets of 4 loop antennas, one for sham and two for exposed animals (changing loops for 900 and 1800 MHz). Animals were exposed 2 hours/day, 5 days/week, for 4 weeks, 2 W/kg of SAR; during the exposure rats were kept in plastic restrainers. DPOAE tests were carried out before exposure, during exposure (i.e. at the end of each week) and after (the day after and one week after); the measurement sessions are performed with animals under general gas anesthesia (isoflurane in O₂, 1.5-2 %). A positive control group of 10 rats treated with kanamycin was also included.

RESULTS: the experiments and the statistical evaluation were performed in blind mode with respect to the exposure conditions (sham or exposed). No statistically significant differences were found in the DPOAE level between exposed and sham group at both frequencies of exposure.

CONCLUSIONS: no effects of GSM modulated 900 and 1800 MHz exposure have been evidenced on OHC's function and structure in this experimental conditions. A similar experimental protocol with higher exposure intensity (4 W/kg) is in program.

This study was founded by: (1) the European Project GUARD "Potential adverse effects of GSM cellular phones on hearing" (FP5,QLK4-CT-2001-00150, 2002-2004); (2) the national research project "Protection of humans and environment from electromagnetic emissions"; (3) a grant from ELETTRA 2000 Consortium.

P-B-131

A NOVEL HEAD-ONLY RF EXPOSURE SYSTEM FOR MICE. R.P. Blackwell, D. Addison, A.L. Bottomley and Z.J. Sienkiewicz, National Radiological Protection Board, Chilton, Didcot, Oxfordshire, OX11 0RQ, UK.

For an integrated project investigating the effects of radiofrequency (RF) fields on gene expression, neurophysiology and animal behaviour in mice, it was necessary to construct an exposure system capable of delivering controlled doses of microwaves, representing realistic handset signals, localised to the heads of the animals. Irradiation was required at one of three frequencies (400 MHz TETRA, 900 MHz GSM and 2200 MHz UMTS) and at local specific energy absorption rates (SARs) of up to 35 Wkg^{-1} . It was also necessary to be able to expose between one and four animals at one time.

The exposure system consists of individual loop antennas for each animal fed via a power splitter from a narrow-band power amplifier driven by a programmable signal source. Careful matching of interconnecting cables and the use of isolators for each antenna minimised interactions and ensured that the power delivered to each antenna was similar within close limits. Separate antenna sets were used for each frequency, tuned for a return loss of $>20\text{dB}$ (with a mouse in the animal holder). All parameters of the exposure system, were controlled by PC using custom software. The exposure mode and level can be easily set for each irradiation at predetermined values with minimal possibility for inadvertent exposure errors. The system maintains a sensibly constant drive to the antennas for the duration of the exposure and also records the exposure history to a file for later inspection.

The system was contained within a large metal outer shielding box. To allow simultaneous irradiation of four animals, this was partitioned into four equal sized compartments, lined on all surfaces by appropriate broad-band, graded absorber material. Each compartment was illuminated with a small light source, and masking noise provided by two externally mounted fans that also provided ventilation within the chamber as a whole. A miniature video camera was positioned above each of the animals to allow them to be observed at all times.

Animals were held immobile using a custom-made acrylic holding tube (and stand). Such holders were necessary to eliminate as far as possible even slight head movements which would affect the local SAR in the head. Using a system of stops and guides, the holders could be located precisely within each partition. Similarly the loop antennas in each compartment could be altered using a highly adjustable acrylic holder and locked into position. In this way the loop antennas could be reproducibly positioned against the same region of the head.

Mapping of the E-fields around the antennas and validation studies have been undertaken. Dosimetry was performed at each frequency using a non perturbing fibre-optic thermometer and mouse cadavers. Exposures using the highest possible power fed to one antenna was used. SARs within the brain were calculated on the basis of the initial temperature rise observed.

Two systems of this design have been successfully used by research teams within the project for the past 18 months.

The work was supported by the Mobile Telecommunications and Health Research Programme but the views expressed are those of the authors.

P-C-132

COMBINED EFFECTS OF PULSED MICROWAVES AND A CNS MITOCHONDRIAL TOXIN ON BEHAVIOR DEPEND ON MICROWAVE-EXPOSURE PARAMETERS. R.L. Seaman¹, M.F. Chesselet², S.P. Mathur¹, C.D. DiCarlo³, S.M. Fleming², J.L. Ashmore¹, T.H. Garza¹, J.M. Morin¹, A.R. Grado³, S.L. Adam^{1,3}. ¹McKesson BioServices at US Army Medical Research Detachment, Brooks City-Base, Texas 78235; ²Dept. of Neurology, UCLA School of Medicine, Los Angeles, CA 90095; ³US Army Medical Research Detachment, Brooks City-Base, Texas 78235, USA.

OBJECTIVE: To test effects of different microwave pulse parameters typical of military applications in exposures at specific absorption rate (SAR) of 0.4 and 4 W/kg on rotenone-induced changes in motor behavior. To obtain results using S-band (2.8 GHz) exposures to compare with the lessening of rotenone-induced deficits seen after L-band (1.25 GHz) exposures.

METHODS: Male Lewis rats (216-293 g) were implanted subcutaneously with 2ML4 Alzet[®] osmotic minipumps (DURECT Corp.) with Teflon[®] flow modulators using aseptic surgical technique. The minipumps delivered 0 or 2 mg/kg/day rotenone in dimethylsulfoxide/polyethylene glycol as an animal model of CNS changes in Parkinson's disease [1]. In three different experiments, 10-13 animals in each condition were exposed for 6 min on post-op days 4 and 5 to 2.8-GHz microwaves applied as 2- μ s pulses at 13 Hz (0.4 W/kg SAR), 20 Hz (0.4 W/kg SAR), or 200 Hz (4 W/kg SAR). A sham-exposed control group was used in each experiment. On post-op day 6, rotenone-induced deficits were quantified by (1) measuring the delay between placement of a forepaw firmly on a flat surface and first movement in a movement-initiation (MI) test and (2) counting the vertical rears made in 5 min in a darkened upright plastic cylinder [2]. The cylinder test was also performed on the day before surgery. Data were tested using ANOVA with rotenone dose and microwave exposure as factors.

RESULTS: No significant change in colonic temperature occurred during any type of exposure. Across experiments, MI time was generally longer and number of cylinder rears was smaller with rotenone, but both behavioral measures were unchanged by microwave exposure. The main effects of rotenone on MI time and cylinder rears were significant at the .01 level in each experiment, with the exception of the 13-Hz MI time ($p=.5$). The main effect of microwave exposure and the rotenone dose-microwave exposure interaction were not significant in any experiment.

CONCLUSIONS: Rotenone had strong, robust effects to increase MI time and reduce number of rears in the cylinder, as expected from our previous work [2]. The lack of effect of exposure to pulsed 2.8-GHz microwaves on rotenone-induced changes, however, contrasted with results of a similar experiment using 1.25-GHz microwaves applied as 6- μ s pulses at 10 Hz also with SARs of 0.4 and 4 W/kg [3]. In this previous experiment, rotenone-treated animals did not show significant deficits in motor behavior after exposure at 0.4 W/kg, i.e., the exposure reduced the effects of rotenone on the measured behaviors. Differences in results between the current experiments and the earlier experiment may be due to differences in microwave frequency, pulse duration, pulse repetition frequency, exposure setup, or some combination of these factors. Identification of critical microwave exposure parameters for the previously observed effects will be essential in optimizing them for reversal of effects of mitochondrial toxins.

Reference.

1. Betarbet R. et al. 2000. Chronic systemic pesticide exposure reproduces features of Parkinson's disease. *Nature Neuroscience* 3:1301-1306.
2. Zhu C. et al. 2003. Chronic intravenous and subcutaneous rotenone infusion: Survival analysis, functional assessment and microglial activation." Society for Neuroscience 23rd Annual Meeting, Program No. 95.1.
3. Seaman R.L. et al. 2003. Effects of exposure to pulsed microwaves on movement initiation in rats exposed to the mitochondrial toxin rotenone. 6th Congress of the European Bioelectromagnetics Association (EBEA). Abstracts, p 27.

Supported by US Army MRMC contract DAMD17-94-C-4069. Investigator(s) adhered to the "Guide for

the Care and Use of Laboratory Animals". The views, opinions and/or findings contained in this report are those of the author(s) and should not be construed as an official Department of the Army position, policy or decision.

P-A-133

STUDENT

THE EFFECT OF A MAGNETIC FIELD AT 9.45 GHz ON THE GROWTH PROCESS OF SILKWORMS. S. Yokoi¹, T. Komuratani², M. Ikeya¹, ²Kinugasa Textile Research Institute, Kyoto, Japan; ¹Department of Earth and Space Science, Graduate School of Science, OSAKA University, Toyonaka, Osaka, 560-0043, Japan.

INTRODUCTION: ESR is a phenomenon of the resonance absorption of electromagnetic wave by unpaired electron spins under a static magnetic field. We measured silkworm eggs (*Bombyx mori*) nondestructively using ESR to investigate the biological material of the embryo at a cell division or at an early stage of the growth process [1]. The magnetic field at 9.45 GHz might cause biological effects on silkworms. So, the effects of the magnetic field at various power levels on silkworm development after the magnetic field exposure were investigated.

OBJECTIVE: To show the effect of magnetic field of microwaves at 9.45 GHz on the development of silkworms from hatching to cocooning.

METHODS: 1. Samples were exposed to a magnetic field of microwaves at 9.45 GHz generated by the microwave unit of the ESR spectrometer during the measurements. 2. Silkworm development were observed until imago.

RESULTS: Hatching ratios of silkworms were found to be decreased by exposure to a magnetic field of microwaves at 9.45 GHz at various power levels under constant thermal conditions. 28.0 % of eggs at a magnetic field power of 10 mW died at the pigmentation stage just before hatching.

DISCUSSION: The magnetic fields of microwaves acted as a fatal stress. Microwave exposure affected the development of surviving larvae for the remainder of the life cycle.

Reference.

1. Yokoi S, Komuratani T, Ikeya M. 2003. Biological rhythms of silkworm egg detected by Electron Spin Resonance (ESR). Appl Radiat Isot. in submitting.

P-B-134

LOW FREQUENCY (50 HZ, 1 MT) MAGNETIC FIELD INDUCE IMPAIRMENT IN *XENOPUS LAEVIS* TADPOLES METAMORPHOSIS. S. Grimaldi, A. Lisi, S. Rieti, M. Ledda, D. Sacco[§], E. D'Emilia[§], E. Rosola. Institute of Neurobiology and Molecular Medicine, CNR, Rome, Italy [§]ISPESL-DIPIA, Rome, Italy.

Amphibians with a larval stage, are distinguished by a distinct phase of morphogenesis named metamorphosis. In anurans, metamorphosis is generally characterized by the transition from an aquatic, fish-like, herbivorous larva (tadpole) to a tetrapodal, carnivorous and often terrestrial adult. Tadpole metamorphosis involves a coordinated series of changes in virtually every tissue of the body: in fact, during this process occur organogenesis and tissue remodelling, each involving a coordinated process of cell proliferation, differentiation and death.

In this work we study the effect of 50 Hz, 1 mT magnetic field on the metamorphosis process and the survival of *Xenopus laevis* tadpoles. On the third day from the oviposition, when occurred the passage from embryo to larval stage, tadpole population was randomly subdivided into four groups, each of 200 individuals, and transferred in four aquariums at a temperature of $26 \pm 0.5^{\circ}\text{C}$. Two aquariums (exposed tadpoles) were then exposed to 50 Hz, 1 mT magnetic field generated in a solenoid, while the other two aquariums (control tadpoles) were maintained in the same room under the same conditions but not exposed to the field. Experiment was performed in the course of the metamorphosis process, lasting approximately for 65 days. Four sets of experiments were performed.

During the course of the experiment, exposed tadpoles showed a significant decrease (2,2%) in daily survival, particularly referred to the first fifteen days, compared to the unexposed (control) tadpoles. In addition to a decrease in tadpole survival, exposure to the field also resulted in a 6-day delay in the rate of metamorphosis compared to the control tadpoles and in a significant reduction in the amount of individuals that reached maturation. The total number of metamorphosed individuals was drastically reduced after 50 Hz exposition, being of 45% for exposed tadpoles and 85% for unexposed (control) tadpoles.

These results indicate that exposure low frequency magnetic field affect the organogenesis and tissue remodelling processes occurring during the tadpoles metamorphosis. Moreover, these findings allow us to consider *Xenopus laevis* tadpoles as sensitive biological indicators of the impact of low frequency magnetic fields to biological systems.

P-C-135**GUARD PROJECT: EXPOSURE SYSTEM, RF DOSIMETRY AND THERMAL IMAGING FOR HUMAN STUDIES ON POTENTIAL HEARING EFFECTS OF CELLULAR PHONE.**

G. Thuróczy¹, B.F. Molnár¹, E. Rahne², J. Bakos¹; ¹Natl. Research Institute for Radiobiology and Radiohygiene, H-1775 Budapest, POB.101., Hungary, ²Professional Industrial Measurement Techniques (PIM) Ltd. Budapest, Hungary.

OBJECTIVE: The main aim of GUARD project is to assess potential changes of the hearing function of animals and humans after exposure to electromagnetic fields produced by cellular phones. The specific aim of this study was to provide exposure system, relevant dosimetry and thermal imaging for the human studies.

METHODS: The Nokia 6310i mobile phone was chosen within the GUARD project which provides all special requirements for the study: the phone has integrated antenna, external antenna connection, dual band, low weight, available PC connection for external PC control (by the PHOENIX program provided by Nokia), it is widely used type in Europe, it is commercially available in the market, it is a relatively recent model. The exposure system was developed also with the assistance from the Nokia Research Center in Helsinki. The RF power of phones was measured using the external RF antenna output. The long term output power stability measurement was made by PC data acquisition during the whole lifetime of the battery. In order to develop a comfortable holder of the phone, a system of phone fixation have been designed with a possibility of freely moving of the subjects head. External RF loads were designed connected to the phone's external antenna output for sham exposure situations. The same size and shape dummy load was also designed in order to provide the double-blind requirements in the protocols. The SAR measurements were made according to the CENELEC requirements using the "touch position" of the phone. The SAR measurements were also performed with and without modeling the ear tube in the liquid phantom. A Janoptik-VarioScan high resolution compact (Infratec) thermocamera was used to assess potential changes of the phone and head skin temperature after exposure. In order to get correct results from the infrared measurement the whole surface of the mobile phone was covered with black mat paint. The warming of the front and the rear surface of the mobile phone was studied with and without external 50 Ω load. The phone was operated at maximal power level (900 MHz, 2W peak; 1800 MHz, 1W peak). The warming up of the human head skin was measured after 10 minutes use of mobile phone.

RESULTS: The RF power uncertainty of the phone during the whole lifetime was below 1 % using the highest peak power level at 900 MHz, 2W, 1800 MHz, 1W respectively. In the first 10 minutes the uncertainty was below 0,4%. No radiated RF fields were measured using the RF load connected to the external antenna output. The SARs at the cochlea region were 0,41 W/kg and 0,19 W/kg at 900 MHz and 1800 MHz respectively. The maximum temperature rise of the mobile phone surface was 6,2 °C and 3.2 °C, at 900/1800 MHz respectively. The warming up of the earlobe and anywhere on the skin of the face was less than 1 °C in all cases.

This study was partially financed by the European Project GUARD "Potential adverse effects of GSM cellular phones on hearing" (European Commission, 5th Framework Program, QLK4-CT-2001-00150, 2002-2004)

P-A-136

EFFECTS OF SHORT-TERM ELF-MF OF 20mT (A COMMERCIALY AVAILABLE POWER-SOURCE OF 50Hz) ON WHOLE RAT EMBRYO CULTURE. T. Ogasawara, F. Hirahara, Department of Obstetrics and Gynecology, Yokohama City University Graduated School of Medicine, 3-9 Fukuura, Kanazawa-ku, Yokohama, Kanagawa, 236-0004, Japan.

OBJECTIVES: It has been controversial that electromagnetic fields generated by electrical apparatus affect human pregnancy. Some guidelines were matched for human beings. Therefore, we consider that it is important mammalian model of experiments on gemetogenetic period. To test this hypothesis, we investigated the ELF-MF on mortality and development of rat embryo and placenta and yolk sac using whole embryo culture system.

METHOD: After sacrificing pregnant Sprague-Dawly rats by cervical dislocation at 9.5 days of embryonic age, whole embryo were dissected and cultured with immediately centrifuged serum for 6 hours using whole embryo culture system. Viable whole embryo was divided into control, sham and ELF-MF of 20mT, a commercially available power-source of 50Hz, or heated exposure for 10 or 20 minutes groups. After following 18 hours culture, morphological change of yolk sac membrane were scanning by electron microscope. Then, embryos that showed regular heart beats were considered survived and crown-rump-length, somites numbers and protein content were measured.

RESULTS: Exposed embryos for 10min. were no difference from other groups. In contrast, exposed embryos for 20min. were showed slightly growth retardation. Exposed conceptive for 20min. were showed cell swelling of surface of yolk sac membrane scanning by electron microscopy. Extension of intercellular spaces were observed, and confirmed to be different from heated groups. We found that the ELF-MF may affect the yolk sac membrane, and no fatal deformation was produced.

CONCLUSIONS: Short-term ELF-MF affects embryonic development, and yolk sac membrane. It was understood that influence went for ELF-MF with a new device, and the further study more is necessary.

P-B-137

STUDY ON TESTICULAR GERM CELL APOPTOSIS OF MICE TO 60 Hz MAGNETIC FIELD EXPOSURE. Y.W. Kim^{1,2}, J.S. Lee^{1,2}, S.S. Ahn³, K.C. Jung⁴, S.K. Lee³, J.Y. Lee⁵, Y.M. Gimm⁶. ¹Institute of Medical Science, ²Department of Microbiology, ³Department of Urology, ⁴Department of Pathology, School of Medicine, Hallym University, Chunchon, 200-702, ⁵Research Institute of Industrial Science & Technology, Pohang, 790-800, ⁶School of Electrical, Electronic and Computer, Dankook University, Seoul, 140-714, Korea.

INTRODUCTION: Extremely low frequency (ELF) fields are defined as those having frequencies up to 300 Hz. 60 Hz electromagnetic (EM) fields were generated from human made sources such as domestic electric devices, electric transport system, etc. Reliable evidence of association between EM field exposure and markers of fertility could not be found in human epidemiological study. Exposure to ELF EM fields has not had significant risk to implantation and developing fetus in animal studies. But in our previous study, continuous exposure of 30 kV/m, 0.5 mT and 1.5 mT for 49 weeks induced the decrease of testis and apoptotic phenomena of spermatogenic cell in mice. This study was the more detail investigation of apoptosis induced ELF magnetic field (MF) in mice.

OBJECTIVES: Investigation of the apoptosis of testicular germ cell induced by the continuous exposure of 60 Hz ELF MF and its some mechanism.

METHODS: Male BALB/c (7 weeks of age) mice were exposed to a 60 Hz MF of 0.1 mT and 0.5 mT continuously, 24 hr/day, for 8 weeks. And male p53 knock-out mice were exposed to a 60 Hz MF of 0.2 mT with same condition above except MF dose. Apoptosis of germ cell in the testis was analyzed by histopathological examination and the TdT-mediated dUTP-biotin nick end labeling (TUNEL) assay to BALB/c and p53 knock-out mice, and flow cytometric examination of isolated spermatogenic cells stained with 7-aminoactinomycin D (7-AAD) to only BALB/c mice.

RESULTS: There was not significant effect on the body weight of mouse exposed to 60 Hz MF. The weight of the testis slightly decreased in the exposed group. Histopathologic examination showed significantly increased incidence of the deaths of testicular germ cells and disorganization of germinal epithelia in the exposed BALB/c mice groups. In the exposed groups TUNEL-positive cells of testis were many and those were mainly spermatogonia, but were rarely in the sham control. Apoptotic, TUNEL-positive, germ cells were significantly increased in mice from the exposed groups compared with the sham control ($P < 0.05$), but the difference between two exposed groups was not statistically significant. Both early and late apoptosis of testicular germ cells in mice from exposed BALB/c mice groups were increased in comparison with sham control used by 7-AAD assay. The p53 is apoptosis-inducing protein, and the increase of this protein induces apoptosis to cell. In histopathologic examination and TUNEL staining of testis of p53 knock-out mice, difference was not found between exposed group and sham control.

CONCLUSION: This study demonstrates that the apoptosis of testicular germ cell could be induced by continuous exposure of 60 Hz MF in BALB/c mice, and suggests that this 60 Hz MF maybe affects integrity of nucleic acid of spermatogenic cell in p53 knock-out mice.

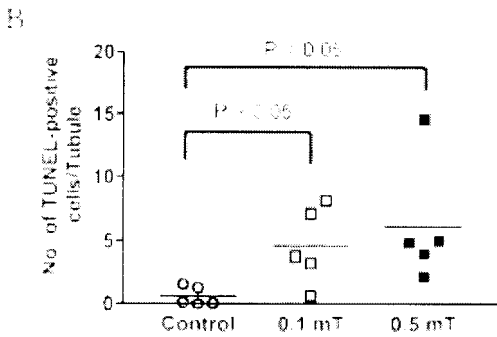
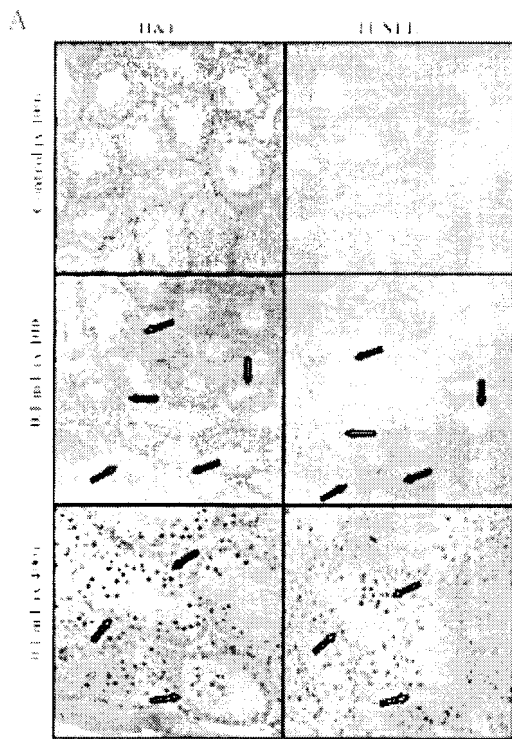


Figure 1: Effects of exposure to 60 Hz magnetic fields on the apoptosis of testicular germ cells. The testicular tissues were stained with H & E (A, left column) or by TUNEL technique (A, right column). TUNEL-positive cells lost from the epithelium (A) and were counted in 100 seminiferous tubules (B). The data represent the results from three independent experiments.

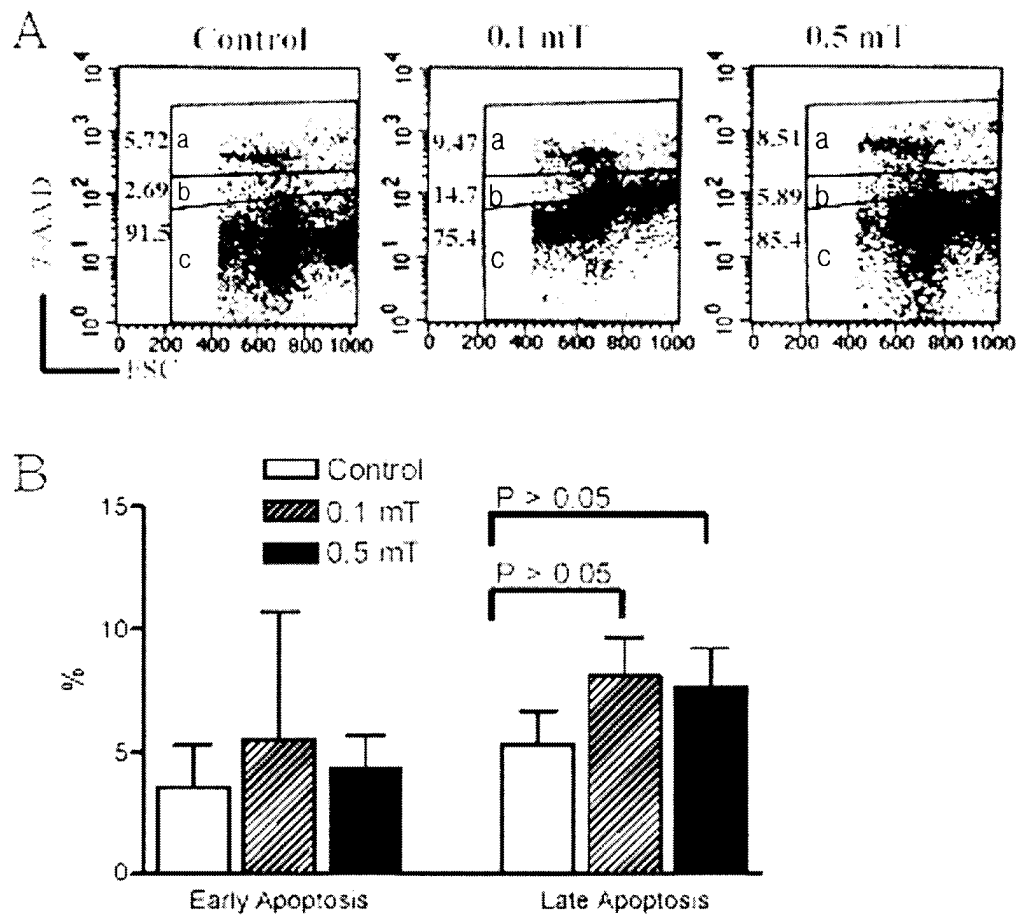


Figure 2: Effects of exposure to 60 Hz magnetic fields on the early and late apoptosis of testicular germ cells. Germ cell rich fractions were separated, and stained with 7-aminoactinomycin D, followed by flow cytometry. The representative data (A) and summary results of flow cytometry (B) are depicted. a, area of normal cells; b, area of early apoptosis; c, area of late apoptosis.

P-C-138

BIOLOGICAL EFFECTS OF 20 KHZ MF EXPOSURE. S.H. Kim¹, D.S. Yoo², Y-M Gimm³, J.K. Pack⁴, H.D. Choi³ and Y-S Lee². ¹College of Veterinary Medicine, Chonnam National University, Kwangju, Korea. ²EME Research Team, Radio & Broadcasting Technology Lab, ETRI, Taejon, Korea. ³Department of Radio Sciences & Engineering, College of Engineering, Chungnam National University, Taejon, Korea. ⁴Lab of Radiation Effect, Korea Institute of Radiological and Medical Sciences, Seoul, Korea.

Sprague Dawley rats (10 males and 10 females per group for sham and magnetic field exposed) were exposed in carousel irradiator to 20 kHz intermediated frequency (IF) magnetic field at 6.5 μ T peak intensity for 8 hrs/day, 5 days/week, for 90 days and 1 year. Urine analysis (pH, serum glucose, protein, ketone bodies, RBC, WBC, glucose, bilirubin, and urobilinogen), blood analysis [WBC, RBC, hemoglobin concentration (HGB), hematocrit (HCT), mean corpuscular volume (MCV), mean corpuscular hemoglobin (MCH), mean corpuscular hemoglobin concentration (MCHC), and platelet (PLT) or thrombocyte count], blood biochemistry (total protein, blood urea nitrogen, creatinine, glucose, total bilirubin, total cholesterol, aspartate aminotransferase, alanine aminotransferase, alkaline phosphatase, and lactate dehydrogenase), and histopathological analysis for organs such as liver, kidney, testis, ovary, spleen, brain, heart, and lung were performed, and there were no significant differences found in the above analyses between IF magnetic field exposed and sham control rats. In addition, in order to evaluate the importance of gestational age to the exposure to 20 kHz sawtooth magnetic field, pregnant ICR mice at gestational days of 2.5 to 15.5 post-coitus which was the most sensitive stage for the induction of major congenital malformations were exposed in carousel irradiator to 20 kHz intermediate frequency sawtooth magnetic field at 6.5 μ T peak intensity for 8 hrs/day. The animals were sacrificed on the 18th day of gestation and the fetuses were examined for mortality, growth retardation, changes in head size and other morphological abnormalities. From the above conditions, it is concluded that the exposure of 20 kHz magnetic field with 6.25 μ T peak intensity does not inflict any adverse effect on pregnant mice fetuses.

P-A-139

STUDENT

EFFECT ON NEURONAL BRAIN ACTIVATION IN MICE FROM PULSED EXTREMELY LOW FREQUENCY MAGNETIC FIELDS. Y. Bureau², K. Marseu¹, A.W. Thomas^{1,2}, F.S. Prato^{1,2}.

¹University of Western Ontario, London, Ontario, Canada; ²Lawson Health Research Institute and Department of Diagnostic Imaging, St. Joseph's Health Care (London), London, Ontario, N6A 4V2, Canada.

BACKGROUND: Pulsed extremely low frequency magnetic fields (PELFMF) have been shown to increase analgesia to hotplate nociception in land snails [1,2] and more recently in mice and humans [3,4,5]. However, little is known about the specific regional brain stimulation that is induced by specific pulsed magnetic fields. Different PELFMF have specific behavioral consequences indicating that unique magnetic field patterns may have different functional consequences (altering behavior, physiology).

OBJECTIVE: To investigate regional activation in mouse brains by pulsed magnetic fields. This will enable us to test magnetic field designs that will target specific brain areas. The brain areas chosen for investigation are the pariaqueductal gray (PAG), the medial (MeA) and central (CeA) amygdala, the locus coeruleus (LC), the anterior cingulate gyrus (CG) and the paraventricular nucleus of the hypothalamus. Note that this is a continuation of an evolving project.

METHODOLOGY: In brief, CD-1 mice were exposed to either; 1) PELFMF ($\pm 200 \mu T_{PK}$, < 500 Hz), 2) discontinuous 60Hz sinusoidal with a refractory period identical to that incorporated in the PELFMF ($\pm 200 \mu T_{PK}$), or 3) ambient MF sham for either 15, 60, or 120 minutes were then euthanized two hours following the termination of treatment. Brains from all mice were processed for regional c-Fos immunoreactivity. C-Fos positive cells were then counted by computer-automated software (Northern Eclipse).

RESULTS: There were no significant effects of the magnetic fields on c-Fos immunoreactivity of the LC, and MeA and CeA. There was, though, a greater density of c-Fos positive cells for the 60Hz pulsed field treated group compared to the other two conditions in the PAG. Also, there was a greater density of c-Fos positive cells in the 60Hz pulsed field treated group in the anterior CG compared to the other two conditions when exposed for 60 minutes. However, more data is required to assess the robustness of the trends presented here.

CONCLUSIONS: Stress related structures such as the LC, MeA and CeA are not differently activated by a specific pulsed magnetic field. However, the PAG and CG, which are associated with pain modulation, show greater activation when exposed to the 60Hz pulsed fields. This is consistent with published data from our laboratory that show a modulation of pain sensitivity in mice and humans using similar fields.

References:

- [1] ^aThomas, A.W., Kavaliers, M., Prato, F.S., and Ossenkopp, K.-P. (1997). *Peptides*, 18(5), 703-709.
- [2] ^bThomas, A.W., Kavaliers, M., Prato, F.S., and Ossenkopp, K.-P. (1997). *Neuroscience Letters*, 222, 107-110.
- [3] Rollman, G., Misener, T., Thomas, A., Prato, F. 24th Annual Bioelectromagnetics Society Meeting, Quebec, Canada, June 23-27th, 2002.
- [4] ^aShupak et al 2004, *Neuroscience Letters*, 354 (1), 30-33.
- [5] ^bShupak et al 2004 *Journal of Pain* (submitted January 2004).

This study was funded by Fralex Therapeutics Inc.; St. Joseph's Health Care (London) Foundation; the Lawson Health Research Institute; the Department of Diagnostic Imaging, SJHC; Natural Sciences and Engineering Research Council of Canada (NSERC); Canadian Institutes of Health Research (CIHR); National Research Council (NRC); the Ontario Research and Development Challenge Fund (ORDCF), Canada Foundation for Innovation (CFI); and the Ontario Innovation Trust (OIT).

THE ENVIRONMENTAL IMPACT OF R.F. ELECTROMAGNETIC FIELDS IN ITALY: MANAGEMENT OF SCIENTIFIC AND SOCIAL ASPECTS. B. Bisceglia¹, M. Boumis² ¹Università del Sannio at Benevento, ² Fondazione Ugo Bordoni – Roma, Italy.

INTRODUCTION: The development and diffusion of telecommunications technologies known in the last few decades have led to a widespread increase of electromagnetic sources over the territory. In Italy, more than in other European Countries, anxiety and fears have arisen. The problem related to the exposure to electromagnetic fields at radio frequency has to be managed at different levels, starting from the local context, which is the closest to citizens, up to the regional, national and international framework.

OBJECTIVES: First of all, citizens will be informed about the electromagnetic field levels actually present in the environment and about the field trends both in the short and long period. Moreover, some complete and systematic information will be given to the scientific community about the temporal and spatial statistics (average and correlation values) of the distribution over the national territory of the electromagnetic fields at radio frequency. Finally, the conditions for a sustainable development of radio communications networks will be constructed, granting transparency and avoiding both unjustified alarm and the proliferation of non-co-ordinate actions originated by Local Administrations.

METHODOLOGY: The treated topic regards several Ministries as well as the Regions, the Provinces and the Municipalities. A homogeneous methodology advantages all the subjects and institutions. The Minister of Communications will nominate a Strategic Committee, where Regions and Local Administrations, supported by Environmental Agencies, will be represented. Ugo Bordoni Foundation is a high-cultured research institute, specialized in telecommunications systems and electromagnetic field topics, which guarantees homogeneous characteristics of the national monitoring network.

CONCLUSIONS: After a few months of activity about 200 wide band measure stations have been installed all over the national territory and over then 400 sites has been monitored during a period of about 300.000 hours.

The experimental results give evidence that the exposure levels are almost always well below thresholds among the most restrictive of Europe.

In the same time, it is evident how correct and complete information helps in increasing public consciousness of the electromagnetic phenomenon, thus reducing the unjustified alarms induced by an incorrect or wrong knowledge of the theme.

P-C-141

RATIONALE FOR THE DRAFT OF CHINA EMF EXPOSURE STANDARDS. H. Chiang Z. Xu. Bioelectromagnetics Lab, Zhejiang University School of Medicine, China.

The main differences (with ICNIRP) and its own rationale are as follows:

(1) There is a body of literature, which reports that health effects can be shown at such a level of radiation that does not produce heating or stimulation. For RF exposure, the SAR thresholds of behavior-disruption have been observed at the levels much lower than 4 W/kg. The bi-phasic changes in immune system were reported at even lower SAR or power densities. In vitro studies, the evidence of RF non-thermal bioeffects is increasing, and the knowledge regarding the molecular mechanisms of low-level EMF potentially adverse health effects is growing. The SAR threshold for the adverse effects in the frequency range from 100 kHz to 10 GHz may be at 0.5 to 1.0 W/kg, rather than 4.0 W/kg. Thus, a whole body average SAR of 0.1 W/kg is chosen as the restriction for occupational exposure, and 0.02 W/kg for general public exposures in the draft of amending China exposure standard. For power frequency (ELF) magnetic field (MF), there is growing evidence that the magnetic fields penetrate cells, tissues and cause bio-effects by themselves. For example, the suppression of gap junction intercellular communication (GJIC) is induced by MF itself rather than the induced electric field. Rapid induction of heat shock proteins by 60 Hz MF exposure at only microtesla level with the related molecular mechanism have been reported. There are many reports showing that 0.1 mT ELF MF exposure may affect cell functions. Coincidentally, adverse health effects induced by 0.1 mT ELF MF exposure were also reported in *in vivo* studies. Since IARC has concluded that the power-frequency MF are possible human carcinogens, and the increasing in the biological plausibility in mechanism and supportive data from animal experimental studies, the exposure limit for ELF MF exposure are suggested to be lower than ICNIRP's.

It is noteworthy that in the research field of bioelectromagnetics, the published reports lacked consistency, and there are many negative results reported. The reason why the pattern of positive and negative reports occurs so commonly are discussed.

(2) Limitation and application of SAR. The SAR is a valid measure of energy absorption rate during RF exposure, but not a quantity indicator of biological effects. For example, the significantly different bioeffects between continuous and intermittent RF exposure, between modulated and unmodulated microwave exposure, under the same SAR questioned the issue of using SAR as a basic restriction. Since the mechanism of low level RF exposure is not well known, the SAR is now useful at extrapolations from animal experiments to human at specific frequencies, but has its limitations. In the draft of amending exposure standards of China, actually the named basic restriction is preliminary restriction. The exposure limits (reference levels) are not only derived from the SAR values, which are also based on exposure duration and considering the data of other factors.

P-A-142

EVALUATION OF HUMAN EXPOSURE TO RF ELECTROMAGNETIC FIELDS FROM MOBILE WIRELESS DEVICES. E.D. Mantiplay, R.F. Cleveland, Jr., M. Perrine, T. Harrington. Office of Engineering and Technology, Federal Communications Commission, Washington DC 20554, USA.

BACKGROUND: The United States Federal Communications Commission (FCC) has adopted limits for human exposure to radiofrequency (RF) electromagnetic fields from RF devices and facilities authorized or licensed by the FCC. These transmitters range from medical implants to high power radars. RF transmitters are classified by the FCC as either fixed, mobile, or portable for regulatory purposes. Compliance is determined by evaluating field strength, power density or specific absorption rate (SAR), as appropriate. The FCC classifies RF devices as "mobile" devices if they are designed to be used at least 20

cm from the user or nearby persons. Devices such as cell phones are classified as “portable” devices (those used closer than 20 cm), and are evaluated in terms of SAR. Mobile RF devices can be evaluated by either SAR or by determining field strength or power density. Section 15.247 of the FCC’s regulations includes rules governing the use of spread spectrum transmitters operating in the 902-928 MHz, 2400-2483.5 MHz and 5725-5850 MHz bands. These devices are permitted to operate at peak conducted output power levels of between 0.125 and 1 watt. Many recently introduced wireless devices used by consumers operate according to these rules. Typical devices authorized under Section 15.247 include cordless telephones, wireless local area network devices (“Wi-Fi”), and wireless computer peripherals. Routine RF exposure evaluation is not required for these devices, but they are required to comply with the exposure limits adopted by the FCC (Title 47 of U.S. Code of Federal Regulations, Section 1.1310).

OBJECTIVE: A study was undertaken to determine exposure levels from typical wireless devices and to determine whether such devices comply with FCC exposure limits under conditions of normal use. This study concentrated primarily on mobile devices and compliance with limits for Maximum Permissible Exposure (MPE) in terms of field strength and/or power density. SAR data, if available, were also analyzed for comparison purposes.

METHODS: Measurements of electric field strength were made using a Wandel and Golterman EMR-30 survey meter probe. DASY free-space E and H-field probes were used where practical for final measurements and for comparison with EMR-30 measurements. Probes were positioned adjacent to the device under test to determine maximum field strength and also in various directions at 5 cm and 20 cm from the device’s antenna. Tests were conducted using typical operating powers and, when achievable, maximum authorized power levels.

RESULTS/CONCLUSIONS: Example preliminary data are given in the table below. The electric field levels measured near the devices listed here were compliant with MPE limits for whole-body exposure. Data for these four devices, all operating near 2.4 GHz are reported below. Devices tested were: (1) a Wi-Fi access point, (2) a Wi-Fi laptop PCMCIA card, and (3) two cordless telephone base stations. This presentation will include all data obtained in this study from typical wireless devices used by consumers. Typical exposure levels will be compared with allowable MPE limits.

Device	Power (mW)	Adjacent Field (V/m)	Field at 5 cm (V/m)	Field at 20 cm (V/m)
Access Point	10	21	14	6
PCMCIA Card	32	15	12	4
Cordless Base 1	57	16	11	3
Cordless Base 2	10	12	10	4

P-B-143

THE PRACTICAL APPLICATION – REALISATION OF THE “ROUND-TABLE-CONSENSUS-MODEL” FOR MOBILE-PHONE-BASE-STATION-SITING. E. Maršálek, Plattform Mobilfunk-Initiativen PMI, Lenaugasse 36, A-3400 Klosterneuburg-Kierling, Austria.

INTRODUCTION: Protests from neighbourhoods occasioned by the planned siting of mobile-phone base-stations are still a world-wide problem for providers and authorities. The legal and practical situation for neighbours of mobile-phone antenna has still not become better, despite WHO recommendation that public involvement and minimisation are essential criteria for acceptance of the antenna-infrastructure for mobile phones.

The every-day-reality in mobile-phone-antenna-siting is still:

a lack of democratic rights and procedures, Governments providing near complete “freedom” for antenna siting in contrast to restrictions placed on other sectors of the private economy that provide facilities and uses for the every-day-life of a major party of the population, international re-insurance companies denying cover of potential EMF-health-risks, health fears of citizens irrespective of the ICNIRP guidelines (even when they are generally met), losses in property values near antennas, increased publicity for suspect shielding-products, and significant problems and costs for mobile-phone providers, public administration and health-insurers as well as private persons.

OBJECTIVE: What procedures and confidence-building measures during the siting-process are necessary for acceptance of the mobile-phone-infrastructure by the public as well as by mobile-phone-users, for minimisation of exposure, for monitoring after installation, for population-health-survey?

METHODS: The siting of mobile-phone antenna should be based on:

1. Exposure minimisation to the minimum needed for the service
2. Minimisation has to be proved, during the planning-phase, with exposure calculations and different siting options
3. Exposure evaluation must include existing HF-EMF sources
4. Open-minded discussion to invoke “new technical strategies” like existing systems of microcells with low-performance, flat-strip-lines-solutions (used now especially in indoor-environments), microcells with nets of “optical fibers” and others.
5. Involvement of communities and concerned public also to guarantee reduction of visual impacts and health fears
6. Industry-independent long-term monitoring of exposure levels after installation.
7. National and local databases of exposure levels from all RF-transmitters free to the public.
8. Use of these databases for evaluation of exposure minimisation
9. For exposure-minimisation, adjustment of existing antennas must, based on application of ALATA (Precautionary Principle), occur within three years of adopting these principles.
10. Reported health problems after installation of antennas must be collected and studied epidemiologically to establish and clarify the reasons for reported health and well-being- problems.

RESULTS: To realise the “round table consensus-model” in daily practice, employees of local authorities should, following a certified training program in co-operation with specialised companies and PMI, calculate the expected exposure for different siting-options as a basis for responsible siting decisions (exposure minimisation). After installation, provider-independent long-term monitoring represents permanent confidence-building measures based on free, publicly available databases.

CONCLUSION: The practical application of the “Round-table Consensus-Model” is an immediately achievable technical problem- and cost-reducing, confidence-building approach. This approach will allow the siting of mobile-phone base-stations based on the Precautionary Principle, to satisfy public requirements, while providing legal regulations for EMF consistent with existing regulations for other agents, like chemicals in the air and water.

Participation is sponsored by the Austrian „Lebensministerium“

P-C-144

THE AUSTRALIAN CENTRE FOR RF BIOEFFECTS RESEARCH (ACRBR) - AN NHMRC CENTRE OF RESEARCH EXCELLENCE. R.J. McKenzie, R.J. Croft, V. Anderson, Australian Centre for Radiofrequency Bioeffects Research, RMIT University, Melbourne, Victoria, 3000, Australia.

OBJECTIVE: The Australian Centre for Radiofrequency Bioeffects Research (ACRBR) is a newly established multi-institutional research centre which seeks to research questions pertaining to possible

health effects of exposure to radiofrequency devices, such as mobile phones and which is funded under the Australian National Health and Medical Research Council (NHMRC) Centres of Research Excellence funding program.

INTRODUCTION: The Centre of Research Excellence in Electromagnetic Energy will combine the efforts of engineers, epidemiologists, physicists, psychophysicists and veterinary pathologists from a number of leading Australian research institutions including RMIT University, the Institute of Medical and Veterinary Science in South Australia (IMVS), Monash University, Swinburne University of Technology and Telstra Research Laboratories (TRL). The centre is funded at \$2.5 M over five years and will undertake a program of research to address the issue of exposure to radiofrequency (RF) devices and health. It will also train new scientists, keep the community informed of ongoing developments and help the development of government policies in this area of considerable public concern.

BACKGROUND: In recent years there have been a number of substantive international reviews on the potential for biological and health impacts from public exposure to the RF emissions of telecommunications technologies, especially with regard to mobile telephony (Royal Society of Canada¹, U.S. GAO², Health Council of the Netherlands³, Stewart Report⁴, ICNIRP Guidelines⁵, French Parliamentary Report⁶, WHO⁷, Zmirou⁸). These reviews have been led by distinguished scientists and public policy makers in their field, and while varying in detail, have produced a consensus view on the highest priority issues to be addressed by ongoing research. Priority research areas identified in these reviews include neurobiological studies, epidemiological studies (both of cancer and non-cancer outcomes), and dosimetry studies. Public information dissemination and consideration of particular population subgroups (e.g. children and ‘electromagnetic hypersensitives’) are also accorded high priority.

METHODS: Neurobiology: One important area where there is a perceived research gap is in the area of potential neurological effects, which will hence be a major focus of this Centre. The proposed studies range from *in vitro* and *in vivo* research studies of RF effects on neuron and neural system functioning in rodents, to that of RF effects on simple neural function, cognition and subjective report in humans. The latter series of studies have been developed to account for the consensus view that more emphasis needs to be placed on possible differences in RF population sensitivity (e.g. youth versus aged, and ‘electromagnetic hypersensitives’).

Epidemiology: Epidemiological studies are an important tool in studying the impact on public health from exposure of whole populations to modern radio technologies. Cancer outcomes in this area of research are already adequately covered the internationally based IARC study. However, epidemiological research investigating associations of mobile phone exposure and non-malignant health outcomes in the general community is less well treated. We propose to undertake a cohort study of teenage school children, an age group identified as a priority research area^{1-2,4-8}, and monitor for an initial period of three years. All subjects will undertake a baseline questionnaire (paying particular attention to evidence of RF-sensitivities and sleep abnormalities), physiological (HR, BP) and cognitive tests. Exposure from normal mobile phone use will be assessed by self report, customer record and physical dosimetry of specific handset type. The establishment of this cohort would also allow for future follow-ups in 5, 10 or 20 years, when any long-term effects may present.

Dosimetry: The technical reviews cited above consistently identified rigorous dosimetry as a key issue for ensuring the validity of results within a given study and consistency of results between studies. This requires that a well-characterised standard methodology and suite of tools be utilised for the provision of dosimetry to research programs that are run within the Centre. The technical reviews have also raised concerns regarding the application of compliance techniques in RF human exposure standards, based on adult models, to children. Further, there remain questions as to applicability of current compliance techniques to the rapidly changing new communications technologies, particularly as they relate to non-handset issues (wireless LANs, mobile data enabled palmtops and laptops etc⁹). Therefore, apart from providing the necessary dosimetry for the other research programs already described, the Centre also proposes to undertake both physical and computational studies to improve the understanding of dosimetric sensitivity to normal population variations such as size, ethnicity, and age and how these impact on current

compliance techniques employing standard human models such as the SAM phantom cited in many protocols (eg CENELEC¹⁰).

CONCLUSIONS: The establishment of the ACRBR is undoubtedly one of the most significant developments in the area of RF bioeffects research in Australia. The Centre will not only advance the international body of knowledge on this subject, but also train new scientists in this multifaceted area of research to carry on the work of the Centre in other institutions in the future. Outcomes of the research will appear in the peer reviewed literature and international scientific fora, and will also be input into public policy and standards setting and regulatory processes. The Centre will also act as a publicly accessible information resource centre on this highly sensitive issue for the general community.

References.

1. C. V. Byus, B. W. Glickman, D. Krewski, W. G. Lotz, R. Mandeville, M. L. McBride, F. S. Prato, and D. F. Weaver, "A Review of the Potential Health Risks of Radiofrequency Fields from Wireless Telecommunication Devices," The Royal Society of Canada, Ottawa RSC.EPR 99-1, March 1999.
2. P. Guerrero and J. P. Finedore, "Research and Regulatory Efforts on Mobile Phone Health Issues," United States General Accounting Office, Washington, Report to Congressional Requesters GAO-01-545, May 2001.
3. Health Council of the Netherlands, "Mobile telephones; an evaluation of health effects," Health Council of the Netherlands, The Hague, Advisory Report No. 2002/01E, January 2002.
4. Independent Expert Group on Mobile Phones, "Mobile Phones and Health," National Radiological Protection Board, Chilton April 2000.
5. International Commission on Non-Ionizing Radiation Protection, "Guidelines for limiting exposure to time-varying electric, magnetic, and electromagnetic fields (up to 300 GHz)," Health Physics, vol. 74, pp. 494-522, 1998.
6. J.-L. Lorrain and D. Raoul, "The possible impact of mobile telephony on health," Parliamentary office of assessment of scientific and technological choices, French National Assembly, Parliamentary report No. 346, November 2002.
7. M. H. Repacholi, "Low-level exposure to radiofrequency electromagnetic fields: health effects and research needs," Bioelectromagnetics, vol. 19, pp. 1-19, 1998.
8. D. Zmirou, B. Veyret, R. de Seze, P. Aubineau, A. Bardou, and M. Goldberg, "Mobile telephones, their base stations and health," Paris, Report to the French Health General Directorate January 2001.
9. D. Black, "Stable standards and new challenges in radiofrequency safety," presented at The Annual Conference of Engineering and Physical Sciences in Medicine, Rotorua, New Zealand, 2002.
10. European Committee for Electrotechnical Standardization, "Basic standard for the measurement of specific absorption rate related to human exposure to electromagnetic fields from mobile phones (300 MHz - 3GHz)," CENELEC EN 50361, 2001.

P-A-145

WHY TO APPLY THE PRECAUTIONARY PRINCIPLE AGAINST MOBILE PHONE BASE STATIONS. R. Santini. National Institute of Applied Sciences (INSA), Villeurbanne, Cedex, 69621, France.

Several arguments can be advanced for applying immediately the precautionary principle to counter the biological effects of cellular phone base stations. Microwave bio effects are known and relearned for more than 40 years: Chronic exposure to microwaves is responsible for the appearance of the microwave syndrome, also called radio frequency sickness, which has been described since the 1960's by researchers of eastern countries. It is characterized by -a debility syndrome (fatigue, irritability, headaches, ...)- a cardiovascular dysfunction syndrome (bradycardia, tachycardia, ...) -a brain dysfunction syndrome (insomnia, concentration difficulties, ...). b Exposure to a mobile cellular telephone generates biological effects: Studies give evidence to a relationship between exposure (number and duration of phone calls)

and the increase in complaints such as headaches, fatigue, feeling of warmth on the ear, feeling of discomfort. ...[1, 2], disturbances to the permeability of the blood-brain barrier [3] - Biological effects are reported by people living in the vicinity of mobile phone base stations: Two studies at least [4, 5] have shown that people living in the vicinity of cellular phone base stations are suffering of microwave syndrome pathologies in relation with their age, their sex and the level of their exposure to microwave power density. 4. Some countries have adopted low exposure limits for their population: In place of 450 and 900 $\mu\text{W}/\text{cm}^2$ (41 and 58 Volts/m) allowed in USA and in Europe for the level of permitted exposition to 900 and 1800 megahertz. Italy adopted 10 $\mu\text{W}/\text{cm}^2$ (6 Volts/m), Luxembourg 3 Volts/m and in Austria the Salzburg resolution recommends 0.6 Volts/m . ~ Sensitivity to microwaves is not the same for all: In 1995 the National Institute of Research and Safety (INRS) concluded after a French Air Force epidemiological study: "There exists indisputably an individual sensitivity to the effects of radio frequencies. Undergoing the same exposure, certain individuals can present with clinical disturbances and others not." [6]. It is equally apparent that children are more vulnerable than adults, due to their developing nervous system and a more intense absorption of electromagnetic energy by their tissues. According to the International Radiation Protection Association (IRPA) this individual sensitivity to radio frequencies would have a genetic basis. ~ Extremely low frequencies (ELF) are present in the mobile telephone signal: It is well known that ELF, like microwaves, have also biological effects at very low values (0.2 to 0.4 μT for the ELF magnetic field), values which are found in the mobile telephone signal.

CONCLUSION: With regard to the preceding.

NEURAL NETWORK MODELS OF THE PERIPHERAL AND THE CENTRAL NERVOUS SYSTEM IN THE PRESENCE OF THE ELECTROMAGNETIC FIELD. A.M. Tranquilli, F. Apollonio, M. Liberti, G. D’Inzeo. ICEmB at Department of Electronic Engineering, “La Sapienza” University of Rome, 00184 Rome, Italy.

OBJECTIVES: An analysis of the possible effects of the interaction between the electromagnetic (EM) field and the nervous system at high and low frequencies is conducted. For this purpose two neural networks are developed: (a) a peripheral network with a pyramidal feed-forward structure [1], and (b) a network simulating a part of the cortical central system composed by excitatory and inhibitory neurons with all-to-all connections [2].

METHODS: For the single neuron an Hodgkin-Huxley (HH) like model with a temperature dependence is used [3]. The synaptic connections between the neurons of the networks are realised with a dynamic synapse model [4]. At high frequencies (~1GHz) only thermal effects are considered, introduced in the network models as a temperature increase. The temperature variations range from 0.1°C, according to the studies on human head exposure to EM fields generated by cellular phones [5], to 1°C limit evaluated by ICNIRP [6]. At lower frequencies (< 70 MHz: human body resonance frequency) the EM field induces a membrane potential given by $\Delta V_m(\theta) = \frac{1.5 E R \cos \theta}{1 + j \omega \tau}$ [7], which gives rise to a current flow across the

membrane due to the presence of the membrane conductance. This current density is directly introduced in the single neuron model. The analysis is made at the power line frequency (50Hz), with current density maximum amplitudes calculated from the EM reference limits given by ICNIRP [6]. Possible effects on the behaviour of the neural networks due to the introduction of the EM field are observed on the time course of the standard deviation (σ_{ISI}), the mean interspike interval (ISI) and the coefficient of variation ($C_V = \sigma_{ISI}/ISI$) of the neural spike trains analysed. For the peripheral network a multiplication factor $Q = \frac{\Delta \omega_s / \omega_s}{\Delta \omega_p / \omega_p}$, proposed

by Adair [1], measures the sensitivity of the network to the changes of the primary neurons firing frequency caused by an external perturbation, in this case the EM field.

RESULTS: Results of the peripheral neural network in the presence of the EM field show that: (a) the maximal effects, high Q values, correspond to those synaptic conductances that present the maximal variability, measured by the coefficient of variation C_V , as shown in Fig. 1 and Fig. 2 for the high frequency case; (b) this amplification is proportional to the number of network layers considered, in Fig. 3 we can see the comparison of Q values between the two-layers and the three-layers network. For the central neural network in the presence of the EM field it is possible to observe: (a) at high frequencies the network model presents linear effects; (b) at 50Hz a greater synchronisation is shown for a particular value of the induced density current than in the case without the EM field; the effect of the field can also be seen directly on the potential waveforms of an excitatory and inhibitory neuron in Fig. 4.

DISCUSSION: The realised networks are valid models of neural networks that can be used for further investigations on the effects of EM fields on the nervous system. The results show different behaviours depending on the network structure and the frequency and amplitude of the EM field.

References

- [1] R.K. Adair: "Simple neural networks for the amplification and utilisation of small changes in neuron firing rates", *Proc. Natl. Acad. Sci USA*, vol. 98, no. 13, pp. 7253-7258, 2001.
- [2] C. Koch, I. Segev: "Methods in Neuronal Modeling", *The MIT Press, Cambridge*, 1998.
- [3] P. Bernardi, G. D’Inzeo, S. Pisa: "A generalized ionic model of the neuronal membrane electrical activity", *IEEE Transactions on Biomedical Engineering*, vol. 41, pp.125-132, 1994.
- [4] A. Destexhe, Z.F. Mainen, T.J. Sejnowski: "An efficient method for computing synaptic conductances based on a kinetic model of receptor binding", *Neur. Comput.*, vol. 6, pp. 14-18, 1994.

[5] P. Bernardi, M. Cavagnaro, S. Pisa, E. Piuze: "Specific absorption rate and temperature increase in the head of a cellular phone user", *IEEE Transactions on Microwave Theory and Techniques*, vol. 48, no. 7, pp. 1118-1126, 2000.

[6] ICNIRP Guidelines: "Guidelines for limiting exposure to time varying electric, magnetic and electromagnetic fields (up to 300 GHz)", *Health Phys.*, vol. 74, no. 4, pp. 494-522, 1998.

[7] C. Polk, E. Postov: "CRC Handbook of biological effects of electromagnetic fields", ed. CRC Press, 1986.

This work is supported by the European Union, V framework under the RAMP2001 Project.

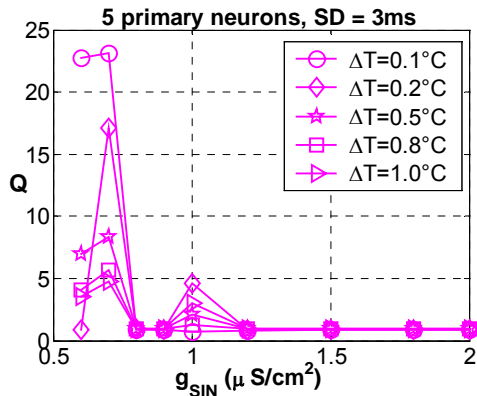


Figure 1: Multiplication factor Q for the peripheral network with 5 primary neurons, starting times with standard deviation $SD=3ms$, high frequency case.

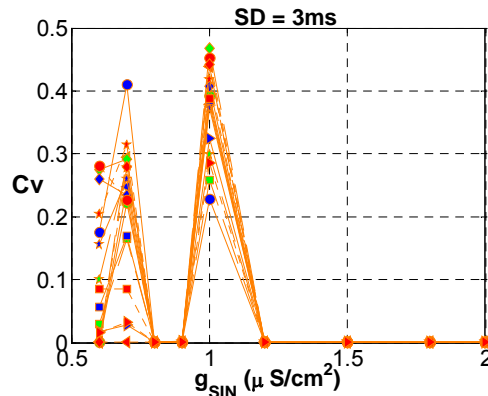


Figure 2: Coefficient of variation for the peripheral network where results for 5, 10, 20 primary neurons are reported all together, starting times with standard deviation $SD=3ms$, high frequency case.

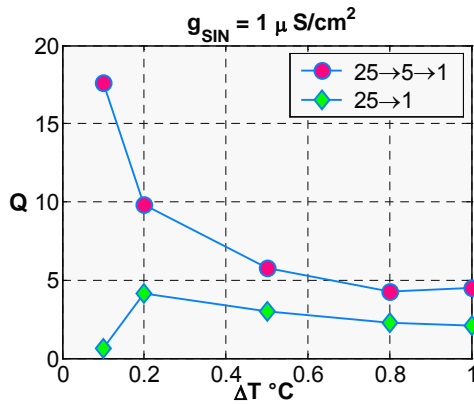


Figure 3: Multiplication factor Q for the peripheral network with 2 and 3 layers, starting times with standard deviation $SD=3ms$, high frequency case.

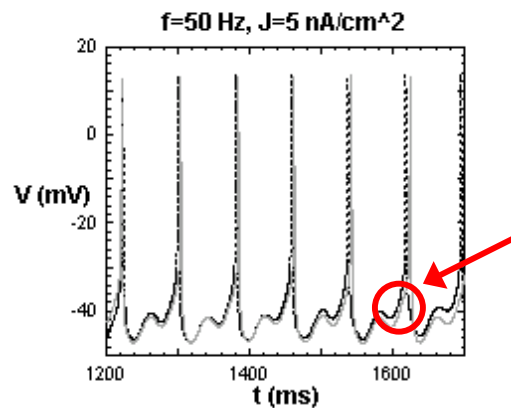


Figure 4: Membrane potential for an inhibitory (solid) and an excitatory (dotted) neuron neural network in the presence of an EM field at 50 Hz.

P-C-147

BIOLOGICAL EFFECTS OF ULTRA-WIDE-BAND PULSES. S.-T. Lu. McKesson BioServices, U.S. Army Medical Research Detachment, Microwave Bioeffects Branch, Brooks City-Base, Texas 78235, USA.

INTRODUCTION: Ultra-Wide-Band (UWB) technology and device are known since 1960. The UWB device is used to transmit and receive an extremely short duration pulse of radio frequency energy, typically a few tens of picoseconds to a few nanoseconds. In addition to military application, UWB device has been used in imaging, vehicular radar, communication, and measurement systems. Newly developed UWB sources are capable of generating hundreds of gigawatts peak power and establishing hundreds of kV/m peak electric field. Safety aspects of high peak power of ultrashort electromagnetic pulses have been questioned and debated. Earliest report on this topic appeared in 1993. Biological database is limited that hinder a judicious promulgation of personnel protection guidelines/standards. Due to ultrashort pulse duration that results in very low duty factor, specific absorption rate and specific absorption, thermal mechanism cannot be used adequately to interpret a few biological effects observed.

OBJECTIVE: The objective of this presentation is to update the current progress in studies of biological effects of UWB pulses that was included in a previous publication [1].

RESULTS: UWB pulses have been used *in vitro* and *in vivo* to elucidate potential biological effects of UWB pulses. Peak e-field intensity ranged from 55 kV/m to 250 kV/m with duty factor between 4.5×10^{-7} to 1.2×10^{-5} . Estimated specific absorption rates ranged between 3.7 mW/kg and 300 mW/kg *in vivo*. Duration of exposure ranged from 25 ms to 30 minutes. Endpoints studied were mutagenesis, UV-induced mutagenesis and recombination, cell cycle progression, p53 target gene transcription, NF- κ B DNA binding activity, endpoints in functional observation battery, swimming performance, brain c-fos protein expression, metazolol-induced seizure, pentylenetetrazol-induced seizure, nociception, morphine-induced analgesia, morphine-induced hyperactivity, L-NAME (N^G-nitro-L-arginine methyl ester) -induced hyperactivity, L-NAME-induced analgesia, nitric oxide production, blood pressure, heart rate, time-domain and frequency-domain heart rate variability, posture-induced alterations in heart rate and blood pressures, development of mammary tumor, and neural and behavioral teratologies. Biological effects were not found when exposure duration was less than 2 minutes. Biological effects observed were: blocking of the L-NAME induced hyperactivity [2], delayed hypotension and increased VLF power spectrum density of the frequency-domain heart variability [3], enhanced nitric oxide production in γ -interferone and lypopolysaccharide stimulated murine macrophages, increased NF- κ B binding activity in human cells [4], more stress vocalization in rat pups, longer medial-to-lateral length in hippocampus and decreased mating frequency [5].

CONCLUSION: Biological effects were observed in cells and animals exposed to UWB pulses at peak e-field around 100 kV/m or less. Additional studies are needed.

References.

- [1] Lu S-T, de Lorge JO (1999) In: "Advances in Electromagnetic Fields in Living Systems", vol. 3, Lin JC ed., Kluwer Academic/Plenum Publishers, NY, NY, pp 207-264.
- [2] Seaman RL, Belt ML, Doyle JM, Mathure SP (1999) *Bioelectromagnetics* 20: 431-439.
- [3] Lu S-T, Mathur SP (2002) In: "Proceedings of the 2nd International Workshop on Biological Effects of Electromagnetic Fields", Kostarakis P ed., pp 409-418.
- [4] Natarajan M, Vijayalaxmi, Szilagy M, Roldan FN, Meltz ML (2003) 25th Annual Meetings of Bioelectromagnetics Society, Maui, HI, USA, June 22-27, p 202.
- [5] Cobb BL, Jauchem JR, Mason PA, Dooley MP, Miller SA, Ziriaux JM, Murphy MR (2002) *Bioelectromagnetics* 21: 524-537.

This work is supported by the U.S. Army Medical Research and Materiel Command under contract DAMD17-94-4069 with McKesson BioServices. The views, opinions and/or findings are those of author

and should not be construed as an official Department of the Army position, policy, or decision unless so designated by other documents.

P-A-148

STUDENT

EFFECTIVE PERMITTIVITY OF BIOLOGICAL MATERIALS: AN ANALYSIS ON THE ROLE OF WATER CONTENT USING MIXING FORMULAS. A. Sadasiva, M.J. Schroeder, R.M. Nelson. Department of Electrical and Computer Engineering, North Dakota State University, Fargo, North Dakota, 58105, USA.

BACKGROUND: A study on the dielectric properties of biological tissues reveals discrepancies in permittivity values published in literature [1]. These discrepancies have made it difficult to accurately determine the electromagnetic field behavior in biological medium and to assess potential health effects. Since the permittivity of a material is a function of the constituent materials, there is a critical need to define the role of these materials in accounting for the variability. Water is a major constituent of biological materials and its relative percentage varies between subjects and changes with age and physiologic state. In the present study we investigate the role of water content on the effective permittivity of biological materials.

OBJECTIVE: To determine whether changes in the volume fraction of water in biomaterials accounts for the discrepancies in permittivity values published in literature.

METHODOLOGY: Theoretical effective permittivity was calculated from the combination of water and biological material through the use of mixing formulas for 3-dimensional asymmetry. Using values obtained from literature, extensive numerical analyses were performed to determine the distribution of effective permittivity for different levels of water concentration (volume fraction) and biological material permittivities. This was repeated for various fluids and frequencies. Various theoretical bounds were tested and the most suitable mixing formulas (Maxwell-Garnett [2] and Bruggemann [3]) were identified using the Weiner [4] and Hashin-Shtrikman [5] limits. Calculations were performed independently using each mixing formula.

RESULTS: Effective permittivity was calculated for particular biological materials and compared to those found in literature. Additionally, cases were performed to analyze general trends in the change of effective permittivity. An example using the Maxwell-Garnett mixing formula at a frequency of 100 MHz is shown in Figure 1. Expected maximum and minimum effective permittivity values are achieved at the 0% and 100% water volume fractions. The darker region of each bar indicates the permittivity range when the water volume fraction is varied over a more physiologically acceptable range of 54% to 80%. For this range, the effective permittivity changes very little when the material permittivity is similar to the water permittivity and up to 20 when its permittivity is much different than water.

CONCLUSION: This study demonstrates that the water concentration of biomaterials can play an important role in the measured permittivity value. The analyses revealed that the physiological levels of the water content in biological materials can account for the variations of permittivity values found in literature. Currently, work is being performed to investigate how the effect of water level on permittivity will affect the distribution and intensity of electromagnetic fields in the body.

References:

[1] <http://www.brooks.af.mil/AFRL/HED/hedr/reports/dielectric/>

[2] J.C.M.Garnett, "Colors in metal glasses and metal films," Trans.R.Soc., vol.CCIII, pp.385-420, 1904.

[3] D.A.G.Bruggemann, "Berechnung verschiedener physikalischer konstanten von heterogenen substanzen, i. dielektrizitatskonstanten und leitfahigkeiten der mischkorper aus isotropen substanzen," Ann. Phys., vol. 24, no. 5, pp.636-664, 1935.

[4] O.Weiner, "Zur Theorie der refraktionskonstanten," Berichtiiber Verhandlungen koniglich-Sachsische Gesellschaft Wissenschaften Leipzig, vol. 62, pp. 256-277, 1910.

[5] Z.Hashin and S.Shtrikman, "A variational approach to the theory of the effective magnetic permeability of multiphase materials," J.Appl. Phys., vol. 33, no. 10, pp.3125-3131, 1962. This work was supported by National Science Foundation – EPSCoR grant #0132289.

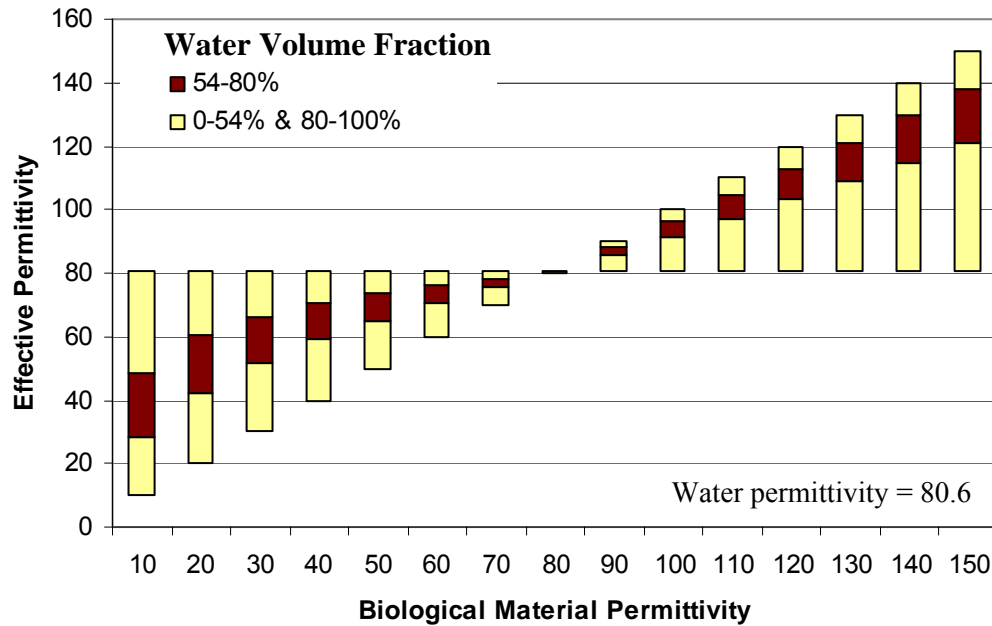


Fig 1: Effective permittivity at various water volume fractions for different values of material permittivity.

P-B-149

STUDENT

THE EFFECT OF FLUID LEVELS ON THE DISTRIBUTION OF ELECTROMAGNETIC FIELDS IN THE BODY. A. Sadasiva, M.J. Schroeder, R.M. Nelson. Department of Electrical And Computer Engineering, North Dakota State University, Fargo, North Dakota, 58105, USA.

BACKGROUND: With growing concern of health threats the effect of electromagnetic (EM) fields on the body has become a major area of research. However, our current understanding of how changes in EM fields affect biosystems is still incomplete. The design and interpretation of various studies on the EM field behavior in biological materials has been complicated by the inadequate characterization of the material characteristics that determine the mechanisms of interaction and energy distribution. In this study we aim to determine the role of one of the confounding variables that affects the electrical characteristics of the materials and hence the EM field behavior in biosystems.

OBJECTIVE: To assess the changes in the EM field distributions and the induced energy levels in biosystems as a result of the change in the material permittivity due to changes in the fluid levels.

METHODOLOGY: This work is the continuation of extensive numerical analyses to determine the effective permittivity values for different levels of biofluid concentrations as obtained from the literature. Theoretical effective permittivity was calculated for various combinations of fluid levels and biological materials through the use of mixing formulas.

The finite-difference time-domain (FDTD) method was used to study the EM field propagation in asymmetrical 3D physiologic models. The modeling and numerical analysis was done using LC (Cray Research Group), a software simulation tool. It simulates the electric and magnetic field intensities using the FDTD method in the time domain. Calculations were performed for different electrical permittivity

values which were obtained for various levels of fluid concentrations in biological materials. Results between different cases were compared and analyzed to determine the changes in the induced energy levels and the distribution of the EM field in the models.

RESULTS: Preliminary analysis revealed that the changes in the effective permittivities due to the fluctuations in the fluid levels of biological materials caused wide variations in the induced energy levels. Also, substantial changes in the distribution and the penetration of the EM fields in the complex biosystem models were observed due to the changes in the amount of reflection seen at the boundaries. These results indicate the importance that biomaterial fluid levels play in EM distribution in the body which in turn can affect the determination of safety limits.

This work was supported by National Science Foundation – EPSCoR grant #0132289.

P-C-150 WITHDRAWN

P-A-151 WITHDRAWN

P-B-152

USING SCALABLE VECTOR GRAPHICS TO MODIFY REALISTIC ANATOMICAL VOXEL MODELS. J.M. Zirix¹, D.D. Cox¹, P.A. Mason², and W.D. Hurt². ¹Naval Health Research Center Detachment, Brooks City-Base, TX 78235-5320, USA; ²Directed Energy Bioeffects Division, Human Effectiveness Directorate, Air Force Research Laboratory, Brooks City-Base, Texas, 78235-5365, USA.

BACKGROUND: The Brooks Anatomical Models are based on a series of images spaced at equal intervals through a volume. The color of each pixel in each image represents the material present in a 3-dimensional volume or voxel. Realistic anatomical voxel models are widely used to calculate specific absorption rates using the finite difference time domain (FDTD) method. However, voxel models are difficult to create and modify. Thus, decisions made when a model was initially created will limit its usefulness. One important limiting decision is voxel size. The FDTD method requires 10 voxels per wavelength. Simply duplicating voxels is not an ideal fix because the “stair steps” of the original model resolution are preserved.

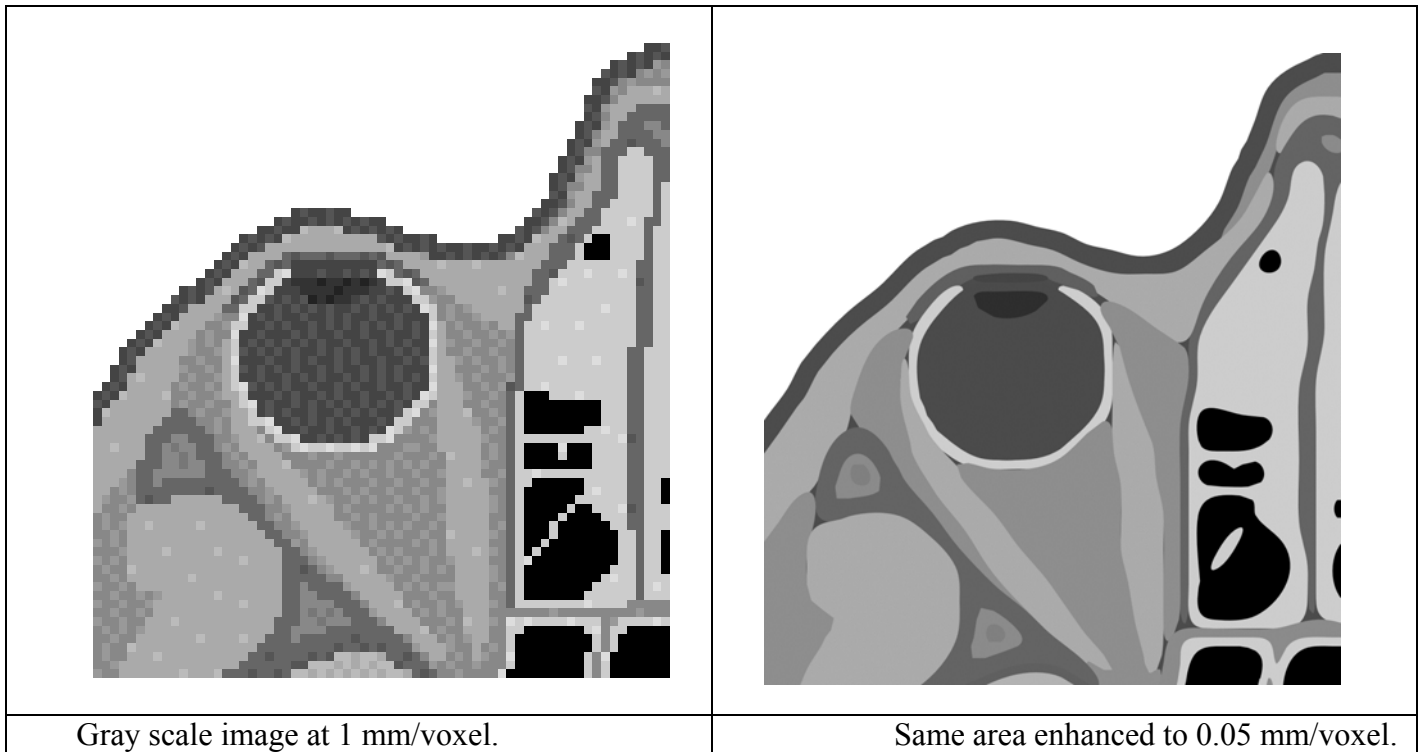
OBJECTIVE: Transform a voxel model into a scalable vector graphics (SVG) format, and then back into voxel format decreasing the voxel size and avoiding the “stair step effect.”

METHODOLOGY: Models based of vector graphics systems (e.g. CAD models) can create many different image resolutions, but these models lack the detail of voxel models. Previous attempts in our laboratory to translate voxel models into vector models produced results which were too large and complex for existing software to manipulate. Recently, the WWW Consortium released the scalable vector graphics (SVG) specification. As an open standard, many independent applications will use this common format. Two Open Source projects already using this format are Autotrace and Sodipodi. Autotrace converts bitmap images into many vector formats including SVG. Sodipodi is an SVG file editor which allows the creation of bitmap images at arbitrary resolutions. Together each image in the series of images of a voxel model could first be translated into a series of SVG files using Autotrace. Then, a new set of images at a higher resolution could be created using Sodipodi. Both of these programs as well as many others are available at <http://www.sourceforge.net>.

RESULTS: A pair of images showing roughly the same area of a single slice of the Brooks Man Model is shown: the original on the left at 1 mm/voxel, and after translation on the right at 0.05 mm/voxel . A twenty-fold increase in resolution. Notice the lack of the stair step effect in the processed image.

CONCLUSION: The resolution of a voxel model shown was increased in two of the model's three dimensions. Applying the same method to the third dimension in a similar fashion would complete the

process. By translating the voxel model into a series of two-dimensional images, the entire voxel model is processed incrementally. Thus, avoiding the problems created by translating the entire model in one step. Other manipulations of the model in the SVG editor are certainly possible.



This work was funded by the U.S. Air Force and U.S. Navy (Project Numbers: 0602236N/M04426.w6, 0601153N/M4023/60182). The views, opinions, and/or findings contained in this report are those of the authors and should not be construed as official Department of the Air Force, Department of the Navy, Department of Defense, or U.S. government position, policy, or decision unless so designated by other documentation. Trade names of materials and/or products of commercial or nongovernment organizations are cited as needed for precision. These citations do not constitute official endorsement or approval of the use of such commercial materials and/or products. Approved for public release; distribution unlimited.

P-C-153

COMPUTATION OF COMPLIANCE DISTANCE NEAR THE BASE STATION PANEL ANTENNA (4X2 DIPOLE ARRAY). J.D. Park¹, H.D. Choi¹, N. Kim², ¹Advanced Radio Technology Department, Electronics and Telecommunications Research Institute, Korea., ²Dept. of Computer & Communication Eng., Chungbuk Nat'l Univ., Korea.

INTRODUCTION: As the cellular phone services are widespread, public awareness of adverse health effects of exposure to EMF from base station antenna is increased. Power density limits for non-occupational and occupational persons were well established in international guidelines [1]. In this paper, power density distribution and compliance distance in the proximity of the base station antenna for the cellular phone service is calculated.

OBJECTIVE: Full wave analysis of near field including radiating near field (Fresnel region)[2] is a very rigorous work, because it takes huge resources of computer memories and time. Objective of this study is to implement methodology of achieving near field distribution from the antenna gain, resulted from FDTD

(Finite Difference Time Domain) simulation. It is so called ‘gain-based model’ [3].

METHODS: As shown in figure 1 (a), An applied antenna is a base station panel antenna (2X4 dipole antenna array), operating in the frequency from 824MHz to 894MHz. In order to calculate power density in reactive near field region ($R < \lambda/4$) and far field region ($R > 2D^2/\lambda$), FDTD method is used (see figure 1 (b)). Where R is the distance between center of the antenna and investigation point, D is length of the antenna, λ is wavelength. Finally, power density in radiating near field region ($\lambda/4 < R < \lambda/4$) is calculated using equation of gain based model(Equation (1)). The power density is compared with human exposure limit level of ICNIRP guideline (shown in Figure 2) [4].

$$E(R, \theta, \phi) \cong \sum_{i=1}^N \frac{\sqrt{30P_i G_i(\theta_i, \phi_i)}}{R} e^{j(kR_i + \psi_i)} \quad (1)$$

Where E is electronic field strength, i is number of each dipole unit, N is number of array, P is input power, G is the antenna gain, k is wave number, ψ is the phase shift constant.

RESULTS: In Figure 2, the distribution of power density near the antenna is shown. According to the ICNIRP guideline, compliance distances toward front direction are calculated to 5.9[m] and 12.1[m] for each occupational and non-occupational persons. As shown in Figure 2 (b) and (c), when the antenna is electrically down-tilted*, main beam direction is considered in calculation of compliance distance.

*Tilted angle is concerned with service coverage area.

References.

- [1] ICNIRP, “Guidelines for Limiting Exposure to Time-Varying Electric, Magnetic, and Electromagnetic Eields (up to 300GHz),” *Health Physics*, vol. 74, no. 4, pp.494-522, April 1998.
- [2] CA Balanis, *Antenna Theory, Analysis and Design, second edition*, (New York: Haper & Row, 1997), pp. 32 - 33.
- [3] A. Faraone, Y. T. Roger, K.H. Joyner, Q. Balzano, “**Estimation of the Average Power Density in the Vicinity of Cellular Base-Station Collinear Array Antennas**”, *IEEE Trans on VT*, vol. 49, pp. 984 – 996, May 2000.
- [4] Z. Altman, B. Begasse, C. Dale, A. Karwowski, J. Wiart, W. Man-Fai, L. Gattoufi, “**Efficient models for base station antennas for human exposure assessment**” *Electromagnetic Compatibility, IEEE Trans on EMC*, vol. 44 , Issue 4, pp. 588 – 592, Nov. 2002.

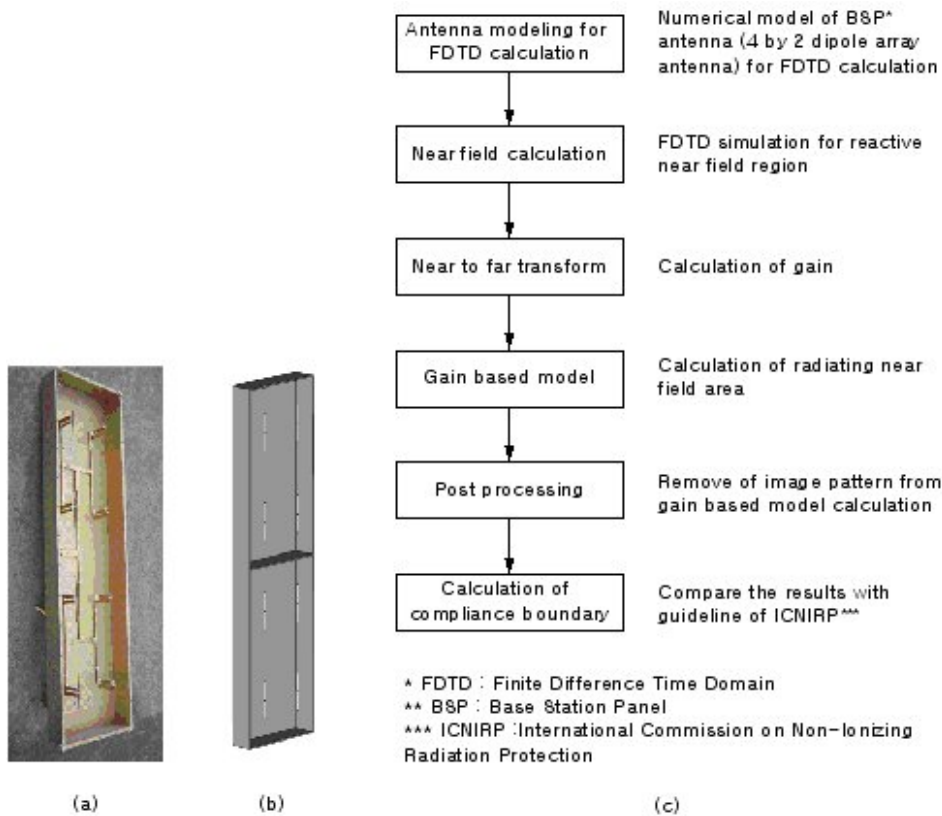


Figure 1: Applied model and Procedure of compliance boundary calculation near the BSP antenna; (a)BSP antenna (b)model for calculation (c) Procedure of compliance boundary

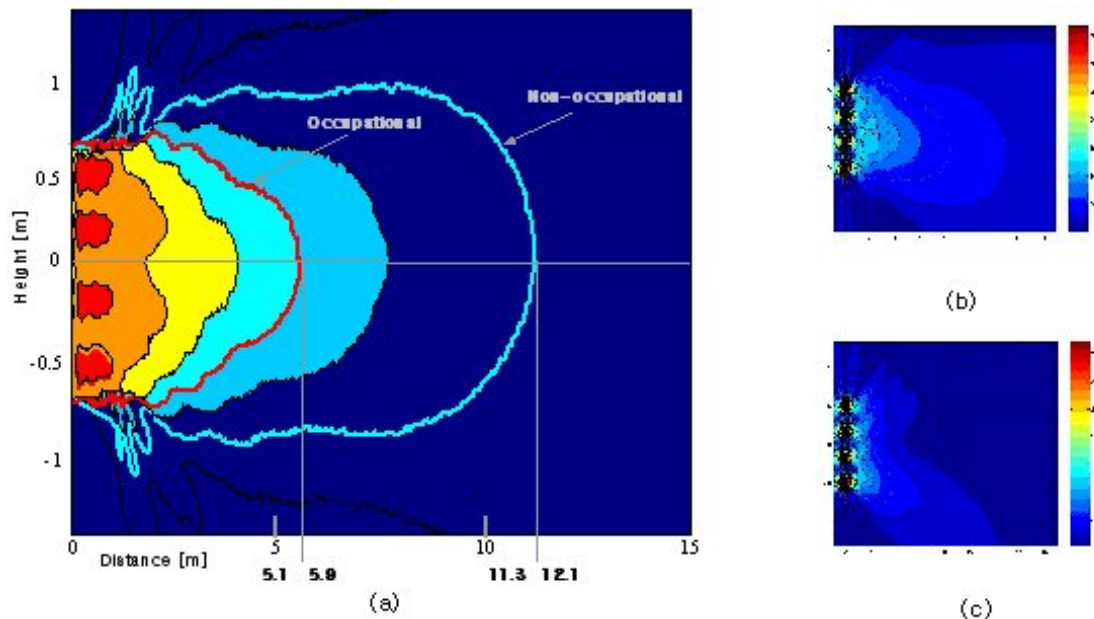


Figure 2: Result of compliance boundary calculation with gain based model; radiating power is normalized to 50[W]; (a) not tilted (b)down tilted by 20° (c)down tilted by 40°

SIGNAL-TO-NOISE RATIO AND SENSITIVITY LIMIT FOR DETECTING MAGNETIC FIELDS USING MAGNETIC RESONANCE IMAGING. T. Hatada, M. Sekino, S. Ueno. Department of Biomedical Engineering, Graduate School of Medicine, University of Tokyo, Tokyo, 113-0033, Japan.

INTRODUCTION: The imaging of magnetic fields produced by local electric currents is important for the mapping the patterns of neuronal activity in the brain. It is difficult, however, to detect the weak transient magnetic fields generated by neural electrical currents. We computed the theoretical sensitivity limits of the magnetic fields from gradient echo (GE) phase images, based on a theory of the signal-to-noise ratio in magnetic resonance imaging.

THEORY: The GE signal intensity S_{GE} can be calculated using the following equation [1],

$$S_{GE} = S_{FID} \times \frac{\{1 - \exp(-T_R/T_1)\} \exp(-T_E/T_2^*)}{1 - \cos\theta \exp(-T_R/T_1)} \sin\theta = N_S V_S \omega_0 (B_1/i) \gamma^2 \hbar^2 B_0 I (I+1) / 3k_B T_S \times \frac{\{1 - \exp(-T_R/T_1)\} \exp(-T_E/T_2^*)}{1 - \cos\theta \exp(-T_R/T_1)} \sin\theta \quad (1)$$

where S_{FID} is the FID signal intensity, N_S is the number of proton spins per unit volume in water ($5.1 \times 10^{18} \text{m}^{-3}$), V_S is the volume of the sample in an image, ω_0 is the resonant frequency, B_1/i is the magnetic field generated by the unit current flowing in the radiofrequency coil, γ is the gyromagnetic ratio of protons ($2.67 \times 10^8 \text{rad/T}\cdot\text{s}$), \hbar is the Planck's constant ($1.05 \times 10^{-34} \text{J}\cdot\text{s}$), B_0 is the static magnetic field, I is the spin quantum number of protons ($1/2$), k_B is the Boltzmann constant ($1.38 \times 10^{23} \text{J/K}$), T_S is the sample temperature, and θ is the flip angle. The Johnson noise produced by the coil and the columnar sample N is

$$N = \{4k_B \Delta f (R_C T_C + R_S T_S)\}^{1/2} = [4k_B \Delta f \{(l/p)(\mu_r \mu_0 \omega_0 \rho / 2)^{1/2} T_C + \frac{1}{8} \sigma_S \omega_0^2 (B_1/i)^2 r_S^4 h_S\}]^{1/2} \quad (2)$$

where Δf is the spectral width, R_C , and R_S are resistances of the coil and the sample, T_C is the coil temperature, l is the coil length, p its circumference, $\mu_r \mu_0$ its permeability, ρ its resistivity, σ_S is the sample conductivity, r_S its radius and h its height. After a two-dimensional Fourier Transformation for reconstructing the GE phase image, the noise in the magnetic fields image σ_B becomes

$$\sigma_B = \frac{1}{\text{SNR}(FI)\gamma T_E} = \frac{N(FI)}{S_{GE}(FI)\gamma T_E} = \frac{nN}{(4/\pi)n^2 n_S^2 S_{GE}\gamma T_E} = \frac{N}{(4/\pi)n n_S^2 S_{GE}\gamma T_E} \quad (3)$$

where n is the number of pixels, and n_S is the data point which corresponds to the diameter of the sample. The noise in the magnetic field image σ_B can be assumed to constitute the theoretical limits of the detectable magnetic field change, since the magnetic field change produced by the weak current can be detected when it is larger than σ_B .

EXPERIMENTS: To investigate the practical value of the detectable magnetic field change, we obtained a magnetic field image using a 4.7 T MRI system under the following conditions. Rectangular current pulses (10mA, 5mA, 2mA, ..., 10 μ A) were applied to the columnar phantom filled with a mixture of 1 % agarose gel and 0.9 % NaCl solution ($r_S = 6.5 \times 10^{-3} \text{m}$, $h_S = 5.0 \times 10^{-2} \text{m}$, $V_S = 6.6 \times 10^{-8} \text{m}^3$, $T_S = 295 \text{K}$, $\sigma_S = 2.0 \text{S/m}$) within the circular surface coil ($l = 8.8 \times 10^{-2} \text{m}$, $p = 5.0 \times 10^{-3} \text{m}$, $\mu_r \mu_0 = 1.26 \times 10^{-6} \text{H}\cdot\text{m}^{-1}$, $\rho = 1.72 \times 10^{-8} \Omega\cdot\text{m}$, $B_1/i = 4.49 \times 10^{-5} \text{T/A}$) to obtain images. Four columnar reference tubes filled with the mixture ($r_S = 1.5 \times 10^{-3} \text{m}$, $h_S = 4.0 \times 10^{-2} \text{m}$, $\sigma_S = 2.0 \text{S/m}$) were located around the phantom to correct the phase shifts. The noise from the references was computed like the sample and added to N . The image parameters were $B_0 = 4.7 \text{T}$, $T_R/T_E/\theta = 900 \text{ms}/5 \text{ms}/90^\circ$, $FOV = 32 \times 32 \text{mm}^2$, $n = 128$, $\Delta f = 80321.3 \text{Hz}$, and the thickness of slice = 0.5mm. In this measurement, $\omega_0 = 1.26 \times 10^9 \text{rad/s}$, $n_S = 52$, $T_1 = 2.50 \text{s}$, $T_2^* = 103.4 \text{ms}$.

Using a theoretical equation, we performed the noise variance simulations of the magnetic field change, modifying the parameters: T_R/T_1 , TE/T_2^* , number of pixels and spectral width.

RESULTS and DISCUSSION: Under these conditions, the theoretical sensitivity limit σ_B was $1.46 \times 10^{-8} \text{T}$. Fig.1 shows dependences of the theoretical sensitivity limits on the following parameters: (a) T_R/T_1 , (b) TE/T_2^* , (c) number of pixels and (d) spectral width. An increase in TR caused a decrease in the theoretical sensitivity limit, while an increase in the number of pixels or the spectral width caused an increase in the theoretical sensitivity limit. Fig.2 (b) shows that there is an optimal value for TE/T_2^* .

References.

- [1] PL Callghan. Principles of Nuclear Magnetic Resonance Microscopy. (1991) Oxford.
 [2] GC Scott, MLG Joy, RL Armstrong, RM Henkelman. (1992) *J Magn Reson* 97: 235-254.

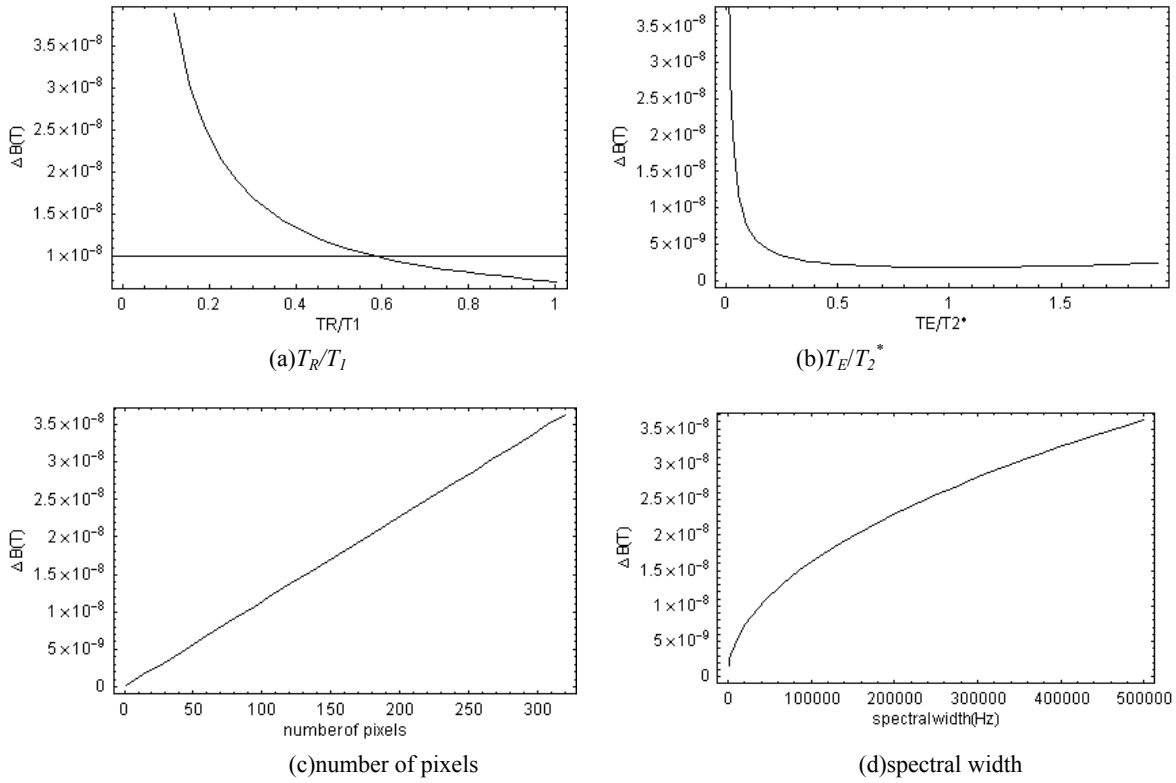


Fig. 1. Dependences of the theoretical sensitivity limit for detecting magnetic field on the following parameters: (a) T_R/T_1 , (b) T_E/T_2^* , (c) number of pixels, (d) spectral width

P-B-155

NOVEL TRANSFER STANDARD FOR SAR-PROBE CALIBRATION IN GSM BANDS. A.P. Sihvonen, T. Toivonen, L. Puranen, K. Jokela. STUK Radiation and Nuclear Safety Authority, FIN-00881 Helsinki, Finland.

INTRODUCTION: Compliance tests of mobile phones are carried out by scanning the electric (E) field in a liquid phantom with a small E-field probe (SAR probe) [1]. An essential requirement for the validity of SAR measurements is the regular calibration, or at least, the regular verification of the calibration of SAR probes in brain simulating liquids. The sensitivity factor of the SAR probe depends also on the data acquisition system connected to the probe and therefore, the probe has to be calibrated together with the SAR measurement system (on-site calibration). However, primary standards consisting of vertical rectangular waveguides with an upper liquid-filled part [2] cannot be used for on-site calibration because they are maintained in a standard laboratory and must not be moved. Thus, it is necessary to develop a transfer standard for on-site calibration of SAR probes.

OBJECTIVE: The objective was to design, construct and test a broadband, compact, light-weight, durable and stable transfer standard which is easy to use for calibration of SAR probes at 900 MHz and at 1800 MHz. Calibration factors obtained at these frequencies can be applied with a sufficient accuracy to predict the factors in other frequency bands used for mobile communication because the frequency response of SAR probes is typically a smooth function decreasing linearly with the frequency.

METHODS: The structure of the transfer standard was designed using analytical calculations and numerical simulations with an XFDTD software (Remcom Inc.). The designed structure consisted of an air-filled double-ridge lower waveguide section and a liquid-filled rectangular upper waveguide section (Fig. 1). The ridges were used to extend the frequency range of the fundamental TE_{10} mode in the air-filled section [3]. They were tapered towards to the liquid-filled section to remove the abrupt change in the cross section which would excite higher order modes in the liquid. The prototype (Fig. 1) was constructed using a standard WR 650 (R14) waveguide (inner dimensions 165.1 mm and 82.55 mm) and inserting ridges (width 20 mm and height 30 mm) into the lower section. The upper section (liquid container) was made replaceable due to different liquids used at 900 MHz and at 1800 MHz. The input and the reflected power were monitored by means of two directional couplers (Arra model 2-3174-20) and zero bias Schottky-diode detectors (Narda model 8506). The output DC voltage was measured with a multimeter. The fundamental TE_{10} mode was excited with a post extending from ridge to ridge. The waveguide feed was matched with tuning screws at 1800 MHz and with an external stripline tuning circuit at 900 MHz. The return loss was measured with a vector network analyzer Hewlett-Packard 8752C. The SAR distribution in the brain simulating liquid was measured by using DASY4 professional dosimetric assessment system (Schmid and Partner AG, Zurich, Switzerland). The transfer standard was calibrated and its stability was studied with an SAR probe ET3DV6 calibrated against the primary standards at 900 MHz and at 1800 MHz.

RESULTS: Broadband matching was not possible but good narrow-band matching was achieved around 900 MHz and 1800 MHz where the return loss measured at the input of the transfer standard was 19 dB and 18 dB, respectively. SAR distributions measured in the E plane at the height of 30 mm from the bottom of the container indicated that no higher order modes propagated in the liquid at 900 MHz. On the contrary, at 1800 MHz higher order modes were found but their effect on the SAR distribution was stable. The main factor for the uncertainty of the SAR probe calibration carried out with the transfer standard was the uncertainty of the calibration in the primary standard (standard uncertainty 3.6% at 900 MHz and 4.0% at 1800 MHz). Other minor uncertainty factors were involved with RF power measurements, temperature dependence of the dielectric properties of the phantom liquids, positioning of the SAR probe and mounting of the liquid container. The estimated uncertainty for the SAR probe calibration in the transfer standard was 9.0% at 900 MHz and 9.8% at 1800 MHz with 95% confidence level.

CONCLUSIONS: The developed transfer standard operates satisfactorily at 900 MHz and 1800 MHz and can be used with a sufficient accuracy for on-site calibration of SAR probes.

References

- [1] CENELEC. European Committee for Electrotechnical Standardization: Basic Standard for the Measurement of Specific Absorption Rate Related to Human Exposure to Electromagnetic Fields from Mobile Phones (300 MHz - 3 GHz), European Standard EN 50361, Brussels, July 2001.
- [2] Jokela K, Hyysalo P and Puranen L. Calibration of specific absorption rate (SAR) probes in waveguide at 900 MHz, IEEE Transactions on Instrumentation and Measurement 1998; 47(2): 432-438.
- [3] Helszajn J. Ridge waveguides and passive microwave components. IEE electromagnetic waves series 49, The Institution of Electrical Engineers. London, United Kingdom, 2000.

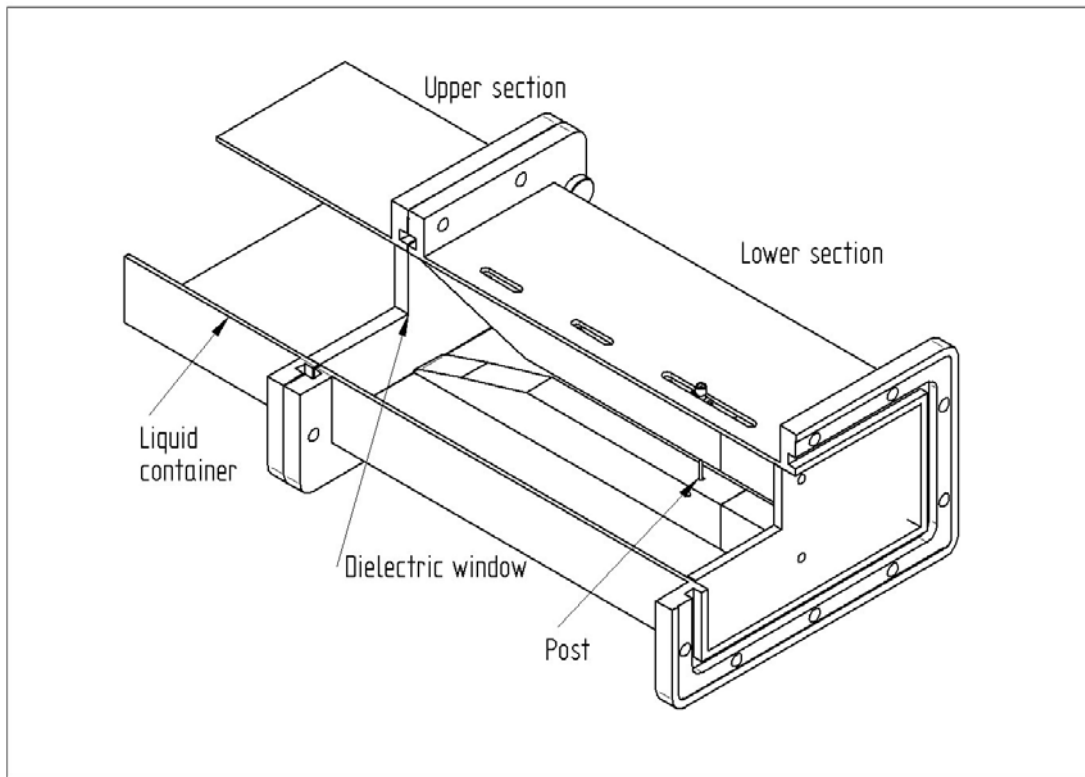


Figure 1. View of the designed transfer standard for SAR probe calibration.

P-C-156
STUDENT

EVALUATION OF CELL COMPARTMENTS DIELECTRIC CONSTANT WITH EXPERIMENTAL TECHNIQUES AND NUMERICAL METHODOLOGIES. C. Merla¹, L. De Gregori², A. Ramundo Orlando², M. Liberti¹, F. Apollonio¹, G. D’Inzeo¹. ¹ICeMB @ Department of Electronic Engineering, “La Sapienza” University of Rome, 00184 Rome Italy, ²ICeMB @ Institute of Neurobiology and Molecular Medicine. CNR, Rome, Italy.

OBJECTIVE: In the study of the interaction between electromagnetic (EM) fields and biological systems, to properly relate the biological effects to the EM exposure, it is crucial to accurately know the field distribution on the biological target down to the single cell level. In this context an accurate dielectric modelling of cell compartments is necessary to proceed to an estimation of EM field distribution [1, 2].

METHODS: For this purpose we have realized a dielectric constant measurement set-up, particularly suitable for liquid solutions [3]. The measurements are conducted in frequency domain using a coaxial cable, the liquid solution under test is inserted between central conductor and external conductor of the

cable, after having previously removed a small fraction of the Teflon filling the coaxial structure. The coaxial cable is directly connected to the network analyzer from which we extract the value of reflection coefficient. The experimental procedure includes an effective calibration with three different standard liquids to deembed the cable mismatch due to connectors and parasitic effects. We obtain the dielectric constant values (real and imaginary part) solving a linear system, which contains the reflection coefficients achieved during the calibration [3, 4]. We simulated the coaxial cable with HFSS software for testing the calibration procedure effectiveness (Fig. 1).

RESULTS: It is possible to estimate dielectric behaviour of cell compartments applying theory of mixtures to measured values of cell solutions [5]. This approach results particularly complex for cell cultures, especially, if we consider a frequency range up to radio-frequency and microwave region. This methodology is based on a multilayered spherical cell model (Fig. 2) accounting not only for the presence of biological membrane (three-layer model) but also considering the presence of two layer of “bound water” on the membrane (five-layer model).

For limiting the estimation complexity and assuring the result’s accuracy, our estimation methodology is applied to mixtures of reverse micelles and to liposomes solutions.

In particular the reverse micelles are a very useful system to estimate the “bound water” dielectric constant. They allow to fix the hydration degree of the structure and to make an accurate study of dielectric phenomena that happened in the “water pool” [2, 3, 6]. Liposome results in well controlled “cell model”: the extra cellular medium is known, the “bound water” close to the membrane is known, due to the previously measurement on reverse micelles, the cytoplasm is known because liposome are synthetic structures and we can choose and measure previously their internal phase. So the only estimation objective is the dielectric behaviour of the membrane.

CONCLUSIONS: This work proposes an experimental method to determine in extremely accurate way the dielectric parameters of a cell model. Hence, with this approach, we try to give the right prominence to the “bound water” role on bioelectromagnetic behaviour of biological structures.

References.

- [1] F.Cleary, “Absorbed Energy Distribution from Radiofrequency Electromagnetic Radiation in a Mammalian Cell Model”, *Bioelectromagnetics*, (16), 160-171, 1995.
- [2] T.Kotnik, D.Miklavcic, “Theoretical Evaluation of the Distributed Power Dissipation in Biological Cells Exposed to Electric Field”, *Bioelectromagnetics*, (21), 385-394, 2000.
- [3] D.Fioretto, G.Onori, “Dielectric Relaxation in Water-Tert-Butanol Mixtures. The Water Rich Region”, *J.Chem.Phys.*, (99/10), 8115-8119, 1993.
- [4] Yan-Zhen Wei, “Technique for Measuring the Frequency-Dependent Complex Dielectric Constant of Liquids up to 20 GHz”, *Rev. Sci. Instrum.*, (60/9), 3041-3046, 1989.
- [5] W.M.Merril, “Effective Medium Theories for Artificial Materials Composed of Multiple Sizes of Spherical Inclusions in a Host Continuum”, *IEEE Trans.Antennas Propagation*, (47), 142-148, 1999.
- [6] M.Freda, “Hydration and Dynamics of Aerosol OT Reverse Micelles”, *J. Molecular Liquids*, (101/1-3), 55-68, 2002.

This work was supported by the European Union, V framework under the RAMP2001 Project.

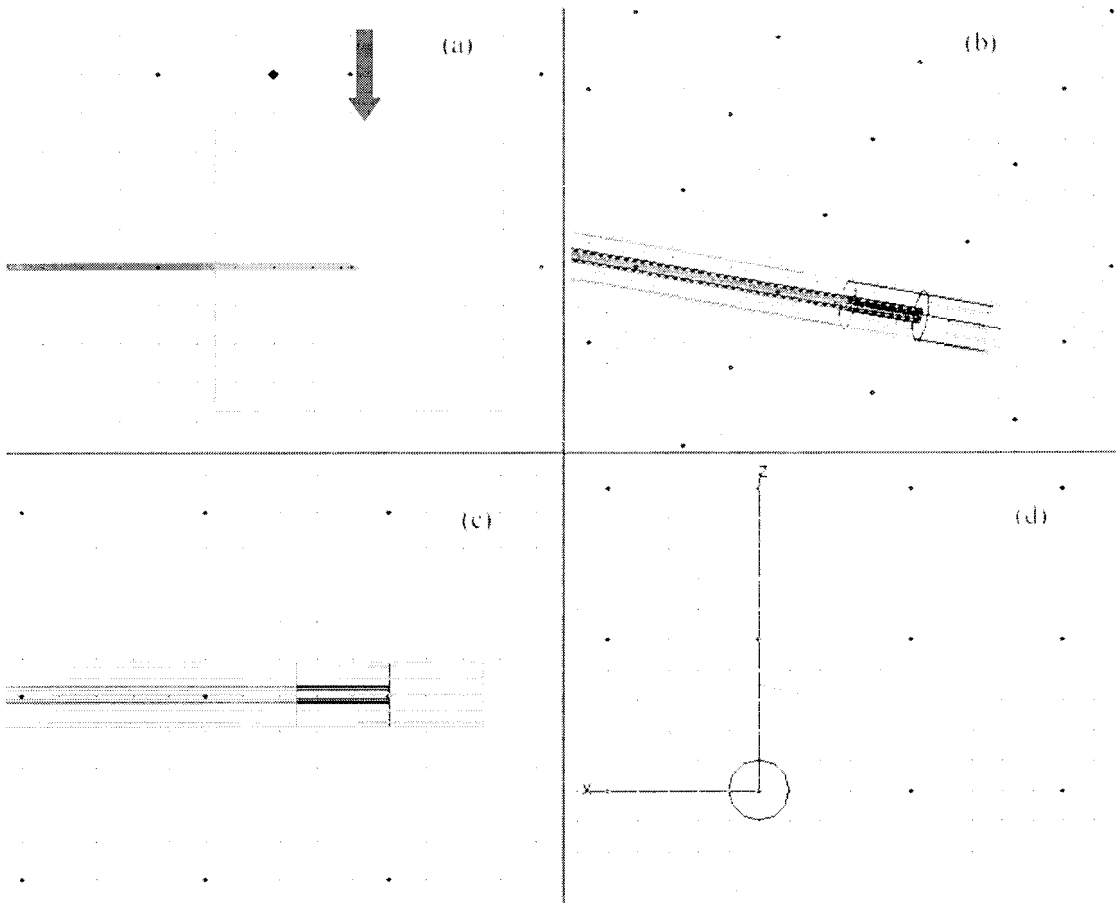


Figure 1
 HFSS simulated coaxial cable structure for testing the calibration effectiveness
 a: the arrow shows the radiation boundary condition adopted in the simulation.
 b: three-dimensional vision of the coaxial structure.
 c: side vision of the coaxial structure.
 d: top vision of the coaxial structure

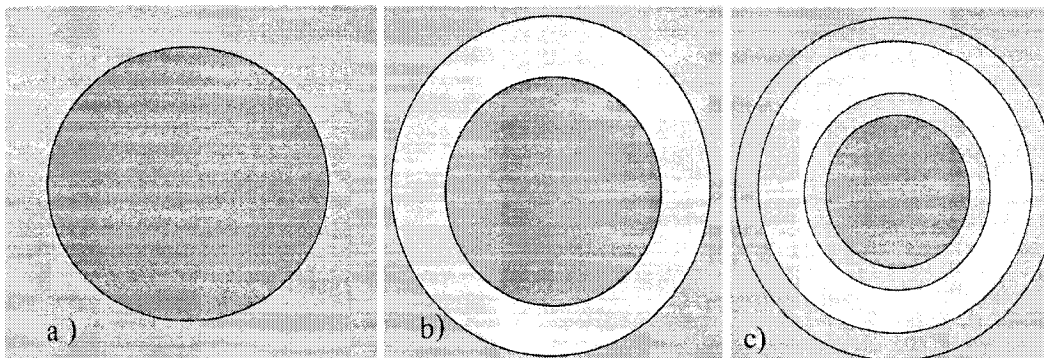


Figure 2
 Different models of cellular structures: a) homogeneous cell model, b) three-layers cell model, c) five-layers cell model

NEW INSTRUMENT FOR MEASUREMENT OF CELLULAR BASE-STATION EMISSIONS. G. Gajda, E. Lemay, A. Thansandote, P. Lemyre and J. McNamee. Consumer & Clinical Radiation Protection Bureau, Health Canada, Ottawa, Ontario, K1A 1C1, Canada.

INTRODUCTION: Along with the wide acceptance of mobile cellular technology by the public there has been a concurrent rise in apprehension about base-station emissions by some segments of society. These concerns have given rise to organized opposition to the siting of existing and proposed base-stations especially near residential and school areas. One factor contributing to these concerns is the lack of current exposure data from existing sites. Because of the low exposure levels encountered, performing measurements with the requisite narrowband instrumentation (i.e. spectrum analyzer) is usually very time consuming and costly.

OBJECTIVES: The objective of this work was to construct and utilize an instrument designed to explore the spatial and temporal variations in exposure levels in locations around cellular base stations in both the 800-900 MHz and 1800-1900 MHz bands. The requirements for the instrument are that it is portable, easy to use and measures the total power density over an entire cellular band in real time. It must be able to record exposure level and geographic position while mounted on a moving vehicle.

METHODS: A block diagram of the instrument is shown in Figure 1. It has two omni-directional antennae, a planar monopole for low angle reception and a planar spiral for high angle reception. Both antennae operate over both cellular bands and are connected through an RF switch to a diplexer. The diplexer separates the signals in the two bands and feeds them to the appropriate receiver. Each receiver filters and detects all signals occurring in its band. Detection is accomplished using a logarithmic amplifier/detector with a 45 dB dynamic range so that the DC output is proportional to the logarithm of the incident power densities at the antennae. The receiver outputs are connected to two of the inputs of a multiplexed analog-to-digital converter (8-bit), which sends the digitally converted power density levels to a computer for storage.

The other part of the system is a commercial Global Positioning Satellite (GPS) receiver (Model G10-RS232, Laipac Technology Inc., Toronto, Canada) which is used to detect the location of the measurement point and send it to the computer for storage. Thus the computer stores three essential pieces of information; the geographic position of the measurement point and the power density in both cellular frequency bands.

RESULTS: Both antennae are mounted on a 64cm x 36cm aluminium groundplane while the electronics enclosure is mounted below. A teardrop-shaped fibreglass cover encloses the antennae and the entire unit is fitted with 4 nylon legs for mounting on a vehicle. In the 800-900 MHz band, reception coverage is a full hemisphere while at the higher band, the response is down 3 dB at 5 degrees elevation. The upper measurement range of power density is 20 mW/m² for the 800-900 MHz band and 200 mW/m² for the higher band, however these can be increased by the connection of calibrated attenuators in front of the receivers. Calibration in both bands and for both antennae yields a worst-case uncertainty of ± 4 dB and is primarily due to variations of the azimuth and elevation patterns of the two antennae and to detector characteristics. Results of surveys performed with the instrument will be presented at the conference.

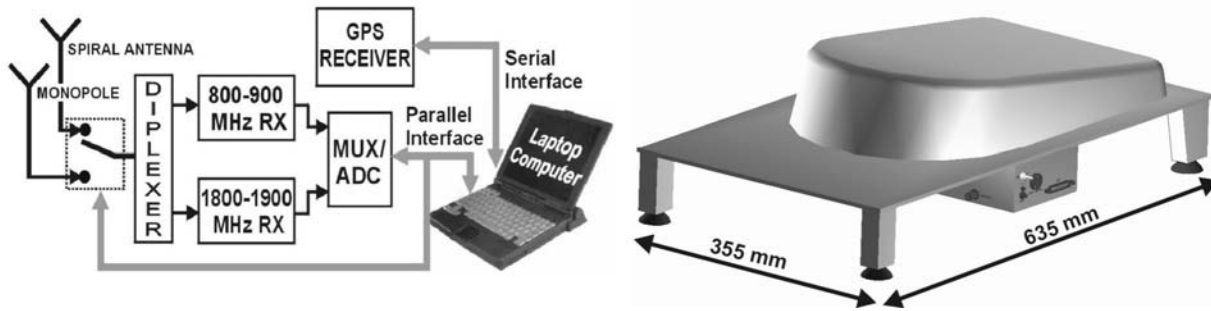


Figure1: Block diagram and drawing of the instrument.

P-B-158

METHOD, MATERIAL AND DEVICE PROVIDING ELECTROMAGNETIC COMPATIBILITY BETWEEN TECHNOLOGICALLY ORIGINATED EMR AND BIOLOGICAL SYSTEMS. I. Smirnov. Global Quantech, Inc., 391 Avenida La Cuesta, San Marcos, CA 93078, USA.

This particular technology relates to subtle electrical effects, and provides some evidence of a fundamental nature on how subtle low frequency electromagnetic fields might be utilized to protect human body against harmful effects of high frequencies electromagnetic radiation. I have focused my efforts on definite polar polymer compound named EMRON (Electromagnetic Radiation Optimum Neutralizer) which is patented in April 2002; US patent No. 6369399 B1, “Electromagnetic Radiation Shielding Material and Device”. This polar polymer material was tested by Underwriters Laboratories and received a UL recognition mark in March 2001. This polar polymer compound can be excited by external high frequencies electromagnetic fields of technological origin in order to generate subtle low frequency oscillations that are biologically very active and beneficial for cellular life structures.

This concept is based on the possibility of existence of resonance phenomenon between polar polymers and biopolymers such as proteins, nucleic acids, lipids, etc. Low frequency patterns generated by defined polar polymer compound can interact with biological systems and transmit the signals that support and improve cellular functions in the body. The mechanism of this process was confirmed by number of studies. The animal (including human) brain is affected by electromagnetic waves to the extent that production of Alpha or Theta waves can be directly induced into brain by carrying an ELF (extremely low frequency, 5-12 Hz) signal on a microwave carrier frequency.

EMRON does not reduce the power of electromagnetic fields. This shielding polar polymer can neutralize negative effects of EMR by changing the quality of the electromagnetic field rather than reducing its power. It “shields” the cellular structures of the body against the harmful effects of EMR that was proved by a number of biological experiments in vitro and in vivo. The radiation is still entering the body but the neutralizing effect of EMRON renders the radiation harmless. There is an obvious parallel here with the pharmacological strategy of attempting to protect against bacterial infection, for example, by taking vitamin C, to fortify the immune system, rather than by wearing a protective mask to simply reduce the intensity of the bacterial field to which a person is exposed.

STRAIN MAPPING OF BIOLOGICAL TISSUES USING DIFFUSION TENSOR MAGNETIC RESONANCE IMAGING. M. Sekino, A. Kaneko, Y. Eguchi, K. Yamaguchi, S. Ueno. Department of Biomedical Engineering, Graduate School of Medicine, University of Tokyo, Tokyo 113-0033, Japan.

INTRODUCTION: Numerous studies on diffusion tensor magnetic resonance imaging (MRI) have shown that diffusion tensor images reflect structure of cell membrane as well as the diffusion coefficient of water [1]. A change in the structure of cell membrane due to an external force or a muscle contraction affects diffusion tensor images, which suggest the potential of imaging strain based on diffusion tensor MRI. In this study, we investigated the effect of strain on diffusion tensor images of muscles using numerical simulation and animal experiment.

METHODS: The finite difference method was used to calculate the signal intensities of diffusion tensor images [2]. Cross section of a muscle fiber without strain was modeled as a $50 \times 50 \mu\text{m}^2$ square. The diffusion coefficient of the intracellular fluid was set to $D = 2.0 \times 10^{-3} \text{ mm}^2 \text{ s}^{-1}$. The pulsed gradients were applied in three directions of $(G_0, 0)$, $(0, G_0)$, and $(G_0/\sqrt{2}, G_0/\sqrt{2})$ with a constant intensity of $G_0 = 50 \text{ mT m}^{-1}$. To investigate the effect of strain, the aspect ratio of the model was varied from 1.0 to 4.0, which corresponded to varying strain from 0.0 to 1.0. For each aspect ratio, the apparent diffusion coefficient (ADC), the mean diffusivity (MD), and the fractional anisotropy (FA) were calculated from the signal intensity. Diffusion tensor images of the isolated frog gastrocnemius muscle were obtained using a 4.7 T MRI system. The muscle was sandwiched between a pair of plastic plates and compressed in the direction perpendicular to the muscle fibers (x direction). Motion probing gradients were applied in the three directions described above. The acquisition parameters were as follows: $\text{TR/TE} = 2000/55 \text{ ms}$, $\Delta = 30 \text{ ms}$, $\delta = 15 \text{ ms}$, and $b = 1006 \text{ s mm}^{-2}$. The ADC, the MD, and the FA were calculated for the images with and without strain.

RESULTS AND DISCUSSION: The case without a strain had an ADC of $1.2 \times 10^{-3} \text{ mm}^2 \text{ s}^{-1}$. An increase in strain caused an increase in the distance between boundaries, which resulted in an increase in the ADC. The ADCs corresponding to the strains of 1.0 and -0.5 were $1.5 \times 10^{-3} \text{ mm}^2 \text{ s}^{-1}$ and $0.8 \times 10^{-3} \text{ mm}^2 \text{ s}^{-1}$, respectively. These results indicate that the ADC monotonically increases with strain. Changes in the MD were below 1 % because the area of the model was kept constant. The model exhibited a certain amount of the FA even without strain because the square-shaped model is not completely isotropic. The FA increased with both positive and negative strains. A strain of 0.8 resulted in a FA value of 0.4. In the frog gastrocnemius muscle without compression, D_{xx} (the ADC in the direction parallel to the compression) was higher than D_{yy} , (the ADC in the direction perpendicular to the compression) which indicated that the muscle had an anisotropy even without strain. The cross-sectional area decreased from 1.56 cm^2 to 1.08 cm^2 . The compression in the x direction caused a decrease in D_{xx} from $1.4 \times 10^{-3} \text{ mm}^2 \text{ s}^{-1}$ to $1.0 \times 10^{-3} \text{ mm}^2 \text{ s}^{-1}$, which was consistent with the result obtained in the simulation. Significant changes were not observed in D_{yy} . The MD decreased with the compression due to a decrease in the cross-sectional area. The FA also decreased with the compression because a decrease in D_{xx} caused a decrease in diffusion anisotropy. Although the simulation was performed with an assumption that the muscle fiber was square-shaped in the case without strain, the muscle fiber exhibited anisotropy in the ADC even without strain. This difference arose a partial discrepancy between the results obtained from the simulation and the experiment. Information on the geometry of muscle fibers without strain and the diffusion coefficient of water in the fibers will enable a quantitative estimation of strain from diffusion tensor images.

References.

[1] Callaghan PT. Principles of nuclear magnetic resonance microscopy. Oxford: Oxford University Press; 1991.

[2] Chin CL, Wehrli FW, Hwang SN, Takahashi M, Hackney DB. Biexponential diffusion attenuation in the rat spinal cord: computer simulations based on anatomic images of axonal architecture. Magn Reson

P-A-160

DESIGN OF AN EXPERIMENTAL SETUP AND PROTOCOL FOR EVALUATING IN VITRO AND IN VIVO POTENTIAL GENOTOXIC AND THERAPEUTIC EFFECTS OF rTMS SIGNALS.

R. Charlet de Sauvage, I. Lagroye, B. Billaudel and B. Veyret. PIOM/Bioelectromagnetics laboratory, ENSCPB/EPHE, University of Bordeaux, Pessac, France.

INTRODUCTION: Repetitive Transcranial Magnetic Stimulation (rTMS) is widely used in clinical practice. Examples of applications are found in neuropsychiatry, particularly for the treatment of drug-resistant depression, either as clinical trials or as routine therapy (Canada, Israel). However, few biological studies have been performed, on possible toxicological effects of rTMS signals or on the molecular mechanisms at the origin of their clinical benefits. In this context, we have developed a specific apparatus allowing a multi-parametric research on biological effects of rTMS.

OBJECTIVES: Our first objective is to evaluate the toxicity of rTMS signals used in clinical trials.

METHODOLOGY: In order to stimulate the cortex, rTMS signals commonly consist of pulsed-magnetic fields with durations between 0.1 and 1 ms, with a repetition rate between 1 and several dozens of Hertz (often 10 Hz), and with a maximum magnetic induction of about 2 Teslas. We have thus built an experimental magnetic stimulator with a repetition rate close to 20 pps. Water cooling is used. Experimental conditions will include unique exposures and sequences of exposition (1 per day during 5 days) to magnetic pulses with one sinusoid (duration 340 μ s), and with an amplitude between 1 and 2 T. Daily doses will be of 1000 magnetic stimulations (Kanno et al, 2003), delivered at a rate ranging from 1 to about 20 pps. Both starting polarities of rTMS signals will be tested *in vivo*. This choice is important since eddy currents in the cortex are rotating in the direction opposite to that in the coil and the cortex threshold is dependent on the direction of the current flow. The influence of repetition rate will be examined and the mapping of the induced electric field will be established for several types of coils, with the goal of inducing electric fields of some hundred V/m. We will evaluate the ability for these signals to induce DNA damages (comet and micronuclei assays) and apoptotic death (flux cytometry). Two protocols are considered: exposing *in vivo* animals whose brain cells will be isolated later or exposing cultured neural cells *in vitro* (human glial U87 and neuronal SH-5YSY cells lines). As far as *in vivo* experiments are concerned, rats will be exposed to rTMS signals produced by a coil placed on the top of the skull. Rats will be restrained during exposure, which necessitates a period of habituation. Possible damages in the cerebral cortex will be compared with those in the rest of the brain, submitted to lower doses of rTMS. Different groups of eight animals will be evaluated: (i) animals exposed to rTMS signal, (ii) control animals for assessing the effects of contention and noise produced by the magnetic stimulator and (iii) cage controls with free movements and unexposed to noise.

CONCLUSION AND PERSPECTIVES: Concerning the mechanisms of possible therapeutic effects such as those on depression, it seems particularly interesting to study the effect of rTMS signals on serotonin receptors of the 5HT1 type (Massot et al, 2000). rTMS may suppress depressive symptoms by decreasing the affinity of type 5HT1 receptors for serotonin. Again, for this second step, two protocols are considered: exposing *in vitro* cell membranes isolated from rat brains and exposing *in vivo* animals whose brain cell membranes will be isolated after exposure. The affinity of the receptors will be determined by the binding method and the serotonin receptors will be localised on brain slices by autoradiography.

This work was supported by a grant from the Conseil Régional d'Aquitaine.

P-B-161

SOME SPATIAL AND TEMPORAL PECULIARITIES OF THE SKIN ELECTRICAL LANDSCAPE AFFECTED BY WEAK CONSTANT MAGNETIC FIELD AND NON-THERMAL MILLIMETER EMF. Y.F. Babich, M.A. Nuzhdina. Institute for Applied Problems of Physics & Biophysics, NAS of Ukraine, 03049-Kiev, Ukraine.

INTRODUCTION: We reported about the mm-EMF-induced electroimpedance waves (in a speed range of Ca^{2+} waves of cell-cell signaling) which have been firstly registered *in vivo* at the Skin Electrical Landscape (SEL) with the aid of our earlier original electrointrosopic device [1,2]. So far, such marked wave-like SEL activity have been revealed only at the biologically active areas, i.e. acupuncture zones, where cell-cell communication level is much higher due to, as reported, the higher density of cells with gap-junctions.

OBJECTIVE: To study the SEL initial and EMF-induced activity at ordinary/singularity-free skin areas both in health and disease, specifically at malignant tumor area (where cell-cell communication is defective or broken). The updated functional imaging setup - Multiparameter Transcutaneous Electrointroscope (MTE) enabled non-invasive, digital, dynamic imaging of the SEL and underlying tissues (spatial resolution <1 mm, scan-speed < 7 cm/s) in 2D spectral electroimpedance (specific conductance and capacitance at 2kHz-1MHz-range and electropotential parameters). The SERs in these parameters, in principle, reflect the 2D electrochemical biotissue characteristics at inter-/intra-cellular and membrane levels correspondingly. The four SER image sequences (30-50 frames of each, interframe period ~ 30s) were registered simultaneously. Our main task was then to reveal significant relative changes in the set of the SERs data.

METHODS: To study initial SER features, the first 4-10 SER images were read out under no outer influence. Then, keeping up the scanning, one of the two test influences – (i) non-thermal mm-EMF (50-70 GHz, <1 mW/sq.cm, 4 min) or (ii) MF (< 1 mT, 4 min) - were applied in immediate proximity to the scan-area. Initial, induced and afteraction SEL dynamics have been graphically and statistically analyzed. Specifically, the through-image-sequence analysis resulted in detailed dispersion maps of the scan-area. The SELs of (i) jellyfishes (45), (ii) healthy (34) and allergic (9) subjects, and (iii) those with cutaneous melanoma (3) were investigated.

RESULTS: May be roughly presented in the table:

Subject	Response in agreed units (0 to 5)	
	mm-EMF	MF
Jelly-fish	0	1-2*
Healthy humans	1-2	1-2
Allergic humans	1 or 5**	No data
Melanoma	0-5***	No data

* Primary response - at the intracellular level, then (with a certain delay) – at the intercellular one.

** At remission and sensitization stages respectfully.

*** No reaction -inside the tumor, max reaction- at its outline, mean one - at remote areas.

In humans, most marked (reversible) reactions were observed at the levels of intracellular media and cellular membranes.

CONCLUSION: The SER dynamics of observed tissues was of chaotic nature; the spread in SER values was spatially dependent on the SER initial pattern. The induced changes of the SER dynamics proved to be highly sensitive indicators of the living tissue response to the weak MF&EMF even for healthy humans and may be used in various bio-medical application, specifically for: real-time assessment of individual

sensitivity to the EMF exposure, early tumor diagnosis and developing new methods of controlled therapy.

References

[1] Babich Y. 2d Int. Conference on Bioelectromagnetism. (Melbourne, Australia, 1998):79-80.

[2] Babich Y., Bakai E. 11th Int. Conference on Electrical Bio-Impedance. Oslo(2001):131-134.

This study was supported by the Science&Technology Center in Ukraine (the financing parties: USA and Canada).

P-C-162

Presented as P-B-98

P-A-163

STUDENT

THE CLUSTERING EFFECT OF PURIFIED EPIDERMAL GROWTH FACTOR RECEPTOR INDUCED BY ELF MAGNETIC FIELD. C. Jia, R. Xia, S. Chen, B. Tian. Key Laboratory of Optical and Magnetic Resonance Spectroscopy, East China Normal University, Shanghai 200062, China.

The oligomerization of Epidermal Growth Factor Receptor (EGFR) has been found after the binding of EGF to the receptor, to initiate the activation of EGFR signal pathway. It is suggested that magnetic field (MF) also induces a similar oligomerization effect of EGFR on cell membranes independent to EGF binding. By using Atomic Force Microscope (AFM) and transmission electron microscope (TEM), we have investigated the effects of the extremely low frequency magnetic field (ELF MF) on the clustering of purified A431 Epidermal Growth Factor Receptor (EGFR). Results from AFM indicated that 30-min exposure of 5 μ g/ml EGFR molecules (in PBS, on a substrate of mica) at room temperature to the field, resulted in obvious clusters for a basal size of the molecule particles: the height of apparent individual basal particles increased from (2.6 \pm 0.2) nm (sham) to (5.2 \pm 0.3) nm, and the half-width from (26.0 \pm 2) nm (sham) to (38.2 \pm 5) nm, suggesting a nearly doubled size of EGFR particles. Besides the existence of the basal clusters, doubled, tripled and even higher degree aggregations of the basal clusters were also observed. A similar effect of an obvious increase in half-width was also conformed by TEM after the MF treatment. This is consistent with the immune-fluorescent labeled EGFR effect from the CHL cell line by using a confocal laser microscope combining, showing that the exposure to the field induces oligomerization of EGFR monomers on cell membrane.

P- B-164 WITHDRAWN

P-C-165

EXPERIMENTAL PREDICTION METHOD FOR EXTREMELY LOW FREQUENCY TRANSIENT MAGNETIC FIELD FROM ELECTRIC APPLIANCES. S.H. Myung, K.H. Yang, M.N. Ju, S.W. Min¹. Electrical Environment & Transmission Group, Electric Power Research Lab., Korea Electrotechnology Research Institute (KERI), Changwon, Gyeongnam 641-120, Korea, ¹Division of Information Technology Engineering, Soonchunhyang University, Asan, Chungnam 336-745, Korea.

BACKGROUND: With biological effects by ELF (Extremely Low Frequency) magnetic field generated from power system, the transient magnetic field (TMF) from electric appliances is a major issue presently. Because the transient magnetic field induces higher current than the power frequency field inside living bodies, transient magnetic field exposure has been much focused [1]. In this paper, it is shown that transient

magnetic field from electric appliances can be characterized as magnetic dipole moment.

OBJECTIVE: Estimation on harmonics characteristics of ELF magnetic fields generated by electric appliances by the use of an equivalent magnetic dipole moment method.

METHODOLOGY: We measured magnetic field distribution around electric appliances in view of harmonics and calculated the amplitude of the magnetic dipole moment, $m=4\pi R^3 B/k\mu_0$ [2]. We adopted an expression of the content of harmonics in magnetic field, $B=B_f(1+\alpha_2^2+\alpha_3^2+\alpha_4^2+\dots)^{1/2}$. B_f is the rms value of the fundamental field component of magnetic flux density, and $\alpha_i(i=2,3,4\dots)$ is fraction of the i^{th} harmonics. This expression can be applied to the equivalent magnetic dipole moment. In addition, a biological interaction parameter M is introduced, $M=f_0 m_f(1+2\alpha_2+3\alpha_3+4\alpha_4+\dots)$, f_0 is the fundamental frequency. This parameter directly represents the index between the magnetic dipole moment and biological interaction based on the current induced inside biological organisms, which is proportional to frequency.

RESULTS: The 20 types of electric appliances used at home and office are examined. The appliances are hair dryer, heater, electric pot, vacuum cleaner, toaster, fan, PC, projectors and so on. When a waveform contains much higher frequency components, it affects the interaction parameter M . For example, a consumption power of hair dryer is about 9 times as large as CRT. However, the interaction M of CRT is reversibly about 8 times as large as hair dryer.

CONCLUSION: The proposed method was applied to 13 types of home appliances (hair drier, heater, vacuum cleaner, toaster etc.) and 7 types of office appliances (personal computer, projectors, printer, monitor etc.), and then their equivalent magnetic dipole moment and harmonic components were estimated. As the results, the useful data for quantifying magnetic field distribution around electric appliances could be obtained. We know most magnetic fields have harmonics and the higher frequency magnetic field may induce higher current inside living body.

References

[1] J. R. Gauger: "Household appliance magnetic field survey", IEEE Trans. Power Apparatus and systems, 104, 9, 2436-2444(1985-9)

[2] International Electrotechnical Commission (IEC): "Measurement of low -frequency magnetic and electric fields with regard to exposure of human beings - Special requirements for instruments and guidance for measurement", IEC Std. 61786(1998)

P-A-166

SKIN HEATING BY MILLIMETER WAVES: THEORY BASED ON A SKIN MODEL COUPLED TO A WHOLE BODY MODEL. D.A. Stewart Jr, T.R. Gowrishankar, G.T. Martin, J.C. Weaver. Harvard-MIT Division of Health Sciences and Technology Massachusetts Institute of Technology, Cambridge, MA 02139, USA.

INTRODUCTION: Human skin can be accidentally or purposefully exposed to millimeter waves (MMW; 3-300 GHz) under a variety of circumstances. At MMW frequencies electromagnetic energy is almost entirely dissipated in the skin's outer regions.

OBJECTIVES: Provide a theoretical basis to explain the thermal response and possible biological outcomes for a series of experiments done with rats exposed to MMW electromagnetic waves.

METHODS: We use a transport lattice system model that incorporates two spatial scales to estimate heating in both human and rat skin in vivo: (1) a layered skin model involving the outer several millimeters of the body, and (2) a whole body model that accounts for the total heat flux and sources, and which provides a changing reference temperature for the skin model. A thermal damage indicator is used to estimate cumulative molecular changes during and after the MMW exposure as a function of location within the skin.

RESULTS: For both human and rat skin in vivo short (10s) exposures to 35 and 94GHz at $1W/cm^2$ have

small predicted damage. In contrast, rat skin exposed *in vivo* to 75mW/cm² for long (50 min) times to both frequencies has very large predicted damage, in agreement with experiments reported in a companion poster (Blystone et al.). Tissue regions with significant thermal damage may release toxic biochemicals which are delivered to other skin regions by diffusion, causing damage at sites which experience insignificant heating. Release and diffusion of such molecules may also lead to systemic damage by diffusive delivery into nearby blood capillaries and removal by perfusion.

This study was supported by an AFOSR subcontract from Trinity University and NIH grant RO1-GM63857

P-B-167

STUDENT

BIOLOGICAL CRITERIA FOR REALISTIC MOBILE PHONE SAFETY STANDARDS. D. Weisbrot¹ M. Blank², H. Lin³ and R. Goodman¹, Departments of Pathology¹ Physiology² and Anatomy³ Columbia University, New York, NY 10032, USA.

INTRODUCTION. Exposure of a variety of *in vivo* and *in vitro* models to mobile phones results in an immediate (within minutes) significant increase in levels of the stress response protein hsp70 by both the low frequency electromagnetic (EM) fields (<3000Hz) and radio frequency (RF) components. This is a non-thermal response. A 70bp nucleotide segment of the HSP70 promoter, containing three nCTCTn consensus sequences, is required for the nonthermal induction of HSP70 expression by EM fields. It is upstream and unlike the consensus sequence required for induction of HSP70 by heat shock. Furthermore, unlike the response to heat shock, elements of MAPK ERK1/2 and p38MAPK cascades respond to EM and RF exposures.

OBJECTIVE. To establish biological criteria for realistic mobile phone safety standards

Materials and Methods. *Drosophila melanogaster* Oregon R were exposed to discontinuous radiation (1 hr twice a day) from a Bosch World 718 GSM mobile phone (SAR 1.4 W/kg) during reproduction and growth.

RESULTS. In more than 50 replicate experiments there was a significant (p=.01) increase in numbers of offspring as well as a doubling of hsp70 levels, SRE-binding and ELK1 phosphorylation as compared with sham exposed samples.

CONCLUSIONS. These data, together with a number of detailed published reports, provide biologically relevant, sensitive and reliable biomarkers that should serve as the basic for establishing realistic safety guidelines for mobile phone emissions, rather than the current practice of using heating as the sole criterion. Reference:

Biological Criteria for Realistic Mobile Phone Safety Standards

David Weisbrot¹ Martin Blank², Hana Lin³ and Reba Goodman¹, Departments of Pathology¹ Physiology² and Anatomy³ Columbia University, New York, NY 10032,

Introduction. Exposure of a variety of *in vivo* and *in vitro* models to mobile phones results in an immediate (within minutes) significant increase in levels of the stress response protein hsp70 by both the low frequency electromagnetic (EM) fields (<3000Hz) and radio frequency (RF) components. This is a non-thermal response. A 70bp nucleotide segment of the HSP70 promoter, containing three nCTCTn consensus sequences, is required for the nonthermal induction of HSP70 expression by EM fields. It is upstream and unlike the consensus sequence required for induction of HSP70 by heat shock. Furthermore, unlike the response to heat shock, elements of MAPK ERK1/2 and p38MAPK cascades respond to EM and RF exposures.

Objective. To establish biological criteria for realistic mobile phone safety standards

Materials and Methods. *Drosophila melanogaster* Oregon R were exposed to discontinuous radiation (1 hr twice a day) from a Bosch World 718 GSM mobile phone (SAR 1.4 W/kg) during reproduction and growth.

Results. In more than 50 replicate experiments there was a significant (p=.01) increase in numbers of

offspring as well as a doubling of hsp70 levels, SRE-binding and ELK1 phosphorylation as compared with sham exposed samples.

Conclusions. These data, together with a number of detailed published reports, provide biologically relevant, sensitive and reliable biomarkers that should serve as the basic for establishing realistic safety guidelines for mobile phone emissions, rather than the current practice of using heating as the sole criterion.

Weisbrot D, Lin H, Ye L, Blank M, Goodman R (2003). Effects of Mobile Phone Radiation on Reproduction and Development in *Drosophila melanogaster*. J Cell Biochem 89: 48-55.
Support from the Robert I Goodman Fund

P-C-168

MOLECULAR MECHANISM FOR THE BIOLOGICAL SIGNIFICANCE OF THE GEOMAGNETIC FIELD. V.N. Binhi. General Physics Institute of the Russian Academy of Sciences, Moscow 119991, Russian Federation.

INTRODUCTION: There are just a few physical explanations of why the presence of the geomagnetic field is important for biological systems to operate. One of them (A. Liboff. Bioelectromagnetics, 18:85–87, 1997) gives a qualitative explanation without means to validate the hypothesis. The theory of quantum interference of the biologically significant ions (V. Binhi. Magnetobiology. Academic Press, San Diego, 2002) explains biological significance of the geomagnetic field quantitatively. However, it is based on the assumption of long-living quantum states of ions inside protein cavities. The assumption is difficult to substantiate. The advanced theory of molecular interference (V. Binhi & A. Savin. Phys. Rev. E, 65(051912):1–10, 2002) is free of that shortcoming and in a good agreement with many experiments on biological effects of weak ELF magnetic fields.

OBJECTIVES: To demonstrate how the theory of molecular interference quantitatively describes the biological effects of “magnetic vacuum”, i.e., the condition of the natural static magnetic field deprivation.

METHODS: The mechanism developed considers dynamics of the density matrix of the molecular groups, which are attached to the walls of protein cavities by two covalent bonds, i.e., molecular gyroscopes. Numerical computations have shown almost free rotations of the molecular gyros; the relaxation time due to van der Waals forces was about 0.01 s for the cavity size of 28 Å. The role of molecular gyros could probably be played by short sections of polypeptides and nucleic acids built inside globular proteins or in cavities between associated globules. In the theory, the formula is derived for magnetic-dependent part of the molecular rotator reaction probability with an active site on the protein cavity wall in ac–dc uniaxial magnetic field:

$$S = \sum_{mm'n} \sigma_{mm'}^2(0) \frac{\sinh^2 \eta + \sin^2 \xi}{\eta^2 + \xi^2} J_n^2 \left[(m - m') \frac{h'}{\Omega'} \right].$$

Here $\sigma_{mm'}$ is the initial populations of the quantum states of the gyroscope, $\eta = \Gamma \tau$ is a parameter where Γ stands for damping and τ for rotator's state lifetime, $\xi = [\omega_{mm'} - (m - m')\omega_g - n\Omega]\tau$ is a parameter with $\omega_{mm'}$ for the Zeeman split, ω_g for characteristic gyro frequency, n for the order of Bessel function J , h' is dimensionless MF amplitude, and Ω' is the dimensionless MF frequency, m is the magnetic quantum number. In the case of the absence of the ac MF $h'=0$, and all J_n in the above formula equals zero except $J_0(0)=1$, then:

$$S = \sum_{mm'} \sigma_{mm'}^2(0) \frac{\sinh^2 \eta + \sin^2 \xi}{\eta^2 + \xi^2}$$

where now $\xi = [\omega_{mm'} - (m - m')\omega_g]\tau$, as $n=0$. The members with small values of ξ mainly contributes to the sum, i.e., the members with $m' = -m$ (then $\omega_{mm'}=0$). Hence, $\xi = -2m\omega_g\tau$. As was shown in the aforementioned article, in MFs of the order of the geomagnetic MF H_{geo} , the value $\omega_g\tau$ is of the order of unit. In addition, ω_g is proportional to the local dc MF. Consequently, $\omega_g\tau \approx H_{dc}/H_{geo} \equiv x$. Here, the

dimensionless variable x is introduced for the local static MF. With the initial k lower equally populated states of the rotating part of a molecular gyroscope, the reaction probability, correct to a multiplier, is equal to

$$S = \sum_{m=0}^k \frac{\sinh^2 \eta + \sin^2 2mx}{\eta^2 + 4m^2 x^2}.$$

The figure below plots a diagram for this dependency $S(x, \eta, k)$ at different values of the parameters.

RESULTS: As is seen, in a wide range of the parameters a significant growth of a gyroscope reaction takes place. This might explain the biological effect of a “magnetic vacuum” condition $H_{ac} \ll H_{dc} \ll H_{geo}$. In other words, it signifies the biological importance of the geomagnetic field. The effect was repeatedly observed in experiments made by many authors. There is a review of those works in this author’s monograph.

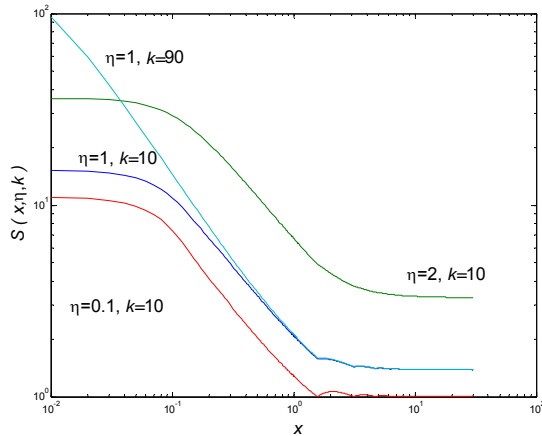


Figure. Growth of the reaction probability of a molecular gyroscope with the reduction of static magnetic field at different values of the parameters.

P-B-169

STUDENT

EXPOSING TO INDUSTRIAL EM FIELDS, STANDARDS, DEVELOPING MEASUREMENT PROCEDURES AND SIMULATION OF MEASUREMENTS. O. Ulukut, S. Comlekci. Department of Electronics and Communication Engineering, Suleyman Demirel University, Isparta, Turkey.

There are widely used of Low Frequency (LF) in Industry and Medicine. In Industrial Frequency Band (150 kHz-30 MHz) there are two distinct and fundamentally different ways of measuring the radiated energy. Such radio frequency radiation has been in use in hospitals (27 MHz Short Wave Diathermy). Diathermy equipments are used at considerable power levels [Franconi, 1991]. This equipment has serious complications with other medical devices [Comlekci et al., 2000]. All equipments must meet the electrical safety standards (e.g. BS 5725 part 1). It is therefore EMC regulations, screening and other solutions will have to be found to solve any problems that may arise [Grant, 1993]. There are more and more current standards for Industrial EM RF. Obviously so much uncertainty occurs. European Commission work on the harmonization of these standards. At very low Industrial Frequencies, the frequency range would have been more limited had a simple resonant rod antennas been used. Below 30 MHz the dipole becomes very large. It is normal practice to use loop antennas below 30 MHz. They are in the far field since at 150 kHz this spacing would have to be over 100 meters. Because loop antennas usually have high Q, they have to be tuned for each frequency of interest if any useful sensitivity is to be achieved, both for electric and magnetic field [Middleton, 1992].

P-C-170

EFFECTS OF A SWITCHED 1.5 Tesla MAGNETIC FIELD ON INTRACELLULAR Ca^{2+} SIGNALING PATHWAYS OF ADRENAL CHROMAFFIN CELLS. T. Ikehara¹, T. Teramoto³, H. Houchi³, K. Hosokawa¹, H. Yamaguchi⁴, Y. Kinouchi², M. Kitamura¹, M. Shono¹, K. Yoshizaki¹, and H. Miyamoto¹. ¹Department of Physiology, School of Medicine, ²Department of Electrical and Electronic Engineering, Faculty of Engineering, ³Department of Pharmacy, School of Medicine, The University of Tokushima 770-8503, ⁴Department of Environmental Physiology, Faculty of Human Life Sciences, Tokushima Bunri University, Tokushima 770-8514, Japan.

OBJECTIVE: We have recently found that the time-varying magnetic field inhibited the Ca^{2+} release from intracellular stores of adrenal chromaffin cells. In this study, we examined to find out the mechanisms that exposure to the magnetic field affected several intracellular Ca^{2+} signaling pathways in the cells.

MATERIALS AND METHODS: HeLa cells and bovine adrenal chromaffin cells were plated on 35-mm culture dishes or cover glasses placed in the same culture dishes. After the cells were attached to the dishes or cover glasses, they were maintained for 2-5 days. Magnetic field is produced by an electromagnet designed and set up by Hitach Metal Indust. Co. (Tokyo, Japan). Magnetic flux density was varied intermittently from 0.07 to 1.5 T at an interval of 3 sec. The cover glasses in culture dishes were put in special incubator to keep their temperature at 37 °C, and then the incubator was placed horizontally in the gap between two poles of the electromagnet. The concentration of intracellular Ca^{2+} ($[\text{Ca}^{2+}]_i$) was measured with Fura 2 by ARGUS 50/CA (Hamamatsu Photonics, Hamamatsu, Japan). Changes in intracellular ATP concentration was measured by luminescence photometer and oxygen consumption was measured by using oxygen probe (YSI 5331). Cells were also observed with a laser scanning confocal microscope (Leica TCS-NT, Hyderberg, Germany).

RESULTS AND DISCUSSION: $[\text{Ca}^{2+}]_i$ of chromaffin cells was increased by addition of acetylcholine or bradykinin. The exposure to the magnetic field for 2 hr inhibited these activators-stimulated increase in $[\text{Ca}^{2+}]_i$ in Ca^{2+} -free medium, but slowed only the decay phase of $[\text{Ca}^{2+}]_i$ after peak in Ca^{2+} containing medium. Also, the intracellular ATP content and oxygen consumption were influenced by the exposure in glucose-free medium. These effects of magnetic field would be related to the eddy current. We have recently found that exposure to a time-varying or ELF magnetic fields affect the several properties of cell membrane. However, mechanism of these influences on Ca^{2+} release from Ca^{2+} stores by the exposure is not yet resolved.

P-A-171

15 YEARS OF RESEARCH INTO THE BIOMEDICAL EFFECTS OF ELECTROMAGNETIC FIELDS AT THE ELECTROPATHOLOGICAL RESEARCH CENTER OF WITTEN/HERDECKE UNIVERSITY – AN INTERIM STATEMENT. J. Reißerweber, A. Wojtysiak*, E. David, Electropathological Research Center, Witten/Herdecke University, D-58453 Witten, Germany.

INTRODUCTION AND OBJECTIVES: This contribution will provide a concise overview over the past research at the Electropathological Research Center (ERC) of Witten/Herdecke University. ERC is Germany's only medical university institute working full-time in the special area of real or hypothetical health effects of electromagnetic fields. The investigated frequencies range from ELF electric and magnetic fields caused by the generation, delivery and use of electricity to HF electromagnetic fields caused by mobile communications. Its long-standing projects have rendered ERC a competent partner in the area of research on electromagnetic field effects on biological systems and man during the past more than 15 years.

EXPERIENCE: The coworkers of ERC dispose of more than 15 years of experience in the following areas:

- conducting own research projects;

- conducting research projects in commission;
- authoring scientific publications;
- providing scientific contributions on the occasion of scientific, public and political events;
- providing consultations of the public on biomedical effects of electromagnetic fields by mail, email or phone;
- writing expert opinions for legal and social courts;
- collaborating with national and European standard-setting committees;

RESEARCH: The following main research projects have been realized so far at ERC:

- Effects of 50 Hz magnetic fields on the circadian rhythmicity of plasma melatonin levels in humans.

This

- program represents endocrinological and chronobiological EMF research;
- Self-reported electromagnetic hypersensitivity in ELF and RF fields as a phenomenon pertaining to the human organism in its entirety including psychological components. This program represents a combined diagnostic and therapeutic approach;
- Influence of circularly polarized 50 Hz magnetic flux densities of 96 μ T on cutaneous microcirculation of the thumb in healthy human volunteers and in persons suffering from self-reported electromagnetic hypersensitivity;
- Migratory behavior and motility of peripheral human lymphocytes in 50 Hz magnetic flux densities of 10 mT. Here a therapeutic field effect is sought for in terms of an enhancement of the immune system;
- As an example for research on biomedical implants within the human body we investigated the electrodynamic disturbances of implanted cardiac pacemakers. Those disturbances can be produced by external low-frequency electric fields of power lines or inductive cooking or be caused by external high-frequency electromagnetic fields of mobile communications; ELF electromagnetic field effects on nerve and muscle cells like excitation;
- Evaluation of consultations of the public on biomedical effects of 50 Hz electric and magnetic fields as a scientific program. New psychological, sociological, economic and political aspects of the public electromagnetic field discussion will be addressed in this context;

The above mentioned research projects will briefly be presented in this contribution and their results and conclusions will be summarized.

MEDICAL COMPETENCE: The phenomenon of self-reported electromagnetic hypersensitivity (see above) is still a problem in modern industrial societies. When persons suffer from uneasiness or dizziness which they subjectively attribute to the hypothetical health effects of weak electromagnetic fields they will need professional help by specialized physicians. This medical help can be provided at ERC. Here electromagnetically hypersensitive persons are taken seriously and their individual situation and subjective burden of suffering are analyzed and categorized. They can participate in a specialized new diagnostic program which will be demonstrated in detail.

PERSPECTIVES AND CONCLUSIONS: As public interest into and concerns about real or hypothetical biomedical effects of electromagnetic fields are as important as before ERC will continue its efforts in future to shed light on the putative or real biomedical effects of electric and magnetic fields and to inform the public about the current state of knowledge.

MEMBERSHIPS: Coworkers of ERC are members of the following scientific bodies:

- Medical Faculty of Witten/Herdecke University
- Bioelectromagnetics Society
- Society for Biomedical Engineering
- German Physiological Society
- German Electrotechnical Committee
- European standard-setting committees
- INTERNET: <http://www.uni-wh.de/de/medi/elpath.htm>

P-B-172

COMPARATIVE ANALYSIS OF SAR INDUCED BY MOBILE PHONE IN CHILD-LIKE HEAD.

A. Hadjem¹, C. Dale¹, D. Lautru², M.F. Wong¹, V. Fouad Hanna², N. Gadi³, I. Bloch³ and J. Wiart¹. ¹ France Telecom R&D, DMR/IIM, 38-40 rue du Général Leclerc, 92794 Issy-les-Moulineaux Cedex 9, France. ; ² Université de Paris 6, Laboratoire LISIF, 4, place Jussieu, 75252 Paris Cedex 05, France. ³ ENST Paris, 46, rue Barrault, 75013 Paris, France.

There is a public concern about possible health impact issued from radio frequency electromagnetic field. Organisms such as ICNIRP and IEEE have set up exposure limits, defined in terms of basic restrictions, to protect public and workers from possible hazards associated to electromagnetic fields overexposure. In line with the compliance analysis with these limits many studies have been done to analyse the SAR in the head of a user.

The wireless system and mobile phone in particular are nowadays used by millions of users including children. Therefore it is of interest to analyse the SAR distribution in the children head

The aim of this study is to analyse the SAR in the children head at different ages. Since the MRI of children heads are not always available, we analyse the SAR in Child-Like (CL) head. These heads are built by deformation of an adult head. Through the literature external shape of human heads and their transformation versus the age have been analysed. The head has been shared in specific volumes having specific ratios (depending on the age) to the adult one. Using these ratios, an adult head has been reshaped by part using relevant parameter and the head. 5, 7, 9, 11, 15 and 19 years old children have been built. The Figure 1 s show an adult head and its transformation into a five years old child.

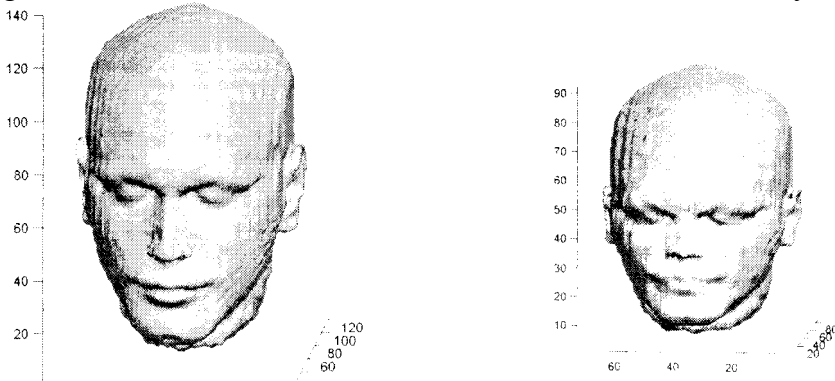


Fig.(1): Example of transformation of an adult head into a five years old child head

The exposure analysis is carried out using FDTD and a numerical model of a phone representative of actual dual band integrated antenna. For the child-like head models with the phone in the CENELEC positions the SAR averaged over 1 and 10 grams as well as the SAR distribution of SAR in tissues are compared to the adult SAR and distribution.

P-C-173

EXPOSURE COMPARISON BETWEEN A MOBILE PHONE AND A BASE STATION AT 900

MHZ, 1800 MHZ AND 2100 MHZ. C. Dale, J. Wiart. France Telecom R&D, DMR/IIM, 38-40 rue du Général Leclerc, 92794 Issy-les-Moulineaux Cedex 9, France.

INTRODUCTION: ICNIRP guidelines have been established to protect public and workers from the exposure to electromagnetic fields. With the wide-spreading of the mobile phone technologies, more and

more questions have been raised by the public and the medias. These questions are more related to base station antennas than to mobile phones, while mobile phone exposure is far more significant since the electromagnetic source is very close the head. Usually, comparisons are made at maximum exposure, possibly averaged over six minutes as required by ICNIRP guidelines for compliance testing. Nevertheless, there is a need to characterise more completely the exposure even well below these limits. One other parameter to describe the exposure is the average value over the day or month.

OBJECTIVES: The aim of this study is to compare the exposure coming from a mobile phone and a base station antenna. This comparison is performed using a 0.3, 1, 1.5 W/kg SAR mobile phone and a base station environmental field of 0.5, 2, 8, 10 V/m. The comparison has first been performed on local and whole body SAR for both situations at 900 MHz, 1800 MHz and 2100 MHz, at the instant of maximum exposure. Then, the analysis has been done on average exposure values over the month.

METHODS: Simulations have been performed using the FDTD method, very useful to take into account strong inhomogeneities. The body model considered is the Visible Man 3D volume made available by Brooks Air Force. The mobile phone has been modelled with a patch antenna. The meshing of the volume is 1 mm in the region of the mobile phone and ear growing non-uniformly till 3 mm on the opposite side. The base station exposure has been modelled first by a plane wave exposure condition, then by a Rayleigh distribution field representing an indoor environment through a Huygens box in the FDTD. To consider the average exposure over the month, a mobile phone use duration of 5 hours per month has been considered, and the variability of the base station traffic has been analysed.

RESULTS: Since the simulations are only performed on the head and shoulders, the whole body exposure had been estimated: for the mobile phone exposure case, it is estimated by dividing the power absorbed in the whole head by the weight of the body – for the base station case, it has been estimated through the average SAR on the head. Simulations at 900 MHz, 1800 MHz and 2100 MHz show that at the instant of maximum exposure, the local and whole body exposure produced by a mobile phone is greater than the exposure to an 8 V/m-base station environmental field. Considering the average exposure over the month, the local exposure produced by the mobile (5 hours during the month) is comparable to an 8 V/m-base station environmental field, while the whole body exposure produced by the base station stays above even though far below the ICNIRP limits specified to protect people from the adverse known effects of electromagnetic fields.

P-A-174

DESTRUCTION OF GASTRIC CANCER CELLS USING MAGNETIZABLE BEADS AND PULSED MAGNETIC FORCE. POSSIBLE RELATIONSHIP BETWEEN BEADS' SIZE AND CYTOCIDAL EFFICIENCY.

H. Yamashita^{1*}, J. Kitayama^{1*}, M. Ogiue-Ikeda^{2*}, S. Ueno², H. Nagawa^{1*}. ¹Department of Surgical Oncology, Graduate School of Medicine, University of Tokyo, Tokyo, Japan. ²Department of Biomedical Engineering, Graduate School of Medicine, University of Tokyo, Tokyo, Japan.

INTRODUCTION: Treatment modalities for eradicating cancer cells using heat from electromagnetic waves and ultrasonic cavitation are widely investigated. We reported a new method to eradicate targeted cells using magnetizable beads and pulsed magnetic forces at the 25th annual meeting. In that report, magnetic force effectively reduced the viability of TCC-S leukemic cells combined with magnetizable beads. However, it remains to be investigated whether this method can be applied for other cell types, and which beads are suitable for this aim. In this study, we used gastric cancer cells and examined the cytotoxic efficiency using two types of magnetizable beads with different size.

MATERIALS & METHOD: MKN45 gastric cancer cells were immunologically combined with magnetizable beads (Dynabeads Pan Mouse IgG (Dyna), diameter = $4.5 \pm 0.2 \mu\text{m}$, magnetic mass susceptibility = $(16 \pm 3) \times 10^{-5} \text{ m}^3/\text{kg}$) or another magnetizable beads (Dynabeads Protein G (Dyna), diameter = $2.8 \pm 0.2 \mu\text{m}$, magnetic mass susceptibility = $(10 \pm 2.5) \times 10^{-5} \text{ m}^3/\text{kg}$). Each beads and mouse anti-CEA

antibodies were mixed gently for 1 hour at 4°C. Then MKN45 cells were incubated with the bead/antibody complexes for another 1 hour. The cell/bead/antibody complexes were purified using a magnetic particle concentrator and suspended in 1 ml of phosphate buffered saline in a 1.5 ml tube. A magnet placed under the tube was used to aggregate the beads. The aggregated beads were then stimulated 20 times or 40 times at 5 sec intervals by a circular-shaped coil (inner diameter = 15 mm, outer diameter = 75 mm), which produced monophasic pulses of 150 μsec in duration and a maximum of 2.4 T at the center of the coil. The magnetic field and the magnetic field gradient near the beads were approximately 2.0 T and 100 T/m respectively, and the magnetic force acting on the aggregated beads was calculated to be approximately 0.036 N and 0.032 N respectively. After stimulation, the viable cells and not viable cells were counted under the microscope and the percentage of destroyed cells were calculated against total cell counts. The morphology of damaged cells were also observed under a scanning electron microscope.

RESULTS & DISCUSSION: The viability of the stimulated cells of the cell/bead/antibody complex was significantly lower than that of the nonstimulated cell/bead/antibody complex. Damage was inflicted by penetration of the beads into the cells or rupturing of the cells by the beads, which was similar with TCC-S cells (Fig 1). MKN45 combined with Pan Mouse IgG showed significantly reduced viability ($55.7\pm 13.4\%$) at 20 times of stimulation and there was no difference in terms of the stimulation number. The viability of MKN45 combined with Protein G showed of $63.9\pm 13.3\%$ at 20 times and of $44.2\pm 7.5\%$ at 40 times of stimulation. However, MKN45 that did not make immunological complex with these beads did not show any significant cell damage under the same magnetic fields.

These results indicate that this method can induce targeted cell damage and that smaller bead may be more suitable for clinical application.

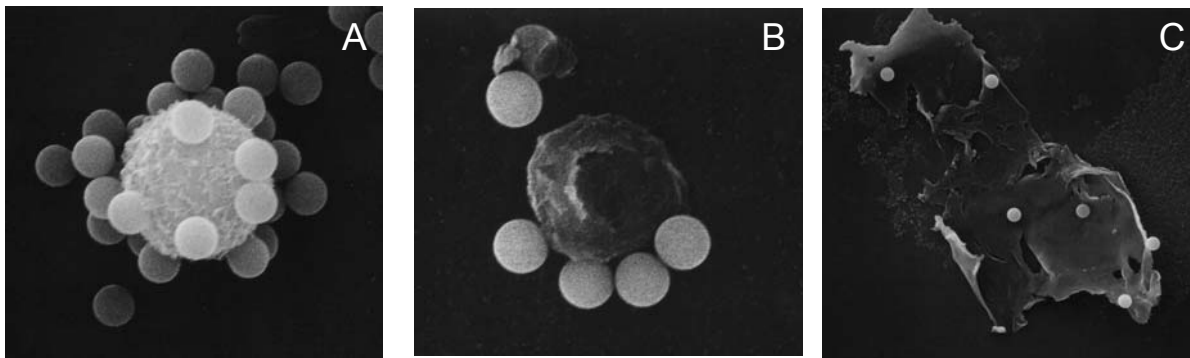


Figure 1. A: Electron scanning micrograph of the nonstimulated cell/bead/antibody complex. B,C: Electron scanning micrographs of cell-bead complexes with Pan Mouse IgG beads (B) or Protein G beads (C) after the magnetic stimulation .

P-B-175

TREATMENT OF PERIPHERAL NEUROPATHY WITH HIGH STRENGTH MAGNETIC FIELDS: A PRELIMINARY STUDY SUGGESTIVE OF NERVE REGENERATION. T.W. Nichols, L.A. Pearce*, D.A. Bonlie. AMRI Pennsylvania 17331, AMRI North Carolina USA, AMRI Int. Calgary Alberta, Canada.

INTRODUCTION: A NIH Consensus Conference on “Alternative Medicine, Expanding Medical Horizons” held in Chantilly Virginia in 1992 and published in December 1994 on “Bioelectromagnetic Therapy,” suggested eight major new applications of the use of electromagnetic fields in medicine include: wound healing, tissue regeneration, immune system stimulation, neuroendocrine modulations, treatment of osteoarthritis, bone repair, electro-acupuncture, and nerve stimulation.

The MME (Magnetic Molecular Energetics) is a treatment method that is hypothesized to address all the

areas above except acupuncture. It was developed by Dean Bonlie D.D.S. at the research laboratory at Magneto, Inc. Calgary Alberta in 1996. The MME is a novel modality consisting of two very large and strong nonpulsed DC electromagnets (3000 to 5000 gauss) with the patient lying in the focal point between a negative pole below and the positive pole above (US patent #6,210,317).

METHOD: Patients with peripheral neuropathy were placed under the subjects lying between two magnets under an IRB protocol. The focus of the MME was on the feet in three diabetic patients, knee in one, and LS spine in two. All patients had a baseline and post Current Perception Threshold (CPT) testing. CPT testing is an effective predictor of symptoms and physical impairment and is obtained with 3 neuroselective frequencies (5, 250 and 2000Hz) to test various nerve fiber types. This was obtained using double-blind testing methodology. ($\pm 20 \mu A$, $p < 0.0006$)

RESULTS: Five patients showed significant improvement with MME therapy, and sustained in most cases more than 1 year. One patient had slight worsening regarding dysesthesiae. His CPT likewise worsened. Treatment times with MME ranged from 12 hrs. to 155 hrs. with a mean of 90 hours.

DISCUSSION: The mechanisms underlying the observed favorable changes are not fully understood. Magnetic fields induce a higher velocity and precession of certain orbiting electrons resulting in enhanced electron transfer and chemical reactions. Free radicals, such as oxygen singlet, superoxide, hydroxyl radicals, hydrogen peroxide, peroxyhydrate and nitric oxide are the cause of many disease at the molecular level, have an odd number of valence electrons. Hence the bonds are not completely satisfied, and there is a net angular momentum and thus react in a magnetic field. In conclusion, the sustained improvement infers that nerve regeneration was induced by the magnetic fields in the majority of these patients. In addition, the CPT changes esp. seen in patient W.Y. were dramatic, rarely seen in prior therapeutic trials, also suggestive of nerve regeneration.

References.

Walleczek J. "Magneticokinetic Effects on Radical Pairs" in *Electromagnetic Fields: Biological Interactions and Mechanisms*. American Chemical Society, 1995 Washington D.C: 395-417.

Pilla, A, A., D.J. Muehsam, and M.S. Markov. A dynamical systems/Larmor precession model for weak magnetic field bioeffects: Ion binding and orientation of bound water molecules. *Bioelectrochemistry and Bioenergetics* 43:239.

Supported by: AMRI International

P-C-176

ELECTROMAGNETIC HYPERSENSITIVITY IS A PROGRESSIVE DISEASE. M.M. Hughes, Hughes Press, Washington, District of Columbia 20037, USA

INTRODUCTION: Electromagnetic sensitivity is a progressive, disabling disease associated with exposure to electromagnetic community to the condition of hypersensitivity to electromagnetic fields created by computers and other electronic equipment.

OBJECTIVE: To alert the bioelectromagnetic community to the condition of hypersensitivity to electromagnetic fields.

SUMMARY: Since 1970, Swedish scientists have documented dermatological symptoms which they report to be the most common to electromagnetic sensitivity. Dr. Bjorn Lagenholm, the Chief of Dermatology at the Karolinska Hospital in Stockholm, attributed skin injuries (dermatitis) and absence of elasticity under the epidermis in young computer operators, to ultraviolet light and x-rays. (Nordstrom, G., *Sick from Computers*, 1989). Also, in a large literature study it was found that screen dermatitis show many similarities with skin damaged by UV light and ionizing radiation. In this study, not only clinical but also immunohistological manifestations were evaluated. (Gangi, S. Johansson, O. *Experimental Dermatology* 6:283-291, 1997).

Dr. William Rea has medically documented the existence of electromagnetic sensitivity in a double blind study. He found primary medical symptoms were neurological, musculoskeletal, respiratory,

gastrointestinal and dermal. He concluded that hypersensitive persons are able to detect and identify weak fields. (Rea, W. Journal of Bioelectricity 10:241-256, 1991). The central nervous system is affected with dizziness, tiredness, headache, epilepsy and slurred speech (Gangi, S. Johansson, O. Experimental Dermatology 6:283-291, 1997).

The World Health Organization found that extremely low frequency magnetic fields are possibly carcinogenic to humans (Group 2B), (WHO, IARC v. 80, p. 338). There are increased reports from electromagnetic sensitive individuals of instances of breast cancer. The value of the negative studies is discounted by the lack of consistent pattern in all of these fields.

CONCLUSION: The international scientists concluded that electromagnetic hypersensitivity is a progressive disease and many afflicted are permanently disabled. The world wide introduction of computers and other electronic equipment into our environment make it urgent that this catastrophic disorder be given widespread attention by the scientific community.

P-A-177

THEORETICAL DERIVATION OF VALID BIOLOGICAL EXPOSURE METRICS FROM MAXWELL'S EQUATIONS OF ELECTROMAGNETISM: CURRENT STATUS RE STATIC FIELDS AND CELLULAR PHONE ANTENNAS. M.A. Lundquist. The Bioelectromagnetic Hygiene Institute, P. O. Box 11831, Milwaukee, Wisconsin 53211-0831 USA

Maxwell's equations of electromagnetism in differential form were the starting point for the derivation. It was assumed that the mechanisms for the interaction of an electromagnetic field with biological tissues are the same as those for its interaction with inanimate matter.

The expression for a biological exposure metric takes the form of an integral equation involving the fields *inside the material medium*. (If a field in air is employed, a trivial solution results.) The general expression for a time-varying field is employed; an expression valid for a static field is obtained by setting all time derivatives in the expression equal to zero.

Results: It was discovered that exposure metrics correspond to conservation laws of physics. In electromagnetic theory, there are *two* such applicable laws: conservation of momentum, and of energy. The latter gives rise to an exposure metric applicable to thermal health effects, while the former produces an exposure metric applicable to athermal (nonthermal) health effects.

A full solution has been obtained only for the special case of a *plane electromagnetic wave* normally incident on a rectangular parallelepiped of a linear isotropic homogeneous lossy medium (because this is the simplest model for which a solution of the integral equations for the two biological exposure metrics can be obtained). The solution confirms that, when the irradiated object has great depth, the *thermal* metric is well approximated by the time-average incident radiation power density, and the *athermal* metric by the time-average volume density of energy stored in the electric and magnetic fields within the medium at the surface of incidence (for a plane wave, this is the radiation power density divided by the speed of light in the medium). [Conventional wisdom employs the radiation power density as the exposure metric, but provides a reliable "safe limit value" only for *thermal* health effects.] Robert K. Adair's assertion¹ (that biological effects of weak fields must depend on the *square* of field strength) is confirmed for the *athermal* metric.

Expressions for static fields produce unexpected results. The biological exposure metric for an electric (magnetic) field does involve the strength of the electric (magnetic) field, but the field strength *by itself* does *not* constitute a valid biological exposure metric [which contradicts conventional wisdom, but explains the curious lack of effect observed in uniform magnetic fields].

A situation of great practical interest is that of a person's head near a linear dipole antenna (simulating the user of a cellular phone). An expression for the field in air around a thin linear antenna exists, but this is valid only when a perfect dielectric surrounds the antenna. Introducing a partially conductive spherical object into the space near the antenna (to model the human head) will alter the distribution of charge on

both the antenna and the introduced object, which changes the field in air around the antenna. Additionally, the integral equations to be solved involve the fields *inside the lossy spherical object*, so there are two major difficulties that to date have prevented the development of theoretically valid biological exposure metrics applicable to the head or brain of a human cellular phone user. [Conventional wisdom teaches that only a thermal hazard to health exists (and if an athermal hazard *does* exist, the “safe limit” for it is not greatly different from that for a thermal hazard), and that the radiation power density constitutes the appropriate biological exposure metric for the human head beside a cellular phone antenna (despite the fact that such a head is in the *near field* of the antenna, where the field configuration is *very different* from that of a plane electromagnetic wave)].

CONCLUSIONS: *Incorrect* exposure metrics are currently being used for *static* fields. This theory *fails* to confirm the conventional (industrial) evaluation of the hazard to a cellular phone user.

Reference.

1. R. K. Adair. Biological responses to weak 60-Hz electric and magnetic fields must vary as the square of the field strength. **Proc. Nat. Acad. Sciences** **91**(20) 9422-5 (Sept. 27, 1994).

P-C-178

DATA FROM CONTROLLED STUDIES OF LABORATORY ANIMALS, PROPERLY INTERPRETED, SHOW THAT CHRONIC EXPOSURE TO LOW-INTENSITY PULSED MICROWAVE RADIATION IS CARCINOGENIC AND TUMOROGENIC. M.A. Lundquist. The Bioelectromagnetic Hygiene Institute, P. O. Box 11831, Milwaukee, WI 53211-0831 USA.

After the U.S. Air Force established its PAVE PAWS radar system, the public began to wonder whether the radiation from it was having an adverse effect on the health of residents living in its vicinity. The first controlled laboratory study ever designed to investigate the health effects of chronic exposure to low-intensity pulsed microwave radiation was carried out in the early 1980s on rats. Its most striking finding was a nearly four-fold increase in the incidence of primary malignant tumors somewhere in the rat's body in the exposed group compared to the control group, which was a highly statistically significant difference. In the scientific paper¹ that reported these results, the authors refused to conclude that this highly statistically significant finding was evidence of a real difference between the two groups, insisting that it was necessary to confirm this finding in an independent study before such a conclusion could be validly drawn. A decade later, a new controlled study conducted on transgenic mice exposed to low-intensity pulsed microwave radiation from a dipole antenna (similar to a cellular phone antenna) once again produced a statistically significant difference in the incidence of non-lymphoblastic lymphoma, with a nearly doubled cancer incidence in the exposed group, compared to the control group. The authors² refused to extrapolate the results beyond the strain of mouse used in the study.

These two studies, which were carried out on specific-pathogen-free (SPF) rodents, both indicated that rodents chronically exposed to low-intensity pulsed microwave radiation were at a greater risk for developing cancer than rodents not so exposed. Since then, more controlled laboratory studies of rodents exposed over a lifetime to low-intensity pulsed micro-wave radiation have been carried out *without* statistically significant results having been obtained!³⁻⁵ Until now, the inconsistent results from the totality of these studies have prevented scientists from drawing any definitive conclusion concerning the carcinogenicity of microwave radiation.

Using a novel statistical technique, the data from the experiments producing results that were *not* statistically significant have been re-evaluated in an effort to answer the following question: Were “*not* statistically significant” experimental results obtained because there was *no real difference* between exposed and control groups, or because the *size of the experiment was too small to provide the statistical power needed* to detect the real differences that were actually present?

RESULTS: It is shown that the experiments³⁻⁵ were all too small (by a factor of 2) to be able to detect the *real* differences that were present between the exposed and control groups.

CONCLUSIONS: When *all* the experiments are evaluated with this fact taken into account, the contradictions are resolved and the experiments overwhelmingly confirm that exposure of rodents to low-intensity pulsed microwave radiation typically *increases* the incidence of malignant tumors—justifying the conclusion that chronic exposure to low-intensity pulsed microwave radiation is carcinogenic—and also of benign tumors of the adrenal gland, which indicates tumorigenicity. Data for exposure to continuous-wave radiation fails to show any evidence of carcinogenicity, indicating that this is associated with the pulsed character of the exposure. [On rare occasions, the incidence of cancer in the exposed group has been *lower* than that in the control group, hinting that conditions may exist under which microwave irradiation can be *anti-carcinogenic!*] The carcinogenic character of cellular phone antenna fields to users is being confirmed by findings in the epidemiological studies of Hardell *et al.*⁶

References.

1. C.-K. Chou *et al.* Bioelectromagnetics 13 (1992) 469-496.
2. M. H. Repacholi *et al.* Radiation Research 147 (1997) 631-640.
3. T. D. Utteridge *et al.* Radiation Research 158 (2002) 357-364.
4. J. C. Toler *et al.* Radiation Research 148 (1997) 227-234.
5. B. C. Zook & S. J. Simmens. Radiation Research 155 (2001) 572-583.
6. L. Hardell *et al.* International Journal of Oncology 22 (2003) 399-407.

P-A-179

A PREDICTED PHOTON CHEMISTRY A.H.J. Fleming*, E.B. Colorio*, Biophotonics Research Institute, Boston, MA 02148, sponsor M.S. Markov, Research International NY 14221

INTRODUCTION: In terms of its rest-mass, the photon is often considered massless within conventional field theories, so its velocity can be frequency dependent, enabling satisfaction of the Planck-Einstein relationship. A massless photon is also historically linked to the vast amounts of energy involved in the industrial and military usage of atomic energy. Some prefer to consider its rest-mass ‘negligible’. While the photon’s energy is insignificant compared to atomic energies, in some milieux it is the predominant source of energy, for instance, in certain important biological processes [1]. This is not to imply relativity is incorrect, rather our concept of mass-point needs rethinking. Searching for a lower limit of the rest-mass and hence the cut-off between classical and quantum electrodynamics involves the accuracy of Coulomb’s electrostatic square law [2]. Avoiding any singularity due to a point-wise mass distribution, a ‘Yukawa’ form is assumed ($F_Y = \frac{1}{r^{2+\epsilon}}$) where charge is spread out over the central region of the photon, or equivalently a Yukawa potential is assumed $\phi_Y = \frac{1}{r^{1+j\mu}}$. Different experiments enable the limit to be tightened downwards. Due to earth’s geomagnetic field, fluctuations in the torque of a Cavendish balance can be observed. The Jovian geomagnetic effect has also been similarly measured. In addition, magnetic fields have been found to permeate the cosmos. This universal magnetism may have arisen if photons possessed mass during the early moments of the big bang. Schumann resonances occur at extremely low frequencies (8, 14, 20, 26, 32 Hz, etc.) and are the result of the earth-ionosphere region having a discrete geometry, a series of spherical layers, that form a large resonant cavity waveguide whose resonances are sensitive to variations in temperature. Using all these methods, the current best-estimate of the lower limit of the photon’s rest-mass is $m_{ph} < 4 \times 10^{-51} \text{ kg}$.

OBJECTIVES: This paper predicts an organization similar to atomic chemistry within the photon and its family of compounds. The study is based on electromagnetic self-field theory (EMSFT) that reveals hitherto undiscovered, exact solutions to Maxwell’s equation [3], [4].

METHOD: In EMSFT the fields are measured between centres of rotation rather than between charge points and can be described as physical spinors. Substituting suitable spinorial field forms into Maxwell’s equations leads to solutions of the hydrogen atom modelled as two point-masses, the electron and the

proton. The full EMSFT solution mirrors the physics obtained by spectroscopy and quantum theory. No new physics is introduced except that the general solution also applies to the simple photon. This implies a sub-photonic structure consisting of two equal and oppositely charged point-masses of equal mass. Similar to standing waves, internal systems of periodically rotating fields can have a mixed field form, for example a positive time exponent associated with the orbital spinor of the E-field $\sigma_o(\mathbf{r}_o, \omega_o) = \hat{r}_o e^{j\phi_o}$, and a negative exponent associated with the cyclotron spinor of the H-field $\sigma_c(\mathbf{r}_c, \omega_c) = \hat{r}_c e^{j\phi_c}$. Internal fields in general have only positive time exponential forms for both the E-and H-field spinors while external, radiating fields have only negative time exponential forms for both spinors. In EMSFT, particle-systems are assumed to consist of internal particles. According to EMSFT, all particles ion a system are related by a mathematics that links the way their internal particles balance each other while in dynamic motion.

DISCUSSION: In analogy to the spectroscopy of the hydrogen atom, the simple photon can exist in a range of states of varying energy. Whereas states of the hydrogen atom form a discrete set for instance, the Balmer series, the simple photon's states form a continuous set. Hence, as delimiters between states are crossed, sudden changes in the electromagnetic field can be encountered. This field mechanism appears to be important in cellular mechanisms such as metaphase and in intracellular mechanisms. This ability of the field to exist in different states varies with temperature, and hence the structure of hydration shells around macromolecules such as microtubules and DNA, also varies with temperature. Such structural mechanisms in the formation of the extracellular matrix may be involved in degenerative diseases as energy inside tissues diminishes with age.

In analogy to atomic elements, photonic 'elements' or compounds are also predicted. The strong nuclear force is known to exist in stable interactions between three quarks. This type of force can only be established if a third vector field, herein termed the nuclear field, exists in addition to the usual electric and magnetic fields. In this case, an extra spinorial motion in addition to the usual orbital and cyclotron motions, and orthogonal to both, must exist. This strong force may be involved in physical and biophysical reactions, in particular, concerning water compounds as the density of water rises and falls in a unique fashion amongst known molecules. This energetic principle based on hydration may be important in both meteorology and inside the cell where cycles based on energy and temperature occur.

This paper presents a new theory of the way photons may interact in biological tissues. What is needed at the start of the 21st century is further investigation of these and future theoretical insights based on EMSFT [5]. There is no doubt that numerical efforts in cellular biology will also be required in the same way that quantum theory and its numerical methods (quantum mechanics) were used to reveal the atomic structure and chemistry in the 20th century [6].

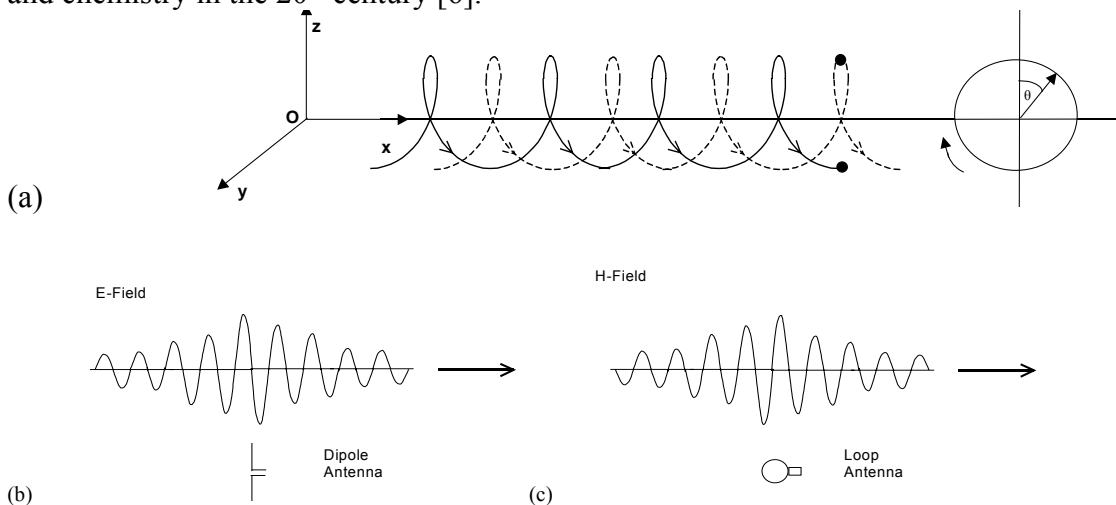


Fig. 1 Electromagnetic field, the wave packet, of a single radiating photon as shown in Figure 1a. The E-field shown in (b) is shifted in phase by 90° from the H-field shown in (c)

References.

- [1] J.D. Jackson, *Classical electrodynamics*, 3rd Edition, Wiley, 1999.
- [2] F.A. Popp, *About the coherence of biophotons*, *Microscopic Quantum Coherence, Proceedings of an International Conference*, World Scientific, 1999.
- [3] A.H.J. Fleming, *Physics Essays*, submitted 2003.
- [4] A.H.J. Fleming *EM self-field theory: the electron in hydrogen atom*. Biophotonics Research Institute; 2003. <http://www.biophotonicsresearchinstitute.com>
- [5] A.H.J. Fleming, E.B. Colorio *The Photon and its energy*. Biophotonics Research Institute; 2003. <http://www.biophotonicsresearchinstitute.com>
- [6] A.H.J. Fleming *Towards computational methods for studying cellular effects due to EM field*. Applied Computational Electromagnetics Conference, Naval Postgraduate College, Monterey, California; March 15-19, 1999.

P-B-180

THE MONITORING OF BTS IN ITALY SHOWS LOWER ENVIRONMENTAL LIMITS ARE ACHIEVABLE. L. Giuliani, F. Boella, ISPESL (Istituto Superiore Prevenzione E Sicurezza Lavoro) - Italian Health Ministry, Venezia, Corso del Popolo, 133.

KEYWORDS: minimisation of exposures, siting of mobile-phone base-stations, environmental limit values

INTRODUCTION: Since 1995, pushed by people who claimed against the cell siting in the neighbourhoods of their residences, the administrations of the cities in Italy developed a policy that was led by the precautionary principle for minimizing the exposure of general public. In 1998 the Italian Government adopted a decree that stated exposure limits lower than IEEE standard limits (C95-2, 1991) or ICNIRP limits (Guidelines, Health Physics, 1998)¹. An environmental exposure limit, named *quality target* was also improved². In Switzerland, the Federal Government adopted an Ordinance (NIRO 29/12/1999) which introduced environmental exposure limits depending on the frequency³. These limits were called *limits for the plants*. The Italian and Swiss limits were both justified by the aim to maintain the exposures levels as low as technologically achievable and the industrial capability to get that limits was tested. After five years of experiences in Italy and four years in Switzerland the BTS monitoring has shown that the quality targets and limits for plants are reached in Italy and in Switzerland. Furthermore almost everywhere lower environmental values for power density have been detected.

OBJECTIVE: To realize georeferenced maps of Pisa and of Venice where buildings are included and where a scale of pseudocolours represents the different exposure levels, showing that levels are lower than 0,1 W/m² everywhere and lower than 0,025 W/m² almost everywhere.

METHODS: Computer simulation of EMF generated by BTS is overlaid to georeferenced maps and a presentation manager provides the scale of pseudocolours. Spot measures are improved to check the simulation.

RESULTS: Thematic georeferenced maps of Venice and Pisa, where the theme is the electromagnetic level at mobile phone frequencies.

CONCLUSION: ALATA principle could be suitable for the application in environmental protection against NIR.

¹ 1 W/m² instead of 2 – 10 W/m² in the range 10 – 3000 MHz.

² 0,1 W/m² in the range 3 MHz – 300 GHz.

³ From 42 until 95 mW/m² in the range 10 – 2000 MHz.

Author Index

- | | | |
|---|-----------------------------------|---|
| Abe, H. 245 | Bianchi, E. 249 | Catalan-Aguilar, F. 84 |
| Adair, E.R. 27, 162 | Billaudel, B. 97, 195, 251, 313 | Cavani, F. 23 |
| Adam, S.L. 278 | Bingle, M. 140 | Cefalas, A.C. 35 |
| Adang, D. 261 | Bingle, M. 128 | Cerna, C. 253 |
| Addison, D. 277 | Binhi, V.N. 185, 318 | Chamberlain, M. 115 |
| Aebersold, R. 72 | Bisceglia, B. 288 | Chan, A. 205 |
| Ahn, S.S. 283 | Bit- Babik, G. 121 | Chan, N. 83 |
| Aizawa, K. 216 | Bitz, A. 30, 258 | Chang, K.T. 109 |
| Allen, M.J. 73 | Bitz, A.K. 139 | Chang, W.H. 109 |
| Allen, S.J. 27, 162 | Blackman, C.F. 206 | Charlet de Sauvage, R. 313 |
| Alsbach, W. 28 | Blackmore, P.F. 6 | Cheben, D. 22 |
| Aly, A. 178, 221, 228 | Blackwell, R.P. 260, 277 | Chen, C.J. 212 |
| Amyan, A.M. 200 | Blank, M. 102, 118, 317 | Chen, G.D. 99 |
| Anderson, V. 292 | Blick, D.W. 27 | Chen, J. 184 |
| Apollonio, F. 63, 67, 152, 295,
307 | Bloch, I. 322 | Chen, N. 197, 233, 245 |
| Arduino, L. 152, 159 | Blystone, R. 84, 253 | Chen, Q. 77 |
| Artemiou, M. 233 | Blystone, R.V. 173 | Chen, S. 315 |
| Asahi, S. 25 | Boella, F. 331 | Chen, S.D. 252 |
| Ashmore, J.L. 278 | Böhler, E. 166 | Chesselet, M.F. 278 |
| Avanesyan, A.S. 217 | Bonlie, D.A. 325 | Chiang, H. 62, 65, 77, 99, 172,
174, 289 |
| Ayrapetyan, S.N. 200, 201,
217, 225, 227, 230 | Booske, J.H. 47 | Cho, J.H. 164 |
| Baba, M. 50 | Bornhausen, M. 260 | Cho, Y.S. 164 |
| Babbitt, J.T. 269 | Bortkiewicz, A. 176, 181 | Choi, H-D. 286 |
| Babich, Y.F. 314 | Bottomley, A.L. 32, 260, 277 | Choi, H-D. 136, 301 |
| Baghdasaryan, N.S. 227 | Boumis, M. 288 | Choi, J.I. 136 |
| Bailey, W.H. 124 | Bowditch, S.C. 185 | Choi, W.-Y. 106 |
| Bakos, J. 281 | Bowman, J.D. 13 | Choi, Y.H. 186 |
| Balcavage, W.X. 96 | Bracken, T.D. 124 | Chou, C.K. 121, 122, 153, 155 |
| Ballen, M. 122 | Brandt, S. 28 | Chretien, P. 61 |
| Balzano, Q. 80, 126 | Brantley, M. 22 | Christ, A. 46, 76 |
| Barbul, A. 204 | Brazzale, A. 276 | Chung, Y.-C. 268 |
| Barnes, F.S. 178, 221, 228 | Brott, B. 253 | Chuyan, E.N. 275 |
| Bartram, R. 32, 260 | Brusil, I.A. 275 | Cleveland, Jr., R.F. 289 |
| Bartsch, B. 86 | Buescher, E.S. 231 | Clothier, R.H. 35 |
| Bassi, A. 182 | Bureau, Y. 272, 287 | Cohen, B.M. 19 |
| Bassi, A. 250 | Burgess, A. 168 | Colas, O. 130 |
| Beebe, S. 197 | Buschmann, J. 30 | Colorio, E.B. 328 |
| Beebe, S.J. 5, 6, 233, 245 | Button, C. 73 | Comlekci, S. 319 |
| Bell, S.L. 12 | Cadossi, R. 23, 120 | Conover, D.L. 13 |
| Bellier, P.V. 170 | Calabrese, M. 224 | Cook, C.M. 179 |
| Belyaev, I. 209, 219 | Cao, X. 69, 226, 251 | Coppage, H. 253 |
| Benane, S.G. 206 | Capri, M. 249 | Cox, D.D. 300 |
| Bernard, N. 61 | Cardis, E. 13 | Craft, C.M. 38 |
| Bersani, F. 57, 195, 249 | Carlezon Jr, W.A. 19 | Crawley, D.A. 41 |
| Bhanushali, A. 86 | Carosella, S. 249 | Cristoforetti, L. 107 |
| | Carson, J.J.L. 54 | Croft, R.J. 292 |
| | Castello, G. 224 | |

Cui, X.....	251	Fitzner, R.....	57, 211	Hadjem, A.....	322
Curran, A.R.....	44, 55	Fleming, A.H.J.....	328	Hagness, S.C.....	47
d'Ambrosio, G.....	224	Fleming, S.M.....	278	Hahn, T.J.....	269
D'Andrea, J.....	90	Forigo, D.....	137, 198	Haik, Y.....	212
D'Arienzo, M.....	42	Foster, K.R.....	126	Hall, E.....	6
D'Emilia, E.....	280	Fouad Hanna, V.....	322	Hamnerius, Y.....	16
D'Inzeo, G. ...	63, 67, 295, 307	Francavilla, M.....	137	Hanazawa, M.....	52
Dale, C.....	322, 323	Franceschi, C.....	249	Hannemann, S.....	240, 242
Dale, C.....	82, 130, 142	Frey, W.....	233, 245	Hansen, V.....	30, 258
Dall'Oca, C.....	120	Fricker, M.....	185	Hansen, V.W.....	139
Damron, T.A.....	73	Fröhlich, J.....	15, 83, 112, 132, 262	Harada, H.....	29
David, E.....	320	Fu, H.Y.....	65	Hardell, L.....	183
De Gregori, L.....	42, 307	Fu, Y.T.....	65	Harms-Ringdahl, M.....	219
Deltour, I.....	13	Fukada, E.....	25	Haro, E.....	97, 251, 273
Dengler, R.J.....	39	Gadi, N.....	322	Harrington, J.....	21
Dertinger, H.....	222	Gadzicka, E.....	176, 181	Harrington, T.....	289
Detlefsen, J.....	260	Gajda, G.....	170, 310	Harrison, P.K.....	32, 257
DiCarlo, C.D.....	278	Galindo, C.....	8, 36, 37	Hashimoto, O.....	146
Ding, G-R.....	244	Gallerano, G.P.....	35, 42	Hata, K.....	79
Ding, G-R.....	220	Galloni, P.....	276	Hatada, T.....	304
Doh, H.J.....	147, 208	Gandhi, O.P.....	87, 158	Haylock, R.G.E.....	260
Domínguez-González, A. .	274	Gargiulo, G.....	249	Hayrapetyan, H.V.....	217
Doria, A.....	42	Garner, A.L.....	197, 207	Heard, A.....	168
Douglas, G.R.....	170	Garza, T.H.....	278	Heetderks, W.J.....	2
Douglas, M.....	122	Gates, L.....	207	Herbst, E.....	271
Douglas, M.G.....	153, 155	Gay, H.....	22	Higashikubo, R.....	231
Dressel, M.....	35	Gerber, H.L.....	182, 184, 250	Hillert, L.....	219
Dronne, V.....	130	Gianni, M.....	63	Hirahara, F.....	282
Dubois, W.....	28	Gilgenbach, R.M.....	207	Hirose, H..	214, 220, 237, 244
Dunbar, K.....	184	Gimm, Y.M.....	283, 286	Hirota, S.....	252, 258, 266
Ebara, H.....	146	Giovenale, E.....	42	Hiwaki, O.....	255
Eberle, J.....	260	Giuliani, L.....	331	Hobson, R.J.....	32
Eggers, J.....	84	Gminski, R.....	211	Holcomb, R.R.....	100, 118
Eggers, J.S.....	173	Goodman, R.....	118	Holden, S.J.....	185
Eguchi, Y.....	235, 247, 312	Goodman, R.....	102, 317	Hong, S.C.....	164
Elder, J.....	81	Gover, A.....	204	Hosokawa, K.....	320
Elías-Viñas, D.....	274	Gowrishankar, T.R.....	4, 316	Hosokawa, K.....	216
Eliran, A.....	204	Grado, A.R.....	278	Houchi, H.....	320
Elliott, P.....	168	Greenebaum, B.....	131	House, D.E.....	206
Engström, S.....	100, 118	Griffin, T.....	72	Huang, T.-Q.....	268
Eom, S.J.....	262	Griffin, T.J.....	57	Huang, L.L.....	252
Erdreich, L.S.....	149	Grimaldi, S.....	223, 280	Huang, T.-Q.....	269
Erhard, M.....	260	Grose, R.I.....	185	Hughes, M.M.....	325
Espinosa, J.M.....	273	Grosse, E.....	35	Hunanyan, A.Sh.....	201
Etou, F.....	255	Grossi, G.F.....	224	Huo, X.L.....	234
Evans, L.O.....	185	Guevara-Guzmán, R.....	274	Hurt, W.D.....	44, 55, 90, 300
Faraone, A.....	121	Guillosson, J-J.....	61	Hyun, Y.J.....	164
Fedrowitz, M.....	31	Gundersen, M.A.....	38	Ikehara, T.....	320
Feychting, M.....	16	Haberland, L.....	28	Ikehara, T.....	216
Fini, M.....	23			Ikehata, M.....	103

Ikeya, M.	279	Kishimoto, T.	252	Lisi, A.	223, 280
Inns, R.H.	185	Kitamura, M.	320	Little, M.	168
Ishido, R.	163	Kitamura, M.	216	Liu, J.	226, 251
Ishii, A.	50	Kitayama, J.	323	Loeser, M.	46
Iskra, S.	134	Klingenböck, A.	46	Loftin, K.C.	197, 245
Isozumi, Y.	229, 244	Kloth, L.C.	24	Logani, M.K.	86
Ito, K.	163	Koana, T.	103	Lopresto, V.	159
Ivancsits, S.	57	Kolb, J.	7, 46, 197, 233, 243, 245, 250	Löscher, W.	31
Izzo, F.	224	Komatsubara, Y.	236	Lovisolò, G.A.	152, 159
Jang, J.-J.	268, 269	Komuratani, T.	279	Lu, D.Q.	62, 65, 77, 99, 172, 174
Jenssen, D.	209	Korenstein, R.	35, 204	Lu, S.-T.	297
Jepsen, P.	35	Korenstein-Ilan, A.	204	Lundquist, M.A.	326, 327
Ji, Z.	47	Kotani, H.	245	Lutman, M.E.	12
Jia, C.	315	Koyama, S.	71, 220, 229, 237, 244	Lymyre, P.	170
Jia, F.	263	Kramer, A.	75	Lyskov, E.	177
Johansson, A.	105, 177	Kummet, T.	21	Maercker, C.	57, 72
Johansson, F.	209	Kundi, M.	142	Malacarne, C.	107
Johnson, D.S.	5, 184	Kuster, N.	15, 16, 46, 72, 75, 76, 83, 112, 132, 249, 262	Malmgren, L.	219
Johnson, M.T.	26, 96	Lagroye, I.	97, 195, 251, 273, 313	Mancini, S.	152, 159
Jokela, K.	129, 306	Lake, D.	22	Mann, S.	13
Joos, T.O.	58	Lambrozo, J.	61	Mannerling, A.C.	33, 240
Jordan, D.W.	207	Lane, R.	185	Mäntele, W.	35
Joseph, W.	92	Lange, S.	242	Mantiply, E.D.	289
Joshi, R.P.	197, 245	Lantow, M.	226	Marcu, L.	38
Ju, M.N.	188, 315	Lanzarini, C.	249	Margulies, B.S.	73
Jung, K.C.	283	Lau, Y.Y.	207	Marino, C.	159, 276
Kaczmarczyk, A.	113	Lautru, D.	322	Markov, M.	194
Kaledzic, N.	177	Ledda, M.	223, 280	Markov, M.S.	100, 205
Kalns, J.	84, 253	Lee, A.K.	136	Markova, E.	209, 219
Kalns, J.E.	173	Lee, J.-J.	269	Maršálek, E.	290
Kanda, M.	11, 122, 155	Lee, J.S.	283	Marseu, K.	287
Kandori, H.	35	Lee, J.-S.	268, 269	Martens, L.	92, 143
Kaneko, A.	312	Lee, J.Y.	283	Martin, G.T.	316
Kang, G.	87, 158	Lee, S.	182, 184	Marttila, E.A.	44, 55
Kapranov, S.V.	185	Lee, S.K.	283	Martynyuk, V.S.	275
Keenliside, L.	189	Lee, Y-S.	286	Masaoka, T.	25
Kelsh, M.	83	Lemay, E.	170, 310	Mason, P.	84, 253
Kelsh, M.A.	15	Lemyre, P.	310	Mason, P.A.	44, 55, 90, 173, 300
Khachatryan, M.G.	225	Lerchl, A.	28, 139, 258	Massa, R.	224
Khan, N.	168	Leszcznski, D.	104, 117	Masuda, H.	52, 251, 252, 258, 263, 265, 266
Kheifets, L.	16, 269	Leszczynski, D.	57, 59, 72	Mathur, S.	47
Kiel, J.	84, 253	Li, H.	62, 172, 174	Mathur, S.P.	8, 36, 278
Kiel, J.L.	173	Li, Q.	87, 158	Mattsson, M.O.	33, 240
Kim, N.	186, 301	Liberti, M.	63, 67, 295, 307	Mazzanti, M.	67
Kim, S.H.	286	Lin, H.	102, 317	Mazzurana, M.	107
Kim, Y.S.	164	Linfield, E.H.	41	McKenzie, R.J.	134, 292
Kim, Y.-W.	283			McLean, D.	13
Kimura, D.	25				
Kinouchi, Y.	320				
Kinouchi, Y.	216				

McLean, M.J.....	100, 118	Nakahara, T.....	214, 229, 244	Pitt, W.....	116
McNamee, J.....	310	Napolitano, M.....	224	Pokovic, D.....	76
McNamee, J.P.....	170	Natarajan, M.....	8, 36, 37	Pontalti, R.....	107
McNeeley, M.....	15	Nayak, B.K.....	8, 36, 37	Poullietier de Gannes, F....	195, 251
McNeely, M.....	83, 149	Neasham, D.....	168	Prato, F.S. ...	23, 179, 189, 272, 287
Meltz, M.....	47	Nelson, D.A.....	44, 55	Preiner, P.....	113
Meltz, M.L.....	8, 36, 37	Nelson, R.M.....	298, 299	Puranen, L.....	306
Merla, C.....	307	Neubauer, G.....	113	Qian, X.....	251
Mesirca, P.....	195, 249	Neubauer, G.G.....	16	Qutob, S.S.....	170
Messina, G.....	42	Ng, E.T.....	55	Rahne, E.....	281
Meyer, F.J.C.....	140	Nichols, T.W.....	325	Ramundo-Orlando, A.	42, 307
Meyer, F.J.C.....	128	Nielson, W.R.....	189	Rathnabharathi, K....	178, 228
Mild, K.H... 33, 105, 177, 183, 240		Nikoloski, N.....	75, 76, 262	Rathnabharathi, K.N.....	221
Millenbaugh, N.....	84, 253	Nindl, G.....	26, 96	Ravazzani, P.....	12, 276
Millenbaugh, N.J.....	173	Nojima, T.....	171, 236	Reinhardt, T.....	30
Milyaev, V.A.....	185	Nuzhdina, M.A.....	314	Reißenweber, J.....	320
Min, S.W.....	133, 315	Nylund, R.....	57, 58, 72	Reivinen, J.....	72
Minko, V.A.....	275	Oesch, W.....	75	Remondini, D.....	57
Miyagawa, N.....	25	Ogasawara, T.....	282	Renshaw, P.F.....	19
Miyakoshi, J..... 71, 171, 214, 220, 229, 236, 237, 238, 244		Ogiue-Ikeda, M.....	323	Resig, P.....	271
Miyamoto, H.....	320	Ogiue-Ikeda, M.....	193	Reyes-Guerrero, G.....	274
Miyamoto, H.....	216	Oh, H.T.....	186	Richards, L.....	185
Miyota, Y.....	160	Ohkubo, C. .52, 252, 258, 263, 265, 266		Rieti, S.....	223, 280
Molchanova, O.P.....	17	Oka, A.....	35	Robertson, J.A.....	272
Molla-Djafari, H.....	142	Okano, H.....	265, 266	Rohan, M.L.....	19
Molnár, B.F.....	281	Okorn, S.....	260	Rollman, G.B.....	189
Morin, J.M.....	278	Onishi, T.....	146, 163	Romanò, M.....	195
Morishita, K.....	25	Osiander, R.....	34	Röösli, M.....	16
Moros, E.....	9	Pack, J.K.....	136, 147, 208	Rosola, E.....	223, 280
Morrissey, J.J.....	11, 81	Pack, J.-K.....	268, 269	Roti Roti, J.L.....	9, 231
Moskovchuk, O.B.....	275	Pack, J-K.....	286	Rowley, J.....	134
Moulton, C.J.....	96	Paffi, A.....	67	Rudiger, H.....	57
Muehsam, D.....	91	Pakhomov, A.....	7	Ruffie, G.....	97
Mueller, J.....	9	Parazzini, M.....	12, 276	Sacco, D.....	280
Murakami, M.....	245	Park, J.D.....	186, 301	Sadasiva, A.....	298, 299
Murphy, M.....	7	Patti, A.M.....	223	Sage, C.....	80
Murphy, M.R.....	90	Pearce, L.A.....	325	Saito, K.....	163
Murray, S.S.....	269	Pedrick, N.....	253	Sakuma, N.....	236
Mylacraine, K.S.....	27, 162	Pellegrino, M.....	67	Sakurai, T.....	71, 229
Myung, S.H.....	133, 188, 315	Perrine, M.....	289	Salvatore, J.R.....	21
Nadon, L.....	13	Perrot, F.....	82	Sanchez, S.....	195, 251
Nafziger, J.....	61	Perrotta, A.....	198	Sandrini, L.....	107
Nagaeva, E.I.....	275	Persson, B.....	219	Sandström, M.....	105, 177
Nagai, T.....	103	Persson, T.....	157	Sannino, A.....	195, 224
Nagawa, H.....	323	Petraglia, G.....	224	Santini, R.....	294
Nagawa, H.....	79	Petrowicz, O.....	260	Saotome, T.....	255
Nakagawa, H.....	245	Pilla, A.A.....	91, 191	Sarimov, R.....	209, 219
		Pinto, R.....	152, 159	Sarimov, R.M.....	185
		Piscitelli, M.....	276		

Sarti, M.	159, 224	Smith, R.R.	231	Thomas, N.....	12
Satoh, K.....	160	Smith, S.J.....	185	Thompson, A.	22
Scampoli, P.	224	Soda, A.	216	Thoss, F.....	86
Scarfi, M.R. 35, 159, 195, 198, 224		Sommer, A.M.	28, 139, 258	Thuroczy, G.	12
Schelkshorn, S.....	260	Song, K.H.	133	Thuróczy, G.	281
Schiavoni, A.....	137, 198	Song, T.	234	Tian, B.	315
Schimmelpfeng, J.....	222	Sorimachi, T.	25	Toivonen, T.....	306
Schlatterer, K.	57, 211	Spadaro, J.A.	73	Tominaga, K.	35
Schmid, G.	142	Spät, D.....	112, 132	Törnevik, C.....	157
Schmid, K.	76	Stangassinger, M.	260	Toutain, Y.....	82
Schneiderman, G.S.....	212	Stensson, O.....	105, 177	Traikov, L.L.....	263
Schoenbach, K.H.2, 5, 6, 7, 46, 197, 231, 233, 243, 245, 250		Stewart Jr., D.A.	316	Tranquilli, A.M.....	295
Scholl, D.M.....	27	Stewart, D.A.....	4	Trillo, M.A.....	206
Scholz, R.....	84	Stohrer, M.....	260	Tsai, M.T.	109
Schroeder, M.J.	298, 299	Stoll, D.	58	Tseng, C.C.	5, 6, 182, 184
Schuderer, J.....	72, 97, 249	Streckert, J.....	30, 139, 258	Tsurita, G.....	79
Schulze, C.H.	24	Stuck, B.	7	Ubeda, A.....	206
Schüz, J.	16, 166	Sun, M.	184	Überbacher, R.....	113
Seaman, R.L.....	278	Sun, W.J.	65	Uebayashi, S.	146, 163
Sekijima, M.....	146, 171, 236	Sun, Y.....	38	Ueno, S.	323
Sekino, M. 192, 193, 241, 255, 304, 312		Suzuki, Y.	50, 103, 237, 238, 258	Ueno, S.	79, 192, 193, 235, 241, 245, 247, 255, 304, 312
Selivanova, G.....	209	Swanson, R.J.	197, 245	Ugolini, L.....	249
Senior, R.S.	124	Swegle, V.M.....	90	Uhler, M.D.....	207
Seo, J.-S.	268, 269	Swicord, M.	121	Ulukut, O.	319
Seo, M.-H.....	106	Swicord, M.L.....	80, 81, 126	Underwood, G.....	32, 257
Setti, S.....	23, 120	Sypniewska, R.....	84, 173, 253	Uney, J.B.	32
Shen, Y.....	41	Szymczak, W.....	176	Uno, T.	52
Sheppard, A.R. 15, 80, 83, 126		Taday, P.....	35	Updahya, P.C.....	41
Shichijo, H.	216	Takashima, Y.	71, 220, 237, 238	Ushiyama, A.	252, 258, 263
Shono, M.....	320	Takeda, H.	171, 236	Vaccari, A.....	107
Shum, M.....	15, 83	Takeuchi, M.	241	Van Kerkhove, M.D.	149
Shupak, N.M.	23, 189	Taki, M.	50, 52, 79, 103, 229, 237, 238, 258	van Wyk, M.J.....	128
Siegbahn, M.	157	Tan, J.	253	VanderVorst, M.A.	261
Siegel, P.H.	39	Tanguy, M-L.	61	Vasilkoski, Z.....	4
Sienkiewicz, Z.J. 32, 260, 277		Tani, K.....	146	Vázquez, M.....	274
Sihvonen, A.P.	306	Tarango, M.	253	Vecchia, P.....	13
Sihvonen, A.-P.....	129	Tattersall, J.E.H.....	32	Verdugo-Diaz, L.....	274
Simeonova, M.....	28	Tattersall, J.E.H.....	257	Vermeeren, G.....	143
Simkó, M.....	226, 240, 242	Tauber, R.....	57, 211	Vernier, P.T.	38
Simonyan, R.H.....	217	Taxile, M.....	97	Veyret, B.....	273
Sisken, B.F.....	205, 271	Templin, M.F.....	58	Veyret, B.....	97, 195, 251, 313
Sivo, F.....	191	Temuryants, N.A.	275	Vijayalaxmi.....	86
Smirnov, I.	311	Teramoto, T.....	320	Vulcano, A.....	223
Smith, A.J.....	32, 257	Thansandote, A.....	170, 310	Wachtel, H.....	167
Smith, J.	205	Thomas, A.W.	23, 179, 189, 272, 287	Waite, L.R.....	96
Smith, J.M.....	271	Thomas, B.W.....	134	Wake, K.	52, 79, 229

Walleczek, J.....	54	Wu, SH.Z.	148	Yoo, D.S.	286
Wan, Q.....	46, 243	Xia, R.	315	Yoo, D.-S.....	106
Wang, D.....	69, 226, 251	Xu, M.	9	Yoshizaki, K.....	320
Wang, S.M.	182, 184	Xu, X.N.....	46, 243	Yoshizaki, K.....	216
Wang, Z-M.	5	Xu, Z.	289	Yuan, H.....	212
Watanabe, H.	52	Xu, Z.P.	62, 77, 99, 172, 174	Yun, J.H.....	136
Watanabe, S.	50, 52, 79, 160	Yamaguchi, H.	320	Yun, J.-H.	106
Weaver, J.C.....	4, 316	Yamaguchi, H.	79, 216	Zeng, Q.L.....	62, 99, 172, 174
Weibezahn, K.-F.....	222	Yamaguchi, K.	312	Zeni, O.....	195, 198, 224
Weisbrot, D.....	317	Yamaguchi, S.	193	Zhang, M.	118
Weng, Y.....	174	Yamamoto, K.	25, 35	Zhang, Q.-M.	214
White, J.....	6	Yamanaka, Y.....	52, 160	Zhang, S.....	226
Whitehead, T.D.....	231	Yamashita, H.....	323	Zhao, M.	69, 226, 251
Wiert, J.....	322, 323	Yan, J.	148	Zhou, C.Q.	182, 184
Wiert, J.....	16, 82, 130, 142	Yang, J.	197, 245	Zhou, E.	178
Wilén, J.....	105, 177	Yang, K.H.	188, 315	Zhou, Q.....	250
Witzmann, F.	253	Yang, W.	234	Zhou, R.....	221, 228
Wojtysiak, A.	320	Yasunaga, K.	171	Ziriax, J.M. 27, 44, 55, 90, 300	
Wong, M.F.....	322	Yauk, C.L.....	170	Ziskin, M.C.....	86
Wong, M.F.....	82	Ye, H.	252	Zmyslony, M.	181
Wright, L.....	22	Yokoi, S.	279	Zorzi, C.....	120
Wu, D.W.....	109	Yonei, S.....	214		